Abstracts Volume

Edited by: Gerardo Carrasco-Núñez Jose Jorge Aranda-Gómez, Michael H. Ort., and J, Jesús Silva-Corona

http://maar2014.geociencias.unam.mx

5th INTERNATIONAL MAAR CONFERENCE

Querétaro, México, November 17-22, 2014

Cinder cones and Aljojuca maar, Puebla, Mexico

THIS BOOK MUST BE CITED AS:

Carrasco-Núñez, G., Aranda-Gómez, J.J., Ort, M.H., Silva-Corona, J.J., 2014, 5th International Maar Conference, Abstracts Volume: Juriquilla, Qro., México, Universidad Nacional Autónoma de México, Centro de Geociencias, 246 pp.

THE ABSTRACTS OF THIS BOOK MUST BE CITED AS THE NEXT EXAMPLE:

Mora-Amador, R., González, G., Alpizar, Y., Ramírez, C., Rouwet, D., 2014, Monogenietic volcanism of Costa Rica back-arc: Aguas Zarcas Piroclastic cones, *in* Carrasco-Núñez, G., Aranda-Gómez, J.J., Ort, M.H., Silva-Corona, J.J., (eds.) 5th International Maar Conference, Abstracts Volume: Juriquilla, Qro., México, Universidad Nacional Autónoma de México, Centro de Geociencias, 82-83.

Design and Technical Edition:
J. Jesús Silva Corona.

Unidad de apoyo editorial,
Centro de Geociencias,
Universidad Nacional Autónoma de México.
October 2014.

Organizing Committee

Chairs

Gerardo Carrasco-Núñez	(gerardoc@geociencias.unam.mx)
Jorge Aranda-Gómez	(jjag@unam.mx)

Members

Pablo Dávila - logistical advisor	(pablo.davila@ipicyt.edu.mx)
Mario López - logistical advisor	(mario_lopr@geociencias.unam.mx)
Michael Ort - logistical advisor	(michael.ort@nau.edu)
Károly Németh- organizing advisor	(K.Nemeth@massey.ac.nz)
José Luis Macías - logistical advisor	(macias@geofisica.unam-mx)

International Advisory Committee

Bernd Zimanowski	(zimano@geologie.uni-wuerzburg.de)
Greg Valentine	(gav4@buffalo.edu)
Guido Giordano	(guido.giordano@uniroma3.it)
Ian Smith	(ie.smith@auckland.ac.nz)
James White	(james.white@otago.ac.nz)
Joan Martí	(joan.marti@ija.csic.es)
Jorg Negendank	(neg@gfz-potsdam.de)
Piero Dellino	(dellino@geomin.uniba.it)
Pierre-Simon Ross	(pierre-simon.ross@ete.inrs.ca)
Shane Cronin	(S.J.Cronin@massey.ac.nz)
Volker Lorenz	(vlorenz@geologie.uni-wuerzburg.de)
Young Kwan Sohn	(yksohn@gsnu.ac.kr yksohn@nongae.gsnu.ac.kr)

Local support

Ulises Álvarez-webmaster	(uma@geociencias.unam.mx)
Juan Manuel López- Technical support	(jmlopez@geociencias.unam.mx)
Emilio Nava- Technical support	(enava@geociencias.unam.mx)
J. Jesús Silva- Technical Editor	(jsilvac@geociencias.unam.mx)

SESSION 1

ORAL PRESENTATIONS AND POSTERS
NOVEMBER 18, 2014

Maars over cones: repeated volcanism in the same location along fissures in western Saudi Arabian volcanic fields

Károly Németh[1], Mohammed R. Moufti[2], Nabil El-Masry[2], Atef Qaddah[2], and Zoltán Pécskay[3]

[1] *Volcanic Risk Solutions, Institute of Agriculture and Environment, Massey University, Palmerston North, New Zealand.* k.nemeth@massey.ac.nz
[2] *Geohazards Research Centre, King Abdulaziz University, Jeddah, Kingdom of Saudi Arabia.*
[3] *Institute of Nuclear Research of the Hungarian Academy of Sciences, Debrecen, Hungary.*

Keywords: scoria cone, crater, monogenetic.

Understanding monogenetic volcanism, in terms of defining eruption volumes, durations, and periodicities, is the subject of much recent research (Németh, 2010). These studies have identified numerous inconsistencies in eruption durations, temporal changes in eruption intensities, eruptive fluxes, chemical compositions and eruption breaks associated with distinct eruptive phases of these typically small-volume volcanoes, which are best defined to be monogenetic. Here we present field data from western Saudi Arabia to demonstrate the variety of rejuvenating volcanism that can occur in nearly the same location over various time scales that can connected with variable levels of geological evidence.

The western margin of the Arabian Peninsula hosts at least 12 extensive volcanic fields that evolved since 10 Ma to recent times, with many of them having volcanic eruptions in the past 10 ka (Coleman *et al.*, 1983) (Fig. 1). Here we explore two extensive intracontinental alkaline basaltic volcanic fields (Harrat Kishb and Hutaymah) located far from the present day Red Sea rift axis (Fig. 1). A common feature of these volcanic fields is the abundance of phreatomagmatic volcanoes such as maars and tuff rings (Camp *et al.*, 1992; Moufti *et al.*, 2013; Pallister, 1985).

Here we selected four maar volcanos with well-exposed tuff ring successions and associated volcanic morphologies (Fig. 2). Al Wahbah is a large maar in the SW edge of the Harrat Kishb (Fig. 2A) with at least two major lava flow fields cut through by a maar crater that is about 2.3 km across (Fig. 3A). A moderately eroded scoria cone and some sporadic lava spatter ramparts sit on the basal pre-maar lava flows. The significance of this maar is that, in spite of a recent Ar-Ar study demonstrating a time gap between the emplacement of the basal lava flows and scoria cones and the inferred timing of maar formation (Abdel Wahab *et al.*, 2014), there is an ambiguity in the stratigraphy; there seems to be no evidence in the stratigraphy of time breaks between the formation of the lava flows and spatter ramparts immediately underlying the tuff ring of the maar. This information was used to interpret the formation of Al Wahbah as being similar to the maars that erupted in Sonora, such as Crater Elegante, where a sudden magma withdrawal facilitated the erupting conduit's access to ground water, leading to a maar-forming explosive eruption followed by Strombolian and effusive phases (Gutmann, 2002).

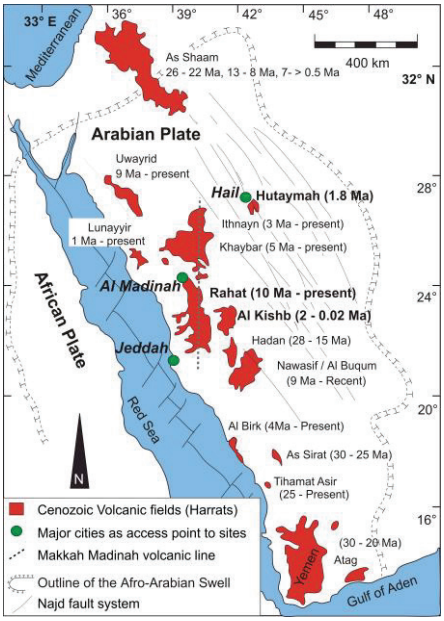

Fig. 1 – Volcanic fields of the Arabian Peninsula with their commonly accepted eruption durations. Harrat Kishb and Hutaymah are generally accepted to be young volcanic fields; however, as has been demonstrated from Harrat Rahat, volcanism seems to have been more widespread and sporadic in the past 10 Ma.

Hutaymah maar in Harrat Hutaymah (Figs 2B and 3B) is slightly smaller than Al Wahbah, and its volcanic edifice shows strikingly similar stratigraphy to Al Wahbah's, having basal lava flows and scoria cones forming the pre-maar successions. The K-Ar ages and the sedimentological observations confirm that these pre-maar volcanics formed significantly prior to the maar, suggesting that the maar erupted in an almost identical location to where a scoria cone had erupted several tens of thousands of years earlier.

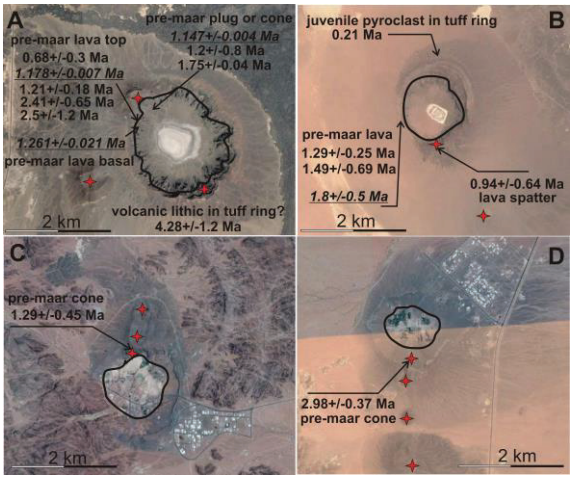

Fig. 2 – Age of various volcanic units of Al Wahbah (A), Hutaymah (B), Jubb (C) and Tabah (D) maars. On "A" italic numbers refer to dates from recent Ar-Ar studies. Italic numbers on "B" refer to previous K-Ar age data.

In other two locations, at the Jubb and Tabah maars (in Harrat Hutaymah), sedimentological and volcanic geomorphology evidence indicates a significant time gap between the formation of pre-maar scoria and spatter cones and the maar. The pre-maar cones have been exhumed and are today located in an erosionally enlarged depression. The pre-maar landforms have been engulfed by medial to distal base surge deposits (Figs 2C, D and 3C, D).

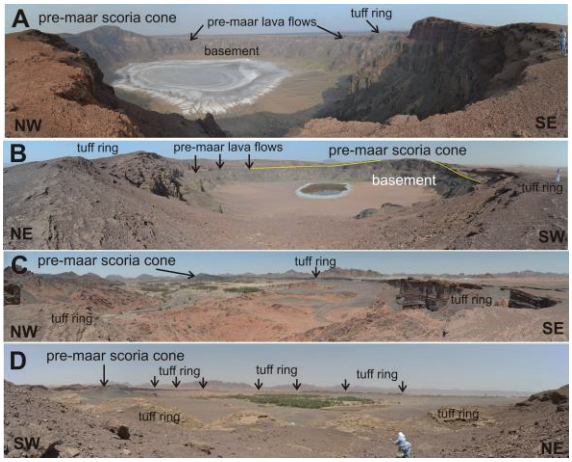

Fig. 3 – Al Wahbah (A), Hutaymah (B), Jubb (C) and Tabah (D) maars erupted in the same location as pre-maar scoria cones and lava flows that had formed along a fissure.

The difficulty, or sometimes impossibility, of recognizing any sedimentological features associated with a time gap between pre-maar volcanoes and maars formed near-identical locations provides a graphic example that care must be taken when inferring that such magmatic explosive and effusive products are immediate precursory events of maar eruptions. It needs to equally considered that, in spite of a general assumption that volcanic eruptions rarely recur in the same location in monogenetic volcanic fields, such scenarios might be more common than we expect.

Acknowledgements

This work was supported by the Volcanic Risk in Saudi Arabia (VORiSA) project, managed by King Abdulaziz University and the University of Auckland.

References

Abdel Wahab, A., Abul Maaty, M.A., Stuart, F.M., Awad, H. and Kafafy, A., 2014. The geology and geochronology of Al Wahbah maar crater, Harrat Kishb, Saudi Arabia. Quaternary Geochronology, 21 (Special Issue: Advances in $^{40}Ar/^{39}Ar$ Dating of Quaternary Events): 70-76.

Camp, V.E., Roobol, M.J. and Hooper, P.R., 1992. The Arabian Continental Alkali Basalt Province .3. Evolution of Harrat Kishb, Kingdom of Saudi-Arabia. Geological Society of America Bulletin, 104(4): 379-396.

Coleman, R.G., Gregory, R.T. and Brown, G.F., 1983. Cenozoic volcanic rocks of Saudi Arabia. Saudi Arabian Deputy Minister of Mineral Resources, Open File Report, 590 USGS-OF93: 1-82.

Gutmann, J.T., 2002. Strombolian and effusive activity as precursors to phreatomagmatism; eruptive sequence at maars of the Pinacate volcanic field, Sonora, Mexico. Journal of Volcanology and Geothermal Research, 113(1-2): 345-356.

Moufti, M.R., Németh, K., El-Masry, N. and Qaddah, A., 2013. Geoheritage values of one of the largest maar craters in the Arabian Peninsula: the Al Wahbah Crater and other volcanoes (Harrat Kishb, Saudi Arabia). Central European Journal of Geosciences, 5(2): 254-271.

Németh, K., 2010. Monogenetic volcanic fields: Origin, sedimentary record, and relationship with polygenetic volcanism. The Geological Society of America, Special Paper 470: 43-66.

Pallister, J.S., 1985. Reconnaissance geology of the Harrat Hutaymah Quadrangle, sheet 26/42A, Kingdom of Saudi Arabia. Open-File Report - U. S. Geological Survey: 82-82.

Reconstruction of the morphological evolution and the eruptive dynamics of the Lechmine n'Aït el Haj Maar in the Middle Atlas karstic province of Morocco.

Sara Mountaj [1], Toufik Remmal [1], Iz-Eddine El Hassani El Amranié[2], Benjamin van Wyk de Vries[3]

[1] *Laboratoire des Géosciences Appliquées à l'Ingénierie d'Aménagement, Faculté des Sciences Aïn Chok, Université Hassan IICasablanca Maroc.* sara.mountaj@gmail.com
[2] *Institut de Recherche Scientifique-Rabat. Maroc.*
[3] *Laboratoire Magmas et Volcans, UMR6524 CNRS, Observatoire du Physique du Globe de Clermont, Clermont-Ferrand II. Université Blaise Pascal- France.*

Keywords: Maar, Karst, Lechmine n'Aït el Haj.

The Lechmine n'Aït el Haj maar is part of a Quaternary volcanic complex in the north east part of the Neogene Middle Atlas volcanic province.

The maar is about 800 m across and 60 m deep. Its lower 30 m cuts into Liassic limestone overlain by thin alluvial and volcaniclastic beds.

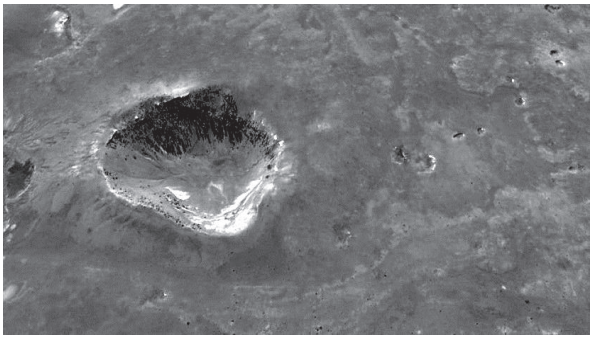

Fig 1. - The Lachemine Maar from Google Earth. The Maar is about 800 m across, and the north is the bottom of the picture. Note small holes to the right of the picture, which are dolines, or karstic collapse features cutting the lava fields. These are termed cryptokarst.

The overall style of the eruptive deposits is phreatomagmatic.

There is a thin basal scoriaceuous bombs unit followed with a coarse breccia unit, rich in limestone blocks that could be related to the initial opening of the maar structure. This is overlain by lenticular units, 1 to 3 m thick, of tuff, rich in dense juveniles, fine ash and limestone lithics.

The limestone fragments can be fresh, have altered limey rims, or be fully altered.

The lenses form larger packets of up to 30 m thick, that thin and thicken rapidly, and form overlapping small tuff cones. These indicate a shifting main explosion point.

Towards the summit, the tuffs are replaced by scoria and lava bomb deposits that form two semi-cricular rings around the maar.

The larger, eastern ring 1 is composed of mostly scoriaceous lapilli and bombs, and can be traced 500 m north to a finely bedded scoria deposit exposed in a large quarry.

The smaller southern and western ring 2 is formed of blocky lava fragments, that are dense and non-vesicular. This deposit sometimes has a fine tuff matrix.

The south west side of the crater is covered with a lava flow, that flows down into the crater. Flow lobes are clearly distinguishable, and the lava clearly arrives at the maar rim and cascades in. No lava is found at in the base of the maar. In contrast there is a small limestone cliff.

Fig 2. - The Lachemine Maar from inside: the tuff cliffs with individual lenses of 1 to 34 m thickness.

As the blocky lava ring 2 contains similar lava to the flow, it is likely that the flow was fragmented by phreatomagmatic activity as it reached the maar floor. This means the ring 2 is a 'rootless ring' rather than a primary eruptive feature.

The ring 1 covers the ring 2 on the eastern side, which indicates that the lava entered the maar after the main tuff cone building phase, but before the end of the non phreatomagmatic scoria ring phase. Thus, the tuff ring – maar, lava flow and scoria ring are part of the same eruptive episode.

Fig 3. - The Lachemine Maar tuff, showing the abundance of Liassic limestone lithics. The notebook is 15 cm across.

Fig. 4. A view over the Lachemine Maar from the rim.

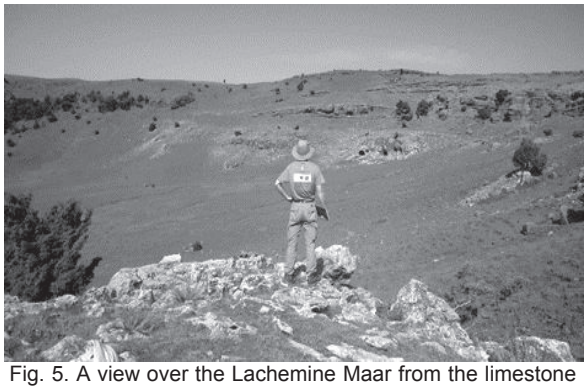

Fig. 5. A view over the Lachemine Maar from the limestone basement exposed in the crater. The Liassic limestone is also at the level of the head, overlain by tuff and topped by the tuff ring 2 blocky lava breccia. The lava flow is on the left hand side.

The sequence of events for the eruption is thus:

1. Start of eruption, with an initial magmatic burst.
2. Interaction with karstic water, to generate strong pheatomagmatic activity and the start of maar formation. This may have been aided by cave systems in the karst, that could be invaded by water and by magma.
3. Progressive growth of the maar by small shifting points of eruption
4. Arrival of the lava flow, and its cascade into the crater. Strong fragmentation of the lava in what must have been a deep water-filled crater. In another part the maar eruption continues, or is mixed with the lava fragmentation.
5. Creation of the blocky tuff cone and a gradual drying of the maar lake.
6. Exhaustion of the water and continued eruption of dry magma from the eastern part of the maar, possible as the lava flow had block and western and southern vents.
7. End of the eruption with final scoria phase.
8. Possible continued sinking of the maar with limestone dissolution.

The sequence seen in the Lechmine n'Aït el Haj maar is repeated in other similar structures in the volcanic field. However some structures form collapse features that cut the tuff ring deposits and lava cascades, suggesting that the maars are commonly deepened by post eruptive karstic processes.

There are many dolines and sink holes that share the same general trends as the volcanoes, indicating a common structural link, and a possible use by magma of the karst system for pathways both to the surface and laterally.

Trachyphonolite, phreatomagmatic eruption in an ocean-island volcano: the Caldera del Rey tuff ring and associated deposits and ash aggregates

Pablo Dávila-Harris[1,2], Michael J. Branney[2] and Richard. J. Brown[3]

[1] *División de Geociencias Aplicadas, Instituto Potosino de Investigación Científica y Tecnológica, San Luis Potosí, México.*
[2] *Department of Geology, University of Leicester, Leicester, U.K.*
[3] *Department of Earth Sciences, Durham University, Durham, U.K.*

Keywords: Phreatomagmatic eruptions, Tenerife, ash aggregates

The Caldera del Rey is a 035˚-trending tuff ring in southwest Tenerife, Canary Islands (Fig. 1). It has a pear-shaped crater and eroded rim, 90 m high, with a narrower SE part, and a wider, 1100 m diameter maar-like northern end excavated into the pre-Cañadas basalt lava basement. Alternating layers of pumice lapilli, lapilli-tuffs and variously stratified tuffs with abundant ash aggregates and impact structures have quaquaversal dips ≤15˚ and centroclinal dips ≤33˚ (Fig 17b). The remnant deposits cover ~3 km^2, with thin distal ashfall layers and thin ignimbrite veneers preserved 4 km from source. Previous accounts (Paradas Herrero and Fernández Santín 1984; Huertas et al., 2002) did not present the stratigraphic relations and proposed correlations with an unrelated pumice-fall layer (Aldea Blanca 'B' from Las Cañadas; see Brown et al., 2003) and the older Casitas Member of the Enramada Formation (Dávila-Harris, P., Unp. PhD thesis, 2009). The formation is subdivided into 6 stratigraphic units (A-F).

The deposits from the Caldera del Rey comprise a local succession of non-welded trachyphonolitic pumice fall layers and stratified tuffs. It records alternating magmatic and phreatomagmatic eruptions from the tuff-ring, on the western margin of Tenerife's southern rift zone (Fig. 1), and is defined at its type location in the outskirts of Las Americas near motorway TF-1, where a basal thin layer of massive ash rests on a palaeosol developed on basalt lava, and is overlain by a thick succession of coarse pumice lapilli and variably stratified lapilli-tuffs. Elsewhere, the formation variously unconformably overlies phonolite lavas, the Adeje Formation, thick fluvial gravels, and the 'Old Basaltic Series' lavas. The top is unconformably overlain by the ~300 ka Aldea Blanca 'B' pumice fall deposit of Brown et al. (2003), by breccia from the Guaza dome and by the Tosca Formation. The Caldera del Rey eruption has been dated by $^{40}Ar/^{39}Ar$ in 0.953 ± 0.01 Ma (see Dávila-Harris, P., Unp. PhD thesis, 2009).

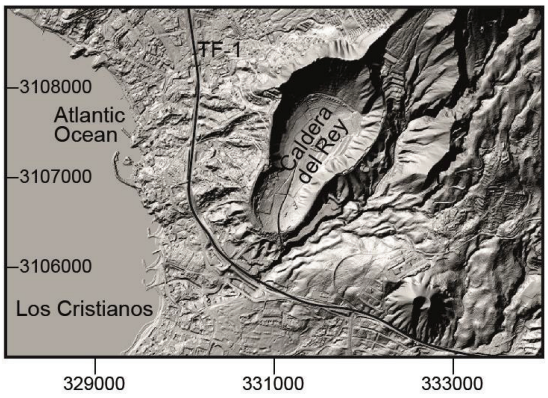

Fig. 1 – Location of the Caldera del Rey tuff ring in southwest Tenerife and 5m DEM showing the pear-shaped crater.

Caldera del Rey eruption summary

The Caldera del Rey eruption began a trachyphonolite intrusion in Tenerife's southern rift zone, causing small phreatomagmatic explosions (phase 1), followed by a relatively sustained sub-Plinian explosive phase (phase 2) that deposited ≤ 8 m thick proximal pumice fall deposit (unit B), proximally with pumice blocks 35 cm in size, over the Los Cristianos region. Intermittent interaction between the erupting magma with groundwater increasingly caused pulsatory phreatomagmatic explosivity (phase 3), with successive ballistic ejections of lithic blocks and short-lived ash aggregate-bearing density currents alternating with further pumice fallout. The abundance of accidental basalt lithic clasts (e.g. unit C) indicates that the activity was probably Ta'alian (Kokelaar, 1983) with explosions sited within a shallow basalt lava aquifer, probably near the top of the Miocene lava basement where the diffuse southern rift cuts the highly irregular sub-Cañadas unconformity. Phases 4-6 involved further phreatomagmatic-magmatic alternations similar to phases 1-3, but involving more water, possibly due to explosive fracturing and excavation of the aquifer. A crater lake may have

developed (Paradas Herrero and Fernández Santín, 1984), but lake deposits have not been observed.

A relatively low, unsteady magmatic eruption column deposited stratified pumice-fall deposits (phase 4) and then became higher and more sustained (unit D grades upwards into coarser, massive and lithic-rich fallout layers). Then a succession of violent, short-lived pyroclastic currents of both fully dilute and granular fluid-based types alternated with intermittent pumice fallout with sporadic influxes of lithic ejecta impacting into the moist-ash (phase 5, unit E). The last density currents and fallout events were probably the most widely dispersed (≤4 km from source; phase 6, unit F). The fine grainsize of many layers in the tuff ring reflects moisture-enhanced proximal deposition caused by aggregation as steam above the volcano condensed (see below). It may also partly reflect steam-enhanced fragmentation, with the eruption reverting to magmatic (pumice fall layers) when ingress of groundwater was temporarily blocked.

Ash aggregation during the Ta'alian eruption

Ash layers (including massive, diffuse-stratified and cross-stratified) in units E and F of the Caldera del Rey contain abundant (≤10-90 %) ash pellets and accretionary lapilli (Fig. 2). Several layers show a vertical sequence comprising a basal massive layer that contains matrix-supported whole and broken accretionary lapilli in its upper part: with height the accretionary lapilli become smaller, closer-spaced, and grade up-sequence into coated ash pellets, and then further up into a thin layer of framework-supported ash pellets that closely resemble the cores of the accretionary lapilli underneath. This sequence is found in many large ignimbrites elsewhere on Tenerife (e.g. Adeje Formation) and elsewhere (Van Eaton *et al*. 2012) and is interpreted as recording the formation within moist ash plumes, of ash pellets that drop into upper levels of pyroclastic density currents, where they accreted concentric ash laminations, thereby transforming into accretionary lapilli, deposited by the density current (Brown *et al*. 2010). As the current wanes, its rate of deposition decreases so the accretionary lapilli became more concentrated with height, while the current competence decreased, recorded by normal grading. Continued pellet fallout from the ash plume after the density current had dissipated, deposited first coated pellets (which fell through dusty moist air) and then pellets (fell through clean air) in the top framework-supported pellet layer. Variations from this sequence, probable arose from the rapidity of successive short-lived density currents, with a more-or-less continuous ash plume over the tuff ring, so that the deposition cycles were interrupted by the next currents before the cycle was complete.

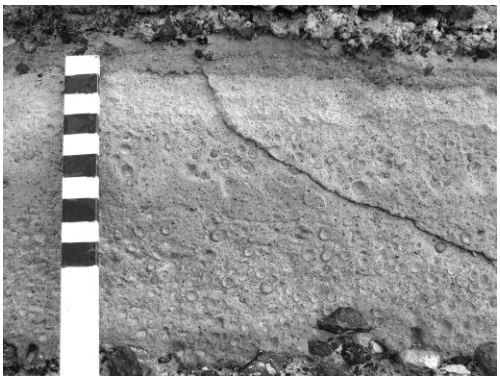

Fig. 2 – Ash aggregates in fines-rich lithofacies of the Caldera del Rey bracketed by lithic-rich layers. In the middle, phreatomagmatic lithofacies (mTacc) grading upwards into near clast-supported pellet layer. Scale shows centimeters.

Acknowledgements

PDH kindly acknowledge fieldwork funds from the Volcanic and Magmatic Studies Group and the University of Leicester.

References

Brown RJ, Barry TL, Branney MJ, Pringle MS, Bryan SE (2003). The Quaternary pyroclastic succession of southern Tenerife, Canary Islands: explosive eruptions, related caldera subsidence and sector collapse. Geological Magazine 140: 265 – 288.

Brown RJ, Branney MJ, Maher C and Dávila-Harris P (2010). Origin of accretionary lapilli within ground-hugging density currents: Evidence from pyroclastic couplets on Tenerife. Geol Soc Am Bull; 122: 305-320

Dávila Harris, P., (2009), Explosive ocean-island volcanism: the 1.8-0.7 Ma explosive eruption history of Cañadas volcano recorded by the pyroclastic successions around Adeje and Abona, southern Tenerife, Canary Islands, Ph.D. Thesis: Leicester, University of Leicester, U.K., 311 p.

Huertas MJ, Arnaud NO, Ancochea E, Cantagrel JM, Fúster JM (2002). 40Ar/39Ar stratigraphy of pyroclastic units from the Cañadas Volcanic Edifice (Tenerife, Canary Islands) and their bearing on the structural evolution. J Volcanol Geotherm Res 115: 351 - 365.

Kokelaar, B. P. (1983). The mechanism of Surtseyan volcanism. *Journal of the Geological Society*, *140*(6), 939-944.

Paradas Herrero, A. and Fernandez Santín, S. 1984. Estudio vulcanológico y geoquímico del maar de la Caldera del Rey, Tenerife (Canarias). Estudios Geológicos 40, 285-313.

Van Eaton, A. R., Muirhead, J. D., Wilson, C. J., & Cimarelli, C. (2012). Growth of volcanic ash aggregates in the presence of liquid water and ice: an experimental approach. Bulletin of volcanology, 74(9),1963-1984.

Phreatomagmatism and phreatomagmatic landforms in the Chaîne des Puys, France

Benjamin van Wyk de Vries[1], Valentin R Troll[2], Sylvia Berg[2], Dougal Jerram[3], Lucia Gurioli[1], Mathieu Colombier[1], Pierre Boivin[1],

[1] *Laboratoire Magmas et Volcans, University Blaise Pascal, Clermont-Ferrand, France. b.vanwyk@opgc.fr*
[2] *Department of Earth Sciences, Solid Earth Geology, University of Uppsala, Sweden.*
[3] *DougalEARTH Ltd. 31 Whitefields Crescent Solihull B91 3NU, U.K.*

Keywords: Phreatomagmatic, Chaîne des Puys, maar.

The Chaîne des Puys, Central France is a monogenetic volcanic field with about 80 edifices with highly variable morphologies, compositions and eruptive styles. The Chain stands on the shoulder of the Limagne Rift. The rift shoulder is composed of Hercynian granite and gneissic basement, cut by small valleys and ravines that descend on one side to the rift, and on the other side of the chain to the Sioule River valley.

There are many tuff rings and maars in the Chaîne des Puys, such as the Gour de Tazenat, Lac Pavin, the Narse d'Espinasse and Beaunit. In addition, many of the scoria cones also contain finely bedded, poorly sorted layers with dense juveniles, suggesting periods of phreatomagmatic activity. The Chaîne des Puys is also famous for its monogenetic domes, and for its intrusion-related uplifts, termed 'craters of elevation' by von Buch (1819). These more acid volcanoes have produced some powerful eruptions that may also have a phreatomagmatic component (Boivin et al 2009).

In this presentation we shall give an overview of the present knowledge of the Chaîne des Puys from a phreatomagmatic perspective. We first describe the hydrogeology of the chain, and then discuss some specific examples of each type of activity.

Hydrogeology: The Chaîne des Puys stands between 5 and 10 km to the west of the Limagne fault. The chain has a continuous cover of volcanic rock, that is rapidly replaced to the east by granitic basement along a line of small hills. In a few places, lavas have flowed through gaps in the hills to descend the fault escarpment to the Limagne Graben. To the west, the volcanic cover is greater, as the lavas have spread out over a broad plateau incised with a few valleys. To the north west, near Volvic, there is a north-easterly oriented drainage system, through which a large part of the Chaîne des Puys water catchment flows.

The granite basement is largely impermeable, and galleries cut into the lavas have uncovered large underground rivers and aquifers at the granite-volcanic contact.

For phreatomagmatism the main source of water is thus found above the basement in the volcanic strata, or to a lesser extent in small streams that flow on the granite basement.

The Beaunit tuff ring is a prime example of the type of maar found in the Chaîne des Puys. It has a characteristic basal deposit rich in fresh granite blocks with a small juvenile fraction. This juvenile fraction itself contains abundant specks of partly-melted xenoliths (*e.g.* buchites). Small amounts of light colored pumice are found concentrated in some bands, which may be the melted fraction of xenoliths that did not mix with the basaltic magma. Going up-sequence, the tuff ring contains more and more juvenile material, which becomes more scoriaceous. The eruption ends with a small scoria cone, that contains abundant frothy, partly melted crustal rocks (pseudopumice) and peridotite xenoliths.

The fresh granite blocks show no sign of interaction with magma, and no juvenile material is found in contact with these clasts. In contrast, the restite is always included in juvenile material and is never found alone. The fresh granite appears to have been thrown out without interacting with magma, while the restite has been produced from an efficient melting episode of granitic rock. The pseudopumice has a similar mineralogy to the restite, but is less fragmented. The glass fraction is found within the pseudopumice, rather than outside as may be the case with the initial deposit's pumice fraction.

We have studied the field relations, the textures and compositions of the basement and magmatic components at Beaunit. We have also taken fresh basement samples and have heated then to near magmatic pressures and temperatures. The resulting textures are identical to those seen in Beaunit and glass compositions from the melted samples are close to those of Beaunit.

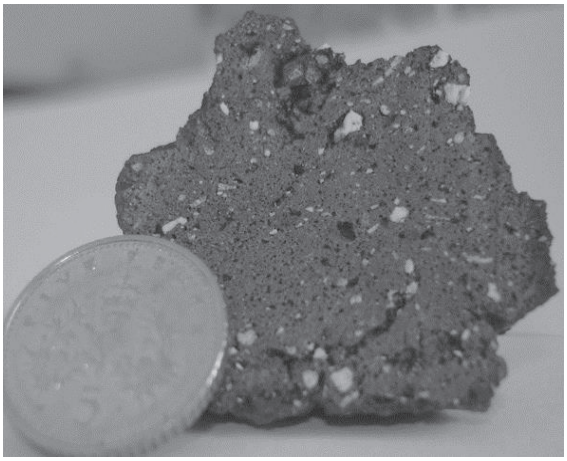

Fig. 1 – Example of the Beaunit Lapilli with flecks of restite – mostly quartz and feldspar. Coin is 1 cm diameter.

We propose a model for Beaunit where ascending basalt mixed strongly with brecciated crust, probably in a local fault zone. The granite quickly melted, rapidly liberating volatiles that rise fast, to create a gas charged, country-rock-rich initial eruption. Magma rapidly followed up, creating an increasingly magmatic gas-powered eruption, as the ratio of crustal gas to magma diminishes. A concomitant influx of water from a local stream may also have contributed to some phreatomagmatic interaction, but this rapidly dried out.

The peridotite may have been scavenged also by the rapid rise following the initial gas rich phase, possible by propagation of a pressure shock downwards. If the model is correct, the highly explosive eruptions in the Chaîne des Puys and similar areas could occur very rapidly, but would be of short duration.

Interestingly, the 19th century volcanologists had initially suggested that gas rich eruptions had formed such deposits, but hydromagmatic theories in the 20th Century have overshadowed their original, perceptive ideas.

Many of the Chaîne des Puys volcanoes have early deposits that are rich in granitic pseudopumice or in granitic restite. This suggests to us that the sequence of events at Beaunit is quite common, and that rising dykes have often been channeled into zones of breccia inherited from the Hercynian tectonics, or the Rift episode, or possibly active faults, where the crust is easily incorporated. Rapid melting of the granite, can thus provide an initial pulse to bring the magma rapidly to the surface.

In contrast to the explosive opening of the basaltic volcanoes, like Beaunit, the acid domes have evidence of having a passive intrusion and effusion episode. The large eruptions from these volcanoes, such as the Killian, the Vasset and the Chopine, contain copious amounts of dense juveniles, that suggest at first inspection to indicate a possible phreatomagmatic origin. These deposits also contain pumice, especially in the upper sequences.

There are two large uplifts, created by intrusions, the Petit Puy de Dôme and the Grosmanaux. The structures on these can be used to estimate the depth of the intrusion (van Wyk de Vries et al 2012), which is near the granite-volcanic contact. Thus it appears that the acid magmas spread out in lacolith-like bodies underneath the volcanics. As this is also the location of the main source of stored water, phreatomagmatic interaction is likely.

It is thus possible that the laccolithic intrusions were periodically disrupted by phreatomagmatic interaction, that triggered the powerful vulcanian events.

A whole range of interactions are seen from the Petit Puy de Dôme that had a small phreatomagmatic eruption, producing a small crater (the 'Nid de la Poule'), to the Killian crater in the Grosmanaux that had five short powerful vulcanian blasts, to the Vasset that had a powerful vulcanian sequence, which left little of the original intrusion intact. The Puy Chopine is a case apart where an intrusion created a small sector collapse and lateral blast.

A final type of phreatomagmatic activity in the Chaîne des Puys is found in the upper layers of scoria cones, such as the Lemptégy volcano. Here the upper layers contain lenses of dense juvenile material and occasional large pseudopumice fragments. These point to a late-stage fracturing and incorporation of granite basement, leading to possible increase gas in and water influx from the fracturing.

References

Boivin, P., Besson, J.C., Briot, D., Camus, G., De Goër de Hervé, A., Gourgaud, A., Labazuy, P., Langlois, E., de Larouzière, F.D., Livet, M., Mergoil, J., Miallier, D., Morel, J.M., Vernet, G., Vincent, P.M., (2009), Volcanologie de la Chaîne des Puys Massif Central Français, 5th Edition, scale 1 : 25 000, 1 sheet.

Von Buch, L., (1819) Observations sur les volcans d'Auvergne: Journal des Mines, v. 13, p. 249-256.

van Wyk de Vries, B, Grosse, P , Marquez, A , Petronis, M S, Kervyn, M , Delcamp, A , Mossoux, S, Troll, V R. (2013). The Chaîne des Puys: how complicated can monogentic get? (Invited) V44C-06 AGU Fall meeting December 2012.

Evolution, structural control and hazards associated with maar volcanism in Central Mexico

Gerardo Carrasco-Núñez[1], Michael H. Ort[2]

[1] *Centro de Geociencias, Universidad Nacional Autónoma de México, Campus Juriquilla, Querétaro, Qro. 76230, México.* gerardoc@geociencias.unam.mx
[2] *SESES, Northern Arizona University, Flagstaff, Arizona, 86011, USA.*

Keywords: maar volcanoes, tectonic regime, volcanic evolution, Mexican volcanism, volcanic hazards.

Monogenetic volcanoes are often thought to have simple eruptive histories but the eruptions and evolution of maar volcanoes are more complex, as they have fluctuating explosive behaviors due to the rapid changes that occur during the magma ascent and interaction with external water.

Maar volcanoes, known in Mexico as xalapazcos (meaning vessel containing sand in the Nahuatl language) or axalapazcos (if they have a lake inside), result from variable magma-water interactions that produce variations in explosivity and eruptive style. In addition to the water/magma ratio, magma extrusion rate, explosion depth variation, increasing cratering, composition and viscosity, etc., local and regional conditions such as the nature of basement rocks and the structural and tectonic regime play important roles in the evolution of these volcanoes.

Although maar volcanoes have a widespread distribution in Mexico, three volcano fields marked by abundant maars are recognized: San Luis Potosí (SLP), Valle de Santiago (VS) and Serdán-Oriental Basin (SOB). The latter two fields belong to the Quaternary Mexican Volcanic Belt province, in contrast with the first one, which is Pliocene and associated with the SE-trending extension of the Basin and Range province (B&RP). Basaltic magmas are by far the dominant type, but rhyolitic maar volcanoes are also present in the SOB and one occurs in the VS.

In an attempt to group the diversity of maar volcanoes because of the contrasts in eruptive style and geologic evolution, Carrasco-Núñez and Ort (2012) proposed three main types of maars: a) La Alberca – Cíntora type, which can be named now as Alchichica type, characterized by a precursor magmatic phase (hawaiian-strombolian activity) followed by a phase of highly explosive phreatomagmatic maar-forming eruptions; b) Atexcac – Tecuitlapa type volcanoes (Carrasco-Núñez *et al.*, 2007; Ort and Carrasco-Núñez, 2009) initiated with surge-dominated eruptions in either karst-fractured or unconsolidated aquifers, with a migration of the eruptive focus along the crater, producing lateral depositional variations and fluctuations in water/magma ratios but with a general drying trend; and c) Hoya Estrada – Tepexitl type (Cano and Carrasco-Núñez, 2008; Austin-Erickson *et al.*, 2011) characterized by rhyolitic tuff-ring activity. They evolve from surge-dominated to fall-dominated activity. During their evolution, dome-building episodes produce generally drier conditions and, in some cases, blast explosions.

A strong tectonic control is observed for the general distribution of the volcanoes in the 3 different volcanic fields. However, the structural setting is distinct for each field: the SLP is mainly controlled by SE-trending structures apparently linked to the B&RP whereas, at the VS, the main NW-trend is cut by a more recent E-W-trending alignment (Fig. 1). The only rhyolitic tuff-ring (Hoya de Estrada) was formed at the junction of these two trends.

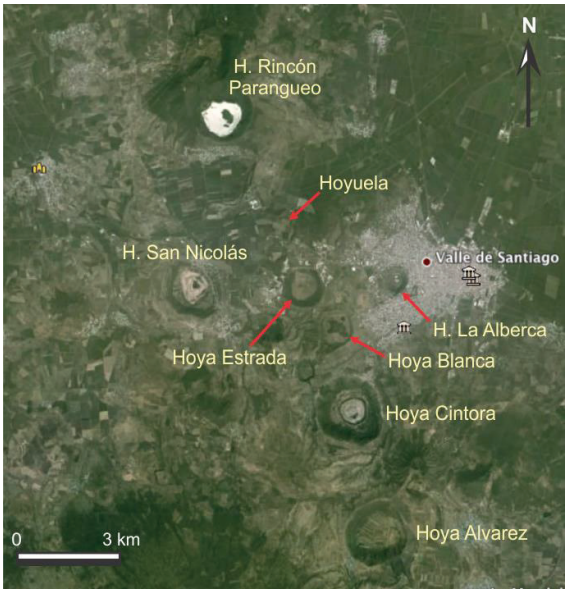

Fig. 1– NW alignment of volcanoes of the Valle de Santiago maar field, which is part of the Michoacán-Guanajuato field, one of the largest monogenetic fields worldwide. Notice also an E-W trend characteristic of the central Mexican Volcanic Belt.

Although a random distribution is observed for most volcanoes in the SOB, a local influence of

shallow crustal fractures seems to control the E-W - trending structures for some of the basaltic volcanoes to the south (Fig. 2A), while the central part is controlled by an apparently older and more developed NW-oriented fracture system, where more viscous rhyolitic domes and maar volcanoes formed (Fig. 2B). The lateral migration of explosion loci observed in the Atexcac, Tecuitlapa and Aljojuca craters of the SOB are, at least in the latter two cases, strongly controlled by the regional stress regime, causing elongated craters shapes oriented in the E-W direction.

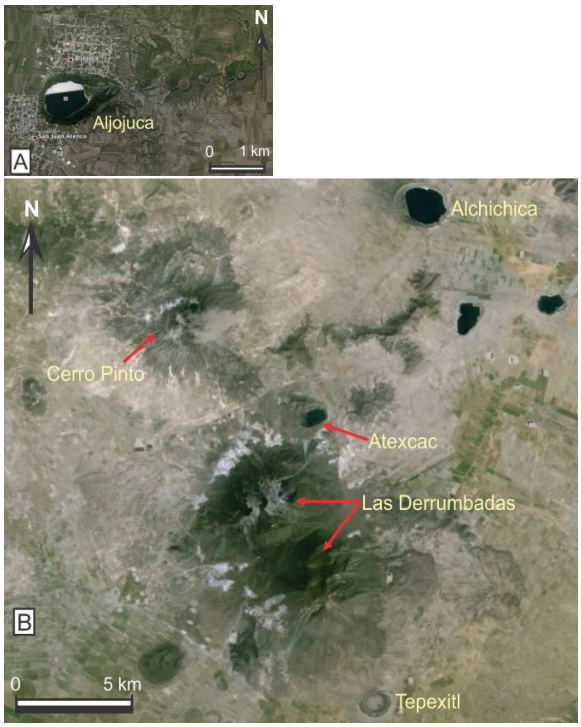

Fig. 2 – A) E-W alignment of cinder cones and the Aljojuca crater (left) in the Serdán-Oriental Basin, eastern Mexican Volcanic Belt. B) NW alignment of rhyolitic volcanism comprising the large Las Derrumbadas domes (Siebe *et al.*, 1995) bounded by the Tepexitl tuff-ring to the south and the Cerro Pinto complex (Zimmer et al, 2007) to the north.

Dating of the three maar fields indicates that the SLP is the oldest field at around 1.1 Ma (Aranda. Gómez and Luhr, 1996), while the VS dates range from 0.4 to 0.1 Ma and the youngest maar volcanism is in the SOB, ranging from 50 ky (Zimmer, 2007; Zimmer *et al.*, 2010) to < 20 ky. New results provide evidence of a Holocene age for the Aljojuca and perhaps also Tecuitlapa craters. On the other hand, even though some volcanoes such as Cerro Pizarro rhyolitic dome (Riggs and Carrasco-Núñez, 2004; Carrasco-Núñez and Riggs, 2008) last erupted around 65 ky, they record repose periods longer than that, implying that future volcanic activity cannot be ruled out. All these features have important implications for hazard assessment of the monogenetic volcanism of the SOB.

Acknowledgements

This work is supported by both and CONACYT grant No. 150900 and PAPIIT grant No. IN106314 Logistical support was provided by Centro de Geociencias (UNAM)

References

Aranda-Gómez, J. J., Luhr, J. F., 1996, Origin of the Joya Honda maar, San Luis Potosí, México: Journal of Volcanology and Geothermal Research, 74, 1-18.

Austin-Erickson, A., Ort, M.H., Carrasco-Núñez, G., 2011. Rhyolitic phreatomagmatism explored: Tepexitl tuff ring (Eastern Mexican Volcanic Belt). Journal of Volcanology and Geothermal Research, 201, 325-341. doi:10.1016/j.volgeores.2010.09.007.

Cano, M., Carrasco-Núñez, G., 2008. Evolución de un cráter de explosión (maar) riolítico: Hoya de Estrada, campo volcánico Valle de Santiago, Guanajuato, México: Revista Mexicana de Ciencias Geológicas, 25 (3), 549-564.

Carrasco-Núñez, G., Riggs, N.R., 2008. Polygenetic nature of a rhyolitic dome and implications for hazard assessment: Cerro Pizarro volcano, Mexico. Journal of Volcanology and Geothermal Research, 171, 307-315.

Carrasco-Núñez, G., Ort, M.H., Romero, C., 2007. Evolution and hydrological conditions of a maar volcano (Atexcac crater, Eastern Mexico). *In* "Maar-diatreme volcanism and associated processes" (Eds. Martin, U., Németh, K., Lorenz, V., White, J.), Journal of Volcanology and Geothermal Research, 159, 179-197.

Carrasco-Núñez, G., Ort, M.H., 2012. Contrasting eruptive styles of Mexican maar volcanoes. Hopi Butes Volcanic field Workshop: Maar-diatreme volcanism, Flagstaff, AZ, USA., abstract volume, oct 2012.

Ort, M.H., Carrasco-Núñez, G., 2009. Lateral vent migration during phreatomagmatic and magmatic eruptions at Tecuitlapa Maar, East-Central Mexico, Journal of Volcanology and Geothermal Research, 181, 67-77.

Riggs, N.R., Carrasco-Núñez, G., 2004. Evolution of a complex, isolated dome system, Cerro Pizarro, central Mexico. Bulletin of Volcanology, 66, 322-335.

Siebe, C., Macías, J.L., Abrams, M., Rodríguez, S., Castro, R., Delgado, H., 1995. Quaternary explosive volcanism and pyroclastic deposits in east central Mexico: implications for future hazards. Geological Society of America Field Guide, 1-47.

Zimmer, B.W., 2007. Eruptive variations during the emplacement of Cerro Pinto dome complex, Puebla, Mexico. MS thesis, Northern Arizona University, 119 pp.

Zimmer, B., Riggs, N.R., Carrasco-Núñez, G. 2010. Evolution of tuff ring-dome complex: the case study of Cerro Pinto, eastern Trans-Mexican Volcanic Belt. Bulletin of Volcanology, 72, 1233-1240.

Phreatomagmatism in the Serdán-Oriental Basin, Eastern Mexican Volcanic Belt

Michael H. Ort[1], Gerardo Carrasco-Núñez[2]

[1] *SESES, Northern Arizona University, Flagstaff, Arizona, USA. michael.ort@nau.edu*
[2] *Centro de Geociencias, Universidad Nacional Autónoma de México, UNAM Campus Juriquilla, Querétaro, México.*

Keywords: Maar vents, Serdán-Oriental, vent migration.

The Serdán-Oriental Basin is located in the Eastern Mexican Volcanic Belt to the north of Volcán Citlaltéptl. The basement rocks are deformed Cretaceous limestone and shale, intruded by isolated small plutons of middle Tertiary age. Quaternary volcanism in the basin is bimodal, dominantly basaltic to basaltic andesite, but with significant rhyolitic volcanism. Volcanic landforms include scoria cones, maars, domes, and small shield volcanoes. The basin itself is a broad depression about 45 x 60 km at ~2300 masl elevation. With no surface streams draining it, groundwater is near the surface and forms large ponds in the summer rainy season. The toba café, an informally named brown reworked tuff of fluvial and eolian origin, is present throughout the basin as well as much of central México. This serves as a shallow aquifer for much of the phreatomagmatism.

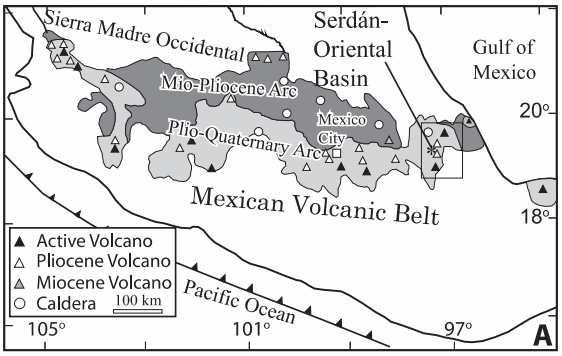

Fig. 1 – Map of the Mexican Volcanic Belt showing the location of the Serdán-Oriental Basin and other features. From Ort and Carrasco-Núñez (2009).

The Serdán-Oriental Basin has more than 10 maar volcanoes, located in the middle and south portions of the basin. Their compositions vary from basalt to rhyolite and some contain a crater lake. General descriptions of these volcanoes and the basin were published by Ordoñez (1905, 1906), Gasca-Durán (1981) and Siebe *et al.* (1995) and studies of individual volcanoes include the multiple-vent Cerro Xalapaxco tuff cone (Abrams and Siebe, 1994), Atexcac basaltic maar (Carrasco-Núñez *et al.*, 2007), Cerro Pinto dome-tuff-ring complex (Zimmer *et al.*, 2011), Tepexitl rhyolitic tuff ring (Austin-Erickson, 2007; Austin-Erickson *et al.*, 2011), and Tecuitlapa maar (Ort and Carrasco-Núñez, 2009). Most of the cinder cones are isolated, although some are aligned along E-W or ENE-WSW orientations, particularly in the south. Two large rhyolitic dome complexes, Las Derrumbadas and Cerro Pizarro, as well as a few smaller domes, also occur within the basin. Here, we will focus on maar volcanoes.

The maars of the Serdán-Oriental Basin yield Ar/Ar dates of latest Pleistocene age (<100 ka) but show a wide range of features. In most cases, the deposits show a general drying trend at the end of the eruptions, although the early and middle parts of the eruptions commonly varied in the amount of water involved.

In many cases (*e.g.* Tecuitlapa and Tepexitl), the tephra deposits (ballistic block, fallout and PDC deposits) contain abundant (commonly dominant) toba café grains, as well as rare blocks of tuff. We interpret this to indicate that the toba café liquefied and flowed into the conduit, a process described by White (1996). Other maars (*e.g.* Atexcac) show little involvement of toba café in the eruptions, but their deposits have abundant blocks of the hard rock types found in their crater walls (*e.g.* lava flows). Thus, both hard and soft rock types appear to have served as the aquifers for the water-magma interaction.

Many of the basaltic maars show evidence of lateral (but little, if any, vertical) migration of the vent location over the course of the eruption. This evidence of vent locations includes duneform axes, ballistic block sag trajectories, changes in lithic fragment types, and grain-size and facies variations. This was interpreted by Ort and Carrasco-Núñez (2009) for Tecuitlapa maar as the result of the high lithologic contrast between the non-consolidated toba café sediments and the underlying fractured bedrock. Water movement in the bedrock was by fracture flow, whereas movement within the sediments was through liquefaction and failure of the deposit. Low magma supply rates allowed collapse of the soft walls of the dike, producing mingling and phreatomagmatic explosions, whereas

the same magma supply rate in fractured bedrock sealed off water access to the magma. The alignment of the vents is parallel to regional structural trends, so was probably set in the underlying bedrock, and the distance that the vent migrated is likely related to the overall dike length. The eruption ended with the formation of a series of scoria cones along the same vent alignment (in reverse chronologic order to the vent migration during phreatomagmatism) and the lack of fluidized sediment coating the scoria-cone clasts implies that the sediment collapse and phreatomagmatic eruptions used up most of the available liquefied sediment, which ended the phreatomagmatic portion of the eruption.

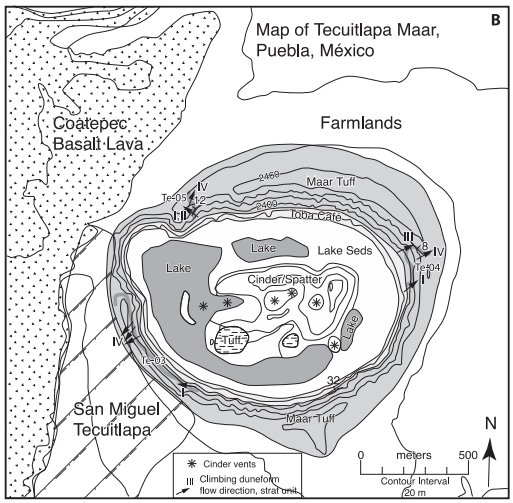

Fig. 2 – Geological map of Tecuitlapa maar, showing evidence for the migration of the phreatomagmatic vents and locations of the scoria-cone vents. From Ort and Carrasco-Núñez (2009).

At Tepexitl, a rhyolitic tuff ring, limited vent migration occurred, but the dominant feature is the development of a dome in the latter period of the eruption, followed by its progressive dissection by phreatomagmatic explosions. Austin-Erickson *et al.* (2008, 2011) offer a model for the interaction of water with the very viscous rhyolitic magma, in which fluidized sediments intrude marginal fractures as they open in the rhyolite magma, creating enough interfacial surface area to initiate phreatomagmatic explosions from within the interior of a rising plug or dome.

Other phreatomagmatic eruptions within the Serdán-Oriental Basin produced basaltic tuff cones in hard-rock substrates and broad and very low-walled basaltic maars in toba café, whereas Cerro Pinto is a pair of nested rhyolitic tuff rings with domes superposed on them. The basin provides a wealth of examples of different types of maars and is an excellent area for their study. We will visit these maars on the post-conference field trip.

Acknowledgements

Logistical support was provided by Centro de Geociencias (UNAM). This work is supported by both CONACYT grant No. 150900 and PAPIIT grant No. IN106314.

References

Abrams, M., Siebe, C., 1994. Cerro Xalapaxco: an unusual tuff cone with multiple explosion craters in central Mexico (Puebla). Journal of Volcanology and Geothermal Research, 63:183–199.

Austin-Erickson, A., Buttner, R., Dellino, P., Ort, M.H., Zimanowski, B., 2008. Phreatomagmatic explosions of rhyolitic magma: experimental and field evidence. Journal of Geophysical Research, 113: B11201, doi:10.1029/2008JB005731.

Austin-Erickson, A., Ort, M., Carrasco-Núñez, G., 2011. Rhyolitic phreatomagmatism explored: Tepexitl tuff ring (Eastern Mexican Volcanic Belt). Journal of Volcanology and Geothermal Research, 201:325-341.

Carrasco-Núñez, G., Ort, M., Romero, C., 2007. Evolution and hydrological conditions of a maar volcano (Atexcac crater, Eastern Mexico). Journal of Volcanology and Geothermal Research, 159:179-197.

Gasca-Durán, A., 1981. Génesis de los lagos-cráter de la cuenca de Oriental. Colección Científica Prehistórica, 98, 57 pp.

Ordóñez, E., 1905. Los xalapaxcos del estado de Puebla. Instituto de Geología. 350–393.

Ordóñez, E., 1906. Los xalapaxcos del estado de Puebla. Instituto de Geología. 350–393 2a parte.

Ort, M.H., Carrasco-Núñez, G., 2009. Lateral vent migration during phreatomagmatic and magmatic eruptions at Tecuitlapa Maar, east-central Mexico. Journal of Volcanology and Geothermal Research, 181:67-77.

Siebe, C., Macías, J.L., Abrams, M., Rodríguez, S., Castro, R., Delgado, H., 1995. Quaternary explosive volcanism and pyroclastic deposits in east-central Mexico: implications for future hazards. Geological Society of America Field Guide, 1–47.

White, J.D.L., 1996. Impure coolants and interaction dynamics of phreatomagmatic eruptions. Journal of Volcanology and Geothermal Research, 74:155–170.

Zimmer, B., Riggs, N.R., Carrasco-Núñez, G. 2010. Evolution of tuff ring-dome complex: the case study of Cerro Pinto, eastern Trans-Mexican Volcanic Belt. Bulletin of Volcanology, 72:1233-1240.

Maar-diatreme volcanoes: their incremental growth and potential maximum size

Volker Lorenz[1], Peter Suhr[2] and Stefan Suhr[3,]

[1] *Physical Volcanological Laboratory, University of Wuerzburg, Pleicherwall 1, D-97070 Wuerzburg, Germany. vlorenz@geologie.uni-wuerzburg.de*
[2] *Sächsisches Landesamt fuer Umwelt, Landwirtschaft und Geologie, (Außenstelle Freiberg), PF 540 137, D-01311 Dresden, Germany. peter.suhr@smul.sachsen.de*
[3] *Université Paris Dauphine and ENS Paris, rue d'Ulm, F-75230 Paris, Cedex 05, France. stefan.suhr@ens.fr*

Keywords: maars, diatremes, growth modeling.

Introduction: Small maar-diatreme volcanoes show a small crater diameter and small crater depth. They are surrounded by a tephra ring that has a small thickness and a relatively small number of phreatomagmatic tephra beds. Small maar craters are underlain by a diatreme of a small diameter and depth as indicated by geophysical investigations. In contrast, large maar-diatreme volcanoes show a larger crater diameter and a deeper crater. The large craters are surrounded by a tephra ring that has a greater thickness and a larger number of tephra beds. A large maar is underlain by a rather large and deep diatreme as shown by geophysical investigations. The individual pyroclastic (i.e. non-reworked) tephra beds in the maar tephra rings are usually of a relatively small thickness (mm to a few dm). Thus, the larger a maar-diatreme volcano is, the longer it has been active.

These relationships led to the growth model for maar-diatreme volcanoes (Lorenz 1986; Lorenz and Kurszlaukis 2007). The model relates downward explosive penetration of the root zone of maar-diatreme volcanoes to the incremental eruptions of country rock clast-rich tephra at the surface. This ejection causes the formation of a mass deficit in the root zone and the consequent collapse of overlying rocks and tephra. That repetitive process results in the formation and growth of the cone-shaped diatreme, the consequent maar crater and lateral retreat of the crest of the tephra ring. The recurrence time of the incremental collapse phases will depend on the rock mechanical parameters of the country rocks, i.e. hard rocks or soft sediments. The intriguing revised model of Valentine and White (2012) does not seriously affect the model described above.

Basis for model calculations: The phreato-magmatic tephra beds of maar tephra rings, on average, represent a comparatively small volume deposited per unit eruption. For the model calculation on the growth of a diatreme we consider only a specific amount of country rock material that is ejected by each eruption during the whole activity of the volcano – irrespective of time involved. For each eruption, we take this amount of ejected country rocks as a layer from the whole wall of the cone-shaped diatreme – with the diatreme wall displaying an inward dip of 82° (Hawthorne 1975). Thus, in this model the country rock material is ejected completely in incremental steps with the result that the diatreme stays open similar to a cone-shaped open pit in mining. In our model, these assumptions have the consequence that after a specific number of eruptions, the volume of the country rocks ejected so far can be related to a specific stage of the incremental growth of the 3-D maar-diatreme volcano.

Denote with V the volume deficit in the maar crater resulting from one explosion. Then the diameter d and depth h of the structure are given by (here we assumed that the geometry is already stabile):

$$d = \frac{1}{2}\sqrt[3]{\frac{3V}{\pi \tan(82°)}n}$$

$$h = \frac{1}{2}\sqrt[3]{\frac{3V}{\pi}\tan^2(82°)n}$$

where n denotes the number of explosions since the formation of the maar-diatreme.

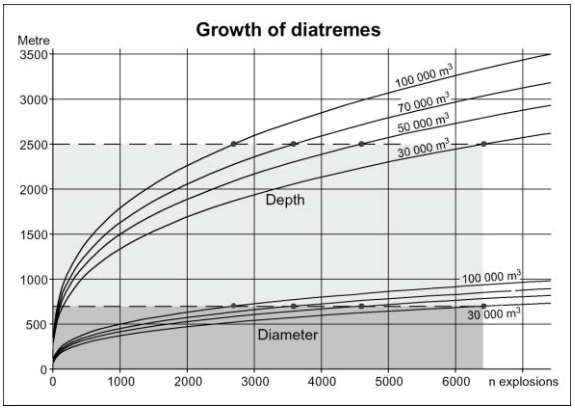

Fig. 1 – Schematic relationship between the number of eruptions of a maar-diatreme volcano (each eruption ejecting a specific unit volume – in series of 30,000, 50,000, 70,000, and 100,000 m³ - and the resulting diameter, respectively the resulting depth of the diatreme. The hatched boundaries of the light and dark grey areas indicate the maximum depth of 2.500 m (light grey area) and diameter (dark area) assumed for natural diatremes.

The model calculations clearly show that during the initial small number of eruptions, ejecting identical country rock volumes, the diameter, circumference and depth of the diatreme grow rather fast. With the steady continuation of the eruptions, however, the growth of the diatreme has to decelerate. The same decrease in growth rate of the volcano size with ongoing eruptions, with equal magma volume per eruption, applies also to scoria cones, strato-volcanoes, shield volcanoes, and extrusive domes.

Natural variations: In nature a series of additional aspects have to be considered during the growth of maar-diatreme volcanoes. The production of magma depends on feeder dyke thickness and its time-dependant production rate and the availability of groundwater depends on the local hydrogeology. Thus, the ratio of magma to groundwater, with which it interacts explosively, could vary and consequently the grain-size of the tephra and the ratio of country rock clasts versus juvenile clasts. The ejected country rock volume per eruption will not be fixed for the many phreatomagmatic eruptions. Some tephra jets might even be so weak as to never reach the crater floor (Ross *et al.* 2008). Some eruptions may result from an individual or a few explosions and some sustained eruptions may result from quite a number of explosions that follow each other rapidly. The incremental eruptions will also vary in terms of their recurrence time.

During the initial period of the formation of a maar-diatreme, country rocks from the diatreme walls and maar crater walls will probably form a high proportion of the material filling the new diatreme. The ongoing eruptions and increase in the size of the maar crater will lead to collapse of larger arcuate slices of country rocks and of the overlying bedded tephra ring and result in debris flows on the crater floor. The syn-eruptive widening and deepening of the maar crater will cause the percentage of country rock clasts from the collapsing crater walls to be larger with respect to the percentages of country rock clasts from deeper lithological levels. With further increase in size of the maar crater the crater as such will also act as a depot center for base surge and tephra fall deposits. These and interbedded lahars form the thick series of bedded tephra known from the upper diatreme level which points to syn- and post-eruptive subsidence. The larger the maar crater will get the slower its crater walls will retreat, the fewer debris flows will form and the larger the relative volume of non-reworked tephra beds will be in the upper diatreme level. There may occur even base surges from weak eruptions that deposit their load only inside the crater.

With the deceleration of the increase in diameter, circumference and depth of the diatreme the recurrence time of wall rock collapse will get longer and longer. In principle, this deceleration of the growth of the diatreme should imply that a small diatreme has only a relatively short root zone underneath whereas a large diatreme might develop a root zone that penetrates much deeper downward before its mass deficit is large enough to trigger another collapse phase of the overlying diatreme and maar crater.

One additional aspect may also have to be taken into account for maar-diatreme volcanoes, is that some basaltic volcanoes (*e.g.*, Paricutin; Surtsey) show a waning phase towards the end of their magma production.

When groundwater stops having sufficient access to the rising magma, magmatic phases, with or without a phreatomagmatic touch, occur in between phreatomagmatic phases. Thus, the volcanic activity might switch to emplacement of dykes, sills or plugs inside the diatreme and finally even to the formation of scoria cones, a lava lake or even a dome on the maar crater floor.

The igneous rocks only participate in filling the diatreme and possibly its maar crater but are not responsible for the formation of the diatreme as such.

Taking into account the assumed average slope angle of diatreme walls of 82^{o} and the maximum assumed depth of diatremes of 2-2.5 km (Hawthorne 1975) as well as the above calculations the diameter of a single diatreme should not exceed c. 600-700 m. If a diatreme has an even larger diameter it is conceivable that such a large diatreme coalesced from two or even more individual diatremes because they had been active simultaneously or because a diatreme had migrated.

References

Hawthorne, J.B., 1975. Model of a kimberlite pipe. Physics and Chemistry of the Earth 9: 1–15.

Lorenz, V., 1986. On the growth of maars and diatremes and its relevance to the formation of tuff-rings. Bulletin of Volcanology 48: 265-274.

Lorenz, V., Kurszlaukis, S., 2007. Root zone processes in the phreatomagmatic pipe emplacement model and consequences for the evolution of maar-diatreme volcanoes. Journal of Volcanology and Geothermal Research 150: 4-32.

Ross, P.-S., Büttner, R., White, J.D.L., Zimanowski, B., 2008. Rapid injection of particles and gas into non-fluidized granular material: volcanological implications. Bulletin of Volcanology DOI: 10.1007/s00445-008-0230-1

Valentine, G.A., White, J.D.L., 2012. A revised conceptual model for maar-diatremes: subsurface processes, energetics, and eruptive products. Geology DOI: 10.1130/G334

Explosion energies and depths at maar-diatremes

Greg A. Valentine, Alison H. Graettinger, Ingo Sonder

Dept. of Geology and Center for Geohazards Studies, University at Buffalo, Buffalo, NY 14260 USA. gav4@buffalo.edu

Keywords: phreatomagmatic, maar-diatreme, scaled depth.

Phreatomagmatic maar-diatremes are a type of volcano that forms primarily by interaction of magma with groundwater, which causes repeated subsurface explosions. Lithic clasts observed in tephra rings are often taken as indicators of the depth to which a diatreme extends, and of the depths of explosions that produced a particular stratigraphic unit of tephra ring deposits. Implicit in the latter is an assumption that a given lithic clast was directly ejected by an explosion at the clast's depth of origin. We use estimates of explosion energy and established relationships for subsurface explosion behavior to test these ideas.

Regimes of behavior associated with subsurface explosions are commonly described in terms of the scaled depth $D_{sc} = d \cdot E^{-1/3}$, where d is the physical depth below the surface and E is the mechanical energy produced by the explosion. For terrestrial gravitational acceleration and typical crustal density, explosions of a wide range of energies, including both chemical and nuclear explosions, have maximum excavation efficiencies, and thus produce maximum crater sizes, when $D_{sc} \approx 0.004$ m $\cdot$ J$^{-1/3}$; thus the optimal excavation depth $d_{opt} \approx (0.004 \text{ m} \cdot \text{J}^{-1/3}) \cdot E^{1/3}$ (*e.g.*, Houser, 1969; Goto *et al.*, 2001). For $D_{sc} > 0.008$ m $\cdot$ J$^{-1/3}$ most explosions are contained in the subsurface and do not eject any material. Therefore, for a given explosion energy E the physical containment threshold is $d_{cont} \approx (0.008 \text{ m} \cdot \text{J}^{-1/3}) \cdot E^{1/3}$. As explosion depth increases from d_{opt} to d_{cont} eruption jets become increasingly vertically focused and reach decreasing heights above the surface (Taddeucci *et al.*, 2013; Graettinger *et al.*, 2014).

The energy source for phreatomagmatic explosions is the heat energy of the magma involved in magma-water interaction. We assume 1-10% efficiency (c_{eff}) in conversion of that heat to mechanical energy during molten fuel-coolant interaction (MFCI); $E = c_p \Delta T \rho_{mag} V \cdot c_{eff}$ (c_p is heat capacity, ΔT is temperature drop, ρ_{mag} is melt density). These efficiencies are consistent with MFCI experiments and theory (Wohletz, 1986; Büttner and Zimanowski, 1998). V is the volume of a magma batch involved in an explosion. The sizes of intrusions in exposed diatremes provide analog information on the volumes of magma batches. The limited data on intrusion dimensions indicate that volumes typically range from ~10^2 – 10^5 m^3, occasionally approaching 10^6 m^3 (Valentine *et al.*, 2014). Explosion energies that could be produced by 10^2 – 10^6 m^3 range from ~3×10^9 J to 3×10^{14} J, accounting for the range of explosion efficiencies. It is likely that smaller volumes in this range, perhaps <10^4 m^3, are more likely to fuel explosions because they can accumulate rapidly before beginning to cool, degas, and crystallize, suggesting energies <10^{13} J. Explosion energy estimates from ballistics and rock fragmentation calculations are also typically 10^{11} – 10^{13} J (*e.g.*, Self *et al.*, 1980; Raue, 2004)

Explosion energy estimates based upon intrusion volumes, ballistics, and rock fragmentation all suggest containment thresholds less than ~170 m (Figure 1), meaning that in most cases only explosions occurring in the upper 200 m (for simplicity) of a typical maar-diatreme will actually erupt. Deeper explosions will only cause subsurface disruption and subsurface debris jets (Ross and White, 2006) with minor or no surface manifestations.

Explosions that are shallower than their containment threshold, but deeper than the optimal crater excavation depth (d_{opt}), will erupt but not necessarily emplace much material onto a tephra

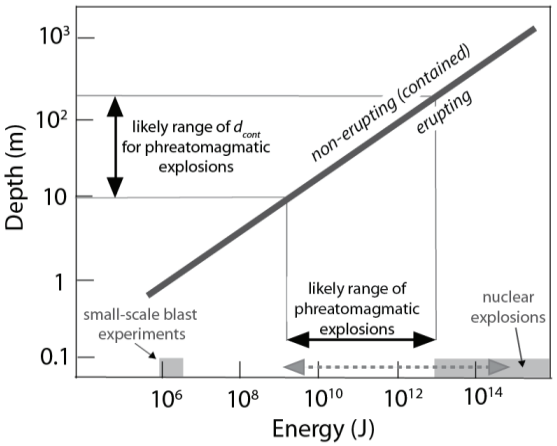

Figure 1. Containment depth (d_{cont}) as a function of explosion energy. Grey dashed line shows potential range of phreatomagmatic explosion energies, with most likely energies ranging from ~10^9 – 10^{13} J. Values corresponding to small-scale blast experiments and nuclear tests indicated for comparison (adapted from Valentine *et al.*, 2014).

ring outside the crater, due to the low rise-height and vertical focusing of their eruptive jets. Deposits in tephra rings likely represent material erupted predominantly from the near optimal scaled depth. Optimal depths are <100 m for the most likely range of magma volumes or energies. As explosion depth increases relative to d_{opt}, ejecta is increasingly likely to fall right back into the crater, until d_{cont} is reached.

Both experimental work and recent field data suggest that a predominance of shallow-derived lithics in tephra ring deposits reflects that eruptions are dominated by shallow explosions (uppermost ~200 m, *e.g.*, LeFebvre *et al.*, 2013; Graettinger *et al.*, 2014); this is consistent with the our analysis using scaled depth relationships for likely explosion energies. The occurrence of some deep-seated lithics in the upper parts of tephra rings, in these natural cases, records mixing of fragmental material within the diatremes due to explosions at a wide range of depths and resulting subsurface debris jets (*e.g.*, Andrews *et al.*, 2014), until some of these lithics are mixed to shallow depths where explosions can eject them. The explosions are caused by repeated injection of small magma batches throughout the diatreme's vertical extent during the lifetime of the volcano. An absence of deep-seated lithics in a tephra ring does not imply absence of deep explosions, only that the lithics did not mix upward sufficiently to be erupted (Graettinger *et al.*, 2014). By extension, the absence of deep-seated lithic clasts in a tephra ring does not necessarily imply a shallow diatreme. Similarly, the deepest-seated lithic clasts in a tephra bed are not necessarily directly related to the location of the explosion and associated magma fragmentation that produced that bed.

Acknowledgements

This work was supported by the 3E Fund at University at Buffalo.

References

Andrews, R.G., White, J.D.L., Dürig,T., Zimanowski, B., 2014. Discrete blasts in granular material yield two-stage process of cavitation and granular fountaining. *Geophysical Research Lett*ers *41*: 422-428, doi:10.1002/2013GL058526.

Büttner, R., Zimanowski, B., 1998. Physics of thermohydraulic explosions. Physical Review E 57: 5726–5729.

Goto, A., Taniguchi, H., Yoshida, M., Ohba, T., Oshima, H., 2001. Effect of explosions energy and depth to the formation of blast wave and crater: field explosion experiment for the understanding of volcanic explosion, Geophysical Research Letters 28, 4287-4290.

Graettinger, A.H., Valentine, G.A., Sonder, I., Ross, P.-S., White, J.D.L., Taddeucci, J., 2014. Maar-diatreme geometry and deposits: subsurface blast experiments with variable explosion depth, Geochemistry Geophysics Geosystems 15: doi:10.1002/2013GC005198.

Houser, F.N., 1969. Subsidence related to underground nuclear explosions, Nevada Test Site. Bulletin of the Seismological Society of America 59: 2231-2251.

LeFebvre, N.S., White, J.D.L., Kjarsgaard, B.A., 2013. Unbedded diatreme deposits reveal maar-diatreme-forming eruptive processes: Standing Rocks West, Hopi Buttes, Navajo Nation, USA. Bulletin of Volcanology 75: 739, doi:10.1007/s00445-013-0739-9.

Raue, H., 2004. A new model for the fracture energy budget of phreatomagmatic explosions. Journal of Volcanology and Geothermal Research 129: 99-108, doi:10.1016/S0377-0273(03)00234-8.

Ross, P.-S., White, J.D.L., 2006. Debris jets in continental phreatomagmatic volcanoes: A field study on their subterranean deposits in the Coombs Hill vent complex, Antarctica. Journal of Volcanology and Geothermal Research 149: 62-84, doi:10.1016/j.jvolgeores.2005.06.007.

Self, S., Kienle, J., Huot, J.-P., 1980. Ukinrek Maars, Alaska, II. Deposits and formation of the 1977 craters. Journal of Volcanology and Geothermal Research 7: 39-65.

Taddeucci, J., Valentine, G.A., Sonder, I., White, J.D.L., Ross, P.-S., Scarlato, P., 2013. The effect of pre-existing craters on the initial development of explosive volcanic eruptions: An experimental investigation. Geophysical Research Letters 40: 507-510, doi:10.1002/grl.50176.

Valentine, G.A., Graettinger, A.H., Sonder I., 2014. Explosion depths for phreatomagmatic eruptions. *Geophysical Research Letters*, doi: 10.1002/2014GL060096

Wohletz, K.H., 1986. Explosive magma-water interactions: Thermodynamics, explosion mechanisms, and field studies. Bulletin of Volcanology 48: 245-264.

Quantitative characterization of the componentry of the ash fraction and the shape of juvenile ash particles in maar deposits (Eifel Volcanic Field, Germany)

Juanita Rausch[1], Bernard Grobéty[1], Pierre Vonlanthen[2]

[1] *Department of Geosciences, University of Fribourg, Chemin du Musée 6, Fribourg, Switzerland, juanita.rausch@unifr.ch*
[2] *Institute of Earth Sciences, University of Lausanne, UNIL Mouline, Building Géopolis, Lausanne, Switzerland.*

Keywords: Eifel Volcanic Field, fractal analysis, automated single particle SEM/EDS analysis.

Maar volcanoes in the Eifel Volcanic Field (Germany), the maar-type locality, generated a large variety of deposits, some of which strongly contrast with the criteria commonly accepted to be diagnostic for phreatomagmatic eruptions. Some of those criteria include well-bedded, dominantly fine-grained (fine ash to lapilli), poorly-sorted and lithic-rich deposits characterized by juvenile particles dominated by angular to cauliflower-shaped morphologies, smooth textures, low vesicularities and a glassy groundmass (i.e. rapid quenched sideromelane glass) (*e.g.* Heiken, 1972; Schmincke, 1977; Fisher and Schmincke, 1984; White and Ross, 2011). All those deposit and particle characteristics suggest the presence of water/steam in the transport and deposition system, as well as particle formation by brittle fragmentation of the magma during water-magma interaction. While those characteristic features are obvious in the East Eifel maar deposits, most of them are not observed in the maar deposits of the West Eifel. In order to decipher the fragmentation mechanisms operating during the East and West Eifel maar eruptions, we carried out a detailed sedimentological, volcanological and geochemical study combined with quantitative componentry and morphological analysis of small volcanic ash particles (< 250 µm) collected from the best exposed tephra ring deposits.

The studied West and East Eifel maar volcanoes can be differentiated by their magma composition and geological setting (Fig. 1). Most West Eifel magmas are highly silica-undersaturated, alkaline (*e.g.* melilite nephelinites), and possibly CO_2-rich, while the East Eifel volcanoes have slightly less silica-undersaturated magma compositions (*e.g.* basanites). The bedrock underlying the studied West Eifel maars consists exclusively of non-porous, consolidated Lower Devonian sedimentary rocks lacking a confined aquifer. These rocks are, however, overlain in the East Eifel by an up to 20 m thick low permeable Tertiary clay layer containing lenses of highly permeable, unconsolidated gravels and sands (Meyer, 1986, 2013), which build a classical confined aquifer.

Most West Eifel maar deposits (*e.g.* Meerfelder Maar, MFM; Pulvermaar, PM; Ulmener Maar, UM; and Oberwinkler Maar, OM) are coarse-grained (Md_{ϕ}: (-1)-(-3.5) phi) and well- to moderately-sorted (σ_{ϕ}: 1.0-2.5). Componentry studies on coarse (32-1 mm ø) and fine fractions (< 250 µm) lead to the conclusion that the coarse-grained character of these deposits is related to the high resistance and degree of consolidation of the underlying bedrock (Lower Devonian sandstone, siltstone and slate), which is hardly fragmented in small (ash-sized) particles. The commonly observed upward increase in juvenile particles and decrease in lithoclasts is interpreted to reflect the increasing stabilization of the crater and conduit walls.

Even though the East and West Eifel maar deposits share some deposit characteristics, fundamental differences in the morphology and internal texture of the juvenile particles were recognized. Based on light microscopy and Scanning Electron Microscope (SEM) studies most juvenile particles from West Eifel maars are round to subround, highly rugose, slightly to moderately vesiculated (5-60 vol. %) and tachylitic, while juvenile clasts from East Eifel maar phases are commonly angular, smooth, poorly-vesiculated (0-15 vol. %) and consist of sideromelane glass (Fig. 1). In order to better assess these differences and because juvenile ash particles hold key information on fragmentation, eruption and transport mechanisms, the shape of the juvenile ash particles was quantitatively characterise by fractal analysis, one of the most powerful methods for the quantification of the shape of complex objects. The fractal method was tested in 3D by analysing particle contours obtained from SEM micro-computed tomography (SEM micro-CT) reconstructions. Subsequently, analyses were performed on a large number of contours (particles of the 125-250 µm sieve fraction) obtained from thin sections. Fractal analyses using the dilation method and the fractal spectrum technique (Maria and Carey, 2002) on West Eifel maar particles yield large small-scale ("textural") dimensions

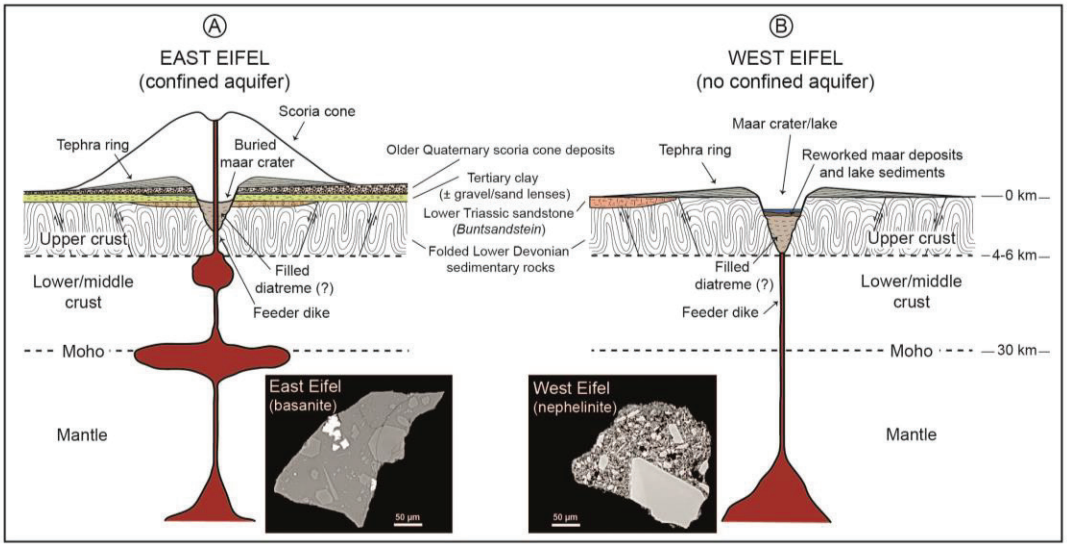

Fig. 1 – Geological and hydrological setting of the A) East Eifel Volcanic Field and the B) West Eifel Volcanic Field, with corresponding juvenile particle types (backscattered electron images).

(D1 > 1.023) compared to classical phreato-magmatic end-members, resembling fractal dimensions of typical magmatic particles and confirming their complex shape at small scales. In contrast, the small-scale ("textural") fractal dimensions of particles from one East Eifel maar phase (EBGU: Eppelsberg Green Unit) are much smaller, coinciding with the fractal dimensions of particles with a phreatomagmatic origin.

In addition, the componentry of the sieve fraction analysed by fractal analysis (125-250 µm) was quantitatively studied by automated single-particle SEM/EDS analysis. The goals were to assess the proportion of magmatic vs. non-magmatic particles in the fine-grained material of Eifel maar deposits and to infer the depth of fragmentation, the eruption style and the influence of the bedrock in the grain size and component distributions of the ejected tephra. In the case of Meerfelder Maar (West Eifel), no significant componentry variations between the coarse- and fine-grained fractions were observed. Based on the occurrence of deep-seated (peridotite) xenoliths within the entire Meerfelder Maar deposit and on the large content of lithoclasts within the lower and middle part of the deposit compared to a much smaller proportion of lithoclasts in the East Eifel maar phase (EBGU), a much greater fragmentation depth is inferred for the Meerfelder Maar eruption.
The later results combined with the characteristics of the deposits and juvenile particles are clear evidence for the phreatomagmatic origin of some of the East Eifel maar phases (*e.g.* EBGU and similar deposits), in which the trigger mechanism is interpreted to have been the shallow interaction of rising magma with groundwater. On the contrary, the various analyses performed in the frame of this study point towards a magmatic pre-fragmentation at depth of the rapid ascending (vesiculating) CO_2-rich magma in the West Eifel maars. In that scenario, limited interaction of the ascending pre-fragmented particle-gas-magma mixture with external water at near-surface levels cannot be ruled out, but it is considered to be uncorrelated with the trigger of the fragmentation process.

Acknowledgements

The Swiss National Science Foundation (Marie-Heim Vögtlin Program) and the University of Fribourg (Switzerland) are kindly thanked for the financial support of this study.

References

Fisher, R.V., Schmincke, H.-U. 1984, Pyroclastic Rocks, Springer, Berlin, 472 pp.

Heiken, G. 1972, Morphology and petrography of volcanic ashes. Geological Society of America Bulletin 83(7): 1961-1988.

Maria, A., Carey, S. 2002, Using fractal analysis to quantitatively characterize the shapes of volcanic particles. Journal of Geophysical Research: Solid Earth (1978–2012), 107(B11), ECV-7.

Meyer, W. 1986, 2013, Geologie der Eifel. Schweizerbart, Stuttgart 614 pp.

Schmincke, H.-U. 1977 Phreatomagmatische Phasen in quartären Vulkanen der Osteifel: Geologisches Jahrbuch 39:3-45.

White, J.D.L., Ross, P.S. 2011, Maar-diatreme volcanoes: A review: Journal of Volcanology and Geothermal Research, 201(1–4):1-29.

Plio-Pleistocene Maar-Diatremes, Mesa Chivato, New Mexico, USA

Fraser Goff[1], John R. Lawrence[2], and Cathy J. Goff[3]

[1] *Department of Earth & Planetary Sciences, University of New Mexico, Albuquerque, NM 87131, USA. candf@swcp.com*
[2] *Lawrence GeoServices Ltd. Co., 2321 Elizabeth St. NE, Albuquerque, NM 87112, USA.*
[3] *Private Consultant, 5515 Quemazon, Los Alamos, NM 87544, USA.*

Keywords: Maars, diatremes, Mesa Chivato.

We describe herein partially buried Plio-Pleistocene maar volcanoes that we recently mapped on southern Mesa Chivato, New Mexico (Fig. 1). Mesa Chivato is a broad, NE-trending highland (elev. ~2600 m) of lava flows, scoria cones, maar craters and deposits, and subordinate trachytic domes emplaced from ca. 3.3 to 1.3 Ma (Crumpler, 1980; Goff *et al.*, 2014). The mesa parallels the NE-SW trend of the Jemez volcanic lineament (JVL), a group of aligned volcanic centers that erupted from Miocene to Quaternary time, and is located about 65 km west of the Rio Grande rift (RGR). Mesa Chivato also flanks the NE side of Mount Taylor (3455 m), a composite alkaline stratovolcano that last erupted about 2.5 Ma (Perry *et al.*, 1990; Goff *et al.*, 2013).

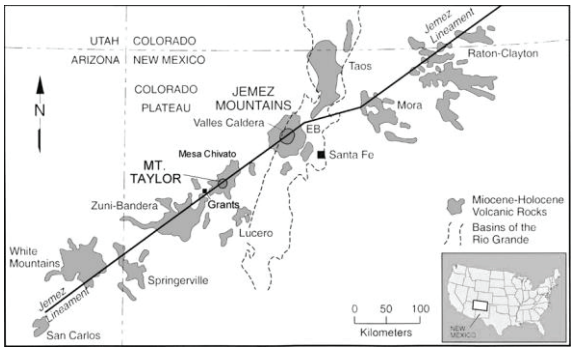

Fig.1 – Map showing location of Mesa Chivato and Mount Taylor with respect to other volcanic centers of the JVL and to basins of the RGR; EB = Española Basin.

Geologic mapping in the Mount Taylor region since 2007 evaluates uranium, coal and water resources, and Plio-Pleistocene volcanism. Laguna Cañoneros quadrangle, which depicts most of southern Mesa Chivato, contains 23 maar craters and roughly 55 scoria cones and fissure vents. The craters are circular to oblong, usually elongated in a NE-SW direction. A few craters appear to be double-maars with adjacent vents located on NE-SW trends. The largest is the western crater of Lagunas Cuatas, which is 1.5 x 0.75 km. The smallest craters, such as Laguna Fria, have diameters ≤150 m. The primary characteristic of the maars is a virtual lack of exposed crater rampart and flanking hydromagmatic deposits typical of tuff rings and tuff cones (Wohletz and Sheridan, 1983; Lorenz, 1986).

Except for remnant craters, the maar volcanoes are surrounded and buried by younger lava flows and scoria cones. In this respect, the Mesa Chivato maars resemble eroded scoria cones surrounded by younger lavas in the Camargo volcanic field, Mexico (Aranda-Gómez *et al.*, 2010). Based on field relations and $^{40}Ar/^{39}Ar$ dates, the Mesa Chivato maar volcanoes formed between 1.9 and 3.2 Ma (Goff *et al.*, 2014).

The best example of a partially buried maar occurs at Laguna Cañoneros (1 x 0.5 km, Fig. 2). Poorly exposed tuff ring deposits partially rim the crater. Two lava flows, one of which is dated at 2.58 ± 0.01 Ma (groundmass), surround the crater and overlie the tuff ring deposits. The excavated drainage from the maar displays about 7 m of planar bedded and cross bedded basaltic hydromagmatic deposits containing a few bomb sags overlain by the flows. An ancient soil horizon containing fragments of trachydacite pumice underlies the hydromagmatic layers. Sanidine from the pumice has an age of 2.700 ± 0.002 Ma. Thus, the maar volcano formed between 2.58 and 2.70 Ma. Beneath the soil is the top of an older basaltic flow (ca. 3.2 Ma).

Fig. 2 – View SW across Laguna Cañoneros maar and basaltic plains of southern Mesa Chivato. Mount Taylor composite volcano (3455 m) rises in far left and Cerro Chivato trachyte dome (3.16 Ma, 2720 m) looms to right.

Our generalized model explains development and resulting field relations of the partially buried maars (Fig. 3). The initial tuff cone/ring is fed from an underlying basaltic diatreme and is built on an older surface of lava with or without soil. Relatively soon thereafter, a younger eruption of lava surrounds the cone/ring before it has completely eroded. With time hydromagmatic beds continue to erode, widening and filling the crater. We believe that the

crater fill deposits are complicated mixtures of eroded hydromagmatic debris, aeolian silt and organic-rich lacustrine beds. Near crater walls, blocks of eroded younger basalt create course talus breccia mixed with marginal crater fill. Primary hydromagmatic beds are preserved where covered by younger lava and exposed along streams that drain the craters. Today, Mesa Chivato maars are mostly dry, but occasionally contain shallow ponds (Goff *et al.*, 2014).

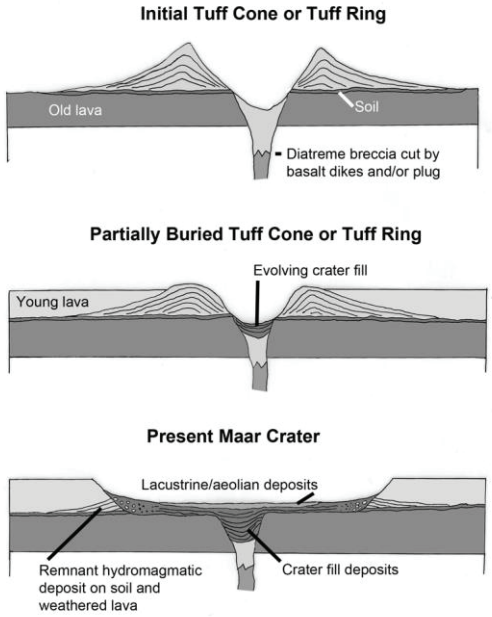

Fig. 3 – Three stage model (not to scale) showing development and evolution of partially buried maars on Mesa Chivato. Volcanic rocks cover ≥1500 m of Jurassic-Cretaceous sandstones, siltstones, shales and coal.

A link between a now-eroded maar and its underlying diatreme (Valentine and White, 2012) is exposed in a deep canyon cutting southern Mesa Chivato (Fig. 4). The diatreme contains abundant blocks of Cretaceous rocks ≤1 m long. A dike cutting the diatreme is dated at 3.07 ± 0.09 Ma (groundmass). The elevation difference between diatreme and flanking basalt-covered mesas is 400 m. Presumably, each Mesa Chivato maar is connected to a basaltic root at similar depths.

The Plio-Pleistocene boundary is a period of dramatic climate change from warmer and wetter to drier and cooler conditions (Zachos *et al.*, 2008, fig. 2). Apparently the Mesa Chivato maars formed during wetter conditions that were normal before 1.9 Ma when groundwater sources were more voluminous. Consequently, a maar-diatreme sequence like Laguna Cañoneros presents an opportunity to drill ±400 m of crater fill deposits and diatreme root to investigate maar processes and climate change from Present to the Plio-Pleistocene boundary.

Fig. 4 – Root zone, Seboyeta Canyon diatreme; 1 = scoria, 2 = hydromagmatic, L = lava infill, 3 = hydromagmatic, D = dikes cutting lava and scoria. Cliffs in background are Cretaceous sandstone and siltstone.

Acknowledgements

W. McIntosh and L. Peters (NMBG&MR) determined the $^{40}Ar/^{39}Ar$ dates cited in this paper.

References

Aranda-Gómez, J.J., Housh, T.B., Luhr, J.F., Neyola-Medrano, C., Rojas-Beltrán, M.A., 2010. Origin and formation of neck in a basin landform: Examples from the Camargo volcanic field, Chihuahua (México). Journal of Volcanology and Geothermal Research 197: 123-132.

Crumpler, L.S., 1980. Alkali basalt through trachyte suite and volcanism, Mesa Chivato, Mount Taylor volcanic field, New Mexico, Part I. Geological Society of America Bulletin 91: 253-255.

Goff, F., Wolff, J.A., Fellah, K., 2013. Mount Taylor dikes. New Mexico Geological Society, 64th Field Conference, Socorro: 159-165.

Goff, F., Kelley, S.A., Lawrence, J.R., Goff, C.J., 2014. Preliminary geologic map of the Laguna Cañoneros quadrangle, Cibola and McKinley counties, New Mexico. New Mexico Bureau of Geology and Mineral Resources Open-file map, 1:24,000 scale. {http://geoinfo.nmt.edu/publications/maps/home.html}

Lorenz, V., 1986. On the growth of maars and diatremes and its relevance to the formation of tuff rings. Bulletin of Volcanology 48: 265-274.

Perry, F.V., Baldridge, W.S., DePaolo, D.J., Shafiqullah, M., 1990. Evolution of a magmatic system during continental extension: The Mount Taylor volcanic field, New Mexico. Journal of Geophysical Research 95: 19,327-19,348.

Valentine, G.A., White, J.D.L., 2012. Revised conceptual model for maar-diatremes: Subsurface processes, energetics, and eruptive products. Geology 40: 1111-1114.

Wohletz, K.H., Sheridan, M.F., 1983. Hydrovolcanic explosions II. Evolution of basaltic tuff rings and tuff cones. American Journal of Science 283: 385-413.

Zachos, J.C., Dickens, G.R., Zeebe, R.E., 2008. An early Cenozoic perspective on greenhouse warming and carbon-cycle dynamics. Nature 45: 279-283.

1 km of syn-eruptive subsidence: deep bedded ultramafic diatremes in the Missouri River Breaks volcanic field, Montana, USA

Séverine Delpit[1], **Pierre-Simon Ross**[1*], B. Carter Hearn Jr[2]

[1] *Institut national de la recherche scientifique, 490 rue de la Couronne, Québec (Qc) G1K 9A9, Canada, rossps@ete.inrs.ca*
[2] *United States Geological Survey, 954 National Center, Reston VA 20192, USA.*

Keywords: diatreme, ultramafic, subsidence.

The ultramafic Eocene Missouri River Breaks volcanic field of north-central Montana includes over 50 diatremes emplaced in a mostly soft substrate (Hearn, 1968). The current erosion level is 1.3-1.5 km below the pre-eruptive surface, exposing the deep part of the diatreme structures and some dikes. Five representative diatremes have been studied by Delpit (2013) and Delpit *et al.* (*in press*). They are 200-375 m across and have sub-vertical walls. Their infill consists mostly of 55-90% bedded pyroclastic rocks with concave-upward bedding (fine tuffs to coarse lapilli tuffs; beds ranging from 3 cm to 10 m thick), and 45-10% non-bedded pyroclastic rocks (medium lapilli tuffs to tuff breccias). In the former, the recognizable deposits of dilute pyroclastic density currents are locally observed. The non-bedded zones form steep columns 15-135 m in horizontal dimension, which cross-cut the bedded pyroclastic rocks. Megablocks of the host sedimentary formations are also present in the diatremes, some being found 1 km or more below their sources (Fig. 1).

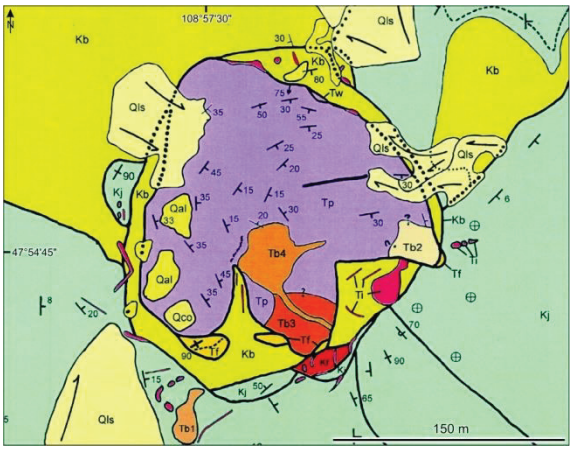

Fig. 1 – Example of a map (prepared by the third author) of an Eocene diatreme in the Missouri River Breaks volcanic field. Upper Cretaceous host formations: Kb = Bearpaw Shale; Kj = Judith River Fm. Sedimentary megablocks and slices in the diatreme: Tw = Wasatch Fm (L. Eocene); Tf = Fort Union Fm (Paleocene); Kf = Fox Hills Sst (U. Cretaceous). Pyroclastic infilling of diatreme: Tp = bedded; Tb1-4 = non-bedded. Other lithologies: Ti = Intrusive igneous rocks (diatreme-related); Qal-Qco-Qls = Quaternary.

Within the bedded pyroclastic rocks, the juvenile fraction (mostly spherical fragments and free altered olivine crystals) varies from 4 to 54% (ave 33%); the lithic fraction varies from 2 to 40% (ave 22%) and the undifferentiated ash fraction represents 5-80% of individual beds (ave 45%). The non-bedded pyroclastic rocks, in contrast, contain 0-28% altered olivine crystals (ave 11%); 13-60% spherical juvenile pyroclasts (ave 34%); 15-65% lithic fragments (ave 39%); and 6-32% undifferentiated ash (ave 16%). Note that the non-bedded material generally contains much less ash than do the bedded pyroclastic rocks.

Ash- to bomb-sized (≤15 cm), non-vesicular, finely crystalline, spherical (to sub-spherical), ultramafic fragments are the principal juvenile component in both bedded and non-bedded pyroclastic rocks. Within the spherical fragments of lapilli size, 67% have a central or eccentric core (lithic clast or altered olivine crystal), coated by ultramafic juvenile material, whereas the other 33% lack cores (Fig. 2). They are accompanied by minor accretionary lapilli and armored lapilli.

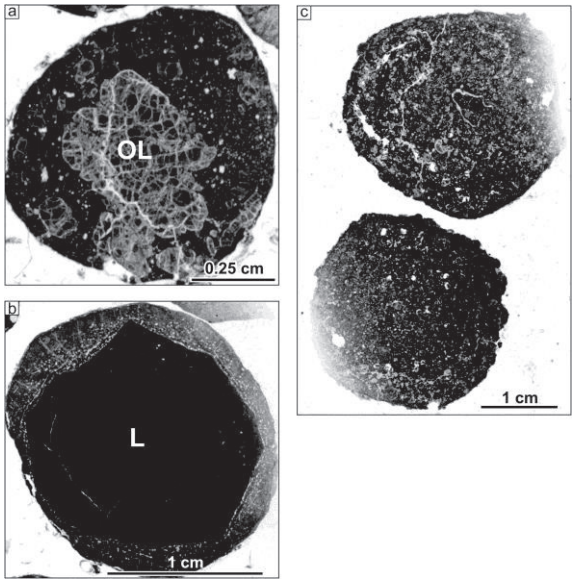

Fig. 2 – Spherical (to sub-spherical) ultramafic juvenile pyroclasts. (a) Cluster of olivine (OL) crystals with thick ultramafic rim. (b) Angular lithic fragment (L) with a relatively thin ultramafic rim. (c) Pyroclasts with no cores.

Our main interpretations are as follows (Fig. 3): (1) the observations strongly support phreatomagmatic explosions as the energy source for fragmentation and diatreme excavation; (2) the bedded pyroclastic rocks were deposited on the crater floor (probably 200-300 m deep), and subsided by 1.0-1.3 km to their current location, with subsidence taking place mostly during the eruption; (3) the observed non-bedded pyroclastic columns were created by debris jets that punched through the bedded pyroclastic material; the debris jets did not empty the mature diatreme, occupying only a fraction of its width, and some debris jets probably did not reach the crater floor; (4) the mature diatreme was nearly always filled and buttressed by pyroclastic debris at depth – there was never a 1.3-1.5 km-deep empty hole with subvertical walls, otherwise the soft substrate would have collapsed inward, which it only did near the surface, to create the megablocks. We infer that syn-eruptive subsidence shifted down bedded pyroclastic material and shallow sedimentary megablocks by 0.8-1.1 km or more, after which limited post-eruptive subsidence occurred (~200 m). This makes these diatremes an extreme end-member case of syn-eruptive subsidence in the spectrum of possibilities for maar-diatreme volcanoes worldwide.

Acknowledgements

The study was funded by NSERC (Discovery grant to PSR) and an INRS start-up grant. We thank V. Lorenz, S. Kurszlaukis and J.D.L. White for discussions during the 2009 Missouri River Breaks field workshop, plus G. Valentine and J.D.L. White for comments on a draft of the Bull. Volc. paper.

References

Delpit, S., 2013. From maar to diatremes: Pali Aike (Argentina) and Missouri River Breaks (United-States) volcanic fields. PhD thesis, Institut national de la recherche scientifique, Québec, Canada, 320 p

Delpit, S., Ross, P.-S., Hearn, B.C., *in press*. Deep bedded ultramafic diatremes in Missouri River Breaks volcanic field, Montana, USA: more than 1 km of syn-eruptive subsidence. Bulletin of Volcanology

Hearn B.C., 1968. Diatremes with kimberlitic affinities in north-central Montana. Science 159: 622-625.

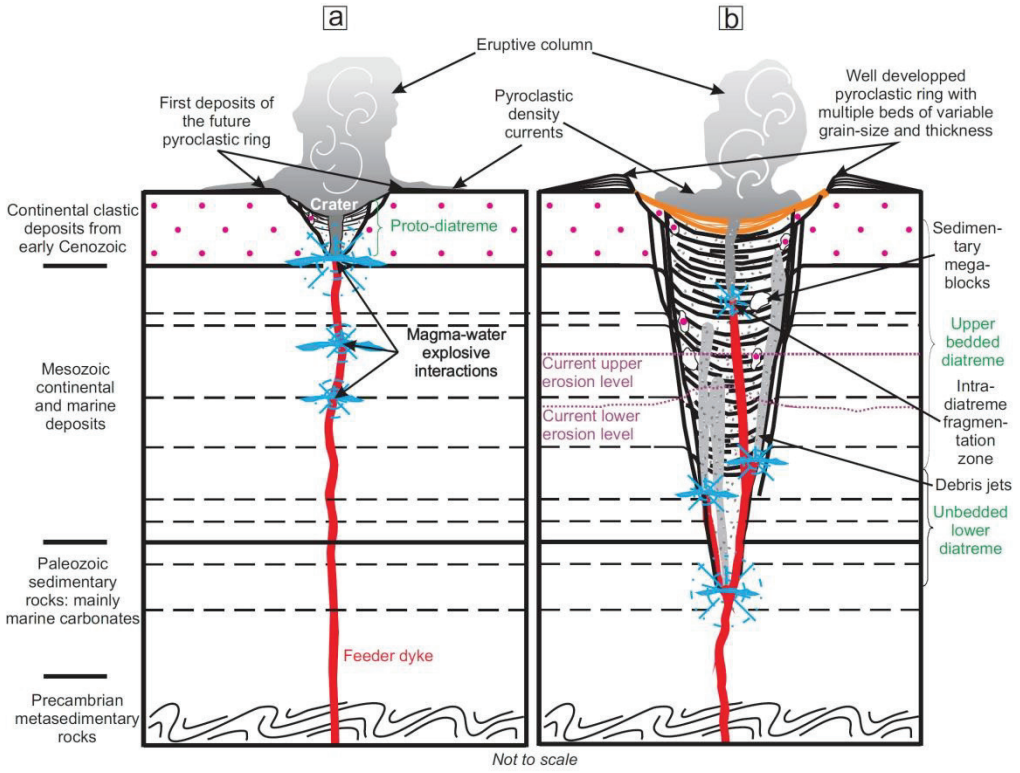

Fig. 3 – Emplacement model for Missouri River Breaks maar-diatreme volcanoes (Delpit *et al.*, *in press*).(a) Magma rises in a dike and interacts explosively with one or more aquifers in the shallow crust. The fragmented material from the shallowest explosions is erupted into the atmosphere, forming an eruptive column, and a crater (plus proto-diatreme) is formed. (b) Towards the end of the eruption, the diatreme is of conical shape with a well developed pyroclastic ring surrounding the maar crater. The upper diatreme is bedded whereas the lower diatreme is not. As a response to syn-eruptive subsidence, the bedded pyroclastic material develops a bowl-shaped structure; megablocks of younger age are now at deeper levels in the diatreme and layers of the country rock record a downward movement along the diatreme walls. Debris jets form at any level within the diatreme as a result of phreatomagmatic explosions and their non-bedded deposits cut pre-existing pyroclastic deposits.

K E Y N O T E

Questions about phreatomagmatic maar-diatreme processes

Greg A. Valentine

Dept. of Geology and Center for Geohazards Studies, University at Buffalo, Buffalo, NY 14260 USA, gav4@buffalo.edu

Keywords: insert, three, keywords.

Maar-diatremes are abundant terrestrial volcanic landforms/structures, and many problems surround their formation. Here I raise some key questions about maar-diatremes, and discuss ongoing work aimed at addressing them. The framework for the questions is provided by a conceptual model that originated, to my knowledge, with Prof. Volker Lorenz, and that has been refined and revised by further research. The conceptual model is one in which individual maar-diatremes are the result of repeated subsurface explosions caused by interaction of ascending magma with groundwater, *i.e.*, they are mainly phreatomagmatic in origin, although volatile-driven (magmatic) eruptive processes may dominate in phases of an eruptive episode. In the words of Prof. Lorenz, maar-diatremes are a type of volcano "that largely prefers to work underground."

One class of fundamental maar-diatreme questions focuses on the mechanisms by which magma and water interact and explode. There are some different perspectives on this process within the volcanological community, but in my opinion the classical process of molten fuel-coolant interaction (MFCI), is the most important (Wohletz, 1986; Büttner and Zimanowski, 1998; and subsequent papers by these authors and their collaborators). Most of our quantitative volcanological understanding of the physics of MFCI is based upon experimental work with injection of water into relatively static melt in a crucible; this experimental foundation, as most participants in this conference will know, has shown that there are four main stages of MFCI: premixing, trigger, thermohydraulic "detonation," and expansion. Most magma-water interaction in maar-diatremes probably takes place in one of two scenarios: (1) magma flowing through a dike with permeable, saturated host rock; or (2) magma intruding unconsolidated sediment or diatreme fill and forming contorted, irregularly shaped bodies with variable enfolding of host material. *How does the geometry of these scenarios influence MFCI?* In the latter scenario, interaction of magma with wet sediment is more likely than interaction with clean water. Lab scale experiments have begun to explore the effects of such "impure" coolants on MFCI (*e.g.*, Schipper *et al.*, 2011); these are an important and necessary step, but natural phreatomagmatic explosions must involve significantly larger masses of melt and coolant than can be studied on the bench top. *What effect does physical scale and multiple pre-mixing "centers" within a magma volume have on MFCI?* Experiments to date have involved systems that are initially relatively static compared to a subvolcanic system with flowing magma. *What is the effect of imposed dynamics on MFCI?* MFCI is often discussed in terms of water:magma mass ratios, but it is not clear whether this is appropriate for a more dynamic system. *Can we define ratios of mass fluxes that constrain explosion processes?* In applying MFCI physics to natural explosions it would be useful to have a simple way to relate magma mass and explosion energy. *Can we constrain a range of efficiencies in conversion of magma thermal energy to mechanical energy of explosion, for masses and geometries that are geologically relevant?* Finally, there remains uncertainty about the depth at which MFCI explosions can take place, except that the hydrostatic pressure should be lower than the critical pressure of water. Lorenz' (1986) classic conceptual model had ever-deepening explosions defined by low hydrostatic pressures as a water table is drawn down, but field evidence (summarized by White and Ross, 2011) strongly indicates that explosions can occur at a range of depths at any given time, rather than simply deepening during an eruptive episode. *What are the pressure controls on MFCI efficiency and what is the hydrostatic pressure field in the dynamic environment of a maar-diatreme?*

Once an explosion has occurred it affects the subsurface and surface. It is important to keep in mind that in the conceptual framework the diatreme is never really empty, but rather is a body of broken up and subsided country rock and eruptive deposits with juvenile pyroclasts and hypabyssal intrusions (see, *e.g.*, White and Ross, 2011; Delpit *et al.*, 2014; note I am focusing on volcanic processes here, and am neglecting post-eruptive subsidence and sedimentation). Field evidence supports the formation of debris jets in the diatreme environment, which result in explosion-driven vertical transport of material. Debris jets in turn play a key role in churning and mixing materials within diatremes. *How do the scales of debris jets vary with explosion energy and depth?* This question in turn relates to the efficiency of upward mixing and downward subsidence within diatremes as a function of MFCI

processes. *What is the role of entrainment as a debris jet injects upward in a diatreme, and how does this affect large-scale mixing?* Many maar-diatremes provide strong evidence for both lateral and vertical shifting of explosion sites during their eruptive episodes. *What are the combined effects of explosions at multiple sites and different times on mixing and subsidence in diatremes and crater formation, and can they be quantified?*

On the surface the effects of some, but probably not all, explosions contribute to eruption processes and crater formation. There is a large literature relating crater size to explosion energy for single explosion scenarios (*e.g.*, chemical or nuclear explosions, or meteorite impacts), when those explosions occur within a certain range of scaled depths (physical depth divided by cube root of explosion energy). When the relationships are applied to maar craters, the resulting energy estimates are very high and require what appear to be unrealistic conditions of magma accumulation and MFCI. In any case, we know that most maar craters are the result of many explosions rather than a single one, and it is the energy of the individual explosions that matter most from a hazards perspective. *Is there a useful relationship between crater size and energy for multiple explosion craters?* As mentioned above many maar-diatremes preserve evidence of both vertically and laterally shifting explosion sites (*e.g.*, Jordan *et al.*, 2013). *What are the effects of a range of scaled depths and lateral locations on the final crater, ejecta dynamics, and eruptive deposits?* Tephra rings preserve diverse pyroclastic deposits, including bedded and cross bedded lapilli tuffs, massive tuff breccias, tephra fall, and ballistic blocks and bombs. Often these are interpreted in terms of different explosion or fragmentation mechanisms, but experiments are showing that eruption jets are strongly influenced by scaled depths and presence or absence of already-formed craters (*e.g.*, Taddeucci *et al.*, 2013; Graettinger *et al.*, 2014). *How much of the diversity of deposits is really related to different explosion mechanisms?*

Although the questions raised here are focused on the maar-diatreme context, I think that there are important implications for explosive volcanism in general. Many hazardous eruptive episodes at composite volcanoes and calderas begin with phreatic and phreatomagmatic explosions. While these phases must have an influence on how each episode unfolds, their details are commonly overprinted by subsequent events or are simply overlooked by volcanologists. Like other monogenetic volcanoes, most maar-diatremes provide the luxury of having been produced by single eruptive episodes that are not overprinted by later activity. In this way we can isolate the effects of subsurface phreatomagmatic processes at maar-diatremes and, potentially, eventually transfer that knowledge to a broader set of volcanological problems. Even without these broader implications, maar-diatremes provide a rich set of problems to tackle with field, experimental, and theoretical approaches in the coming years.

Acknowledgements

The author's work is supported by the 3E Fund at University at Buffalo and by the U.S. National Science Foundation. Many collaborators have contributed to my thinking on maar-diatremes and to the questions posed here and I thank them immensely, especially James White, Pierre-Simon Ross, Alison Graettinger, Ingo Sonder, Jacopo Taddeucci, and Bernd Zimanowski.

References

Büttner, R., Zimanowski, B., 1998. Physics of thermohydraulic explosions. Physical Review E 57: 5726–5729.

Delpit, S., Ross, P.-S., Hearn Jr., B.C., 2014. Deep-bedded ultramafic diatremes in the Missouri River Breaks volcanic field, Montana, USA: 1 km of syn-eruptive subsidence. Bulletin of Volcanology 76: 832.

Graettinger, A.H., Valentine, G.A., Sonder, I., Ross, P.-S., White, J.D.L., Taddeucci, J., 2014. Maar-diatreme geometry and deposits: subsurface blast experiments with variable explosion depth. Geochemistry Geophysics Geosystems 15: doi:10.1002/2013GC005198.

Jordan, S.C., Cas, R.A.F., Hayman, P.C., 2013. The origin of a large (< 3 km) maar volcano by coalescence of multiple shallow craters: Lake Purrumbete maar, southeastern Australia. Journal of Volcanology and Geothermal Research 254: 5-22.

LeFebvre, N.S., White, J.D.L., Kjarsgaard, B.A., 2013. Unbedded diatreme deposits reveal maar-diatreme-forming eruptive processes: Standing Rocks West, Hopi Buttes, Navajo Nation, USA. Bulletin of Volcanology 75: 739, doi:10.1007/s00445-013-0739-9.

Lorenz, V., 1986. On the growth of maars and diatremes and its relevance to the formation of tuff rings. Bulletin of Volcanology 48:265-274.

Schipper, C.I., White, J.D.L., Zimanowski, B., Büttner R., Sonder, I., Schmid, A., 2011. Experimental interaction of magma and "dirty" coolants. Earth and Planetary Science Letters 303:323-336.

Taddeucci, J., Valentine, G.A., Sonder, I., White, J.D.L., Ross, P.-S., Scarlato, P., 2013. The effect of pre-existing craters on the initial development of explosive volcanic eruptions: An experimental investigation. Geophysical Research Letters 40: 507-510, doi:10.1002/grl.50176.

White, J.D.L., Ross, P.-S., 2011. Maar-diatreme volcanoes: A review. Journal of Volcanology and Geothermal Research 201:1-29.

Wohletz, K.H., 1986. Explosive magma-water interactions: Thermodynamics, explosion mechanisms, and field studies. Bulletin of Volcanology 48: 245-264.

A generic emplacement model for the Chidliak kimberlites, Baffin Island, Nunavut

Stephan Kurszlaukis[1], Jennifer Pell[2] and Alexandrina Fulop[1]

[1] *De Beers Canada Inc., 250 Ferrand Drive, Suite 900, Toronto, ON, Canada.*
[2] *Peregrine Diamonds Ltd, Vancouver, BC, Canada.*

Keywords: kimberlite, pipe, emplacement.

The Chidliak kimberlite field (Pell et al., 2013) is located on the Hall Peninsula of Baffin Island and consists of at least 67 kimberlite occurrences. An additional three kimberlites have been discovered in the adjacent Qilaq project area. The kimberlite field has a known extent of approximately 70x40 km, and most of the pipes discovered to date occur in the southern portion of the field. The emplacement ages range from 156-138 Ma, with a peak of magmatic activity between 150-143 Ma (Heaman et al., 2011). Conodont data derived from limestone xenoliths suggest that at the time of emplacement the basement rocks were covered with about 300m of Paleozoic limestone (Zhang and Pell, 2014). The present day country rocks are comprised of Archean rocks, predominantly orthogneisses and paragneisses. All limestone strata are eroded.

Most of the kimberlite occurrences are pipes, with a minor number of occurrences related to dykes. The feeder dyke system has a pronounced N to NNW direction with only a few dykes deviating from this direction. The dykes often have several eruptive centres located on them. For example, the CH10 and CH20 kimberlites appear to be minor eruptive centres adjacent to the CH6 pipe. The eruptive centres have significantly different sizes mostly ranging from an estimated 0.25 to 2 ha. The kimberlite material filling the smallest eruptive centres is usually comprised of coherent kimberlites (CK), while the larger centres show volcaniclastic kimberlite (VK) infills. The VKs are both primary pyroclastic (PK) as well as resedimented (RVK) in nature. A special type of VK is a dark rock that has a coherent appearance; however, textural features in many of these rocks suggest that they are reconstituted and are best interpreted as agglutinated tuffs. These rocks are called apparent coherent kimberlites (ACK). With the exception of ACK, some VK deposits show a mixture of basement and limestone xenoliths but are usually dominated by limestone fragments. The ACK show low dilution that is dominated by basement xenoliths and only on occasion by limestones.

The pipes mostly have surface areas of 2 ha or less; many have been discovered that are 1 ha or less. Larger pipes, up to 4 ha in size, have been defined by drilling and some geophysical anomalies suggest pipes of over 4 ha are present, but they seem to be the exception. Large sized pipes exceeding 10 ha in surface area have not yet been discovered.

Drilling information suggests that the pipes are steep sided and often inclined towards the SSW. However, it is not clear at this stage whether the apparent inclination of the pipes is a result of structural control during emplacement (along inclined faults or other structures) or is due to post-emplacement tilting.

The Chidliak kimberlite field shows a number of volcanological features that are rather unique for kimberlites and which are more typical for basaltic monogenetic fields. The most significant and unusual features for a kimberlite field are the predominance of eruptive centers ≤ 1 ha in size and the frequent appearance of ACK. In few pipes the latter is sandwiched in between PK or RVK deposits and shows a gradual transition zone between the adjacent volcaniclastic units and the ACK. On occasions, the ACK itself still shows remnants of reconstituted juvenile pyroclasts, giving evidence for a once fragmental nature of the rock. The alternation of xenolith-rich PK deposits with abundant xenolith-poor, agglutinated ACK deposits suggests that the fragmentation mechanism has changed (on occasions several times) during the emplacement history of a pipe. The unusual high abundance of ACK's in the pipes may also explain the predominance of sub-hectare eruptive centers in the field, since these xenolith-poor reconstituted spatter deposits testify to hot, low-energy fragmentation of magma that filled in a pipe rather than excavated it. Further evidence to the existence of hot magma is presented in Pell et al (submitted) on conodont geothermometry.

The amount of erosion since emplacement is unknown. Superficially, the predominance of pipes filled with coherent-looking kimberlite suggests significant erosion down to the root zone level. However, under close examination, only relatively few of the smallest pipes qualify as real root zones. In contrast, many features present in the volcaniclastic pipe infills support deposition on crater floors, as it is testified by the presence of RVK's (as expressed by xenolith-rich talus deposits with debris and grain flows) or base surge deposits. However, the volcaniclastic deposits are in most

cases massive or only crudely bedded. This observation, together with the scarcity of fine, well-bedded tuffs and the absence of crater lake deposits, suggests that the structural level of most of the pipes is in the middle diatreme zone.

Some of the volcaniclastic units are almost exclusively dominated by limestone xenoliths, while the ACK are dominated by basement fragments. This observation allows conclusions on crater depth and morphology: for limestone-rich PK's, the root zone with its explosion chambers must have originally resided in the Paleozoic limestone level. If the root zone would be located deeper in the basement, the volcaniclastic deposits would have to contain a significant amount of basement xenoliths, too. Similarly, the crater floor of RVK's that are highly enriched in limestones must have resided in the limestones. If the Chidliak pipes had deep craters in the basement, a mixture of basement and limestone xenoliths would have to be expected. Therefore, all limestone xenolith-rich volcaniclastic deposits must have originally been produced in the limestone cover and later, during pipe growth, subsided into the current basement level.

In some pipes, basement xenolith-rich VK's (RVK forming talus deposits and ACK) are underlain by limestone-xenolith rich volcaniclastic deposits. This constellation suggests that the explosion chambers in the root zone were located in the basement and basement-rich debris was ejected to the surface through feeder conduits piercing through the overlying limestone-rich tephra filling the diatreme. The presence of RVK's almost entirely comprised of basement debris is more difficult to explain, since the sedimentation of limestone xenoliths has to be temporarily suppressed. This can be achieved by wide and shallow craters present in the Paleozoic sediments which are undercut by vents of narrow feeder pipes excavating the basement. The inner crater slopes of the large maar craters could be veneered by basement debris ejected from the rather small vents in the maar crater floor, effectively subduing limestone sedimentation from the inner slopes of the maar crater. However, direct evidence for these large maar craters is no longer present since the Paleozoic sequence is entirely eroded.

For our generic emplacement model, the contrasting aquifer situation at the time of emplacement in between the Paleozoic cover sequence and the underlying basement is of high importance. Some large limestone xenolith blocks in the pipes suggest that significant aquifers were present in the limestone sequence. These aquifers were most likely strata-bound and showed a high groundwater recharge rate. In a limestone basin scenario they were possibly even of artesian nature. In contrast, the supply of groundwater in the basement was limited and restricted to (sub)vertical faults and joint systems. A kimberlite dyke rising to surface would have encountered little or no water along faults in the basement, while in the limestones there would have been widespread and rich stratabound aquifers. Magma that came into contact with the abundant groundwater in the limestones would have had plenty of opportunity to react explosively by phreatomagmatic explosions. The high recharge rate of the stratabound aquifers would have hampered downward growth of the explosion site and the repeated eruptions from the same depth level would have generated large and shallow maar craters. However, if a maar crater was able to grow deeper it would ultimately have reached the basement level with its generally "dry" conditions or only very limited, localized groundwater supply in faults crosscutting the dykes. In the basement, phreato-magmatic explosions would have become rather the exception than the rule and phreatomagmatic explosions would have alternated with periods of limited groundwater supply, resulting in low energy, hot and "dry" fragmentation of the magma. This process would have led to the alternation of volcaniclastic, xenolith-rich deposits with ACK. During pipe growth, ejection of fragmented material to the surface creates a volume deficit in the root zone which is compensated by subsidence of the overlying diatreme tephra. This process allows for limestone rich VK's in basement level.

Our emplacement model differs from conventional volatile-driven emplacement models and explains the observed features by the variable reaction of rising magma with groundwater.

Acknowledgements

The authors thank Peregrine Diamond Ltd and De Beers Canada Inc for permission to publish.

References

Pell, J., Grutter, H., Neilson, S., Lockhart, G., Dempsey, S., Grenon, H., 2013. Exploration and discovery of the Chidliak Kimberlite Province, Baffin Island, Nunavut: Canada's newest diamond district. In: Pearson, D.G., et al. (eds.) Proceedings of the 10th International Kimberlite Conference, Volume 2. 209-227.

Heaman, L.M., Grutter, H.S., Pell, J., Holmes, P., Grenon H., 2011. U-Pb geochronology, Sr- and Nd-isotope compositions of groundmass perovskite from the Chidliak and Qilaq kimberlites, Baffin Island, Nunavut. Extended abstract No 193, 10th International Kimberlite Conference.

Zhang, S., Pell, J., 2014. Conodonts recovered from the carbonate xenoliths in the kimberlites confirm Paleozoic cover on the Hall Peninsula, Nunavut. Can. J. Earth Sci. 51, 142-155l dx.doi.org/10.1139/cjes-2013-0171.

Influence of the basement in the eruptive dynamics of El Puig d'Àdri tephra ring combining fieldworks and geophysical surveys

Dario Pedrazzi[1,2], Xavier Bolós[2], Stéphanie Barde-Cabusson[2] and Joan Martí[2]

[1] *Centro de Geociencias, UNAM, Campus Juriquilla, Querétaro, México. d_pedrazzi@yahoo.com*
[2] *Institute of Earth Sciences Jaume Almera, ICTJA-CSIC, Group of Volcanology.SIMGEO (UB-CSIC) Lluis Sole i Sabaris s/n, 08028, Barcelona, Spain.*

Keywords: Garrotxa Volcanic Field, Phreatomagmatism, Geophysics.

Tephra rings are monogenetic landforms with successions commonly interpreted to be deposited predominantly by pyroclastics density current such as base surges (Dellino *et al.* 1990, 2004a, 2004b, Dellino 2000, Dellino and La Volpe 2000). Scoriaceous fall deposits are common in tephra rings successions and are interpreted to be the result of an intermittent magma/water interaction (Houghton *et al.* 1999).

El Puig d'Àdri tephra ring is one of the most representative edifice of the Garrotxa Volcanic Field (GVF) (0.6–0.01 Ma), which is part of the Catalan Volcanic Zone (CVZ) (NE of the Iberian Peninsula) (Fig.1), one of the Quaternary alkaline volcanic provinces associated with the European Cenozoic Rift System (Martí *et al.* 1992, Dèzes *et al.* 2004).

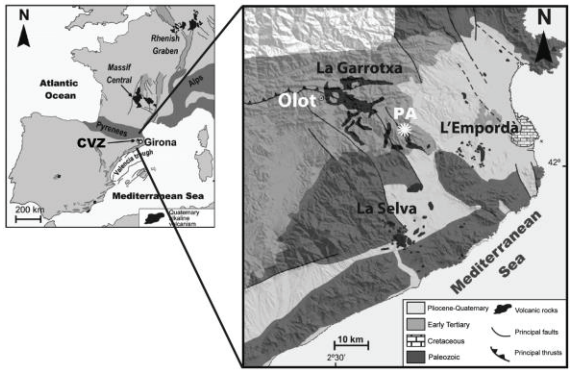

Fig. 1 – Simplified geological map of the Catalan Volcanic Zone (CVZ) and the three subzones; La Selva (7.9–1.7 Ma), L'Empordà (12–8 Ma) and La Garrotxa (0.5–0.01 Ma). PA indicates the position of El Puig d'Adri Volcano (Modified from Guérin *et al.* 1986 and Martí *et al.* 1992).

The area is bounded to the East by the Amer Fault and to the West by the Llorà Fault. These two regional conjugated Neogene normal faults have a transtensional component (Goula *et al.* 1999; Olivera *et al.* 2003). They are responsible for the distribution of volcanism in the area, as well as seismicity and the fluvial network (Saula *et al.* 1996; Martí *et al.* 2011; Bolós *et al.* submitted).

El Puig d'Àdri volcano was emplaced above Paleocene and Eocene materials (red sandstones, marls and limestones) covered by Neogene alluvial sediments mostly at the southern side.

The construction of this volcano involved the superposition of three volcanic vents (Fig. 2) with a main edifice constituted by a tephra-ring of 850 m in diameter, a small scoria cone at the western side of the tephra ring and a new scoria cone further SE. This last forms the main relief of the volcano and covers most of the previous structures (Martí *et al.* 2011).

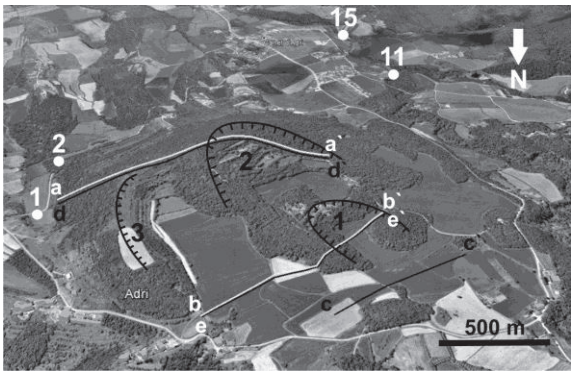

Fig. 2 – Google Earth image of El Puig d'Adri volcano showing part of the tephra ring (3 in black) and the two subordinate scoria cones (1-2 in black). Reference zone is 31N. White dots and numbers indicate the locations of the representative stratigraphic columns. White lines show the ERT profiles and black lines the SP profiles.

A total of 5 different stratigraphic units were identified in El Puig d'Àdri deposits (Fig. 3). The eruption started with an explosive phreatomagmatic event followed by a Strombolian episode of limited extent. The activity returned to a stronger phreatomagmatic phase generating pyroclastic surges and explosion breccias along with a pyroclastic flow that extended to the south for more than 3 Km. A final Strombolian phase gave rise to the construction of the main scoria cone, with the deposits covering most of the proximal phreatomagmatic products. The eruption ended with an effusive phase that generated two lava flows causing the breaching of the northwestern flank of the scoria cone

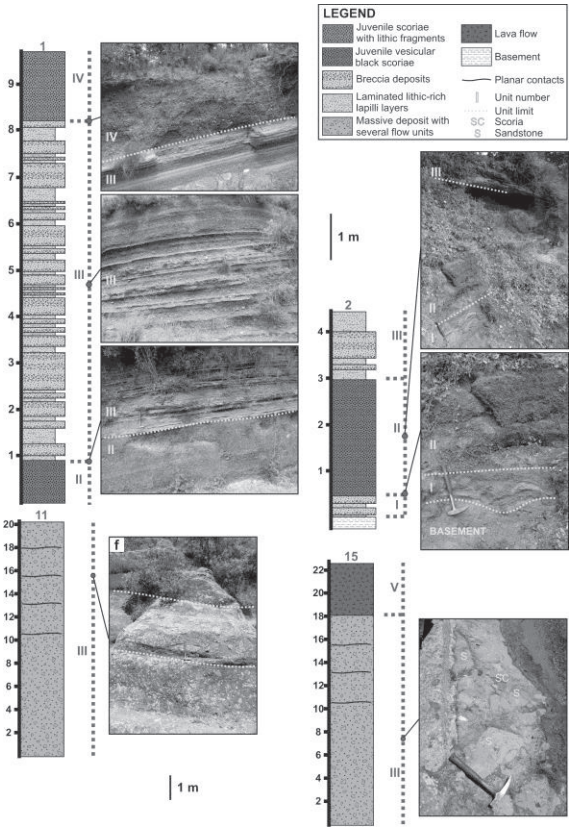

Fig. 3 – Representative stratigraphic columns of the deposits at El Puig d'Adri ed Strombolian unit, III-stronger phreatomagmatic phase generating pyroclastic surges, and explosion breccias and a pyroclastic flow deposit, IV-second Strombolian phase, V-effusive phase. Columns refer to numbers in Figure 2.

Componentry analysis suggests that the explosions took place in the sandstones/marls basement although the second Strombolian phase of the eruption shows a notable increase of limestone fragments, suggesting a switch of the explosion locus. This is also suggested by the position of the second scoria cone respect to the tephra ring and first Strombolian edifice.

A complementary geophysical survey was performed using Electrical Resistivity Tomography (ERT) and Self-Potential (SP) (Fig. 3). The description of one of the three ERT profiles presented here is described in Barde-Cabusson *et al.* (2013) and allowed distinguishing phreatomagmatic and Strombolian deposits at depth. Two SP profiles confirmed the results obtained. Furthermore Phreatomagmatic and Strombolian deposits are here described in detail as units or phases of the eruption and related to this previous study. Two additional ERT profiles helped to understand the continuation of the volcanic deposits at depth and to describe the pre-volcanic basement, which is constituted of limestones, marls and sandstones with different hydrogeological characteristics. Geological and geophysical surveys, thus, allowed interpreting the eruptive dynamics of this complex volcano and to determine the role played by the basement. These results can be extrapolated to other phreatomagmatic volcanoes alternating phreatomagmatic and Strombolian phases and built up on hard basement.

References

Barde-Cabusson, S., Bolós, X., Pedrazzi, D., Lovera, R., Serra, G., Martí, J., Casas, A., 2013. Electrical resistivity tomography revealing the internal structure of monogenetic volcanoes. Geophysical Research Letters 40(11): 2544-2549.

Dellino, P., 2000. Phreatomagmatic deposits: fragmentation, transportation and deposition mechanisms. Terra Nostra 6(2000): 99-105.

Dellino, P., Frazzetta, G., La Volpe, L., 1990. Wet surge deposits at La Fossa di Vulcano: Depositional and eruptive mechanisms. Journal of Volcanology and Geothermal Research 43(1–4): 215-233.

Dellino, P., Isaia, R., La Volpe, L., Orsi, G., 2004a. Interaction between particles transported by fallout and surge in the deposits of the Agnano-Monte Spina eruption (Campi Flegrei, Southern Italy). Journal of Volcanology and Geothermal Research 133(1-4): 193-210.

Dellino, P., Isaia, R., Veneruso, M., 2004b. Turbulent boundary layer shear flows as an approximation of base surges at Campi Flegrei (Southern Italy). Journal of Volcanology and Geothermal Research 133(1-4): 211-228.

Dèzes, P., Schmid, S.M., Ziegler, P.A., 2004. Evolution of the European Cenozoic Rift System: interaction of the Alpine and Pyrenean orogens with their foreland lithosphere. Tectonophysics 389(1–2): 1-33.

Goula, X., Olivera, C., Fleta, J., Grellet, B., Lindo, R., Rivera, L.A., Cisternas, A., Carbon, D., 1999. Present and recent stress regime in the eastern part of the Pyrenees. Tectonophysics 308(4): 487-502.

Houghton, B.F., Wilson, C.J.N., Smith, I.E.M., 1999. Shallow-seated controls on styles of explosive basaltic volcanism: a case study from New Zealand. Journal of Volcanology and Geothermal Research 91(1): 97-120.

Martí, J., Mitjavila, J., Roca, E., Aparicio, A., 1992. Cenozoic magmatism of the Valencia trough(western Mediterranean): relationship between structural evolution and volcanism. Tectonophysics 203: 145-165.

Martí, J., Planagumà, L., Geyer, A., Canal, E., Pedrazzi, D., 2011. Complex interaction between Strombolian and phreatomagmatic eruptions in the Quaternary monogenetic volcanism of the Catalan Volcanic Zone (NE of Spain). Journal of Volcanology and Geothermal Research 201(1–4): 178-193.

Olivera, C., Fleta, J., Susagna, T., Figueras, S., Goula, X., Roca, A., 2003. Seismicity and recent deformations in the northeastern of the Iberian Peninsula. Física de la Tierra 15: 111-114.

Saula, E., Picart, J., Mató, E., Llenas, M., Losantos, M., Berasategui, X., Agustí, J., 1996. Evolución geodinámica de la fosa del Empordà y de las Sierras Transversales. Acta Geologica Hispánica 29: 55–75.

Understanding the structure of a large basaltic maar volcano through three-dimensional potential field modelling, Lake Purrumbete Maar, Newer Volcanics Province.

Jackson C. van den Hove, Laurent Ailleres, Peter G. Betts and Ray A.F. Cas

School of Geosciences, Monash University, Clayton, Victoria 3800, Australia.

Keywords: large maar, subsurface structure, potential field modelling.

Lake Purrumbete Maar (LPM) is situated in the intaplate basaltic volcanic field of the Newer Volcanics Province in western Victoria, south-eastern Australia. It represents one of the largest maar volcanoes in the world with a near circular crater up to 2800 m in diameter, which is host to a 45 m deep crater. Accessory lithincs present in the tuff ring deposits suggest explosive fragmentation has occurred to a depth no greater than 250 m. Irregular shapes and peperitic textures observed within marl accessory lithics suggest it was poorly consolidated when eruptive activity took place. LPM presents an interesting case, given the combination a large, circular maar crater coupled with a shallow inferred depth of fragmentation. In order to understand how large maar volcanoes like LPM form, the types of diatreme, vent and dyke structures that it is associated with must also be understood. LPM has experienced negligible post-eruptive erosion; therefore little information can be gleaned on the morphology of its diatreme, vent and feeder dyke structures.

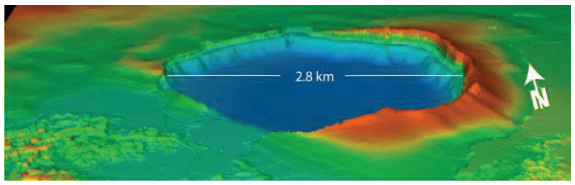

Fig. 1 – Digital terrain model and bathymetry model of Lake Purrumbete Maars crater and tuff ring. VE = 3.

In cases where little to no exposure of diatreme structures exists, geophysical potential field modelling represents an invaluable tool for gaining information on subsurface structures (Blaikie *et al.*, 2014; Blaikie *et al.*, 2012). Geophysical modelling based on gravity, magnetic, electromagnetic and seismic methods has been successfully applied to characterise the architecture of maar diatremes, vents and feeder dykes (Blaikie *et al.*, 2014; Blaikie *et al.*, 2012; Cassidy *et al.*, 2007; Matthes *et al.*, 2010; Mrlina *et al.*, 2009; Schulz *et al.*, 2005). Forward and inverse modelling the subsurface architecture of young, uneroded maar volcanoes allows us to make associations between the still intact maar crater, deposits observed within the tuff rim and subsurface features associated with the diatreme, vent and feeder dykes (Blaikie *et al.*, 2014; Blaikie *et al.*, 2012).

Ground-based gravity and magnetic data was collected over and around LPM, for application toward forward modelling of the subsurface architecture associated with the maar. Twenty six E-W oriented lines and six tie lines of magnetic data were collected over the lake providing a high data density. The collection of gravity data presented a unique challenge due to the nature of measuring small changes in gravitational forces (<1 mGal), associated with the maar, on an inherently unstable water body. Twenty-five usable gravity readings were measured over the lake.

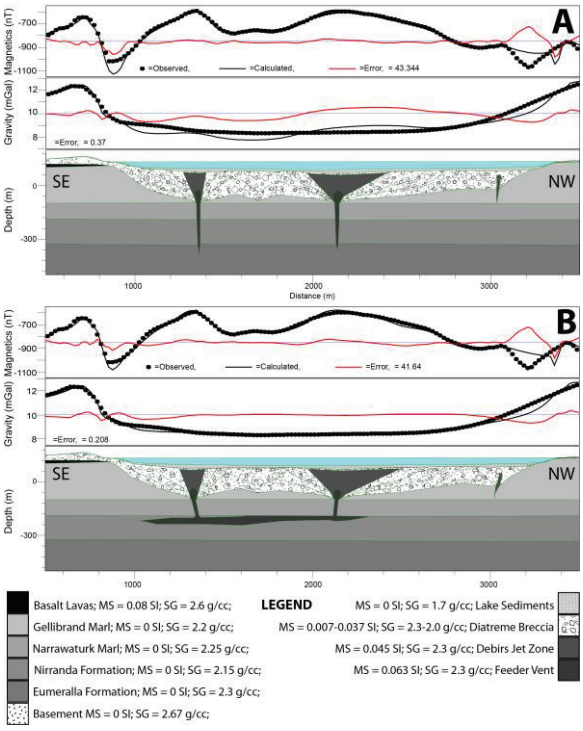

Fig. 2 – 2D forward model profiles across Lake Purrumbete Maar.

The magnetic anomaly over LPM shows three large, irregular shaped high amplitude magnetic anomalies associated with major eruption points within the

crater. Several other odd shaped high magnetic anomalies are also present, which are uncertain as to whether they represent minor eruption points or areas of thick juvenile basaltic infill. Four 2D profile forward models transecting LPM were produced using GM-SYS software, to satisfy observed anomalies from gridded RTP magnetic and free-air gravity data. Five eruption points and an undulating shallow bowl shaped diatreme structure were modelled to satisfy the magnetic response. Vents were modelled with a low angled open bowl shape, having been feed from a thin point source dkye. A second profile completed along the NW-SE profile includes a large sill body at 350 m depth (figure 2). This was better able to satisfy the observed gravity response in the model, which shows low amplitude, long wavelength high anomaly below the three main eruption points. 2D Forward models were used to produce a 3D model, which itself is used as an initial reference model for 3D geometry and property inversions to test the validity of modelled features.

Geometry inversions on the diatreme suggest the major vents likely occur to a greater depth (390 m depth when magnetic susceptibility of the diatreme is optimized at 0.0242 SI) than is incorporated in the initial reference model, which was built with a maximum diatreme depth of 250 m, based on erupted lithics (figure 3). Constrained and unconstrained heterogeneous inversions also suggest diatreme and vent structures occur to greater depths and that there is likely a greater proportion of high magnetic (basaltic) material at depth beneath LPM.

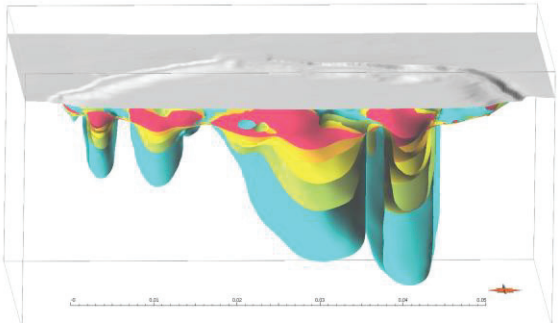

Fig 3 – Range of diatreme geometries inverted to satisfy the observed magnetic response, based on a range of magnetic susceptibilities applied to the diatreme. Deeper diatremes have lower magnetic susceptibilities; shallow diatremes have higher magnetic susceptibilities.

Interpretation of and forward and inverse modelling based on magnetic and gravity potential fields suggest that three major factors have contributed to the large size of LPM. 1) Greater maximum depth of explosive fragmentation than previously inferred by erupted accessory lithics (Inversions on a geophysical forward model of LPM suggests a greater diatreme and vent depth, than is inferred by excavated accessory lithics within the maar rim, which suggest no greater depth than 250 m). 2) Poor consolidation of the sediments within which explosive fragmentation has been hosted. Allowing efficient crater wall collapse during explosive fragmentation and liquification of sediments (marl lithics show poor consolidation indicators such as peperite and thermal baking). 3) Migration of the eruption locus, resulting in multiple, coalesced eruption points making up the eruption centre (multiple magnetic highs within the area of the maar crater). Results from geophysical interpretation and modelling suggest it is also likely a shallow sill or sill complex exists below LPM, as Inferred by the high gravity response (dense basalt) below the eastern part of the crater. This may have allowed for a broad area of terminal feeder dykes sourced from the sill.

Acknowledgements

References

Blaikie, T.N., Ailleres, L., Betts, P.G. and Cas, R.A.F., 2014. Interpreting subsurface volcanic structures using geologically constrained 3D gravity inversions. Examples of maar-diatremes, Newer Volcanics Province, south-eastern Australia. Journal of Geophysical Research: Solid Earth: 2013JB010751.

Blaikie, T.N., Ailleres, L., Cas, R.A.F. and Betts, P.G., 2012. Three-dimensional potential field modelling of a multi-vent maar-diatreme — The Lake Coragulac maar, Newer Volcanics Province, south-eastern Australia. Journal of Volcanology and Geothermal Research, 235–236(0): 70-83.

Cassidy, J., France, S.J. and Locke, C.A., 2007. Gravity and magnetic investigation of maar volcanoes, Auckland volcanic field, New Zealand. Journal of Volcanology and Geothermal Research, 159(1-3): 153-163.

Matthes, H., Kroner, C., Jahr, T. and Kämpf, H., 2010. Geophysical modelling of the Ebersbrunn diatreme, western Saxony, Germany. Near Surface Geophysics, 8: 311-319.

Mrlina, J., Kämpf, H., Kroner, C., Mingram, J., Stebich, M., Brauer, A., Geissler, W.H., Kallmeyer, J., Matthes, H. and Seidl, M., 2009. Discovery of the first Quaternary maar in the Bohemian Massif, Central Europe, based on combined geophysical and geological surveys. Journal of Volcanology and Geothermal Research, 182(1-2): 97-112.

Schulz, R., Buness, H., Gabriel, G., Pucher, R., Rolf, C., Wiederhold, H. and Wonik, T., 2005. Detailed investigation of preserved maar structures by combined geophysical surveys. Bulletin of Volcanology, 68(2): 95-106.

Maar geophysics: Valle de Santiago study

Vsevolod Yutsis[1], José Jorge Aranda-Gómez[2], Jorge Arturo Arzate Flores[2], Harald Bohnel[2], Jesús Pacheco Martínez[3] and Héctor López-Loera[1]

[1] *Instituto Potosino de Investigación Científica y Tecnológica, San Luis Potosí, Mexico. vsevolod.yutsis@ipicyt.edu.mx*
[2] *Centro de Geociencias, UNAM, Campus Juriquilla, Querétaro, México.*
[3] *Universidad Autónoma de Aguascalientes, México.*

Keywords: maar, diatreme, integration.

Knowledge about maar-diatreme systems is usually based on surface observations on either the volcanic (maar) or on (the partially exposed by erosion) subvolcanic part of the system (diatreme). The morphology of the maar craters, often bounded by steep scarps excavated in the country rock, as well as the sedimentological features and lithological variations in the pyroclastic successions near the craters, allow inferring the basic vulcanological evolution of these structures. However, maar-diatreme systems have a post-eruptive evolution dominated by erosion and mass-wasting that modifies the crater itself and the pyroclastic rampart around it. Formation of perennial lakes after the end of the eruption is a common, nearly universal, process once the phreatomagmatic explosions end (Lorenz, 1986). Notable exceptions to this may occur in those systems where volcanic activity continues inside the crater for a significant period, creating lava lakes and/or cinder or spatter cones that significantly raise the bottom of the crater above the water table, such as it happened in La Breña maar (Aranda-Gómez et al., 1992). In those maar-diatreme systems where a perennial lakes are formed, there is also a protracted history of sedimentation and/or subsidence, that may last for tens of millions of years (e.g. Suhr et al. 2006) and produce very thick lacustrine successions above the diatreme. Relatively old maar-diatreme systems, where the original craters are still preserved, almost never allow the direct study of the lacustrine successions and in most exposed diatremes they were nearly completely or completely eroded. Thus, the only way to study them is by direct drilling (e.g. Kienel et al., 2009) and/or by the combined use of several geophysical methods, in order to infer some geometric and/or geologic features beneath the surface below the maar (e.g. Schultz et al., 2005). In this paper we report the results obtained by the combined use of several geophysical methods, including gravity, magnetic and audio-magnetotelluric (AMT), applied to three of the Valle de Santiago maars (Cíntora, San Nicolás and Rincón de Parangueo: Fig. 1), which are located in the northern part of the Mexican Volcanic Belt (MVB).

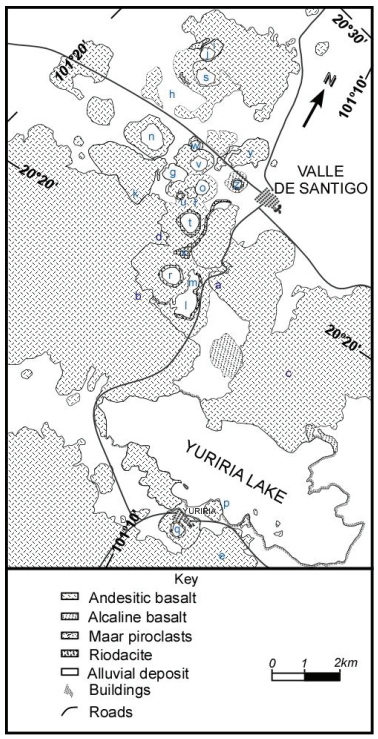

Fig. 1 – Generalized geologic map of the region between Valle de Santiago and the Yuriria Lake, Guanajuato, Mexico. s = Rincón de Parangueo, n = San Nicolás, and t = Cíntora

The MVB is an active continental arc related to subduction of the Rivera and Cocos plates underneath the North America plate. The MVB consists of nearly 8,000 volcanic structures and some intrusive bodies, exposed along a belt which stretches from the Pacific coast to the shores of the Gulf of Mexico (Demant, 1978). This magmatic arc can be divided into three domains: the western, central and eastern sectors, which display significant differences in the type of volcanism and chemical composition of their magmas. The Valle de Santiago area is located in the northern part of the central sector, and it is part of the Michoacán-Guanajuato Volcanic Field. The Valle de Santiago maars occur on a 7 x 50 km, N25°W-trending belt, which extends between the Yuriria lake (Fig.1.) and Irapuato city.

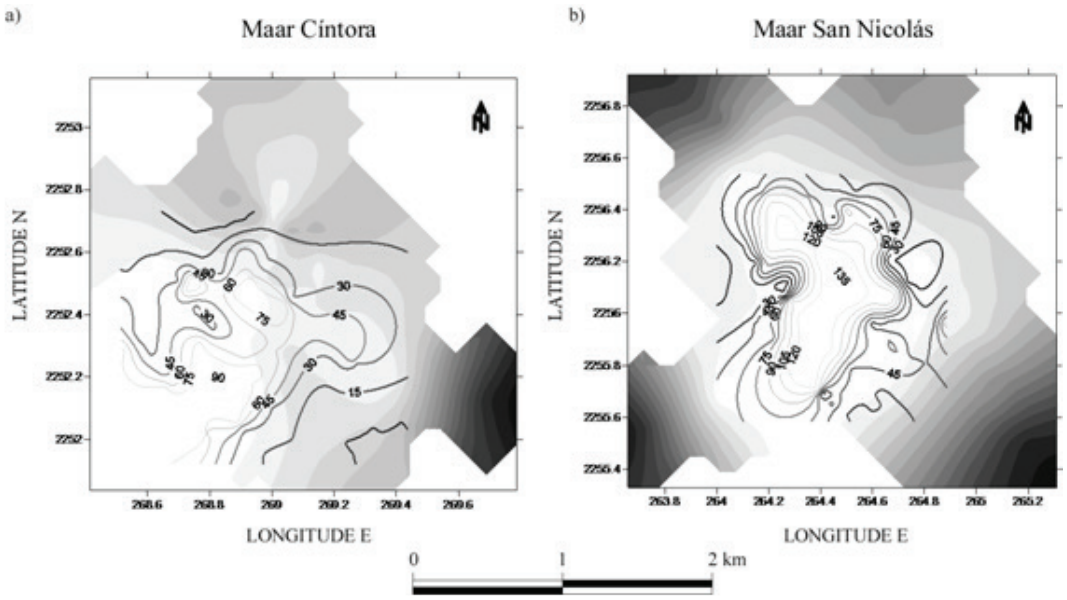

Fig. 2 – Inferred thickness (in meters) of the lake sediments in the Cíntora (a) and San Nicolás (b) maars. Based on gravity models.

Gravity and magnetic profiles were obtained in Cíntora, San Nicolás and Rincón de Parangueo. These maars used to have perennial lakes and were gradually desiccated in the 1980's (Aranda-Gómez et al., 2013). The stratigraphy beneath the bottom of the crates was modeled with three layers. The upper layer corresponds to lake sediments with densities ranging between 1.4 and 1.8 g/cm^3. Underneath the lake sediment layer, there is a body which represents a diatreme made of volcanic breccia, with an inferred density between 2.0 and 2.4 g/cm^3. Finally, the country rock around the lake sediments and underlying diatreme was modeled as igneous rocks with densities between 2.7 and 3.0 g/cm^3. This choice for the country rock is justified as on the walls of the crater of all the studied maars are exposed intermediate to mafic lava flows. The thickness of the lacustrine sediments in Cíntora maar varies from 0 m, near the walls of the crater, to 75-80 m in the center of the basin (Fig. 2a). Lacustrine sediments in San Nicolás maar may reach a thickness of 130 m in the center of the basin (Fig.2b). A seismic refraction study realized in San Nicolás maar shows two layers with velocities 600 and 2000 m/s, respectively. These values correspond layer 1 (lake sediments) and layer 2 (diatreme) of the gravity model. An interesting feature found in the geophysical data collected at the Rincón de Parangueo maar is that the general trend of both gravity and magnetic anomalies is N45°E. This trend contrasts sharply with that in the N25°W-trending maar lineament near Valle de Santiago (Fig. 1), and with the regional aeromagnetic anomalies in the region. These data combined with AMT soundings

Acknowledgements

CONACYT (129550) grant is acknowledged.

References

Aranda-Gómez, J.J., Luhr, J.F., Pier, J.G., 1992, The La Breña-El Jagüey maar complex, Durango, México: I. Geological Evolution. Bulletin Volcanology 54: 393-404.

Aranda-Gómez J.J, Levresse, G., Pacheco Martínez J., Ramos-Leal, J.A., Carrasco-Núñez, G, Chacón-Baca, E., González-Naranjo, G., Chávez-Cabello, G., Vega-González, M., Origel, G., Noyola-Medrano,C., 2013, Active sinking at the bottom of the Rincón de Parangueo Maar (Guanajuato, México) and its probable relation with subsidence faults at Salamanca and Celaya. Boletín de la Sociedad Geológica Mexicana 65(1): 169-188.

Demant, A., 1978, Características del Eje Neovolcánico Transmexicano y sus problemas de interpretación: Universidad Nacional Autónoma de México, Revista del Instituto de Geología 2: 172–187.

Lorenz, V., 1986. On the growth of maars and diatremes and its relevance to the formation of tuff rings. Bulletin Volcanology 48:265-274

Schultz, R., Buness, H., Gabriel, G., Pucher, R., Rolf, C., Wiederhold, H., Wonik, T., 2005, Detailed investigation of preserved maar structures by combined geophysical surveys. Bulletin of Volcanology 68: 95-106. Kienel, U. Et al., 2009. First lacustrine varve chronologies from Mexico: impact of droughts, ENSO and human activity since AD 1840 as recorded in maar sediments from Valle de Santiago: J Paleolimnol 42: 587-609

Suhr, P., Goth, K., Lorenz, V., Suhr, S., 2006, Long lasting subsidence and deformation above maar-diatreme volcanoes – a never ending story. Zeitschrift der Deutchen Gesellschaft für Geowissenschaften 157(3): 491-511.

Geophysical modeling of a phreato-magmatic explosion (maars) field in central-eastern Mexico

Román Álvarez

Instituto de Investigaciones en Matemáticas Aplicadas y en Sistemas, Universidad Nacional Autónoma de México, México D.F. 04510, México. roman.alvarez@iimas.unam.mx

Keywords: Phreato-magmatic explosions, Maars, Oriental-Serdán basin.

The Oriental-Serdán basin (mean elevation 2350 m) is located in the eastern margin of the Trans Mexican Neovolcanic Axis (Fig. 1) where a group of maars and volcanic cones coexist. The area is flanked by major volcanic structures: Cofre de Perote (4282 m) and Pico de Orizaba (5700 m) the highest mountain in Mexico, to the east of the field, and Malinche (4461 m) to the west. To the north, Los Humeros caldera is a 24 km-diameter volcanic structure where geothermal energy is being exploited. The early inhabitants of the area distinguished between "xalapazcos", dry craters, and "axalapazcos", craters with a lake, or maars. Bazán (1959) made a geomorphologic, geohydrologic, and geologic description of the basin noting that its drainage has no exterior outlet and rain water forms shallow lakes and a considerable ground water system, conditions that unquestionably favor phreato-magmatic explosions in the area. The distribution of maars and volcanic cones exhibits a roughly N-S trend that parallels the Cofre de Perote-Pico de Orizaba volcanic chain. The sources of heat to induce such explosions appear to be ascending rhyolitic domes (Alvarez et al., 1976); in two of them, Cerro Pizarro and Cerro Pinto, rhyolites have emerged after the explosion took place, since Cerro Pizarro is piercing the explosion crater and Cerro Pinto is located on the southern rim of a 3 km diameter explosion crater called Tepeyahualco (Maupomé et al, 1975).

An aeromagnetic survey flown over several of these structures at elevations above ground ranging from 100 to 300 m attempted at establishing geophysical criteria to discriminate between the structures (Alvarez et al., 1976) concluding that volcanic cones show the strongest magnetic anomalies resembling a dipolar field, explosion craters with an ash ring show weak magnetic anomalies, and collapse structures with no obvious ash ring may show a strong anomaly, a weak anomaly, or no anomaly at all. However, no attempt was made at modeling such responses.

A geological reconnaissance study (Yáñez-García and Casique-Vázquez, 1980) established a regional, widespread distribution of Cretaceous limestone formations that outcrop throughout the area and in some places may be the aquifer confining formation. To the north of Las Derrumbadas rhyolitic domes four explosion craters are located filled with water. That is also the area with the lowest terrain elevation in the basin (Fig. 1)

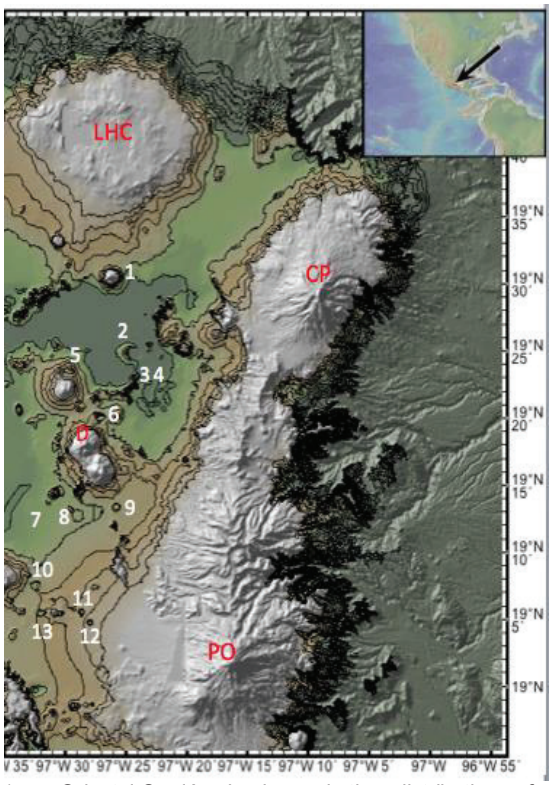

Fig.1 – Oriental-Serdán basin and the distribution of explosion craters. Contours from 2000 to 2250 m in 50 m intervals are shown in black. The lowest elevation occurs between Las Derrumbadas (D) rhyolitic domes and Los Humeros Caldera (LHC), CP Cofre de Perote, PO Pico de Orizaba. 1. Cerro Pizarro, 2. Alchichica, 3. La Preciosa, 4. Quecholac ,5. Tepeyahualco, 6. Atexcac, 7. La Hacienda, 8. Buenavista, 9. Tepexitl, 10. Tecuitlapa, 11 Xalapazco Grande, 12. Xalapazco Chico, 13. Aljojuca. Topography from Ryan et al. (2009).

and thus the water table is above the bottom of the craters, creating the lakes. However, the water level differs (Fig. 2) between the craters: Alchichica 2320 m while La Preciosa, and Quecholac 2340 m, indicating that the water level is locally controlled by underground barriers. To the south of Las

Derrumbadas two craters of considerable depths (Xalapazco Grande: 70 m; Xalapazco Chico: 150 m) are nevertheless dry (Fig. 3) since they occur up slope on the foothills of Pico de Orizaba volcano; their bottoms are ~80 m above the water table at nearby Aljojuca crater to the west.

Fig. 2 – Alchichica, La Preciosa, and Quecholac maars. They occur in the lowest topographic elevation of the basin. La Preciosa and Quecholac may be the result of multiple explosions.

Fig. 3 – Tecuitlapa, Aljojuca, Xalapazco Grande, Xalapazco Chico and the Zotoltepec cones at the center exemplify the type of short distances in which volcanism can change expression in this area, from craters with a lake, to craters without it, to monogenetic cones.

In the present study an attempt is made at mapping the underground distribution of the rhyolites and mafic bodies that are the sources of heat that create explosions or volcanic cones.

Previous electrical vertical soundings (Palacios-Hartweg and García-Velázquez, 1981) and the aeromagnetic map NAMAG (2002) of the area reduced to the pole are used to model several profiles across the volcanic field to depths of 4-5 km. Preliminary observations suggest that underground rhyolite formations display mushroom-like distributions in the vicinity of the outcropping domes.

Acknowledgements

This work was supported by PAPIIT-UNAM Grants IN111110-1, IN111110-2, IN100912-1 and IN-100912-2.

References

Alvarez, R., Maupomé, L. and Tejera, A. 1976. Magnetic comparison of explosion craters and volcanic cones. Geofísica Internacional, 16, 63-94.

Bazán, B.S, 1959. Levantamiento geológico como base para una clasificación de suelos, efectuado en la cuenca de Oriental-Serdán, estados de Puebla, Tlaxcala y Veracruz. Tesis profesional, 53p, ESIA, Instituto Politécnico Nacional, México DF.

Maupomé, L., Alvarez, R., Kieffer, S.W., and Dietz, R.S., 1975. On the terrestrial origin of Tepexitl crater, Mexico. Meteoritics, 10, 209-214.

NAMAG, 2002. Magnetic Anomaly Map of North America. US Department of the Interior and US Geological Survey.

Palacios-Hartweg, L.H. and García-Velázquez, H. 1981. Informe geofisico del proyecto geotérmico Los Humeros -Derrumbadas Estados de Puebla y Veracruz. Comisión Federal de Electricidad, 99p, México, DF.

Ryan, W.B.F. Carbotte, S.M., Coplan, J.O. O'Hara, S., Melkonian, A., Arko, R., Weissel, R.A., Ferrini, V., Goodwillie, A., Nitsche, F., Bonczkowski, J., Zemsky, R., 2009. Global-multi-resolution topography synthesis, Geochemical, Geophysical Geosystems, 10, doi; 10.1029/2008GC002332.

Yáñez-García, C., Casique-Vázquez, J., 1980. Informe geológico del proyecto geotérmico Los Humeros-Derrumbadas. Comisión Federal de Electricidad, unpublished report, México, DF.

K E Y N O T E

Small scale basaltic systems are a window to the mantle

Ian E.M. Smith

School of Environment, The University of Auckland, Private Bag 92019, Auckland, New Zealand. ie.smith@auckland.ac.nz

Keywords: Monogenetic volcano, volcano field, mantle melts.

Basaltic volcanic systems are the surface expression of mantle kinematics and partial melting processes. Their scale ranges through many orders of magnitude from Large Igneous Provinces (LIPs) characterized by very high magma production rates through an intermediate range found in the island and seamount chains of the ocean basins and in the continental volcanoes associated with crustal extension, to very small-scale systems expressed at the Earth's surface as fields of small basalt volcanoes associated with very low rates of magma flux and formed over time periods comparable to or longer than those of LIPs. In terms of scale basaltic systems occur as a continuous spectrum although partitioning into discrete entities provides an arbitrary but useful practical framework.

Small scale basaltic magmatic systems (magma flux ~10^{-5} km^3/year) are expressed at the surface of the Earth as fields of small volcanoes occurring as maars, scoria cones and lava fields; each volcano represents an episode (batch) of magma generation and the concept of monogenetic volcanos arises from this observation. Their underlying magmatic plumbing system is physically dispersed and differs from the focused conduit system of large volcanoes. Timescales of individual eruptions from monogenetic volcanoes are short (<10^2 years) although the duration of their parental systems may be long (up to 10^4 years).

An extremely significant observation is that systematic sampling through monogenetic volcanoes show geochemical variations which reflect the processes of melt extraction and deep fractionation that occur in their near source environments; they thus provide a unique window on the way that the mantle behaves. In this way they are different from larger scale systems in which magmas can be profoundly modified by fractionation, mixing and assimilation during their transit through the lithosphere. Geochemical investigations into variations in small basaltic volcanoes have provided new insights into how the mantle yields its partial melts.

There are a number of compositional trends that are recognized as common to small scale basaltic volcanoes in general as well as trends that are interpreted to be specific to particular magmatic processes.

General trends are

1. In an individual eruption sequence initial magmas are relatively evolved and as eruptions proceed the composition of magmas becomes less evolved.
2. Within monogenetic volcano fields, temporally closely spaced eruptions are compositionally distinct indicating contemporaneous discrete magma generation/ segregation episodes.
3. The typically fine scale variations observed in small volcanic cones become less distinct as the volumes of magma batches increase.
4. Fine-scale variations suggest that deep seated processes are reflected in their systematic occurrence at the surface pointing to little or no changes during ascent and therefore to very rapid ascent rates.
5. Correlation of chemical composition with magma volume. Smaller volumes are more under-saturated in terms of SiO_2 and are basanites and nephelinites; larger volumes trend toward oversaturation in SiO_2 and are alkali basalts transitioning to tholeiites.

Specific tends observed in individual eruptive centres are:

1. Continuous compositional variation as an eruption progresses from more evolved to less evolved (*e.g.*Smith et al, 2008)
2. Distinct changes within an eruption sequence signifying the arrival of a new magma in the near surface conduit (*e.g.* McGee *et al.*,2012).
3. Complex variation patterns (Brenna *et al.*, 2011).

These patterns of geochemical variation in small scale basaltic systems are interpreted to be due to processes that occur within the source and near source regions by combinations of partial melting, fractional crystallization and magma mixing. In any particular volcano field there is a combination of fundamental parameters linked to a particular crustal environment and tectonic setting. In individual volcanoes within a field variation in the combination of processes produce distinct geochemical trends.

A general model for monogenetic systems

Small scale basaltic magmatic systems typically produce discrete batches of magma that are erupted to the surface to form monogenetic volcanoes. Repeated episodes of magma formation result in fields of monogenetic volcanoes. Basaltic magmas are produced by partial melting of the mantle which, although primarily peridotitic potentially has an eclogitic component that may be related to earlier tectonic episodes thus mantle sources are likely to be heterogeneous on an decimeter to meter scale.These different components will have different melting characteristics.

Variations in the composition of primary magmas in monogenetic systems are due to variations in the chemical and mineralogical composition of their mantle source and different degrees of partial melting.. These explain the general points above. A recent example of this is presented by McGee et al 2012 who explain the eruption of two distinct primary magmas by the sequential production and extraction of a low temperature fraction (eclogitic) and high temperature fraction (peridotitic) during a single eruptive event

References

Brenna, M., Cronin, S.J., Németh, K., Smith, *I.E.*M., Sohn, Y.K., 2011. The influence of magma plumbing complexity on monogenetic eruptions, Jeju Island, Korea. Terra Nova 23, 70–75.

McGee, L. E., Millet, M-A, Smith, *I.E.*M., Nemeth, K., Lindsay, J.M. 2012. The inception and progression of a monogenetic eruption: Motukorea Volcano, the Auckland Volcanic Field, New Zealand. Lithos 155, 360-374.

Smith, *I.E.*M., Blake, S., Wilson, C.J.N., Houghton, B.F. 2008. Deep-seated fractionation during the rise of a small-volume basalt magma batch: Crater Hill, Auckland, New Zealand. Contributions to Mineralogy and Petrology 3155: 511-527.

Volcano-sedimentary characteristics in the rift-margin Abu Terifyia basin, Cairo-Suez District, Egypt: Example of dynamics and fluidization over volcaniclastic beds by emplacement of syn-volcanic basaltic rocks

Khalaf, E.A., El Manawi, A., Hammed, M.S., Abdel Motelib, A.

Cairo University, Faculty of Science, Geology Department, Egypt.

Keywords: peperite, fuel-coolant interactions, thermohydraulic interactions.

Neogene peperites have been identified for the first time at the **Abu Terifyia basin, Egypt**. This finding is significant for the reconstruction of Neogene evolution in the Abu **Terifyia** region. The peperites form successions up to 200 m thick interbedded with basaltic lava and sedimentary rocks. Four types of peperites are described and interpreted as resulting from basaltic lava bulldozed into wet, unconsolidated sediments to produce both blocky and fluidal peperite at their lower contacts. Carbonate occur in the lowermost part of the peperite-bearing succession. Southward, the succession becomes thinner and changes into basaltic lava and interlayered sandstone, volcaniclastic sediments, associated with carbonate horizons. Seven facies types are recognized in the peperite succession, including four facies (A, B, C and D) of peperites distinguished by the shapes of the juvenile clasts and the properties of sediment matrix. Facies E consists of basalt flows and sediments and facies F of basalts with intercalated sediment. In addition, facies G represents peperite-fed debris-flow deposits that overlie the main peperite–lava succession. The peperite-bearing units probably formed at a water depth of less than 3 km and are generally undeformed, occurring in continuous stratigraphic sections distributed regionally over a distance of 100 km. Soft-sediment deformation structures adjacent to the flows, irregularly shaped vesicles in the sediments, and sediments filled vesicles in the mafic lava all indicate the sediment was wet at the time of flow emplacement. Evidence for the mafic magma interacting with wet sediment includes sediment-filled vesicles in basalt, quartz-filled vesicles in the sediments and angular, non-vesicular shards of basalt in clastic dykes.

Some peperites are inferred to record 'frozen' coarse mixing-stage fuel-coolant interactions (FCIs), and hence can be used in attempts to determine specific parameters related to phreatomagmatic fragmentation, such as water/magma mass ratios, confining pressures, and vent-region hydrology. The presence of both fluidal and blocky juvenile clasts, combined with physical aspects of the sediment-lava contacts, suggest that 'frozen' coarse mixing-stage fuel-coolant interactions (FCIs) was a potential fragmentation mechanism within these systems. The change from fluidal to blocky peperite texture may also be controlled in part by the magma temperature and/or confining pressure, and the generation and maintenance of a steam film at the magma/wet sediment interface. A number of factors may have inhibited further explosive activity in these peperite-forming mixing events, including anisotropic saturation of the host sediment, low confining pressures and water/melt ratios, and damped explosive interactions resulting from increased density, viscosity, and surface tension of sediment-water coolants. Nevertheless, these deposits record localized thermohydraulic interactions between magma and wet sediment, and provide valuable information about the geometry and mixing ratios present during peperite formation.

First evidence of phreatomagmatic volcanism in Harrat Al Birk along the Tihamat Asir in SW Saudi Arabia

Károly Németh[1], Nabil El-Masry[2] and Mohammed R. Moufti[2]

[1] *Volcanic Risk Solutions, Institute of Agriculture and Environment, Massey University, Palmerston North, New Zealand.* *k.nemeth@massey.ac.nz*
[2] *Geohazards Research Centre, King Abdulaziz University, Jeddah, Kingdom of Saudi Arabia.*

Keywords: sideromelane, Surtsey, maar.

The intracontinental Al Birk volcanic field in SW Saudi Arabia formed alkaline basaltic volcanoes, such as scoria and spatter cones, extensive lava fields and lava domes/dome coulees (Brown et al., 1989 and references therein). The field consists of two parts. The main part is in the north (Fig. 1) and is located in an area about 100 km long and 50 km wide between the present Red Sea coastline and the Red Sea coastal escarpment. It comprises over 200 individual eruptive centres. Scattered individual volcanic regions are also known in the southern part of the coastal plain, an area commonly referred to as Tihamat Asir (Vincent, 2008). Northern Harrat Al Birk is located ~100 km north of Jizan City (Fig. 1), and is composed of a ridge of basal lava flows that formed a few millions of years ago and host scattered young scoria and spatter cones (< 2 Ma) (Brown et al., 1989). South of the Ad Darb transform fault (Fig. 1), in the Asir coastal plain, there are small volcanic fields also composed of scoria cones and unconfined lava fields. Historic eruptions are suspected in this region, such as at Jabal Ba'a and Jabal al Qishr scoria cones or in the Harrat Gar'atain (Jiratan) (Fig. 1), but these have not yet been confirmed convincingly (Brown et al., 1989). However, these reports indicate that this region is a potentially active volcanic area. The harrat is largely dominated by scoria and spatter cones associated with extensive lava flows and so far no evidence has been found to support phreatomagmatic eruptions in the history of Harrat Al Birk, in spite of its proximity to the Red Sea and the abundant alluvial valleys in the coastal plain (Vincent, 2008). Here we describe the first evidence that phreatomagmatic eruptions played an important role in the growth of at least two of the young volcanoes of the field, and therefore that phreatomagmatism should be considered as a potentially destructive eruption scenario for any future eruptions. Near the city of Sabya (Fig.1), two well-distinguished large scoria cones and associated lava fields dominate the landscape: Jabal Akwa Al Shamiah in the north and Jabal Akwa Al Yamaniah in the south (Fig. 1). At Jabal Akwa Al Yamaniah an upper lava field surrounds the westward breached scoria cone and the lava field seems to be ponded and banked against an obstacle, forming a curved area about 3 km from the scoria cone. A basal lava field spread about 6 km from the cone and formed a flat surface ~50 m below the upper lava field. Quaternary aeolian deposits hosting archaeological sites cover both lava fields.

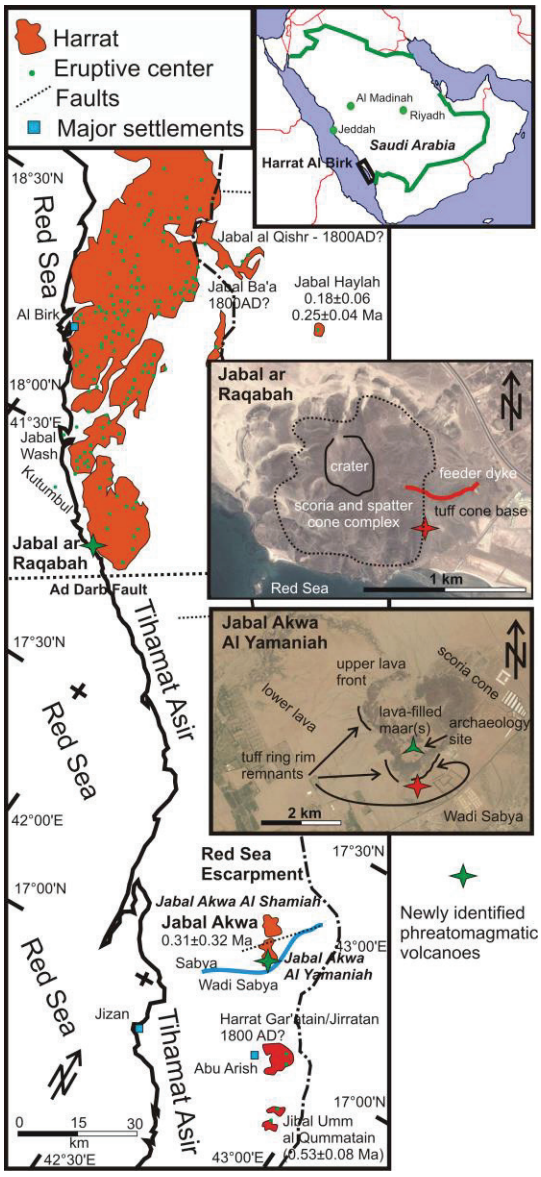

Fig. 1 – Harrat Al Birk in SW Saudi Arabia.

Tuff deposits intercalated with a fluvial terrace along the Wadi Sabya and aeolian deposits in the south of Jabal Akwa Al Yamaniah, have been identified previously below the upper lava flow; however, their origin and significance was not discussed further (Dabbagh *et al*., 1984).

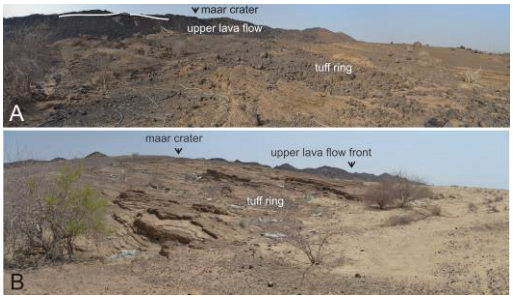

Fig. 2 – Preserved tuff ring sections of Jabal Akwa Al Yamaniah looking toward the NE (A) and toward the E (B).

These deposits are well-bedded, dune-bedded accidental lithic-rich tuff and lapilli tuff beds that are in angular unconformity with the thick upper lava flow fronts of Jabal Akwa Al Yamaniah's entire southern and eastern margin. The gently dipping yellow tuff beds are inferred to be part of a former gently sloping volcanic edifice such as a tuff ring (Fig. 2). The lapilli tuff beds are rich in angular, moderately vesicular glassy pyroclasts that are commonly altered to red to brown palagonite, suggesting phreatomagmatic explosive fragmentation of the participating magma. The abundant accidental lithics from every known crustal rock types and mantle-derived nodules suggest significant excavation and cratering, which is best explained to be a result of maar-diatreme eruptions over a prolonged period of activity (White and Ross, 2011). The nearly 40 m thick pyroclastic succession shows a general trend of fining upward, from a lithic-dominated lapilli tuff and tuff breccia in the base that gradually transforms to a better sorted, finer grained and more juvenile-rich, rhythmic tuff and lapilli tuff nearer the top (Fig. 2). Jabal ar Raqabah is located on the present day Red Sea coast (Fig. 1) and consists of a basal phreatomagmatic lapilli tuff-dominated succession that is capped by a lava spatter and scoria-dominated edifice (Fig. 3). Feeder dykes with chilled margins can be recognized (Fig. 3A). The base of the succession is rich in chilled blocky pyroclasts, cauliflower bombs and evidence of pyroclastic density current transportation (Fig. 3B) typical for an emergent, Surtseyan-style volcano (White and Houghton, 2000). The basal phreatomagmatic succession of Jabal ar Raqabah is different from those identified at Jabal Akwa Al Yamaniah in terms of its abundance in juvenile chilled pyroclasts, small amounts of crustal accidental lithic fragments, and the general textural features that are more consistent with a tuff cone forming eruption and interaction between rising magma and shallow sea.

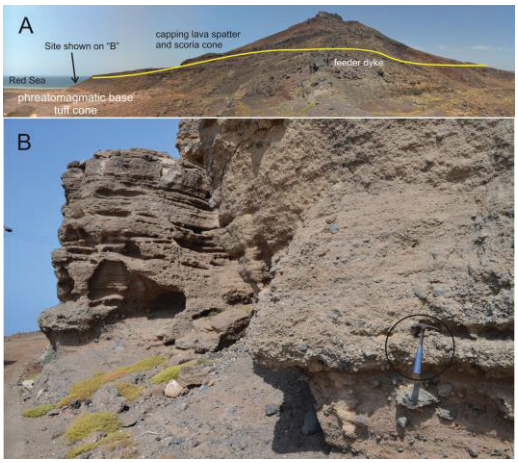

Fig. 3 – Jabal ar Raqabah basal phreatomagmatic succession (B) that is capped by a lava spatter and scoria edifice frequently cross-cut by dykes (A).

Jabal Akwa Al Yamaniah and Jabal ar Raqabah are the first volcanoes where basal phreatomagmatic pyroclastic successions have been identified in SW Saudi Arabia. They record two different eruption scenarios where violent phreatomagmatic explosive eruptive phases occurred upon interaction between rising magma and the ground water table (Jabal Akwa Al Yamaniah) or the shallow sea (Jabal ar Raqabah).

References

Brown, G.F., Schmidt, D.L. and Huffan Jr, A.C., 1989. Geology of the Arabian Peninsula, Shield area of western Saudi Arabia. U.S. Geological Survey professional paper, 560-A,: 1-188.

Dabbagh, A., Emmermann, R., Hoetzl, H., Jado, A.R., Lippolt, H.J., Kollmann, W., Moser, H., Rauert, W. and Zoetl, J.G., 1984. The development of Tihamat Asir during the Quaternary. In: A.R. Jado and J.G. Zoetl (Editors), The Quaternary period in Saudi Arabia Volume 2. Springer-Verlag, Vienna, Austria, pp. 150-173.

Vincent, P., 2008. Saudi Arabia - An environemental overview. Taylor and Francis, London, 309 pp.

White, J.D.L. and Houghton, B.F., 2000. Surtseyan and related eruptions. In: H. Sigurdsson, B. Houghton, S. McNutt, H. Rymer and J. Stix (Editors), Encyclopedia of Volcanoes. Academic Press, New York, pp. 495-512.

White, J.D.L. and Ross, P.S., 2011. Maar-diatreme volcanoes: A review. Journal of Volcanology and Geothermal Research, 201(1-4): 1-29.

The Yuriria – Valle de Santiago – Irapuato maar lineament (Guanajuato, México); an overview

José Jorge Aranda-Gómez[1], James F. Luhr[2ψ], Todd B. Housh[3ψ] and Oscar Carranza-Castañeda[1]

[1] *Centro de Geociencias, UNAM, Campus Juriquilla, Querétaro, México. jjag@geociencias.unam.mx*
[2] *Department of Mineral Sciences, Smithsonian Institution, Washington, D.C., USA.*
[3] *Department of Geological Sciences, University of Texas at Austin, Austin, Texas, USA.*
[ψ] *Deceased.*

Keywords: intra-plate magma, crustal xenolith, megacryst.

Maar volcanoes belonging to this lineament were first described by Ordóñez in 1900; his landform map clearly depicts that 8 of the 10 maars shown near Valle de Santiago form a N25ºW, 18 km long, linear array, while the other two maar craters, together with one of the maars in the NW lineament form an intersecting, E-W, 6 km long linear array. However, as pointed out by Murphy (1986), the maars around Valle de Santiago are part of a larger N25°W lineament, which extends from the southern shore of lake Yuriria (Yuriria maar: 20°12.322', -101°7.762') to the outskirts of the city of Irapuato (Irapuato N maar: 20°37.963', -101°19.066'). Thus, the NW maar array is nearly 55 km long and it is better described as an elongated volcanic cluster with an 8 – 10 km width. In addition to the maar volcanoes near Valle de Santiago, we have identified in the same region two more maars located near the rhyolitic dome complex of Cerro Huanímaro, which we refer to as the Cerro La Lobera maar (20°22.899', -101°27.025') and the Jarrillas maar (20°21.256, -101°29.446'). An articulated fossil horse (Equus aff. *E. mexicanus,* Late Pleistocene) was found in intermediate to distal surge beds exposed at the town of Charco de Pantoja (20°23.422', -101°21.134'). The fossil did not display any evidence of transport or attack by scavengers, so it is reasonable to assume that it was killed and immediately buried by a surge cloud. Therefore a phreatomagmatic eruption occurred close to the place where the horse was found. However, there is no obvious maar crater nearby, so we assume that the low hill located immediately south of the town may represent the remnants of one more maar. Taking into account the Cerro La Lobera maar and the Charco de Pantoja cryptic maar (?), it turns out that the EW maar alignment is a 27 km long. In addition to these maar lineaments, we found in the area with the highest vent density another N55°E linear trend composed by 9 cinder cones.

The study region is located in the northern end of the Trans Mexican Volcanic Belt (TMVB) and in the northwestern part of the Michoacán Guanajuato Volcanic Field (MGVF: Hasenaka and Carmichael, 1985), which is a broad area (~40,000 km²) characterized by a large concentration of monogenetic vents (~1040) that lacks large active composite volcanoes. In addition to the monogentic volcanoes, there are more than 300 medium-sized continental shield volcanoes in the MGVF. In general, shield volcanoes are more degraded than neighboring cinder cones, thus they seem pre-date the small monogentic vents. Monogenetic volcanoes in the MGVF form several distinct clusters with a higher vent density and in places they define local alignments. Shield volcanoes occur in the same area, but they are not clustered or define distinct alignments (Hasenaka, 1992). Statistical studies (e. g. Connor, 1990) have shown vent alignments in the MGVF. Two types of orientations appear. Type 1 is oriented NNE-SSW near the Pacific coast and changes gradually to ENE-WSW northward. Type 2 is WNW-ESE and occurs throughout the field. Type 1 vent lineaments are parallel to the conspicuous Chapala-Tula fault system, which follows the trend of the TMVB for 450 km, from the Guadalajara triple point to an area located north of Mexico City. The northeastern part of the MGVF ends at the Taxco-Querétaro Fault System (TQFS), which is NS to NNW- trending array of normal faults that crosses the central part of the TMVB. These faults occur over a region located between Querétaro city, where faults trend N25°W, and the NS Penjamillo graben, which is located ~70 km west of Valle de Santiago. It appears that magma ascent along the NW-trending maar lineament is related to the TQFS.

We collected and analyzed a large number of rock samples (~60) in the studied area. Sampling was focused mainly on the Quaternary monogenetic volcanoes. However, in some of the maars, like Hoya Cíntora and Hoya de Álvarez, our samples include pre-maar lavas, which probably were issued from older shield volcanoes and at least two samples from two shield volcanoes located south of the Yuriria lake (Cerro Santiago: 20º11.613', -101º5.785'; Cerro El Capulín: 20º10.349',-101º7.801').We found that many of the samples collected from the monogenetic volcanoes are

mildly alkaline, while those samples that came from the older shields are subalkaline. SiO_2 content in the rocks ranges between 76.9 and 47.2 wt% and nearly 20% of the samples have small amounts ($\leq$ 5%) of nepheline in the norm, while the rest have hypersthene or hypersthene + quartz. Most samples plot in the alkaline field in a TAS diagram and ~1/3 of the samples are sodic, while the rest are potasic. Some of the Quaternary magmas involved in the phreatomagmatic eruptions and in the formation cinder cones and associated lava flows carried megacrysts and/or feldspathic granulites to the surface, and at least one of our samples contain deformed olivine xenocrysts derived from mantle peridotites. So far, we have not found xenoliths or megacrysts in the lavas of the shield volcanoes. K-Ar ages of the volcanoes range between 6.9 and 0.07 Ma, with the Miocene age obtained in a shield volcano and the Quaternary ages in the small monogenetic volcanoes (Murphy, 1986). We obtained $^{40}Ar/^{39}Ar$ ages for six Quaternary samples. San Nicolás and Hoya Blanca samples yield negative weighted mean ages that are interpreted as "zero ages" (they are too young to be dated with the method). The ages of samples collected at Cerro San Andrés (0.605 Ma), Cerro Buenavista (0.386 Ma), Cerro Las Silletas (0.068 Ma), and the Santa Rosa maar (0.137 Ma) are interpreted as eruption ages.

The Valle de Santiago region is located a short distance from present day boundary between the Mexican Basin and Range province (MBRP) and the TMVB. Quaternary volcanic rocks in the MBRP are mafic alkaline and often contain mantle (spinel lherzolite) and/or crustal (feldspathic granulite) xenoliths and/or complex sets of megacrysts similar to those documented in the Valle de Santiago maars. We also note that the N25°W orientation of the most conspicuous vent alignment in the area is similar to the Cenozoic normal fault pattern of the southern end of the MBRP (*e.g.* Henry and Aranda-Gómez, 1992) and unlike other vent alignments documented elsewhere in the MGVF. As pointed out by Luhr *et al.* (2006) for Valle de Santiago and other occurrences of alkaline intra-plate type magmas in the TMVB, the Valle de Santiago magmas appear to be the "product of involvement during subduction zone partial melting of the same mantle source that feeds the intra-plate type magmas generated beneath the [MBRP]" (Luhr *et al.*, *op.cit.*, p.13). What it appears extraordinary in Valle de Santiago, in comparison with other intra-plate magma localities in the TMVB, is the presence of deep crustal xenoliths and xenocryst derived from them or from mantle rocks in the products of some of the maars and cinder cones. Thus, it appears that lithospheric extension in the region was sufficient to allow ascent of the magmas without losing part of their load of xenoliths of deep-seated rocks. The region between Valle de Santiago and Yuriria is characterized by a high density of vents, with more than 100 volcanoes in a relatively small area. Intense fracturing of the crust in the region is suggested by the N25°W, N55°E and EW vent alignments. Normal faults in the area are remarkably scarce in comparison with nearby areas. We attribute this to "normal fault suppression" as crust dilation was accommodated by dike injection rather than by fault slip.

The large number of maars, together with the flat terrain in the region locally known as El Bajío, and the fact that the Río Lerma lacks a well defined channel in the area suggest the existence of a large lake in the area. However, there are no significant exposures of its sediments. Erosion of some volcanic structures near Valle de Santiago suggests that water surface in this hypothetical lake reached 1800 masl. A good candidate to block the water flow in the paleo Lerma river is the master fault on the western side of the NS-trending Penjamillo graben.

Acknowledgements

Financial support for this research was provided by Conacyt grant 129550 to J. Aranda.

References

Aranda-Gómez, J.J., Housh, T.B., Luhr, J.F., Carrasco-Nuñez, G., 2002, Geología de la región de Valle de Santiago (Guanajuato): Informe preliminar: GEOS, vol. 22, núm. 2, p.39

Connor, C.B., 1990, Cinder cone clustering in the TransMexican volcanic belt: Implications for structural and petrological models: Journal of Geophysical Research, v. 95, p. 19395-19405

Hasenaka, T., 1992, Contrasting volcanism in the Michoacán-Guanajuato volcanic field, central Mexico: Shield volcanoes vs. cinder cones, *in* K. I. Aoki, ed., Subduction volcanism and tectonics of western Mexican volcanic belt, Sendai, Japan, The Faculty of Science, Tohoku University, p. 142-162.

Hasenaka, T., and I. S. E. Carmichael, 1985, The cinder cones of the Michoacan-Guanajuato, central Mexico: their age, volume, and distribution, and magma discharge rate: Journal of Volcanology and Geothermal Research, v. 25, p. 104-124

Henry, C.D. and Aranda-Gómez, J.J., 1992, The real southern Basin and Range: Mid- to late Cenozoic extension in Mexico: Geology, v.20, p.701-704.

Luhr, J. F. *et al.*, 2006, México's Quaternary volcanic rocks: Insights from the MEXPET petrological and geochemical data base: GSA Sp. Paper 402, p 1-44

Murphy, G. P., 1986, The chronology, pyroclastic stratigraphy, and petrology of the Valle de Santiago maar field, central Mexico: Master of Science thesis, University of California, Berkeley, 55 p

Ordoñez, E.,1900, Les volcans du Valle de Santiago, Memrias Sociedad Científica Antonio Alzate, 14: 299-326

Stratigraphy and radiocarbon dating of phreatomagmatic deposits on the northern shoreline of Lake Kivu (DRCongo)

Sam Poppe[1], Benoît Smets[2,3,1], Montfort Bagalwa Rukeza[4], Antoine Fikiri[4], Albert Kyambikwa Milungu[4], Didier Birimwiragi Namogo[4], **Audray Delcamp[1,*]**, Matthieu Kervyn[1]

[1] *Department of Geography, Vrije Universiteit Brussel, Brussels, Belgium. sam.poppe@vub.ac.be; *adelcamp@vub.ac.be*
[2] *European Center for Geodynamics and Seismology, Walferdange, Luxembourg.*
[3] *Royal Museum for Central-Africa, Tervuren, Belgium.*
[4] *Goma Volcano Observatory, Goma, Democratic Republic of Congo.*

Keywords: Phreatomagmatism, radiocarbon-datation, Virunga.

The active volcanoes Nyamulagira and Nyiragongo are part of the Virunga Volcanic Province (VVP), within the western branch of the East-African Rift. Nyiragongo lies to the immediate North of the cities of Goma (East-DRCongo) and Gisenyi (Rwanda) and its central crater holds a permanently active lava lake. Nyamulagira lies to the North-West of the former, and has been erupting lava flows every 1-4 years over the past century.

While many satellite spatter-and-scoria cones are scattered within these volcanoes' lava fields, several satellite tuff cones and a maar volcano lie markedly within 1-2 km from the northern shoreline of Lake Kivu (Fig.1).

Denaeyer (1975) reported the presence of these satellite volcanoes, and more recently Capaccioni *et al*. (2003) analysed the overall geochemistry of the deposits. The dynamics and timing of these past eruptions hence remains poorly understood, while these eruptive centers are located in a densely urbanized area. We present the stratigraphy of the best exposed satellite edifices, along with radiocarbon dates of palaeosols retrieved below the lava flows that cover the cone-and-maar deposits.

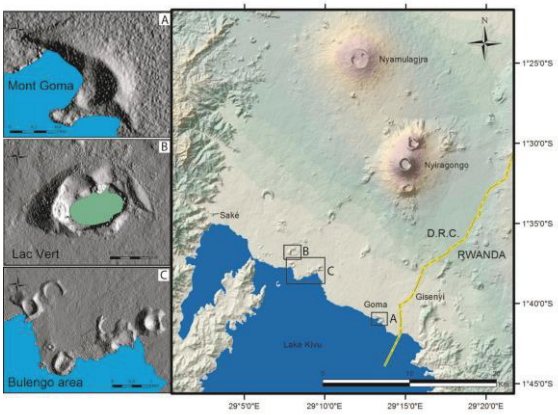

Fig. 1 – Hillshade DEM image of the northern shoreline of Lake Kivu with Nyamulagira and Nyiragongo volcanoes. Insets: A. Mont Goma tuff cone; B. Lac Vert maar and tuff ring; C. The Bulengo area (6 tuff cones).

Mt Goma is a complex tuff cone constructed during at least three eruptive stages with undefined time lags in between, around at least three craters, dissected to the South by Lake Kivu (see Fig.1A).

The oldest eruptive phase has deposited decimetric cross-laminated layers of low-vesicular and angular lapilli in an abundant matrix of fine ocher ash, and beds of centimetric ash-armored lapilli, with sporadic decimetric lithic older lava blocks. This points towards a significant magma:water interaction from the southernmost crater, with an instable ash column as the result.

The second phase displays a thick package of centimetric laminae of finer and coarser, ocher to black ash, with impact sags below up to m-size ballistic lithic blocks. Cross-lamination, wavy bed-forms and erosive channels testify the occurrence of base surge pulses from an instable ash column, as the result of pulsating magma:water interaction in the central crater.

The third phase consists of plane-parallel centimetric laminae of brown to black scoriaceous coarse ash to fine lapilli, with both lithic blocks and scoria bombs. While cross-laminations and wavy bed forms are lacking here, sporadic base surges eroded decimetric channels.

The Mt Goma eruptive sequence is interpreted to result from a decrease in water:magma ratio, and thus probably in explosive dynamics of the eruptive activity, with recurrent collapse of the eruptive column and formation of (mildly) wet base surges.

The pyroclastic deposits of Mt Goma are covered by more recent lava flows. Two samples of the uppermost mafic ash below the lava yield ages between 0.6 and 0.9 ka BP, thus a *minimum* age for the last phase that constructed Mt Goma.

Lac Vert is a maar volcano consisting of 2-3 craters - the deeper of which is filled with green water providing the maars name – and an adjacent tuff ring (Fig. 1B). The ejecta tuff ring consists of 2 phases. The lowermost visible sequence starts with a chaotic polygenic lithic breccia, comprising several types of older lava flows, aggregates of older ash-

and-lapilli tuff blocks and basement granites. Lithic blocks range in size from centimetric to metric, demonstrating a high explosivity through magma/water interaction during this phase. The breccia grades upward into a bedded lithic breccia with an overall fining-upwards trend of the matrix, and an upward-increasing content of low-vesicular juvenile lapilli. This bedded sequence contains wavy bed-forms with metric wavelengths, cross-laminations, and decimetric ballistic lithic blocks with impact sags.

An abrupt contact separates the bedded breccia, from a cover of brown to black, centimetric laminae of alternating coarse to fine scoriaceous ash without lithics. This contrast suggests a switch to a violent Strombolian phase at Lac Vert, possibly from a different crater than the first phase.

A terrestrial gastropod shell in the clearly weathered top of the bedded breccia, at the outer base of Lac Vert, was dated at 1.3 -1.4 ka BP, while its surrounding palaeosol was dated between 2.1 and 2.5 ka BP in two separate locations. Two samples from the upper scoriaceous ashes below a more recent lava flow covering the Lac Vert ash-and-lapilli tuffs date at 0.35 - 0.45 ka BP. We thus suggest a time gap of at least ~1000 years must exist between both eruptive phases within the maar – ejecta rim complex of Lac Vert, with the youngest and least explosive eruptive phase occurring more recently than ~1.3 ky.

At least seven additional tuff cones with each at least one incompletely exposed phreatomagmatic eruptive phase are present in the Bulengo area, to the immediate West of Goma (Fig.1C). Assuming Lake Kivu must have reached its approximate current water level ~10 ka BP, and at least 10 phreatomagmatic eruptive centers are present close to the lake shoreline, the average recurrent rate of a phreatomagmatic eruption originating from Nyiragongo volcano could be roughly estimated at ~1000 years in the area.

Additionally, Ross *et al*. (2014) recently identified numerous relatively older tuff cones on the northernmost lake floor of Lake Kivu, below the present water level and 'off-shore' of the above presented edifices.

In conclusion, bedding structures in satellite edifice deposits along the northern shoreline of Lake Kivu suggest the occurrence of phreatomagmatic eruptive activity and the occurrence of base surge events, with plausible severe impacts on the close surroundings of such eruptive centres. Due to the dense urbanization surrounding the observed tuff cones and maars, notably Mont Goma and Lac Vert, the potential intermediary explosive nature of future eruptive outbreaks close to Lake Kivu is a key element of volcanic hazard in the Saké-Goma-Gisenyi urban area. The eruptive history and dynamics of these phreatomagmatic cones should be completed and analyzed further, in order to provide a more robust assessment of the 'explosive' volcanic hazard in the area.

Acknowledgements

This work has been carried out in the framework of the project 'Geo-Risk in Central-Africa' (GeoRisCA; http://georisca.africamuseum.be), and is supported by the Belgian Science Policy (BELSPO). The GVO personel is thanked for logistic support during field work. Palaeosol and gastropod shell samples have been dated by radiocarbon at Beta Analytic lab, Florida, USA.

References

Capaccioni, B., Vaselli, O., Santo, A.P. and Yalire, M.M., 2003. Monogenic and polygenic volcanoes in the area between the Nyiragongo summit crater and the Lake Kivu shoreline. Acta Volcanologica, 14 :1-2, 129-136.

Denaeyer, M.E., 1975. Le glacis des volcans actifs au Nord du Lac Kivu. Mémoires du Museum national d'Histoire Naturelle, Série C, Sciences de la Terre, 33, 79 pp.

Ross, K.E., Smets, B., De Batist, M., Hilbe, M., Schmid, M. and Anselmetti, F.S., 2014. Lake-level rise in the late Pleistocene and active subaquatic volcanism since the Holocene in Lake Kivu; East African Rift. Geomorphology, in Press.
DOI:10.1016/j.geomorph.2014.05.010

The subsurface morphology and eruptive histories of complex maar volcanoes within the Newer Volcanics Province, south-eastern Australia - Insights from potential field modelling.

Jackson van den Hove, Teagan Blaikie, Laurent Ailleres, Peter Betts, Ray Cas

School of Geoscience , Monash University, Melbourne, Australia.

Keywords: Geophysical modelling, diatreme, Newer Volcanics Province

In order to better characterise the eruptive histories and subsurface structures of several maar volcanoes from the 4.5 Ma-4.5 ka Newer Volcanics Province of south-eastern Australia, forward and inverse geophysical modelling is combined with a study on the geology of the volcanic centres. The maar volcanoes under investigation include the Lake Purrumbete, Red Rock Volcanic Complex, Ecklin maar, and the Mount Leura Volcanic Complex. These volcanic centres represent a range of the different sizes and eruptive histories observed within maar volcanoes in the region. These maars are hosted in the weakly lithified sedimentary sequences of the Otway Basin.

Lake Purrumbete Maar is a large maar complex comprised of several coalesced eruption points, which has experienced largely phreatomagmatic eruption styles. Ecklin maar is a small, simple maar volcano, also showing dominantly phreatomagmatic eruptive styles. Mount Leura consists of a large maar crater and overlapping tuff rings, with up to 16 scoria cones contained within the centre. Red Rock is one of the most complex volcanic centres within the province, and is host to over 40 separate eruption points forming numerous poly-lobate maars and a scoria cone complex.

Understanding the subsurface of these volcanoes is an important step towards fully understanding eruption processes and assessing volcanic hazards in the region. However, there is no exposure of subsurface volcanic structures within the Newer Volcanics Province so potential field modelling techniques are relied upon to image the volcanic conduit (Blaikie *et al*., 2014a).

To achieve this, high resolution gravity and magnetic data were acquired across each of these maars and the data was modelled in two and three dimensions to understand the subsurface morphology and petrophysical property distributions within the subsurface. In each case the depth of the maar diatreme was also constrained by examining lithic fragments contained within pyroclastic deposits and determining their origin within the well constrained stratigraphy of the Otway Basin.

The magnetic anomaly over LPM shows three large, irregular shaped high magnetic anomalies associated with major eruption points within the crater. Several other odd shaped high magnetic anomalies are also present, which are uncertain as to whether they represent minor eruption points or areas of thick juvenile basaltic infill.

The geophysical signature of the Ecklin maar consists of two corresponding short-wavelength Bouguer gravity and magnetic highs in the centre of the crater, superimposed on a longer wavelength Bouguer gravity and magnetic low. These anomalies were reproduced during forward and inverse modelling by two shallow coalesced diatremes structures (Figure 1c). The centres of the two diatremes are denser and have a higher magnetic susceptibility, representing the higher volume volcanic debris contained within the vent. The overall structure of this maar-diatreme is typical of a maar volcano hosted in weakly lithified sediments (*e.g.* Auer *et al*., 2007).

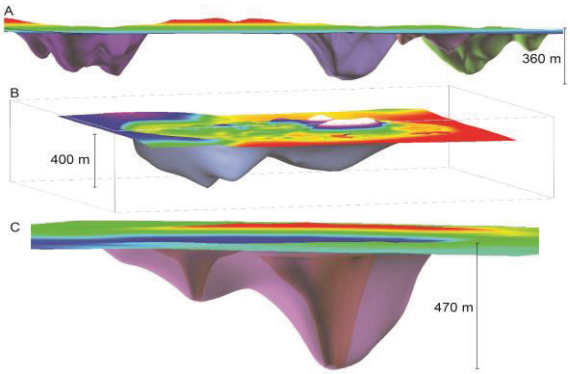

Fig. 1 – Example of the 3D models generated from geophysical modeling of a) Red Rock, b) Mount Leura, c) Ecklin (modified after Blaikie *et al*. 2014b).

Gravity and magnetic surveys over Mount Leura revealed a large Bouguer gravity high within the centre of the maar crater with a corresponding magnetic high which is related to the larger scoria cones and underlying lava flows (Figure 2). Magnetic anomalies are variable across other parts

of the complex due to dispersed scoria cones within the coalesced maar/tuff cone craters. Magnetic highs are typically observed over the cones, however they do not always have a corresponding gravity anomalies. Modelling revealed two shallow coalesced diatremes overlain by a thick lava flow and scoria deposits (Figure 1b).

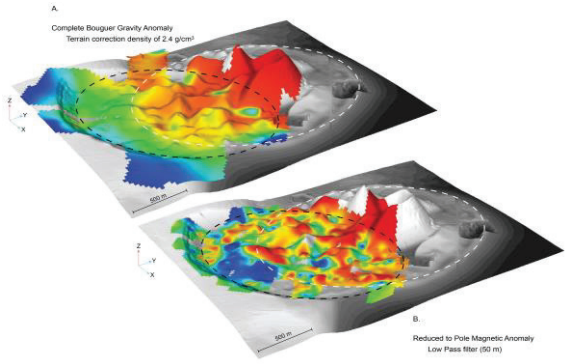

Fig. 2 – Example of the complex geophysical response seen at Mount Leura (modified after Blaikie *et al. 2014a*).

Geophysical signatures across the maars contained within the Red Rock Volcanic Complex are highly variable, with some maars displaying corresponding short-wavelength Bouguer gravity and magnetic highs, others corresponding lows, and some with magnetic anomalies but no gravity anomalies. Alternating scoria and ash layers are observed within the ejecta rims of the maars, and provide evidence that they frequently fluctuated between magmatic and phreatomagmatic explosive activity. This suggests that dykes have risen through the diatreme to the near surface and may be preserved within the diatreme where they could be detected by the implementation of a high resolution survey. The short wavelength, positive gravity and magnetic anomalies identified within a number of maars at Red Rock were reproduced during forward and inverse modelling by several sub-vertical dykes that have intruded the diatreme. Modelling of diatremes revealed complex coalesced structures, suggesting that the eruption points frequently migrated during the formation of the complex (Figure 1a). The diatremes are shallow and bowl-shaped, indicating that the soft sediment in which the volcano is hosted influenced its final geometry.

By comparing the geophysical signature and eruptive histories of these case studies, several geophysical trends correlating to different eruptive histories have been identified (Blaikie *et al*., 2014a). Where corresponding Bouguer gravity and magnetic lows are detected across a volcanic crater, all the available magma was fragmented by magma-water interaction and the resulting pyroclastic debris were deposited on the surface or within the diatreme. The Bouguer gravity low arises because of low density pyroclastic debris and lake sediments infilling the crater.

Maars with corresponding short wavelength gravity and magnetic highs indicate the presence of subsurface basalt, possibly in the form of a dyke or sill. If the anomalies are broader with a higher amplitude, it is thought that ponding of magma at the surface of the vent has occurred. The presence of dykes and/or magma ponds within the diatreme suggests a lack of groundwater was available for magma to interact with during the eruption, which facilitated magma rising upwards through the diatreme to erupt magmatically.

Recognising these trends, and how they relate to the eruptive histories of the maars have assisted in understanding the evolution of these volcanoes, and may assist in future interpretations of potential field data. Within the Newer Volcanics Province, shallow maar diatremes with multiple vents are commonly observed (*e.g*. Blaikie *et al*., 2014a; Blaikie *et al*., 2012; Jordan *et al*., 2013), suggesting vent migration, rather than the downward propagation of explosions is the main cause of for crater widening.

References

Auer, A., Martin, U. and Németh, K., 2007. The Fekete-hegy (Balaton Highland Hungary) "soft-substrate" and "hard-substrate" maar volcanoes in an aligned volcanic complex - Implications for vent geometry, subsurface stratigraphy and the palaeoenvironmental setting. Journal of Volcanology and Geothermal Research, 159(1-3): 225-245.

Blaikie, T.N., Ailleres, L., Betts, P.G. and Cas, R.A.F., 2014a. A geophysical comparison of the diatremes of simple and complex maar volcanoes, Newer Volcanics Province, south-eastern Australia. Journal of Volcanology and Geothermal Research, 276: 64-81.

Blaikie, T.N., Ailleres, L., Betts, P.G. and Cas, R.A.F., 2014b. Interpreting subsurface volcanic structures using geologically constrained 3-D gravity inversions: Examples of maar-diatremes, Newer Volcanics Province, southeastern Australia. Journal of Geophysical Research: Solid Earth, 119: n/a-n/a.

Blaikie, T.N., Ailleres, L., Cas, R.A.F. and Betts, P.G., 2012. Three-dimensional potential field modelling of a multi-vent maar-diatreme - the Lake Coragulac maar, Newer Volcanics Province, south-eastern Australia. Journal of Volcanology and Geothermal Research, 235-236: 70-83.

Jordan, S.C., Cas, R.F.A. and Hayman, P.C., 2013. The origin of a large ([>3]km) maar volcano by coalescence of multiple shallow craters, not deep excavation: The late Pleistocene Lake Purrumbete maar, Newer Volcanics Province, southeastern Australia. Journal of Volcanology and Geothermal Research 254: 5-22.

The maars of the Tuxtla Volcanic Field: the example of "Laguna Pizatal"

J. M. Espindola[1], A. Zamora-Camacho[1], A. Hernandez[2], E. Alvarez del Castillo[2], L. Godinez[3]

[1] *Instituto de Geofísica, Universidad Nacional Autónoma de México, México D.F. 04510,México.*
[2] *Facultad de Ciencias, Universidad Nacional Autónoma de México, México D.F. 04510,México.*
[3] *Instituto de Geografía, Universidad Nacional Autónoma de México, México D.F. 04510,México.*

Los Tuxtlas Volcanic Field (TVF), also known as Los Tuxtlas massif, is a structure of volcanic rocks rising conspicuously in the south-central part of the coastal plains of eastern Mexico. The TVF seems related to the upper cretaceous magmatism of the NW part of the Gulf's margin (e.g. San Carlos and Sierra de Tamaulipas alkaline complexes) rather than to the nearby Mexican Volcanic Belt.

The volcanism in this field began in late Miocene and has continued in historical times, The TVF is composed of 4 large volcanoes (San Martin Tuxtla, San Martin Pajapan, Santa Marta, Cerro El Vigia), at least 365 volcanic cones and 43 maars.

In this poster we present the distribution of the maars, their size and depths. These maars span from a few hundred meters to almost 1 km in average diameter, and a few meters to several tens of meters in depth; most of them filled with lakes.

As an example on the nature of these structures we present our results of the ongoing study of "Laguna Pizatal" or "Pisatal" (18° 33'N, 95° 16.4´, 428 m a.s.l.) located some 3 km from the village of Reforma, on the western side of San Martin Tuxtla volcano. "Laguna Pizatal" is a maar some 500 meters in radius and a depth about 40 meters from the surrounding ground level. It is covered by a lake 200 m^2 in extent fed by a spring discharging on its western side. We examined a succession of 15 layers on the margins of the maar, these layers are blast deposits of different sizes interbedded with surge deposits. Most of the contacts between layers are irregular; which suggests scouring during deposition of the upper beds. This in turn suggests that the layers were deposited in a series of explosions, which mixed juvenile material with fragments of the preexisting bedrock. We were unable to find the extent of these deposits since the surrounding areas are nowadays sugar cane plantations and the lake has overspilled in several occasions.

Magmatic and phreatomagmatic eruptions of Takuhiyama tephra cone, Oki Dozen in the Japan Sea off SW Japan

Kazuhiko Kano[1], Nobuyuki Kaneko[2], and Tokiko Tiba[3]

[1] *The Kagoshima University Museum, Kagoshima University, 21-30, Kagoshima, Japan. kano@kaum.kagoshima-u.ac.jp*
[2] *Institute for Geo-Resources and Environment, Geological Survey of Japan, AIST, Tsukuba, Japan.*
[3] *Emeritus Research Fellow, National Museum of Nature and Science, Tokyo, Japan.*

Keywords: tephra cone, eruption mechanism, welding.

Oki Dozen is a caldera volcano surrounded by sea. Since its birth about 6 Ma ago in the Japan Sea, 60 km north of the Shimane Peninsula, SW Japan, this old volcano has been subjected to surface erosion but still preserves the original volcanic structure (Tiba *et al*., 2000).

The topographic basement of Oki Dozen volcano is 50–60 m below sea level with a basal diameter of 18–24 km. The caldera floor is 8–10 km across and 30–50 m below sea level. The somma is composed mainly of trachybasalt to trachyandesite lava flows with ridge up to 435 m above sea level wich is divided into four sectors by completely or partly submerged incised valleys.

The Takuhiyama tephra cone occupies the northern central part of the caldera floor and is composed mainly of trachyte welded tuff to tuff breccia, rising 452 m above sea level. This cone has lost its upper part by erosion and part of the early construct is exposed (Fig. 1) representing a wide opening or tephra ring.

Late Middle Miocene quartz syenite and older sedimentary rocks are exposed on the northern side of the cone. They are partly overlain by the tephra wich flowed out of the crater and that enclose the lower construct. The contact wall with the lower construct is inward inside at an angle of 40–80º with a circular trace and likely shapes a funnel with an aperture of 3 or 4 km (Fig. 1). Providing further evidence for this funnel structure, welding and bedding planes also dip inward at an angle of 20–90º with strike lines mainly parallel to the contact wall and dips outward in the area outside the contact wall.

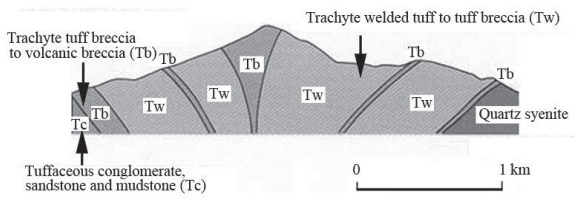

Fig. 1 – An E-W cross section of the Takuhiyama tephra cone.

Fig. 2 – Irregularly curved blocks in welded tuff breccia. A v-shaped block in the center shows a fibrous texture.

Fig. 3 – A block-sag in intensely-welded, well-stratified tuff.

The cone-building welded tephra comprises glassy lenses, millimeters to centimeters thick, and millimeters to tens of centimeters long, and a dark, homogeneous matrix of fragmental volcanic glass and feldspar and other crystals. The Tephra has crude columnar and platy joints. Where welding is not so intense, glassy lenses or blocks locally retain a fibrous texture reminiscent of pumice with irregularly curved external forms (Fig. 2). Each bed unit bed is meters to tens of meters in thickness, and it is poorly sorted, mostly non-stratified, normally graded at its top, and in some cases, overlain by bedded tuff.

The welded tuff to lapilli tuff that forms the outer slope of the tephra construct locally forms 10–30-m-thick successions of well-sorted and -stratified multiple beds (Fig. 3). On the other hand, the crater-infilling welded succession is intercalated with non-welded minor successions composed of poorly sorted breccia to tuff breccia, well sorted and stratified lapilli tuff to tuff, and subordinate epiclastic rocks in the basal, middle and upper central parts (Fig. 1).

Fig. 4 – Explosion breccia composed mainly of the fragments of welded tuff, lapilli tuff and tuff breccia.

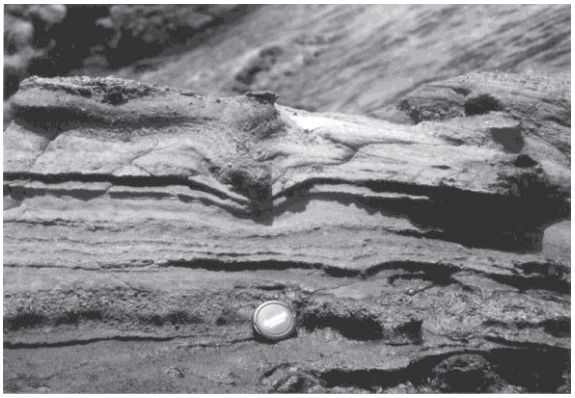

Fig. 5 – A block-sag in well-stratified tuff and lapilli tuff. Accreationary and lithic lapilli concentrate in a lower layer.

In the non-welded successions, breccias are mostly non-stratified, poorly sorted, and mainly supported mainly by meter- to centimeter-size fragments of trachyte welded tuff to tuff breccias, quartz syenite and other minor basement rocks (Fig. 4). They are inversely to normally graded and change upwards to poorly sorted tuff breccia and further up to well-stratified lapilli tuff to tuff with a total unit bed thickness of meters to tens of meters. The non-welded tuff to lapilli tuff comprises many blocky ash grains and contains block-sags, accretionary lapilli, and tiny vesicles in the fine ash matrix (Fig. 5), suggesting a phretomagmatic origin. Tuffaceous conglomerate, sandstone and mudstone locally underlie or overlie the succession of these non-welded pyroclastic rocks. The major constituent fragments are epiclastic, identical to the associated pyroclastic rocks and are rounded to some extent, though meter-size blocks of syenite are locally predominant over the epiclasts near the vent wall.

The Takuhiyama tephra beds have features of pyroclastic density current deposits and are mainly welded, suggesting an explosive subaerial magmatic eruption. Irregularly curved exterior of the juvenile fragments likely represent fluidal deformation during their emplacement. Intensely welded, well-stratified lapilli tuff and tuff demonstrate syn-depositional, instantaneous welding of hot, fluid particles carried by dilute pyroclastic density currents as envisaged for a high-grade ignimbrite (Branney and Kokelaar, 1992). Resulting deposits were sufficiently stiff to form sag structures by impact of blocks on them (Fig. 5).

Instantaneous welding and rapid cooling of the welded bed likely mantled the crater to minimize the access of water to the conduit. Degassing from the succeeding magma, however, plausibly caused explosive eruptions to disrupt the welded rocks. This allowed permeation of external water to the conduit and thus, would have induced eruptions of wet pyroclastic surges with explosive magma-water interaction and deposition of stratified lapilli tuff and tuff from the surges.

The source of the external water is not clear. Where mantled by welded pyroclastic rocks, the crater have likely collected and reserved rain or snow-melt water. Seawater could have been also likely to flow into the crater with a storm, global sea level rise, collapse or erosion of the crater rim, or subsidence of the basement. Permeation of underground water to the conduit was perhaps plausible to occur through cracks or joints developed in the basements rocks but must have been significantly prevented by the welded crater-infillings. Epiclastic beds were presumably produced by repeated explosions or wave actions in the crater water, and partly ejected onto the surrounding rim deposits. They were also likely produced by sea wave action on the surrounding shore and carried into the crater by storms.

References

Branney, M.C. and Kokelaar, P., 1992. A reappraisal of ignimbrite emplacement: progressive aggradation and changes from particulate to non-particulate flow during emplacement of high-grade ignimbrite. Bulletin of Volcanology, 54: 504-520.

Tiba, T., Kaneko, N., Kano, K., 2000. Geology of the Urago district. Geological Survey of Japan, 74 p. with a geological sheet map at 1:50,000 (in Japanese with English abstract)

Stratigraphy of the Aljojuca Maar Volcano (Puebla, México)

Lorena de León Barragán[1*] and Gerardo Carrasco-Núñez[1]

[1] *Universidad Nacional Autónoma de México, Centro de Geociencias, UNAM, Campus Juriquilla, Querétaro, México.*
ldeleon@geociencias.unam.mx

Keywords: Aljojuca, maar, volcanic stratigraphy, xalapaxcos.

The Aljojuca crater is located at the Serdan-Oriental Basin, which belongs to the Eastern Neogene-Quaternary Sector of the Transmexican Volcanic Belt. The Serdán-Oriental Basin is characterized by monogenetic bimodal volcanism (Riggs and Carrasco-Núñez, 2004) that is built on a >45 km thick crust at about 360-420 km distance from the Mexican trench (Mori and Gómez-Tuena, 2012). This volcanism consist of a set of rhyolitic domes, basaltic cinder cones, lava cones and maar volcanoes. There are about a dozen maar volcanoes, which vary in composition from rhyolitic (*e.g.* Tepexitl, Austin-Erickson *et al.*, 2011) to basaltic (e.g Atexcac, Carrasco-Núñez *et al.*, 2007). They have diverse shapes and some of them include a lake inside, while others are mainly dry.

According to Lorenz´s classification (1986), the Aljojuca crater is a maar volcano type (Mexican xalapazco) because it exposes a pre-maar lithology, which is composed of a basaltic lava flow, and a sequence of pyroclastic and sedimentary deposits. The crater has a elliptical shape (Fig. 1) of about 1.6 km at the major axis, 0.9 km at the minor axis, and a maximum depth of 50.6 m (Wogau-Chong, 2013). Additionally, the crater shows a major elongation to the east forming an alignment with three scoria cones (E-W), similar to the dominant fault system for the central Transmexican Volcanic Belt (Suter *et al.*, 1992), which probably suggest a progressive migration of the vent, along that trend.

Fig. 1 – Aljojuca Maar Volcano with a view to the west.

With the aim to understand the intensity of magma-water interactions that take place during the eruption, and the consequent evolution and development of the shape of the volcanic edifice, we present a preliminary report of the stratigraphic record. In order to characterize the maar deposits, we describe a stratigraphic section at the W crater wall (Fig. 2). The pre-maar rocks in this area are composed of a lower volcano-sedimentary sequence and sedimentary layers, overlain by a vesicular basaltic lava flow, which is in turn overlain by a 0.6 m thick paleosoil and volcaniclastic deposits of maar.

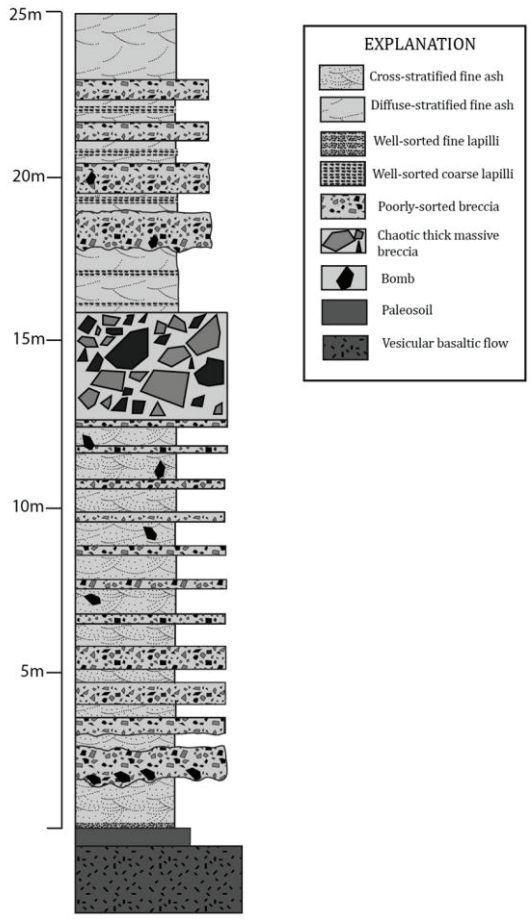

Fig. 2 – Stratigraphic section, at W Aljojuca‘s crater wall.

The maar sequence can be divided into 5 different units. The sequence starts at the base of the section with a layer of a) well- sorted fall deposit, composed of black scoria of 2-3 cm, which is overlain by 0.7-1.5 m-thick stratified sequence of fine ash showing cross stratification (Fig. 3) with abundant accretionary lapilli of 2-8 mm; b) an alternated sequence of 3.9 m-thick consisting of poor-sorted breccias and ash beds with some 0.1 m blocks that caused incipient deformation sags; c) stratified sequence of 6.8 m, dominated by ash beds and some blocks, but without deformation sags; d) a chaotic poorly-sorted and mostly clast-supported massive thick breccia, e) an alternated stratified sequence of 9 m-thick, composed of coarse lapilli with ash beds; the thickness of ash beds increases to the top of the sequence. All previous stratigraphic features suggest a variable explosive activity, from short-lived dry pulses followed by wet layers at the base, and then drier conditions dominated, to finally return to wetter conditions towards the top of the deposits.

Based on stratigraphic field relations with volcanism nearby along with preliminary ^{14}C dating from a palaeosoil deposit underlying the Aljojuca Maar-forming sequence, a Holocene age is proposed for this volcano, having important implications for hazard assessment.

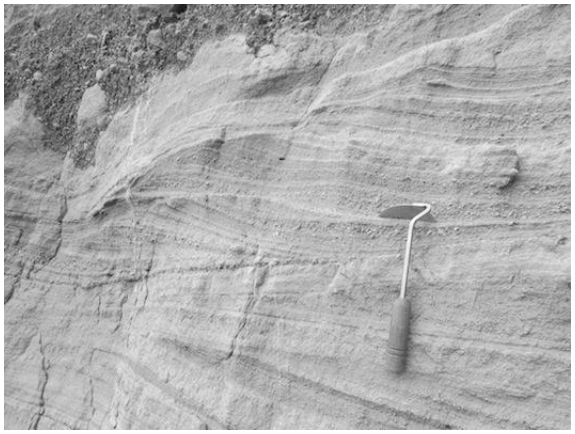

Fig. 3 – Photograph showing the base of the stratigraphic section (unit a) in contact with a poorly-sorted breccia (unit b), at the western crater´s wall.

Acknowledgements

This work has been supported by CONACyT 150900 and PAPIIT IN106314 grants. Logistical support was provided by Centro de Geociencias, Universidad Nacional Autónoma de México.

References

Austin-Erickson, A., Ort, M., Carrasco-Núñez, G., 2011. Rhyolitic phreatomagmatism explored: Tepexitl tuff ring (Eastern Mexican Volcanic Belt). Journal of Volcanology and Geothermal Research 201: 325-341. Doi: 10.1016/j.volgeores.2010.09.007.

Carrasco-Núñez, G., Ort., M.H., Romero, C., 2007. Evolution and hydrological conditions of a maar volcano (Atexcac crater, Eastern Mexico). "Maar-diatreme volcanism and associated processes" (Ed. Martin, U., Németh, K., Lorenz, V., White, J.) Journal of Volcanology and Geothermal Research 159: 179-197.

Lorenz, V, 1986. On the growth of maars and diatremes and its relevance to the formation of tuff rings. Bull. Volcanol. 48: 265–274.

Mori, L., Gómez-Tuena, A., 2012. Geochemical recycling and magma generation in the Eastern Trans-Mexican Volcanic Belt: The case study of the Serdán-Oriental Basin, Cordilleran Section Meeting, 2012, Insituto de Geología, UNAM.

Riggs, N., Carrasco-Núñez, G., 2004. Evolution of a complex, isolated dome system, Cerro Pizarro, central México. Bull. Volcanol.66: 322-335. Lindsay, J., Marzocchi, W., Jolly, G., 2010. Towards real-time eruption forecasting in the Auckland Volcanic Field: application of BET_EF during the New Zealand National Disaster Exercise 'Ruaumoko'. Bulletin of Volcanology 72: 185-204.

Suter, M., Quintero, O., Johnson, C., 1992. Active faults and state of stress in the central part of the trans-Mexican volcanic belt.1. the Venta de Bravo fault. J. Geophys. Res. 97: 11983-11993.

Wogau-Chong, K., 2013: Estudio de magnetismo ambiental para la determinación de paleoclimas y paleoambientes, en la Cuenca de Serdán-Oriental. Juriquilla Qro., Universidad Nacional Autónoma de México, Centro de Geociencias, Ms.C. Thesis.

Temporal evolution and growth of the Barombi Mbo Maar (Cameroon): Constraint from juvenile pyroclast distributions

Boris Chako Tchamabe[1], Takeshi Ohba[1], Gábor Kereszturi[2], Issa[1], Károly Németh[2], Seigo Ooki[1], Gregory Tanyiléké[3] and Joseph V. Hell[3]

[1] *Tokai University, Hiratsuka, Japan. boris.chako@yahoo.fr*
[2] *Volcanic Risk Solutions, Institute of Agriculture and Environment, Massey University, Palmerston North, New Zealand.*
[3] *Institute of Mining and Geological Research (IRGM), PO Box 4110, Yaoundé, Cameroon.*

Keywords: maar-diatreme, juvenile pyroclasts, crater.

Although maar-diatreme volcanoes, are known to have a relatively short eruptive life ranging from days to up to years, they can go through very complex fragmentation processes including multiple phases and diverse eruption styles. The understanding of these complex eruption processes is usually based on sedimentological description of their pyroclastic record and on morphological appraisal of particles accumulated in ejecta rings around the maar craters. However, the relationship between the eruption process and the plumbing system beneath maars are still poorly understood (*e.g.* Valentine, 2012).

The study of accidental lithic clast population provides valuable keys for understanding the cratering process and diatreme growth during maar forming eruptions. However, constrains on the growth of the maar-diatreme based on accidental lithic clast populations in the pyroclastic deposit may requires good knowledge of the substrate geology, including individual thickness of each country rock unit. Such data are generally not available at many maars.

In this study, the juvenile content distribution throughout the pyroclastic sequence of the Barombi Mbo Maar (BMM) is examined to attempt to understand its diatreme and ejecta ring growth. The BMM is the largest maar in Cameroon, with a crater diameter of ~2.5 km. The crater rim consists of about 100 m-thick pyroclastic succession preserved mostly at the eastern margin of the maar. The edifice-building deposit was subdivided into three eruptive units based on their volcano-sedimentary facies characteristics (*e.g.* Chako Tchamabé *et al.* 2013). The deposits are inferred to represent fundamentally two end-members of eruption styles; "dry" magmatic and "wet" phreatomagmatic.

K-Ar ages obtained from different units of the pyroclastic succession as well as the identification of paleosoil horizons in the tuff ring deposits suggested the polycyclic nature of the BMM. The first volcanic episode occurred ~0.51 Ma ago, the second at ~0.2 Ma and the latest one ~0.08 Ma ago thes ages suggest that the BMM could be a nested and amalgamated maar-diatreme complex where recurrence of eruptions took place in the same place over long time.

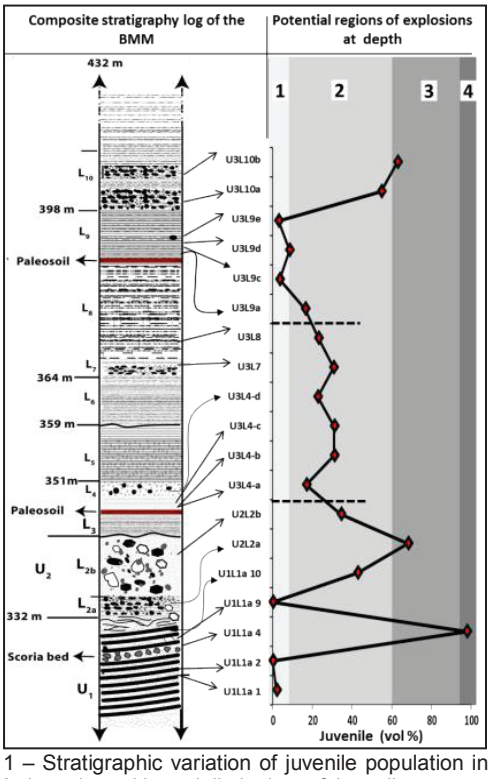

Fig. 1 – Stratigraphic variation of juvenile population in the BMM deposits, with a delimitation of juveniles proportion that might reflect a potential model of explosions during maar-diatremes formation. Dashed lines represent paleosoils.1 = deep-seated explosions with limited ejection of juveniles + extensive entrainment of fragmented lithics. 2 = deep- and shallow-seated explosions + common entrainment of juveniles and fragmented lithics. 3 = explosions taking place at shallow-seated explosions + common ejection of juvenile with limited entrainment of fragmented lithics. 4 = very shallow (near surface) gas-driven explosions with ejection of more juveniles (>90 vol %). These domains are mainly based on the first episode deposits i.e. before the first paleosoil. They also well-define the third episode deposits although the very rich-juveniles domain is not observed therein.

Based on the sedimentary characteristics, a model of evolution of the BMM is summarized in Fig. 2. The most interesting characteristic of the evolution of the BMM is the apparent fluctuation of

juvenile content as a function of stratigraphic height (Fig. 1). The observed fluctuation of the juvenile proportion within maar deposits might be linked to the variations in magma fluxes and depth of explosion during the course of eruptions. This could therefore suggest connection between the upper diatreme/crater excavations zone (ca. <100 m) with the growth of the ejecta rings. It can also be the result of the lateral and/or vertical mobility of the explosion sites in the diatreme (*e.g.* Ort and Carrasco-Nunez 2009; Kurszlaukis and Fulop 2013), which has in turn an influence on the growth of diatreme and ejecta rings.

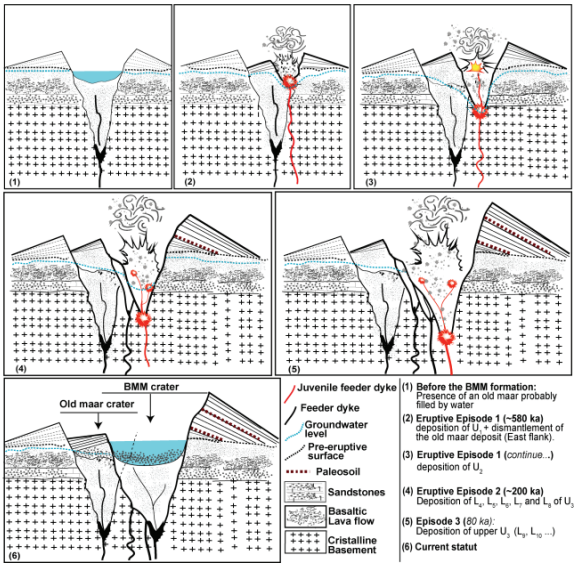

Fig. 2 – Evolution of the BMM maar-diatreme. The current situation of the diatreme is assumed to be an amalgamation of the three possible small diatremes formed during the different eruptive episodes.

Based on the proportion of juvenile clasts in the deposits, four domains at where explosions could take place to produce a relative amount of juveniles are proposed in Fig. 1. These domains suggest that explosions taking place at a deeper position might entrain extensive amount of lithic from the mostly lithic-dominated upper crater infill deposits, thus depositing juvenile-poor tephra beds (<10 vol%). Layers with a juvenile content of 10-60 vol%, for example, could be the result of deep to shallow-seated explosions, with a common entrainment of lithics from the crater infill region. On the other hand, explosions occurring at shallower positions, or near the surface, could produce mainly juvenile-rich beds (>90 vol%).

The presented model for exemplifying lithic and juvenile proportion and their fluctuation in the stratigraphic record is promising, however, it should be investigated further to unravel the link between upper diatreme excavation processes and ejecta ring growth.

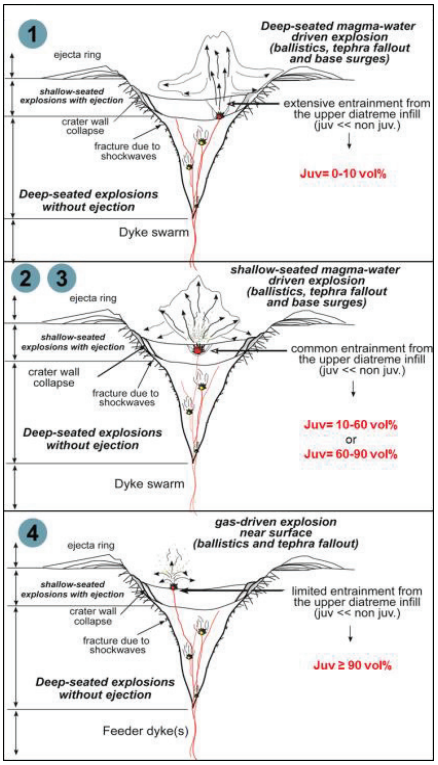

Fig. 3 – A model for explosion depth for maar-diatreme based on juvenile proportion in U_1+U_2 deposits units of the BMM. Cartons 1, 2-3, and 4 correspond to the sketches of the explosions for domains delimited on Figure 1. Carton 2-3 explain the same explosion pattern with the difference that juvenile contents vary from 10-60 vol% in 2 and 60-90 vol% in 3.

Acknowledgements

This work is conducted under the funding of the SATREPS-IRGM project, coordinated by Prof. Takeshi Ohba and Dr. Gregory Tanyiléké.

References

Chako Tchamabé, B., Youmen, D., Owona, S., Issa, Ohba, T., Németh, K., Nsangou, M.N., Asaah, A.N. E., Aka, F.T., Tanyileke G., Hell J.V. 2013. Eruptive history of the Barombi Mbo Maar, Cameroon Volcanic Line, Central Africa: Constraints from volcanic facies analysis. Centr European J Geosci 5(4): 480-496 [Doi: 10.2478/S13533-012-0147-2.]

Kurszlaukis, S., Fulop, A. 2013. Factors controlling the internal facies architecture of maar-diatreme volcanoes. Bull Volcanol 75:761, [DOI: 10.1007/s00445-013-0761-y.]

Ort, M.H., Carrasco-Núñez, G. 2009. Lateral vent migration during phreatomagmatic and magmatic eruptions at Tecuitlapa Maar, east-central Mexico. J. Volcanol Geotherm. Res. 181(1-2): 67-77 [DOI:10.1016/j.jvolgeores.2009.01.003.]

Valentine, G.A. 2012. Shallow plumbing systems for small-volume basaltic volcanoes, 2: Evidence from crustal xenoliths at scoria cones and maars. J. Volcanol. Geotherm. Res. 223-224: 47-63 [DOI: 10.1016/j.jvolgeores.2012.01.012.]

Stratigraphy of Xico: A tuff ring situated at the southeastern part of the Mexico basin

I. Gallegos-Meza[1], **F. García-Tenorio [1, 2]**, J.L. Macías[2]

[1] *ESIA,Ciencias de la Tierra, Instituto Politécnico Nacional, México. ritzelgame@outlook.es*
[2] *Instituto de Geofísica, Ex-Hacienda de San José de La Huerta C.P. 58190, Morelia, Michoacán, México.*

Keywords: Basin of Mexico, tuff ring, phreatomagmatic crater.

The tuff ring of Xico is located at the southeastern edge of the Mexico City metropolitan area. The crater sits at the edge of the remnants of the Lake of Chalco and the city of the same name. Since prehispanic time (~550 AC) the crater of Xico has been used to perform ceremonial rituals. In the local "náhuatl" language means "xictli" = Navel. Xico is located in the central part of the Trans-Mexican Volcanic Belt (TMVB). The volcano has been mapped by several authors (Mooser, 1975; Vázquez and Jaimes, 1989) as a Quaternary volcano. It is a low relief tuff cone with a 1.5 km wide crater and 70 m deep internal walls and gentle slopes (50º).The volcano was excavated through the lacustrine sequence of the Chalco Lake. The volcanic sequence is best exposed on the northern slopes of the crater that consist of:

1) A basal deposit (>50 m thick) composed of a brown to dark-gray indurated layer with vesicles and occasional accretionary and armored lapilli. Followed by an interbedding of massive layers (5 to >110 cm thick) of ash and fine lapilli and wave to cross laminated layers (1 to >50 cm thick) of ash and lapilli with lenses. This deposit is made of basaltic-andesitic lithics, scoria and pumice clast.

2) A dark-gray, massive, 40-m thick, lava flow exposed to the NE part of the crater. It is 1.3 km long and 1.1-0.75 km wide with an A-A type surface. In hand specimen, the rock consists of phenocrysts of plagioclase, pyroxene and olivine for which, it was classified as a basaltic andesite. The lava flow was emitted from the NE side of the crater through a NW-SE fissure or fault (Fig. 1b).

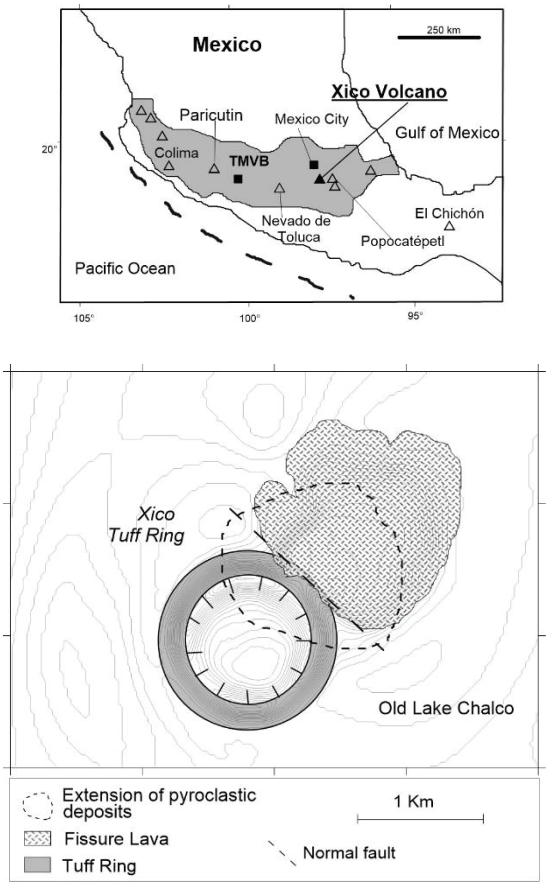

Figure 1. a) Location map of the TMVB and Xico volcano, b) Simplified geological map of the volcano.

3) A beige, massive, matrix-supported, ≤2 m thick layer made of medium to fine ash size particles rich in plagioclase and pyroxene crystals with scarce lithics, scoria and pumice clasts. It overlies the lava flow partly covering the northern and northeastern slopes of the tuff ring (Fig. 2). This distribution of the deposit suggests that it was associated to the emission of the lava flow along an E-W fissure or fault (Fig. 1b).

4) Two dark to light-gray (1-3 cm) clast-supported layers rich in coarse ash pumice (fig. 3) covered by massive and laminated layers (2-8 cm thick) made of coarse ash to fine lapilli particles rich in scoria, pumice, lithics and crystals. The deposit lies on paleosols developed atop the lava flow and crops out on the northern and northwestern parts of the tuff ring. These layers are covered by brown paleosols, one of them is rich in orange pumice and green lithic (hornfels) characteristic of the 14 ka Tutti Frutti pumice fall deposit of Popocatépetl volcano (Siebe *et al*. 1995; Siebe *et al*. 2005).

A preliminary interpretation of the stratigraphic sequence suggests that activity at Xico started with a series of phreatomagmatic explosions (1) that emplaced base surges involving a basaltic andesitic magma followed by the emission of a lava flow (2) from the northeast external crater rim followed by pulsating explosions that emplaced pyroclastic density currents (3) and fallouts (4). Xico´s sequence covers a paleosol and underlies the ~14 ka Tutti Frutti eruption of Popocatépetl volcano.

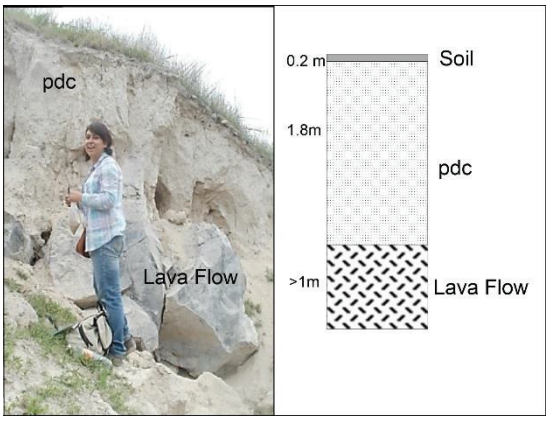

Figure 2. Photograph of an outcrop of the northern part of Xico volcano showing lava flows covered by an ash pyroclastic density current (pdc).

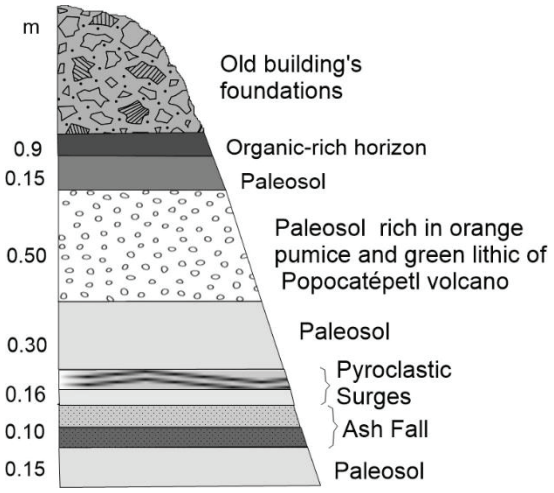

Figure 3. Composite stratigraphic column showing Xico's pyroclastic deposits, paleosols, and anthropogenic horizons.

References

Mooser, F., 1975, Historia geológica de la Cuenca de México, en Memoria de las obras del sistema de drenaje profundo del Distrito Federal, México, D.F., DDF, T. 1, 7-38.

Siebe, C., Macías, J.L., Abrams, M., Rodríguez Elizarrarás, R.S., Castro, R., Delgado, H., 1995, Deposits in East-Central México: Implications for Future Hazards: Geological Society of America, 1, 1-48.

Siebe, C., Macías, J.L., 2004, Volcanic hazards in the Mexico City metropolitan area from eruptions at Popocatépetl, Nevado de Toluca, and Jocotitlán stratovolcanoes and monogenetic scoria cones in the Sierra de Chichinautzin Volcanic Field: Geological Society of America, Fieldtrip Books 1, 77 pp.

Vázquez-Sánchez, E., and Jaimes-Palomera, L.R., 1989, Geología de la cuenca de México: Geofísica Internacional, v. 28, p. 133-190.

Eruptive dynamics of the Joya Honda maar, San Luis Potosí, México: Interpreted from stratigraphy and SEM analysis

Ricardo Saucedo[1], Wilfredo Gómez[1], Edwin Rivera[1], José Luis Macías[2], Yam Zul E. Ocampo[3], José R. Torres[1], Francisco Galindo[4], María del Carmen Ojeda[4], Gerardo Carrasco[5] and Teresa Scolamacchia[6].

[1]*Instituto de Geología Universidad Autónoma de San Luis Potosí (UASLP), México, rgiro@uaslp.mx*
[2] *Instituto de Geofísica, Universidad Nacional Autónoma de México (UNAM), Ex-Hacienda de San José de La Huerta C.P. 58190, Morelia, Michoacán, México.*
[3] *Facultad de Ingeniería, Área de Ciencia de la Tierra UASLP San Luis Potosí, México.*
[4]*Instituto de Metalurgia, UASLP San Luis Potosí, México*
[5]*Centro de Geociencias, UNAM, Campus Juriquilla, Querétaro, México.*
[6]*University of Munich, Department of Earth and Environmental Sciences (Geophysics), Germany.*

Keywords: Joya Honda crater, Maar, magmatic-hydromagmatic activity.

The Joya Honda maar (JHm) is located in central Mexico, 35 km N-NE of the city of San Luis Potosí. It belongs to the Plio-Quaternary Ventura-Espiritu Santo (CVVES) monogenetic alkaline volcanic field that is located in the eastern part of the Mesa Central province (Luhr *et al*. (1989); Aranda-Gómez *et al*. (1993); Aranda-Gómez *et al*. (2005)). The crater was excavated some ~0.3 Ma ago through Cretaceous limestones. The crater has an elliptical shape (~1.3 × 0.88 km wide) and a maximum depth of ~270 m with its major axis oriented to the ENE-WSW. The pyroclastic sequence of the JHm extends preferentially towards the NW-NE, 7 km from the source. At the crater rim, these deposits are 60-80 m thick on the NE-NW and 1-15 m thick on the S-SW wall.

Stratigraphy

A composite stratigraphic column of the JHm sequence is made of five deposits types separated by textural changes. These deposits have substantial differences among their granulometric distributions, and componentry. In fact, juvenile clasts through the sequence have clear differences in vesicularity, density, and morphology observed under the SEM. With this information, we interpreted the five deposits as different eruptive phases of the JHm eruption that consist from base to top of:

1) light-gray, basal fallout deposit clast-supported scoria beds interbedded with cross-stratified beds with soft sedimentary deformation (some up to 30 cm thick) that crops on NE and SW well crater. These beds are interpreted as strombolian fallouts and pyroclastic density currents (surges).

2) dark-gray, clast-supported layer rich in scoria fragments and xenoliths (spinel lherzolita and feldspathic granulite; Gómez Aranda and Luhr, 1996) up to 1 m thick interpreted similar to a spatter deposit that crops on the southern flank.

3) light-beige, cross-stratified, dune, layers rich in accretionary lapilli varying in thickness from 3 to 30 m covered by a 1.6 m thick, matrix-supported layer with blocks and ash interpreted as from phreatomagmatic explosions deposits that crops around the crater.

4) dark-gray, clast-supported layer (≤4 m thick) rich in scoria fragments and mantle xenoliths, interpreted as a fallout deposit that crops on the southern flank.

5) light-gray and light yellow for palagonite alteration, clast-supported scoria-rich layers fallout interbedded with occasional intercalations of cross-stratified layers base surge. All these layers have a total thickness of ~60 m (NE-NW wall) and ~7 m (S-SW wall). These layers are interpreted as a series of mamatic and hidromagmatic explosion deposits.

Preliminary Interpretation

The five eruptive phases identified indicate that the JHm eruption occurred as a series of explosions that started as magmatic explosions of Strombolian activity emplacing a basanite scoria with a low content of mantle xenoliths alternating with hydromagmatic pulses with the generation of base surges.

The eruption continued with hydromagmatic explosions yet followed by Strombolian activity to finally end with a violent Strombolian or micro-Plinian (Valentine and Gregg, 2008; Otterloo and Cas, 2013) phase that emplaced fallout beds interrupted by sporadic pyroclastic density currents surges.

The changes found in the eruptive dynamics of the JHm eruption respond to variations in the amount of magma-water interaction with time and space. These variations must have been subordinated

to factors as: speeds of magma rising, available groundwater, discharge rate, and magma degassing. Magma rise was also controlled by the geological and structural conditions dominated by the NE-SW fault system (López-Loera *et al*., 2008).

The distribution and textural characteristics of the deposits suggest that simultaneous or alternating vents could have worked during the eruption and possibly along a fissure.

Acknowledgements

This research was supported by grants from CONACYT (101548) and FAI-UASLP (04-25.25) to R. Saucedo.

References

Aranda Gómez, J.J., Luhr, J.F. Housh, T.B., Valdez-Moreno, G. and Chavez-Cabello, G. 2005. El vulcanismo tipo intraplaca del Cenozoico tardío en el centro y norte de México: Boletín de la Sociedad Geológica Mexicana, Volumen Conmemorativo del Centenario, Temas Selectos de la Geología Mexicana. Tomo LVII, núm. 5, 187-225.

Aranda-Gómez, J.J. y Luhr, J.F. 1996. Origin of the Joya Honda maar, San Luis Potosí, México: J. Volcanol. Geotherm. Res. 74:1-18.

Aranda-Gómez, J.J., Luhr, J.F. y Pier, J. 1993. Geología de los volcanes cuaternarios portadores de xenolitos provenientes del manto y de la base de la corteza en el estado de San Luis Potosí: Universidad Nacional Autónoma de México, Instituto de Geología, Boletín 106: 1-22.

López-Loera, H., Aranda-Gómez, J.J., Arzate, J.A., Molina-Garza, R.S. 2008. Geophysical surveys of the Joya Honda maar (México) and surroundings; volcanic implications: J. Volcanol. Geotherm. Res. 170: 135–152.

Luhr, J.F., Aranda Gómez, J.J. y Pier, J.G. 1989. Spinel lherzolite bearing, quaternary volcanic centers in San Luis Potosí, México. I. Geology, Mineralogy, and Petrology, J. Geophys. Res. 94 No. B6: 7916- 7940.

Otterloo, J., Cas A.F., R., Sheard, M. J., 2013, Eruption processes and deposit characteristics at the monogenetic Mt. Gambier Volcanic Complex, SE Australia: implications for alternating magmatic and phreatomagmatic activity: Bull. Vulcanol. 75:737: 1.21.

Valentine, G.A., Gregg, T.K.P. 2008. Continental basaltic volcanoes-processes and problems: J. Volcanol. Geotherm. Res. 177: 857-873.

Petrology of the Hopi Buttes Volcanic Field: implications for near-surface volcanism

Bruce Kjarsgaard[1], Nathalie Lefebvre[2], Michael H. Ort[3], Jorge Vazquez[4], James D.L. White[2], Kaj Hoernle[5]

[1] *Geological Survey of Canada, Ottawa, Ontario, Canada. Bruce.Kjarsgaard@NRCan.gc.ca*
[2] *University of Otago, Dunedin 9054, New Zealand.*
[3] *Northern Arizona University, Flagstaff, Arizona, U.S.A.*
[4] *Stanford University, Stanford, California, U.S.A.*
[5] *GEOMAR, Kiel, Germany.*

Keywords: Hopi Buttes, magma chamber, volcanism.

We present preliminary results from a petrological study of igneous rocks of the Hopi Buttes Volcanic Field (HBVF), situated at the southern margin of the Colorado Plateau, to better understand the potential influence of magmatic processes on surface volcanism. The suite of 88 samples consists of coherent/intrusive rocks (sills, dykes, plugs, flows) and fragmental rocks (spatter dykes, agglutinates and juvenile material from diatremes) rocks. The majority of samples are from recent fieldwork (2009 - 2012), but include data compiled from the literature. The samples covers a wide geographic spread of the HBVF (Fig. 1), however, the northwestern quadrant of the field has not been sampled.

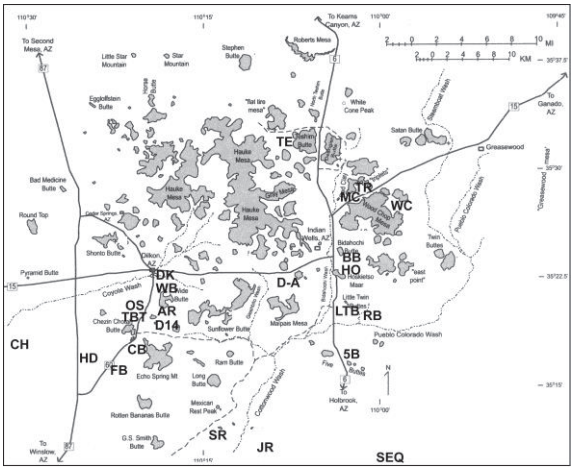

Fig. 1 – Hopi Buttes Volcanic Field. Sample locations indicated by bold letters (e.g., SEQ, RB, SR).

Utilizing the IUGS total alkalis – silica classification for volcanic rocks, the samples all fall in the basanite – tephrite field (Fig. 2). Previous petrographic results have variably classified the HBVF rocks as nephelinite, limburgite, and mochiquite. Normative mineral calculations indicate no samples can be classified as melanephelinite or nephelinite (modal nepheline to low, and/or albite to high). We suggest that the most robust classification for HBVF samples is limburgite (IUGS: pyroxene, olivine and opaques in a glassy groundmass with the same minerals). At HBVF, monchiquite samples are identical to limburgite, with the addition of amphibole (kaersutite) and/or mica (biotite) crystals, which tend to be present as large megacrysts (i.e., of cognate origin). We suggest that due to the geochemical similarity of samples classified as limbugite and monchiquite, the latter are best described as heteromorphs, which have crystallized from a near identical 'limburgite' melt that is more volatile-rich (H_2O).

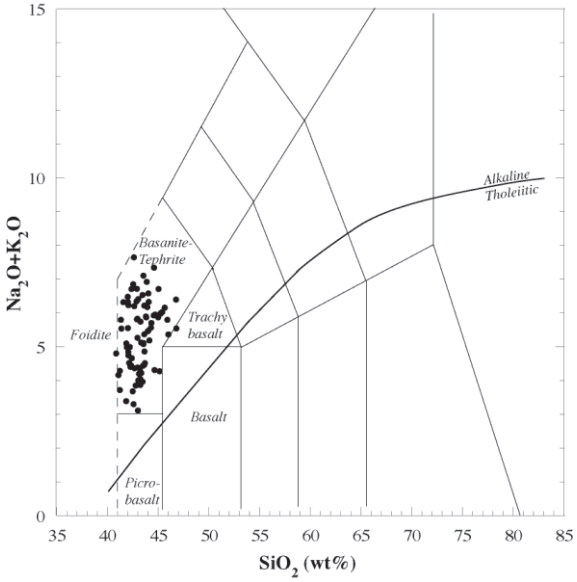

Fig. 2 – Total alkalis versus silica, Hopi Buttes samples.

Results from whole-rock geochemical studies are consistent with a well-defined fractionation trend e.g., increasing alkalis at near-constant SiO_2 (Fig. 2). Fractionation trends are well displayed on Harker diagrams (MgO on x-axis), as illustrated for compatible (Ni) and incompatible (Ce) elements (Figs 3a, b).

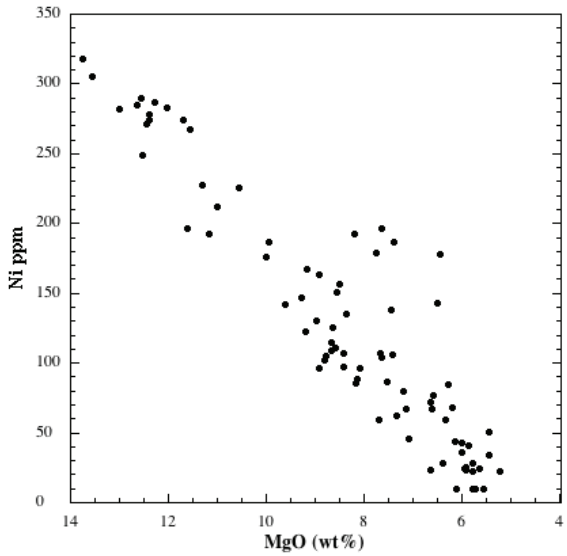

Fig. 3a – MgO vsersus Ni for HBVF samples.

The most primitive HBVF samples have ~12-13.5 wt% MgO with ~250-300 ppm Ni and 350-550 ppm Cr i.e., candidates for primary mantle melts. Based on current sampling, the most primitive rocks are from the southern and southeastern HBVF (Southeast Quarry, Round Butte, Little Twin Peaks, Standing Rocks East; Fig. 1). Intrusive rocks span the range of MgO concentration (13.5 – 5 wt%), whereas fragmental rocks consistently have < ~9 wt%. Rarely, individual volcanic centers are geochemically distinct and deviate from the HBVF trend, for example, fractionated Hoskietso samples are exceptionally incompatible element enriched (Fig. 3b).

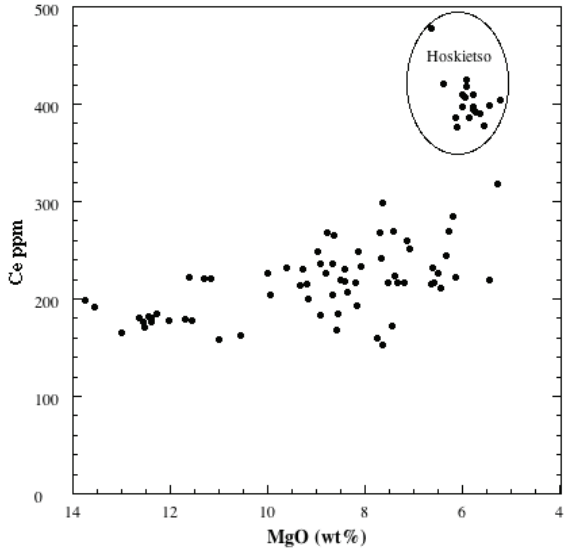

Fig. 3b – MgO vsersus Ce for HBVF samples.

A number of observations made from fieldwork, petrographic and geochemical studies are consistent with the idea that magma chamber processes are important in the HBVF. We note the following: (1) well-defined geochemical fractionation trends; (2) the presence of large, cognate kaersutite and biotite megacrysts, interpreted to be formed in an environment with increased pH_2O; (3) large, reverse zoned, pyroxene crystals, with iron-rich cores that have initially crystallized from a fractionated melt; (4) glomerophyric pyroxene 'aggregates', and; (5) the extreme rarity of lower crustal and spinel peridotite xenoliths, and absence of garnet peridotite xenoliths (due to high density settling).

At Hopi Buttes, volcanism is strongly influenced by near-surface phreatomagmatic processes. However, what are the potential influence(s) of magma chamber processes on near surface volcanism? Primitive versus fractionated melts have differing volatile solubility, density and viscosity. Magma chambers can variably 'accumulate' and/or buffer volatiles. In addition, depending on if the magma chamber is deep (lower- to mid-crustal) or high level, will influence the response time and potential volume of magma delivery to the surface. At the Castle Butte Trading Post spatter dyke - maar system, complex magma diversion and magma withdrawl define quite interesting shallow plumbing system dynamics. Are these plumbing dynamics consistent with a shallow, or deeper level magma chamber?

Acknowledgements

We thank the Navajo Nation Minerals Department for the required permit to conduct geologic investigations on the Navajo Nation.

Ten diatremes in three days in the Navajo volcanic field, Navajo Nation, Arizona and New Mexico, USA

Pierre-Simon Ross[1], James D.L. White[2]

[1] *Institut national de la recherche scientifique, Québec (QC), Canada, rossps@ete.inrs.ca*
[2] *University of Otago, Dunedin, New Zealand, james.white@otago.ac.nz*

Keywords: diatreme, minette, pyroclastic rocks.

The Navajo volcanic field (NVF) covers about 14,000 km^2 (this study) in the central part of the Colorado Plateau; it spans portions of Arizona, Colorado, New Mexico and Utah (Fig. 1). Over 80 Oligocene to Miocene (28-19 Ma) volcanoes and intrusive features are known in the NVF (Semken, 2003). Dikes and diatremes ("necks") are the main exposed features due to significant post-emplacement erosion; shallower features such as maars and lava flows are only preserved in a few areas such as Narbona Pass (Brand *et al.*, 2009). Scoria cones are not known but are likely represented by dikes at the current erosion level.

The predominant magma type in the NVF is minette, a potassic mica lamprophyre with about 50% SiO_2 (phenocrysts of dark mica, clinopyroxene, ±olivine in a dark aphanitic groundmass; Roden, 1981). Nine of the ten volcanoes visited by the authors in March 2014 were formed by explosive eruptions of the minette magma.

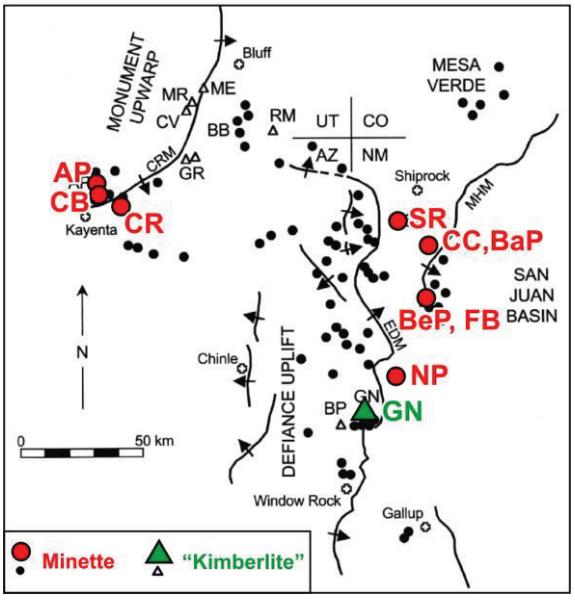

Fig. 1 – Sketch map of the NVF, modified from Semken (2003). Sites visited: **AP** = Agathla Peak, **BaP** = Barber Peak, **BeP** = Bennett Peak, **CB** = Chaistla Butte, **CC** = Cathedral Cliff, **CR** = Church Rock, **FB** = Ford Butte, **GN** = Gneen Knobs, **NP** = Narbona Pass, **SR** = Ship Rock.

A few diatremes of the NVF instead consist of "serpentinized ultramafic microbreccia" (SUM), which was formerly called "kimberlite". According to Semken (2003) these rocks contain "xenocrysts of olivine, enstatite, chrome diopside, chlorite, garnet, titanoclinohumite, oxide minerals, and apatite, as well as abundant crustal and mantle xenoliths" in a fine matrix, but no identifiable juvenile particles. Green Knobs, the tenth site visited by the authors, is a good example.

The most famous minette diatreme in the NVF is the 480 m-tall Ship Rock (Delaney, 1987). The 450 m-high Agathla Peak, another minette diatreme near Kayenta, is also an important landmark (Fig. 2), visible from a distance of 80 km (Williams, 1936); both are considered sacred by the Navajo people and were only examined from a distance. Due to space constraints only two of the ten visited sites will be briefly described in this abstract: Cathedral Cliff and Green Knobs, in the New Mexico part of the field.

Fig. 2 – Agathla Peak viewed from the west. The neck (eroded diatreme) sits on a pedestal of Chine Formation.

Cathedral Cliff (Fig. 1: **CC**) is a minette diatreme >250 m in diameter. We found no information on this volcano in the literature. It is located 14.5 km SE of Ship Rock, where Delaney and Pollard (1981) estimate ~1 km of erosion to the current land surface (Mancos Shale). The Cathedral Cliff diatreme infill is dominated by pyroclastic rocks with very minor coherent minette. The

pyroclastic rocks range from bedded to non-bedded, from coarse tuff to tuff breccia (lapilli tuffs dominate), and from lithic-rich to juvenile-rich. The lithic population includes abundant loose quartz grains. The bedded pyroclastic rocks dip steeply (~75°) inward on the E and S sides of the diatreme; these beds display low-angle cross bedding and are interpreted mostly at base surge deposits.

A sub-vertical column of non-bedded pyroclastic rocks, ~9 m in width, cuts disrupted bedded rocks on the SW side of the diatreme (Fig. 3). This column is interpreted to reflect the passage of one or several debris jets through the existing diatreme fill (see White and Ross, 2011). The N and NE sides of the diatreme expose mostly non-bedded pyroclastic rocks, locally with large sedimentary megablocks. Country rock breccias occur on the S side. The inferred erosion level of ~1 km indicates deep subsidence of the bedded pyroclastic rocks within the diatreme.

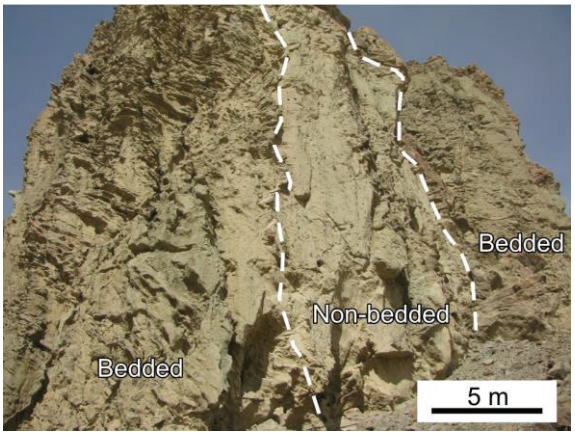

Fig. 3 – The minette diatreme at Cathedral Cliff (SW side, near-vertical face).

The **Green Knobs** (Fig. 1: **GN**) SUM diatreme (Allen and Balk, 1954; Akers *et al*. 1971; Smith and Levy, 1976) is approximately 800 m in diameter and circular in map view. The pale green rocks are clearly to cryptically bedded with inward dips ranging from ~80-85° near the margins of the diatreme to sub-horizontal toward the centre. The grain-size is mostly lapilli tuff. The average constituents are 12% lithic fragments, 43% crystal fragments (mostly olivine, pyroxene, quartz, and feldspar), and 45% fine matrix (Smith and Levy, 1976). The main types of lithic fragments are gneiss, granite, sandstone, shale and peridotite (Akers *et al*, 1971). The reported absence of juvenile clasts in this and other SUM diatremes is very intriguing. Volatiles apparently rose from the mantle and carried the olivine and other xenocrysts, also sampling the crust along the way. The gas-solids mixture finally erupted explosively to form a diatreme (and presumably an ejecta ring and crater). SUM diatremes occur in areas where minettes are also found (sometimes in the same diatreme, *e.g.* Buell Park, BP on Fig. 1), suggesting an association. According to Roden (1981), the volatiles that created the SUMs were either liberated from the garnet peridotite mantle during intrusion of minette magma into it, or they dissociated as a supercritical phase from the minette magma. Alternatively, the juvenile fraction in the SUMs may be "hiding" in the 45% optically irresolvable matrix.

Acknowledgements

Field work on the Navajo Nation was conducted under a permit from the Navajo Nation Minerals Department, Window Rock, Arizona.

References

Akers JP, Shorty JC, Stevens PR (1971) Hydrogeology of the Cenozoic igneous rocks, Navajo and Hopi Indian Reservations, Arizona, New Mexico, and Utah. USGS Professional Paper 521-D, 18 pp.

Allen JE, Balk R (1954) Mineral resources of Fort Defiance and Tohatchi quadrangles, Arizona and New Mexico. New Mexico Bureau of Geology and Mineral Resources, Bulletin 36, 192 pp.

Brand BD, Clarke AB, Semken S (2009) Eruptive conditions and depositional processes of Narbona Pass Maar volcano, Navajo volcanic field, Navajo Nation, New Mexico (USA). Bull. Volc. 71:49-77.

Delaney PT (1987) Ship Rock, New Mexico: the vent of a violent volcanic eruption. Geological Society of America, Centenial Field Guide - Rocky Mountain Section, pp 411-415.

Delaney PT, Pollard DD (1981) Deformation of host rocks and flow of magma during growth of minette dikes and breccia-bearing intrusions near Ship Rock, New Mexico. USGS Professional Paper 1202, 61 pp.

Roden MF (1981) Origin of coexisting minette and ultramafic breccia, Navajo volcanic field. Contrib. Min. Pet. 77:195-206.

Semken S (2003) Black rocks protruding up: the Navajo volcanic field. In: Lucas SG, Semken SC, Berglof WR, Ulmer-Scholle DS (eds) Geology of the Zuni Plateau. New Mexico Geological Society, Fall Field Conference Guidebook 54, pp 133-138.

Smith D, Levy S (1976) Petrology of the Green Knobs diatreme and implications for the upper mantle below the Colorado Plateau. Earth Planet. Sci. Lett. 29:107-125.

White JDL, Ross P-S (2011) Maar-diatreme volcanoes: a review. J. Volcanol. Geotherm. Res. 201:1-29.

Williams H (1936) Pliocene volcanoes of the Navajo-Hopi country. Geol. Soc. Am. Bull. 47:111-17.

Structure of the Pliocene Camp dels Ninots maar-diatreme (Catalan Volcanic Zone, NE Spain)

Oriol Oms[1], Xavier Bolós[2], Stéphanie Barde-Cabusson[2], Joan Martí[2], Albert Casas[3], Raúl Lovera[3] Mahjoub Himi [3,4], Bruno Gómez de Soler[5,6], Gerard Campeny Vall-Llosera[5,6], Dario Pedrazzi[2], Jordi Agustí[7].

[1] *Universitat Autònoma de Barcelona. Geology Department. Campus Bellaterra, Fac. Ciencies.08193 Bellaterra, Spain. Joseporiol.oms@uab.cat.*
[2] *Institute of Earth Sciences Jaume Almera, ICTJA-CSIC, Group of Volcanology. SIMGEO (UB-CSIC) Lluis Sole i Sabaris s/n, 08028 Barcelona, Spain.*
[3] *Economic and Environmental Geology and Hydrology Group, Department of Geochemistry, Petrology and Geological Prospecting, Faculty of Geology, University of Barcelona, Martí i Franqués s/n, Barcelona, Spain.*
[4] *Ecole Nationale des Sciences Appliquées d'Al Hoceima (ENSAH), University Mohammed Premier, Ajdir, Al Hoceima, Morocco*
[5] *Institut Català de Paleoecologia Humana i Evolució Social (IPHES), C/ Escorxador s/n, 43003 Tarragona, Spain.*
[6] *Àrea de Prehistòria, Universitat Rovira i Virgili (URV) Avinguda de Catalunya 35, 43002 Tarragona, Spain.*
[7] *ICREA Research Professor. IPHES-URV.*

Keywords: maar lake, diatreme, Catalan Volcanic Field, fossil.

The sedimentary infill of maar lakes is of potential interest to perform environmental reconstructions during Earth and life history. This is because such lakes enhance fossil preservation in their anoxic bottoms. Water stratification and anoxia are the result of the isolation from running waters and lake morphology. Such lakes are generally relatively deep if compared with their width, which is controlled by shape of the diatreme. Issues such as the effect of substrate rocks (soft *vs* hard maars) and processes are of crucial importance to understand the structure of the volcano itself. So that, paleolimnological determinations are not only based on the study of sediments or organism, but also on associated volcanism.

The sediments infilling several Quaternary and Holocene maars provide pollen and petrologic records that are used as successful paleoclimate proxies. Also, important paleontological sites with exceptional preservation are found in maar lakes (such as Messel and Eckfeld in the Eocene of Germany among so many others).

The studied structure (Figure 1) is located at the surroundings of Caldes de Malavella village (Girona province, Spain). Geologically it belongs to the Catalan Coastal Ranges, which is and alpine orogen that underwent an extensional phase during the Neogene, leading to the formation of several fault-bounded basins. Such faults are linked to the Catalan volcanic field (see summary in Bolós *et al* 2014). The faults bounding the La Selva Basin (LSB in figure 1A) contain maar lakes such as that of La Crosa de Sant Dalmai (Bolós *et al*., 2012) and the El Camp dels Ninots here studied.

First geological descriptions of the layers at Camp dels Ninots (Vidal, 1882) considered them to be of lacustrine origin, but no volcanic structure was considered. The work by Vehí *et al*. (1999) identified these lacustrine sediments to be the infill of a maar. This maar remained largely unknown since it hardly has any geomorphological evidence of the tephra ring. First fossil remains were reported by Vicente (1985), but recent research at Camp dels Ninots has lead to the discovery of a large amount of fossils representing the whole biota (Gómez de Soler *et al*., 2012) at 3 Ma. Large bovids, tapirs and rhinoceros are commonly found at this site. Small vertebrate (fishes, amphibians, reptiles, invertebrates etc.) are also common together with large plant remains. Camp dels Ninots has also been the target of a very detailed paleoenvironmental record based on pollen (Jiménez-Moreno *et al*., 2014).

Our study intended to reconstruct the structure of the maar by combining direct acquisition of geological data (surface mapping, sediment coring and logging, and outcrop trench description) with near surface geophysics that included gravimetry, magnetometry, self-potential, electrical resistivity tomography (ERT) and ground penetrating radar. The use of electrical resistivity tomography has been proved to be a very useful tool to obtain the internal structure of monogenetic volcanoes (Barde-Cabusson *et al*., 2013). That was the case of our study, which 9 transects (see Figure 1B) were compiled with 9 logs, to get a clear 3D structure of the maar. It can be easily identified the tephra ring, the maar infill and the different substrate (hard and soft, in SE and NW, respectively). Gravimetry is also a useful tool (see Barde-Cabusson *et al*., 2014) and permitted the identification of the diatreme root and the main faults affecting the hard rock basement.

In conclusion, the general structure of the Camp dels Ninots volcano (diatreme and faults location etc.) can be obtained with an accurate integration of geological and geophysical data.

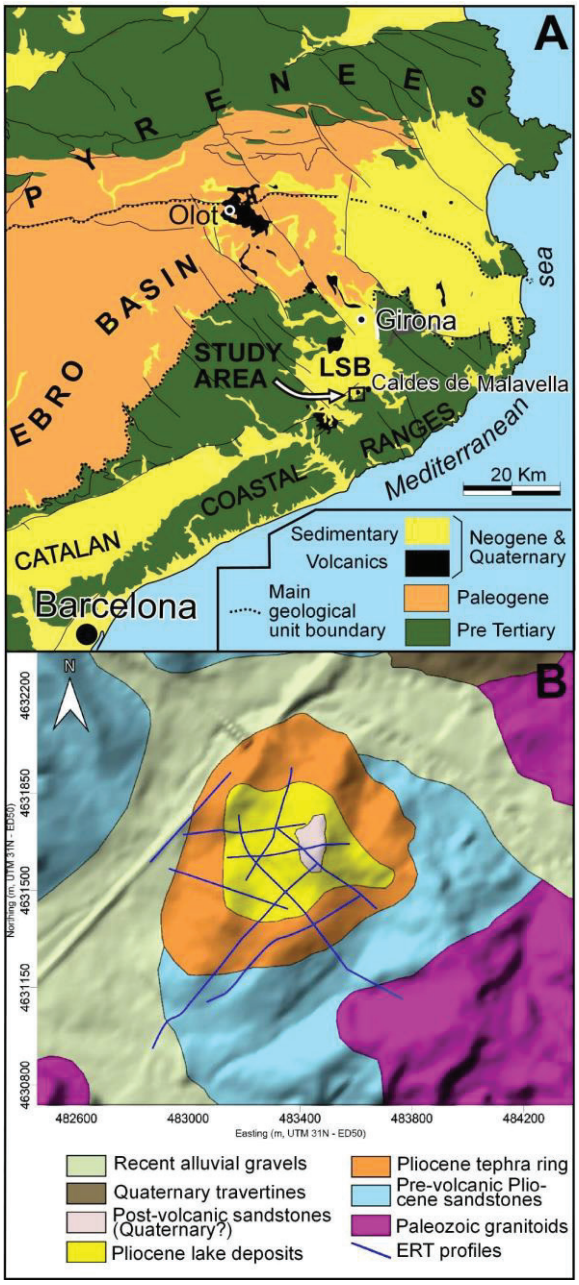

Fig. 1 – A) Geological Map of Western Catalonia. B) El Camp dels Ninots volcano with location of the studied ERT profiles.

Acknowledgements

This study was partially funded projects CGL2012-38358, -434-C03-03, -481 of the Spanish Government, by Generalitat de Catalunya and by the European Commission (FT7 Theme: ENV.2011.1.3.3-1; Grant 282759: "VUELCO"). Caldes de Malavella townhall kindly provided fieldwork logistics.

References

Gómez de Soler, B., Campeny Vall-llosera, G., van Der Made, J., Oms, O., Agustí, J., Sala, R., Blain, H.-A., Burjachs, F., Claude, J., García Catalán, S., Riba, D. and Rosillo, R. (2012): A new key locality for the Pliocene vertebrate record of Europe: the Camp dels Ninots maar (NE Spain). – Geologica Acta, 10 (1): 1–17.

Barde-Cabusson, S., Bolós, X., Pedrazzi, D., Lovera, R., Serra, G., Martí, J., Casas, A., 2013. Electrical resistivity tomography revealing the internal structure of monogenetic volcanoes. Geophysical Research Letters 40, 2544-2549.

Barde-Cabusson, S., Gottsman, J., Martí, J., Bolós, X., Camacho, A.G., Geyer, A., Planagumà, L., Ronchin, E., Sanchez, A., 2014. Structural control of monogenetic volcanism in the Garrotxa volcanic field (Northeastern Spain) from gravity and self-potential measurements. Bulletin of Volcanology 76, 788.

Bolós, X., Barde-Cabusson, S., Pedrazzi, D., Martí, J., Casas, A., Himi, M., Lovera, R., 2012. Investigation of the inner structure of La Crosa de Sant Dalmai maar (Catalan Volcanic Zone, Spain). Journal of Volcanology and Geothermal Research 247–248, 37-48.

Bolós, X., Planagumà, L., Martí, J., 2014. Volcanic stratigraphy and evolution of the Quaternary monogenetic volcanism in the Catalan Volcanic Zone (NE Spain). Journal of Quaternary Science.

Jiménez-Moreno G, Burjachs F, Expósito I, Oms O, Carrancho Á, Villalaín JJ, Agustí J, Campeny G, Gómez de Soler B, van der Made J. 2013. Late Pliocene vegetation and orbital-scale climate changes from the western Mediterranean area. Global Planet Change. 108:15–28.

Vehí, M., Pujadas, A., Roqué, C., Pallí, L., 1999. Un edifici volcànic inèdit a Caldes de Malavella (La Selva, Girona): El volcà del Camp dels Ninots. Quaderns de la Selva 1, 45–67.

Vicente, J., 1985. Troballa d'un *Leptobos* a Caldes de Malavella (La Selva). Societat d'Història Natural, Butlletí del Centre d'Estudis de la Natura del Barcelonès Nord, 1(1), 86-88.

Vidal, Ll.M., 1882. Estudio geológico de la estación termal de Caldas de Malavella (Gerona). Boletín de la Comisión del Mapa Geológico de España, 9, 65-91.

High-Resolution Geophysical Surveys and Modeling to Constrain Maar Geometry and Structural Control of Rattlesnake Crater, San Francisco Volcanic Field, Arizona

Anita Marshall, Sarah Kruse, Charles Connor, Rocco Malservisi

[1] *Department of Geosciences, University of South Florida, Tampa, Florida, USA.* amarshall3@mail.usf.edu

Keywords: geophysics, magnetic inversion, structural control.

Located 25 kilometers east of Flagstaff, Arizona, Rattlesnake Crater is a maar volcano in the San Francisco Volcanic Field. The oblong crater is approximately 1.4 kilometers at its widest point, with a crater floor at roughly the same elevation as the surrounding terrain. The crater is surrounded by an uneven tuff ring which is overlapped by a scoria cone volcano on the southeastern side. Improved understanding of its formation and evolution requires geophysical study because there are very few outcrops, and no digging is permitted on site. Geologic features related to the crater are further obscured by deposits from the overlapping scoria cone, as well as tephra from eruptions at nearby Sunset Crater.

We present the updated results of detailed magnetic and gravity surveys in and around Rattlesnake Crater. Field work completed in the summer of 2014 is added to data collected in 2012 (Fig. 1) in order to expand the magnetic map to include the entire tuff ring and more of the surrounding area.

The magnetic survey was completed on foot with a 50 - 100 meter line spacing over the entire survey area. Gravity readings were taken every 100 meters inside the crater and every 1000 meters outside the crater on intersecting survey lines; one running west to east, and another roughly north to south. Ground penetrating Radar profiles of the tuff ring using 50 and 100 MHz antenna were also collected as supporting data to the magnetic survey.

Anomalies in the crater include a substantial NW-SE trending elongate magnetic anomaly (1400 nT) on the west side of the crater and a smaller offset anomaly near the center of the crater. A positive gravitational anomaly (+1.0-1.5 mGal) was observed over the crater as well.

There is a clear linear trend observed with the strongest magnetic anomalies and the vent locations on the adjacent cinder cone. This may be evidence of structural control from a pre-existing fracture on this particular maar (Fig 2).

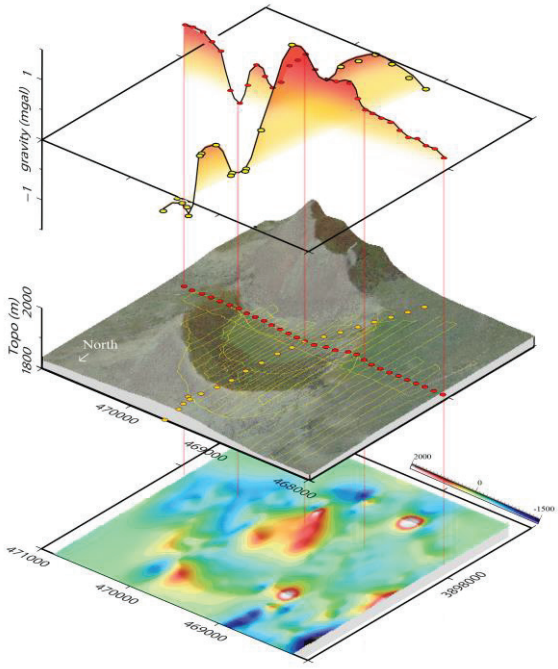

Figure 1. Results of the original survey at Rattlesnake Crater. The top layer shows Bouger gravity data illustrating a +1.4 nT anomaly over the crater. The second layer shows the field site with magnetic survey track lines in yellow, and gravity survey points as circles. The third layer shows the magnetic data with an upward continuation of 50 meters.

An unexpected result from the first survey was the distinctive positive magnetic anomalies observed in the tuff ring. An anomaly on the northwest side of the tuff ring is also located very close to a previously unmapped lava flow, and aligns with the observed linear trend (Fig. 2). Because the focus of our original survey was the crater, we only surveyed part of the tuff ring, and anomalies in the tuff ring itself were not well constrained. During our second trip, an expanded survey allowed us to get a more detailed look at anomalies in the tuff ring.

Possible explanations of positive magnetic signatures in the tuff ring could include a high emplacement temperature, late-stage igneous intrusions, or the remnants of older volcanic structures obscured by the eruption of the maar.

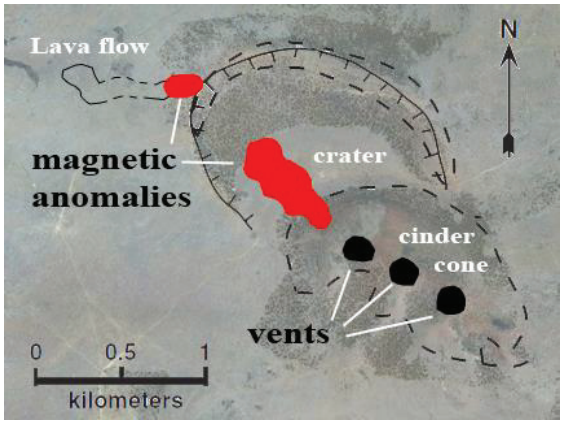

Fig 2.Rattlesnake Crater and its adjacent cinder cone. Geologic contacts from Valentine 2012. Note the strong linear trend of volcanic vents and magnetic anomalies.

A 2D model of the gravity and magnetic data was constructed to estimate the depth and geometry of the maar diatreme, as well as the possible morphology of an intrusive structure detected inside the crater. The data was modeled as an intrusive igneous structure with a shallow horizontal component surrounded by thermally magnetized diatreme fill.

A new 3D magnetic inversion model was created with the updated survey data using the inversion code developed by Laura Connor and Chuck Connor. The resulting 3D inversion is compared to the 2D model. The models are also compared to size and depth estimates calculated by Valentine (2012 using xenolith content.

Acknowledgements

This paper is the result of a group effort by the geophysics graduate students and faculty at USF. The survey crew included the listed authors plus Laura Connor, Makan Karegar, Aleeza Harburger, Jacob Richardson, Leah Courtland, Alexandra Farrell, Henok Kiflu, Christine McNiff, Mary Njoroge, Nate Nushart, and Kyra Rookey. Thanks for your hard work in the field!

Partial funding was obtained from the Geologic Society of America's Graduate Student Research Grant Program.

References

Valentine, G., 2012. Shallow plumbing systems for small-volume basaltic volcanoes, 2: Evidence from crustal xenoliths at scoria cones and maars. Journal of Volcanology and Geothermal Research, 223-224, 47-63.

Preliminary results on the application of Geophysical Methods in La Joyuela maar, Ventura Volcanic Field, central Mexico

Jesús Galván[1], David Torres[2], Ignacio Paz[1], Osvaldo Varela[1], Iyotirindranath Thompson[1], Héctor López[2] and Pablo Dávila-Harris[2]

[1] *Posgrado en Geociencias Aplicadas. Instituto Potosino de Investigaciones Científica y Tecnológica A. C., San Luis Potosí, S.L.P, México, jesus.galvan@ipicyt.edu.mx*
[2] *División de Geociencias Aplicadas. Instituto Potosino de Investigaciones Científica y Tecnológica A. C., San Luis Potosí, S.L.P, México.*

Keywords: magnetic, maar, Joyuela.

The purpose of this study is to characterize the Joyuela maar volcanic structure with in the Ventura Volcanic Field, located 31 kilometers at the north of the city of San Luis Potosi. The estimated age of the Joyuela is around 1.4 million years (K/Ar; Aranda-Gomez, 1996) see Figure 1.

La Joyuela maar, with its horseshoe shape has a diameter larger than 1,500m and a depth of 100m from the top to the base of the in filled crater. The crater walls expose Mesozoic limestone and shale from the Cuesta del Cura and La Peña formations, unconformably overlained by strombolian volcanic spatter grading into a thick phreatomagmatic pyroclastic sequence in proximal facies that thins towards the south-west (Dávila, 2003).

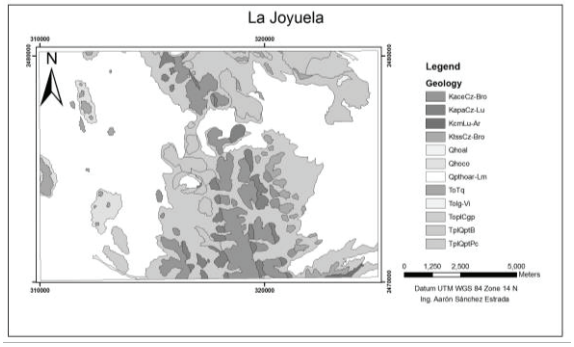

Fig. 1 –In this picture show geology in the area.

This study focuses on the magnetic characterization of the crater with the purpose of identifying a possible diatreme, assumed to exist at depth. Potential geophysical methods such as magnetic and gravity surveys can give information about different materials. In Magnetism we measurement the different magnetic susceptibility presents on materials which we expect to be between the alluvium and the diatreme.

To characterize La Joyuela, 7 magnetic sections were performed with NE-SW direction and separation of 250 meters between them. The space between the stations was of 50m, however when the gradient changed quickly the value was changed to 25m when. The acquisition of the information was made with three magnetometers, two geometrics G -856 and one GEM GSM -19. Geometrics G-856 was used as a base station taking measurements every 3m to carry out the diurnal correction.

To determine the residual magnetic field, that allows, remove the magnetic contribution due to the nucleus, and observe susceptibility induced by surface rocks. The average was obtained in all the raised lines and the values acquired were subtracted to get residual magnetic field. A residual magnetic field plan was generated. We applied reduction to the pole with a magnetic inclination of 59.13° and a declination of 5.73° but analyze the information as if we were on the pole without distortion.

Figure 2 shows the results of the magnetic survey where it is possible to observe the edge of the crater. The high magnetic that are generated are due to the main structure which is found at the north side becoming less intensive around La Joyuela and with a horseshoe shape. West of the structure high values can be perceived, these are caused by a basalt dome that surface. To the east of the structure pyroclastic domes are encountered; these are exposed on Highway 57.

At center of La Joyuela, a zone of low magnetic field value can be distinguished. This may be interpreted as the alluvium fill that could probably covers the diatreme or explosive breccias deep within the structure. At the center of the maar, a small magnetic high can be observed. This anomaly value, with other higher values surrounding it, is presumed to be the response caused by the maar diatreme.

We have also used aerial magnetic data to support our observations. The analysis of the aerial magnetic information consisted on the reduction to the pole. Additionally the pseudo gravity filter in horizontal gradient was defined to determine the general aspects of the area. To define the magnetic domains we used in reduce to pole and the upward continuation filter.

The aerial magnetic map contour, shows that the Joyuela mar geologic structure are in the limits of two aerial magnetic domains, associated one with a volcanic unit, and the other with a sedimentary geologic unit (López et.al. 2008).

This work will be complemented with gravity data and electric and electromagnetic surverys. With gravity data we expect to see density contrasts at depth which can be inferred as the presence of a possible diatreme or eruptive breccia beneath. Finally, magnetotelluric surveys will also be made to dig deeply and with less uncertainty to resolve the presence or not of a diatreme structure.

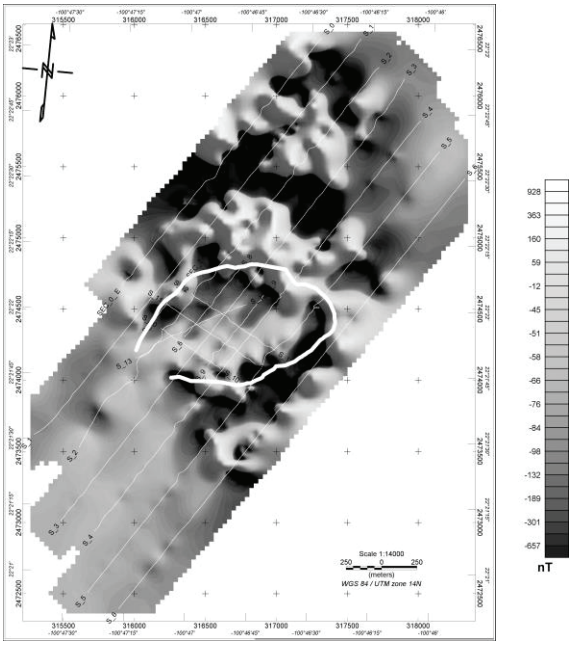

Fig. 2 – Ground magnetometry of "La Joyuela" showing 14 raised sections. The horseshoe-shaped line defines the limits of the caldera.

All these information gathered, will help to generate two-dimensional models to simulate the underground structure beneath the La Joyuela maar volcano.

Acknowledgements

We appreciate the support given during the fulfillment of the field surveys and lab work to the Instituto Potosino de Investigación Científica y Tecnológica, A.C. (IPICYT). We acknowledge help from students Aarón Sánchez and Alejandro Rosas for the support acquiring field data.

References

Aranda G.J.J., Luhr, J.F, 1996. Origin of the Joya Honda maar, San Luis Potosí, México. Journal of Volcanology and Geothermal Research 74, 1-18.

Baranov, V., 1957. A new method for interpretation of aeromagnetic maps: Pseudo gravimetric anomalies. Geophysics 22, 359-383.

Baranov, V., Naudy, H., 1964. Numerical calculation of the formula of reduction to the magnetic pole. Geophysics 29, 67-79.

Dávila, H.P., 2003. Historia eruptiva del crater "La Joyuela", San Luis Potosi. Thesis, Area Ciencias de la Tierra. Facultad de Ingenieria. Universidad Autonóma de San Luis Potosí. México 112pp.

López, L.H., Aranda, G.J.J., 2008. Geophysical surveys of Joya Honda Maar (México) and surroundings; volcanic implications. Journal of Volcanology and Geothermal Research 170 (3-4),135-152

López L.H., 2002. Estudio de Anomalías magnéticas y su relación con las estructuras geológicas y actividad eruptive de los complejos volcánicos actives de Colima y Popocatépetl, México. Ph D. Thesis, Instituto de Geofísica, Universidad Nacional Autónoma de México. 232 pp.

Teagan, N.B., Laurent, .A., 2012. Three-dimensional potential field modeling of a multi-vent maar-diatreme – The lake Coragulac maar, Newer Volcanics Province, south-easter Australia. Journal of Volcanology and Geothermal Research 235-236: 70-83.

Wiliam J.H., Ralph R.B. Von F., Afif H.S., 2013. Gravity andMagnetic Exploration Principles, Practices and Applications:Cambridge.

Robert J. Lillie., 1999. Whole earth geophysics an introductory test book for Geologists & Geophysicists: Prentince Hall.

White. J.D.L., 1991. Maar-diatrema phreatomagmatis mat Hopi Buttes, Navajo Nation (Arizona), USA, Bullentin of Volcanology 53, 431-446.

Characterization of past phreatomagmatic eruptions in the Auckland Volcanic Field, New Zealand

Javier Agustín-Flores[1], Károly Németh[1], Shane Cronin[1], Jan Lindsay[2], and Gábor Kereszturi[1]

[1] *Volcanic Risk Solutions, Massey University, Palmerston North, New Zealand. j.agustinflores@massey.ac.nz*
[2] *School of Environment, The University of Auckland, Private Bag 92019, Auckland, New Zealand.*

Keywords: phreatomagmatism, substrate, water-magma ratios.

The Auckland Volcanic Field (AVF) (Fig. 1) comprises about 52 individual olivine-rich alkali basalts and basanite eruption centres over an approximate area of 360 km^2. The minimum DRE volume of the eruption products of the AVF is 1.7 km^3 (Kereszturi *et al*., 2013). Eruptions have been sporadic since 250 ka, but more frequent since ~50 ka (Bebbington and Cronin, 2011). The outstanding feature of the AVF is the abundance of volcanic products inferred to be the result of explosive phreatomagmatic eruptions with approximately 75% of the volcanoes in the AVF showing evidence of phreatomagmatism at least in their initial stage of eruptive phases.

As a general outline, the northern part of the AVF (Fig. 1) is characterized by a pre-eruptive substrate composed of the >300 m-thick, aquifer-bearing sequence of Miocene-aged sandstones and mudstones, whereas in the southern AVF (Fig. 1) the volcanoes erupted through the same rocks, but with a 10-60 m+ cap of unconsolidated and saturated Plio-Pleistocene, shallow marine to fluvio-lacustrine sediments. This implies that at least two substrate types prevail in the AVF (Fig. 1): (1) hard substrate in the northern AVF and (2) a shallow soft substrate capping the Miocene rocks to the south. Two of the studied volcanoes, Motukorea and North Head, occur in situation (1) in the northern AVF (Figs. 1,2), while Maungataketake is situated to the south in substrate type (2) (Figs. 1,2).

The mixing ratio of magma to water is conventionally regarded as the main factor that contributes to the explosive potential of phreatomagmatic volcanoes (*e.g.* Sheridan and Wohletz, 1983; Kokelaar, 1986). However, vent-specific factors influence the geometry and nature of magma-water interaction and create distinctive volcanoes with a range of eruptive processes (White, 1996). These factors include substrate lithological and hydrogeological characteristics, tectonic/faulting patterns, surface water, magma confinement pressure, and magma composition. Relating these factors in a quantitative way to assessing hazard remains stalled however because the role of each factor in modifying phreatomagmatic eruptions is not well known.

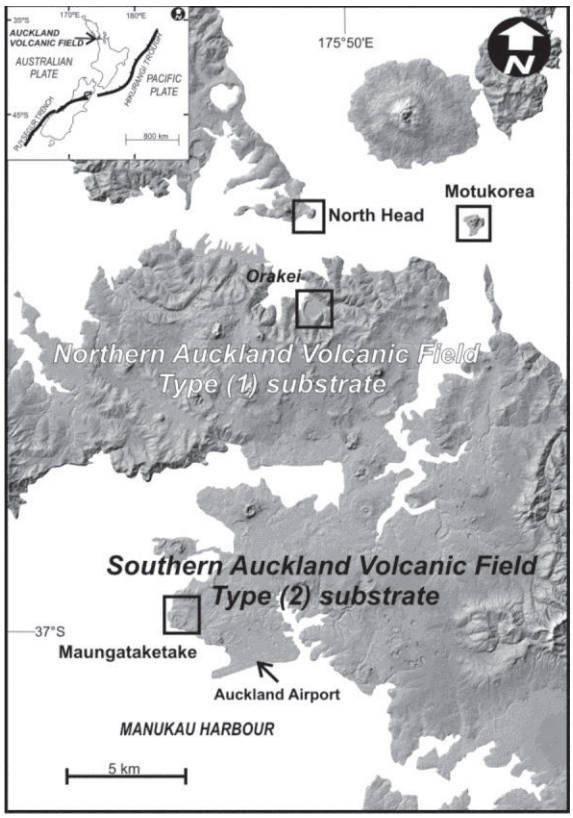

Fig. 1 – Location of the studied volcanoes within the Auckland Volcanic Field

Our approach to addressing this knowledge gap was to analyse the morphological, stratigraphic, and sedimentary deposit characteristics of volcanoes with similar composition and size, but in differing eruption site conditions. Using pyroclast and volcano-sedimentary characterization, coupled with the inference of the syn-eruptive geological and hydrogeological substrate conditions, we have been able to determine the role of the substrate in influencing the first stages of magma intrusion and eruption. At Motukorea (Agustín-Flores *et al*, in prep), its location primarily substrate type (1) (Fig. 2) we find ~60 vol.% of accidental fragments from the Miocene rocks in the tephra ring. The hard, but

fractured substrate promotes energetic explosions between confined magma and water within narrow cracks and fractures. This produces highly energetic wet and dry base surges. An exhaustion of the ground-water during this eruption was followed by its re-infiltration into the diatreme. Further downward excavation brought access to water from deeper fracture-hosted aquifers to fuel phreatomagmatic explosions. By contrast, in Maungataketake (Agustín-Flores *et al*, 2014) (Fig. 2), the thick upper soft substrates promoted dominantly mild to weak shallow seated explosions restricted to within the unconsolidated sediments as evidenced by the 65 vol.% accidental fragment from this lithology. This produced dominantly wet surges and the water table remained stable throughout the eruption. Collapse and flow of liquefied, saturated sediment led to little downward excavation and focusing of magma-water interaction. In addition to our research, a recent study on Orakei volcano (Németh *et al*., 2012), erupted through substrate type (1) (Fig. 1), illustrates an example of a fault/valley constrained eruption system, where the confinement of magma in a narrow area led to a small volume, but highly explosive phreatomagmatic eruption. Here some surface unconsolidated Plio-Pleistocene sediments were present (few meters), and a fair bit of material was milled in the eruptive vent. Yet the overall presence of Miocene rock-fragments within the deposits indicates efficient disruption of this type of substrate, nevertheless in a more focused way than at Maungataketake.

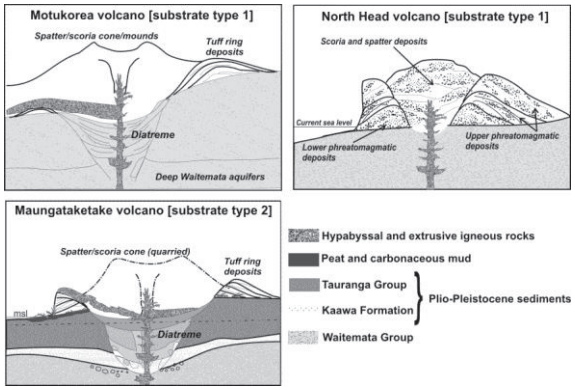

Fig. 2 – Cartoons representing the hypothetical cross-sections of the studied volcanoes and the substrate involved in the eruptions.

Although broadly similar geologically, the three eruptions described represent substantially different hazard scenarios. The third environmental influence on phreatomagmatic eruption style is exhibited at North Head volcano (Agustín-Flores *et al*., in revision) (Fig. 2), where shallow sea water (<16 m) covered the eruption site. Here, unlike the other AVF centres, the North Head tephra has little country rock material (>90 vol.% juvenile fragments in tuff cone deposits) and deposits are dominated by collapsing Surtseyan style tephra jets and weak up-rush generated surges.

Although tuff ring/maar-diatreme-related explosive phreatomagmatic eruptions producing violent base surges have dominated the past hazards in the Auckland field (*e.g.*, Németh *et al*., 2012), less energetic Surtseyan-type eruptions or shallow soft-sediment influenced eruptions may be of greater likelihood. Recognising that over 90% of the AVF lifespan involved lower glaico-eustatic sea levels, it must be noted that for future forecasting that around 35% of the field is now covered by water (Fig. 1). Recognizing the broad spectrum of phreatomagmatic eruptions within hard and soft substrates, as well as very shallow water environments in the AVF is a key component to a more precise understanding of the range and likelihood of future hazard in the area.

Acknowledgements

This research is supported through grants by the Volcanic Risk Solutions (Massey) and part of the research supported by the NZ FRST-IIOF Grant "Facing the challenge of Auckland's Volcanism" (MAUX0808), and the DEVORA project.

References

Agustin-Flores, J., Nemeth, K., Cronin, S., Lindsay, J., Kereszturi, G., Brand, B., Smith, I.E.M., 2014. Phreatomagmatic eruptions through unconsolidated coastal plain sequences, Maungataketake, Auckland Volcanic Field (New Zealand). Journal of Volcanology and Geothermal Research. 276: 46-63.

Bebbington, M.S., Cronin, S.J. 2010. Spatio-temporal hazard estimation in the Auckland Volcanic Field, New Zealand, with a new event-order model. Bulletin of Volcanology DOI: 10.1007/s00445-010-0403-6.

Kereszturi, G., Németh, K., Cronin, J.S., Agustin-Flores, J., Smith, I.E.M. and Lindsay, J., 2013. A model for calculating eruptive volumes for monogenetic volcanoes – Implication for the Quaternary Auckland Volcanic Field, New Zealand. J Volcanol Geoth Res, 266: 16-33.

Kokelaar, P., 1986. Magma-water interactions in subaqueous and emergent basaltic volcanism. Bulletin of Volcanology 48: 275-289.

Németh, K., Cronin, S.J., Smith, I.E.M., Agustín-Flores, J., 2012. Amplified hazard of small-volume monogenetic eruptions due to environmental controls, Orakei Basin, Auckland Volcanic Field, New Zealand. Bull Volcanol, 74: 2121-2137.

Sheridan, MF, Wohletz, KH, 1983. Hydrovolcanism: Basic considerations and review. Journal of Volcanology and Geothermal Research 17, 1-29.

White, JDL, 1996. Impure coolants and interaction dynamics of phreatomagmatic eruptions. Journal of Volcanology and Geothermal Research 74: 155-170.

Deposits associated to San Diego Maar volcano (Colombia)

Maria Luisa Monsalve[1], Ivan Darío Ortíz[1], and Gianluca Norini [2]

[1] *Grupo Geotérmia, Servicio Geológico Colombiano, Bogotá, Colombia.* mmonsalve@sgc.gov.co

Keywords: San Diego Maar, phreatic -phreatomagmatic activity, Acretionary lapilli.

Maar volcanoes are not common in Colombia. Geothermal exploration by the Colombian Geological Survey, in the San Diego area (Caldas), allowed to characterize the volcanic structures in the area and the identification of the related deposits. The San Diego maar is located north of Colombia's Central Range, and it is displaced about 90 km northeast of the active northern segment. maar is nearly circular pyroclastic ring, 2.7 km in diameter. Its crater is occupied by a lake (Figure 1). A "plug" or dome (Morro de San Diego) is located in its NE portion. This vent was previously called the "volcano of San Diego" by Toro (1988). Norini (2013) and Monsalve and Ortíz (2014) suggested the presence of another concatenated pyroclastic ring, which may be preserved in the NE sector of the dome.

Figure 1. San Diego maar structure and the “morro” of the same name.

The first studies on these structures were carried out in the 80´s by Toro (1989), Toro (1991), who recognized San Diego volcano, and the geothermics national reconnaissance identified the maar structure.

Field work in the area allow to identified deposits associated with phreatic to phreato – magmatic activity, consisting of pyroclastic breccias, flows and surges with a wide distribution in the area, forming the tuff ring of San Diego maar. Powerful and very fine ash deposits with significant variation in facies and abundant accretionary lapilli associated with intense phreatic activity seems to be associated with a dacitic – ryolithic tuff cone giving rise to magmatic phase of “Morro the San Diego” dome. Other Important local deposits of accretionary lapilli, located south of San Diego structure, suggests another possible phreatic vent, not yet recognized.

The main sequence of San Diego maar deposits, outcrops almost uninterrupted around the structure forming the tuff ring, but not in equal proportions, showing variations of the eruption styles, between relatively dry and wet phreatomagmatic conditions. In general, all the deposits found in the area are deeply weathered.

Three main eruption phases are recognized, and a probable volcanic hiatus between the basal phase and the uppermost phases, is marked by the presence of a thick pumice fall deposit that seems to be associated to a different vent (Escondido de Florencia volcano), which is located nearly 20 km southwest of the maar. The hiatus suggests that the San Diego magmatic system may have reactivated. The pyroclastic succession shows how complicated the evolution of maar volcanoes can be, and raises also the question from other authors (*i.e.* Jordan et al., 2013. Ngwa, et al., 2011) if these systems are actually monogenetic.

The depositional sequences are defined by abrupt changes in clast size, dominant facies, block abundance and composition. Evidence for water in the eruptive system includes, among others, abundant, accretionary lapilli, bedding, and lithics, in the maar deposits, originate from country rock formations. Changes in dominant facies and facies patterns define distinct units, which reflect changes in eruptive dynamics with time. The early eruptions are interpreted to have been dominated by phreatomagmatic blasts, which caused a progressive deepening of the eruptive center, followed by a transition to dominantly magmatic behavior in the upper sequence, tuff cone and plug dome growth occurring at the later stage of maar activity.

Deposits associated with San Diego Maar

The lowermost unit corresponds to a succession of coarse lithic-rich breccia with blocks up to 20 cm in diameter, and matrix supported breccia. The lithics are gneiss and schists accidental fragments with subordinate dacitic – ryolithic fragments coated by a glass (?) derived clay. Towards the southern sector, this deposit overlies the metamorphic basement at the base of pyroclastic ring.

Between the lowermost unit and the upper ones, a argillaceous yellow pumice deposit is found in most of the maar sequence outcrops.

The normal graded pumice deposit is composed of porphyritic fibrous pumice lapilli, in less proportion grey lava lapilli and accidental lithics of granodiorite which seems to comes from the basement of the "Escondido de Florencia" volcano, has an age of 30 Ka.

The intermediate maar phase is a diluted CDP sequence. The best exposition is in the northeastern part of the rim. It consist of at least four main levels (2.5m. thick), distinguishable by color and grain size (very fine to medium ash) and lamination: The lower part of the sequence is constituted by beige gray alternating laminations continues toward the top with a yellowish to brown laminated deposit, followed by a massive fine grained yellowish unit with sporadic intercalations of light gray levels and finally, at the top of the sequence, a massive package of dark gray color and irregular thickness is exhibited.

The upper phase of the maar rim is the most widely distributed deposit around San Diego structure, reaching up to 15 m of thickness at its ENE edge. The unit consists of laminated medium to coarse ash and lapilli, composed by crystals, altered and fresh lithics and some pumice fragments. The deposit varies, in a transitional way to a massive coarse ash unit with the same components.

"Morro de San Diego"

An irregular dome landform, 350 m tall, is located in the northeastern side of the "Laguna de San Diego" lake. The Morro de San Diego Dome is formed by a biotite rhyolite porphyry with a 69% SiO2 content (Toro, 1989). The dome is partially surrounded by a massive, compact, gray deposit of very fine to medium ash, with 67% SiO2 content, showing vertical and horizontal variations of facies, given by the grain size, lithic and accretionary lapilli content. Its main characteristic is the accretionary lapilli content, wich locally form highly enriched layers. The outcrops of these deposits usually form vertical walls up to 8 m high. This deposit is thought to have preceded the emergence of the dome.

Probably, before the final magmatic phase, a tuff cone (a closely related to phreatic – phreatomagmatic activity structure (Wohletz, and Heiken, 1992)), built at the east edge of the maar. The tuff cone is now eroded and filled by the plug or San Diego dome, and correspond to the last magmatic stage (magmatic) of the maar construction.

References

Wohletz, K.H., and Heiken, G. 1992. Volcanology and Geothermal Energy. Berkeley: California University Press. 432 p.

Jordan, S.C., Cas, R.A.F, Hayman, P.C. (2013) The origin of a large (>3 km) maar volcano by coalescence of multiple shallow craters: Lake Purrumbete maar, southeastern Australia. Journal of Volcanology and Geothermal Research 254,5–22.

Monsalve & Ortiz, 2014. Reconocimiento vulcanológico área geotérmica de San Diego. SGC, informe interno, 35 p.

Ngwa C.N., Suh C.E., Devey C.W. (2010). Phreatomagmatic deposits and stratigraphic reconstruction at Debunscha Maar (Mt Cameroon volcano) Journal of Volcanology and Geothermal Research 192, 201–211.

Norini, G., 2013. Bases metodológicas para estudios de volcanotectónica en áreas de interés geotérmico: Informe final de la primera etapa del estudio de geología estructural en el área geotérmica del Volcán de San Diego. 32 p. Bogotá (Colombia) – Milán (Italia). SGC informe interno.

Toro (1988). Etude du volcan de San Diego (Caldas), et des depots de Nariño (Antioquia), Colombie. Contributions a l'etude des tephras en climats tropicaux humides, Memoire de fin d'etude.

Toro (1989). Caracterización del vulcanismo de San Diego y estudio de los depósitos de San Diego (Caldas) y de Nariño (Antioquia), Colombia. Memorias del V congreso Colombiano de Geología, Bucaramanga. Marzo 14 -17, p 419 – 440.

Toro 1991. Geología de la zona del volcán de San Diego, departamento de Caldas Colombia. Simposio Magmatismo Andino. Manizales Colombia.

Dyke disintegration: shallow interaction between dykes and host-rock in the root zone of maar-diatreme volcanoes, and their link to surface eruptions

Charlotte E McLean[1] and David J. Brown[1]

[1]*School of Geographical and Earth Sciences, University of Glasgow, Glasgow, G12 8QQ, UK c.mclean.1@research.gla.ac.uk*

Keywords: high-level, dyke, disintegration.

At shallow stratigraphic levels within maar-diatreme volcanoes, dykes can be emplaced into water-saturated, unconsolidated or partially consolidated host-rock. This can occur in the root zone or in intra-diatreme fragmentation zones, where dykes are emplaced into volcaniclastic diatreme fill (White and Ross, 2011). As magma enters this so-called "soft-rock" environment, ponding becomes more frequent due to the density contrasts and differences in lithostatic strength between diatreme deposits and country rock, and influences how the intrusion is emplaced (Lorenz and Haneke, 2004). Unconsolidation and water-saturation of diatreme deposits supports sub-surface magma-sediment interactions and secondary phreatomagmatic explosions (Kokelaar, 1986). This can lead to peperite formation and thermal mobilisation of host-sediments directly surrounding dykes, which can subsequently aid the disintegration of dykes upon emplacement.

In this study, we document basaltic dykes that have been emplaced at much higher stratigraphic levels within maar-diatreme volcanoes than previously recognised, and also provide evidence for dykes directly feeding "surface" extrusion events. The overall dyke geometries and degree of dyke fragmentation have been investigated at two localities (Carboniferous maar-diatremes in Fife, Scotland and Quaternary Surtseyan-type tuff-rings located on the south coast of Iceland), to establish host-rock controls on dyke emplacement into maar-diatreme volcanoes, the stratigraphic level of dyke termination and disintegration, and the potential feeding of "surface" eruptions. At both locations, shallow dykes and inclined sheets intrude volcaniclastic sediments and intra-"vent" deposits. A variety of interactions are seen, including: 1) complex dyke disintegration from coherent dykes, through dykes with brecciated carapaces, to coherent clastogenic bodies (Fig. 1); 2) fluidal and blocky peperites on a range of scales (Fig. 2); and 3) fluidisation of host-sediments. This dyke disintegration occurs at much higher levels than previously recorded (<10 m below surface), and locally, we record dykes directly feeding "surface" extrusion events (hyaloclastite/lapilli-tuff and breccia).

By studying the complexity of how intrusions interact with host-rock in the shallow sub-surface, the scales at which they interact, and the intrusion geometries, a reconstruction of the shallow sub-surface volcanic plumbing network of maar-diatreme volcanoes can be established. This work will significantly improve our understanding of the structure of these volcanoes, how extrusive volcanic processes are potentially fed, and provide a detailed model of the plumbing systems/conduits beneath volcanic edifices.

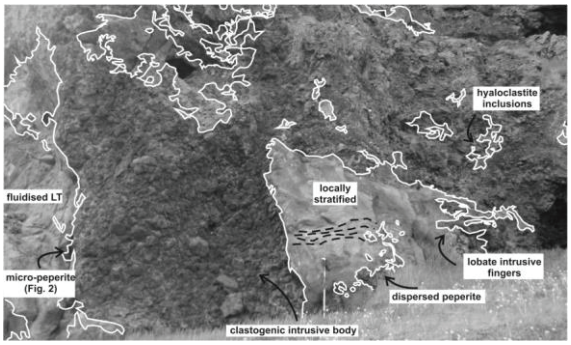

Fig. 1 – Clastogenic intrusive body cross-cutting locally stratified hyaloclastite lapilli-tuff (LT). Host-rock consists of hyaloclastite tuff-ring and has locally fluidized by intrusive bodies. Walking pole for scale.

Fig. 2 – Micro-peperite at edge of clastogenic intrusive body

References

Kokelaar, B. P. 1986. Magma-water interaction in sub aqueous and emergent basaltic volcanism. Bulletin of Volcanology. 48: 275-289.

Lorenz, V., and Haneke, J., 2004. Relationship between diatremes, dykes, sills, laccoliths, intrusive-extrusive domes, lava flows, and tephra deposits with unconsolidated water-saturated sediments in the late Variscan intermontane Saar-Nahe Basin, SW Germany: Geological Society, London, Special Publications, 234: 75-124.

White, J.D.L, Ross, P.S., 2011. Maar-diatreme volcanoes: a review. J Volcanology Geothermal Research 201: 1–29

Volcanology and Geochemistry of the Befang-Oshieng volcano (Oku Volcanic Field- Cameroon Line)

Ngahane Mbami L., Juinang Dieugnou J, Tchouankoue J.P., Azeuda k., Mouafo L., Temdjim R.

University of Yaounde I, Department of earth Sciences, P.O. Box 812 Yaounde-Cameroon. lindangahane13@yahoo.fr

Keywords: Maar, Befang, Cameroon.

The Cameroon Volcanic Line (CVL) is a huge tectonomagmatic structure characterized by a N30°E alignment of oceanic and continental volcanoes and plutovolcanic bodies over a distance of more than 1500 km. It is the unique example on Earth of an active intraplate alkaline tectonomagmatic alignment simultaneously developed into both oceanic and continental domains (Deruelle *et al.*, 2007).

Field work and photo-interpretation (Tchoua, 1974; Gouhier *et al.*, 1974; Cornacchia and Dars, 1983; Déruelle and Régnoult, 1983), as well as remote sensing and autocorrelation analyses of surface distribution of sub-volcanic and volcanic complexes (Moreau *et al.*, 1987) revealed four main networks of rectilinear lineaments or directions of rocks fracturing associated with the CVL:

-The N-S trend also termed the Pan-African belt trend,
-The N70° trend also called the Adamawa trend, straighting W-E in Northern Cameroon,
-The N135° trend or the Upper Benue trend and
-The N30° trend or the CVL trend.

Several hypothesis to explain the origin of the CVL have been formulated. Amongst others are :

-Epeirogenic movements that generated horsts and grabens bordered by boundary faults trending SW-NE (Gèze, 1943; Vincent, 1970; Gouhier *et al.*, 1974; Déruelle, 1982),
-A rifting (Vincent, 1970; Tchoua, 1974; Lasserre, 1978; Fitton, 1983),
-Rejuvenation of ancient faults (Déruelle, 1982; Déruelle et al, 1983; 1984; Nni, 1984),
-An ancient hot spot (Fitton and Hughes, 1977; Fitton, 1980; Dunlop and Fitton, 1981; Fitton, 1983),
-A southernmost geostructure of a Pelusium megashear system, which extends from the Amazon basin to Anatolia, via the Atlantic equatorial fracture zone and across Africa from the Gulf of Guinea to the Nile Delta (Neev *et al.*, 1982),
-A mega left-lateral shear zone (Moreau *et al.*, 1987). According to this theory, the N70° Adamawa fault zone, a Pan-African fracture reworked during Albian-Aptian times, is the only shear zone of continental scale that could have initiated "en echelon" mega-tension gashes within the CVL during a Cainozoic left-lateral transcurrent movement.

In the Southern Continental part of the Line, there is a concentration of maar volcanoes around the city of Wum. The maar set includes Nyos, Kuk, Benakuma and Oshieng volcanoes; the latter being only studied in a reconnaissance fashion by Peyronne (1969). The Oshieng maar is located at ca. 60 km from lake Nyos which was the site of a gas burst that killed more than 1746 people in 1986 and at it is less than 3 km uphill of a hydroelectric power plant project (the Mentchum river Power plant). Thus, the Oshieng maar may be surrounded by water of the dam reservoir.

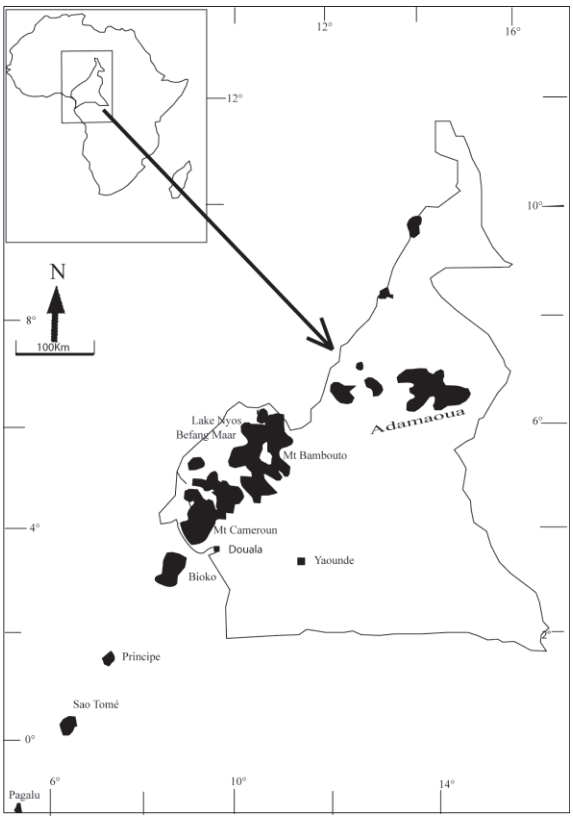

Fig. 1 – Location of the Befang maar volcano in the Cameroon Volcanic Line.

The Befang maar volcano reaches an altitude 753 m and it is higher than the lake (Oshien) level of 703 m The maar crater was excavated in a Neoproterozoic granito-gneissic basement. The base of the volcanic sequence is made up of a small basalt flow that extends over ca. 2 km in the eastern side of the volcano. Phreatomagmatic products which are made up of vesicular basalt, mantle xenoliths and granite-gneisses accidental fragments derived from the basement form bedded deposits on the south western side of the volcano (Fig. 2).

The Befang maar volcano is thought to be a polygenetic volcano resulting from two types of volcanic activity: a fissural event that originated the basalt flow and a phreatomagmatic event that lead to the formation of the pyroclastic deposits.

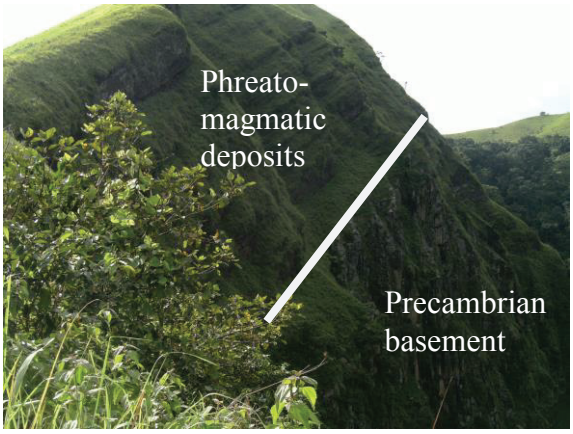

Fig. 2 – Stratified pyroclastic deposits expose at the western side of the volcano.

The Befang volcano is very probably a polygenetic volcano with its lake sharing some common features with lake Nyos: subcircular shape, euxinic conditions. Its proximity with a power plant project adds to the interest in a detailed study of the lake.

References

Tchouankoue J. P., Temdjim R. et Tchawoua C. (2003). Microstationhydroelectrique: nouvelle solution pour le degazage du lac de Nyos au Cameroun. Bull. Soc. Volc. Europ., Genève., Vol. 7 pp. 9-15.

Temdjim R., Tchouankoue J. P. et Tchoua F. M. (2000). Decouverte d'un maar trachytique dans la Ligne Volcanique du Cameroun: le maar Mbalang-Djalingo dans le district volcanique de Ngaoundere (Adamaoua, Centre Cameroun). Bull. Soc. Volc. Eur., vol. 4, pp. 9-14.

Temdjim R. (2012) Ultramafic xenoliths from Lake Nyos area, Cameroon Volcanic Line.: petrography, mineral chemistry, equilibration conditions and metasomatic features. Chemie der erde, Vol. 72, 1, 39-60.

Volcanology and Geochemistry of the Nyos volcano (Cameroon Volcanic Line)

Nkouamen Nemzoue P.N., Ayaba F., Tchouankoue J.P., Moundi A., Azeuda K., Temdjim R.

University of Yaounde I, Department of Earth Sciences, P.O. Box 812 Yaounde-Cameroon
peguynoel@ymail.com

Keywords: Maar, Nyos, Cameroon.

The Nyos volcano (6°26'78'' N, 10°17'76''E) is located in the southern continental part of the Cameroon Volcanic Line, a chain of Cenozoic volcanoes with no clear age progression. Its origin is still unclear and the nature of its magmatic rocks poorly known. (Fig1).

The Nyos volcano is well known for having been the site of a gas busrt from its lake that killed 1746 people in 1986. Following the catastrophe, the Nyos maar has been subject to intense scientific activities mainly the study of the degassing process of the lake, but little interest has been devoted to the volcanological and geochemical environment of formation of the maar.

Most recent report on lake Nyos degassing and management (Evans et al., 2012) indicates that degassing is steadily reducing gas amounts at the bottom of the lake and that gas pressure at the deepest part of the lake has been reduced by ~2.5 times from a maximum content measured in 2001 when the first pipe was installed. The total CO_2 in the lake has been reduced by 40% since 2001, from ~710,000 to 425,000 metric tons.

The natural dam impounding the upper 40 m of the lake at its spillway has been too strengthened in order to reduce the danger of the dam falling and creating a flood that could reach into Nigeria and affect up to 10,000 people in areas located below the lake.

The maar crater is now occupied by a lake and it is formed of a wall of Precambrian granite to the East and of volcanic debris to the West. Phreatomagmatic deposits from the western part of the crater are formed by accidental fragments derived from the granitic basement, olivine basalt, and mantle xenoliths. Clast size can reach 30 cm (basalt) nearer to the crater and less than 1 mm in the most distal deposits (>3 km from the lake).

The Nyos volcano is a monogenic volcano that shows relatively large pyroclastic deposits for a single volcanic event. The formation of the volcano may have been favoured by an intense fracturation of the Precambrian basement as shown by the basalt dykes intruding the granitic wall of the crater (Fig 2).

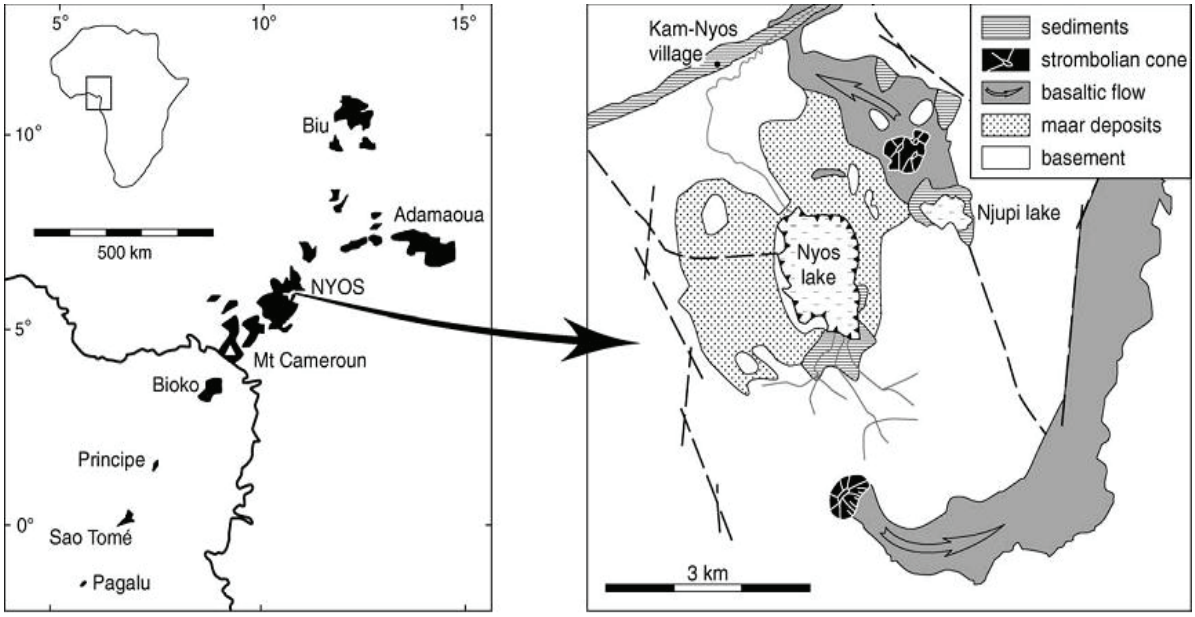

Fig 1. Geological map of the Nyos area.

Fig 2: basaltic dyke in the granitic wall of Nyos volcano crater.

References

Tchouankoue J. P., Temdjim R. et Tchawoua C. (2003).Microstation hydroélectrique: nouvelle solution pour le dégazage du lac de Nyos au Cameroun. Bull. Soc. Volc. Europ., Genève., Vol. 7 pp. 9-15.

Tchouankoue J. P. et Tchoua F. M. (2000). Découverte d'un maar trachytique dans la Ligne Volcanique du Cameroun: le maar Mbalang-Djalingo dans le district volcanique de Ngaoundéré (Adamaoua, Centre Cameroun). Bull. Soc. Volc. Eur., vol. 4, pp. 9-14.

Temdjim R. (2012) ultramafic xenoliths from Lake Nyos area, Cameroon Volcanic Line.:petrography, mineral chemistry, equilibration conditions and metasomatic features. Chemie der erde, Vol. 72, 1, 39-60.

Evans W., Kling G., Tanyileke G., Kusakabe M., Yoshida Y. (2012). Preliminary report of the June 2012 field expedition to lakes Nyos and Monoun, Cameroon. Report, USGS, 19 p.

Volcanology and Geochemistry of the Kuk volcano (Nyos Volcanic Field- Cameroon Line)

Ayaba F., Nkouamen Nemzoue P.N., Moundi A., Tchouankoue J.P., Azeuda K., Temdjim R.

University of Yaounde I, Department of earth Sciences, P.O. Box 812 Yaounde-Cameroon. billbliss88@yahoo.fr

Keywords: Maar, Kuk, Cameroon.

The Cameroon Volcanic Line (CVL) is a 100 km wide alignment of plutonic anorogenic complexes, volcanoes and volcanic fields located along a tectonic corridor, which trends N30° over 1600 km (Fig. 1). It is a "Y-shape" structure stretching from the Island of Pagalu, located in the Atlantic Ocean, through Mount Cameroon, near the coast, to the Ngaoundere Plateau, where it splits into two branches, one running eastward to Sudan and the other northward to the Biu Plateau in Nigeria.

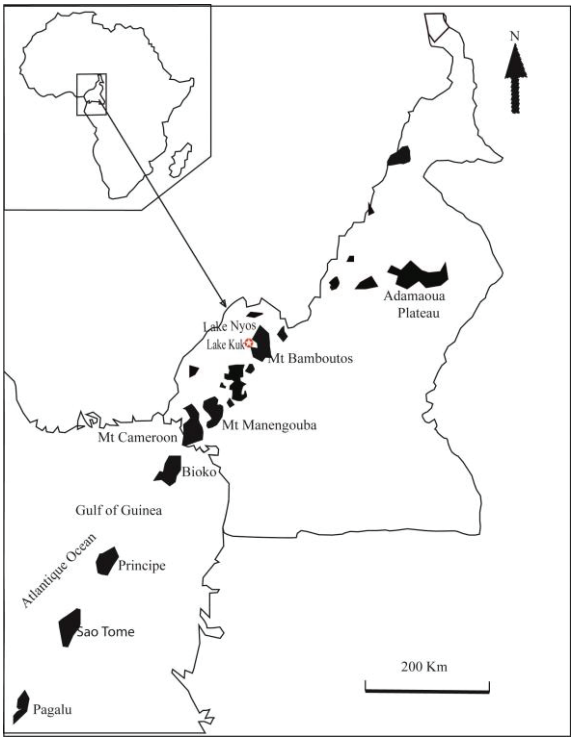

Fig.1 – Localization of Kuk volcano (star) in the Cameroon Volcanic Line (black).

From a geomorphlogical point of view, the CVL is a succession of horsts and grabens (Gèze, 1943; Tchoua, 1974, Déruelle et *al.*, 1983). Horsts are covered by large polygenetic volcanoes and plateaus, whereas grabens are characterized by monogenetic volcanic fields.

Numerous tectonic and petrologic problems – amongst others, lithospheric or asthenospheric origin for basaltic magmas (Dunlop, 1983; Halliday et *al.*, 1988; 1990; Lee et *al.*, 1994; Nkoumbou et *al.*, 1995), the differences between monogenetic and polygenetic volcanoes (Sato et *al.*, 1990), the magmatic differenciation processes involved in the evolution of the CVL (Déruelle et *al.*, 1991; Marzoli et *al.*, 1999) – fuel the debate on the CVL and so far no consensus has been arrived at yet. It should be noted that most studies on the CVL were carried out on large volcanoes; only few studies have been realized on small volcanoes such as the Kuk volcano, despite their great number and varieties.

The Kuk maar (6° 23' '30'' N, 10°11'00''E) is located in the center of the continental part of the Cameroon Volcanic Line, at ca. 10 km west of Nyos maar. The Nyos maar has been a site of CO2 gas emission that killed over 1700 people in 1986. Despite its closeness to Lake Nyos, there is little or no literature on the Kuk volcano. Lake Kuk covers a surface area of 400 m2 and has a maximum depth 47 m. Within the pyroclastic deposits (Fig. 2) can be found large mantle xenoliths accompanied by granite xenoliths, which were transported to the surface by the rising magma. The inferred age of the Kuk maar is late Tertiary to Quaternary age.

Fig.2 – Contact between the basement and pyroclastic deposits. Note the red soils formed from the weathering of the basement granite at the bottom.

Basaltic clasts in the phreatomagmatic deposits associated to the maar range in size from 60 cm near

to the crater to less than 2 mm in the Kuk village, 4km west of the lake.

From the various lithologies identified in the field, it appears that the Kuk volcano is monogenetic.

The Kuk and Nyos maars are similar n many aspects. Therefore, a particular attention needs to be devoted to a detailed study of this maar.

The aim of our research is to map and sample all the lithological units associated with the Kuk maar in order to decipher the eruption dynamics. Thin and polished thin sections shall be prepared from the samples for both petrographic and mineralogical studies. Major, and trace element, including REEs, will be anlyzed on the samples. Since Lake Kuk maar has not been dated, we will also be doing Ar-Ar dating on the samples. This geochemical information will enable us to infer the mantle source composition of the magmas, the degree of partial melting, the various geochemical processes through which the magma underwent before eruption at the surface. On the long run, we shall also be sampling the bottom waters of the lake to see whether there has been any accumulation of CO2 with time as with Lake Monoun to the south and Lake Nyos to the east.

References

Deruelle,, B.C. Moreau, & E. N Nsifa, (1983): Sur la recent eruption du Mont Cameroun (16th Oct-12th Nov. 1982) C.R. Acad. Sci. Paris 296

Geze B. (1943); Geographie physique et Geologie du Cameroun Occidental Memoires du Museum National d'histoire Naturelle/, 226 Pages,

Tchoua F, (1973): Sur l'existence d'une Phase initiale ignimbrite dans le volcanisme des Monts Bambouto (Cameroun), Presente par Mr, Marcel Roubault, C,R,Acad,Sc,Paris 276,

Tchouankoue J.P. et Tchoua F. M. (2000). Découverte d'un maar trachytique dans la Ligne Volcanique du Cameroun: le maar Mbalang-Djalingo dans le district volcanique de Ngaoundere (Adamaoua, Centre Cameroun). Bul . Soc. Volc. Eur., vol. 4, pp. 9-14.

Tchouankoue J. P., Temdjim R. et Tchawoua C. (2003). Microstation hydroelectrique: nouvelle solution pour le dégazage du lac de Nyos au Cameroun. Bull. Soc. Volc. Europ., Genève, v. 7, pp 9-15.

Temdjim R. (2012) Ultramafic xenoliths from Lake Nyos area, Cameroon Volcanic Line: petrography, mineral chemistry, equilibration conditions and metasomatic features. Chemie der erde, Vol. 72,1, 39-60

.

Volcanology and Geochemistry of the Benakuma volcano (Oku Volcanic Field- Cameroon Line)

Juinang Dieugnou J., Ngahane Mbami L., Tchouankoue J.P., Mouafo L., Azeuda K., Temdjim R.

University of Yaounde I, Department of earth Sciences, P.O. Box 812 Yaounde-Cameroon.
juinangjoseline8@yahoo.fr

Keywords: Maar, Benakuma, Cameroon.

The Cameroon Volcanic Line is an active, intraplate, tectonomagmatic zone developed on both oceanic and continental lithosphere. It is oriented N30°E and extends through Cameroon, from the Gulf of Guinea to Chad, for more than 1500 km. Volcanic activity along the Cameroon Volcanic Line started during the Eocene with the emplacement of peralkaline rhyolites in southern Chad at Ca. 68 Ma (Mbowou *et al*., 2012) and plateau basalts for its southern continental part ca.51 Ma ago (Moundi *et al.*, 2007). The most recent eruptions along the Line took place in 1999 and 2000 at Mount Cameroon, which is located at the transition between continental and oceanic crusts (Figure 1)

Basaltic volcanism is dominant in the CVL, but in the central-northern areas of the Line, erupted more evolved magmas and sequences resulting from phreatomagmatic explosions formed maar craters with minor pyroclastic rings formed by explosion breccias. In the southern continental part of the Cameroon Volcanic Line is locate, the Benakuma maar, which is unique in the Line, as it is a maar produced by evolved magmas (trachytes, phonolites).

The Benakuma volcano (6° 25' 29.1'' N, 09° 56' 41.8'' E reaches at altitude of 990 m, and it belongs to the Wum volcanic field, which is mostly known by the Nyos maar (Figure 1).

The Benakuma volcano was produced by phreatomagmatic activity after an initial trachybasaltic fissural phase. The main phreatomagmatic phase produced a consolidated ash (Figure 2). This pyroclastic deposit occurs mainly south of the crater, around spillway of the crater lake.

Lake Benakuma is peculiar as it lacks aquatic animals. It has a water temperature above regional mean values (*e.g.* 22 °C at lake Nyos. Recent landslides occurred on the steep northern part of the crater.

The Benakuma volcano is slightly different from the other maar volcanoes of the southern continental part of the Cameroon Volcanic Line as it was formed by more differentiated magmas.

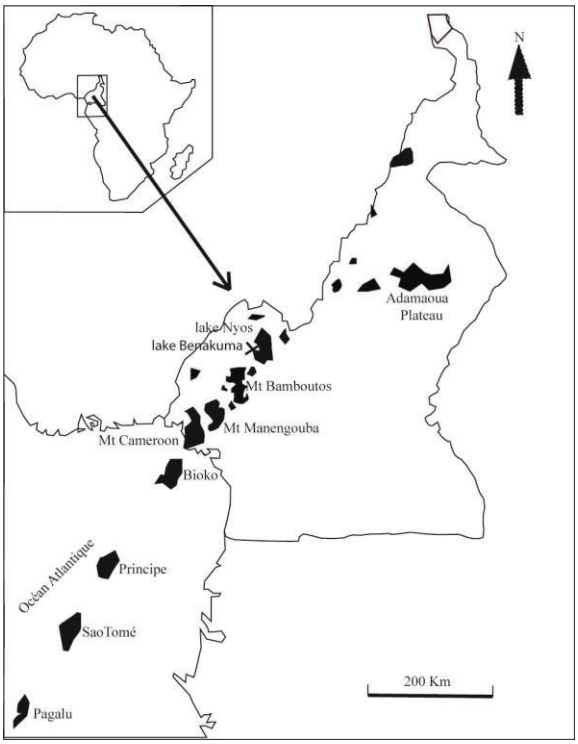

Fig. 1 – Localization of lake Benakuma (star) in the Cameroon Volcanic Line (black).

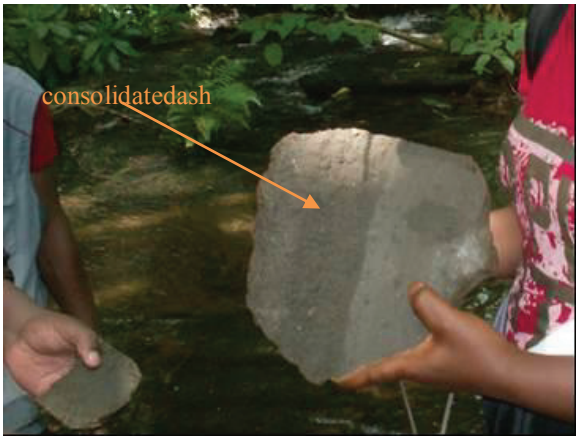

Fig. 2 – Consolidated ash collected at pyroclastic deposits of the Benakuma volcano.

References

Tchouankoue J. P., Temdjim R. et Tchawoua C. (2003). Microstationhydroelectrique: nouvelle solution pour le degazage du lac de Nyos au Cameroun. Bull. Soc. Volc. Europ., Genève., Vol. 7 pp. 9-15.

Tchouankoue J. P. et Tchoua F. M. (2000). Decouverte d'un maar trachytique dans la Ligne Volcanique du Cameroun: le maar Mbalang-Djalingo dans le district volcanique d'Adamaoua, Centre Cameroun). Bull. Soc. Volc. Eur., vol. 4, pp. 9-14.

Temdjim R. (2012) ultramafic xenoliths from Lake Nyos area, Cameroon Volcanic Line.: petrography, mineral chemistry, equilibration conditions and metasomatic features. Chemie der erde, Vol. 72, 1, 39-60.

Monogetic volcanism of Costa Rica back-arc: Aguas Zarcas Pyroclastic cones

Raúl Mora-Amador[1], Gino González[1], Yemerith Alpizar[1] Carlos Ramírez[1], and Dmitri Rouwet[2]

[1] *Escuela Centroamericana de Geología, Centro de Investigaciones en Ciencias Geológicas, Red Sismológica Nacional; Universidad de Costa Rica UCR, San Pedro de Montes de Oca, San José, Costa Rica.* raulvolcanes@yahoo.com.mx
[2] *INGV, Bologna, Italy.*

Keywords: Monogenitic, back-arc, Costa Rica.

Monogenetic volcanic fields are important manifestations of magmatic activity in almost every tectonic setting, although they are most commonly formed in continental regions (Németh, 2010).

In the Costa Rica back-arc region the only monogenetic volcanic located in the back-arc region is formed by at least 12 pyroclastic cones and 5 more volcaneoes that remain to be confirmed (Fig. 1 and Table 1).

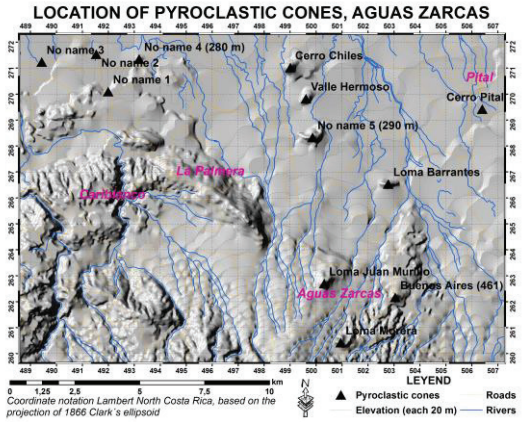

Fig. 1 – Location of Aguas Zarcas monogenetic field.

Name	X Coordinate	Y Coordinate	Elevation (m a.s.l.)	Height (m)
No name 1	491991.0	270095.0	94.12	<20
No name 2	491533.0	271533.0	80.00	<20
No name 3	489432.0	271234.0	280.00	<20
No name 5	499867.0	268330.6	125.32	100
Loma Barrantes	502779.7	266533.8	280.00	80
Valle Hermoso	499610.3	269820.1	200.00	60
Cerro Chiles	499006.7	271017.0	240.00	120
Loma Juan Murillo	500313.5	262696.4	500.00	40
Loma Morera	500948.1	260424.3	620.00	80
Buenos Aires	503047.9	262161.4	460.00	60
No name 6	493184.5	271346.3	138.29	40
Cerro Pital	506418.9	269403.5	180.00	20

Table 1. Name and locatation of pyroclastic cone.

The only isotopic age reported for one of these cones 300,000 years old (Ponce, 1993). However, it is clear that these cones were not formed at the same time, as it can be inferred from cone morphologies, that suggests significant differences in erosionand weathering of the pyroclastic material in the cones (Figure 2).

Fig. 2 –Juan Murillo Hill is theonly pyroclastic cone in the Aguas Zarcas region with an obvious crater.

The only study that described the morphology of the volcanoes in this field is Martens (2004), who pointed out that the back-arc cones in Costa Rica have gentler outer slopes and are lower (Figure 2) than those volcanoes found in the rest of country perhaps as a consequence of to being more mafic and/or more eroded and older.

In the region of Muelle de San Carlos (west side of Figure 1), three nameless cones define an E-W alignment, while the cones of Los Chiles, Valle Hermoso, an unnamed vent and Barrantes Hill define a NW-SE lineament in the eastern part of the volcanic field The volcanoes located in the SW corner of Figure 1 are not clearly related to those above.

More field work is needed to understand the tectonic relationship of these pyroclastic cones.

We are working in the a first detailed description of the stratigraphy of this volcanic field. Quarries are the best localities available to study the pyroclastic deposits in the area.

The best outcrop is present at the Los Chiles hill (figure 3); where an excellent stratification is observed. The pyroclastic deposit is formed by alternating beds lapilli and ash, with sporadic pumice layers.

Fig. 3 – Los Chiles hill, the biggest pyroclastic cone at the Aguas Zarcas region. At least 4 lava flows originated from the eastern side of the cone.

The studied stratigraphic sequence are formed by clast-supported lapilli with inverse graded bedding (Figure 4). Lapilli and pumice are porous (25%), with a reddish color, and with a bread like crust texture on their surface. We identified plagioclase and pyroxene phenocryst with the handlens.

Fig. 4 – Lapilli and ash deposit with reversed graded bedding exposed in Los Chiles hill.

Seen under the microscope, the rocks are vesicular, with hypocristalyne matrix (40%). Estimated modal content in the studied rocks is plagioclase (30%), augite (15%), hematite (5%). Based on this information, the studied rocks are classified as andesitic.

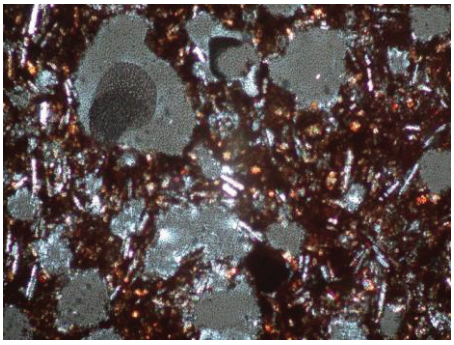

Fig. 5 – Photograph of thin section.

During 2014 and 2015 field work as well as laboratory research will be conducted to study the details of this field of pyroclastic cones.

References

Martens, U., 2004; Aspectos morfométricos de los conos de scoria de Costa Rica. – Rev. Geol. Amér. Central, 30: 15-29.

Németh, K., 2010. Monogenetic volcanic fields: Origin, sedimentary record, and relationship with polygenetic volcanism, in Cañón-Tapia, E., and Szakács, A., eds., What Is a Volcano? Geological Society of America Special Paper 470: 43–66.

Poncia, C., 1993. II Complesso alcalino-subalcalino Platanar-Aguas Zarcas (Costa Rica): genesi dei magni e relazione tra tettonica e vulcanismo. -79 p. Tesis, Univ. degli Studi di Milano, Dipartimento di Science della Terra.

Surtsey blocks & bombs: dikelets, magma-tephra mingling, and episodes of maar-like country-rock ejection

James D.L. White[1], Sveinn P. Jakobsson[2] and C. Ian Schipper[3]

[1] *University of Otago, Dunedin, New Zealand. james.white@otago.ac.nz*
[2] *Icelandic Institute of Natural History, Reykjavik, Iceland.*
[3] *Victoria University, Wellington, New Zealand.*

Keywords: surtseyan.

Surtsey's eruption lasted from 1963 into 1967 with growth of 4 separate eruptive centers along the 4.5 km long Surtsey fissure. Syrtlingur and Jolnir ~ 0.07 km^3 each, plus Surtla (~0.01 km^3), are half the volume of Surtsey below sea level (~0.3 km^3). Syrtlingur and Jolnir also formed islands, but only Surtsey remains, the other two having been eroded below sea level within months of their last activity. Surtsey's explosive activity gave way after 6 months to fountaining and lava effusion, but it was more than 3 years into the eruption when the last pyroclastic activity at Jolnir ended.

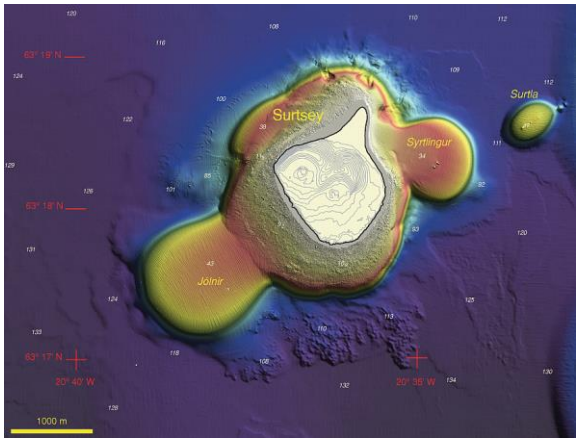

Fig. 1 – 2007 bathymetric map of Surtsey from the Surtsey Research Progress Reports (Jakobsson *et al.*, 2009).

A core through Surtsey was acquired in 1979, reaching almost to the pre-eruption seafloor (Jakobsson and Moore, 1982). Near the base of the hole, unlithified pyroclastic deposits were encountered, and sampled as drill cuttings. These are highly vesicular, and many show large populations of small, spherical to sub-spherical vesicles. Examination of the core and dozens of thin sections reveals strong palagonite rims on pyroclasts at many intervals in the core, developed particularly well on highly vesicular and originally glassy pyroclasts. In the uppermost several meters armoured lapilli are present, along with "vesiculated tuff". We see no evidence for deep subsidence of surficial deposits at the site cored, and our working hypothesis is that an eruption stratigraphy can be established from the drillsite.

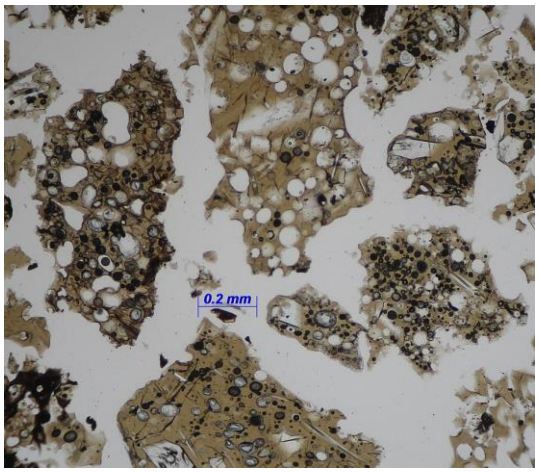

Fig. 2 – Fresh pyroclasts, base of the Surtsey drillhole (118 mbsl) comprise sideromelane and varied populations of phenocrysts and vesicles.

On the emergent cone, a notable feature not previously emphasized is an abundance in certain layers of blocks from pre-eruption seafloor sedimentary rock. These layers make up a small proportion of the volcano, but indicate that at multiple times, extending to very near the end of the

Fig. 2 – Large clasts (10-20 cm): dike fragment (lower left), seafloor sediment (upper left), and a glassy composite bomb *(right)*.

explosive phases of Surtsey's eruption, material from 200 m or more below sea level was being ejected to the surface. Surtsey's ejecta contains no fragments of pillow lava, but there are abundant fragments of dikes characterized by parallel bands of vesicles and, on many fragments, a single or paired chilled margins. Many of these exhibit strong cracking and a cauliflower-like appearance on one side, but they are not true cauliflower bombs.

Juvenile bombs and lapilli are characteristally composite. They consist of tachylite and have weakly fractured glassy surfaces. Many have contorted internal structures in which pyroclasts are entwined with stretched and bubbled coherent basalt. Such textures developed through strong 'recycling' processes that allowed capture of older pyroclasts within new ones through in-vent welding and agglutination, or/and by capture of particles within magma that was subsequently disrupted.

Fig. 3 – Composite bomb (~20 cm): numerous small lapilli are visible inside the bomb, many lying within cavities that fit around them.

The evidence for ubiquitous hot-state particle recycling supports models involving particulate slurries in the vent (Kokelaar 1983; 1986), while providing constraints on timescales for interaction and subsequent fragmentation and ejection. Ejection of subvolcanic sedimentary blocks at different times during the eruption, including during the last explosive phase implies further complications in vent conditions. If the blocks were excavated and directly ejected from depth, a vent open to the atmosphere would seem necessary (see Moore, 1984). Alternatively, stepwise upward block transport, as argued for diatremes (Valentine and White, 2012; Valentine *et al.*, 2014), could take place in a vent persistently filled or partially filled with debris.

Acknowledgements

Field work on Surtsey takes place under the auspices of the Surtsey Research Society. JDLW was supported by an Otago Research Grant.

References

Jakobsson SP, Moore JG (1982) The Surtsey research drilling project of 1979. Surtsey Research Progress Report 9:76-93

Jakobsson SP, Thors K, Vésteinsson AT, Ásbjörnsdóttir L (2009) Some aspects of the seafloor morphology at Surtsey volcano: The new multibeam bathymetric survey of 2007. Surtsey Research 12:9-20

Kokelaar P (1983) The mechanism of Surtseyan volcanism. Journal of Geological Society of London 140:939-944

Kokelaar P (1986) Magma-water interactions in subaqueous and emergent basaltic volcanism. Bull Volcanol 48:275-289

Moore JG (1985) Structure and eruptive mechanisms at Surtsey Volcano, Iceland. Geol Mag 122:649-661

Valentine GA, White JDL (2012) Revised conceptual model for maar-diatremes: Subsurface processes, energetics, and eruptive products. Geology 40(12):1111-1114

Valentine GA, Graettinger AH, Sonder I (2014) Explosion depths for phreatomagmatic eruptions. Geophys Res Lett 41(9):2014GL060096.

SESSION 2 and 3-1

ORAL PRESENTATIONS AND POSTERS

NOVEMBER 19, 2014

Using tephrochronology for cross-correlating drill-cores in maar sediments: a case study from the West Eifel Volcanic Field

Michael W. Förster[1], Frank Sirocko[2]

[1] *Johannes Gutenberg University, Institute for Geosciences, J.-J.-Becher-Weg 21, D-55099 Mainz, Germany.* foermich@students.uni-mainz.de
[2] *Johannes Gutenberg University, Institute for Geosciences, Workgroup: climate and sediments, J.-J.-Becher-Weg 21, D-55099 Mainz, Germany.* sirocko@uni-mainz.de

Keywords: Tephrochronology, Eifel, Drill-cores.

Tephrochronology is based on widely dispersive volcanic ash layers which are used to date stratigraphic units. Most tephrochronological studies applied geochemical observations *e.g.* Pouclet and Juvigne (2009). This study however, uses the specific ratios of different grain types in the volcanic ash.

To reconstruct the tephrochronology of the Eifel Volcanic Fields, the sediments of their maar volcanoes were studied. These tend to form sedimentary environments especially in mountainous regions. The sediments were probed (drilled) by the Eifel Laminated Sediment Archive (ELSA) project (Sirocko *et al.* 2013). Overall, ten localities were sampled: Aueler Maar, Dehner Maar, Merscheider Maar, Rother Maar, Hoher List Maar, Oberwinkler Maar, Jungferweiher Maar, Holzmaar, Eigelbach Maar and Walsdorfer Maar. All cores show a variety of ash layers at different depths. The cores averaged 80 m in length. For the purpose of analyzation, the ashes were sieved to a fraction of 250 to 100 µm. The next step was to search for grains of reddish sandstone, grayish sandstone, quartz, amphibole, pyroxene, scoria and pumice, sanidine, leucite and mica. Afterwards 100 grains per probed ash were sorted into these groups. The count rates for each grain were converted into vol.-% abundances. Three main types of ashes could be identified (see Fig. 1):

Phreatomagmatic ashes are rich in accidentally introduced host-rock. The ratios of which vary with the diatremes geographic location.

Strombolian ashes are rich in pyroxene and scoria. Ideally, these ashes contain only small amounts of host-rock fragments. However, there are also intermediate compositions consisting of both phreatomagmatic and strombolian ashes. This indicates an early maar volcanic stage in the evolution of a scoria-cone.

Tephra enriched in sanidine and pumice are referred to as evolved ashes. The source of which resulting from a (sub)-plinian eruption of a large volcano.

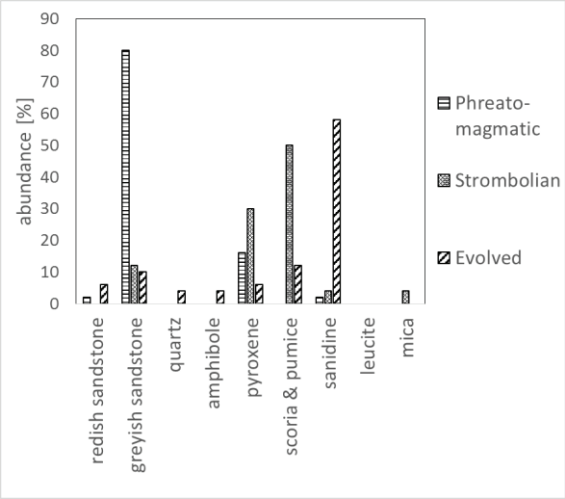

Fig. 1 – Three main types of ashes: Phreatomagmatic – containing major amounts of accidentally introduced host-rocks, strombolian – rich in scoria and pyroxene, evolved – mostly sanidine and pumice.

The pattern of the grain-count ratios give each ash-layer an individual fingerprint: Some ash-layers are easily recognized, because they are either enriched or lack specific grains completely. Ashes of similar appearance can be distinguished by their position within the cores and their relative age. Deep insights into the local eruption history were gained by applying this method to the Eifel Volcanic fields: Eleven characteristic ash layers were distinguished, spanning a time interval of about 200,000 years with the 215,000 BP Hüttenberg-Tephra as oldest and 12,900 BP Lake Laach Tephra as the youngest. The cores were correlated with ash deposits collected from tuff-walls of the eruption centers. To ensure a cross section over the eruption sequence, tephra was collected from the debris at the foot of the exposed outcrops. After comparing 40 different ash layers from exposed volcanic tuff walls, seven of the eleven ash layers from the drill-cores could be assigned to the eruption centers: Lake Laach at 12,900 BP, Wartgesberg at 30,000 BP, Boos at 33,000 BP, Dreiser Weiher at 41,000 BP, Dümpelmaar at 116,000 BP, Wehr-volcano with

Glees-tephra at 151,000 BP and Hüttenberg-tephra at 215,000 BP. The tephra of the Dreiser Weiher maar is of special interest: This tephra contains a significant amount of 20 vol.-% sanidine. Due to its mineral content, the magma of the Dreiser Weiher is very mafic, enriched with ultramafic xenoliths of the lithospheric mantle. Therefore, the sanidine grains must be xenocrysts, as both mineral species do not coexist together. A possible source could be a solidified, evolved magma-chamber encountered by the explosions of the diatreme.

The correlation of the eleven ash layers enabled the drill-cores to be arranged into a chronological order. Between 200,000 BP and 180,000 BP many strombolian ash-layers are found in the Walsdorf core. Probable sources are the basanitic to tephratic scoria-cones of the East Eifel Volcanic Field. Most maar volcanoes seem to have erupted in two brief periods of time at around 100,000 BP and 60,000 BP, suggesting an episodic volcanism of the West Eifel Volcanic Field. After the large eruption of Wartgesberg at 30,000 BP no activity is known to have occurred in this region, suggesting that the West Eifel Volcanic Field entered a dormant phase. This was interrupted only once by the formation of the minor Ulmener Maar volcano at 11,000 BP.

References

Pouclet, A., & Juvigne, E. (2009). The Eltville Tephra, a late pleistocene widespread tephra layer in Germany, Belgium and the Netherlands; symptomatic compositions of the minerals. Geologica Belgica, 12.

Sirocko, F., Dietrich, S., Veres, D., Grootes, P. M., Schaber-Mohr, K., Seelos, K., ... & Grim, S. (2013). Multi-proxy dating of Holocene maar lakes and Pleistocene dry maar sediments in the Eifel, Germany. Quaternary Science Reviews, 62, 56-76.

Lacustrine sediments as result of an occasional volcanic lake by drainage natural damming and implication with paleoclimate (Colima volcano, Mexico)

Matteo Roverato[1], Lucia Capra[2]

[1] *Departamento de Geologia Sedimentar e Ambiental (GSA), Instituto de Geociências (IGC), USP, Brasil, roteo@hotmail.com*
[2] *Centro de Geociencias, Universidad Nacional Autónoma de México, UNAM Campus Juriquilla, Querétaro, México.*

Keywords: Colima volcano, natural dams, volcanic lakes.

Volcanic lakes are water bodies frequently hosted by stratovolcano's summit craters or maar structures formed by strong hidrovolcanic activity.

Crater- and maar lakes have, due to their specific formation and characteristic morphology, a high potential for the development and preservation of seasonally laminated sediments (Mingram *et al.*, 2004) but they are not the only water volcanic basins that could record important environmental informations.

In some cases, lakes form in other volcanic setting that not implies the direct relationship with craters. The obstruction of the hydrological network is a phenomena that can give rise to a natural dam. This can occur when an important volume of rock is rapidly mobilized obstructing main rivers. Landslides in narrow valleys that generally fill the river bed creating an impoundment, represent the most common case (Capra, 2007).

Thus, volcanic lakes also form by blockage of the drainage system by pyroclastic flows, debris flows or debris avalanche deposits that act as natural debris dams. These occasional lakes are less common than crater lakes but also represent important events worldwide (Capra *et al.*, 2002; Clavero *et al.*, 2002; Cortez *et al.*, 2010; Kataoka *et al.*, 2008; Macias *et al.*, 2004; Waythomas, 2001) that can record many phenomena processes related to the volcanic activity and paleoclimate variations.

Lake sediments are, along with tree rings, glacier ice and speleothems, one of the most important terrestrial archives of palaeoenvironmental and palaeoclimatic information with up to seasonal resolution.

Tens of meters thick (> 40 m) sequence of lacustrine sediments outcrops at the very top of the "Los Ganchos" ravine in the western sector of the Colima volcano at ca.13 km from the actual summit.

These sediments are the result of the ravine damming by two debris avalanche deposits (Cortez *et al.*, 2010) and temporary lakes formation occurred during the numerous sector collapses that characterized the Colima volcano during its eruptive history (Cortes *et al.*, 2010; Komorowski *et al.*, 1997; Roverato *et al.*, 2011).

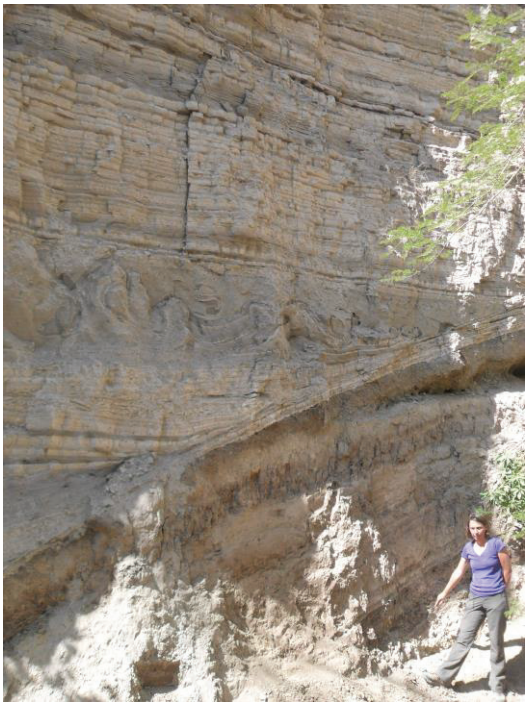

Fig. 1 – The picture shows the lacustrine sequence lying on top of a paleosol that yields an age of ca. 8000 yr cal. BP. The scale-person steps on a debris avalanche deposit.

Three aspects are here considered: 1) the relationship between the drainage natural damming and the occasional lake formation, 2) geochronological data provided by organic material found in the lacustrine sequence and 3) the recorded paleoclimate changes.

Two main lacustrine sequences were recognized.

The older lacustrine sediments yield a maximum age of ca. 8000 yr cal. BP based on ^{14}C dates of

organic matter and sweet-water bivalve shell found at the very top of the sequence that shows a high degree of pedogenization. This sequence displays scattered gypsum crystals that suggests important implication of climate variations. In fact selenite gypsum "desert rose" typically form in arid sandy conditions, such as the evaporation of a shallow salt basin. This arid climate condition at ca. 8000 yrs cal. BP possibly correlate with δ18O data from speleothem analysis that also point to dryer conditions in sothwestern Mexico (Bernal *et al.*, 2011). This lacustrine sequence represents an accident linked to the emplacement of a debris avalanche deposit in a narrow valley, which is giving important information on the paleclimate reconstruction of the area, where no other proxy for climate variation are available.

The younger sequence is possibly associated to temporary lake formed (ca. 0,2 km^3 of water volume) after the emplacement of the 3600 yrs BP debris avalanche (Cortes *et al.*, 2010).

References

Bernal, J.P., Lachniet, M., McCulloch, M., Mortimer, G., Morales, P., Cienfuegos, E., 2011. A speleothem record of Holocene climate variability from southwestern Mexico. Quaternary Research 75: 104-113.

Capra, L., Macias, J.L., 2002. The cohesive Naranjo debris-flow deposit: A dam breakout flow derived from the Pleistocene debris-avalanche deposit of Nevado de Colima Volcano (Mexico). Jouranal of Volcanology and Geothermal Research 117: 213–235.

Capra, L., 2007. Volcanic natural dams: identification, stability, and secondary effects. Natural hazards 43: 45-61.

Clavero, J.E., Sparks, R.S.J., Huppert, H.E., 2002. Geological constraints on the emplacement mechanism of the Parinacota avalanche, northern Chile. Bull. Volcano 64:40–54.

Cortes A., Macías, J. L., Capra, L., L., Garduño-Monroy, V. H., 2010. Sector collapse of the SW flank of Volcán de Colima, México. The 3600 yr BP La Lumbre-Los Ganchos debris avalanche and associated debris flows. J. Volcanol. Geotherm. Res. 189 (1-4): 52-66.

Komorowski, J. C., Navarro, C., Cortes, A., Saucedo, R., Gavilanes, J. C., Siebe, C., Espindola, J. M., Rodriguez-Elizarraras, S. R., 1997. The Colima Volcanic Complex. Field guide 3, Int. Assoc. Volcanol. Chem. Earth's Inter., General Assembly, Puerto Vallarta.

Macías, J.L, Capra, L, Scott, K.M, Espindola, J.M, Garcia-Palomo, A, Costa, J.E, 2004. The 26 May 1982 breakout flows derived from failure of a volcanic dam at El Chichón, Chiapas, Mexico. Geol Soc. Am. Bull. 116: 233-246.

Mingram, J., Allen, J.R.M., Brüchmann, C., Liu, J., luo, X., Negendank, J.F.W., Nowaczyk, N., Schettler, G., 2004. Maar- and crater lakes of the Long Gang Volcanic Field (N.E. China)—overview, laminated sediments, and vegetation history of the last 900 years. Quaternary International 123-125:135-147.

Roverato, M., Capra, L., Sulpizio, R., Norini, G., 2011. Stratigraphic reconstruction of two debris avalanche deposits at Colima Volcano (Mexico): Insights into pre-failure conditions and climate influence. J. Volc. Geoth. Res. 207: 33-46.

Waythomas, C.F., 200. Formation and failure of volcanic debris dams in the Chakachatna River valley associated with eruptions of the Spurr volcanic complex, Alaska. Geomorphology 39: 111-12.

A fluviolacustrine sediment archive of the Late Weichselian Pleniglacial from the SE part of the Quaternary West Eifel Volcanic Field

Luise Eichhorn[1], Thomas Lange[1], Ulrich Polom[2], Michael Pirrung[1], Georg Büchel[1], Martin Heimann[3]

[1] *Friedrich Schiller University Jena, Institute of Earth Sciences, 07749 Jena, luise.eichhorn@uni-jena.de*
[2] *Leibniz Institute for Applied Geophysics, Stilleweg 2, 30655 Hannover, Germany.*
[3] *Max Planck Institute for Biogeochemistry,Hans-Knöll-Straße 10, 07745 Jena, Germany.*

Keywords: Sediment archive, Late Weichselian Pleniglacial, Quaternary West Eifel Volcanic Field.

The Quaternary West Eifel Volcanic Field is situated in the western part of Germany between Ormont and Bad Bertrich. It covers an area of 600 km² and is characterized by highly silica-undersaturated foiditic magmas (Büchel 1994, Schmincke 2007). In the SE part of the West Eifel Volcanic Field an accumulation of maars like Meerfelder maar, Dauner maar group, Holzmaar, Sprinker maar and Pulvermaar is notable – all eruptions dated within the Weichselian Pleniglacial (72-13 ka) (Negendank 1989, Woda *et al.* 2001, Schaber *et al.* 2005).

During the Weichselian Pleniglacial low temperatures (mean annual temperature -7 to -2°C) and continuous permafrost leading to low biological productivity and prominent wind activity roughly describe the environmental conditions (Huijzer *et al.* 1998). Due to the low organic content in preserved sediments, ^{14}C dating and an environmental reconstruction of that time interval using terrestrial organic micro or macro remains as proxies is difficult. Therefore, sediment archives containing indicators of environmental conditions like drop stones, bedded sediment or tephra layers are of high interest.

In this study, a fluviolacustrine sediment archive from the Late Pleniglacial is presented. At around 31 ka BP the Wartgesberg-Volcano Complex started eruptions and filled the originally V-shaped Alf valley with lava and tephra leading to a dammed lake (Hemfler *et al.* 1991, Pirrung *et al.* 2007). Main focus of this study is the reconstruction of the preexisting V-valley and the fluviolacustrine sedimentation history indicating environmental changes in the catchment area between 30 and 22 ka BP. Therefore, 16 sediment core lithostratigraphies distributed over five kilometers horizontal distance, geomorphological observations and geophysical methods (magnetic survey and shear wave seismic measurements) help to characterize and quantify the sediments. Combining preserved prevolcanic geomorphological relief features from the digital terrain model (one to five meter resolution) and magnetic anomalies, former erosion banks and meanders were identified. By using preserved features of the past course of the Alf River, core lithostratigraphy and seismic data, the sedimentation history is reconstructed. Moreover, the eruption history of volcanoes in the immediate vicinity will be discussed again with regard to this study.

References

Büchel, G., 1994. Volcanological Map West- and Hocheifel. Mainz.

Hemfler, M., Büchel, G., 1991. Influente Verhältnisseals Folge der Trinkwassergewinnung im Alfbachtal bei Strohn (Westeifel). Pollichia 78: 35-83.

Huijzer, B., Vandenberghe, J., 1998. Climatic reconstruction of the Weichselian Pleniglacial in northwestern and central Europe. Journal of Quaternary Science 13(5): 391-417.

Negendank, J. F. W., 1989. Pleistozäne und holozäne Maarsedimente der Eifel. Zeitschrift der Deutschen Geologischen Gesellschaft 140:13-24.

Pirrung, M., Büchel, G., Köppen K.-H., 2007. Hochauflösende fluviolakustrine Sedimente des jüngeren Pleistozän aus dem Alfbachtal bei Gillenfeld (Westeifel) - erste Ergebnisse. Mainzer geowissenschaftliche Mitteilungen 35: 51-80.

Schaber, K., Sirocko, F., 2005. Lithologie und der Eifel. Mainzer geowissenschaftliche Mitteilungen 33: 295-340.

Schmincke, H.-U., 2007. The Quaternary Volcanic Fields of the East and West Eifel (Germany). Mantle Plumes. J. R. Ritter and U. Christensen, Springer Berlin Heidelberg: 241-322.

Woda, C., Mangini, A., Wagner, G.A., 2001. ESR dating of xenolithic quartz in volcanic rocks. Quaternary Science Reviews 20(5): 993-998.

Trends in Holocene environmental and climatic changes in central Mexico

Margarita Caballero[1], Socorro Lozano[2], Beatríz Ortega[1], Estela Cuna[1, 3], Edyta Zawizsa[4], Gabrieal Vázquez[5]

[1] *Laboratorio de Paleolimnología, Instituto de Geofísica, Universidad Nacional Autónoma de México (UNAM), Ciudad Universitaria, Coyoacán 04510, México City, México.* maga@geofisica.unam.mx
[2] *Instituto de Geología, UNAM, Ciudad Universitaria, Coyoacán 04510, México City, México.*
[3] *Posgrado en Ciencias Biológicas, UNAM, Ciudad Universitaria, Coyoacán 04510, Mexico City, México.*
[4] *Institute of Geological Sciences, Polsih Academy of Sciences, Warsow, Poland.*
[5] *Instituto de Ecología AC, Xalapa, Veracruz, México.*

Keywords: Holocene, paleolimnology, paleoclimatology.

Central Mexico is characterized by an intense Neogene volcanism centered at the Trans Mexican Volcanic Belt (TMVB), a volcanic chain that crosses central Mexico in an E-W transect at about 21-19ºN. The TMVB has several crater lakes, most of which are small (<1 km2) with depths ranging from a few meters (2 to 4 m) up to 65 m.

Crater lakes in central Mexico are ideal sites for the study of Holocene climatic trends. These lakes have high sedimentation rates and their sediments are rich in pollen, diatoms and other biological remains that allow reconstructions of past environmental, ecological and climatic changes.

Fig. 1– Location of research sites in central Mexico. Shaded represents the Trans-Mexican Volcanic Belt.

Here we present result from palaeoenvironmental research undertaken in four of these lakes located along an E-W transect across the TMVB (Fig. 1): Lago Verde, La Luna, Tacámbaro and Santa María del Oro. The main proxies used are magnetic susceptibility, charcoal, pollen, diatoms and cladocera. All records have reliable chronologies based in 14-C dates (all) and 210-Pb (Lago Verde, La Luna).

The records presented here extend to the early Holocene (ca. 9 ka BP, Tacámbaro), the mid Holocene (5 ka BP, SMO) and the late Holocene (2.5 and 1 ka BP, Lago Verde and La Luna). These records give evidence of human occupation in their basins (presence of *Zea mays*) frequently associated with evidences of high environmental impact (charcoal, high magnetic susceptibility). Depending on the time span of the sequence and its geographic location, intervals of high human impact can be identified during the Classic (AD 100-900), Post-Classic (ca. AD 1200-1350), or Colonial times (late 16th century), giving evidence of the long history and high density of human occupation in this culturally diverse region (Mesoamerica). In most of the records, however, modern human impact is also important.

Main longer term climatic trend is a mid-Holocene transition that can be related with dryer and less seasonal climates (cooler summers and warmer winters). The main shorter term trends involve relatively dry climates during the Classic (AD 100-900), a shift to moister climates at some time between AD 900 and 1200 and the cooling of the Little Ice Age starting at about AD 1400 and extending until 1910. This cool period is recorded as a dry interval in regions that currently have a negative water balance; in regions with a positive water balance the drying trend is not evident. The coolest intervals during the LIA correlate with Spörer and Mounder minima in solar activity. The second was the period with the coldest conditions, from 1660 to 1760. Modern global warming trends can be identified in at least two of these lakes.

Reconstruction of the Eocene Messel Maar

Georg Büchel[1] and Michael Wuttke [2]

[1] *Friedrich-Schiller-Universität Jena, Institut für Geowissenschaften, Burgweg 11, 07749 Jena,Germany. georg.buechel@uni-jena.de*
[2] *Landesamt für Denkmalpflege Rheinland-Pfalz, Erthaler Hof, Schillerstr. 44, 55116 Mainz, Germany. michael.wuttke@gdke. rlp.de*

Keywords: Messel, compaction, diatreme.

The Messel pit fossil site, labelled by UNESCO as World Heritage, is the site richest in fossils in the world for understanding the living environment of the Eocene. For the interpretation of the fossils it is very important to have a well evolved model about the architecture of the depositional area. The Messel deposits were formed in a maar crater. We will present reflections about the reconstruction of the middle Eocene Messel-Maar-Volcano located on the Sprendlingen horst near Darmstadt, Germany.

The early Palaeozic plutonites and metamorphic rocks are overlain by a maximum of 63 m thick Permian sediments and thin Pleistocene and Quaternary sediments. In our presented model we will postulate a significantly higher original thickness of the Permian sediments.

Today the first subaquaceously deposited sediments in the original maar crater occur in a depth of -134 m a.s.l., which is known from a recent research drilling. Hence the depth of the boundary between the lowest part of the original maar crater and the uppermost part of the underlying diatreme is fixed. Above, the partly sandy lower Messel formation follows. It reaches up to 8 m a.s.l.. The fossil-rich finegrained organic middle Messel formation extends to 168 m a.s.l.. This altogether amounts to 305m thick compacted lake sediments above the diatreme up to the recent land surface.

For the evaluation of the height of the denudation around the maar volcano we assume that today the youngest maar crater sediments reach up to a height of 232 m a.s.l. This means that the total thickness of the known crater sediments amounts to around 370 m.

In the meantime, compaction of crater sediments and diatreme filling took place. We calculated a minimum model, with a mechanical compaction for the total Messel formation, from the start until the end of the sedimentation a porosity decrease of 10% (from40% to 30%) and an another decrease until today of 10% (from 30% to 20%). This makes sense from the sedimentological perspective. The depth of the diatreme we figure as 1000 m. So we get a result, for the earlier land surface being located around 300 m (468 m a.s.l.) higher than today. Alternatively, in a maximum model we calculated the compaction of the finegrained organic sediments until the end of the sedimentation of the upper Messel formation from an original porosity of 60% to 40% to a recent porosity of 40% to 20%. The depth of the original diatreme is accounted for as 2000m. So we get a result of around 600 m (768 m a.s.l.) for the higher position of the earlier land surface compared to today, in the maximum model.

We calculate the original diameter of the maar crater based on the total thickness of the crater sediments. At the end of the sedimentation theis thickness is calculated as 437 m. Often recent maars show a ratio of the depth of the crater to the original diameter of around 1 : 5. Applying this to the Messel volcano, the diameter was more than 2 km. This is substantially more than the recent extension of the crater sediments indicate. The original shore line was located at least 500m inland from the recent Messel pit.

The dip of the recent contact between the crater sediments and the Paleozoic plutonic and metamorphic rocks is about 60°. Seismic measurements indicate a steeper inclination with depth (70° and more). So what we can see today is the upper part of the diatreme in which the central crater sediments have been compacted and subsided. So the beautiful fossils owe their conservation to the compaction of the diatreme.

Introduction to the research progress of Sifang Mountain Tianchi

Jiali Liu[1], Qiang Liu[1], Jiaqi Liu[1], Jing Wu[1] and Guoqiang Chu[1]

[1] *Division of Cenozoic Geology and Environment, Institute of Geology and Geophysics Chinese Academy of Sciences, Beijing, China.* liujiali@mail.iggcas.ac.cn

Keywords: Crater Lake, climate change, EASM.

Sifang Mountain Tianchi (49° 22′ 32.97″ N, 123° 27′ 49.90″ E, altitude: 933 m asl) is a circular crater lake which located on the northeast of the Hulunbeier City, Inner Mongolia Province, China (Fig.1-A). For regional geological, it sites in the Nuomin River-Kuile River volcanic area which compose the Great Xing'an Range Quaternary volcanic area with the Halaha River-Chaoer River volcanic area (Fig.1-D). It was formed by volcanic eruptions during the late-Pleistocene (0.128±0.01Ma) (Zhao, 2010).The hilltop is about 500 meters from east to west, over 300 meters from north to south.

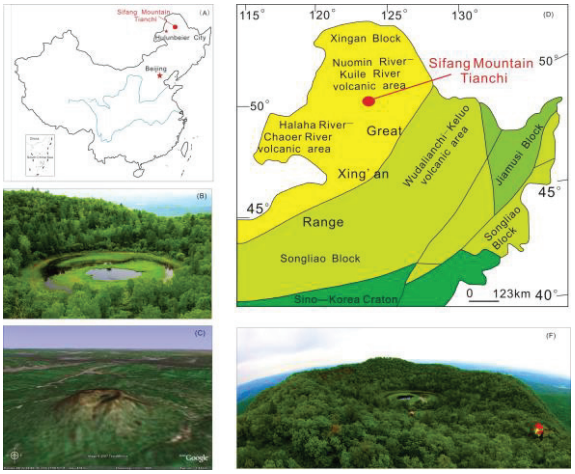

Fig. 1 – (A) Location of the Sifang Mountain Tianchi; (B) Close-range diagram of the Sifang Mountain Tianchi; (C)Satellite image of the Sifang Mountain Tianchi (modified from Google Earth) (D) Geological map of Northeast China; (F) Distanced-range diagram of the Sifang Mountain Tianchi (modified from Wu *et al.*, 2001).

A series of overlapping cores gravity cores and piston cores) have been retrieved from Sifang Mountain Tianchi in March, 2012. The core was transported upright back to the laboratory. In the laboratory, the cores were split, opened and sampled. The cores were split in half lengthwise. One half was used for geochemical analyses, whereas the other half was used for preservation. Cores were cut into 1-cm discs. In our study, 489 samples were used for analyzing TOC and TON by vario EL cube which was produced by Elementar Analysensysteme GmbH in Qinghai Institute of Salt Lakes, Chinese Academy of Sciences; 102 samples were used for determining $\delta^{13}C_{org}$ (‰) by Finnigan MAT 251 in State Key Laboratory of Loess and Quaternary Geology, Institute of Earth Environment, Chinese Academy of Sciences.

In order to build reliable high-precision the ^{14}C age timescale, we equidistantly picked leaves, fruits, seeds and other plant residues in the lake sediments as far as possible. 16 samples were determined by Poznan Radiocarbon Laboratory, Adam Mickiewicz University; Calibrated age was obtained after correction using the CALIB-602(http: // calib.qub.ac.uk/calib/) programme. Then, we obtained the calibrated age sequence of the Sifang Mountain Tianchi sediment profile via the linear interpolation-extrapolation method. Finally, we built up the Depth-Age model of the Sifang Mountain Tianchi sedimentary sequence (Fig.2).

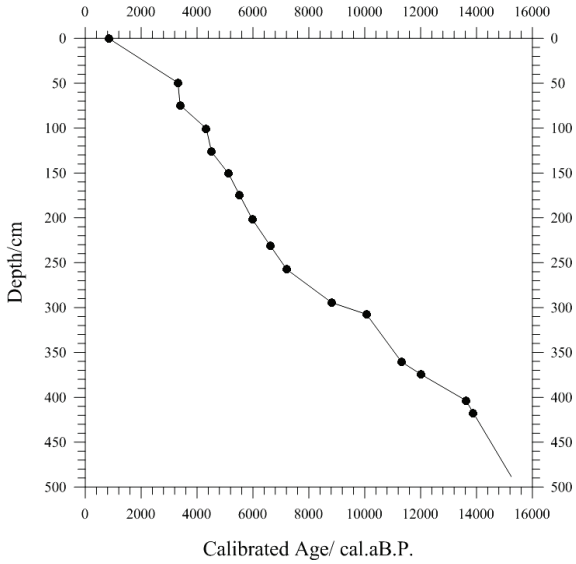

Fig. 2 – The Depth-Age model of the Sifang Mountain Tianchi sedimentary sequence.

The variation tendency of the $\delta^{13}C_{org}$ (‰) of the Sifang Mountain Tianchi sedimentary sequence （Fig.3） has been expressed by a curve. Fig.4 shows the deviation from the mean of the Sifang Mountain Tianchi sediment $\delta^{13}C_{org}$ (‰) series. The zero line indicates -26.94‰; this is the mean of the $\delta^{13}C_{org}$ (‰) values over the entire sedimentary

sequence. We can't discuss scientific views in detail just because we haven't obtained all the data of TOC, TN and other proxies.

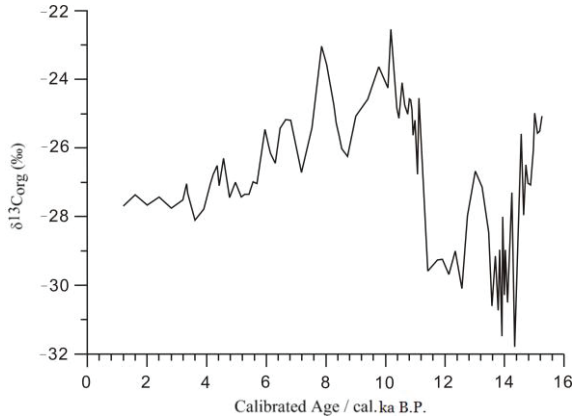

Fig. 3 – The variation tendency of the $\delta^{13}C_{org}$ (‰) of the Sifang Mountain Tianchi sedimentary sequence.

Since the lower the amount of $\delta^{13}C_{org}$, the higher the precipitation or intensity of the monsoon, and vice versa (Hong *et al.*, 2003, 2005). Research studies examining lake sediments and loess paleosol have suggested an abrupt strengthening of the East Asian Summer Monsoon (EASM) during the YD interval (An *et al.*, 1993; Wang *et al.*, 1994; Zhou *et al.*, 1996). We gallantly assumed that the climate of the YD cold period in northeast China is wet which is attributed to the occurrence of sea surface temperature variations from the El Nino-like pattern in the Equatorial Pacific Ocean Which is similar to the anomalous distribution of wet in the north and dry in the south over the Chinese mainland on an interannual scale (Hong, *et al.*, 2010).

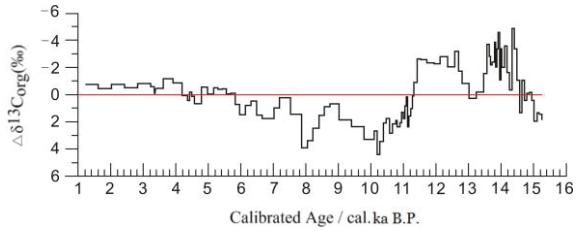

Fig. 4 – The deviation from the mean of the Sifang Mountain Tianchi sediment $\delta^{13}C_{org}$ (‰) series.

The assumption which was mentioned before is quite audacious and vague. The climate variation which should been concluded is still needed more evidences and proxies. The further works in the future may give us more inspiration.

Acknowledgements

We are grateful to all the teachers in the State Key Laboratory of Loess and Quaternary Geology, Institute of Earth Environment, Chinese Academy of Sciences and Qinghai Institute of Salt Lakes, Chinese Academy of Sciences for their helps during the experiment periods.

This research was supported by the National Natural Science Foundation of China (41320104006; 40872206; 41272392).

References

An, Z.S., Porter, S.C., Zhou, W.J., Lu, Y.C., Donahue, D.J., Head, M.J., Wu, X.H., Ren, J.Z.,Zheng, H.B., 1993. Episode of strengthened summer monsoon climate of Younger Dryas age on the loess plateau of central China. Quaternary Research 39: 45-54.

Hong, Y.T., Hong, B., Lin, Q.H., Zhu, Y.X., Shibata, Y., Hirota, M., Uchida, M., Leng, X.T., Jiang, H.B., Xu, H., Wang, H., Yi, L., 2003. Correlation between Indian Ocean summer monsoon and North Atlantic climate during the Holocene. Earth and Planetary Science Letters 211: 371-380.

Hong, Y.T., Hong, B., Lin, Q.H., Shibata, Y., Hirota, M., Zhu, Y.X., Leng, X.T., Wang, Y., Wang, H., Yi, L., 2005. Inverse phase oscillations between the East Asian and Indian Ocean summer monsoons during the last 12000 years and paleo-El Niño. Earth and Planetary Science Letters 231: 337-346.

Hong, B., Hong, Y.T., Lin, Q.H., Shibata, Y., Uchida, M., Zhu, Y.X., Leng X.T., Wang, Y., Cai, C.C., 2010. Palaeogeography, Palaeoclimatology, Palaeoecology 297:214-222.

Wang, S.M., Ji, L., Yang, X.D., Xue, B., Ma, Y., Hu, S.Y., 1994. The record of Younger Dryas event from sediment in Zalairoer Lake, Inner Mongolia. China Science Bulletin 39: 348-351.

Zhao, Y.W., 2010. Study on geology and geochemistry of Quaternary volcanoes in the Da Xing'an Ling Mountains. Doctor thesis. Institute of Geology, China Earthquake Administration.Beijing, China.

Paleoenvironmental reconstruction of a potential maar-diatreme system in the Siberian Traps

Kirsten E. Fristad[1] and Henrik Svensen[2]

[1] *ORAU/NASA Postdoctoral Program, NASA Ames Research Center, Moffett Field, California 94035, USA* Kirsten.E.Fristad@nasa.gov
[2] *Centre for Earth Evolution and Dynamics (CEED), The University of Oslo, Oslo, Norway*

Keywords: Siberian Traps, hydrothermal vent, end-Permian.

The Siberian Traps large igneous province comprises lava flows, pyroclastic deposits, and a network of sills and dikes that were emplaced in the Tunguska Basin sediments in Eastern Siberia. Hundreds of brecciated pipe structures, or diatremes, associated with the Siberian Traps have also been identified throughout the Tunguska Basin (Fig. 1) (Svensen et al., 2009; Von der Flaass and Naumov, 1995). These relict hydrothermal structures are rooted at approximately 4 km depth and were formed by interaction between Siberian Trap sill intrusions and water-petroleum-bearing horizons of the Cambrian evaporite-carbonate sequence in the Tunguska Basin (Von der Flaass, 1992). Soviet iron ore prospecting in the 1980's led to extensive mapping and sampling of the diatremes via hundreds of boreholes as many contain large magnetite ore bodies. Recent work examining the role of the Siberian Traps volcanism on the end-Permian mass extinction has renewed interest in the degassing potential of these diatremes. Svensen et al. (2009) proposed that significant volumes of carbon were thermogenically released from petroleum and organic matter deposits in the Tunguska Basin during Siberian Trap sill emplacement and diatreme formation. Thus, the diatremes may have acted as conduits for the release of toxic and greenhouse contact metamorphic gases, leading to environmental crisis at the end-Permian.

In the southern-most Tunguska Basin, crater deposits are preserved in twelve of these diatremes in a similar morphology to maar-diatreme volcanoes (Fig. 2). Given their timing relative to Siberian Traps formation and the end-Permian extinction (Ankudimova and Naumov, 1992; Burgess et al., 2014; Visscher et al., 2010), the maar-like crater sediments provide a unique window into the continental paleoecology of Siberia and hydrothermal degassing through the underlying diatreme at the time of formation.

An expedition to the Bratsk region in the southern Tunguska Basin in 2006 identified and sampled several intact drill cores through the East and West Oktyabrsk crater sediments and underlying diatreme.

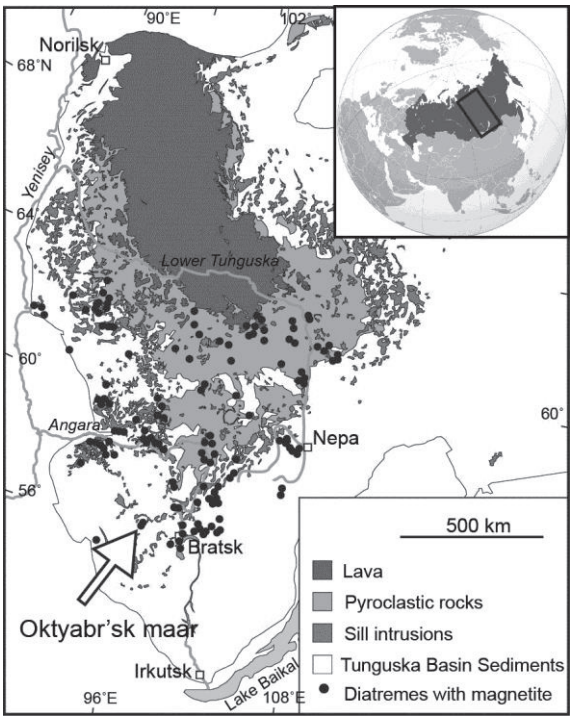

Fig. 1 – Geologic map of the Siberian Traps province and magnetite-bearing diatremes in Eastern Siberia.

We present analyses of material from the 1.3 km long s26 and s160 cores drilled through West Oktyabrsk diatreme and crater.

We report on the petrographic, geochemical and isotopic analyses of the Oktyabrsk lacustrine crater sediments with the goal of assessing their source and reconstructing the crater lake environment throughout its history. The volcaniclastic-rich carbonate-cemented sediments are consistent with maar-diatreme volcano origins and a rich organic matter and palynomorph record reflects the influence of the underlying hydrothermal system on lake conditions. We find that viewing the Oktyabrsk complex through a maar-diatreme paradigm may be useful for better understanding the formation history and environmental impact of these structures at the end-Permian.

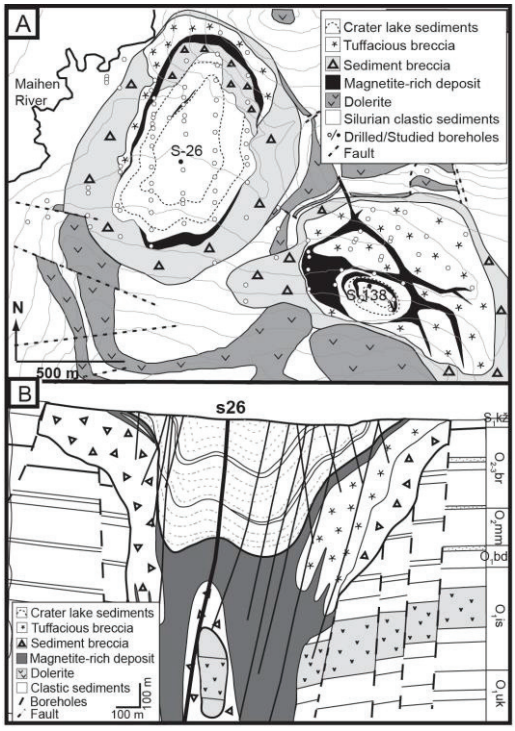

Fig. 2 – Geologic maps of the Oktyabrsk complex based on borehole data in A) map view and B) cross-section (Western crater).

Acknowledgements

We thank Sverre Planke for organization of the fieldwork, Stephane Poulteau and Clement Ganino for help during sampling, Øyvind Hammer for statistics assistance, K. Backer-Owe for lab assistance. K.E.F. acknowledges funding from the Norwegian Research Council YFF grant and NASA/ORAU Postdoctoral Program.

References

Ankudimova, L. A., and Naumov, V. A., 1995, The first pollen assemblages from volcanogenic sediments of middle angara region: Trans. Russ. Acad. Sci., v. 340, p. 72-74.

Burgess, S., Bowring, S., Shen, S. 2014. High-precision timeline for Earth's most severe extinction. Proceedings of the National Academy of Sciences DOI: 10.1073/pnas.1317692111.

Svensen, H., Planke, S., Polozov, A. G., Schmidbauer, N., Corfu, F., Podladchikov, Y., and Jamtveit, B., 2009, Siberian gas venting and the end-Permian environmental crisis: Earth Planet. Sci. Lett., v. 277, p. 490-500.

Visscher, H., Svensen, H., Looy, C., Fristad, K. E., Polozov, A. G., and Planke, S., 2010, Palynological constraints on timing and duration of Siberian Traps volcanic events, 7th EGU General Assembly, Volume 12, Geophys. Res. Abstr. p. 11100.

Von der Flaass, G. S., 1992, Magmatic stage in evolution of the Angara-Ilim type ore-forming system: Russ. Geol. Geophys., v. 33, p. 67-72.

Von der Flaass, G. S., and Naumov, V. A., 1995, Cup-Shaped Structures of Iron Ore Deposits in the South of the Siberian Platfrom (Russia): Geol Ore Deposit, v. 37, p. 340-350.

Impact of environmental changes on lacustrine dynamics in the Lake Pavin over the last 7,000 years (French Massif Central)

Léo Chassiot[1], Emmanuel Chapron[1,2], Aude Beauger[3], Yannick Miras[3], Patrick Albéric[1], Grégoire Ledoux[4], Patrick Lajeunesse[4], Markus Schwab[5], Anne-Lise Develle[6], Fabien Arnaud[6], Anne-Catherine Lehours[7], Christian Di Giovanni[1] and Didier Jézéquel[8]

[1] *ISTO, UMR 7327, CNRS, Université d'Orléans, BRGM, Orléans, France.* leo.chassiot@cnrs-orleans.fr
[2] *GEODE, UMR 5062, CNRS, Université Toulouse 2, Toulouse, France.*
[3] *GEOLAB, UMR 6042, CNRS, Université Blaise Pascal, Clermont-Ferrand, France.*
[4] *CEN, Université Laval, Québec, Canada.*
[5] *GFZ, Postdam, Germany.*
[6] *EDYTEM, UMR 5204, CNRS, Université de Savoie, Le Bourget du Lac, France.*
[7] *LMGE, UMR 6023, Université Blaise-Pascal, Aubière, France.*
[8] *LGE, UMR 7047, Université Paris Diderot, IPGP, Paris, France.*

Keywords: Maar, paleolimnology, hazards.

Lake records provide insight into the interactions between human societies, past climate and the natural environment. Maar lake basin fills are key sites for paleoenvironmental studies covering the Holocene and periods beyond (Negendank and Zolitschka, 1993, Augustinus *et al.*, 2012). They also could record sedimentary events linked to natural hazards specific to volcanic area such as crater outburst and limnic eruption (Anzidei *et al.*, 2008, Chapron *et al.*, 2010). Lake Pavin (French Massif Central, France) located in Western Europe is a meromictic maar formed ca. 7,000 years ago (Gewelt and Juvigné, 1988, Chapron *et al.*, 2010). This lake is almost circular with an area of 44 ha and a maximum depth of 92 meters with anoxic waters below 60 meters depth. Recent studies on the water column confirm the presence of methane and carbon dioxide in these anoxic waters (Fig. 1, Busigny *et al.*, 2014 and references therein).

Up to now, few paleoenvironmental studies have been made in this young French volcanic region (Lavrieux *et al.*, 2013) and specifically on sediments accumulated in the central basin in the Lake Pavin (Stebich *et al.*, 2005, Schettler *et al.*, 2007, Chapron *et al.*, 2012). Moreover, questions remain about the evolution of limnic and trophic status of this meromictic maar lake and hazards associated to it. For these reasons, this study focused on sedimentary deposits using geophysical mapping techniques (multibeam bathymetry and high-resolution seismic reflection) and sediment cores retrieved both in shallow water environments and within anoxic waters in the deep central basin (Fig. 1).

Multi-proxies analyses were carried out on sediments including X-Ray fluorescence, spectrophotometry and organic geochemistry by Rock-Eval pyrolysis. Radiocarbon dating has been performed both on leaves debris and bulk sediment in order to establish a depth-age model (Blaauw, 2010).

Results report gas-rich sediments consisting primarily of diatoms, deposited in three sedimentary environments: a littoral area, a plateau clipped by a landslide scar in the northern part of the lake and a flat central basin surrounded by steep slopes (Chapron *et al.*, 2010, 2012).

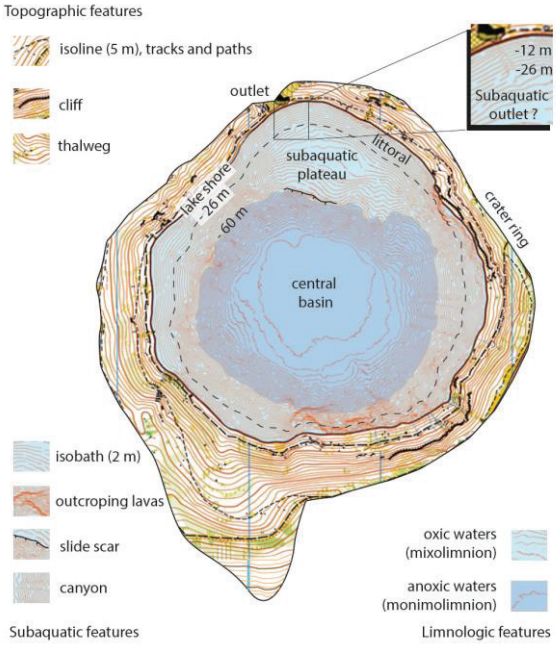

Fig. 1 – Geomorphological and bathymetric map of Lake Pavin and its catchment

In the central basin (Fig. 1), a 14 m long core has been retrieved, covering the last 7,000 years. The depth-age model is relevant with previous studies and has been confirmed by regional earthquakes recorded in the lake. The sediment is mainly composed of two in-situ diatomite units separated by a massive unit resulting from an instantaneous

deposit dated ca. AD 1300 and originating from the slide scar identified at the edge of the plateau (Chapron *et al.*, 2010, 2012). Change in diatom and pollen assemblages, but also in mineral and organic content reflects evolution in the trophic status of the lake from its origin to the present day, with a gradual transition from a young lacustrine system fed by allochthonous material to an organic maar with strong algal supplies. Elementary content of sediments allow us to estimate the amount of exported material towards the lake and the in-situ production. Although, the record of titanium along the core reflects an allochthonous contribution to sediment which may be related to climate triggers. Variation in this record highlights periods of enhanced supplies from the catchment.

On the plateau (Fig. 1), acoustic mapping and sedimentary analyses indicates a slump deposit surrounded by diatomites. This slump is dated around AD 600 and may have been caused by a crater outburst that was followed by a water-level drop in the lake and a catastrophic flood in the valley downstream.

On the littoral environment, which consist of brownish sediments (Fig. 1), two erosive layers made of sand and/or leaves have been correlated to previously mentioned events (AD 600 and AD 1300). They have been deposited after wave action on the banks of the lake, generated by mass wasting deposits in the central basin and the plateau. The major lake-level drop is also confirmed by the changes in the composition of the sedimentary organic matter after AD 600.

Finally, this study provides new elements on the trophic status evolution of maar Lake Pavin and information about sedimentation patterns due to climate through the late Holocene in the French Massif Central. This study also illustrates the instability of such gas-rich sediments, which can be easily reworked because of regional trigger and may cause mass wasting deposits. Because catastrophic phenomena can occur into meromictic maar lakes, further evaluations have to be made to define the role of gravitational processes on natural hazards linked to meromictic maar lake.

Acknowledgements

Authors would like to thank contributors to projects MEEDDAT and DICENTIM (and many else…) to provide us data and sedimentary material for studying the Lake Pavin.

References

Anzidei, M., Carapezza, M.L., Esposito, A., Giordano, G., Lelli, M., Tarchini, L., 2008. The Albano maar lake high resolution bathymetry and disolved CO2 budget (Colli Albani volcano, Italy): constrains to hazard evaluation, Journal of Volcanic and Geothermal Research, 171, 258-268.

Augustinus, P., Cochran, U., Kattel, G., D'Costa, D., Shane, P., 2012. Late Quaternary palolimnology of Onepoto maar, Auckland, New Zealand: implications for the drivers of regional paleoclimate. Quaternary International 253, 18-31.

Blaauw, M., 2010. Methods and code for 'classical' age-modelling of radiocarbon sequences. Quaternary Geology 5, 512-518.

Busigny, V., Planavsky, N.J., Jézéquel, D., Crowe, S., Louvat, P., Moureau, J., Viollier, E., Lyons, T.W., 2014. Iron isotopes in a Archean ocean analogue. Geochimica et Cosmochimica Acta 133, 443-462.

Chapron, E., Albéric, P., Jézéquel, D., Versteeg W., Bourdier, J.-L., Sitbon, J., 2010. Multidisciplinary characterisation of sedimentary processes in a recent maar lake (Lake Pavin, french Massif Central) and implication for natural hazards. Natural Hazards and Earth System Sciences 10, 1-13.

Chapron, E., Ledoux, G., Simonneau, A., Albéric P., St-Onge, G., Lajeunesse, P., Boivin, P., Desmet, M., 2012. New evidence of Holocene Mass Wasting Events in recent volcanic lakes from the French Massif Central (Lakes Pavin, Montcineyre and Chauvet) and implications for natural hazards. In: Yamada *et al.* (eds.) Submarine Mass movements and their consequences. Advances in natural and technological hazards research 31.

Gewelt, M., Juvigné, E., 1988. Téphrochronologie du Tardiglaciaire et de l'Holocène dans le Cantal, le Cézallier et les Mont Dore (Massif central, France) : résultats nouveaux et synthèse. In: Bulletin de l'Association française pour l'étude du quaternaire 25 : 25-34.

Lavrieux, M., Disnar, J.-R., Chapron, E., Bréheret, J.-G., Jacob, J., Miras Y., Reyss, J.-L., Andrieu-Ponel, Valérie, Arnaud, F., 2013. 6700 yr sedimentary record of climatic and anthropogenic signals in Lake Aydat (French Massif Central). The Holocene 23, 1317-1328.

Negendank, J.F.W., Zolitschka, B., 1993. Paleolimnology of European Maar Lakes. Lectures Notes in Earth Sciences 49, 509 pp.

Schettler, G., Schwab, M.J., Stebich, M., 2007. A 700-year record of climate change based on geochemical and palynological data from varved sediments (Lac Pavin, France). Chemical Geology 240, 11-35.

Stebich, M., Brüchmann, C., Kulbe, T., Negendank, J.F.W., 2005. Vegetation history, human impact and climate change during the last 700 years recorded in annually laminated sediments of Lac Pavin, France. Review of Palaeobotany and Palynology 133, 115-133.

Hydrogeochemical characterization and microdiversity in Extreme Environmental of Mexico: Case Rincon de Parangueo, Guanajuato

María Elizabeth Hernández Zavala[1], José Alfredo Ramos Leal[1], Ángel Gabriel Alpuche Solis[2], María Isabel Isordia Jasso[2], Mayra Janeth Esparza Araiza[2], Janete Morán Ramíez[1], Ulises Rodríguez Robles[3], Rosa María Fuentes Rivas[1], and Rosalba Castillo Collazo[2].

[1] *División de Geociencias Aplicadas, IPICYT, San Luis Potosí, México,* maria.hernández@ipicyt.edu.mx
[2] *División de Biología Molecular, IPICYT, San Luis Potosí, México.*
[3] *División de Ciencias Ambientales, IPICYT, San Luis Potosí, México.*

Keywords: Hydrogeochemical, microbiodiversidad, extremófilo.

Introduction

The study site is a crater lake located in the southern part Guanajuato state, near the state of Michoacán. The maar is located at 20° 25' N, 101° 15'W and it is 1700 m a.s.l. The average annual temperature varies between 18 and 20 ºC. The annual rainfall varies between 600 and 800 mm. According to INEGI's classification, the study area is located in the municipality of Valle de Santiago, Guanajuato, within the province of the Central Volcanic Belt.

The volcano Rincón de Parangueo is a maar. The gradual dessication of the lake was caused by human activities and urban growth that demanded a lot of wells drilled, this affected the deep aquifer, lowering their levels. As a consequence of the decrease in the water volume there was and increase in the salts concentration in the water. Today Crater of Parangueo is an extreme halophilic environment type (Figure 1), with a large halófila microbiodiversity. Base on its physicochemical characteristics, the site compares to other similar planets; which helps us to know, understand and find the primitive conditions of our planet Earth, hence the importance of describing the conditions under which life could start and develop on Earth. Biology in this type of environment, it is the least studied, so in this paper intends to perform physicochemical measurements in water and sediment samples; as well as molecular testing, microbiological microorganisms in such media.

There are microorganisms that remain unidentified to date, so conservation of samples is important in biotechnology, pharmaceutical, food research and the evolution of microbes found.

The study site is located in a broad valley and south of the maar is a highland formed by late Tertiary and Quaternary volcanoes.

Terrestrial vegetation in the inner slopes of the crater Parangueo is formed by bushes, thistles and cacti.

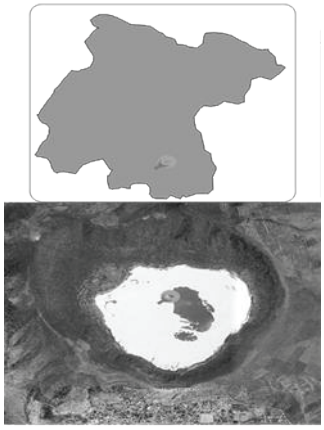

Fig. 1 – Rincón de Parangueo, Guanajuato.

Materials and methods.

Two samples (water and sediment) were collected during the rainy season. Later in the dry season samples are being analyzed were taken. They were divided for chemical, molecular, physical microbiological studies.

Fig. 2 – View of Crater-Lake of Rincon of Parangueo, Guanajuato.

Sediment and water sampling. For this study, water samples were collected in Nalgene bottles. These samples were used for chemical analyzes (cations, anions and trace) and isotopes.

A spatula was used to collect sediment samples in plastic bags. These were used for microbiological and molecular analysis.

In situ measurement of physicochemical parameters. An alkalinity test kit of Hanna Instruments was used. To obtain the parameters of pH, ORP, conductivity, water temperature, dissolved oxygen, total dissolved solids, salinity, atmospheric pressure, using HI 9828 Multiparameter.

Microbiological methods. Potato Dextrose Agar medium was prepared MDC Brand, Brand MP YPD, Middle Chu used Gómez *et al.*, 2009. Were used in aerobic and anaerobic conditions at 28 °C.

Molecular biology. A modified protocol proposed by Gabor *et al.* (2003) was used for the extraction of DNA samples. Identification of microorganisms was performed by amplifying the region with universal 16S rDNA oligos 533F (5'-GTGCCAGCMGCCGCGGTAA-3'), 1391R (5'-GACGGGCGGTGTGTRCA-3') (Bond *et al.*, 2000). The amplified fragments were cloned into pGEM T-easy vector (Promega). Sequencing of the clones obtained was performed at the 3130 Genetic analyzer Applied Biosystems (LANBAMA).

Results

The first campaigns in the crater-lake of Rincón de Parangueo to collect water and sediment were held during the rainy season of 2013 (2 samples, September 27) and during the dry season of 2014 (7 samples, April 23).

The physicochemical characteristics of the study site are presented in the following table, in which, alkaline water is observed in Rincon de Parangueo and its electrical conductivity is remarkably high.

Table of Results of Rincon de Parangueo, anions studied in September 2013.

Sitio	Cráter-lake
pH	10.16
ORP	112.9
Temp.	25.4
STD	17.01
OD	243
Conductivity	26370
Alcalinity	$3x10^{-12}$ mg/L
NO_2-	0.39
$(NH_4)NO_3$	0.87
NO_3-	3
SO_4	360
Cl-	6.5
PO_4	2.57
Si-	3.34
F-	$0.22x10^{-13}$

Microbial diagnostics in the water sample in the rainy season, showed Penicillium sp, bacilli (gram positive), gram positive cocci and bacilli. In the sediment were observed Aspergillus sp, sterile mycelium, 2 different types of bacilli size using gram positive and gram negative cocci and Arthrospira platensis.

In the microbiological diagnosis, fungi, bacteria and cyanobacteria were developed as shown in the figures from left to right: Penicillim sp (fungus), gram positive bacteria and Arthrospira platensis (cyanobacteria).

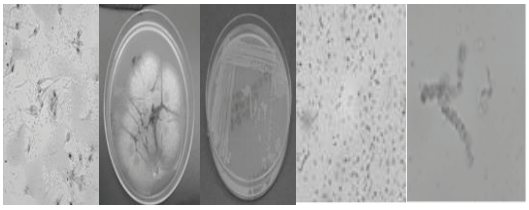

In molecular tests such oligos were used because they can identify bacteria and archaea. Samples are examined in the sequencing process.

Conclusions

The physicochemical study confirms through its parameters is an extreme halophile site. On the other hand, was isolated in means of short-term conservation different microorganisms can continue to study and learn some biotechnological application. Molecular studies have been amended several protocols to achieve the extraction of DNA.

The first results of this work show great microbiodiversity, the importance of extremophiles can contribute to the development of new biotechnological applications; however, the lake is increasingly affected by anthropogenic activities whereby the preservation of the ecosystem and the conservation of its microbiodiversity necessary.

References

Gómez N. *et al*. 2009.Conceptos y técnicas en Ecología Fluvial. Fundación BBVA.

Gabor, E., De Vries, Erik J., Janssen Dick B.,2003. Efficient recovery of environmental DNA for expression cloning by indirect extraction methods. FEMS Microbiology Ecology 44: 153-163.

Pacheco J. *et al.* 2012. Avances en el entendimiento del hundimiento del cráter-lago rincón de parangueo, Valle de santiago, Guanajuato. 13 Seminario de Investigacion. Universidad Autónoma de Aguascalientes.

Philip L. *et al.* 2000. Phylogeny of Microorganisms Populating a Thick, Subaerial, Predominantly Lithotrophic Biofilm at an Extreme Acid Mine Drainage Site. Applied and environmental microbiology. Vol. 66, No. 9: 3842–3849.

Paleontology of Foulden and Hindon Maars, Waipiata Volcanic Field, southern New Zealand: key sites for reconstructing early Miocene Southern Hemisphere mid-latitude terrestrial paleoecosystems

Uwe Kaulfuss[1], Daphne E. Lee[1], Jennifer M. Bannister[2], Jon K. Lindqvist[1], John G. Conran[3], Tammo Reichgelt[1], Elizabeth M. Kennedy[4] and Dallas C. Mildenhall[4]

[1] *Department of Geology, University of Otago, PO Box 56, Dunedin, New Zealand.* uwe.kaulfuss@otago.ac.nz
[2] *Department of Botany, University of Otago, PO Box 56, Dunedin, New Zealand*
[3] *ACEBB, School of Earth & Environmental Sciences, Benham Bldg DX 650 312, University of Adelaide, Australia.*
[4] *GNS Science, PO Box 30368, Lower Hutt, New Zealand.*

Keywords: maar lake, fossil, New Zealand.

Foulden Maar and Hindon Maar are two partly eroded maar–diatreme volcanoes in the monogenetic, early to mid Miocene Waipiata Volcanic Field, Otago, southern New Zealand that preserve highly fossiliferous, laminated lacustrine diatomite deposited in former maar lakes. Numerous plant and animal fossils collected at both sites provide exceptional windows into mid-latitude lake and forest ecosystems in the Miocene of New Zealand. The diversity and maar–type quality of preservation confirms these are fossil *Lagerstätten* comparable to famous European maars of Eckfeld, Enspel, Messel and Randeck: they are as yet unrivalled in the Southern Hemisphere.

Paleontological research since 2003 (*e.g.* Lindqvist and Lee, 2009; Bannister *et al.* 2012; Lee *et al.* 2007, 2012; Reichgelt *et al.* 2013; Mildenhall *et al.* 2014) has established the paleoenvironment at Foulden Maar as that of a ~1000 m diameter maar lake, free of benthic organisms in deeper parts but inhabited by a lake–locked species of *Galaxias* (southern Hemisphere family Galaxiidae), freshwater eels and aquatic insect larvae. The lake was surrounded by an evergreen Lauraceae–dominated notophyll vine forest with diverse understory components, lianes, epiphytes and several canopy layers, growing on fertile volcanic soils and probably including some forest openings at the lake's margin. More than 100 species from 35 plant families identified to date from micro and macrofossils indicate that modern equivalents of the Foulden Maar paleoforest are to be found in Queensland, Australia.

Regarding the fossil record of terrestrial arthropods, Foulden Maar is by far the most informative site in New Zealand. About 20 spider and insect families have been identified from the orders Araneae (spiders), Plecoptera (stoneflies), Blattodea: Termitoidea (termites), Hemiptera ('bugs'), Coleoptera (beetles), Hymenoptera (wasps and ants), Trichoptera (caddisflies), and Diptera, which largely represent a fauna typical of soil, leaf litter and forest floor habitats: large–winged and flying insects are comparatively rare. Many of the fossil taxa have close relatives in the modern New Zealand biota, but some are now locally extinct.

Based on the varved character of the diatomite, compositional affinities of the fossil biota to modern taxa, and CLAMP and Bioclimatic Analysis of leaves, a mesothermal, seasonal paleoclimate with mean annual temperatures at 18.5–19.5 °C and mean precipitation rates at 1700–2000 mm per year has been reconstructed for the site. The earliest Miocene age (~23.2 Ma) of Foulden Maar is well–constrained by palynology, radiometric dating of volcanics and magnetostratigraphy.

Comparatively little is known about the geology and paleontology of Hindon Maar (c. 25 km SSE of Foulden), where preliminary research commenced in 2014. The presence of a maar–diatreme structure has been inferred from a subcircular magnetic anomaly c. 1000 m in diameter, filled in at near-surface levels by very fossiliferous, laminated diatomite and exhibiting outcrops of weathered lapilli tuff at its margins, in a monogenetic volcanic setting. Excavations in two test pits near the centre of the inferred maar crater have yielded a wealth of animal and plant fossils (Fig. 1), which show a quality of preservation similar to that from Foulden Maar, but with a different taxonomic composition. The preliminary age determined for Hindon Maar is early Miocene (23–16 Ma), based on a palynological sample: we plan to obtain a more precise age from additional pollen samples and, if possible, radiometric ages from associated volcanics. The most common fossils at Hindon Maar are again floral remains such as leaves (mainly *Nothofagus* (southern beech), but also *Ripogonum*, conifers and cycads), flowers with *in situ* pollen, fern fronds, seeds and fruits, which together are indicative of a

Nothofagus/podocarp forest growing under humid, warm temperate to subtropical conditions around the maar–lake. This is in marked contrast with the subtropical Lauraceae–dominated evergreen rainforest that surrounded Foulden Maar.

Fish fossils appear more abundant at Hindon Maar: several dozen specimens include larval to adult stages of one or more taxa within Galaxiidae but have not yet been studied in detail. Some include fish skin and mouthparts. Also abundant in terms of specimen numbers and diversity are insects, which currently comprise ~60 specimens belonging to the orders Hemiptera, Hymenoptera, Trichoptera and, in particular, Coleoptera, with weevils being particularly diverse.

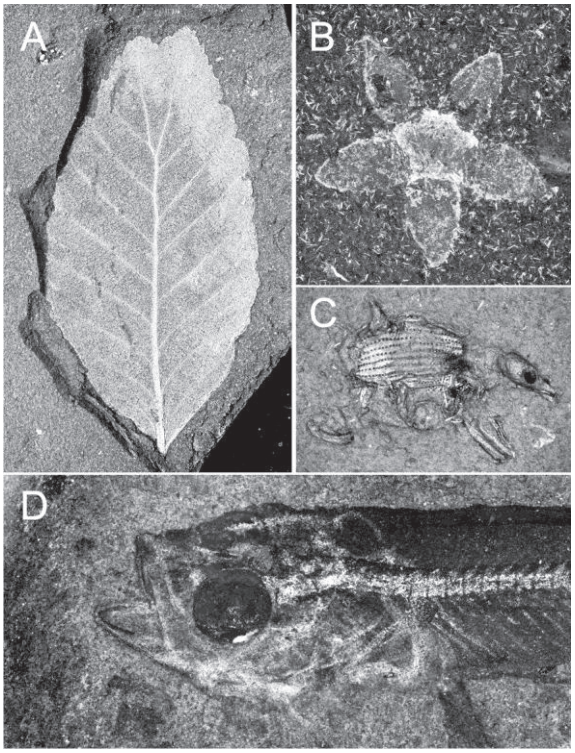

Fig. 1 – Examples of early Miocene fossils from Hindon Maar. A, leaf; B, flower; C, weevil, D galaxiid fish.

While fossils at Foulden Maar and Hindon Maar allow detailed reconstructions of their respective local paleoecosystems, the obviously different floral and faunal spectrum at these spatially (and temporally?) separated sites provide the opportunity to test environmental and climatic factors influencing terrestrial diversity in southern New Zealand in the Miocene. For example, the insect families and genera identified from both sites are largely present in the modern NZ fauna (although many have their highest modern diversity in subtropical and tropical regions elsewhere in the Pacific region); but so far no families are common at Foulden and Hindon. Whether this reflects coeval variation between local ecosystems and/or environment and climate–related ecological changes over time (*e.g.* Hindon is probably closer to the Miocene Climatic Optimum than Foulden) will be the subject of future study, as will be the geology of the Hindon Maar and nearby magnetic anomalies.

Both Foulden and Hindon Maars are crucial in reconstructing past lake and forest ecosystems in southern New Zealand, in particular the terrestrial arthropod component, which has been virtually absent at other Cenozoic sites. This underlines the importance of maar lake sediments as fossil and climate archives in New Zealand and elsewhere.

Acknowledgements

We thank the Gibson and Neehoff families and Featherston Resources for kindly allowing us access to the sites, and the Marsden Fund and the Division of Science, University of Otago, for financial support.

References

Bannister, J.M., Conran, J.G. Lee, D.E., 2012. Lauraceae from rainforest surrounding an early Miocene maar lake, Otago, southern New Zealand. Review of Palaeobotany and Palynology 178: 13-34.

Lee, D.E., Conran, J.G., Lindqvist, J.K., Bannister, J.M., Mildenhall, D.C., 2012. New Zealand Eocene, Oligocene and Miocene Macrofossil and Pollen Records and Modern Plant Distributions in the Southern Hemisphere. Botanical Review 78: 235-260.

Lee, D.E., McDowall, R.M., Lindqvist, J.K., 2007. *Galaxias* fossils from Miocene lake deposits, Otago, New Zealand: the earliest records of the Southern Hemisphere family Galaxiidae (Teleostei). Journal of the Royal Society of New Zealand 37: 109-130.

Lindqvist, J.K., Lee, D.E., 2009. High-frequency paleoclimate signals from Foulden Maar, Waipiata Volcanic Field, southern New Zealand: An Early Miocene varved lacustrine diatomite deposit. Sedimentary Geology 222: 98-110.

Mildenhall, D.C., Kennedy, E.M., Lee, D.E., Kaulfuss, U., Bannister, J.M., Fox, B., Conran, J.G., 2014. Palynology of the early Miocene Foulden Maar, Otago, New Zealand: Diversity following destruction. Review of Palaeobotany and Palynology 204: 27-42.

Reichgelt, T., Kennedy, E.M., Mildenhall, D.C., Conran, J.G., Greenwood, D.R., Lee, D.E., 2013. Quantitative palaeoclimate estimates for Early Miocene southern New Zealand: Evidence from Foulden Maar. Palaeogeography, Palaeoclimatology, Palaeoecology 378: 26-44.

Wavelet analysis of chlorophyll time series from Alchichica maar lake (Mexico)

Benjamín Quiroz-Martínez[1], Javier Alcocer Durand[2], David Alberto Salas de León[3], and Circe G. González[2]

[1] *Colección Nacional de Crustáceos, Instituto de Biología, Universidad Nacional Autónoma de México, México.* *bquirozm@gmail.com*
[2] *Proyecto de Investigación en Limnología Tropical, FES Iztacala, Universidad Nacional Autónoma de México, México.*
[3] *Laboratorio de Oceanografía Física, Instituto de Ciencias del Mar y Limnología, gUniversidad Nacional Autónoma de México, México.*

Keywords: Wavelets, Chlorophyll *a*, Lake Alchichica.

An eleven-year data set (1999-2010) of monthly temperature profiles from Lake Alchichica, Mexico, was used to perform nonlinear analysis of a time series using, time series decomposition, temporal autocorrelation functions and wavelet analysis to characterize the fluctuations of phytoplankton biomass expressed as chlorophyll *a* (Chl-a) over time. Wavelet analysis is quickly becoming a well known and important addition to the available set of tools of time series analysis; it performs a time-frequency analysis of the signal, which permits the estimation of the spectral characteristics of the signal as a function of time Mallat (1998) and then the identification of different periodic components and their time evolution all along the time series Cazelles et al (2008) . Phytoplankton biomass expressed as Chl-a is directly related to the total production of lakes Melack (1976). Spatial and temporal changes in Chl-a are primarily controlled by nutrients, light and temperature in the water column, factors that also determine the size spectrum and species composition of the phytoplankton Talling and Lemoalle (1998) and Adame *et al.* (2008). We compiled an eleven year time series of phytoplankton biomass (Chl-a concentration) from tropical Lake Alchichica and used wavelet analysis to extract the dominant periods of variability and the recurrence strength at those periods. We analyze whether phytoplankton biomass fluctuates over a consistent annual cycle in Lake Alchichica and whether characteristic phases and amplitudes of variability exist.

Lake Alchichica (2.3 km^2) is almost circular and has a maximum depth of 62 m (mean, 40.9 m). The lake is fed by saline, alkaline groundwater (TDS = 8.3–9.0 g L^{-1}, pH = 8.7–9.2) dominated by sodium, magnesium, chloride and bicarbonate ions Vilaclara *et al.* (1993), Alcocer *et al.* (2000), Filonov *et al.* (2006). Alchichica is warm monomictic. Annual mixing takes place from late December to early March during the cold dry season. During the warm rainy season from late March to early December, the lake remains stratified Alcocer *et al.*, (2000).

Two distinctive phytoplankton blooms occur during the year Alcocer and Lugo (2003). A winter diatom bloom takes place during the mixing period Oliva *et al.*, (2001) and a spring cyanobacteria Bloom occurs during early stratification around May Lugo *et al.*, (2000). Results showed a dominant and characteristic cycle with a period of 12 months, clearly associated to its hydrodynamics (thermal stratification) typified as warm monomixis.

Fig. 1 – Maar Lake Alchichica.

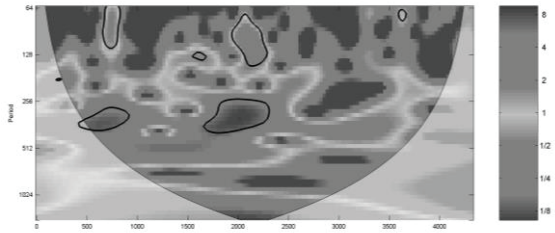

Fig. 2 – Wavelet analysis for the characterization of periodic frequencies of Chl-a time series

Contrary to the clear seasonal pattern, we found no interannual patterns or clear thermal trends. The lack of interannual patterns in Lake Alchichica is not unique, for example, Berman *et al.* (1995) found the same lack of interannual patterns in their analysis of a temperature time-series of 21 years in Lake Kinneret, Israel. Lake Alchichica resulted thermally regular and highly predictable.

Acknowledgements

This project was financially supported by the Consejo Nacional de Ciencia y Tecnología (CONACyT) project 103332, and the Dirección General de Asuntos del Personal Académico de la UNAM (DGAPA) projects IN221009 and 215212. Thanks are due to Luis A. Oseguera for field and laboratory support.

References

Adame, M.F., J. Alcocer, *et al.* (2008) Size-fractionated phytoplankton biomass and its implications for the dynamics of an oligotrophic tropical lake. Freshwater Biology, 53, 22-31.

Alcocer J., Lugo A., Escobar E., Sánchez M.R. & Vilaclara G. (2000) Water column stratification and its implications in the tropical warm monomictic Lake Alchichica, Puebla, Mexico. Verhandlungen Internationale Vereinigung für theoretische und angewandte Limnologie, 27, 3166–3169.

Alocer J. & Lugo A. (2003) Effects of El Niño on the dynamics of Lake Alchichica, central Mexico. Geofísica Internacional, 42, 523–528

Cazelles, B., M. Chavez, *et al.* (2008) Wavelet analysis of ecological time series. Oecologia, 156(2), 287-304.

Filonov A., Tereshchenko I. & Alcocer J. (2006) Dynamic response to mountain breeze circulation in Alchichica, a crater lake in Mexico. Geophysical Research Letters, 33, L07404, DOI: 10.1029/2006GL025901.

Lugo A., Alcocer J., Sánchez M.R., Escobar E. & Macek M. (2000) Temporal and spatial variation of bacterioplankton abundance in a tropical, warm-monomictic, saline lake: Alchichica, Puebla, Mexico. Verhandlungen Internationale Vereinigung fuür theoretische und angewandte Limnologie, 27, 2968–2971.

Mallat, S. (1998). A wavelet tout of signal processing. Academic Press, San Diego: 832 pp.

Melack, J.M. (1976) Primary productivity and fish yields in tropical lakes. Transactions of the American Fisheries Society, 105, 575-580.

Oliva M.G., Lugo A., Alcocer J., Peralta L. & Sánchez M.R. (2001) Phytoplankton dynamics in a deep, tropical, hyposaline lake. Hydrobiologia, 466, 299–306.

Talling, J.F., J. Lemoalle (1998). Ecological Dynamics of Tropical Inland Waters. Cambridge University Press, Cambridge: 452 pp.

Vilaclara G., Chávez M., Lugo A., González H. & Gaytán M. (1993) Comparative description of crater-lakes Basic chemistry in Puebla State, Mexico. Verhandlungen Internationale Vereinigung für theoretische und angewandte Limnologie, 25, 435–440.

Bacteria associated with microbialites from Rincón de Parangueo, Guanajuato

Adriana Espino del Castillo [1], Hugo Beraldi-Campesi [2], José Jorge Aranda-Gómez[3]

[1] *Departamento de Procesos y Tecnología, UAM-Cuajimalpa, México D.F. adrianaecr@gmail.com*
[2] *Instituto de Geología, Universidad Nacional Autónoma de México, Ciudad Universitaria, 04510 México D.F.*
[3] *Centro de Geociencias, Universidad Nacional Autónoma de México, UNAM Campus Juriquilla, Querétaro, México.*

Keywords: Rincón de Parangueo, microbialites, bacteria.

The Rincón de Parangueo maar used to have a perennial lake at its bottom. The lake was desiccated in the 1980's and now lake sediments are exposed at the crater's bottom, except in a reduced area which contains a highly evaporated playa-lake (Fig. 1). Near the former coast of the lake it existed a calcareous platform which now displays a great abundance and variety of hydromagnesite- and aragonite-rich microbialites. These microbialites are concentrated between the former coast of the lake and a 15 m high topographic scarp (Fig. 1). Evaporites, such as trona [$Na_3(CO_3)(HCO_3)\cdot 2(H_2O)$] and other sodium carbonates such as thermonatrite [$Na_2CO_3\cdot H_2O$], natrite [Na_2CO_3], and eitelite [$Na_2Mg(CO_3)_2$], together with halite [NaCl] and silvite [KCl] are present in the exposed sediments, indicating that the water was highly alkaline. Present day evaporated water has a pH = 10-11 (Aranda-Gómez *et al.*, 2013).

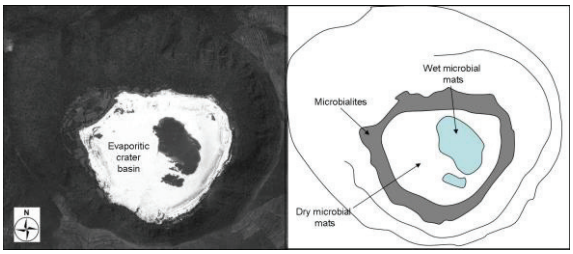

Fig. 1 – The former extent of Rincón de Parangueo perennial lake can be inferred from white lake sediments distribution. The sketch-map on the right shows the location of the calcareous platform where some of the studied samples were collected. Present day playa- lake where wet microbial mats were collected is also shown in the map.

Rincón de Parangueo microbialites (Fig. 2) can be classified as oncolites (laminated, non-attached structures), stromatolites (laminated and attached structures), and thrombolites (clotted, attached and non-attached structures). They vary greatly in size (from a few mm to several dm in diameter per individual structure) and shape (from nearly spherical to highly elongate forms). The size variation depends on microbialite location within the calcareous platform, as the largest stromatolites occur near an annular fault system at the top of the topographic scarp. This fault system is related to active subsidence and probably reflects the location of the buried contact between the country rock-diatreme (see Aranda-Gómez *et al.*, this volume). The fact that the largest stromatolites occur near the inferred location of the buried ring fault of the diatreme, and the shape of some of the stromatolite mounds (similar to that seen in hotspring sinter deposits), suggests that the diatreme's ring fault may have channeled mineral-rich hot water that favored stromatolite growth. By contrast, smaller onclolites are widespread elsewhere in the calcareous platform and they nucleated on a variety of inorganic (*e.g.* rock fragments) and organic (*e.g.* plant debris) materials.

Fig. 2 – Microbialites from Rincón de Parangueo. Left: Oncolites. Right: stromatolites (sometimes with internal thrombolitic fabric). Scale bar = 1 m.

As is the case with other types of microbialites (Walter, 1976), the presence of microorganisms was necessary for the formation of Parangueo's microbialites. The presence of bacteria associated with Parangueo's microbialites can be visually confirmed in crosscut sections that reveal the typical green pigmentation of cyanobacteria near the surface of the structures (Fig. 3a). The unquestionable presence of cyanobacteria can be further confirmed by keeping fragments of microbialites wet in the laboratory until the greening of the surface is evident

(Fig. 3b). However, it is expected that in addition to cyanobacteria, other types of bacteria will be present in such microenvironments, as it occurs with most microbial communities.

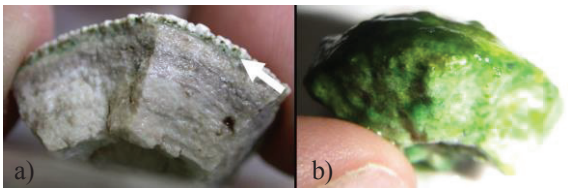

Fig. 3 – Cyanobacteria in Parangueo's microbialites. Left: green layer near the microbialite surface (arrow). Right: Same fragment of microbialite 1 week after being wetted in the laboratory. Note the green veneer of cyanobacteria covering the whole piece.

To better understand the nature of Parangueo's microbialites and the microbial ecology of the crater lake, we used the PCR-DGGE technique (Muyzer & Smalla, 1998) to determine the type of bacteria that are dominant in these microbialites. We also analyzed the bacterial composition of microbial mats collected in wet samples collected in the playa-lake (Fig. 1), in order to establish whether the microbial consortia associated with the microbialites is indigenous or not. Such comparison was necessary to evaluate if the microbial communities associated with Parangueo's microbialites represent the original consortia that formed them, or whether they are recent endolithic communities.

We found that microbialites are dominated by Cyanobacteria related to the Oscillatoriales, Firmicutes related to *Bacillus* sp., Mollicutes related to *Spiroplasma* sp., and Betaproteobacteria related to *Polynucleobacter* sp. or *Sulfuricella* sp. The wet microbial mats are dominated by Cyanobacteria related to *Calothrix* sp., *Cylindrospermum* sp., *Anabaena* sp. or *Nodularia* sp.; Actinobacteria and Gram-positive cocci were represented by single, unresolved sequences related to *Actinomyces* sp. and *Anaerococcus* sp., respectively. Flavobacteria are represented by sequences related to *Aestuariicola* sp., *Tenacibaculum* sp., *Lutimonas* sp., and *Polaribacter* sp.; Betaproteobacteria are represented by sequences related to *Piscinibacter* sp., *Roseateles* sp., and *Schlegelella* sp. The dry microbial mats are dominated by the Betaproteobacteria with sequences related to *Piscinibacter* sp., *Roseateles* sp., and *Schlegelella* sp. Cyanobacteria might have been present in the dry microbial mats, but no sequences were successfully retrieved from them.

Overall, the diversity found is distinctive for microbialites, and a few genera are common in both the wet and dry microbial mats (Table 1). Relatedness of sequences obtained from this study to sequences from public databases (GenBank) may indicate a distinction between indigenous and allochthonous bacteria. This may suggest that the present day communities associated with microbialites may be the original microbialite-building organisms, and not necessarily post-microbialite, endolithic communities. However, this needs further investigation to reach a final conclusion.

	Microbialites	Wet Microbial Mats	Dry Microbial Mats
Cyanobacteria	Oscillatoriales *Schizothrix* *Phormidium*	*Calothrix* *Cylindrospermum* *Anabaena* *Nodularia*	
Firmicutes	*Bacillus*		
Mollicutes	*Spiroplasma*		
Betaproteobacteria	*Polynucleobacter* *Sulfuricella*	*Piscinibacter* *Roseateles* *Schlegelella*	*Piscinibacter* *Roseateles* *Schlegelella*
Actinobacteria		*Actinomyces*	
Gram-positive cocci		*Anaerococcus*	
Flavobacteria		*Aestuariicola* *Tenacibaculum* *Lutimonas* *Polaribacter*	

Table 1. Genera found in microbialites, and in wet and dry microbial mats from Parangueo lake, based on partial 16S rRNA sequences.

Additionally, the inevitable presence of well-adapted microbes in Parangueo when the microbialites formed, is expected to have produced changes in the morphological development of the microbialites, as well as in their inner fabrics – such as porosity, density, and laminations. Thus, a biosignature could be characterized through the recognition of the biotic participation in the development of these microbialites. This also needs further investigation.

Acknowledgements

We thank Dr. Sylvie LeBorgne from UAM-C for her technical support, and Dr. Teresa Pi for XRD analyses. Research was supported by PAPIIT (IN109410) and Conacyt (129550) grants to Aranda.

References

Aranda-Gómez, J.J., Levresse, G., Pacheco Martínez, J., Ramos-Leal, J.J., Carrasco-Núñez, G., Chacón-Baca, E., González-Naranjo, G., Chávez-Cabello, G., Vega-González, M., Origel, G., Noyola-Medrano, C., 2013, Active sinking at the bottom of the Rincón de Parangueo Maar (Guanajuato, México) and its probable relation with subsidence faults at Salamanca and Celaya. Boletín de la Sociedad Geológica Mexicana 65(1): 169-188.

Muyzer G, Smalla K (1998) Application of denaturing gradient gel electrophoresis (DGGE) and temperature gradient gel electrophoresis (TGGE) in microbial ecology. Antonie Van Leeuwenhoek 73: 127-141.

Walter MR (1976) Stromatolites. In Developments in Sedimentology, 20 (ed. Walter MR). Elsevier, Amsterdam, 790 pp.

K E Y N O T E

Volcanic and hydrogeological hazards related to maar-diatreme volcanoes and distributed volcanic fields

Volker Lorenz

Physical Volcanological Laboratory, Department of Geography and Geology, University of Wuerzburg, Pleicherwall 1, D-97070 Wuerzburg, Germany. *vlorenz@geologie, uni-wuerzburg.de*

Keywords: maar-diatreme volcanoes, distributed volcanic fields, volcanic hazards.

Many areas of the world are subject to maar-diatreme volcanism and related distributed volcanic processes – formation of scoria cones, lava flows, domes, and tuff-ring-diatreme volcanoes. The highly explosive violence of maar and tuff-ring volcanoes is the most dangerous threat to human life in monogenetic volcanic fields. Growth of world population, settlements and economic development in and around active volcanic areas resulting in terrestrial and aerial transport and construction of many transport line systems make maar- and tuff-ring-related hazards and mitigation of hazards highly important issues. Therefore, maar and tuff-ring hazards must be investigated intensively and hazard maps must be made in order to be prepared and react fast when maar eruptions will occur in or near populated areas (Lorenz 2007).

Questions that will be asked prior to such expected explosive eruptions are: where will the eruptions occur, how powerful will they be, what are their characteristic hazards, how far will the individual hazards reach, how long might the volcano/es erupt, will there be a change from explosive phreatomagmatic to magmatic eruptions or vice versa, what will be the effects on humans, lifestock, agriculture, forests, local and regional infrastructure, air transport, and local, regional and international economy?

Very little is known about the pre-eruptive hazards of maar-diatreme and tuff-ring volcanoes except about the potential seismic hazard. Much more is known about possible syn-eruptive hazards for these volcano types but usually not in sufficient society-relevant detail (Lorenz 2007, Lorenz & Kurszlaukis 2007). A series of hazard scenarios can and should be deduced by the analysis of historic maar eruptions, but also of Holocene, Pleistocene and some Tertiary maar and tuff-ring craters and their tephra rings – and of the fill of Tertiary and older diatremes. These hazard scenarios should include the magmatic characteristics of the distributed volcanic field, good age data for the existing volcanoes to work out characteristics of the volcanic activity within the past lifetime of the particular distributed field, data of the topography, elevation, host-rock properties, structural aspects, stress field, hydrogeology and surface water properties. As all these characteristics vary from one volcanic field to another so vary some of the eruption and hazard characteristics. Another important aspect is that such maar and tuff-ring volcanoes as well as scoria cones may form only individually or that sometimes scoria cones and their lava flows form jointly with several explosive maar volcanoes along an eruptive fissure system that may be a few km long – with the consequence that the proximal hazard zones not a circular area surround an elongate volcanic system.

Discussions of hazards of eruptions within distributed volcanic fields, rarely tackle the important aspect of much more powerful eruptions. In central areas of many Western European volcanic fields intermediate magmas also formed maar-diatreme volcanoes, even with a dome inside their craters as happened, e.g., in the Chaîne des Puys in central France. However, even more voluminous and very powerful eruptions can take place in these central areas of monogenetic volcanic fields, as happened, e.g., in the East Eifel Volcanic Field. There, the phonolitic Rieden and Wehr volcanoes erupted several times and the Laacher See volcano erupted so far only once – but it erupted c. 6.4 km^3 of phonolitic magma (DRE) (Schmincke 2004).

An important variable is the host "rock" environment of the distributed volcanic field. One end member is the hard rock environment consisting of rather impermeable rocks and the other end member is a soft sediment environment with aquifers in coarse-grained sediments and aquicludes in fine-grained sediments in between. In a hard rock environment there exist aquifers of mostly vertical to near-vertical orientation in joint and fault zones along which groundwater, mineral, thermal, and CO_2 water flow and form springs. The more such a fracture zone is hydraulically active the more pronounced a valley is forming during regional uplift.

A good example for an uplifted hard rock environment is the West Eifel in Germany with its one Holocene, but mostly Pleistocene nephelinite, leucitite, basanite, and tephrite volcanoes (Lorenz & Zimanowski 2008). Most of the country rocks in the West Eifel consist of rather impermeable slates, greywackes, and quartzites. Out of c. 280 volcanoes about 98 maars and tuff-rings (and a few scoria rings) are known (Seib et al. 2013) and nearly all of them are

located in distinct valleys (Lorenz & Zimanowski 2008). They usually erupted phreatomagmatically from the beginning to the end of their of their activity which points to the availability of groundwater in more or less vertically oriented, hydraulically active fracture zones below the valley floors. Magnetic mapping showed, however, that in about 50 % of the maar-diatremes there had been a final phase of intrusion of a dyke or possibly even formation of a small scoria cone on the crater floor – that, similar to the late scoria cone inside Ukinrek East Maar/Alaska later became covered by lake sediments. The other c. 180 volcanoes consist of scoria cones that are located on the valley slopes or on plateaus. 57 % of the scoria cones formed lava flows that flowed towards or into neighboring valleys. Out of the 180 scoria cones about two thirds are known to be underlain by an initial maar. Thus, they started with a typical phreatomagmatic phase but then changed rather suddenly into a magmatic scoria production phase. This change indicates that there was sufficient ground water supply available for the initial phreatomagmatic phase but then, during ongoing magma rise, sufficient groundwater was not available anymore to continue the phreatomagmatic activity. Some of the scoria cones had also intermittent phreatomagmatic phases. Some of these scoria cones that formed within an initial maar crater are located on shallow usually dry valleys and thus obviously on fracture zones with some hydraulic activity. Thus, despite the fact that the country rocks are quite impermeable in the West Eifel Volcanic Field - as in many other distributed volcanic fields - there had been a very large number of volcanoes that erupted phreatomagmatically, either continuously or at least distinctly initially or intermittently. The number of the phreatomagmatically active volcanoes in the West Eifel Volcanic Field, therefore, had been almost 220, i.e. almost 80 % of the total. In this volcanic field a number of scoria cones and maars formed on the same eruptive fissure system almost simultaneously.

Since in the West Eifel not only most of the maar volcanoes are located in valleys but also many villages and small towns, the latter frequently 3-5 km apart from each other, future explosive volcanism in the West Eifel might severely effect some villages or small towns and the respective transport lines as has been pointed out already previously (Lorenz 2007). Depending on the length and intensity of the phreatomagmatic eruptions and wind directions, aviation in the airspace of the nearby airports of Frankfurt, Cologne-Bonn, Düsseldorf, Luxemburg, Saarbrücken, and Frankfurt-Hahn - all between 45 and 160 km away from potential West Eifel maar eruptions - and business at surrounding European international airports might get also stopped for weeks, months or, in a worst case scenario, for several years.

The soft sediment environment is represented by graben structures that displays syn-sedimentary volcanism as occurred, e.g., in the Basin-and-Range Province in northern Mexico and the Western U.S.A., in the European Cenozoic Rift System (ECRIS), the Late Herynian/Variscan Permo-carboniferous intermontane basins, or in coastal environments. One example is, e.g., the Late Variscan Permocarboniferous intermontane Saar-Nahe Basin with its Lower Permian intensive syn-sedimentary volcanism (tholeiitic basalts to rhyolites and alkalifeldspar trachytes) (Lorenz & Haneke 2004, Lorenz 2008). The volcanism led to formation of c. 26 diatremes, c. 20-30 dykes, many sills, 15 laccoliths, 3 intrusive-extrusive domes, many lava flows - reaching a thickness of up to 1000 m in the Baumholder area - and widespread tephra deposits. The majority of the several thousand meters of pre-volcanic sediments in the Saar-Nahe Basin consisted of fine-grained muds and silts as well as of badly sorted fine- and medium-grained sands. Due to their cumulate thickness and related compaction they cannot have been very permeable. Whereas the many sills intruded mostly finegrained muds and silts, the investigated diatremes is located on faults assumed to have been both active syn-sedimentarily and hydraulically (Lorenz & Haneke 2004, Lorenz 2008).

Several hydrogeological hazards associated with maar-diatremes were dealt with by (Lorenz (2007).

References

Lorenz, V., 1987. Syn- and posteruptive hazards of maar-diatreme volcanoes. Journal of Volcanology and Geothermal Research 159: 285-312.

Lorenz, V., 2008. Explosive maar-diatreme volcanism in unconsolidated water-saturated sediments and its relevance for diamondiferous pipes. Zeitschrift der Deutschen Gemmologischen Gesellschaft 57: 41-60.

Lorenz, V., Haneke, J.,2004. Relationship between diatremes, dykes, sills, laccoliths, intrusive-extrusive domes, lava flows, and tephra deposits with unconsolidated water-saturated sediments in the Late Variscan intermontane Saar-Nahe Basin, SW Germany. In: Breitkreuz, C., Petford, N. (eds.), Physical geology of high level magmatic systems. Geological Society, London, Special Publications 234: 75-124.

Lorenz, V., Kurszlaukis, S., 2007. Root zone processes in the phreatomagmatic pipe emplacement model and consequences for the evolution of maar-diatreme volcanoes. Journal of Volcanology Geothermal Research 150: 4-32.

Lorenz, V. & Zimanowski, B. 2008. Volcanology of the West Eifel Maars and its relevance to the understanding of kimberlite pipes. 9th International Kimberlite Conference, field trip, 7-10 & 16-18. August 2008, 9IKC, Frankfurt, 11-16. August 2008.

Schmincke, H.-U., 2004. Volcanism. 324 p., Berlin, Heidelberg, New York (Springer Verlag).

Seib, N., Kley, J., Büchel, G., 2013. Identification of maars and similar volcanic landforms in the West Eifel Volcanic Field through image processing of DTM data: efficiency of different methods depending on preservation state. International Journal of Earth Sciences (Geologische Rundschau) 102: 875-901.

The behavior of small scale basaltic systems

Ian E.M. Smith[1], Lucy E McGee[2]

[1] *School of Environment, The University of Auckland, Private Bag 92019, Auckland, New Zealand. ie.smith@auckland.ac.nz.*
[2] *Centro de Excelencia en Geotermia de los Andes, Universidad de Chile, Santiago, Chile.*

Keywords: monogenetic volcano, Auckland Volcanic Field, basalt geochemistry.

Fine-scale sampling through the deposits of small basaltic volcanoes reveals consistent trends in the chemical composition of magmas erupted over relatively short time scales. These trends provide a basis for understanding the geochemical behavior of monogenetic magmatic systems.

There are a number of compositional trends that are recognized as common to small scale basaltic volcanoes in general as well as trends that are interpreted to be specific to particular magmatic processes.

General trends are

1. In an individual eruption sequence initial magmas are relatively evolved and as eruptions proceed the composition of magmas becomes less evolved.
2. Fine-scale compositional variations suggest that deep seated processes are reflected in systematic compositional patterns at the surface pointing to little or no modification during ascent and therefore to very rapid ascent rates.
3. The typically fine scale variations observed in small volcanic cones become less distinct as the volumes of magma batches increase.
4. Within monogenetic volcano fields, temporally closely spaced eruptions are compositionally distinct indicating contemporaneous discrete magma generation/ segregation episodes.
5. There is a correlation of chemical composition with magma volume. Smaller volumes are more under-saturated in terms of SiO_2 and are basanites and nephelinites; larger volumes trend toward oversaturation in SiO_2 and are alkali basalts transitioning to tholeiites.

Specific tends observed in individual eruptive centres are:

1. Continuous compositional variation as an eruption progresses from more evolved to less involved (e.g .Smith et al, 2008)
2. Distinct changes within an eruption sequence signifying the arrival of a new magma in the near surface conduit (e.g. McGee et al.,2012).
3. Complex variation patterns (Brenna et al., 2011).

These patterns of geochemical variation in small scale basaltic systems are interpreted to be due to processes that occur within the source and near source regions by combinations of partial melting, fractional crystallization and magma mixing. In some examples there is also evidence for low pressure fractionation processes. In any particular volcano field there is a combination of fundamental parameters linked to a particular crustal environment and tectonic setting. In individual volcanoes within a field, variation in the combination of processes produces distinct geochemical trends.

In the following discussion we present a generalized model for the geochemical behavior of monogenetic basaltic systems.

A general model for monogenetic systems

Small scale basaltic magmatic systems typically produce discrete batches of magma that are erupted to the surface to form monogenetic volcanoes. Repeated episodes of magma formation result in fields of monogenetic volcanoes. Basaltic magmas are produced by partial melting of the mantle which, although primarily peridotite, potentially has an eclogite component that may reflect a previous tectonic (subduction-related) episode. These different components will have different melting characteristics (see below). Mantle sources are likely to be heterogeneous on a decimeter to meter scale.

Variations in the composition of primary magmas in monogenetic systems are due to variations in the chemical and mineralogical composition of their mantle source and to different degrees of partial melting. Although these are independent variables they can act together. These variables explain general points 4-5 above. A recent example of this is presented by McGee et al. (2012) (Fig.1) who explain the eruption of two distinct primary magmas in a single cone building episode by the sequential production and extraction of a low temperature fraction (eclogitic) and high temperature fraction (peridotitic).

In addition to variations in the chemical composition of primary magmas, monogenetic cones also typically show systematic compositional

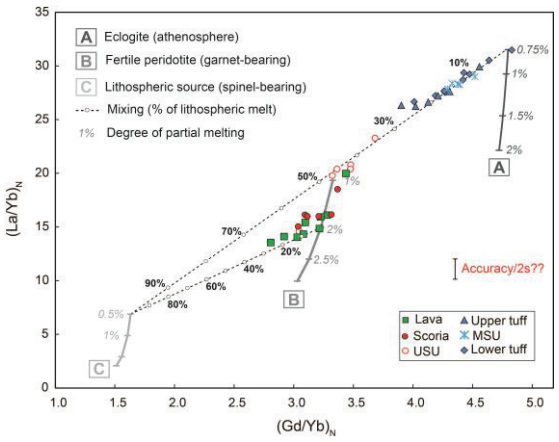

Fig. 1 – $(La/Yb)_N$ vs. $(Gd/Yb)_N$ (normalised to primitive mantle for Motukorea Volcano in the Auckland Volcanic Field . Variation patterns within the stratigraphic sequence from the early stage of the eruption (lower tuff, MSU, upper tuff) to the later stages (USU, scoria, lava) illustrate melting and mixing processes which create the observed chemical trends between the dominantly phreatomagmatic and dominantly magmatic phases of the eruption. Solid lines show melting of three sources based on those modelled for the AVF in McGee et al., (*2013*): Line **A** denotes melting of eclogite veins, Line **B** denotes melting of a fertile asthenospheric garnet peridotite source and Line **C** denotes melting of more depleted lithospheric spinel-bearing peridotitic source. Italicised numbers in all models denote degrees of partial melting. Bold numbers on mixing lines show percentage of lithospheric melt. For further details see McGee et al., (2012).

variations correlated with stratigraphy which is a proxy for time through an eruption sequence. Several types of variation are observed.

Simple variation in which the earliest magma erupted with relatively evolved chemical characteristics (low Mg, Ni, Cr and high LIL elements and HFS elements) are followed progressively by magmas with less evolved chemical characteristics (e.g. Smith et al., 2008). These variations are explained by crystal fractionation either at near source depths (clino-pyroxene dominated fractionation trends) or in the upper low pressure levels of the conduit system (olivine dominated fractionation trends).

More complex variation trends are observed where more than one magma batch occurs so that magma mixing as well as within batch fractionation processes create a variety of trends within a stratigraphic framework.

An important observation is that in magmatic systems where magma volumes are larger, the subtle trends observed in small-scale systems become increasingly less obvious. This is logical because convection and consequent mixing inevitably occurs in larger volumes and they have a greater capacity to interact with the rocks through which they pass.

An exciting conclusion is that small scale basaltic systems have a unique capacity to reveal the details of source mineralogy, partial melting and melt extraction processes through detailed study in a way that larger systems cannot

Acknowledgements

This work forms a part of the DEVORA project studying the Auckland Volcanic Field and funded through the Earthquake Commission of New Zealand

References

Brenna, M., Cronin, S.J., Németh, K., Smith, I.E.M., Sohn, Y.K., 2011. The influence of magma plumbing complexity on monogenetic eruptions, Jeju Island, Korea. Terra Nova 23, 70–75.

McGee, L. E., Millet, M-A, Smith, I.E.M., Nemeth, K., Lindsay, J.M. 2012. The inception and progression of a monogenetic eruption: Motukorea Volcano, the Auckland Volcanic Field, New Zealand. Lithos 155, 360-374.

McGee, L. E.; Smith, I. E. M.; Millet, M-A.; Handley, H. K.; Lindsay, J. M. 2013. Asthenospheric Control of Melting Processes in a Monogenetic Basaltic System: a Case Study of the Auckland Volcanic Field, New Zealand. *Journal of Petrology* 54, 2125-2153 doi:10.1093/petrology/egt043.

Smith, I.E.M., Blake, S., Wilson, C.J.N., Houghton, B.F. 2008. Deep-seated fractionation during the rise of a small-volume basalt magma batch: Crater Hill, Auckland, New Zealand. Contributions to Mineralogy and Petrology 3155: 511-527.

Spatial density analysis of volcanic vents as a tool to infer subsurface magma pathways

Aurelie Germa*, Laura Connor, Chuck Connor, Rocco Malservisi, Jacob Richardson and Aleeza Harburger.

[1] *School of Geosciences, University of South Florida, 4202 E Fowler Ave., Tampa, Florida, USA.*
* *agerma@usf.edu*

Keywords: spatial density, distributed volcanic fields, magma focusing, vent clusters.

Distributed volcanic fields often contain a large number of small-volume basaltic volcanoes along with one or more silicic central volcanoes that are long-lived and voluminous due to the development of shallow reservoirs (Bacon, 1985; Davidson and de Silva, 2000). One challenge of volcanic hazard assessment in distributed fields is to constrain the location of future activity given the unknown and generally unobserved subsurface location of melts and preferential magma pathways. Consequently, a key feature of any hazards analysis is how to relate the geologic record of past eruptive activity to the expected location of future events.

The lateral extent of distributed volcanic fields is defined by the area that encloses all eruptive vents at the surface and is believed to reflect the extent of the source at depth (Kiyosugi et al., 2010). Within a field, clusters of mafic volcanoes and the presence of polygenetic edifices denote zones of high magma flux and recurrence rate (Kereszturi and Nemeth, 2012; Conway et al., 1998; Martin, 2004), whereas areas of distributed mafic volcanism represent zones of lower flux. The high magma flux beneath polygenetic edifices may capture rising dikes and focus magmas, enhancing magma lensing mechanisms and the development of silicic reservoirs (Karlstrom et al., 2009; Muller et al., 2001). Additionally, voluminous edifices act as magma filters and prevent dense mafic magmas from reaching the surface. This results in a shadow zone surrounding the central silicic system, controlled by the edifice's radius, where mafic magmas are absent (Bacon, 1985; Pinel and Jaupart, 2000). Subsequently, the spatial distribution of mafic vents studied over long time periods may provide clues to the subsurface structure of a volcanic field including its magma sources and preferential magma pathways thereby, improving the assessment of volcanic hazards.

The questions we address are: How does the spatial distribution of eruptive vents at the surface reveal the location of magma sources or focusing? To what extent does edifice load or the shallow reservoirs affect the vertical and lateral ascent and migration of mafic magmas and cluster development?

We investigate five volcanic fields in different tectonic settings (i.e. continental arc and intraplate) in the western U.S.A.: Mt Adams (MA, Washington), Three Sisters volcanic cluster (TSVC, Oregon), Lassen volcanic area (LVA, California), San Francisco volcanic field (SFVF, Arizona), and Springerville volcanic field (SVF, Arizona). Each field contains hundreds of monogenetic volcanoes that are widely distributed, and often grouped into clusters. Monogenetic vents are generally absent from silicic edifices except at Mt Adams, South Sister and Lassen Peak that have chains of silicic domes on their flanks. Springerville is the only field where there is no polygenetic edifice present. An investigation of the spatial density of eruptive vents (number of vents per unit area, Fig. 1) allows us to locate vent clusters, i.e. areas where volcanic activity has been more intense, possibly revealing the location of magma sources at depth or preferential magma pathways in the crust. Additionally, we explore the influence of edifice load and shallow reservoirs on surface patterns of mafic volcanism by modeling bulk magma transport and storage in the crust as the non-linear flow of a viscous fluid within a homogeneous porous medium (Bonafede and Cenni, 1998; Bonafede and Boschi, 1992). By comparing output data from numerical simulations to the flux revealed at the surface by our spatial density analysis, we gain insights into the processes in the subsurface controlling the location of mafic volcanism. These data are augmented by incorporating published material such as geophysical or petrogenetic data that reveal the current distribution of melts in the crust or mantle.

Our results indicate that spatial density is generally lower by one order of magnitude at intraplate than at continental arc distributed volcanic fields (Fig. 1).

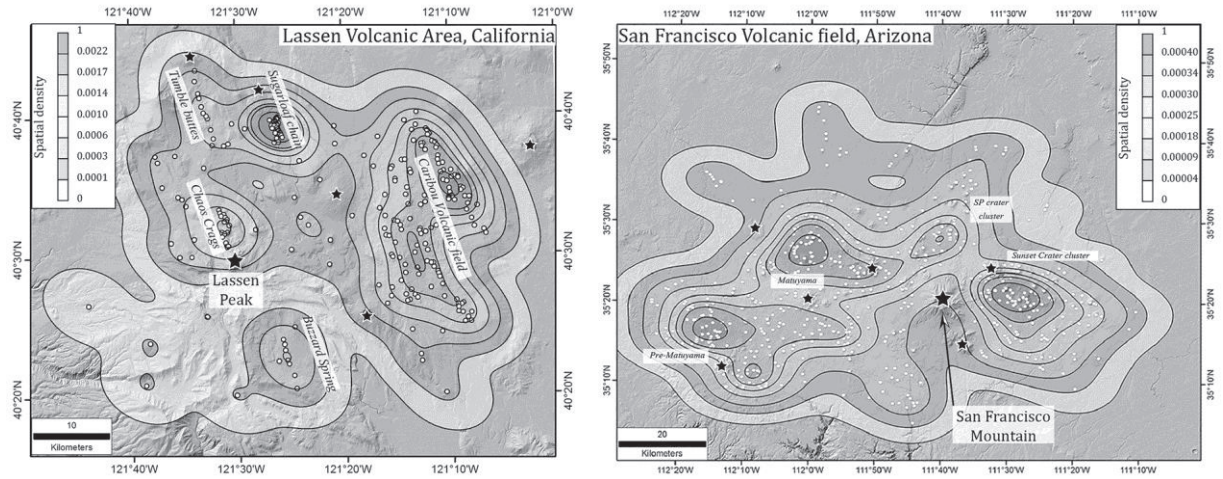

Fig. 1 – Spatial density map of monogenetic vents (white circles) at Lassen Volcanic area, California, and San Francisco Volcanic field, Arizona. Silicic polygenetic edifices are locates with black stars. Spatial density is calculated using an elliptical smoothing bandwidth determined with a SAMSE selector (Duong, 2007).

In the arc fields, clusters are narrow and elongated, parallel to the arc and to coeval regional fault systems. In the LVA (Fig. 1) and south of Mt Bachelor, clusters correspond to individual chains of vents, grouped in terms of age or geochemistry. In the SFVF (Fig. 1), the clusters mimic the migration of volcanism in the SFVF (Harburger, 2014). The two western clusters include vents older than 1 Ma whereas the eastern clusters have been the locus of the most recent volcanic activity in the SFVF (Tanaka, 1986). Moreover, in all fields, the clusters are spatially separated by the presence of polygenetic edifices. The spatial density of monogenetic vents agrees well with models of volcanism in these fields and allows identification of zones where magma fluxes are higher. Consequently, our method provides tools to standardize data collection and analysis and to improve hazard assessment efforts.

References

Bacon, C.R., 1985. Implications of silicic vent patterns for the presence of large crustal magma chambers. J Geophys Res, 90(B13): 11243.

Bonafede, M., Cenni, N. (1998). A porous flow model of magma migration within Mt. Etna: The influence of extended sources and permeability anisotropy. Journal of volcanology and geothermal research, 81(1), 51-68

Bonafede, M., Boschi, E. (1992). A porous-flow model of flank eruptions on Mount Etna. Journal of volcanology and geothermal research, 49(3), 349-363.

Conway, F.M., Connor, C.B., Hill, B.E., Condit, C.D., Mullaney, K. and Hall, C.M., 1998. Recurrence rates of basaltic volcanism in SP cluster, San Francisco volcanic field, Arizona. Geology, 26(7): 655-658.

Davidson, J. and de Silva, S., 2000. Composite Volcanoes. In: Sigurdsson (Editor), Encyclopedia Of Volcanoes. Academic Press, pp. 663-681.

Duong, T., 2007. ks: Kernel Density Estimation and Kernel Discriminant Analysis for Multivariate Data in R. Journal of Statistical Software, 21(7): 1-16

Harburger, A.M., 2014. Probabilistic modeling of lava flows: A hazard assessment for the San Francisco Volcanic Field, Arizona, University of South Florida, 78 pp.

Karlstrom, L., Dufek, J. and Manga, M., 2009. Organization of volcanic plumbing through magmatic lensing by magma chambers and volcanic loads. Journal of Geophysical Research: Solid Earth, 114(B10): B10204.

Kereszturi, G. and Nemeth, K., 2012. Monogenetic Basaltic Volcanoes: Genetic Classification, Growth, Geomorphology and Degradation.

Kiyosugi, K., Connor, C., Zhao, D., Connor, L. and Tanaka, K., 2010. Relationships between volcano distribution, crustal structure, and P-wave tomography: an example from the Abu Monogenetic Volcano Group, SW Japan. Bull. Volc., 72(3): 331-340.

Martin, A.J., 2004. Modeling long-term volcanic hazards through Bayesian inference: An example from the Tohoku volcanic arc, Japan. J Geophys Res, 109: 1-20.

Morgan, P., Sass, J.H. and duffield, W., 2004. Geothermal Resource Evaluation Program of the Eastern San Francisco Volcanic Field, Arizona.

Muller, J.R., Ito, G. and Martel, S.J., 2001. Effects of volcano loading on dike propagation in an elastic half-space. Journal of Geophysical Research: Solid Earth, 106(B6): 11101-11113.

Pinel, V. and Jaupart, C., 2000. The effect of edifice load on magma ascent beneath a volcano. Philos. Trans. R. Soc. London, A, 358: 1515-1532.

Tanaka, K.L., Shoemaker, E.M., Ulrich, G.E. and Wolfe, E.W., 1986. Migration of volcanism in the San Francisco volcanic field, Arizona. Geol. Soc. Am. Bull., 97(2): 129-141.

Monogenetic volcanism and seismicity the Mexico City area

Ana Lillian Martin-Del Pozzo*, Luis Quintanar, Carmen Jaimes, and Amiel Nieto

Instituto de Geofísica, Universidad Nacional Autónoma de México, Ciudad Universitaria, México D.F. 04510. México.
**analil@geofisica.unam.mx*

Keywords: Chichinautzin,seismicity, monogenetic.

The Chichinauzin monogenetic field is a large active field in southern Mexico City with volcanism spanning about 40Ka. Over 300 monogenetic volcanoes formed mostly by Strombolian eruptions that cluster into 22 eruptive events with a frequency of about 1000–2000 years. Composition varies from dacitic to basaltic which is reflected in the flow features (thick viscous to fluid lava flows). Scoria cone height ranges from 100-300m and radius from 100–500 m. Volumes vary from less than 0.1 to 3.8 km³. The youngest of these volcanoes are basaltic; Xitle and Chichinautzin, lie within Mexico City (more than 20 million people) and 18 km to the south. The lava flows from Chichinautzin Volcano reached 5 km from present day Cuernavaca (580,000people) and 4 km from Tepoztlán (15,000people) and other small towns. The pahoehoe lavas from Xitle were fed by a complex system of multiple level large lava tubes controlled by the steep topography and flatter lake plain of Mexico City. These flows dammed the rivers on the west that fed the lake on which Mexico City is built and covered the Pre-Colombian City of Cuicuilco 2000 yBP, forcing the inhabitants to migrate. Chichinautzin volcano on the other hand, formed on an east-west fissure that produced a central cone and many flows that were observed by dwellers**.**

Although cone alignment can be speculated in several directions, individual vents and many cone clusters are emplaced in an east-west direction, as are small faults. Some of them are active and seismicity shows they have east-west normal fault focal mechanisms with minor-lateral slip. Most of the seismic events are 6–15km deep and cluster in the northwestern part of the field, although three recent events are also located just south of Chichinautzin volcano, in the central part of the field.

Ash from renewed volcanism in this area would be fairly local but since the area is heavily populated, it would cause an important impact. It is highly probable that a new monogenetic volcano would be basaltic and have fluid lavas. The Sierra Chichinautzin is also a main recharge area for the ground water in Mexico City.

Volcano-structural analysis to investigate the plumbing system and the origin of La Garrotxa monogenetic Volcanic Field (NE Iberia)

Xavier Bolós[1], Joan Martí[1], Laura Becerril[1], Llorenç Planagomà[2], Pablo Grosse[3], Stéphanie Barde-Cabusson[1]

[1] *Institute of Earth Sciences Jaume Almera, ICTJA-CSIC, Group of Volcanology. SIMGEO (UB-CSIC) Lluis Sole i Sabaris s/n, 08028 Barcelona, Spain.* xavier.bolos@gmail.com
[2] *Tosca Environmental Services. Parc Natural de la Zona Volcànica de la Garrotxa, c/Santa Coloma, 17800 Olot, Spain.*
[3] *CONICET and Fundación Miguel Lillo, Tucumán, Argentina.*

Keywords: Volcano-structural, Garrotxa monogenetic Volcanic Field, plumbing system.

In monogenetic volcanic fields the distributions and magnitudes of different stress fields can be related to the tectonic and gravitational forces that, in turn, are linked to basement geometry, local topography, stress changes occurring during dyke propagation, and stress barriers related to structural discontinuities and rheological changes in stratigraphic successions (Gretener, 1969; Clemens and Mawer, 1992; Gudmundsson, 2003; Tibaldi, 2003; Acocella and Tibaldi, 2005; Gudmundsson and Philipp, 2006; Kavanagh *et al.*, 2006; Tibaldi *et al.*, 2014). Deciphering the potential pathways that magma uses to reach the surface is of crucial importance when conducting hazard assessment in volcanic areas.

The complexity of subsurface plumbing systems in monogenetic volcanism ensures that such systems are difficult to predict and rarely accessible for study and so other methods are needed for understanding the structural setting of a volcanic area and the pathways used by magma on its ascent to the Earth's surface.

In La Garrotxa Volcanic Field (GVF) similar geophysical studies have been conducted in the last years and have permitted to establish the stratigraphy of the area and the shallow structure beneath the volcanic deposits (Bolós *et al.*, 2012, 2014a, 2014b; Barde-Cabusson *et al.*, 2013, 2014).

This volcanic field is related to the Neogene-Quaternary European Rift system and is the youngest representation of monogenetic volcanism in the Iberian Peninsula. It encompasses over 50 well-preserved volcanoes in an area of about 600 km^2 lying between the cities of Olot and Girona (NE Spain).

In this study we investigate the relationship between the Neogene extensional tectonics and the spatial distribution of the volcanoes in the area. The analysis includes the geostatistical distribution of faults, fissures and vents, as well as morpho-structural lineaments, and the morphometrical analysis of volcanic cones and craters. As well, we use the location of the regional seismicity registered since 1978 and the sites of freshwater springs and mantle-derived gases as indicators of active faults and open fractures. Finally, we consider the location of the volcanoes with ultramafic xenoliths as a way of identifying the deepest fractures in the zone and estimating magma ascent velocities.

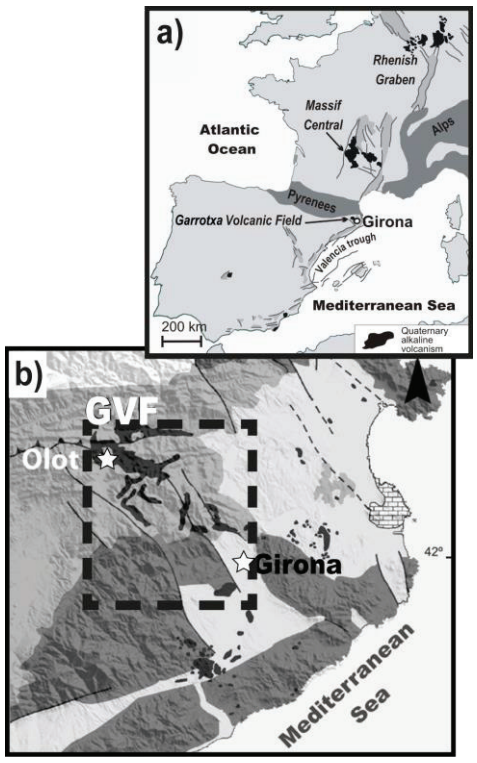

Fig. 1 – a) Simplified map of the distribution of the European rift system. b) Simplified geological map of the Catalan Volcanic Zone (Modified from Guérin *et al.*, 1985).

The results obtained show that this volcanic area consists of an extensional basin delimited by two principal faults that permitted the ascent of magma from either the source region or from shallower reservoirs located at the base of the crust. Towards

the upper part of the crust, magma transport was captured by shallow extensional secondary faults whose formation is linked to the slight trans-tensional movement of the main bounding faults. Our study provides evidence of how the local stress field and contrasts in rheology could have controlled magma migration, which suggests that precise knowledge of the stress configuration and distribution of rheological and structural discontinuities in such regions is crucial in the forecasting of monogenetic volcanism.

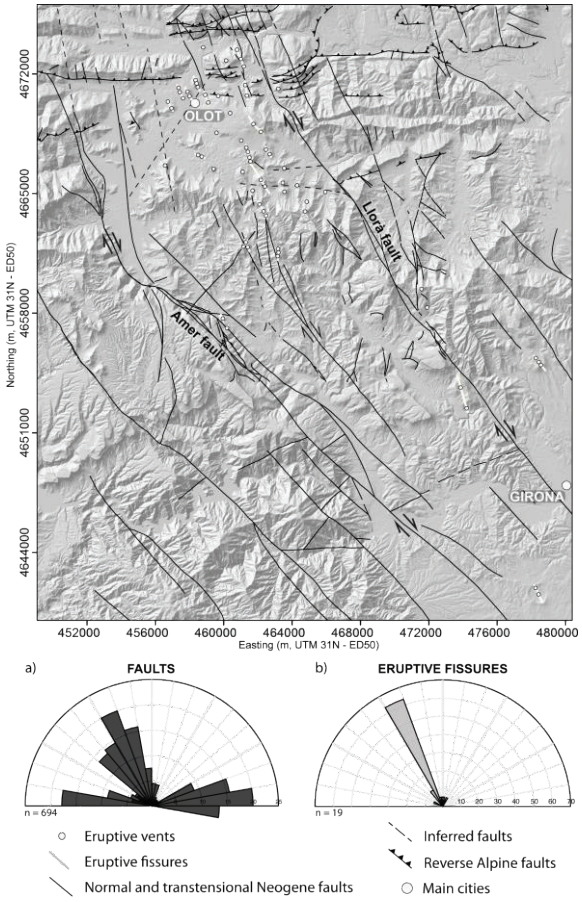

Fig. 2 – Volcano-structural map of La Garrotxa Volcanic Field. a) Rose diagram of faults; Neogene faults are represented in dark grey, and Alpine reverse fauls in light grey. b) Rose diagram of eruptive fissures.

Acknowledgements

This study was partially funded by the European Commission (FT7 Theme: ENV.2011.1.3.3-1; Grant 282759: "VUELCO") and Beca Ciutat d'Olot en Ciències Naturals. We are grateful to La Garrotxa Volcanic Zone Natural Park for their support throughout this study. We would like to thank Emilio Casciello, Núria Bagués, Joan Andujar, Pierangelo Romano, Dario Pedrazzi, Daniele Giordano, Jorge Galve, Xavier Castelltort and Daniel Nadal for their suggestions during this research. We also thank Enric Vinyanls for providing us unpublished information on seismic studies of the study area.

References

Acocella, V., Tibaldi, A., 2005. Dike propagation driven by volcano collapse: a general model tested at Stromboli, Italy. Geophysical Research Letters 32.

Barde-Cabusson, S., Bolós, X., Pedrazzi, D., Lovera, R., Serra, G., Martí, J., Casas, A., 2013. Electrical resistivity tomography revealing the internal structure of monogenetic volcanoes. Geophysical Research Letters 40, 2544-2549.

Barde-Cabusson, S., Gottsman, J., Martí, J., Bolós, X., Camacho, A.G., Geyer, A., Planagumà, L., Ronchin, E., Sanchez, A., 2014. Structural control of monogenetic volcanism in the Garrotxa volcanic field (Northeastern Spain) from gravity and self-potential measurements. Bulletin of Volcanology 76, 788.

Bolós, X., Barde-Cabusson, S., Pedrazzi, D., Martí, J., Casas, A., Himi, M., Lovera, R., 2012. Investigation of the inner structure of La Crosa de Sant Dalmai maar (Catalan Volcanic Zone, Spain). Journal of Volcanology and Geothermal Research 247–248, 37-48.

Bolós, X., Barde-Cabusson, S., Pedrazzi, D., Martí, J., Casas, A., Lovera, R., Nadal-Sala, D., 2014a. Subsurface geology in the monogenetic La Garrotxa Volcanic Field (NE Iberian Peninsula). International Journal of Earth Science.

Bolós, X., Planagumà, L., Martí, J., 2014b. Volcanic stratigraphy and evolution of the Quaternary monogenetic volcanism in the Catalan Volcanic Zone (NE Spain). Journal of Quaternary Science.

Clemens, J.D., Mawer, C.K., 1992. Granitic magma transport by fracture propagation. Tectonophysics 204, 339-360.

Gretener, P.E., 1969. On the mechanics of the intrusion of sills. Canadian Journal of Earth Sciences 6, 1415–1419.

Gudmundsson, A., 2003. Surface stresses associated with arrested dykes in rift zones. Bulletin of Volcanology 65, 606-619.

Gudmundsson, A., Philipp, S.L., 2006. How local stress fields prevent volcanic eruptions. J. Volcanol. Geotherm. Res. 158, 257-268.

Kavanagh, J.L., Menand, T., Sparks, R.S.J., 2006. An experimental investigation of sill formation and propagation in layered elastic media. Earth Planetary Science Letters 245, 799-813.

Tibaldi, A., 2003. Influence of cone morphology on dykes, Stromboli, Italy. Journal of Volcanology and Geothermal Research 126, 79-95.

Tibaldi, A., Bonali, F.L., Corazzato, C., 2014. The diverging volcanic rift system. Tectonophysics 611, 94-113.

Monogenetic volcanism with 3D X-ray vision: Advances and opportunities of rapid, high-throughput olivine and particle size/shape/porosity analysis

Matthew Pankhurst[1], Kate Dobson[2,3], Dan Morgan[1], Sue Loughlin[4], Thor Thordarson[5], Peter Lee[2,3], and Loic Courtios[2,3]

[1] *School of Earth and Environment, University of Leeds, Leeds, UK. m.j.pankhurst@leeds.ac.uk*
[2] *Manchester X-ray Imaging Facility, School of Material, The University of Manchester, Oxford Rd., M13 9PL, UK*
[3] *Research Complex at Harwell, Rutherford Appleton Laboratories, Didcot, Oxfordshire, OX11 0FA, UK.*
[4] *British Geological Survey, Edinburgh, EH9 3LA, UK.*
[5] *Institute of Earth Science, University of Iceland, Sæmundargötu 2, 101 Reykjavik, Iceland.*

Keywords: olivine, X-ray, micro-computed-tomography.

Olivine ~$(Mg,Fe)_2SiO_4$~ is common within magmas that supply mafic monogenetic volcanic fields. The Mg# (Mg_{mol} / (Fe_{mol} + Mg_{mol}) of olivine is an important parameter that can serve as a proxy for the state of evolution of an equilibrium melt. Thus knowing the Mg# of olivine offers a fundamental petrogenetic perspective of such systems. Crystal chemical- and size- distributions give insight to processes such as magma mixing and wall-rock magma interaction. Geo-barometry, -thermometry and crystal timescales can all often be applied when the Mg# of olivine is known, which offers an integrated 4D view of magmatic processes.

With increasing complexity/scale of a given system, these approaches must necessarily require correspondingly larger datasets to maintain a high degree of confidence in interpretations. However, generating large enough datasets to constrain 4D magmatic processes tightly by conventional techniques (electron microprobe: EPMA; scanning electron microscopy: SEM and electron backscatter diffraction EBSD) is extremely resource intensive. As such this limits the rate at which we can conduct research as well as our capacity to quickly understand new, potentially hazardous eruptions.

Here we present current work upon a recently described application of X-ray micro-computed tomography (XMT) that address these problems. We present details of both the method development and results of recent applications. XMT measures the X-ray attenuation of an object in 3D, by digitally reconstructing stacked radiographs taken at intervals around 180° or 360°. Since the X-ray attenuation of an object is proxy for its density, and the density of olivine is dictated by its Fe content (Fig. 1a), we may use X-ray attenuation as a sensitive proxy for olivine Mg# (Fig. 1b). The practical outcome is that the greyscale value of a region of olivine mapped by XMT can thus be used to infer the Mg# relative to other regions/grains, recently demonstrated by Pankhurst *et al.* (2014) (Fig. 1c). Influence of trace elements (*e.g.* Ni, Mn) in magmatic olivine is negligible.

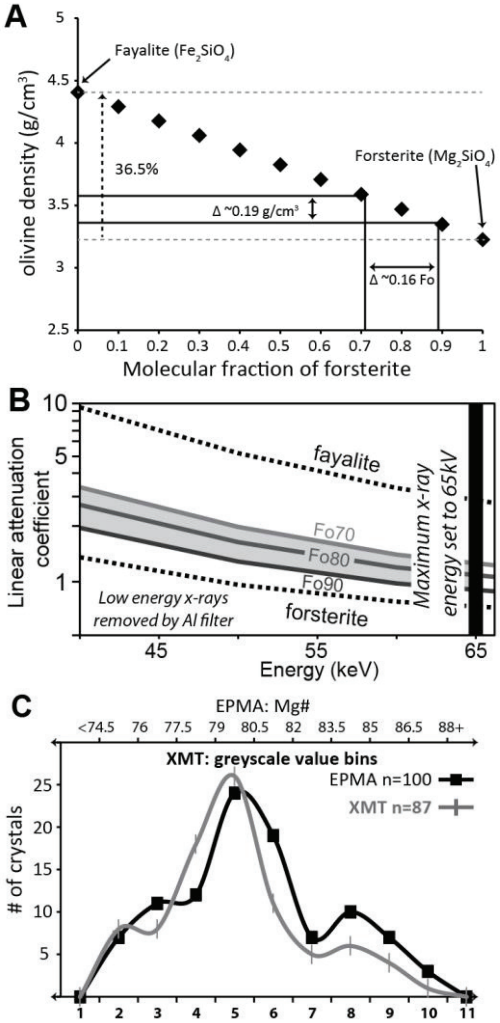

Fig.1 – A) Density varies as a linear (within analytical error) function against forsterite content (Fo or Mg#). B) The linear X-ray attenuation of the olivine solid-solution ranges by ~one order of magnitude. C) EPMA vs. XMT olivine crystal

chemical populations of a sample of Icelandic tephra demonstrating proof of concept of the technique. From Pankhurst *et al.* (2014).

One major advantage of XMT is the minimal sample preparation requirements. All that is necessary is that the sample is fixed onto a stage and presented to the beam. If the material is granular it may be contained by low-X-ray attenuating material (usually thin walled plastic tube/straw). No mounting in resin, polishing or coating is required. Another advantage is the rapid analysis, which allows high throughput: ~20 min scan per sample is often adequate. Voxel resolution of ~2 μm is typical, which allows high confidence in features ~10 μm in diameter (features smaller than this suffer from potential partial-volume effects). Furthermore, since XMT constrains the 3rd dimension, true volumetric analysis of crystal/domain sizes and shapes, and 3D petrographic relationships can be understood.

One disadvantage of XMT is that laboratory sources emit polychromatic X-ray beams (cf synchrotron which emits monochromatic beams), which leads to phenomena such as beam hardening, whereby the object itself filters the beam (preferentially low energy "soft" X-rays).

The vast majority of XMT applications require qualitative data only, however, for our purposes we require quantitative data, and thus repeatable absolute greyscale values. This exposes another disadvantage of XMT, for beam instability and X-ray source target (usually tungsten) sputtering results in significant drift from run to run.

Here we overcome these issues by forward modeling, constructing and testing an X-ray phantom (Fig. 2). A plastic vessel whose walls are studded with geometric shapes of mineral and/or glass of different Fe content represent a collection of internal X-ray attenuation standards that are scanned with each sample. The scale of each mineral/glass particle and smoothness of the surfaces is known (the material is precision laser-cut and imaged using SEM), thus edge effects such as beam hardening and partial volume issues are also constrained.

Since the technique is rapid and high-throughput, characterizing the olivine and it's attendant petrogenetic information from entire terranes is now becoming feasible. Furthermore, the calculation of both particle and crystal volume/shape distributions are straightforward directly from XMT data, which we explore here briefly, using examples of recently erupted natural tephra from Iceland. These natural data may be used as inputs into the next generation of numerical modeling of flow and eruption.

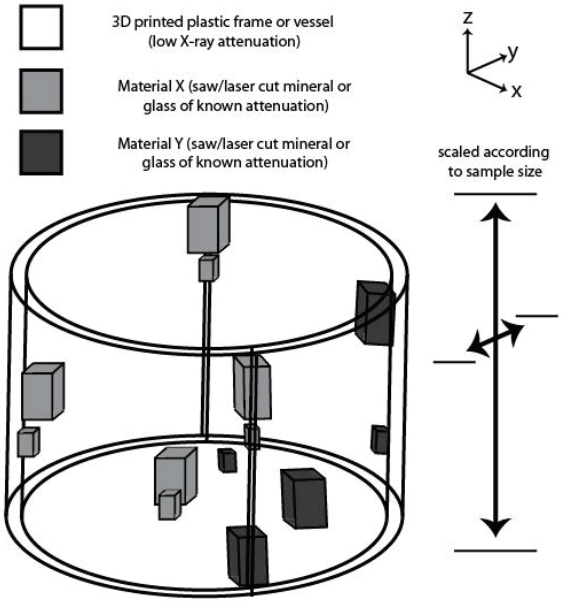

Fig. 2 – Schematic of X-ray phantom design, whereby the sample is placed within the vessel, itself studded with material of known composition, structure, size and shape. These particles act as standards, such that a correction can be applied to the attenuation of the sample, and edge effects may be quantified specific to each scan

Acknowledgements

The Natural History Museum, London, is thanks for supplying material that aided the initial investigations into X-ray attenuation of the olivine solid-solution series.

References

Pankhurst, M.J., Dobson, K.J., Morgan, D.J., Loughlin, S.C., Thordarson, T., Courtios, L. & Lee, P.D. 2014. Directly monitoring the magmas fuelling volcanic eruptions in near-real-time. Journal of Petrology 55: 671-684.

K E Y N O T E

How Exploitation, Science, and Geotourism Interact in a Monogenetic Volcanic Field – the West-Eifel example

Peter Bitschene[1,2]

[1] *Gerolstein Museum of Natural History, Hauptstraße 72, 54568 Gerolstein, German. info@naturkundemuseum-gerolstein.de*
[2] *TW Gerolsteiner Land GmbH, Gerolstein, German.*

Keywords: exploitation, science, geotourism.

Progress and communication in a modern world more and more rely on the global interaction between economy, politics, and science. Advances and communication in volcanology is also increasingly linked to the interaction between natural sciences, human and social sciences, and institutions dealing with volcanic emergencies and risks. Consequently, our session entitled "Monogenetic volcanism and mineral resources, quarries, land management, and geotourism" clearly states that the field of volcanology is opening widely towards economic issues, environmental and heritage protection, and geotourism.

The Westeifel Volcanic Field (WEVOF) comprises roughly about 350 volcanic cones, lava flows, and maars, has an intraplate setting amidst the European plate, ranges in age from about 700,000 to 11,000 years BP, is nearly exclusively alkaline basaltic in composition, and is famous for being the region with the type location, where the term "maar" has been coined (Steininger, 1820).

This lecture addresses the coherence between economy, science, and geotourism in Central Europe's best investigated monogenetic volcanic field – the Eifel. The method employed is basically "story telling", which in geotourism is the most successful tool to reach out to the public in general. Of course, time is too short to cover all aspects of a monogenetic volcanic field with roughly 350 volcanic centers covering an area of about 2,000 km^2. The aspects addressed here are economic exploitation and resulting environmental and social problems, scientific progress, and geotourism. The WEVOF – in politics and land management better known as "Vulkaneifel" - was the first geopark world wide that had volcanism as a prime asset.

Economic exploitation: Recent findings suggest that the ice-age hunters already visited the West Eifel ca. 30.000 years ago. Monogenetic volcanism was also active at that time. Thus it seems probable that the early Cromagnon families have witnessed one or the other volcanic eruption (Fig. 1).

Fig. – 1. About 30,000 years ago small monogenetic volcanoes erupted basaltic pyroclasts and lava flows in the West Eifel Volcanic Field – probably witnessed by early man.

The first proven use of the local basaltic rocks came from early hunters and settlers, which used hatches and axes made from local basalt. Celtic and Roman times settlers then widened the use of basalt with carving milling stones out of basaltic blocks.

Also, in the 1st Century AD basaltic palagonite tuff was already used for buildings and foundations. During medieval times through to the 18th Century milling stones were carved out of porous basalt in caves, which were dug into the volcanic cones. Although the milling stone caves count into the dozens, their environmental impact was negligible, but the human toll was enormous. Somewhere in the 19th Century, and throughout the 20th and 21st Century open pit quarrying started because the basaltic rocks became a prime material for: milling stones, building material, monuments, street and highway construction, air and water filtering, river and sea coast shelter.

Today, a single basalt quarry delivers up to 35,000 tons per year. The benefits from basalt quarrying are quite clear: income for entrepreneurs, local workers, and villages, which take in their share per ton. This also results in an appreciable tax income for County and State. Secondary benefits are the use of open pits for geotourism, breeding of endangered species such as owls, and dump sites for organic and inorganic waste. And, to state it clear, science benefits: only quarries show a true 3-dimensional picture of the architecture of an Eifel volcano, and the best and freshest samples of course come from active quarries. But, the threads are also quite clear: complete mountains vanished, noise and dust arise, and shakes and quakes due to the use of explosives put people, wildlife, and human housing at risk; rain water storage is diminished and water tables fall once an ash and scoria cone is gone; uncontrolled dumping in quarries has already contaminated ground water and soil; and once too many quarries gape into the landscape, then geotourism will also vanish leaving an agonizing West Eifel behind.

Scientific progress: In the early days of basalt exploitation the mere survival of the local population and the revenue for the owners were the only reason to deal with the West Eifel volcanoes and basalts. It were the Godfathers of German natural sciences GOETHE and HUMBOLDT, who came to the Eifel for scientific investigations, and to solve the enigmatic "Plutonism" *vs*. "Neptunism" controverse. But the WEVOF is most famous for the term "maar", which was coined by J. Steininger in the 1820ies. He saw and described the maars and their surrounding tuff walls and concluded that they are volcanic in origin. This holds true until today, and maars are now found worldwide, including wonderful examples in Mexico! Besides the scientific progress STEININGER stood for, it should be mentioned that he taught no other than his pupil KARL MARX how to observe, describe and evaluate nature. This eventually had two results: Karl Marx became a vivid lay geologist, and obviously he employed his teacher's way of geologic interpretation to social issues. Also bold, it is fair to say that the Eifel maars taught STEININGER, and STEININGER taught MARX, and that without the maars maybe "MA(A)RXISM" never ever may have been invented! More an anecdote than sober science, this shows how far reaching intra plate monogenetic volcanism can be!

Geotourism: The first geotourists in the Eifel have already been mentioned: GOETHE, HUMBOLDT, and many, many more were still to come. In the 1980ies the first geo paths were developed in the West Eifel culminating in the creation of Germany's first geopark around Gerolstein. The city of Gerolstein and its surrounding have seen geo-tourists with explicit interest for rocks, fossils, and minerals for more than 200 years. It is the home town of Germany's top selling premium mineral water, but also Germany's youngest lava flow (Sarresdorf lava flow) crops out here, and Germany's most complete monogenetic volcanic complex (Rockeskyller Kopf) lies around the corner. These geo-assets and political will then converged into today's Vulkaneifel Nature- and Geopark, one of the 4 founding members of the European and Global Geoparks Network. Geotourism and geopark now pose triple win situations: Creation of work and revenue, protection of geo heritage, and an attractive Vulkaneifel county. But without 200 years of quarrying and scientific progress, geopark and geotourism would not have been started yet! A classic geopark observation is that with the argument to protect the geoheritage locals and tourist are not allowed to collect rocks and fossils in the field, but the rude exploitation of rocks in quarries is allowed.

Conclusion: What has been described here vertically and chronologically, today is intrinsically horizontally intertwined as follows: On one side, open pit quarrying in the WEVOF was and still is the basic requirement for direct regional revenue increase, geoscientific investigations, and geotourism. On the other side, uncontrolled over-exploitation of quarries and new open pit quarries will undoubtedly destroy our geoheritage and put at risk the needed equilibrium between exploitation, science, and geotourism in the WEVOF.

References

Steininger, J. 1820. Die erloschenen Vulkane in der Eifel und am Niederrheine. 182 p., Mainz, Kupferberg.

Río Cuarto Maar: A Nyos type lake? (Costa Rica)

María Martínez

Observatorio Sismológico y Vulcanológico de Costa Rica Universidad Nacional, OVSICORI-UNA, Campus Omar Dengo, Heredia, Costa Rica. maria.martinez.cruz@una.cr

Keywords: maar, Río Cuarto, volcanic lakes.

Río Cuarto maar lies 18 km to the north of Poás volcano massif, along a 27 km long fracture zone cutting Poás. This fracture zone starts with the Sabana Redonda cinder cones on the southern flank of Poás massif, through Botos cone, Poás active crater, von Frantzius cone, and Congo stratocone, ending with the Hule and Río Cuarto maars (Fig. 1).

There are a very few studies on the Río Cuarto maar and several hypotheses on its origin. Sapper (1925) interpreted it as an explosion crater. Geo-archaeology data have been used to constrain on the formation and activity of Río Cuarto maar. It suggests that an episode of volcanic activity originating in Río Cuarto took place sometime around 3 ka B.P. or earlier (3–4 ka). This event involved a small amount of magma, i.e. 0.008km^3, as suggested by the scarsed amount of volcanic tephra present around the maar.

The Río Cuarto lake (361m a.s.l.) is also known as the Laguna de los Misterios ("Lake of Mystery", probably due to its relative seclusion and its characteristic periodic and unexplained phenomena of mass fish death), or as Laguna Kopper (after the landowner's family name). It is within a crater with a rim that reaches some 52 m above the water level (412m a.s.l.). The crater rim has an E–W axis of 847 m, a mean width of 707 m, and the lake has an E–W axis of 758 m, a mean width of 581 m, and a surface of 0.33 km^2.

The lake has a maximum depth of 66 m, making it the deepest natural lake in Costa Rica (Horn and Haberyan, 1993). A bathymetric study by Gocke *et al.* (1987) showed a mean depth of 45.5m, corresponding to a water volumen of 15×10^6 m3.

Lake surface water temperature has been observed to vary between 24.6 and 29.9°C, whereas the temperature of the hypolimnion at 60m fluctuates only between 24.2 and 24.4 °C (Gocke *et al.*, 1987, 1990; Haberyan and Horn, 1999). The depth of the boundary layer between the oxic and anoxic water bodies varies between 25 m (January–February) and 20 m (May–June). About 55% (mean value) of the total lake water body is permanently anoxic (Gocke *et al.*, 1987).

Reports of ocassional lake water overturns that cause sudden mass killing of fish and fauna and changes in the colour of the Río Cuarto lake, have been recorded since the first published mention of these phenomena at Río Cuarto by Sapper (1925). He reported that in 1924 the lake had a temperature of 23°C, and that a local informant sustained that on Sunday 30th, May of 1920 at 1 p.m., a black and then white smoke rose from the central part of the lake.

In Río Cuarto lake, at the beginning of some years, the green water have adopted a yellow-reddish colouration accompanied by massive fish mortality. As Gocke *et al.* (1987, 1990) pointed out, the wind cannot play a larger role, but only a minor role in the mixing process, since the lake is well sheltered by its relatively high and steep rims. They proposed that a possible explanation could be that long periods of anomalously cold weather (in December-January-February), combined with extremely strong winds, favouring the cooling of the surface and making it denser, and then the lake overturned. As a result, hypolimnetic Fe^{2+} mixed into the epilimnion, which is then oxidized to insoluble yellowish $Fe(OH)_3$, producing a very low oxygen concentration.

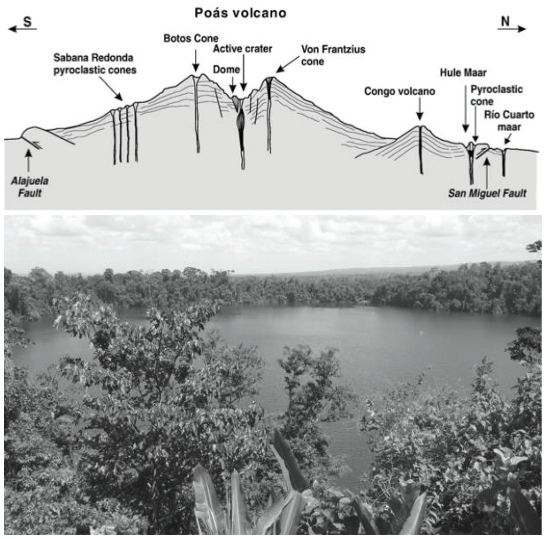

Fig. 1 – The Río Cuarto Maar located northward Poás volcano, along a 27 km north-south long fracture zone cutting Poás.

Based on the profiles of Fig. 2, the deep layers of the lake below 25-26 metres are normally never mixed with the surface waters. This has far reaching consequences for the oxygen budget. The depth of the lower limit of the O_2-containing surface waters

lies at 22metres, which means that about 55% of the total water volumen is permanently anoxic. Figure 2 shows that the hydrogen sulphide concentrations in the hypolimnion increased to 6 µmol/L. However, the H_2S concentration constitutes only a rather small part of the O_2 deficiency in the hypolimnion. The greatest part of the oxygen deficiency, which was about 1 mg O_2/L as an annual mean, is most probably caused by the relatively high concentration of ferrous compounds in the deep water.

The lake waters may have overturned at least once between 1978 and 1991 (Haberyan and Horn, 1999). Recent oral communications from the owner of the land where the lake sits reveal that such events occur every 6–7 years. The most recent events have been witnessed in January 1997 and February 2010. According to local people, the lake had very occasionally turned into a yellow-reddish discolouration accompanied by massive fish mortality. A posible explanation could be that hypolimnetic Fe^{2+} was mixed into the epilimnion, which was then oxidized to insoluble yellowish $Fe(OH)_3$. The fish mortality might be caused merely by severe depletion of oxygen concentrations.

However, the question that still arises is whether massive fish mortality is due to the mixing of oxygenated and anoxic waters and/or accumulation or sudden emission of volcanic gases. In any case, the dimensions of these reservoirs are limited by the continuous gas dispersion through the lake surface, which is favored by the dominant convective regime resulting in frequent mixing of water strata. Therefore, in these systems the hazard related to the possible occurrence of Nyos-type gas eruptions (i.e. Kusakabe, 1996) can be considered negligible or very local, but important if tourists camp near the lake shoreline.

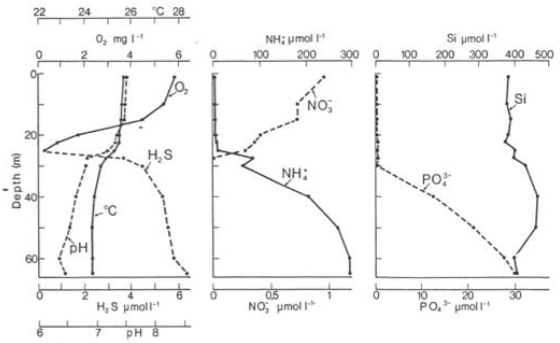

Fig. 2 – Vertical distribution of temperature, pH, O_2, H_2S, and some nutrients.

References

Alvarado, G., Soto, G., Salani, F.M., Ruiz, P., Hurtado de Mendoza, L, 2011. The formation and evolution of Hule and Río Cuarto Maars, Costa Rica. Journal of Volcanology and Geothermal Research, 201: 342-356.

Gocke, K., Bussing, W., Cortés, J, 1987. Morphometric and basic limnological properties of the Laguna de Río Cuarto, Costa Rica. Rev. Biol. Trop., 35(2): 277-285.

Gocke, K., Bussing, W., Cortés, J., 1990. The annual cycle of primary productivity in Laguna de Río Cuarto, a volcanic lake (maar) in Costa Rica. Rev. Biol. Trop. 38 (2B), 387–394.

Haberyan, K.A., Horn, S.P., 1999. Chemical and physical characteristics of seven volcanic lakes in Costa Rica. Brenesia 51, 85–95.

Haberyan, K.A., Horn, S.P., Umaña V., G. 2003. Basic limnology of fifty-one lakes in Costa Rica. Rev. Biol. Trop., 51(1): 107-122.

Horn, S., Haberyan, K.A., 1993. Physical and chemical properties of Costa Rican lakes. Natl. Geogr. Res. Explor. 9 (1), 86–103.

Kusakabe, M., 1996. Hazardous Crater Lakes. In: Scarpa, R., Tilling, R.I. (Eds.), Monitoring and Mitigation of volcano Hazards. Springer, pp. 573–598.

Sapper, K., 1925. Los Volcanes de la América Central. Max Niemayer, Halle (Saale). 144 pp.

Ecology of chironomids (Insecta: Diptera) from maar lakes in east-central, Mexico

Liseth Pérez[1], Carolina Vergara[2], Alberto Araneda[2], Julieta Massaferro[3], Socorro Lozano[1] and Margarita Caballero[4]

[1] *Instituto de Geología, Universidad Nacional Autónoma de México, Ciudad Universitaria, 04510, Distrito Federal, México. lcpereza@geologia.unam.mx*
[2] *Grupo de Estudios Paleolimnológicos (GEP), Unidad de Sistemas Acuáticos, Facultad de Ciencias Ambientales, Universidad de Concepción. Casilla 160-C, Concepción, Chile.*
[3] *CENAC-APN, CONICET, San Martin 24, 8400, Bariloche, Argentina.*
[4] *Instituto de Geofísica, Universidad Nacional Autónoma de México Ciudad Universitaria, 04510, Distrito Federal, México.*

Keywords: ecology, chironomids, Nearctic-Neotropical transitional zone.

Chironomids are non-biting midges (Insecta: Diptera) and are one of the most dominant groups of aquatic insects in fresh waters. They are true flies, but spend most of their life cycle in aquatic habitats (Armitage *et al.* 1995). Chironomids are frequently used as to track past environmental change, especially in lakes of the northern Hemisphere, because they are highly sensitive to changes in temperature, pH, dissolved oxygen concentration, trophic status, water depth, among others (Pérez *et al.* 2013).

Most paleoenvironmental studies based on chironomids are known for the Palearctic zone and there are only few for the southern Neotropical zone (Argentina, Brazil, Chile, Colombia). Pérez *et al.* (2013) established established a multi-bioproxy (microcrustaceans, diatoms and chironomids) training set (63 waterbodies) for the lowlands and highlands of the Yucatán Peninsula and surrounding regions (México,Guatemala and Belize).

Lakes in the Trans-Mexican Volcanic Belt (TMVB) central Mexico are abundant and are located in the transitional Nearctic-Neotropical zone. There are only few studies dedicated to the aquatic bioindicator fauna in central Mexico. This is the first study based on the chironomid fauna and ecology in 5 maar lakes (Alchichica, Aljojuca, La Preciosa, Tecuitlapa, Quechulac). The main objective is to study the modern chironomid diversity and species ecological preferences, and their potential as paleoenvironmental indicators.

Surface sediments containing chironomids were collected from the lake deepest point and littoral zones using an Ekman grab and a hand net (90 μm), respectively. Limnological variables (pH, temperature, dissolved oxygen, conductivity, TDS, etc.) were measured with a multiparemetric sonde at each collection site and the water chemical composition was determined in the laboratory. Chironomid head capsules were extracted from all surface sediments using a Bogorov sorting tray and fine forceps. Due to the lack of taxonomic keys, most organisms were identified down to genera level. Identification followed Ruiz-Moreno *et al.* (2000), Trivinho-Strixino and Strixino (1999).

A total of 13 genera were identified. Widely distributed genera included *Chironomus*, *Cricotopus* and *Dicrotendipes*. Lake Tecuitlapa displayed the highest diversity (8 genera), followed by Alchichica (5 genera) and Aljojuca (4 genera). The dominant ions in waters of these lakes were Na, Mg, HCO_3, CO_3, and Cl. The high diversity in lake Tecuitlapa suggests that this is an ideal environment for chironomid development, because it is a large shallow lake with abundant macrophytes. Genera restricted to lake Tecuitlapa were *Ablabesmyia*, *Endochironomus*, *Einfeldia*, *Micropsectra*, and *Paratanytarsus*. Preliminary results from a study carried out in 28 lakes in central Mexico, reports *Micropsectra* only for lake Tecuitlapa, suggesting that this is a good indicator for littoral zones, warm (≤26 °C) and alkaline waters (pH ~10.3), similarly to the genera *Einfeldia*, *Endochironomus* and *Paratanytarsus*.

Species collected only in lake Alchichica were *Labrundinia*, and *Pseudosmittia*, which shows their tolerance to high conductivities (≤15000 μS/cm). *Pseudosmittia* has been generally found in the "splash zone" of lakes. Other studies have shown that *Dicrotendipes* can feed on "aufwuchs", which could explain its presence in lake Alchichica.

Multivariate statistics will be used to determine the most important environmental variable(s) that control(s) the chironomid distribution in the study area. This information will complement the training set that is being established in central Mexico for a future development of chironomid transfer functions and down-core application. Here, we show that chironomids in the studied maar lakes are highly sensitive to changes in environmental variables showing their potential as paleoenvironmental indicators. Future studies will attempted to retrieve

multiple cores from maar lakes for a future application of transfer functions to fossil species assemblages, and the quantitative reconstruction of important environmental variables.

Acknowledgements

We would like to thank all participants in our field trips: Edyta Zawisza, Alexander Correa-Metrio and Esperanza Torres and the staff of the Department of Analytical Chemistry of the Institute of Geophysics, Universidad Nacional Autónoma de México, especially María Aurora Armienta for the water chemical analysis. We also thank the agencies and institutions that provided financial support: CONACYT (project number 167621), National Science Foundation (NSF award number 0902864) and the Instituto de Geología, Universidad Nacional Autónoma de México.

References

Armitage, P.D., Cranston, P.S, Pinder, L.C.V., 1995. The Chironomidae: biology and ecology of nonbiting midges. Chapman and Hall, London, England.

Pérez, L., Lorenschat, J., Massaferro, J., Pailles, C., Sylvestre, F., Hollwedel, W., Brandorff, G.-O., Brenner, M., Islebe, G., Lozano, S., Scharf, B., Schwalb, A., 2013. Bioindicators of climate and trophic state in lowland and highland aquatic ecosystems of the northern Neotropics. Revista de Biología Tropical 61: 603-644.

Trivinho-Strixino, S, Strixino, G., 1999. Insectos dípteros quironomídeos, p.141-148. In Ismael D, Valenti W C, Matsumura-Tundisi T Rocha O (eds) Biodiversidade do estado de São Paulo Brasil, 176 pp.

Ruiz-Moreno, J., Ospina-Torres, R., Riss, W., 2000. Guía para la identificación genérica de larvas de quironómidos (Diptera: Chironomidae) de la Sabana de Bogotá. II Subfamilia Chironominae. Caldasia 22: 15-33.

Enspel Crater Lake: A Maar-like structure with an unusual high crater wall and fossiliferous lake sediments (Oligocene, Germany)

Michael Wuttke[1], Thomas Schindler[1] & Martin Koziol[2]

[1] *Generaldirektion Kulturelles Erbe, Direktion Landesarchäologie, Referat Erdgeschichte, Große Langgasse 29, D-55116 Mainz, Germany, michael.wuttke@gdke.rlp.de and thomas.schindler@gdke.rlp.de*
[2] *Maarmuseum Manderscheid, Wittlicher Strasse 11, D-54531 Manderscheid, maarmuseum@t-online.de*

Keywords: deep lake, black pelite, debris flows.

The Enspel maar volcano is part of the Tertiary volcanic field of the High Westerwald. It lies in the center of the Mid European Cenozoic Volcanic Field. The volcano was formed as the middle of three NNW-SSE oriented diatrems. It was a small trachytic caldera or a pumice volcano. After the end of the eruption (dated by a lava flow within posteruptive breccias, owing an isotopic age of 24,79 ± 0,05 Ma; Mertz et al. 2008) the diatreme filled with groundwater. The resulting lake was deep. The crater rim with steep inner slopes was unbroken up to the end of the sedimentation period. There was no fluvial input. Alluvial inputs (mud flows) derived from gullies on the crater's inner rim.

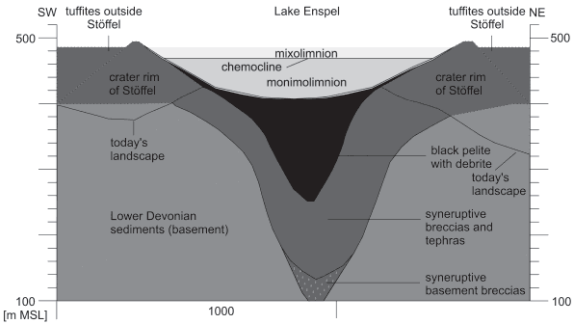

Fig. 1 – Reconstructed cross-section of lake Enspel (changed after Schindler and Wuttke 2014.)

Some of these sediments were deposited temporarily in alluvial fans. Pyroclastic fallout deposits from volcanic eruptions accumulated there as well. Crater floor subsidence, episodic heavy rains, and earthquakes triggered flank collapses and slides on the alluvial fan slopes and led to the creation of thick debris flows on the lake bottom. These debris flows are partly correlatable over the entire profundal zone. During normal sedimentation times, laminated black shale sedimentation occurred. Herein, many aquatic and terrestrial fossils are preserved (Poschmann et al. 2010). 230.000 years after onset of lake sedimentation, a basaltic lava flow, caused by a nearby eruption, filled the lake up in one go.

References

Mertz, D.F., Renne, P.R., Wuttke, M., Mödden, C. 2007. A numerically calibrated reference level (MP28) for the terrestrial mammal-based biozonation of theEuropean Upper Oligocene. Int. J. Earth Sci. (Geol. Rundsch.) 123: 353-361.

Poschmann, M., Schindler, T., Uhl, D. 2010. Fossil-Lagerstätte Enspel–a short review of current knowledge, the fossil association, and a bibliography, in Wuttke, D., Uhl, D., and Schindler, T., eds., The Fossil-Lagerstätte Enspel - exceptional preservation in an Upper Oligocene maar; Palaeobiodiv. Palaeoenv. 90: 3-20.

Schindler, T., Wuttke, M. 2014 (submitted). A revised sedimentological model for the Late Oligocene Crater Lake Enspel (Enspel Formation, Westerwald Mountains, Germany), in Wuttke, M. and Schindler, T. eds., The Fossil-Lagerstaette Enspel – reconstructing the palaeoenvironment with new data on fossils and geology; Palaeobiodiv. Palaeoenv.

Magnetic mineralogy records from volcanic lakes in central Mexico

Beatriz Ortega[1], Margarita Caballero[1], Socorro Lozano[2], Gabriel Vázquez[3]

[1] *Instituto de Geofísica, Universidad Nacional Autónoma de México (UNAM), Ciudad Universitaria, Coyoacán 04510, México City, bortega@geofisica.unam.mx*
[2] *Instituto de Geología, UNAM, Ciudad Universitaria, Coyoacán 04510, México City.*
[3] *Escuela Nacional de Estudios Superiores de Morelia, UNAM.*

Keywords: Environmental magnetism, paleolimnology, paleoclimatology.

Modern lakes in volcanic settings exhibit a large range of physicochemical characteristics in response to their morphology, water chemistry, regional climate, groundwater regime, tectonism, and the type of volcanic activity and its composition. All these factors affect the lacustrine deposition in different manners, resulting in great assortment of sediment types. Lacustrine sediments are common archives past environmental conditions, and the understanding of climatic and environmental changes is achieved from the analysis of biological, geochemical and mineralogical records. Magnetic mineralogy has become an important proxy of environmental change; therefore it is necessary to comprehend the processes that control the formation, accumulation, and transformation of magnetic minerals in order to construct an accurate model of past environmental changes.

In this work we present the example of three volcanic lakes located in the Transmexican Volcanic Belt in central Mexico, which exhibit different processes that transform the primary magnetic mineralogy record. These lakes are, from west to east, Santa María del Oro (Nayarit), Tacámbaro (Michoacán) and Lago Verde (Veracruz). In this geological setting volcanic activity has played a major influence on sediment magnetic properties, as a purveyor of Ti-magnetites/Ti-maghemites, and as a factor of instability in the environment. Combined magnetic mineral and non-magnetic analyses were conducted on lacustrine sediments. Non-magnetic studies comprise organic and inorganic carbon content, geochemical (XRF) and mineralogical (XRD) analysis, pollen and diatom analysis, and direct microscopic observations. Mineral magnetic methods include the analysis of laboratory induced magnetizations (k, ARM, SIRM and S ratios) and low temperature demagnetization of the saturation magnetization. Ratios of geochemical (Fe, Ti), and ferrimagnetic (χf) and paramagnetic (χp) susceptibility (χ) data, are used as parameters for magnetite dissolution ($\chi p/\chi$, $Fe/\chi f$), and precipitation (χ f/Ti) of magnetic minerals. The combined multiproxy analysis allows distinguishing main periods and variations of erosive terrigenous input, redoximorphic iron mineral diagenesis and biogenic productivity, which reflect variability of past environmental conditions.

Santa María del Oro

Laminated sediments recovered from Santa Maria del Oro lake span the last 2,600 years. Laminations are caused by alternations of their main components: lithogenic detritus, biogenic and authigenic carbonates, and amorphous material from biological and volcanic remains. Horizons characterized by high inorganic carbon content, authigenic siderite, and the dissolution of the finest ferrimagnetic mineralogy (magnetite) in reductive conditions, are upward followed by an increase in the concentrations of fine grained ferrimagnetic minerals. This sequence represents dissolution-precipitation cycles of magnetic minerals by anoxic/oxic variations in the water-sediment interface during warmer and dryer periods.

Lago Verde

Magnetic and non-magnetic mineral analyses conducted on a lacustrine sequence from Lago Verde, in the tropical coast along the Gulf of Mexico, covers the last 2000 years. The site witnessed the transformation of the environment since the early Olmec societies until forest clearance in the last century. Anoxic reductive conditions are evident in most of Lago Verde's sedimentary record. Intense volcanic activity and anoxia are recorded before AD 20, leading to the formation of framboidal pyrite. Increased erosion, higher evaporation rates, lower lake levels, anoxia and reductive diagenesis in non-sulphidic conditions are inferred for laminated sediments between AD 20–850. This deposit matches the period of historical crisis and multiyear droughts that contributed to the collapse of the Maya civilization. Dissolution of

magnetite, a high organic content and framboidal pyrite point to anoxic, sulphidic conditions and higher lake levels after AD 850, which broadly coincide with the increased precipitation documented during the Medieval Warm Period (AD 950–1350) in the northern tropical and subtropical regions of the American continent. Higher erosion rates reflect destruction of the rainforest over the last 40 years.

Tacámbaro

A 8.4 m core of laminated sediments collected in Lake Tacámbaro (Michoacán, central Mexico), spans the last ca. 9,000 years. Non-diamagnetic susceptibility (knd) and ARM are proxies for the abundance of (ferri)magnetic grains. Ti is associated to allochthonous component (here mostly volcanic origin). Si/Ti represents biogenic silica (mostly diatoms), and S/Ti reflects variability of organic matter. Diagenesis of Fe-bearing sediments is evident, as lower concentration of ferrimagnetic minerals coincides with higher total organic carbon and diatom abundance. Reductive diagenesis and precipitation of Fe sulphides, pyrite and greigite, is inferred in several horizons from proxies of higher organic productivity, reductive magnetite diagenesis, sulphur precipitation, finer magnetic grain sizes and higher coercivity minerals. At the time of the arrival of Spaniard to this region, exacerbated erosion is evident from the increase of mineral magnetic and terrigenous input to the lake.

Acknowledgements

This work wes funded bay several projects: DGAPA IN107902, IN107928, IN203102 IN113408, and CONACyT G28528T.

Ecology of testate amoebae in 5 maar lakes in Puebla, Mexico

Itzel Sigala[1], Socorro Lozano[1], Jaime Escobar[2, 3], Liseth Pérez[1] and Elvia Gallegos-Neyra[4]

[1] *Posgrado de Ciencias Biológicas, Instituto de Geología, Universidad Nacional Autónoma de México (UNAM), A.P. 70-296, 04510 México, DF, México. itzelsr@yahoo.com.mx*
[2] *Departamento de Ingeniería Civil y Ambiental, Universidad del Norte, Km 5 Vía Puerto Colombia, Barranquilla, Colombia.*
[3] *Center for Tropical Paleoecology and Archaeology, Smithsonian Tropical Research Institute (STRI), Panama City, Panama*
[4] *Laboratorio de Investigación de Patógenos Emergentes, Unidad de Investigación Interdisciplinaria para las Ciencias de la Salud y Educación (UIICSE). Facultad de Estudios Superiores, Iztacala, UNAM.*

Keywords: testate, amoebae, ecology.

Testate amoebae (also referred as thecamoebians) are single-celled ameboid protozoa in which the cytoplasm is enclosed within an external shell or discrete test and where pseudopodia emerge. These tests cover a broad range of sizes and range between 20µm and 400µm

Some species have an autogenous test that can be proteinaceus, siliceous or, rarely, calcareous, whereas other species present xenogenous test formed by agglutinated organic or mineral particles captured from their surrounding enviroment (Meisterfeld 2002 a,b).

In recent classifications (i.e. Corliss, 1994) this group is divided in two classes inside the Phylum Rhizopoda, based in their pseudopodia. For ecologic and paleoenviromental studies, however, they altogether are classified as a functional group (Medioli and Scott, 1988).

There are few ecological studies from tropical latitudes. Investigations done on tropical lakes describe thecamoebians taxa but pay little attention to the environmental controls on their distribution (Escobar *et al.*, 2005).

Testate amoebae can be very useful as environmental and paleoenvironmental indicators because of their high abundance and species diversity, widespread distribution, easy identification, and good preservation in sediments.

The aim of this research was to study the environmental conditions that can be important for the presence of testate amoebae in five maar lakes (Alchichica, Aljojuca, La Preciosa, Tecuitlapa and Quechulac) located in Puebla, Mexico. This results are part of a more extensive study that tries to establish an ecological training set in the central region of Mexico.

The sediment samples for thecamoebian quantitative analysis were collected with an Ekman grab from the littoral zones and deepest point of each lake. Several environmental parameters were taken at each collection site with a multiparametric sonde (pH, temperature, dissolved oxygen, conductivity, TDS) and parallel water samples were collected for water chemical composition analysis in the laboratory. Sediments were sieved with a 53µm sieve, and tests were extracted with a fine paintbrush.

We identified 11 species in all maar lakes. Lake Aljojuca has the greatest diversity and abundance of testate amoebae, particularly in the littoral zone, while no organisms were found in the littoral zone of Lake Quechulac. In other lakes the diversity was similar in littoral and lake's deepest point samples.

Some species and varieties that have not been previously reported for Mexico were recorded in some of these lakes. The more represented genera were *Arcella* and *Centropyxis*.

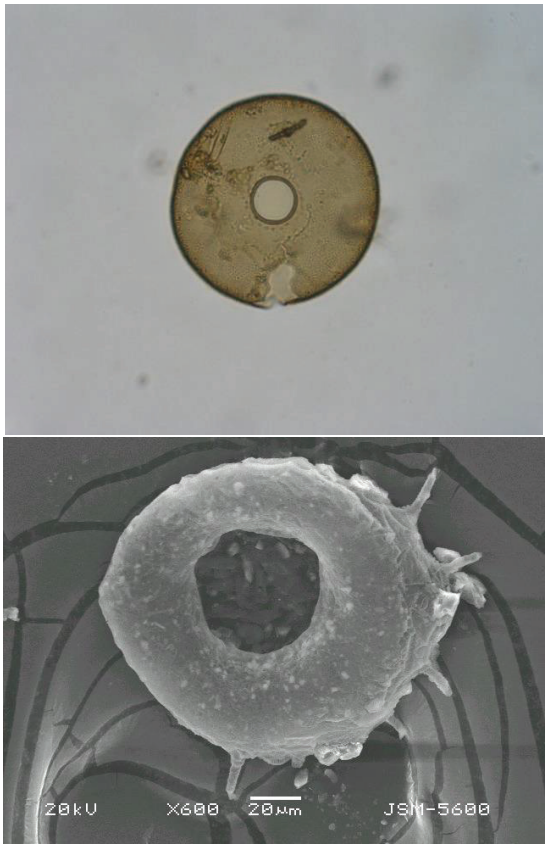

Fig. 1 – Up, *Arcella vulgaris*, 400x DIC; Down, *Centropyxis aculeata*, 600x SEM. Both from Aljojuca lake.

In Lake Alchichica lake we see an important difference between the species present in the littoral and bottom samples. This lake is one of the deepest in Mexico and is a warm monomictic lake circulating in winter and stratified over the rest of the year which could partly explain this change in the thecamoebian species assemblages.

In Lake Tecuitlapa we found only two individuals. This lake is characterized by its high levels of PT, DIN, DIC and SiO_2 and seems unfavorable conditions for the development of amoebae testate.

Multivariate statistics will be applied to determine the variables that control the distribution and abundances of testate amoebae species in the study area. It is highly important to continue with this study to better understand the seasonal variations of the thecamoebians assemblages.

Acknowledgements

We thank Margarita Caballero and Edyta Zawisza (Instituto de Geofísica, UNAM), Alexander Correa-Metrio and Esperanza Torres (Instituto de Geología, UNAM) for field work. We also thanks to María Aurora Armienta and the staff of the Department of Analytical Chemistry of the Institute of Geophysics, Universidad Nacional Autónoma de México for the water chemical analysis. Special thanks to Mariela Esquivel and Alejandro Ángeles for their help in field and laboratory work, as well as the Posgrado de Ciencias Biológicas, UNAM, CONACYT (project number 167621), National Science Foundation (NSF award number 0902864) and the Instituto de Geología, Universidad Nacional Autónoma de México for financial support.

References

Corliss, J.O. 1994. An interim utilitarian hierarchical classification and characterization of the Protists. Acta Protozoologica, 33: 1-51.

Dalby, A.P., Kumar, A., Moore, J.M., Patterson, R.T. 2000. Preliminary survey of Arcellaceans (Thecamoebians) as limnological indicators in tropical Lake Sentani, Irian Jaya, Indonesia. Journal of Foraminiferal Research, 30(2): 135-142.

Escobar, J., Martínez, J.I., Parra, L.N. 2005. Thecamoebians (Testaceous Rhizopods) from a tropical lake: La Fe Reservoir, Antioquia, Colombia. Caldasia, 27(2): 293-298.

Escobar, J., M. Brenner, T.J. Whitmore, W.F. Kenney y J.H. Curtis. 2008. Ecology of testate amoebae (thecamoebians) in subtropical Florida lakes. Journal of Paleolimnology, 40(2): 715-731.

Ogden C.G., Hedley, H. 1980. An atlas of freshwater testate amoebae. Oxford Universtiy Press, Hampshire, 222 pp.

Medioli, F.S., Scott, D.B. 1988. Lacustrine thecamoebians (mainly arcellaceans) as potential tools for palaeolimnological interpretations. Palaeogeography, Palaeoclimatology, Palaeoecology,62: 361-386.

Meisterfeld, R. 2002a. Order Arcellinida Kent, 1880. In: Lee J.J., G.G Leedale y P. Bradbury (eds). The illustrated guide to the protozoa, vol. 2. Society of protozoologists, Lawrence, Kansas, USA, pp 827–860.

Meisterfeld, R. 2002b. Testate amoebae with Wlopodia. In: Lee J.J., G.F. Leedale, P. Bradbury (eds). The illustrated guide to the protozoa, vol. 2. Society of protozoologists, Lawrence, Kansas, USA, pp 1054–1084.

Mitchell, E.A.D., Charman, D.J., Warner, B.G.. 2008. Testate amoebae analysis in ecological and paleoecological studies of wetlands: past, present and future. Biodiversity and Conservation, 17: 2115-2137.

Tropical, high altitude, mountain lakes El Sol and La Luna, Nevado deToluca, México: Seasonal and interannual limnological dynamics

Diana Ibarra[1], Javier Alcocer[2] and Luis A. Oseguera[2]

[1] *Posgrado en Ciencias del Mar y Limnología, FES Iztacala, Universidad Nacional Autónoma de México, Av. de los Barrios No. 1, Los Reyes Iztacala. 54090 Tlalnepantla, Edo. de México, México.* melanosim@hotmail.com
[2] *Proyecto de Investigación en Limnología Tropical, FES Iztacala, Universidad Nacional Autónoma de México, Av. de los Barrios No. 1, Los Reyes Iztacala. 54090 Tlalnepantla, Edo. de México, México.*

Keywords: High mountain lakes, climate change, Limnology.

Tropical high mountain lakes are located above the timberline (around 3,500 and 4,800 m a.s.l., Margalef, 1983). They receive about the same sunlight along the year (Lewis, 1996), are mostly polymitic (Thomasson, 1956), display low temperatures (Thomasson, 1956), and receive high amounts of UV radiation; (Löffler, 1964; Sommaruga, 2001). These lakes waters are poorly-mineralized, are acidic with low dissolved organic matter concentrations (Sommaruga, 2001).

High mountain lakes are mostly located in remote and undisturbed areas of the planet. Their environmental conditions turn these lakes vulnerable to acid rain, air pollutants and climate change. This "susceptibility" makes them natural sentinels of global change. However, to be used as sensors of global or local change it´s necessary to know their natural limnological variability to differentiate from the anthropogenic change.

Lakes El Sol and La Luna are two high mountain lakes inside the crater of the Nevado de Toluca volcano (19°06´N, 99°45´W, 4200 m a.s.l.), Central Mexico. Both lakes are perennially astatic, this is, their levels rise and fall as a result of the precipitation-evaporation balance, but do not dry up (Alcocer *et al.,* 2004). Twenty-year data (1921–1980) from the ''Nevado de Toluca'' weather station (19º 07' N, 99º 45' W, 4,140 m a.s.l.) report average monthly mean temperatures ranged between 2.8ºC in February and 5.8ºC in April, with an annual mean temperature of 4.2ºC. Total annual precipitation is 1243.5 mm, ranging from 17.2 mm in December to 270 mm in July (García, 1988). Maximum water depth of El Sol is 15 m (mean depth 6 m), with a surface area of 237,321 m^2. Maximum water depth of La Luna is 10 m (mean depth 5 m) with a surface area of 31,083 m^2 (Alcocer *et al.,* 2004).

This project proposed to characterize the seasonal (intra-annual) and interannual variability of lakes El Sol and La Luna by analyzing two annual cycles: 2000-2001 and 2006-2007. We measured the main physical and chemical parameters: temperature, pH, dissolved oxygen, conductivity and nutrients (nitrites, nitrates, ammonium, dissolved inorganic nitrogen, soluble reactive phosphorus, soluble reactive silica) as well as phytoplankton biomass expressed as the concentration of chlorophyll *a*.

The inter-annual comparison showed no variation in water temperature ($p>0.05$). Dissolved oxygen was higher in El Sol in the 2006-2007 period with a differences of 0.7± 0.1 mg/L in El Sol and 0.2±0.2 mg/L in La Luna. The pH augmented from 2000-2001 to 2006-2007 ($p<0.05$), 1.2±0.9 units in El Sol and 0.7±0.4 units in La Luna. Conductivity was higher in El Sol in the 2006-2007 period with a difference of 42.1±5.5 µS/cm; opposite, in La Luna was higher in the 2000-2001 period with a difference of 7.6±1.7 µS/cm ($p<0.05$). Both lakes became more turbid from 2000-2001 to 2006-2007 ($p<0.05$). In El Sol turbidity augmented 9±4% an in La Luna 18 ±1%. In El Sol, nitrites, nitrates, ammonium and dissolved inorganic nitrogen were higher in the 2000-20001 period ($p<0.05$; differences of 1.85±2.99 µg/L, 58.73±36.3 µg/L, 14.12±1.7 µg/L and 76.64±30.8 µg/L, respectively). Opposite, soluble reactive phosphorus and soluble reactive silica were higher in the 2006-2007 period ($p<0.05$; differences of 8.5±6 µg/L and 2069.31±352.4 µg/L, respectively). In La Luna, nitrites, ammonium and soluble reactive silica were higher in the 2006-2007 period ($p<0.05$; differences of 1.21±0.5 µg/L, 4.08±4 µg/L and 225.25±34.6 µg/L, respectively). Nitrates and dissolved inorganic nitrogen were higher in La Luna in 2000-2001 ($p<0.05$; differences of 182.01±21.6 µg/L and 176.88± 42.42 µg/L, respectively). Soluble reactive phosphorus showed no differences between both sampling periods ($p>0.05$). The phytoplankton biomass diminished in both lakes from 2000-2001 to 2006-2007 ($p<0.05$). The difference in El Sol was of 0.02 µg/L and the difference in La Luna was of 0.01 ±1.01 µg/L.

Comparison between lakes showed no variation in the water temperature in both annual periods ($p>0.05$). Dissolved oxygen was similar in 2000-2001 ($p>0.05$) between both lakes. In the 2006-2007 period, the dissolved oxygen in El Sol was higher

than in La Luna ($p<0.05$) with a difference of 0.3±0.1 mg/L. In both annual periods, El Sol was more alkaline than La Luna; in 2000-2001 the difference was of 0.8 pH units and in 2006-2007 was of 1.3±0.5 pH units. In both periods, El Sol showed higher conductivity values than La Luna: 2.3±0.1 µS/cm in 2000-2001 and 52±3.7 µS/cm ($p<0.05$). In both periods, La Luna was more transparent than El Sol ($p<0.05$). In the 2000-2001 was 34 ± 6 % and in 2006-2007 period was 24 ± 11%. In the 2000-2001 period El Sol had higher concentrations of nitrates, soluble reactive phosphorus and soluble reactive silica ($p<0.05$; differences of 2.2±3 µg/L, 1.83±0.9 µg/L and 51.6±28.2 µg/L respectively). In La Luna there were higher values for nitrates and dissolved inorganic nitrogen ($p<0.05$; differences of 250.7±16.3 µg/L and 249.7±34.1 µg/L, respectively). In 2006-2007 El Sol showed higher concentrations of soluble reactive phosphorus and soluble reactive silica ($p<0.05$; differences of 10.62±5.4 µg/L and 1895.66±346 µg/L, respectively). In the same period, La Luna had higher values for nitrites, nitrates, ammonium and dissolved inorganic nitrogen ($p<0.05$; differences of 0.86±0.49 µg/L, 127.42±41.6 µg/L, 21.16±1.5 µg/L and 149.46±39.12 µg/L, respectively). El Sol display higher Chlorophyll *a* concentration ($p<0.05$). The difference in the 2000-2001 period was 1.2 ±0.63 µg/L and the difference in the 2006-2007 period was 1.23 ±0.38 µg/L.

References

Alcocer, J., Oseguera, L. A., Escobar E., Peralta L., Lugo A., 2004. Phytoplankton biomass and water chemistry in two high mountain lakes in Central Mexico. Arctic, Antarctic and Alpine Research 36 (3): 342-346.

García, E., 1988. Modificaciones al sistema de clasificación climática de Köppen. Instituto de geografía, Universidad Nacional Autónoma de México, Mexico, D.F.

Löffler, H., 1964. The limnology of tropical high-mountain lakes. Verhandlungen Internationale Vereinigung für Theoretische und Angewandte Limnologie 15: 176-193.

Lewis M. Jr., 1996. Tropical lakes: How latitude makes a difference. Perspectives in Tropical Limnology :43-64.

Margalef, R., 1983. Limnología. Omega. Barcelona, 1010 pp.

Sommaruga, R., 2001. The role of solar UV radiation in the ecology of alpine lakes. Journal of Photochemistry and Photobiology 62: 35-42.

Thomasson, K., 1956. Reflections on Arctic and Alpine Lakes. Oikos 7: 119-143.

C-O-B isotopic evolution of lacustrine microbialites of Rincón de Parangueo maar, México

Gilles Levresse[1], José Jorge Aranda-Gómez[1], Claire Rollion Bard[2], Mariano Cerca-Martínez[1], Luis Rocha-Treviño[3], Jesús Pacheco-Martínez[4], José Alfredo Ramos -Leal[4], Vsevolod Yutsis[4], and Jorge Arzate-Flores[1]

[1] *Centro de Geociencias, Universidad Nacional Autónoma de México, UNAM Campus Juriquilla, Querétaro, México.*
[2] *Institut de Physique du Globe de Paris, France.*
[3] *Posgrado en Ciencias de la Tierra, Centro de Geociencias, Universidad Nacional Autónoma de México, UNAM Campus Juriquilla, Querétaro, México.*
[4] *Centro del Diseño y la Construcción, Universidad Autónoma de Aguascalientes, Av. Universidad 940, Aguascalientes, Ags. México.*
[4] *División de Geociencias Aplicadas, Instituto Potosino de Investigación Científica y Tecnologica, San Luis Potosí, SLP, México.*

Keywords: maar subsidence, microbialite, stable isotopes.

The Parangueo crater-lake was a small perennial, alkaline lake located inside of a maar in Guanajuato state, central Mexico. Together with other three nearby maar crater-lakes, Parangueo was gradually desiccated in the second half of last century, as a consequence of rapid drawdown in the regional Valle de Santiago-Salamanca aquifer (Aranda-Gómez et al., 2013). Today the crater acts as playa-lake with a small amount of water after the rainy season that tends to evaporate during the dry season. The decrease in water level inside the crater exposed large areas covered by nearshore microbialites. These organogenic structures range in size from individual oncoliths up to several centimeters in diameter, to stromatolite colonies (bioherms) tens of meters in length and up to 1.5 meters high.

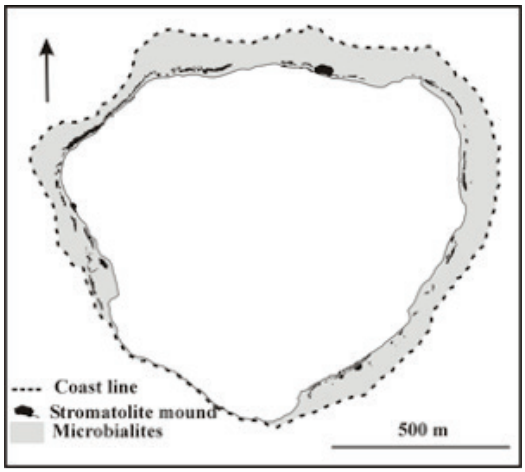

Fig.1– Schematic map of the parangueo paleo crater-lake.

In general, there are two dominant types of modern carbonate structures present in the shoreline/nearshore area of the former Parangueo perennial lake: (i) microbialites, including large coalesced biohermal structures, (ii) "pavements" (biostromes), and local laminated coatings developed on rocks and/or pieces of wood that fell inside the lake while it still had water, and (iii) cemented calcareous siltstones and breccias. Although these various types of microbialites are readily identified in field exposures and some of them form mappable units, their distributions are not mutually exclusive. All modern carbonate structures in Parangueo can occur together, adjacent to each other, or superposed on one another at one location. The calcareous crusts, microbialites, and "hardgrounds" (weakly lithified shallow lake floor) extend basin ward as much as 200 m to a few tens of meters from the former perennial lake shore. The highest elevation at which the lithified carbonates have been found above of the present-day playa-lake level is about 22 m, but this height difference is related in part to post-desiccation subsidence of the bottom of the lake.

Because of the wide variety of morphologies and compositions exhibited by the lithified shoreline carbonate sediments, few generalizations can be made about them. Lithologies recognized include micritic limestone and dolostone lying on top of calcareous siltstones. The rocks range from strongly lithified to weakly consolidated and friable. On most exposures along the topographic scarp caused by subsidence (Aranda-Gómez et al., 2013), it can be seen that on top of the micritic carbonates grew biohermal structures. Rock colors range from predominantly light grey to light brown in both, the micritic carbonates and in the oncoliths and stromatoliths. The surface of many of the exposed microbialites is altered to various shades of grayish-green when algal pigments are still present. The microbialites interiors show bands with distinct brownish to black staining (Fig. 2a).

The most common carbonate minerals in the Parangueo microbialites are magnesian calcite,

calcite, and aragonite. The leiolitic interiors of the larger microbialites are dominated by magnesian calcite. The outer rims of the larger microbialites and the laminated small pinnacles are composed of hydromagnesite. The pavement hardgrounds and the carbonate crusts developed on rocks located near the shore are magnesian calcite, hydromagnesite or more rarely trona.

We analyzed the laminated internal structure (Fig. 2) in a single stromatolith (2,4 cm of diameter, Fig. 2a) collected in one of the bioherms, which is located 10 m away from the former eastern lake shore. It is inferred that the microbialite formed in shallow water and carbonate precipitation was caused by a living algae colony.

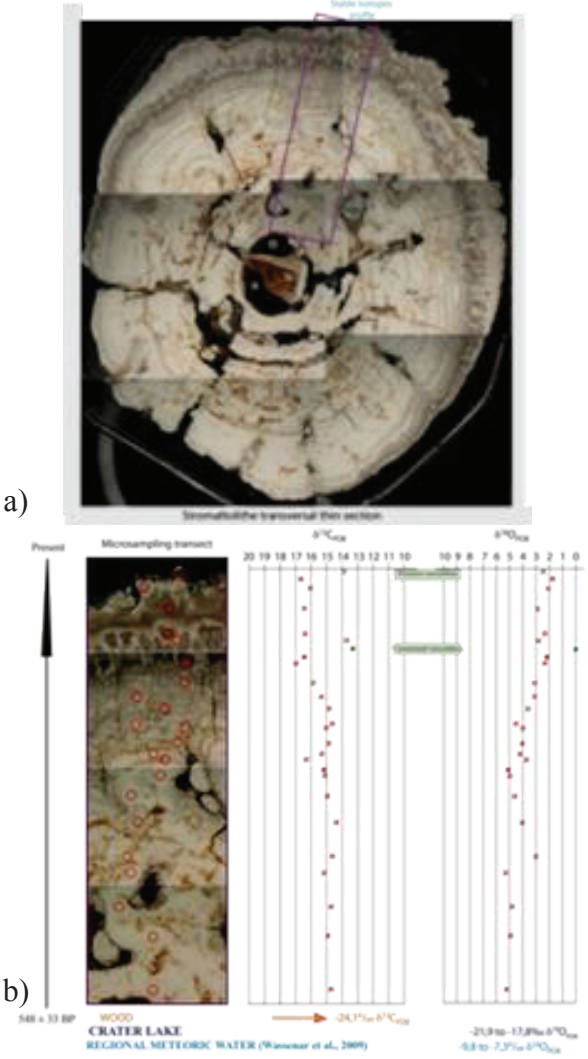

Fig.2 (a)- Photomicrograph mosaic of the studied stromatolite. Note the laminated structure near the outer rim and the leiolitic core. Carbonate precipitation started around a piece of wood that probably fell into the lake. The purple rectangle corresponds to the region where microanalyses were performed. (b) On the left is shown a close up of the area where microanalyses were done (red circles). Carbon and oxygen isotopic variations along the core to rim transect.

The age of the central wood piece was determinated by ^{14}C dating method in the AMS laboratory from Arizona University, Tucson. The analysis yielded an age of 548 ± 33 Before Present, suggesting a growing rate for the microbialite close to 0.4 millimeter per year. $\delta^{13}C$, $\delta\ ^{18}O$ and δB analyses were obtained in the carbonates, and the $\delta^{13}C$, $\delta\ ^{18}O$ results are shown in Figure 1. From the center to the outer border, the oxygen $\delta^{13}C$, $\delta\ ^{18}O$ and δB values vary respectively from 14.75 ± 0.03 to 16.68 ± 0.03 ‰, from 5.35 ± 0.07 to 1.76 ± 0.07 ‰ and from 32.4 ± 0.9 to 16.7 ± 1.2 ‰, respectively. All isotopes show a sinusoidal variation with a general depletion trend for oxygen and boron and enrichment for carbon. The paleothermometric interpretation of the $\delta^{18}O$ variation in the microbialite is necessarily based on the assumption that the oxygen isotope fractionation between the water and the precipitated carbonate is produced in equilibrium. Unfortunately the composition of the present-day, highly evaporated, lake water is not representative of the composition of the lake water prior to the perennial lake desiccation. Thus, isotopic values in the water in the lake's remnants are not in equilibrium with the carbonate.

Acknowledgements

Financial support for this project was provided by PAPIIT (IN109410) & CONACyT (129550) grants to J. Aranda.

References

Aranda-Gómez, J.J., Levresse, G., Pacheco Martínez, J., Ramos-Leal, J.A., Carrasco-Núñez, G., Chacón-Baca E., González-Naranjo, G., Chávez-Cabello G., Vega-González, M., Origel, G., Noyola-Medrano, C., 2013, Active sinking at the bottom of the Rincón de Parangueo Maar (Guanajuato, México) and its probable relation with subsidence faults at Salamanca and Celaya. Boletín de la Sociedad Geológica Mexicana 65(1): 169-188.

Wassenaara, L.I., Van Wilgenburgb, S.L., Larsonc, K., Hobsona, K.A., 2009, A groundwater isoscape (δD, $\delta^{18}O$) for Mexico. Journal of Geochemical Exploration, 102, 123-136.

Phosphorus utilization potential in extant microbialites of Alchichica maar lake, Mexico

Patricia Valdespino-Castillo[1,2], Rocío J. Alcántara-Hernández[2], Javier Alcocer[3], Miroslav Macek[3], Martín Merino-Ibarra[4] , Luis A. Oseguera[3], Fermín S. Castillo[4], Antonio Cruz[5], Osiris Gaona[2] and Luisa Falcón[2]

[1] *Posgrado en Ciencias del Mar y Limnología, Universidad Nacional Autónoma de México, Ciudad Universitaria, México, D.F., Mexico.* pancronica@gmail.com
[2] *Departamento de Ecología Evolutiva, Instituto de Ecología, Universidad Nacional Autónoma de México, Ciudad Universitaria, México, D.F., Mexico.*
[3] *Facultad de Estudios Superiores Iztacala, Universidad Nacional Autónoma de México,Edo. de México, México.*
[4] *Departamento de Ecología Acuática, Instituto de Ciencias del Mar y Limnología, Universidad Nacional Autónoma de México, Ciudad Universitaria, México, D.F., Mexico.*
[5] *Facultad de Ciencias, Universidad Nacional Autónoma de México, Ciudad Universitaria, México, D.F., Mexico.*

Keywords: phosphorus remineralizing bacteria, low-calcium environment, DOP utilization.

Phosphorus utilization by prokaryote communities has taken place through life history by genetic units that had evolve from ancient times but whose identity is largely unknown. Present communities associated to potential phosphorus transformations may help us to gain insight on the evolution of these metabolic tools.

Alchichica maar lake, is located in the easternmost part of the Transvolcanic belt, Puebla, Mexico. Littoral zone of Alchichica lake exhibits a ring of microbialites of two different morphologies and age of origin: columnar type and spongy type. Lake Alchichica water environment exhibits a particular geochemistry (see Armienta *et al.* 2008, Kazmierczak *et al.* 2011), similar to that of the ancient soda ocean (*sensu* Kempe and Degens 1985) where Mg:Ca ratio is high and calcium concentration is relatively low, compared to other systems such as seawater.

These extant microorganism communities have been the study model for a survey of genetic markers associated to prokaryote phosphorus transformations. A gene survey of calcium-dependent metalloenzymes (alkaline phosphatase *phoX*) showed a different abundance and diversity of this genetic marker in microbialite metagenomes. Ca^{+2} and Mg^{+2} function as cofactors of bacterial alkaline phosphatases studied, the natural availability of these metals has been posed to explain presence and diversity of these enzymes (Sebastian and Ammerman 2009, Luo *et al.* 2009).

Geochemical features of the system were used to frame phosphorus utilization genes in the present conditions of Alchichica lake microbialites, that exhibit a particular mineral composition dominated by hydromagnesite-magnesite (Kazmierczak *et al.* 2011).

Calcium-dependent metallophosphatases *phoX* were present and abundant in this low-calcium environment.

Affiliation of the alkaline phosphatases found indicate that heterotrophic bacteria play a fundamental role in dissolved organic phosphorus (DOP) utilization.

Our findings showed a broad genetic potential for DOP utilization in lake Alchichica present conditions (such as pH, phosphorus status and geochemical composition of the aquatic environment) that are suitable for the activity of the predicted enzymes.

Sequences found (alkaline phosphatase *phoX*) were compared *in silico* with *phoX* from other environmental studies that show contrasting ambient conditions (phosphorus availability, trophic state, calcium and magnesium concentration).

An OTU-based analysis showed that *phoX* diversity was similar among systems surveyed although no phylotypes were shared (Fig. 1).

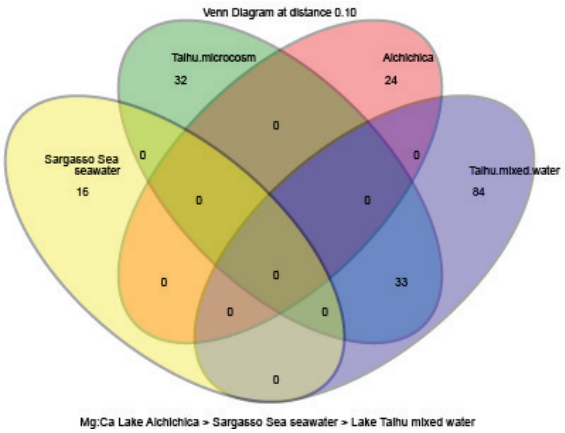

Fig. 1 – Venn´s diagram showing alkaline phosphatase *phoX* phylotypes (cutoff = 0.10) from aquatic systems of contrasting characteristics (Lake Alchichica, Sargasso Sea seawater and Lake Taihu mixed water and a microcosm study). In the figure is shown the Mg:Ca ratio gradient among studied systems.

These results intend to gain insight on the identity of phosphorus mineralizing bacteria, particularly for DOP utilization, where heterotrophic groups seem to play a major role. The cross-system analysis performed show a panorama of diversity of alkaline phosphatase enzymes in natural waters with contrasting geochemical characteristics.

Acknowledgements

We thank Luis A. Oseguera, Sergio Castillo, Antonio Cruz, Rigoberto Vicencio Pérez, Bernardo Valdespino, Rubén Pérez Ishiwara and Osiris Gaona Pineda for technical support.

References

Armienta, M.A., Vilaclara, G., De la Cruz-Reyna, S., Ramos, S., Ceniceros, N., Cruz, O., Aguayo, A., Arcega-Cabrera, F. 2008. Water chemistry of lakes related to active and inactive Mexican volcanoes. Journal of volcanology and Geothermal Research 178(2): 249-258.

Kazmierczak, J., Kempe, S., Kremer, B., Lopez-Garcia, P., Moreira, D., Tavera, R. 2011. Hydrochemistry and microbialites of the alkaline crater lake Alchichica, Mexico. Facies 57: 543-570.

Kempe, S., Degens, E.T. 1985. An early soda ocean?. Chemical Geology 53(1): 95-108.

Luo, H., Bennera, R., Long, R.A., Hu, J. 2009. Subcellular localization of marine bacterial alkaline phosphatases. Proceedings of the National Academy of Sciences USA 106: 21219-21223.

Sebastian, M., Ammerman, J.W. 2009. The alkaline phosphatase PhoX is more widely distributed in marine bacteria than the classical PhoA. ISME Journal 3: 563-572.

Paleoecological reconstruction during the late Holocene Maar La Alberca, Valle de Santiago, in the State of Guanajuato, Mexico

Valerio Castro Lòpez[1], Gabriela Dominguez[2], Isabel Israde[1]

[1] *Geociencias y Planificación del Territorio, UMSNH, Morelia, Michoacán, México.* salix@live.com.mx
[2] *Facultad de Biología, UMSNH, Morelia, Michoacán, México.*

Keywords: Pollen, Reconstruction, Maar.

At the end of the last glacial period, started the last interglacial, which is named the Holocene and covers the last 11000 years. This period is characterized by warmer climate than the last glacial period. One hypothesis about the global warming during the Holocene is related to Northern Hemisphere insolation, which reached its maximum at the beginning of the Holocene. Seasonal changes in solar radiation modify the atmospheric circulation pattern and cause the melting of the Laurentide ice sheet (Roberts 1998).

The Holocene is broadly recognized as a period of short-term climatic variability, on decadal to century level scales. Current understanding of climate changes in Central Mexico spanning the entire Holocene is sparse, in part because of the paucity of continuous sediment records and well-dated proxies. The Holocene climate in Mexico was highly variable. The early Holocene in the Upper Lerma Basin was cold, based on glacial advances on the Nevado de Toluca and Iztaccihuatl Volcanoes (Lozano-García *et al.*, 2005). The middle Holocene appeared to be dry, as was indicated by studies of several lake cores located around Central Mexico. In contrast, the late Holocene is generally characterized by short dry/wet cycles.

La Alberca is a crater lake aligned along a fault system NW-SE inside the Michoacán-Guanajuato volcanic field in the Transmexican Volcanic Field, which crosses Central Mexico along an east-west trend. The region contains more than 1000 volcanic structures (Hasenaka and Carmichael 1985). The volcanism of the region is product of subduction of the Cocos Plate under the Pacific Plate and vent location appear to be influenced the presence of NE-SW fault and fractures systems (Pasquaré *et al.*, 1991).

The Valle de Santiago maars are located in the state of Guanajuato south of the City of Salamanca, at the northern limit of the Mexican Volcanic Arc. It is near the border between arid northern México and tropical to subtropical high pressure climatic systems that dominate the central and southern Mexico. The rainfall distribution, as in all central Mexico, is controlled in part by the subtropical high pressure, the latitudinal migration of the InterTropical Convergence Zone (ITCZ), which brings humid air from the Gulf of México and the Caribbean and the westerly winds that carry moisture from the Pacific during the summer rainy season.

La Alberca is located at 20° 23.35´ N, 101° 12.10´ O, at an altitude of 1690 m a.s.l.

Regional climate, according to Rzedowski and Rzedowski (1987), is semi warm, subhumid and temperate subhumid with summer rains. The annual precipitation ranges from 679 to 1000 mm, falling 90% of the rain between may and october. Significant evaporation occurs between march and may. The mean annual temperature is 19 °C.

An 11 m long core was recovered from a locality close to the center of the maar using a Russian corer. As the Russian corer recover half tubes 50 cm long, we extracted two copies of every level sampled. Every core section was wrapped in plastic foil, marked and taken to the laboratory. Sediment samples were taken at regular 5 cm intervals for analyses of pollen, charcoal and elemental analysis. 7 samples were taken for AMS, and calibrated using calib 7.0.

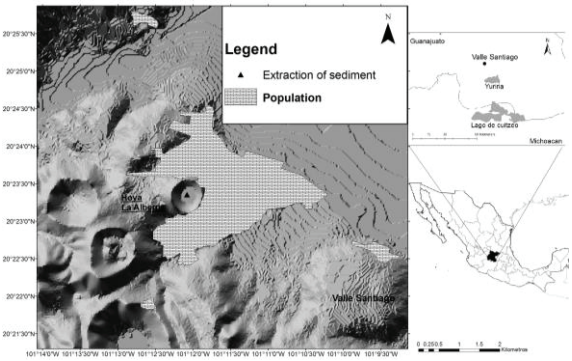

Fig. 1 – A sediment core was extracted from the center of the crater of La Alberca maar at Valle de Santiago, Guanajuato, Mexico.

Results and Discussion

The sedimentary sequence is dominated by clay sediments facies, with layered clay, lime sediments, and lime-clay sediments. Three tephra layers were found at depths of 784-785 cm, 335-336 cm, and 165-166 cm.

For the paloinological analysis, only the most representatives pollen taxa were used. Such as Salix, *Alnus, Pinus, Quercus*, Ulmaceae, Leguminoseae, Gamineae, Compositae, Cyperaceae. The climatic

conditions during the middle Holocene were variables, a dry period is observed ca. 6672 to 5367 yrs. B.P., during this period the lake level was low. This dry conditions existed by clay materials. And the vegetation was dominated by a pine forest. Humid conditions are established by ca. 5360 a 5000 yrs b.P., allowing a vegetation with *Quercus, Alnus* and *Taxodium*. During this periods wild fires were intense and frequents. These humid conditions were reported also for different cores from the maar de San Nicolás, mar Rincón de Parangueo, the Lerma, Zacapu, Chalco and Tlapacoya; González-Quintero *et al.* (1986); Neiderberger (1987): Xelhauntzi-López (1995) Caballero *et al.* (2002); Park *et al.* (2010). Although other records report a dry climate during the middle Holocene that caused a hiatus in sedimentation. This hiatus is caused by a strong erosion process or for tectonics like was reported for Cuitzeo, Zacapu and. Zirahuén; Israde-Alcántara *et al.* (2010); Arnault *et al.* (1997); Ortega *et al.*, (2002, 2010).

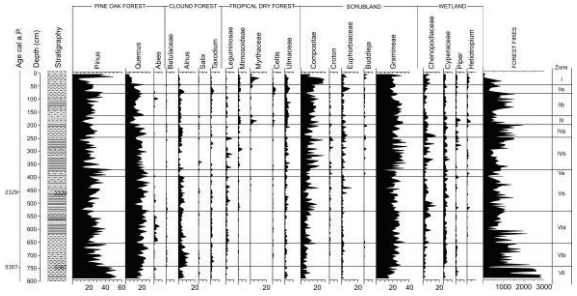

Fig. 2 – Diagram of the main pollen taxa in La Alberca, Valle de Santiago, Guanajuato.

During the late Holocene the climate conditions were variables. The vegetation was dominated by a scrubland and a tropical dry forest and high values in elements like Ti, Fe, Al, K. During the humid periods *Quercus*, *Alnus* and *Pinus* increased and low values of Ti, Fe, Al, K and Ca/Ti y Ca/K, P/P+Q are observed.

The driest period was recorded from 1400 to 255 yrs. bP. (550 a.d. a 1438 a.d.), drought which caused the dominance of elements resistant to such as Gramineae, Leguminosae, Mimosoideae, Ulmaceae, and Euphorbiaceae. This extreme dry conditions are related with the highest values in Ca/Ti, Ca/K and P/P+Q. This drought reached its climax at 486 years b.P. (1463 a.d.), causing strong evaporation and high salinity in the lake. This same arid condition were reported for the maar de San Nicolás, Rincón de Parangueo, la Piscina de Yuriria, Cuitzeo, Zacapu, Pátzcuaro, Zirahuén, Chalco y Chignahuapan; Xelhuantzi-López (1994); Metcalfe *et al.* (2000); Caballero *et al.*, (2002); Ortega *et al.* (2010); Park *et al.*, (2010); Israde-Alcántara *et al.* (2010).

Acknowledgements

We thank Dulce and Verónica for their help in fieldwork and the to the people of Valle Santiago, Guanajuato and laboratory of paleoenvironments, UMSNH.

References

Arnauld, C., S. E. Metcalfe y P. Petrequin. 1997. Holocene climatic change in the Zacapu lake basin, Michoacán: synthesis of results. Quaternary International: 173-179.

Caballero, M., B. Ortega, F. Valadez, S. Metcalfe, J. L. Macias y Y. Sugiera. 2002. Sta. Cruz Atizapan: a 22-ka lake level record and climatic implications for the late Holocene human occupation in the Upper Lerma Basin, central Mexico. Palaeogeography, Palaeoclimatology. Palaeoecology 186: 217-235.

González-Quintero, L. 1986. Análisis polínicos de los sedimentos. En: Lorenzo, J.L., L. Mirambell (Eds.). Tlapacoya: 35,000 años de historia del Lago de Chalco. Colección Científica, Serie Prehistoria, Instituto Nacional de Antropología e Historia, 157-166.

Hasenaka, T., I.S.E. Carmichael. 1985b. A compilation of lozation, size, and geomorphological parameters of volcanoes of the Michoacan-Guanajuato Volcanic Field, central Mexico. Geofis. Int., 24 (4): 577-607.

Israde-Alcántara, I., R. Velázquez-Durán, M. S. Lozano-García, J. Bischoff, G. Domínguez-Vázquez y V. H. Garduño-Monroy. 2010. Evolución Paleolimnológica del Lago Cuitzeo, Michoacán durante el Pleistoceno-Holoceno. Boletín de la Sociedad Geológica Mexicana 62 (3): 345-357.

Lozano-García S., L. Vazquez-Selem. 2005. A high- elevation Holocene pollen record from Iztaccihuatl volcano, central México. The Holocene 15, 3. 329-338

Metcalfe, S.E., S.L. O'Hara, M. Caballero y S.J. Davies. 2000. Records of Late Pleistocene Holocene climatic change in Mexico-a review. Quaternary Science Reviews 19 (17): 699-721.

Neiderberger, C. 1987. Paleopaysages et archéologie pre-urbaine de Bassin de Mexico. Collection Etudes Mesoaméricaines. Centre d'Etudes Mexicaines et Centraméricaines, México, D.F.

Ortega, B., C. Caballero, S. Lozano-García, I. Israde-Alcántara y G. Villaclara 2002. "52000 years of environmental history in Zacapu basin, Michoacán, México: the magnetic record". Earth and Planetary Science Letters 202: 663-675.

Ortega, B., G. Vázquez, M. Caballero, I. Israde-Alcántara, S. Lozano-García, P. Schaaf y E. Torres. 2010. Late Pleistocene: Holocene record of environmental changes in Lake Zirahuen, Central Mexico. J Paleolimnol 44: 745-760.

Pasquaré, G., L. Ferrari, V. Garduño, A. Tibaldi, L. Vezzoli. 1991. Geology of the central sector of the Mexican Volcanic Belt, states of Guanajuato and Michoacan: Boulder, CO, Geological Society of America, Map and Chart Series MCH072, 1 mapa con texto, 22 p.

Park, J., R. Byrne, H. Bohnel, R. Molina-Garza y M. Conserva. 2010. Holocene climate change and human impact, central Mexico: a record base on maar lake pollen and sediment chemistry. Quaternary Science Reviews 29: 618-632.

Roberts, N. 1998. The Holocene, and Environmental History. Second Edition. Blackwell, Oxford, 316pp.

Rzedowski, J. y G. Calderón de Rzedowski. 1987. El bosque tropical caducifolio de La región Mexicana del Bajío. Trace 12: 12-21.

Xelhuantzi-López, M.S., 1995, Palynologie et palèoenvironnement du bassin de Zacapu, Michoacán, Mexique, depuis 8000 ans. Geofisica internacional 34 (2): 239-248.

Vegetation Change in Northeast China of Late Pleistocene based on the pollen records from Moon and Sifangshan crater lakes

Jing Wu, Qiang Liu, Luo Wang, Guoqiang Chu, Jiali Liu and Jiaqi Liu

Key Laboratory of Cenozoic Geology and Environment, Institute of Geology and Geophysics, Chinese Academy of Sciences, Beijing, China wujing@mail.iggcas.ac.cn

Keywords: Crater Lake, palynology, climate change.

Global climatic systems have experienced various dramatic variations during the transition from the last glacial maximum (LGM) to the Holocene in the past 21,000 years. Some of these high-frequency oscillations on millennial and centennial timescales are the widely-reported such as the Heinrich event 1 (H1), the Bølling- Allerød warm phases and Younger Dryas (YD) cold periods (Dansgaard *et al.*, 1993; Bond *et al.*, 1997; Bard *et al.*, 2000; Wang *et al.*, 2001). These events may be not global distributed, and their geographical unevenness is still a significant debate (Clark *et al.*, 2002; Kiefer *et al.*, 2005). Although the accumulation of understanding on those millennial and centennial-timescale climatic oscillations speed up during recent decades, reliable records are still inadequate to map their regional manifestation worldwide, which will further our understanding not only on linkages between different climate systems, but also on climatic connections between distant regions.

The Great Khingan Mountain range is located in the Northeast China as the watershed of Inner Mongolia Plateau and Songliao Plain. It is one of the areas where the high-resolution and well-dated record spanning the late Pleistocene is inadequate. This range is not only the transitional zone between boreal and temperate forests from the north to the south, the transitional zone between woodland and grass land from the east to the west, but is also the northeast margin region of modern East Asian Summer Monsoon (EASM). East Asian Monsoon (EAM) is one of important components of worldwide spread monsoon phenomenon, which is the linkage of the marine and terrestrial system, the atmosphere and hydrosphere. The structures and mechanism of EAM have been explored without fully understanding on the regional differences in recent decades (Heusser and Morley, 1997; Wang *et al.*, 1999; An, 2000; Wang *et al.*, 2001; 2008; Yuan *et al.*, 2004; Yancheva *et al.*, 2007). These features make the geologic files from the region controlled by EAM record not only the matter and energy circulation between the global atmosphere, ocean, land and ice systems (An, 2000), but also the regional characteristics.

This study focuses on the vegetation reconstruction and climate change based on pollen assemblages of the Lake Moon and Lake Sifangshan lacustrine sediment sequence from last glacial to Early Holocene in the Great Khingan Mountain range and also on its comparison with records from the region relative to East Asian Monsoon and the North Atlantic region. It is hoped that regional differences and commonalities of the millennial and centennial-timescale climatic oscillations during the last deglacial can be depicted, and the understanding of potential mechanistic linkages of the Great Khingan Mountain range and key regions of climate change can be improved.

Lake Moon (47°30′N, 120°52′E, 1190m a.s.l) is one of crater lakes within the Aershan-Chaihe Volcanic Field, Inner Mongolia, which is almost circular with 220m diameter. Lake Sifangshan (49°23′N, 123°28′E, 933m a.s.l) is a circular crater lake located in Nuomin volcanic area, Inner Mongolia Province, whose diameter is even smaller as 30m.

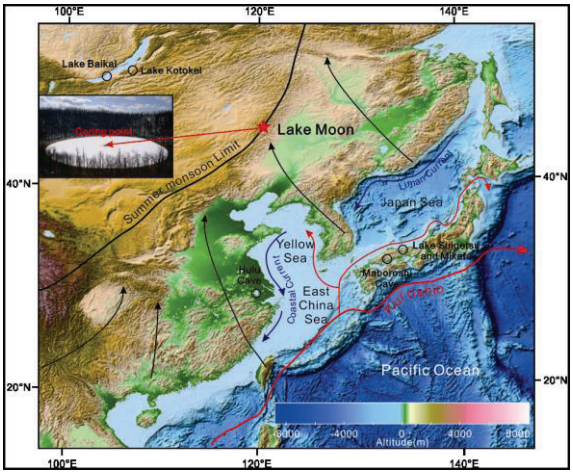

Fig. 1 – Locations of Lake Moon, Sifangshan, Baikal, Kotokel, Suigetsu and Mikata, and Hulu and Maboroshi caves with atmospheric circulation in summer. Black arrows show seasonal dominant wind vectors and the red arrow points to the location of coring point of Lake Moon.

The climate of the study area around Lake Moon and Sifangshan are characterized by relative low humidity and large seasonal temperature variability, because the locations of them are on the northwestern front of EASM and governed by the Siberian air mass in winter. As the plants would not grow under the severe climate in winter, the relative temperature around Lake Moon and Sifangshan based on pollen records represents the intensity of EASM, which is influenced by the behavior and temperature of the Pacific air mass in summer.

According to the curve of relative temperature and humidity reconstructed based on pollen records of Lake Moon and Sifangshan, the temperature change in study area is synchronous and correlative with the North Atlantic region (Fig. 2). The onset of first deglacial warming occurred at ca. 20.3 cal. ka B.P. followed by the H1 and Younger Dryas respectively appeared at 18.0 and 12.8 cal. ka B.P. shows climate changes are synchronous with those of Asian caves and Greenland ice cores. The finding that the amplitude of Younger Dryas event was much reduced in East Asia support that this cooling event was probably triggered by a melt water pulse into the North Atlantic thermohaline circulation. The temperature of East Asian Monsoon region depend on solar insolation and North Atlantic thermohaline circulation, while the local humidity is site specific based on different position on surface air gradient of EAM.

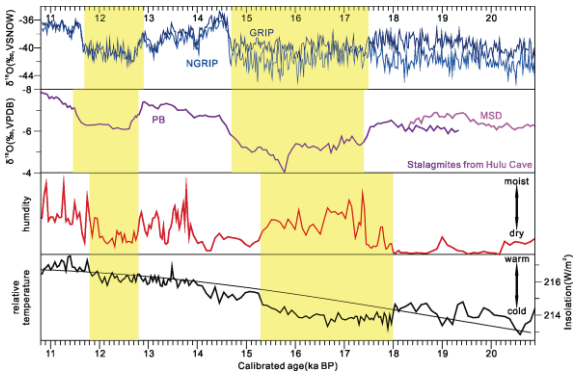

Fig. 2 –The relative temperature and humidity reconstructed based on pollen records of Lake Moon and Sifangshan. The temperature change tendency in study area is synchronous and correlative with the $\delta^{18}O$ caves of Hulu Cave and ice cores of Greenland.

The mechanism responsible for the regional climate changes surrounding the Lake Moon and Sifangshan refers the matter and energy circulation between the global atmosphere, ocean, land and ice systems like insolation, thermohaline circulation and surface air-pressure gradient. The force of the transition from glacial to interglacial is likely derived by the insolation change. In contrast, the cold stadial like the H1 and Younger Dryas has their probable origin in the North Atlantic. The temperature decreasing under the higher temperature condition during the YD brought a steeper surface air-pressure gradient decreasing between Eastern Eurasia and the Pacific in summer, which was responsible for reduction of the EASM and resulted in negative vapor transport from the Pacific to the region near the Lake Moon and Sifangshan. Nevertheless, the local humidity surrounding the Lake Moon and Sifangshan do not lie on the action of the EASM but the insolation during the H1 when the temperature is relatively low. The fact that the pollen records captured most millennial and centennial-timescale climatic oscillations equivalent to the North Atlantic assume the temperature and humidity signal of study area is very sensitive to the intensify change of EASM, as the study site is very close to the present northwestern the limit front of the EASM. The teleconnection between the East Asia and the North Atlantic is obvious. The regional characteristics determine the specific reaction of study site to the factors driven the climate change, resulted that the different scenes in EAM region since LGM. Meanwhile the different indexes like pollen and stalagmite in East Asia have different sensitivity to the driven factors or the processes of climate change, which caused the different duration of lags to the climate signals from trigger regions.

Acknowledgements

This research was supported by the National Natural Science Foundation of China (40872206; 41272392; 41202259; 41320104006).

References

An, Z., 2000. The history and variability of the East Asian paleomonsoon climate. Quaternary Science Reviews 19, 171-187.

Bard, E., Rostek, F., Turon, J.-L., Gendreau, S., 2000. Hydrological Impact of Heinrich Events in the Subtropical Northeast Atlantic. Science 289, 1321-1324.

Bond, G., Showers, W., Cheseby, M., Lotti, R., Almasi, P., deMenocal, P., Priore, P., Cullen, H., Hajdas, I., Bonani, G., 1997. A Pervasive Millennial-Scale Cycle in North Atlantic Holocene and Glacial Climates. Science 278, 1257-1266.

Wang, Y.J., Cheng, H., Edwards, R.L., An, Z.S., Wu, J.Y., Shen, C.-C., Dorale, J.A., 2001. A High-Resolution Absolute-Dated Late Pleistocene Monsoon Record from Hulu Cave, China. Science 294, 2345-2348.

Clark, P.U., Pisias, N.G., Stocker, T.F., Weaver, A.J., 2002. The role of the thermohaline circulation in abrupt climate change. Nature 415, 863-869.

Kiefer, T., Kienast, M., 2005. Patterns of deglacial warming in the Pacific Ocean: a review with emphasis on the time interval of Heinrich event 1. Quaternary Science Reviews 24, 1063-1081.

The potential of lacustrine ostracodes, thecamoebians, and chironomids from maar lakes in east-central Mexico as paleoenvironmental and climatic indicators

Liseth Pérez[1], Sergio Cohuo[2], Itzel Sigala[1,3], Jaime Escobar[4], Carolina Vergara[5], Alberto Araneda[5], Julieta Massaferro[6], Socorro Lozano[1] and Margarita Caballero[7]

[1] *Instituto de Geología, Universidad Nacional Autónoma de México (UNAM), Ciudad Universitaria, 04510, Distrito Federal, México. lcpereza@geologia.unam.mx*
[2] *Institut für Geosysteme und Bioindikation, Technische Universität Braunschweig, Langer Kamp 19c, 38106 Braunschweig, Alemania.*
[3] *Posgrado en Ciencias Biológicas, Universidad Nacional Autónoma de México (UNAM), Ciudad Universitaria, 04510, Distrito Federal, México.*
[4] *Departamento de Ingeniería Civil y Ambiental, Universidad del Norte, Km 5 Vía Puerto Colombia, Barranquilla, Colombia.*
[5] *Grupo de Estudios Paleolimnológicos (GEP), Unidad de Sistemas Acuáticos, Facultad de Ciencias Ambientales, Universidad de Concepción. Casilla 160-C, Concepción, Chile.*
[6] *CENAC-APN, CONICET, San Martin 24, 8400, Bariloche, Argentina.*
[7] *Instituto de Geofísica, Universidad Nacional Autónoma de México (UNAM), Ciudad Universitaria, 04510, Distrito Federal, México.*

Keywords: (paleo)bioindicators, Neartic-Neotropical transitional zone, paleoenvironment.

Aquatic environments of central Mexico are highly important for modern and past biological and ecological studies, because they are located in the transitional zone between the Nearctic and Neotropical ecozones. The bioindicator fauna of this transitional zone has remained poorly known despite the fact that a full understanding of their taxonomy and ecology is a pre-requisite for reliable paleoenvironmental reconstructions. Some paleolimnological studies based on ostracodes have been conducted in a zone in east-central Mexico locally known as the "Axalapascos", which is particularly characterized by its high endemism.

We studied the taxonomy and ecological preferences of modern ostracodes, thecamoebians and chironomids from a total of 5 maar lakes (Alchichica, Aljojuca, La Preciosa, Tecuitlapa, Quechulac) with the ultimate objective to test their potential as paleobioindicators of environmental and climatic changes. Surface sediments for quantitative faunal analysis were collected from the lake deepest point and littoral zones. Environmental variables (pH, temperature, dissolved oxygen, conductivity, TDS, etc.) were measured in situ with a multiparemetric sonde at every collection site. Parallel water samples were collected for water chemical composition analyses in the laboratory.

Seven ostracode species were identified. However, species diversity per site was not higher than 3 species. For instance, in Lake Alchichica, the largest, deepest and most saline studied maar lake, two ostracode species were collected. The dominant species in the area was *Eucandona* cf. *patzcuaro* and *Limnocytherina axalapasco*. *Eucandona* cf. *patzcuaro* displayed morphological discrepancies with the type material of *E. patzcuaro* and its taxonomic position is currently under investigation. The new species *Limnocytherina axalapasco* Cohuo, Pérez & Karanovic 2014 displays intraspecific variability among populations of the region (La Preciosa and Quechulac). *Limnocytherina* is a genus conformed by 12 species; its previously known distribution in the American continent was known to be exclusively on the north (Nearctics), but until our study little was reported about its distribution from Mexico (transitional zone) and Central America (Neotropics), this record extends the distribution zone for this genus. Lakes La Preciosa, Quechulac and Alchichica share species in common, differing from the fauna from lakes Aljojuca and Tecuitlapa. Preliminary results of a study of the ostracode fauna from lakes across the Trans-Mexican Volcanic Belt (TMVB) suggests that maar lakes in east-central Mexico possess particular species assemblages that differ from the rest of studied lakes.

Thecamoebian and chironomid species richness was higher than for ostracodes. A total of 11 thecamoebian species and 13 chironomid genera were identified. The highest thecamoebian species richness was reported in lake Aljojuca (n=7) and Alchichica (n=5). For chironomids, 8 genera were reported in lake Tecuitlapa. Lake Aljojuca is characterized by HCO_3>>Cl>SO_4 -- Na>Mg>>Ca waters, Lake Alchichica by Cl>>CO_3>SO_4 -- Na>>Mg and lake Tecuitlapa by CO_3>>Cl -- Na. The thecamoebian genus *Arcella* is widely distributed in the study area. Other genera present in the lakes were *Difflugia, Centropyxis* and

Pseudodifflugia. *Chironomus*, *Cricotopus* and *Dicrotendipes* were the most distributed chironomid genera. Genera restricted to lake Tecuitlapa were *Ablabesmyia*, *Endochironomus*, *Einfeldia*, *Micropsectra*, *Paratanytarsus*, and genera living only in lake Alchichica included *Labrundinia*, and *Pseudosmittia*.

We will use multivariate statistics to reveal the most important variable(s) that determine(s) the bioindicator distribution in the area, which will suggest the variable(s) that could be use for the development of transfer functions. Such transfer functions could be apply to fossil species assemblages in sediment cores retrieved from the area. Our study provides important taxonomic and ecological information for species living in maar lakes from east-central Mexico and highlights their potential as paleobioindicators. This will improve the interpretation of fossil species assemblages in sediment cores from maar lakes in east-central Mexico.

Acknowledgements

We would like to thank all participants in our field trips: Edyta Zawisza (PAN, I. Ciencias Geológicas, Polonia), Alexander Correa-Metrio and Esperanza Torres (Instituto de Geología, UNAM). Special thanks go to María Aurora Armienta and the staff of the Laboratory of Analytical Chemistry of the Institute of Geophysics, Universidad Nacional Autónoma de México for the water chemical analysis. We also thank the agencies and institutions that provided financial support: CONACYT (project number 167621), National Science Foundation (NSF award number 0902864) and the Instituto de Geología, Universidad Nacional Autónoma de México.

Environmental magnetism study for the determination of paleoclimates and paleoenvironmental conditions in Serdan Oriental Basin.

Kurt Wogau Chong[1], Harald Böhnel[1], Kenneth L. Verosub[2], Tripti Bhattacharya[3], and Roger Byrne[3]

[1] *Centro de Geociencias, Universidad Nacional autónoma de México, UNAM Campus Juriquilla, Querétaro, México.* *kurtwogau@gmail.com, hboehnel@geociencias.unam.mx*
[2] *University of California, Davis campus, California, USA, klverosub@ucdavis.edu*
[2] *University of California, Berkeley campus, California, USA, tripti@berkeley.edu, arbyrne@berkeley.edu*

Keywords: Cantona, paleoclimates, paleoenvironmental.

Aljojuca lake is located in the Serdán Oriental basin in the state of Puebla, in the eastern part of the Transmexican Volcanic Belt. Three lake sediment cores were recovered for studying the magnetic mineralogy (see figure 1), establish the paleo environmental conditions of the area and gather data of the secular variation for the Holocene in Mexico.

Core images and magnetic concentration-dependent parameters were used to correlate the core sections and then build a compound core. The length of this core is 1171.2 cm and the maximum age is 5460 years according to five C-14 ages. The core was subdivided into seven zones with similar behavior of the magnetic concentration-dependent parameters. The results shows that the main magnetic minerals in Aljojuca lake are magnetite and titanomagnetite, with the rare presence of hematite and iron sulfurs like pyrrhotite. The principal magnetic grain size observed in the sediments is pseudo single-domain, determined from King and Day plots. Comparing the results of magnetic mineralogy with different climatic proxys in the center of Mexico we discovered that between zones I to IV the high concentration of sandy facies, related to high values of magnetic concentration-dependent parameters, were formed in wet weather conditions. In zone V we relate high concentration of organic matter to more reducing conditions during the dry climates. This episode coincides with the fall of prehispanic city of Cantona around 950 a.C. Zones VI and VII are characterized by anthropogenic activity (García Cook and Martínez, 2005).

Fig. 1– Figure shows the location of the three cores taken from the Aljojuca lake, for the paleoclimate and paleoenvironmental study.

References

García Cook .A., Martínez C.Y., 2005. Proyecto Arqueológico Cantona y del Norte de la Cuenca de Oriental: "Informe de los trabajos en campo llevados a cabo en la temporada 2004". Archivo Técnico de la Coordinación Nacional de Antropología, INAH,Mexico.

Detailed geologic map of the bottom of Rincón de Parangueo maar, México: evidence of active subsidence

José Jorge Aranda-Gómez[1], Luis Rocha-Treviño[2], Jesús Pacheco-Martínez[3]

[1] *Centro de Geociencias, Universidad Nacional Autónoma de México, UNAM, Campus Juriquilla, Querétaro, México.* *jjag@geociencias.unam.mx*
[2] *Posgrado en Ciencias de la Tierra, Centro de Geociencias, Universidad Nacional Autónoma de México, UNAM, Campus Juriquilla, Querétaro, México.*
[3] *Centro del Diseño y la Construcción, Universidad Autónoma de Aguascalientes, Av. Universidad 940, Aguascalientes, Ags.México.*

Keywords: maar subsidence, gravity tectonics, mud diapirism.

We show in this poster a 1.1,000 scale geologic map of Rincón de Parangueo (RP) as a visual complement of the data discussed in two other works (Aranda-Gómez *et al.* and Espino del Castillo *et al.*, this volume) presented in this 5th International Maar Conference. Additional information about RP can be found in Aranda-Gómez *et al.* (2009, 2013) and in the 5IMC intra-conference field trip guidebook. The large number, variety, and size of the structural features exposed on the dry bed of the desiccated lake in RP, makes it virtually impossible to show these features in regular slides presented in a talk, thus we believe it is worth showing the map.

Methods

Geological data compiled in the field was plotted on a topographic map prepared by us with two Sokia SET610k total stations. Contour lines shown on the base map were calculated on the basis of nearly 4700 triangulation points measured from 8 points located in terrain above the lake bed. Contour lines, spaced 0.50 m, were calculated with Surfer 8 Golden software, using the kriging interpolation method. We began the geologic map project at a 1:2,000 scale, as the size of the printed map was more manageable in the field. Soon, it was obvious that many structural features could not be plotted at this scale. Location of the data points was obtained in the field with a Ashtech Mobilemapper 10 GPS, which has an approximate horizontal precision of 1 m. We found that in most places within the crater the GPS yielded reliable locations. One exception is in the SW portion of the basin, where the crater walls are closer to the lake coast (Fig. 1). As we advanced in the mapping project we found that many features, such as the fracture sets exposed on the topographic scarp were not well depicted in the topo map, and mapping each fracture with the GPS was a unwieldy task. Thus, we order a low altitude flight above the crater and obtained color digital photographs with and estimated resolution of 10 cm per pixel. In addition, the air photos form stereopairs that can be studied and interpreted with a regular stereoscope. These air photos were also used to prepare an orthophoto of the crater's bottom.

Detailed geologic mapping was performed only at the lake's bottom and its immediate surroundings. Figure 1 shows the crater's edge and the inferred maximun extent of the lake prior to desiccation. The blue line (coast) roughly correspond with the 1722 m contour line. However, there are several places where subsidence is already affecting talus deposits located between the coast and the crater's wall.

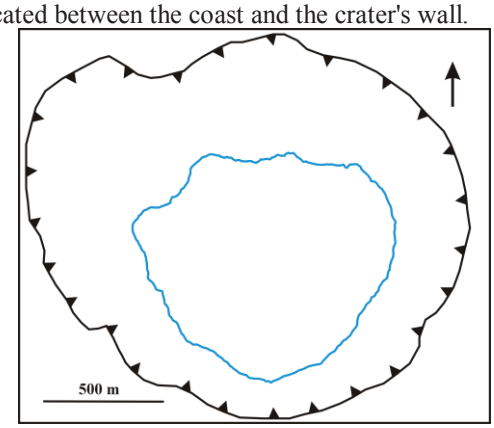

Fig. 1 Coast line of the lake (blue) and maar crater rim. Figures 2-4 only show the coast line in blue

Stratigraphic units

Close to the coast, the lake had a calcareous platform formed by aragonite and hydromagnesite microbialites. Microbialite structures have different morphologies (Espino del Castillo *et al.*, 2014), but stromatolites form mounds up to 1 m high, while oncolits and trombolites form a flat, thin (< 0.3 m) layer. Stromatolite mounds form a discontinuous ring, which was located 100 – 300 from the coast, except in the SW part of the basin where stromatolites grew directly on talus deposits. Therefore, in that area the platform did not existed or was substantially reduced.

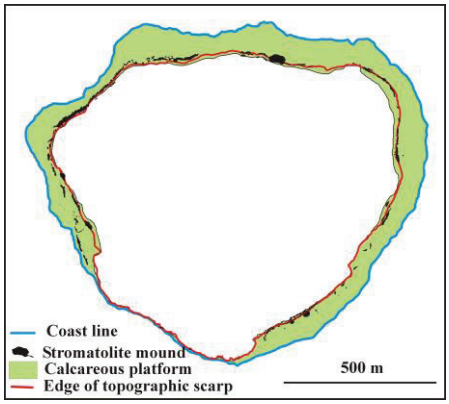

Fig. 2. Extent of the calcareous platform near the coast (blue line). Mounds made of stromatolites form a discontinuous ring. Note that the edge of the main topographic scarp and subsidence-related normal faults coincide with the stromatolite ring.

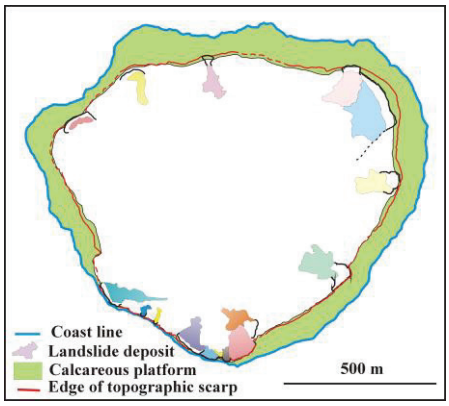

Fig. 3. There is a high concentration of landslides in the area where the calcareous platform is very narrow. Therefore, it is possible that this feature was destroyed by slope processes.

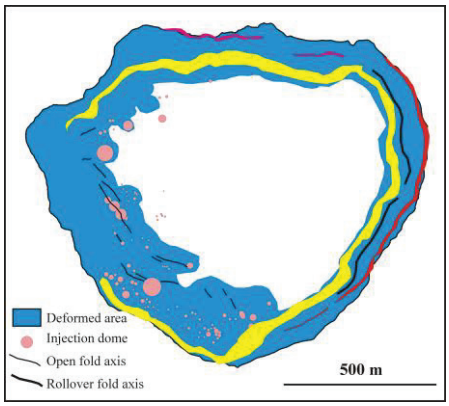

Fig. 4 Width of the deformed area and dome and fold distribution. Some of the largest dome clusters occur in areas covered by landslide deposits. The yellow area corresponds to the main scarp fault system. The red area follows the listric fault system. Note presence of rollover folds in the eastern part of the deformed area

From the edge of the calcareous platform toward the depocenter, lake sediments are calcareous muds also composed by aragonite and hydromagnesite. Near the depocenter, at the edge of the present day playa-lake, occur evaporitic crusts made of trona, halite, silvite and other calcium carbonates. We made the distinction between depositional mud facies based on the presence of parallel laminations or convoluted bedding. Chaotic megabreccias occur near landslide scars exposed on the scarp

Structures

The width of the area affected by subsidence-related deformation varies from one place to other areas affected by deformation **Style 1** described by Aranda-Gómez *et al.* (2014) are relatively narrow and lack the presence of injection domes near the base of the scarp (Fig. 4). The width of the deformed area where **Style 2** and **Style 3** are present is considerably wider. Injection domes occur as isolated clusters or as lineaments associated with open folds (Fig. 4). Some clusters coincide with areas covered by landslide deposits

Acknowledgements

Research supported by Papiit (IN109410) & Conacyt (129550) grants to J. Aranda. Nuri López Báez assisted in the field.

References

Aranda-Gómez, J.J Chacón-Baca, E., Charles-Polo, M., Solorio-Munguía, J.G., Vega-González, M., Moreno-Arredondo, A., Origel-Gutiérrez, G., 2009, Collapse structures at the bottom of a recently desiccated maar lake: Rincón de Parangueo maar, Valle de Santiago, México. 3rd International Maar Conference, Asociación Geológica Argentina, Publicaciones especiales Serie D, Núm. 12.

Aranda-Gómez, J.J Levresse, G., Pacheco Martínez, J., Ramos-Leal, J.A., Carrasco-Núñez, G., Chacón-Baca E., González-Naranjo, G., Chávez-Cabello G., Vega-González, M., Origel, G., Noyola-Medrano, C., 2013, Active sinking at the bottom of the Rincón de Parangueo Maar (Guanajuato, México) and its probable relation with subsidence faults at Salamanca and Celaya. Boletín de la Sociedad Geológica Mexicana 65(1): 169-188.

Aranda-Gómez, J.J. Cerca M., Rocha-Treviño, L., Pacheco-Martínez, J., Levresse, G., Ramos-Leal, J.A., Yutsis,V., Arzate-Flores, J., 2014, Structural analysis of subsidence-related deformation at the bottom of Rincón de Parangueo maar, México (this volume).

Espino del Castillo, A., *Beraldi-Campes, H., Aranda-Gómez J.J.*, 2014, Bacteria associated with microbialites from Rincón de Parangueo, Guanajuato (this volume).

.

Structural analysis of subsidence-related deformation at the bottom of Rincón de Parangueo maar, México

José Jorge Aranda-Gómez[1], Mariano Cerca[1], Luis Rocha-Treviño[2], Jesús Pacheco-Martínez[3], Gilles Levresse[1], José Alfredo Ramos -Leal[4], Vsevolod Yutsis[4] and Jorge Arzate-Flores[1]

[1] *Centro de Geociencias, Universidad Nacional Autónoma de México, UNAM, Campus Juriquilla, Querétaro, México.* *jjag@geociencias.unam.mx*
[2] *Posgrado en Ciencias de la Tierra, Centro de Geociencias, UNAM, Campus Juriquilla, Querétaro, México*
[3] *Centro del Diseño y la Construcción, Universidad Autónoma de Aguascalientes, Ave. Universidad 940, Aguascalientes, Ags.*
[4] *División de Geociencias Aplicadas, Instituto Potosino de Investigación Científica y Tecnologica, San Luis Potosí, SLP IPICYT*

Keywords: maar subsidence, gravity tectonics, mud diapirism.

Rincón de Parangueo (RP), together with other three nearby maar crater-lakes, was gradually desiccated in the second half of last century, as a consequence of overdraft in the regional Valle de Santiago-Salamanca aquifer (Aranda-Gómez et al., 2013). Overdrafting has caused land subsidence and development of faults both inside the RP maar and in nearby Salamanca city. However, the rate of normal fault displacement and the complexity of associated deformation near the faults inside RP is significantly higher than those observed elsewhere in the region. So far, none of the other three desiccated crater-lakes display any structural evidence of subsidence in their lake beds. Thus, special conditions must be present in RP, which we believe are related with mass removal of evaporite minerals from the crater by brine infiltration toward the aquifer (Aranda-Gómez et al., 2013).

The most conspicuous feature at RP lake bottom is a 15 m high topographic scarp located near the former shore. The scarp has an annular shape and it is nearly continuous, but its width and slope varies from place to place around the center of the lake. Detailed 1:1000 geologic mapping has shown that the scarp in most places might be interpreted as a monocline modified by normal faults and by mass movement along the slope. Basinward tilt angles in the dry, finely laminated mud blocks exposed across the scarp usually range between 10° and 30º but in isolated places are up to 50º. The scarp is also the locus of an annular, segmented, down toward the lake, high angle, normal fault system. The initial structure in the scarp must have resembled folds formed by differential compaction over an underlying structure (Skuce, 1996), and later were modified by normal faults propagating toward the surface from the tip of the underlying structure (Whitjack, 1990). Location of both, monocline and annular fault system, suggest that normal faults nucleated and propagated toward the surface from a buried topographic accident, which may represent the diatreme-country rock contact at depth (Fig. 1, C-D).

Two conspicuous sets of tensional open fractures are exposed on the scarp. One set is parallel to the scarp and the other is perpendicular to it. Separation between the mud blocks across the fractures varies from few centimeters up to two meters. These fracture sets are interpreted as the products of mud expansion in sediment that is sliding down towards the lake's center. Some of the scarp-parallel open fractures evolve to normal faults and concentrate vertical throw caused by downward movement of the sediment. Thus, some of the normal faults exposed in the scarp are unusual because despite being high angle structures, they may have larger heave than throw. Deformation is a combination of downward movement along the scarp and simultaneous translation of sediments towards the depocenter, in unconfined conditions.

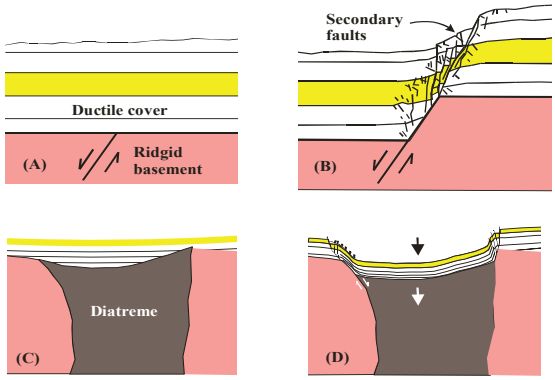

Fig.1 (A)-(B) Experimental clay model of extensional fault-propagation fold associated with an upward-propagating, normal fault involving a rigid basement and a ductile sedimentary cover (Whitjack et al., 1990). (C)-(D) deformation at RP lake sediments occurred above the buried contact diatreme-country rock. “Normal movement” in the system is mimicked by differential compaction of the wet lake sediments at the bottom of the maar.

There are at least three different deformation styles developed along the scarp. We enlist the observed structures in the order they are found when moving from the center of the lake in a landward direction: **Style 1** consists of the monocline modified by 3 to 5 high angle normal faults, a rollover anticline, and a

secondary graben associated with a listric normal fault (Fig. 2B) located close to the crater wall. The slope of the scarp in areas affected by **Style 2** is lower than in the other two styles (Fig. 2) and the width of the deformed area is wider, involving areas located between the break of the slope and the center of the lake; near the base of the scarp occur aligned domes and few open folds that are followed by the monocline, which is modified by a series (7 -10) of normal faults where heave is larger than throw, and finally at the top of the scarp there is a platform gently tilted towards the lake, which represents the undeformed bottom of the lake. **Style 3** is formed by mud injection domes and folds near the base of the scarp, formed by a single, high angle normal fault, which is partially covered by talus deposit, and a basinward tilted platform located between the top of the scarp and the former lake coast. The monocline is not present in the area that displays Style 3 of deformation (Fig. 2D).

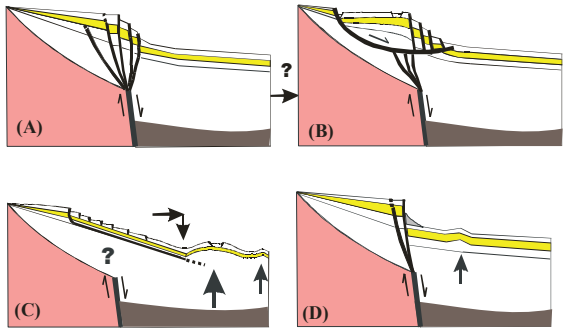

Fig. 2. Deformation styles documented in RP lake sediments. (A)-(B) correspond to Style 1; we view (B) as a modification of (A), caused by slope processes. (C) Style 2. (D) Style 3, note the monocline absence.

There are several places where the monocline has been affected by slope processes as rotational landslides or topples. Most of these features are obvious on the scarp as they left "scars" with a characteristic crescent shape and, in most of them, there are landslide deposits made of chaotic megabreccias at their base. It is worth mentioning that some of the landslides scars lack a clear megabreccia at their base, and microfolds are abundant at the laminated mud in the area. Therefore, we conclude that some of the landslide scars correspond to events that occurred when the lake still had water.

We recognize domes formed by vertical mud injection near the scarp. These domes generally occur between the scarp and the depocenter of the lake. The size of the base in the domes ranges between 50 and 2 m and their height between 10 and 0.5 m. The largest domes also have two fracture sets: one radial and the other concentric. Two different mud facies are exposed on the flank of the domes: 1) coherent blocks made of finely laminated mud, similar to the mud exposed in the monocline, 2) massive mud with a characteristic "pop corn texture" displayed on the dry surfaces, which is interpreted as mud extruded thru the fractures. Some of the domes formed as a direct response to subsidence, specially in the areas affected by Style 2 of deformation, where they form alignments associated with open folds. There, the mud blocks on the scarp are sliding on layer-parallel detachment surfaces, which are flat (non-listric), except near the top of the topographic scarp, where they become nearly vertical and are exposed as high angle normal faults. Very slow extrusion of mud from tensional fractures in the domes indicates that underneath a thin crust of dry mud exposed on the surface, there is wet, plastic mud. Thus, the formation of the dome chains and associated folds is caused by the sediments load and the pressure exerted by them as they move along the detachments and reach the bottom of the scarp. Domes are also common in areas covered by landslide megabreccias. These domes may appear isolated or form clusters; their formation mechanism is slightly different, as upward mud movement appears to be caused by the weight of the megabreccia resting atop of a thin crust of dry mud. RP is a striking example of active subsidence, gravity-induced deformation, and mud tectonics.

Acknowledgements

Research supported by Papiit (IN109410) & CONACyT (129550) grants to J. Aranda. Nuri López Báez assisted in the field.

References

Aranda-Gómez, J.J., Levresse, G., Pacheco Martínez, J., Ramos-Leal, J.A., Carrasco-Núñez, G., Chacón-Baca E., González-Naranjo, G., Chávez-Cabello G., Vega-González, M., Origel, G., Noyola-Medrano, C.,, 2013, Active sinking at the bottom of the Rincón de Parangueo Maar (Guanajuato, México) and its probable relation with subsidence faults at Salamanca and Celaya. Boletín de la Sociedad Geológica Mexicana 65(1): 169-188.

Skuce, A.G., 1996, Forward modelling of compaction above normal faults: an example from the Sirte Basin, Libya" In Buchanan,P.G. and Nieuwland,D.A. Modern Developments in Structural Interpretation, Validation and Modelling. London Geological Society Special Publications 99. 135–146.

Whitjack, M.O., Olson, J., Peterson. E., 1990, Experimental models of forced extensional folds. AAPG Bull 74: 1038-1054.

GPR survey and physical experiments of the subsiding lacustrine sequence of Rincón de Parangueo maar, Guanajuato México

Mariano Cerca-Martínez[1], Luis Rocha-Treviño[2], José Jorge Aranda-Gómez[1], Dora Celia Carreón-Freyre[1]

[1] *Centro de Geociencias, Universidad Nacional Autónoma de México, Campus Juriquilla, Querétaro, México, mcerca@geociencias.unam.mx*
[2] *Posgrado en Ciencias de la Tierra, Centro de Geociencias, Universidad Nacional Autónoma de México, Campus Juriquilla, Querétaro, México.*

Keywords: maar subsidence, GPR survey, physical experiments.

Rincón de Parangueo maar, located in the N portion of the Michoacán – Guanajuato volcanic field, in the northern part of the Trans Mexican Volcanic Belt, was gradually desiccated in the last part of the XX century, as a consequence of over exploitation of the regional Salamanca – Valle de Santiago aquifer (Aranda-Gómez *et al*., 2013). Groundwater withdrawal resulted in accelerated subsidence and faulting in the dry lake bed. Sinking of the crater's bottom produced a ring – fault system near the coast line of former lake, which is exposed on a 15 m high topographic scarp. Other structural features observed in the lake sediments are two sets of open fractures exposed along the scarp; one of the sets is parallel to the trend of the scarp and the other is perpendicular. The scarp is continuous and was produced by initial downsagging of the sediments, followed later by additional inclination of the laminated mud, and formation segmented normal faults with the hanging walls towards the lake center. We recognize two contrasting styles of deformation, which we interpret as products of a combination of gravitational and mud tectonics in unconfined sediments. The eastern sector of the topographic scarp is characterized by the presence of rollover anticlines with secondary crestal grabens developed in a block that overlies a listric normal detachment fault. On the western sector of the basin, the topography of the scarp is attenuated (as compared with the eastern sector), rollover folds and secondary crestal grabens are absent, and mud domes and folds are developed in the dry mud at the base of the scarp. Depth and separation of both fracture sets are more pronounced in the western sector than in the rollover domain.

To document the deformation, in addition to detailed (1:1,000 scale) geologic mapping, we performed a GPR survey, which included two profiles across the lake basin. Each profile is ~1000 m long and data was continuously recorded across the lake bottom We used a SIR-20 equipment with a 200 MHz antenna. Processing of the GPR raw data included a detailed topographic correction based on a topographic map, with a contour level spacing of 1 m that we prepared with total stations. Reflectors in the GPR images were correlated with layers observed in small excavations made in the lacustrine sequence; this allowed us to estimate a wave propagation velocity of 0.075 m/ns. Shallow reflectors recorded in the images are interpreted as sedimentary layers, fractures, faults, or mud domes as observed in unstacked profiles. Likewise, we found that the radar signature of continuous reflectors can be related with the spatial distribution of evaporites in the lake sediments. Evaporites are now mostly concentrated in the area near the lake remnants, where lake water has experienced many cycles of evaporation in the recent past. We believe that evaporites precipitated as the alkaline lake shrunk, but the evaporites have been lixiviated and transported towards present day playa-lake by rain water. The complete GPR profiles allowed the identification of major deformation structures and they give further insights on the differences in the structural styles along the ring fault. The GPR results were of great importance for a better understanding of the geometry and distribution of structures near the surface related to land subsidence in the fine grained materials.

Different factors such as differences variations in the geometry of the diatreme – country rock contact may have influenced the location and characteristics of the structures now seen on the surface. For example, a buried step-like feature in that contact may force the location of the fractures and faults that now form the main scarp. To explore systematically this hypothesis we have produced a series of physical experiments of the deformation observed at the lake sediments in the maar. The analogue models attempt to reproduce the desiccation and sinking of the bottom of the lake sediments and the nucleation and propagation of faults and fractures toward the surface. The granular material used is hollow microspheres with an apparent density of 700 kg/m^3, size of ca. 80 μm, and high cohesion. Initially, the material was saturated with water. The material was

contained in a rigid bowl with a half sphere shape. We placed underneath the microspheres plasticine features that simulate different geometries in the underlying country rock and/or country rock-diatreme contact. Plasticine was used to simulate the buried topography underneath the lake sediments as it is an incompressible material at the experimental strain rate used. Experimental variation included changes in the geometry of step-like features below the sediments, which tended to cause differential compaction in the wet sediments as they lost water. The water was drained from the experiments in order to drive deformation of the granular material.

All models produced an initial depression in the center of the bowl. Later, the deformation propagated from the center to the edges of the bowl. Irregularities in the basement localized deformation and fractures propagated upward to the surface mimicking the geometry of the basement faults.

Acknowledgements

Research supported by PAPIIT (IN109410) and CONACyT (129550) grants to J. Aranda., Diego Gracia Marroquín and Ricardo Carrizosa assisted in laboratory (Centro de Geociencias, Universidad Nacional Autónoma de México).

References

Aranda-Gómez, J.J., Levresse, G., Pacheco Martínez, J., Ramos-Leal, J.A., Carrasco-Núñez, G., Chacón-Baca E., González-Naranjo, G., Chávez-Cabello G., Vega-González, M., Origel, G., Noyola-Medrano, C., 2013, Active sinking at the bottom of the Rincón de Parangueo Maar (Guanajuato, México) and its probable relation with subsidence faults at Salamanca and Celaya: Boletín de la Sociedad Geológica Mexicana 65(1), 169-188.

.

It takes two to Tango. Or: How polygenetic is a monogenetic volcano?

Alexandrina Fulop and Stephan Kurszlaukis

De Beers Canada Inc., 250 Ferrand Drive, Suite 900, Toronto, ON, Canada. alexandrina.fulop@debeersgroup.com

Keywords: *monogenetic, polygenetic, kimberlite.*

In the classic definition of a monogenetic volcano, these volcanoes are typically considered to erupt only once and to be thus short-lived. The initial definitions are very specific about the requirement of a single eruptive episode and the freezing of the intra-pipe volcanic conduit which connects the vent to the magmatic source as described by Francis (1993) and Francis & Oppenheimer (2003). Walker (2000) defined a monogenetic volcano as a single eruption with a small and episodic magma supply and the freezing of the pathway which is no longer the favoured route for a subsequent eruption. Connor and Conway (2000) further refine the definition to single episodes of volcanic activity that can last days, years or decades, without subsequent eruptions. A general problem with these definitions is that the terms "eruption" or "episode" are poorly defined in that, strictly speaking, and eruption is a single event and an episode is either a continuous eruption or a series of eruptions over a certain time interval. If the latter, the time gaps in between the single eruptions need to be better defined and separated from a real hiatus in primary volcanic activity. In the same way, a hiatus needs to be better defined as to whether it is a break in primary pyroclastic activity or whether it would include resedimentation (or other) processes that can still occur when primary activity has ceased.

However, small volcanoes are still often called "monogenetic" although, under close examination, they have revealed histories of multiple eruptions.

Recent studies demonstrate that the facies architecture of a "monogenetic volcano" can be very complex and exhibit longer eruption durations and hiatuses than expected (Nemeth, 2010). Changing eruptive styles in terms of intensity, level of interaction with external water and magma chemistry during repeated episodes of eruption or from one episode to the other are now frequently documented in volcanoes still classified as "monogenetic" and overlap with the classical definitions of polygenetic volcanoes.

Francis (1993) and Francis & Oppenheimer (2003) classify the existence of two or multiple eruptive episodes through single or multiple vents and plumbing systems connected to a single or multiple magmatic sources as polygenetic volcanism. Walker

(2000) classifies a polygenetic volcano as a volcano that erupts repeatedly and is fed by a large and persistent magma supply following the same, still hot pathway. Suggesting the rather gradual distinction between monogenetic and polygenetic volcanoes, Lexa et al. (2010) introduces "the presence or absence of a significant period of erosion implying a longer lasting break in volcanic activity" as best criterion to distinguish between monogenetic and polygenetic volcanoes.

In our study of a complex kimberlite maar-diatreme volcano, we put both monogenetic and polygenetic definitions to a test.

The Tango Extension kimberlite pipe is one of 18 pipes discovered by De Beers in the Attawapiskat kimberlite field, Ontario, Canada.

Extensive drilling of the pipe resulted in the construction of a geological model that revealed the complex facies architecture of the volcano. In fact, the volcano is comprised of two amalgamated pipes:

an older pipe, Tango Extension Deep (TED), which is cut along its northern margin by the smaller Tango Extension (TE) pipe.

The resulting volcano is a pipe-in-pipe structure that is called the Tango Extension Super Structure (TESS).

The emplacement history of TED begins with a shallow maar crater that was subsequently filled with resedimented tephra from the initial phreatomagmatic explosions and large volumes of country rock displaced from the crater wall. In a subsequent hiatus the material filling this initial maar crater was solidified by pervasive hydrothermal carbonatization. Renewed magma ascent led to strong phreatic explosions in deeper levels than the maar crater, as it was indicated by a high abundance of cognate xenoliths of earlier consolidated maar crater infill and xenolith blocks derived from deeper strata. The following hiatus in volcanic activity led to a shallowing of the crater due to resedimentation, and the development of soil horizons along the margins of the crater. Within the crater center a lake was developing that grew as the crater was filled in. Simultaneously, the intrusion of

a small kimberlite batch into the subsurface feeder/plumbing system led to a concealed explosion in the basement that was not strong enough to crater. However, this explosion was pre-weakening the basement and had as such an important influence in later intruding magma that could slightly shift the focal point of explosions and with that the root zone of the later developing diatreme. The explosion in the basement was followed by magma intruding into the diatreme fill and fragmenting in weak magmatic explosions close to the crater floor where a spatter cone or a lava lake filling the crater with an apparent coherent kimberlite was formed. This final episode of volcanism in TED occurs during ongoing background resedimentation of tephra onto the crater which ends when the tephra ring is entirely eroded. However, even after the erosion of the tephra ring the crater formed a depression that was then exclusively filled by epiclastic material from the surrounding land surface, leading to a still preserved over 130 m thick mudstone basin as the final crater infill of TED. After this significant hiatus a reactivation of the plumbing system triggers a second episode of volcanism, leading to the emplacement of the younger TE pipe. The pre-weakened basement enables magma rising on a slightly different pathway close to the root zone and enhances the likelihood of explosive interaction of magma with the aquifer at the basement/Paleozoic interface. Repeated phreatomagmatic explosions cut through the northern portion of the precursor TED pipe capped by the thick mudstone basin, and forms the steep sided explosive crater of the younger TE pipe. Ongoing volcanism triggered a series of mass exchange processes between the TE and the partly consolidated TED structure in the attempt of the system to re-equilibrate itself: the slump of the soft, unstable upper portion of the TED mudstone basin as well as mudstone blocks from deeper levels of the TED crater infill into the TE crater together with the overlying TE tephra ring; the collapse and subsidence of the TED pipe fill adjacent to TE; the subsidence of a large country rock floating reef on the south side of TED towards the root zone of TED, and also the subsidence of the TE diatreme fill towards the root zone. The significant mass movements compensate for the mass deficit generated during the emplacement of the TE structure.

The emplacement of the TSS clearly shows that the feeder system underneath a maar-diatreme volcano can be reactivated after significant duration(s) of volcanic inactivity. The hiatuses observed in the emplacement of the TESS were also long enough to fully freeze the feeder dykes. As a consequence, the subsequently intruding magma used different pathways in the pre-weakened substructure of the volcano as it is indicated by the shift of the root zone in between the two pipes.

So is the Tango Extension superstructure a monogenetic or a polygenetic volcano? It actually qualifies as a polygenetic volcano in that it shows multiple eruptive episodes with different magma batches (mantle extraction events), significant hiatuses with erosion of the tephra ring, freezing and shifting of the plumbing system and at least a partial consolidation of tephra filling the diatreme. However, the emplacement of the two pipes is still closely related to each other, in that the plumbing system from the mantle to the upper crust has certainly been re-used and the final shift of the feeder dyke into the migrating root zone must have occurred in very close proximity to the root zone only. In the big picture, the emplacement of TESS was also very short lived in comparison to the volcanic activity in the entire volcanic field, which spans over several million years (Januszczak et al, 2013).

Acknowledgements

The authors thank De Beers Canada Inc. for permission to publish.

References

Connor, C.B., Conway, F.M. 2000. Basaltic volcanic fields, in Sigurdsson, H., Houghton, B., McNutt, S.R., Rymer, H., Stix, J., eds., Encyclopedia of Volcanoes, Academic Press: 331-343.

Francis, P. 1993. Volcanoes: a planetary perspective. Clarendon Press 443p.

Francis, P. and Oppenheimer, C. 2003. Volcanoes. Oxford University Press 521p.

Januszczak, N., Seller, M. H., Kurszlaukis, S., Murphy, C., Delgaty, J., Tappe, S., Ali, K., Zhu, J., and Ellemers, P. 2013. A Multidisciplinary Approach to the Attawapiskat Kimberlite Field, Canada: Accelerating the Discovery-to-Production Pipeline. Proceedings of 10th International Kimberlite Conference, Springer: 157-162.

Kurszlaukis, S. and Fulop, A. 2013. Factors controlling the internal facies architecture of maar-diatreme volcanoes. B Volcanol. 75: 761.

Lexa, J., Seghedi, I., Németh, K., Szakács, A., Konecný, V, Pécskay, Z., Fülöp, A., Kovacs, M. 2010. Neogene-Quaternary Volcanic forms in the Carpathian-Pannonian Region: a review. Cent. Eur. J. Geosci. 2(3): 207-270.

Nemeth, K. 2010. Monogenetic volcanic fields: Origin, sedimentary record, and relationship with polygenetic volcanism. The Geological Society of America, Special Paper 470: 43-66.

Walker, G.P.L. 2000. Basaltic volcanoes and volcanic systems, in Sigurdsson, H., Houghton, B., McNutt, S.R., Rymer, H., Stix, J., eds., Encyclopedia of Volcanoes, Academic Press: 283-289.

Volcanic Geology (radiometric dating, geochemistry) of the Paracho-Cherán area, Michoacán, México: Preliminary results

Juan Ramón de la Fuente, Claus Siebe, Marie-Noëlle Guilbaud, and Magdalena Oryaëlle Chevrel

Departamento de Vulcanología, Instituto de Geofísica, Universidad Nacional Autónoma de México, Coyoacán, C. P. 04510, México D. F.

Keywords: Shield volcano, scoria cone, geochronology.

The Plio-Quaternary Michoacán-Guanajuato Volcanic Field (MGVF) is located in the central part of the Trans-Mexican Volcanic Belt and covers an area of ~40,000 Km^2. It includes >1000 monogenetic scoria cones and associated lava flows, ca. 300 shield volcanoes, tens of lava domes, and only a dozen of phreato-magmatic vents (Hasenaka and Carmichael, 1985). Large strato-volcanoes that are so typical for subduction-related volcanic arcs are absent, except for V. Tancítaro (3840 m asl) that is nevertheless believed to be extinct (*e.g.* Ownby *et al.*, 2006). Eruptive products in the MGVF are predominantly calc-alkaline andesites, but a wide range in compositions (ol-basalts to rhyolites, including exotic alkaline varieties) can be found.

The fame of the MGVF is related to the fact that it hosts Paricutin, a scoria cone born in a corn-field in 1943. This eruption lasted until 1952 and motivated first modern volcanological studies in the area. Most of these works focused on Paricutin, and few addressed the regional volcanic geology of the area (Williams, 1950). First comprehensive studies considering the entire MGVF include those by Hasenaka and Carmichael (1985; 1987), followed by Connor (1987), Ban *et al.* (1992), Roggensack (1992), and Hasenaka (1994).

Some conclusions reached by these authors (*e.g.* the southward migration of volcanic activity) remain however debatable due to the lack of sufficient reliable information (especially radiometric data and

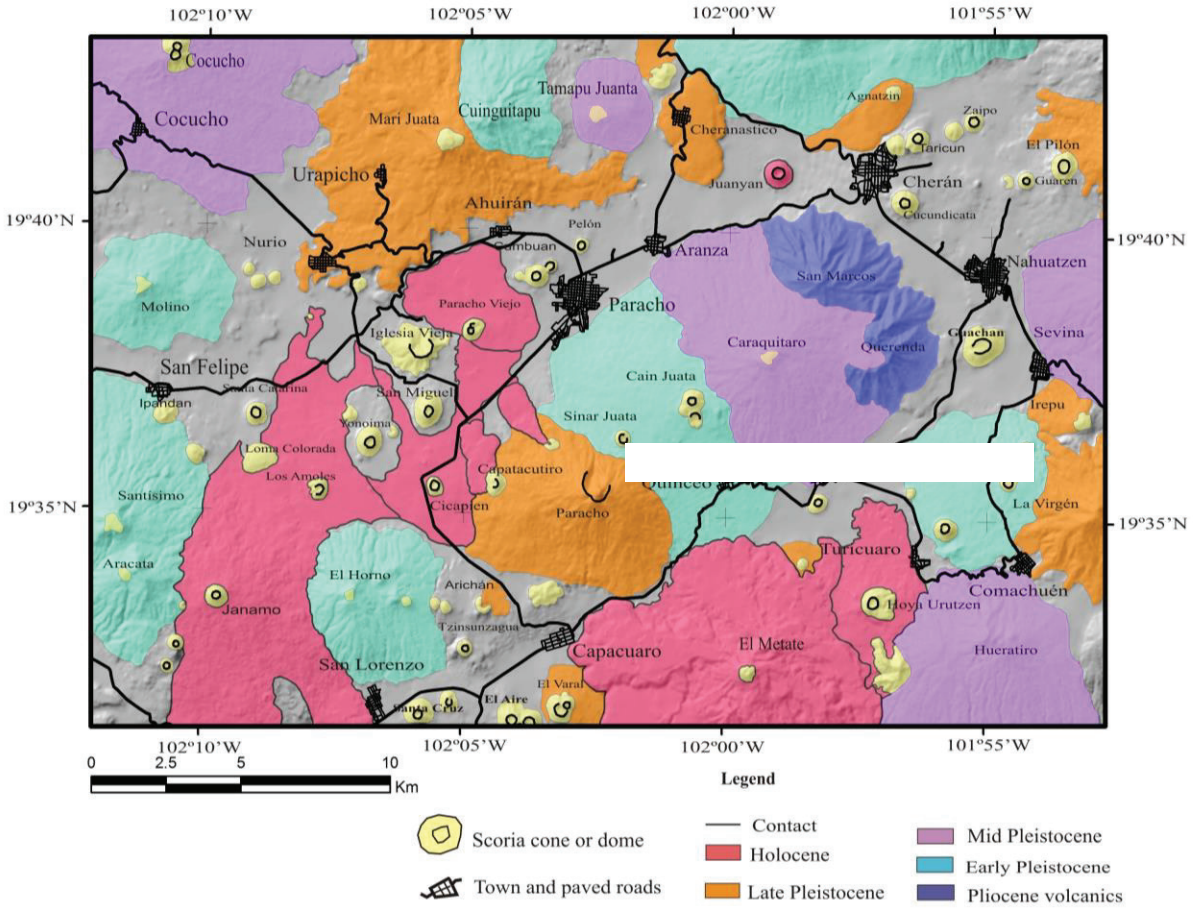

Fig. 1 – Map of Paracho-Cherán area.

erupted volumes). Because of the large extension of the MGVF and remoteness of some sectors, detailed mapping and radiometric dating were not undertaken until recently. First detailed maps and systematic radiometric age data sets of discrete areas were published recently by Ownby *et al.* 2011 (Tancítaro-Nueva Italia area) and Guilbaud *et al.* 2011, 2012 (Jorullo and Tacámbaro-Puruarán areas). These areas are however all located near the volcanic front and the present study focuses on the Paracho-Cherán area, located in the heartland of the MGVF. Following the same methodology as employed in the recent works, we intend to analyze the composition and mineralogy (petrography, major and trace elements, Sr-Nd-Pb isotopes) and radiometrically date (^{14}C, $^{40}Ar/^{39}Ar$) as many volcanoes within the study area as possible. With this new data in hand, we will be able to determine with precision eruption rates and compositional trends over time. Comparing with previous results from areas located towards the arc front will allow to test hypotheses about the origin and evolution of the entire MVGF (*e.g.* Siebe *et al.*, 2013). Furthermore, we will be able to better estimate the probability of recurrence of volcanic activity in this area.

The Paracho-Cherán study area (Fig. 1) covers ~580 km^2 and contains 53 monogenetic scoria cones (and associated lava flows) and 19 medium-sized volcanoes (shields and domes). First results from ^{14}C dating indicate that at least 7 scoria cones (Janamo, Capatacuatiro, Cicapién, cone on Paracho NW flank, Hoya Urutzen, Paracho Viejo, and Juanyán; Fig. 2) and one shield volcano (El Metate, see Chevrel *et al.*, this conference proceeding) have formed in the Holocene. In contrast, many of the volcanoes have morphologies suggesting older ages spreading from Pliocene to late-Pleistocene (Fig. 1). The most common rocks encountered are andesites with a typical mineral paragenesis that includes olivine, plagioclase, pyroxene, (and sometimes hornblende) in a glassy groundmass with feldspar microlites.

Fig. 2 – Aerial photograph of Cerro Juanyan (view from the NE). This Holocene cone is ca. 10,000 yrs B.P.

Acknowledgements

Costs were defrayed from projects CONACyT-167231 and UNAM-DGAPA IN-109412-3 granted to C.S., and CONACyT-152294 granted to M.N.

References

Ban, M., Hasenaka, T., Delgado-Granados,H., Takaoka, N., 1992. K-Ar ages of lavas from shield volcanoes in the Michoacán-Guanajuato volcanic field, México. Geofis. Int. 31(4): 467-473.

Connor, C. B., 1987. Structure of the Michoacán-Guanajuato Volcanic Field, Mexico. J. Volcanol. Geoth. Res. 33: 191-200.

Guilbaud, M-N., Siebe, C., Layer, P., Salinas, S., Castro-Govea, R., Garduño-Monroy, V.H., Le Corvec, N., 2011. Geology, geochronology, and tectonic setting of the Jorullo Volcano region, Michoacán, México. J. Volcanol. Geoth. Res. 201: 97-112.

Guilbaud, M-N., Siebe, C., Layer, P., Salinas, S., 2012. Reconstruction of the volcanic history of the Tacámbaro-Pururarán area (Michoacán, México) reveals high frequency of Holocene monogenetic eruptions. Bull. Volcanol. 74: 1187-1211.

Hasenaka, T., Carmichael, I.S.E., 1985. The cinder cones of Michoacán-Guanajuato, Central Mexico: Their age, volume and distribution, and magma discharge rate. J. Volcanol. Geoth. Res. 25: 105-124.

Hasenaka, T., Carmichael, I.S.E., 1987. The cinder cones of Michoacán-Guanajuato, Central México: Petrology and chemistry. J. Petrol. 28: 241-269.

Hasenaka, T., 1994. Size, distribution and magma output rates for shield volcanoes of the Michoacán-Guanajuato volcanic field, Central Mexico. J. Volcanol. Geotherm. Res. 63:13– 31.

Ownby, S., Delgado-Granados, H., Lange, R.A., Hall, C.M., 2006. VolcánTancítaro, Michoacán, México. $^{40}Ar/^{39}Ar$ constraints on its history of sector collapse. J. Volcanol. Geoth. Res. 161: 1-14.

Ownby, S.E., Lange, R. A., Hall, C.M., Delgado-Granados, H., 2011. Origin of andesite in the deep crust and eruption rates in the Tancítaro-Nueva Italia region of the central Mexican arc. Bull. Geol. Soc. Am. 123 (1-2): 274-294.

Roggensack, K., 1992. Petrology and geochemistry of shield volcanoes in the central Mexican Volcanic Belt. PhD-thesis, Dartmouth College, Hanover, New Hampshire, 179 p.

Siebe, C., Guilbaud, M-N., Salinas, S., Layer, P.W., 2013. Comparision of the volcanic geology of the Tacámbaro-Puruarán (arc front) and the Zacapu (arc inland) areas in the Michoacán-Guanajuato volcanic field, Mexico. IAVCEI 2013 Scientific Assembly, July 20-24. Kagoshima, Japan, Abstract Volume.

Williams, H., 1950. Volcanoes of the Paricutin region, México: Geologic investigations in the Paricutin area, México. US Geol. Survey Bull. 965-B: 165-279.

Gravimetric constrains on the structure of the subduction zone associated with the Michoacán-Guanajuato monogenetic field

Balam Molina de Artola[1], Marie Noëlle Guilbaud[1], Vladimir Kostoglodov[2]

[1] *Departamento de Vulcanología, Instituto de Geofísica, Universidad Nacional Autónoma de México, C.U., México City, México.* coatl@ciencias.unam.mx
[2] *Departamento de Sismología, Instituto de Geofísica, Universidad Nacional Autónoma de México, C.U., México City, México.*

Keywords: subduction zone, free air anomaly, Bouguer anomaly.

The Michoacán-Guanajuato volcanic field (MGVF) located in the central sector of the Trans-Mexican Volcanic Belt (TMVB) is the largest monogenetic field in the world. It includes more than 1,000 volcanoes covering an area of ca. 40,000 km^2, with ca. 1000 small-sized volcanoes (principally scoria cones), ca. 400 medium-sized volcanoes (dominantly shields) and only two large stratovolcanoes (Tancítaro and Patamban) that are considered extinct (Hasenaka and Carmichael, 1985). Volcanic activity began in the Late Pliocene (5 Ma) in this field and continued up to recent times, the last eruption forming the Paricutin cone was in 1943-1952, hence the field can be considered as potentially active (Guilbaud *et al.*, 2012).

Monogenetic fields are generally associated to zones in extension where distributed magma generation, a thin crust, and abundant extensional faults favor the ascent and eruption of small batches of poorly-differentiated magmas. Hence, they are not common in subduction settings where instead localized magma generation and a thick crust favor the formation of large stratovolcanoes.

The location of this very large MGVF in a subduction setting is thus evidently "anomalous" and this is still unclear which of the factors is important, i.e., whether the subduction setting or the crustal structure is atypical and allows such field to exist.

The structure of the subduction zone in Michoacán has been subjected to ample debate, and several authors have even proposed that the volcanism could be related to some intraplate-type setting (mantle plume or continental rift), on the basis of the occurrence of OIB type magma compositions.

The cutoff of the Wadatti-Benioff zone at approx. 100 km depth and hence lack of seismic activity at depth below the volcanic zone has been the main cause of this uncertainty. Recent work have allowed the structure of the subduction zone to be known in just a few transects across the TMVB but the structure in the MGVF zone is still largely unknown.

The aim of this work is to use gravity anomalies, together with topography and seismic data, to constrain in general the structure of the subduction zone below the MGVF.

Gravity data coverage is not homogeneous in México. For the purpose of this work, we analyzed the data from two sources: 1) database available from the Scripps Institution of Oceanography (SIO) platform (Sandwell and Smith, 1997, 2009) derived from the Satellite Geodesy data (Geosat and ERS-1) in the ocean and from the Earth Gravitational Model 2008 (EGM2008) (Pavlis *et al.*, 2012) on land; 2) digitalized readings from the gravity map constructed from a set of irregularly-distributed field data (De la Fuente *et al.*, 1991). Both types of data give similar results at large scale and we report here only the results based on the SIO data.

The mapping of the SIO data (Fig. 1) in the MGVF area reveals several important characteristics. From the ocean to land and perpendicular to the coastline, the free air anomaly map (Fig. 1A) is characterized by: 1) weak positive anomalies in the sea floor far from the trench, 2) a pronounced negative anomaly at the Meso-America Trench (MAT), followed by 3) a pronounced positive anomaly at the Sierra Madre del Sur (SMS) old volcanic range, 4) a negative anomaly in the depression of the Balsas River (BR) and 5) varying positive anomalies on the volcanic highland plateau. The volcanic field itself presents four main positive anomalies, two of them associated with the two largest volcanoes of the field: V. Patamban (130 mGal) and V. Tancítaro (230 mGal) (1 and 2 in Fig. 1A) and the other two characterized by regions with a high density of volcanic centers (3 and 4 in Fig. 1A). In comparison, the main lacustrine basins in the volcanic field correspond to weak positive anomalies (Pátzcuaro: 10 mGal, Cuitzeo: 4 mGal, Zirahuén: 60 mGal and Yuriria: 10 mGal).

The simple Bouguer anomaly map of the MGVF (Fig. 1B) shows less local variations and more regional behavior, as expected by the correction introduced for the varying topography across the region. The coastline keeps a well defined positive anomaly (50-70 mGal) with only one discontinuity

near to Lázaro Cárdenas Canyon that has values ranging from -80 to -60 mGal. The frontal part of the field (from Apatzingan to the V. Paricutin) characterized by irregularly spaced scoria cones presents a negative anomaly ranging from -130 to -90 mGal (region I in Figure 1B). The interior of the MGVF with the highest densities of volcanic centers coincides with a negative anomaly ranging from -190 to -220 mGal (region II in Fig. 1B). The western border of the field, from Zamora to Lake Chapala, is defined by a less-pronounced negative anomaly (-170 to -150 mGal, region III in Fig. 1B). Finally the N and NE boundaries of the field (region IV in Fig. 1B) marked by lower densities of volcanoes and dominated by shield volcanoes shows similar negative anomaly as the central region (region II).

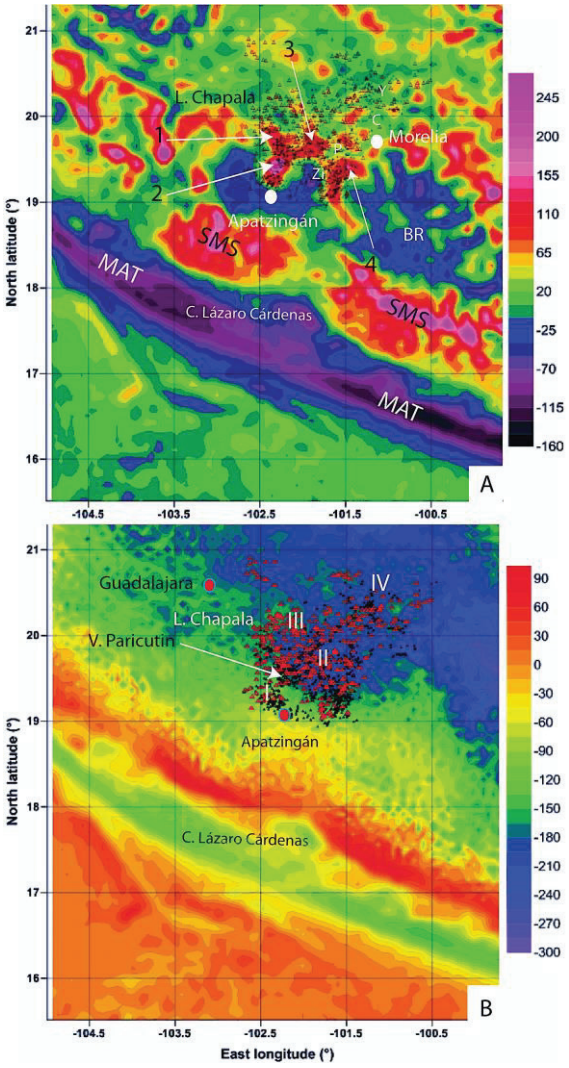

Fig. 1 – A) Free Air and B) Bouguer anomaly maps of the MGVF area. MAT = Meso-America Trench, BR = Balsas River ; Lakes: Zi = Zirahuén, P = Pátzcuaro, C = Cuitzeo, Y = Yuriria. Open red triangles represents medium sized volcanoes (shields mainly) and black triangles small sized volcanoes (scoria cones mainly) in the MGVF. Numbers correspond to text description.

Preliminary interpretations

Large-scale variations in free air and Bouguer gravity anomalies observed across the coastline in the study area are typical for subduction zones around the world, the negative anomaly at trench relating to the accumulation of low density sediments in an accretionary prism at the trench, while the positive anomaly at forearc is related to the flexure of the sinking lithosphere.

The volcanic field is associated with a strong negative Bouguer anomaly that changes sharply across the eastern and western borders of the field, suggesting sharp lateral changes in the geometry of the subducting slab as suggested by studies of regional seismic waveforms for the eastern border (*e.g.* Dougherty *et al.* 2012).

Within the volcanic field, while Bouguer anomalies are roughly uniform, free air anomalies show large variations. As described before, large positive values correspond to regions with elevated topography that also coincide with areas with more intensive volcanic activity (largest volcanoes in the field or higher density of scoria cones). This suggest some localization in the volcanic and magmatic activity that may be related to the geometry of mantle melt sources.

Acknowledgements

This study was supported by CONACYT project no. 152294 granted to M.N.G.

References

De La Fuente, M., Mena, M., Aiken, C.L.V., 1991. Cartas gravimétricas de la República Mexicana: UNAM. IGF, scale, 1(3,000,000).

Dougherty, S. L., Clayton, R. W., Helmberger, D. V., 2012. Seismic structure in central Mexico: Impliations for fragmentation of the subducted Cocos plate. J Geophys Res: Solid Earth (1978-2012), 117(B9).

Guilbaud, M. N., Siebe, C., Layer, P., Salinas, S., 2012. Reconstruction of the volcanic history of the Tacámbaro-Puruarán area (Michoacán, México) reveals high frequency of Holocene monogenetic eruptions. Bull Volc: 74 (5), 1187-1211.

Hasenaka T., I. S. E. Carmichael., 1985. The cinder cones of Michoacan-Guanajuato, central Mexico: Their age, volume and distribution and magma discharge rate. J Volcanol Geotherm Res: 25(1), 105-124.

Pavlis, N. K., Holmes, S. A., Kenyon, S. C., Factor, J. K., 2012. The development and evaluation of the Earth Gravitational Model 2008 (EGM 2008). J Geophys Res: Solid Earth, 117(B4).

Sandwell, D. T., W.H. F. Smith., 2009. Global marine gravity from retracked Geosat and ERS-1 altimetry: Ridge Segmentation versus spreading rate. J Geophys Res: Solid Earth, 114(B1).

Tectono-volcanic relationships between the Limagne fault and the Chaîne des Puys

Benjamin van Wyk de Vries[1], Audray Delcamp[2], Mathiue Kervyn[2], Tatum Miko Herrero[3], Mahar Lagmay[3]

[1] *Laboratoire Magmas et Volcans, University Blaise Pascal, Clermont-Ferrand, France. b.vanwyk@opgc.fr*
[2] *Department of Geography, Vrije Univieristiteit Brussel, Belgium. delcampa@tcd.ie*
[3] *National Institute of Geological Sciences, University of the Philippines, Dilliman Campus, Quezon City, the Philippines.*

Keywords: *Limagne Rift, Chaîne des Puys, Tectono-volcanic.*

This abstract presents a discussion about the relationships between faulting and monogenetic volcanism using the example of the closely associated Chaîne des Puys and Limagne Fault (Fig 1). The 80 strong monogenetic alignment is sited on the western shoulder of the Limagne Rift, in the Auvergne Region of Central France. It is currently a UNESCO World Heritage candidate site.

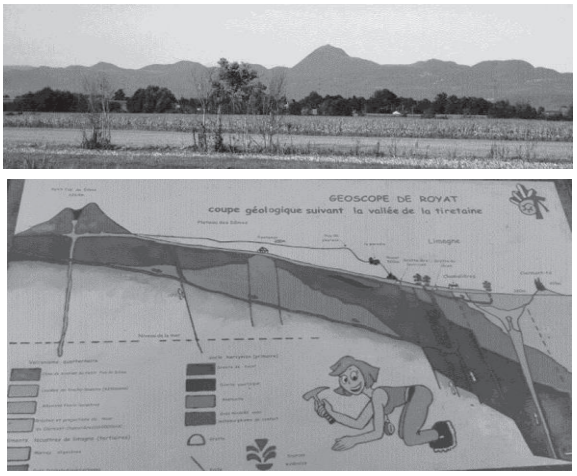

Fig. 1 – Above, a view of the Limagne Fault and the Chaîne des Puys with the Puy de Dôme in the centre. Below, a cross-section of the fault and Chaîne des Puys taken from the Geoscope round walk on the Limagne Fault. On the far right is the black Catherdral of Clermont-Ferrand, and the Clermont maar, then going left, the fault and escarpment, the plateau of Hercynian orogenic rocks and then the Chaîne des Puys.

The close proximity of the Limagne Fault to the Chaîne des Puys has been noted for a long time. In fact, if the Limagne fault had not raised the Chaîne relative to the Limagne Rift, to create a spectacular skyline of volcanoes, there would probably not have been so much interest in them.

The relationship is also a hot recent topic of debate (e.g. Maccaferri *et al.* 2014), and this presentation gives some of the morpho-structural background to this.

Early geologists such as Elie de Beaumont, Davy, Lyell, Murchison, and Von Humbolt, were as much concerned with explaining the escarpment by catastrophism or uniformitarianism, as they were with battling over neptunism and plutonism, or craters of elevation.

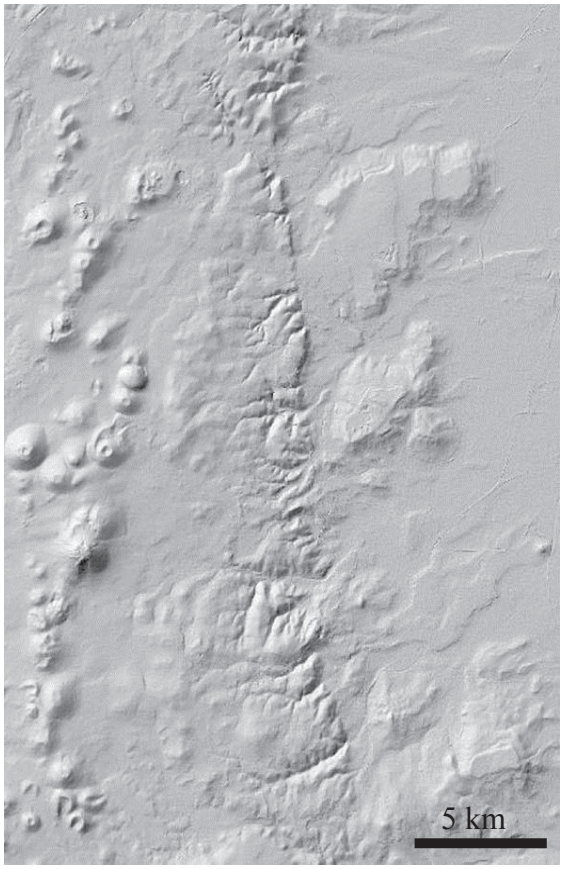

Fig. 2 – Shaded Relief image of the Chaîne des Puys and the Limagne Fault. From this it can be seen that the monogenetic alignment generally follows the fault, but groups of volcanoes cluster on trends that strike more NNE to NE in the the north of the area. This trend is also found in the faults, and Hercynian dykes, indicating a strong local structural control on the location of vents, as well as the more general parallelism.

The questions still stands as to what relationship the monogenetic volcanoes have to the fault, and perhaps: are the volcanoes monogenetic because of the fault? - seeing as just to the south of the rift,

stand the Mont Dore-Sancy and Cantal stratovolcanoes off the main rifted area.

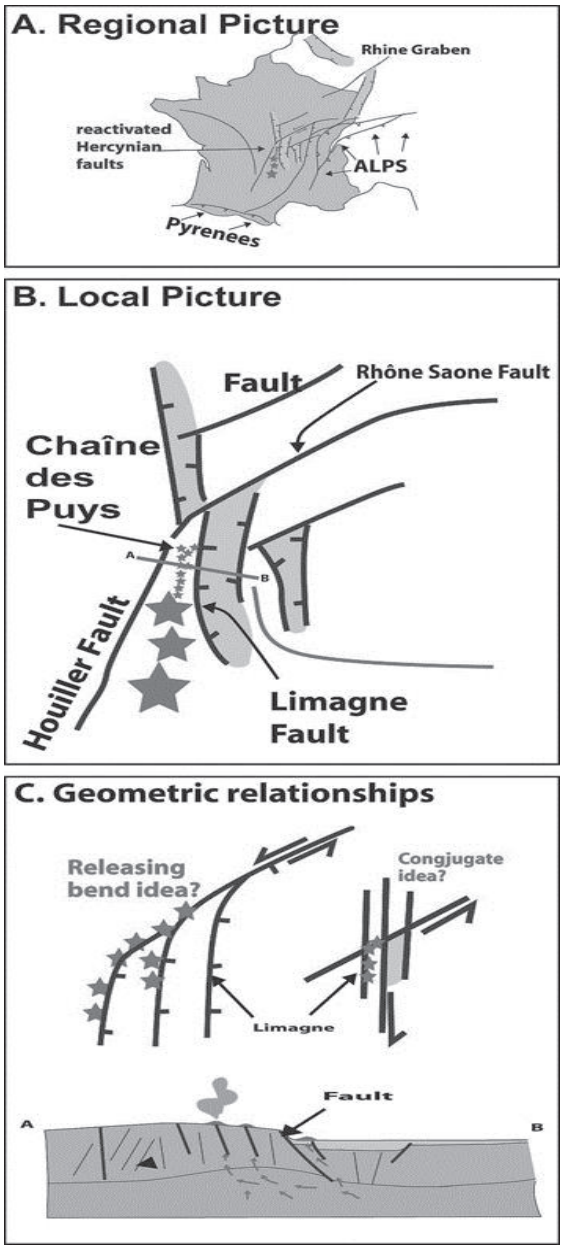

Fig. 3 – Structural and Volcanic relationships between the Limagne Fault and the Chaîne des Puys. **A.** Regional situation with the Limagne Rift as part of the Western European Rift: the Limagne is linked to the Rhine Graben by a NE-SW-trending transfer system. **B.** Local situation with the main stratovolcanoes (big stars) and the fault parallel Chaîne des Puys. **C.** Geometric relationships and possible links. Either the Chaîne des Puys is forming a releasing bend type structure, or it is related to a conjugate set of Hercynian -inherited faults. The Cross-section shows the possible migration of magma from the rift to the rift shoulder (van Wyk de Vries *et al.* 2012), a situation suggested by the modelling of Maccaferi *et al.* (2014).

Considering the spatial-temporal relationship, it becomes clear that there are volcanoes on the fault, in the rift, and behind the footwall, but with different ages and configurations.

Early volcanoes are cut by the faulting, showing a potential linkage, later volcanoes, as a whole, follow generally the main structural NS trend of the rift, but in detail group around a more NE-SW trend, that can be related to Hercynian structures, and to a major transfer fault linking the Limagne Rift to the Rhine Graben (Fig. 3). These trends host some of the youngest volcanoes, and the fault appears to have been more recently active in this area, and the area of some damaging historic earthquakes.

Considering the proximity of the fault as an influence in the monogenetic nature of the volcanism, more needs to be known about the state of faulting in the Tertiary, Quaternary and Holocene in the Massif Central. However, the area of the Chaîne de Puys is highly heterogeneous, with complex associations of Hercynian and Tertiary structures, and thus the crustal structure may be compatible with multiple pathways, and thus a monogenetic tendency.

In conclusion, there is a probably spatial and temporal structural link between the the Chaîne des Puys and the Limagne Rift, partly inherited for both from the Hercynian crust and lithosphere.

Acknowledgements

We thank the Chaîne des Puys and Limagne Fault UNESCO World Heritage project for their support and encouragement for this research.

References

Maccaferri F, Rivalta E, Keir D, Acocella V., 2014. Off-rift volcanism in rift zones determined by crustal unloading. Nature Geoscience 7, 297–300 doi:10.1038/ngeo2110

van Wyk de Vries B Tiu G, Mossoux S, Kervyn M Lagmay, 2012. Structural control of the Limagne Rift Fault on the Chaîne des Puys (Invited) V53C-2855 AGU FALL meeting December 2013

Updated perspectives regarding the West-Eifel volcanism

Jennifer Günther [1,2], Dejan Prelevic[1] and Martin Koziol[2]

[1] *Institute of Geosciences, Johannes Gutenberg University Mainz, Becherweg 21, D-55099 Mainz, Germany.*
[2] *Maarmuseum Manderscheid, Wittlicher Strasse 11, D-54531 Manderscheid. Germany.* maarmuseum@t-online.de

Keywords: West-Eifel volcanic field, geomorphologic detailed relief, geochemical analyses.

The volcanoes of the Eifel have been intensively researched and interpreted for over 200 years. Scientific research started at the 18th century. Johann Steininger published the first, thorough description of the West Eifel in 1819. It was he who introduced the specialist term ”*maar*” for the funnel-shaped volcano current today. In 1853, he published the ”Geognostic map of the Eifel” containing all important, geological entities, as well as the 3 volcanic fields ”West, High and East Eifel”. One indispensable map of the West Eifel is by Eilhard Mitscherlich & Justus Roth from 1865. The famous naturalist Alexander von Humboldt, under whom Steininger studied, traveled around the West Eifel in 1845. In his work ”*Kosmos*” in 1858 he published his findings on the volcanoes of the West Eifel, confirming Mitscherlich’s opinion that maars are formed by phreatomagmatic processes. With his ”Geognostic guide to the volcanic series of the “Vorder-Eifel” in 1861, Heinrich von Dechen wrote a standard work on the area that is still important today. You will find further informations in the publication by Lutz & Lorenz, 2009.

The start into more recent volcano research and the general geology of the Eifel succeeds best by means of the comprehensive ”Geology of the Eifel, 2013" by Wilhelm Meyer and the Geological Guide to “Trier and surroundings, 2012" by Wolfgang Wagner, Friedrike Kremb-Wagner, Martin Koziol & Jörg F. W. Negendank. The colleagues and their study groups named there have been studying the volcanoes of the (West-) Eifel in the past decades. In 1994, Georg Büchel published the important ”Vulcanological map of the West Eifel". So in the past few years, many doctoral, diploma, MSc and BSc theses have been produced about the volcanoes in the West Eifel.

We have begun in the SE (Manderscheid – Daun – Gillenfeld – Bad Bertrich) of the West Eifel (600 km^2 with 270 volcanoes) to archive and work through many of these works with a focus on the geochemistry and petrography of the respective vulcanites. Based on the indications obtained, the locations were checked on site, mapped and samples were taken. These are needed, on the one hand, for new analyses and thin sections, on the other hand, a research collection of volcanic rocks is being compiled at Maarmuseum Manderscheid.

Four volcanic regions have been brought together: 1. Bad Bertrich 2. Wartgesberg – Pulvermaar –Holzmaar Group, 3. Volcanoes around Daun, 4. Meerfeld-Mosenberg volcano group.

In the following the 1.600 m long SE-NW extending “Bad Bertrich” volcanic system (Meyer, 2013) is presented as an example. It lies in the lower "Üßbach-valley” by "Bad Bertrich" with the "Kennfus" plateau located above it. In the SE, it begins with the reddish-brown tuffs of the “Facher Höhe” scoria cone. Following further NW, the “Dachskopf” scoria cone with its dark welding cinders, lapilli tuffs and basalt blocks is situated. The lava flow ”Dachslöcher” poured out from this over the valley of the ”Müllischwiese” into the "Üßbach-valley”. There, in the "Üßbach-valley”, a great basalt lava flow outcrops that can be detected down into the ”Römerkessel” at "Bad Bertrich". Between ”Dachskopf” and ”Falkenley” lies the 600 m large and 100 m deep, elliptically formed ”Hardt-Maar”. Located above, the badly eroded strato volcano “Falkenley” is situated from which a united lava flow (“Hüstchen” & “Falkenley”) descended to the “Müllischwiese”. The small scoria cones ”Hüstchen” and ”Tümmelbusch” are located on the plateau of “Kennfus”. In the NW, the ”Kennfus-Maar” concludes the chain of volcanoes (Lorenz & Büchel 1980). During field work, we detected a black colored layer of maar tephra of 20 cm thickness underlying the reddish-brown scoria of “Hüstchen”. We interpret this previously unknown tephra layer (Fig. 1) as the product of the initial maar phase of the quaternary (new) ”Hüstchen-Maar”.

Fig. 1 – Maartephra “Hüstchen-Maar”.

In the Eifel, 2/3 of the scoria cones started in this way, then the supply of water was interrupted and a scoria cone was suddenly formed above the initial maar funnel. The chain of volcanoes consists of six scoria cones, three maars, one large lava flow and

some smaller ones. All the volcanic structures can be reached and detected. Today, everything is completely covered in vegetation. Active lava pits do not exist anymore.

In order to check the terrain data, with the help of digital satellite data from the Rhineland-Palatinate State Office for Surveying Geobase Information, we had the 3D structures of the Bad Bertrich volcanoes calculated at the Institute of Physical Geography & Environmental Change of the University of Basel and converted into a geomorphologic detailed relief (Fig. 2). The outcrops seen in the terrain can thus be confirmed. In addition, through the detailed depth of definition in space, further new, previously invisible structures also appear.

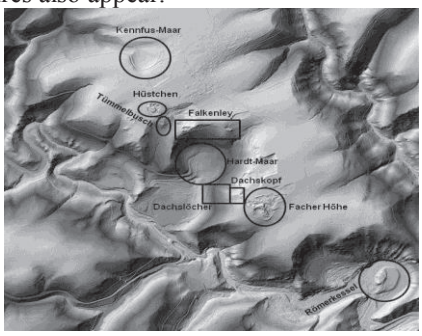

Fig. 2 – Detail relief of Bad Bertrich volcanic system.

Existing data from the comprehensive work by H. Mertes on the West Eifel field (1983) were supplemented by our geochemical analyses. The analyses of the "Bad Bertrich" vulcanites prepared by means of X-ray fluorescence produced high Mg contents of between 11.7–13.5 weight %, SiO_2 contents of between 41.6 – 43.9 weight % and an alkalinity of between 4.2–4.8 weight % . With the help of the TAS-diagram (Le Bas *et al.* 1986, Fig. 3), the rocks can be classified into the field of basanites. A classification adapted to the West Eifel gives an assignment to the "ONB suite" (ON = olivine-nephelinite & B = basanite, Mertes 1983). High Mg figures between 0.67- 0.73 and high Cr & Ni contents (540-733 ppm & 240-316 ppm) point to low degrees of differentiation and the primitive character of the vulcanites. The variations in trace

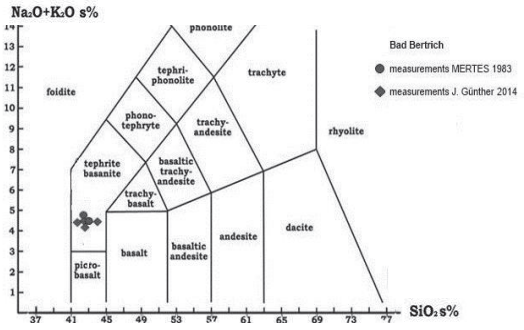

Fig. 3 – TAS diagram after Le Bas et al. (1986): plotted data from the eruption centers of Bad Bertrich volcanic system.

elements indicate a slightly varying degree of differentiation of the rocks. The scoria cones of "Hüstchen" and "Tümmelbusch" show the highest degree of differentiation of "Bad Bertrich" vulcanites and are thus the latest products of this volcanic system. The petrography confirms the chemical finding. The mineral content again speaks for an assignment of the vulcanites to the field of basanites (QAPF-diagram after Streckeisen 1979). Their matrix contains clinopyroxenes, leucite, nepheline and plagioclase. Olivine and augite are to be observed as phenocrystals that are partially zoned. The latest findings confirm that these alkaline rocks, greatly undersaturated in SiO_2, typical for the most recent phase of West Eifel volcanism, are minimally differentiated and very close in their chemical composition to the primary magma coming from the upper mantle of the Earth (Schmincke 2007).

Acknowledgements

In the coming years we want to continue the project in the West Eifel and extend it over the High Eifel into the East Eifel. Achim Brauer (German GFZ Potsdam), Bernd Zolitschka & Andreas Klügel (Univ. of Bremen), Konrad Hammerschmidt (Free Univ. of Berlin), Wilhelm Meyer (Univ. of Bonn), Nikolaus Kuhn & Samuel Kuonen (Univ. of Basel), Klemens Seelos (Univ. of Mainz), Andreas Schüller (Vulkaneifel Nature- and Geopark) and Mayor Wolfgang Schmitz (District of Manderscheid) have provided support. We thank Andrea Brockes for helping by the English translation.

Web page: www.maarmuseum.de / www.geopark-vulkaneifel.de / www.vulkanerlebnis-mosenberg.de

References

Le Bas, M.J. *et al.* (1986). A chemical classification of volcanic rocks Based on the Total Alkali-Silica Diagram. Journal of Petrology, 27(3): 745-750.

Lorenz, V. & Büchel, (1980a). Zur Vulkanologie der Maare und Schlackenkegel der Westeifel. Mitt. Pollichia, 68, pp. 29-100.

Lutz, H. & Lorenz, V. (2009). Die Vulkaneifel und die Anfänge der modernen Vulkanologie - eine geo-historische Quellensammlung. Mainzer naturwiss. Archiv, 47, pp. 193-261, 20 figures.

Mertes, H. (1983). Aufbau und Genese des Westeifler Vulkanfeldes. Inst. für Geologie d. Ruhr-Univ., Bochum, 415 pp.

Meyer, W. (2013). Geologie der Eifel. 4. Edition, XIV, 704 pp., 157 figures, 12 tables, 8 panels.

Schmincke, H.U. (2007). The Quaternary Volcanic Fields of the East and West Eifel (Germany). In: J.R.R. Ritter und U.R. Christensen (Ed.), Mantle plumes a multidisciplinary approach Springer, Berlin, pp. 501.

Wagner, W.H., Kremb-Wagner, F., Koziol, M. & Negendank, J.F.W. (2012). Trier und Umgebung. 3. Edition, X, 396 pp., 170 figures, 13 tables, Collection of Geol. Leaders, Vol. 60.

Effects of tectonic activity in the maar type volcano of Teremendo (Michoacán, México)

Diana C. Soria Caballero[1], Victor Hugo Garduño Monroy[2]

[1] *Posgrado en Ciencias de la Tierra, sede Geología, Universidad Nacional Autónoma de México Ciudad Universitaria México, DF, dianscc@hotmail.com*
[2] *Instituto de Investigaciones en Ciencias de la Tierra, UMSNH, Morelia, Michoacán, México*

Keywords: TMVB, faults, maar Teremendo, MAFS.

The Teremendo volcano is a monogenetic cone located at 0242840.52, 2192043.65 UTM, 30 km to NW of Morelia, Michoacán (fig. 1). This volcano belongs to a series of monogenetic cones and domes with Quaternary age, developed in the Michoacán – Guanajuato volcanic field (MGVF). The MGVF was formed during the last period of volcanic activity in the Trans-Mexican Volcanic Belt (TMVB) (Hasenaka and Carmichael, 1985; Ferrari, 2000; Garduño-Monroy *et al.*, 2009).

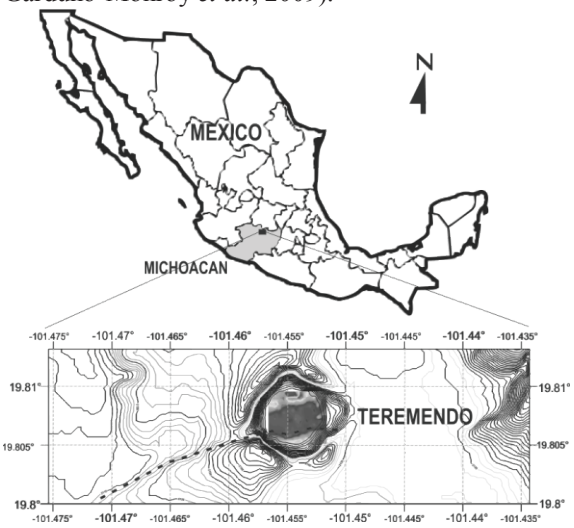

Fig. 1 – Localization of Teremendo volcano, in the state of Michoacán, México (Contours with difference of 5m, the dotted line indicate the fault line and the magnetic anomaly obtained in the lake).

Three eruptive periods has been proposed for the construction of Teremendo volcano (fig. 2). First, a period of effusive activity caused the emplacement of ca. 100m thick lava flows, with andesitic – balsaltic composition. This sequence is followed by a 30 cm deposit of soil (andosol). The second eruptive phase correspond to explosive activity (strombolian type), which formed small deposits of debris flows (ca. 60cm thick) and 1m thick layers of scoria falls, slightly inclinated. Above this, another inactivity period allows the formation of a 25 cm soil (andosol). The third eruptive period is a phase of phreatomagmatic activity (phreatoplinian type), which one deposited a 40 cm thick debris flow and culminate with a 3m sequence of basal pyroclastic surges with pseudostratification. The deposit has a unimodal granulometry, with sizes from coarse ash to fine lapilli. A high content of accretionary lapilli suggest a Surtseyan eruption. Mineralogically, the surges contain abundance of pumice, plagioclases and amphibole. Several accidental lithics with structures of ballistic impacts associated are observable through the sequence. The pyroclastic surges are radially deposited to 2km from the eruptive center, with an inclination of 26°NE. Additionally, this deposit is affected by normal faults with NW-SE and ENE-WSW directions. The top of the sequence is cover for a recent soil (andosol) with thickness from 20cm to 1.2m.

During the periods of explosive activity, the phreatic level was reached, forming the lake inside the crater of Teremendo volcano, which one remains to our days. The volcano has an area of 1.1 km^2 in the base, 0.6 km^2 in the crater and 0.16 km^2 in the lake. It is aligned in NNW-SSE direction with four smaller but contemporary monogenetic cones. The lake shows a linear shape, has a volume of $1x10^6$ m^3 and an average depth of 6 m (max. of 11 m) (Chacón-Torres pers. comm.). The water column is divided in two zones: the superficial, oxygenated and warm waters (0 to 3m depth), and the deep, anoxic and cold waters (3m to bottom).

The volcanic deposits and lacustrine sequences are afectted by an ENE–WSW fault segment belong to the Morelia-Acambay fault system (Rodríguez-Pascua *et al.*, 2000; Szynkaruk *et al.*, 2004; Garduño-Monroy *et al.*, 2009). Is a 2.1km long normal fault, with the hanging block falling in NNW direction, and a slip rate of 0.5mm/year (Suter *et al.*, 2001). It is a part of a regional structure of 26km long, with en echelon geometry and N84°-87° direction.

The activity of this fault has been related to changes in the geomorphology of the area, generating a *seismic landscape* (Michetti *et al.*, 2005; McCalpin, 2009). Landscape analysis and fieldwork, suggests that the fault caused the collapse of the top of a semi-shield volcano nearby (named

"Picacho"), displacing an area of 1 km^2 in SW direction (fig. 2). At the west, the fault shows a 2m height scarp that displaces recent soil (fig. 2). Under the lake, the fault trace is defined through a series of bathymetric, seismo-acoustic and magnetometric profiles. This shows a small displacement of the lacustrine floor and the coincidence of the fault and the volcanic vent (fig.1). We suggest that the emplacement of the volcano was favored by a zone of crustal weakness, previously generated by the fault. At the east wall of the crater, the fault cut and displaces the upper volcaniclastic sequence (fig. 2). In the outcrop a large amount of faults and fractures are recorded, following two main directions: N80-100° and N130-170°. However, a group of small faults is differentiated and associated to rearrangement of the materials, which have a brittle behaviour to the strains.

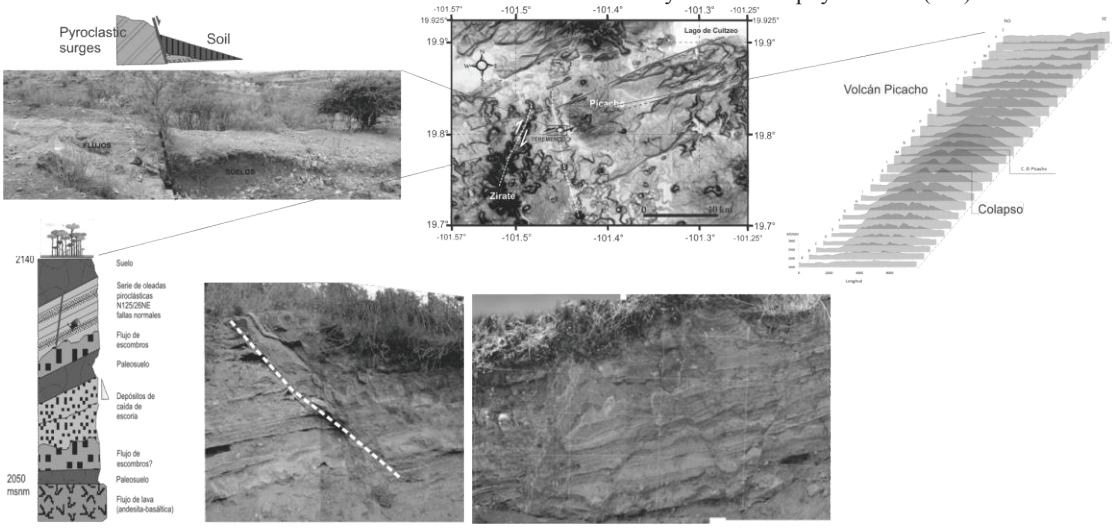

Fig. 2 – Localization of the fault structures in the Teremendo volcano and the collapse in the Picacho volcano. Details of the scarp at the W edge, volcanic stratigraphy and details of faulting and fracturing in the pyroclastic surges sequence.

According to the results the fault segment that affects the Teremendo maar, has been active since late Pleistocene to recent times. Estimations of *potentiality* considers that the regional structure can produce seismic events with magnitudes of Mw≥6 (M=5.08+1.6*log(LSR), Wells and Coppersmith (1994)). However, further work is required to improve the estimations of seismic hazard in this area (Smith *et al.*, 1996).

Acknowledgements

This is a project supported by CONACyT about the study of the activity of MAFS. Thanks to Neftalí Razo Pérez for the comments to this text.

References

Ferrari, L. 2000. Avances en el conocimiento de la Faja Volcánica Transmexicana durante la última década. Boletín de la Sociedad Geológica Mexicana. Vl. LIII: 84-92.

Garduño-Monroy, V.H., Chávez-Hernández, J., Aguirre-González, J., Vázquez-Rosas, R., Mijares-Arellano, H., Israde-Alcántara, I., Hernández-Madrigal, V.M., Rodríguez-Pascua, M.A., Pérez-López, R. 2009. Zonificación de los periodos naturales de oscilación superficial en la ciudad de Pátzcuaro, Mich., México, con base en microtremores y estudios de paleosismología. Revista mexicana de ciencias geológicas. 26 (3): 623 – 637.

Hasenaka, T., Carmichael, I.S.E. 1985. The cinder cones of Michoacan – Guanajuato, central Mexico: their age, volume and distribution, and magma discharge rate. Journal of Volcanology and Geothermal Research. 25 (1 - 2): 105 – 124.

McCalpin, JP. 2009. Paleoseismology. International Geophysics. V.95. 2da. Edición. Elsevier. 613 pp.

Michetti, A.M., Audemard, F.A., Marco, S. 2005. Future trends in paleoseismology: Integrated study of the seismic landscape as a vital tool in seismic hazard analyses. Tectonophysics. 408 (1-4). 3 – 21.

Rodríguez Pascua, M.A., Calvo, J.P., De Vicente, G., Gómez, G.D. 2000. Soft-sediment deformation interpreted as seismites in lacustrine sediments of the Prebetic Zone, SE Spain, and their potencial use as indicators of earthquake magnitudes during the Late Miocene. Sedimentary Geology 135: 117-135.

Smith, R.P., Jackson, S.M., Hackett, W.R. 1996. Paleoseismology and seismic hazards evaluations in extensional volcanic terrains. J. Geophyical Research. 101: 6277– 6292.

Suter, M., López-Martínez, M., Quintero-Legorreta, O., Carrillo-Martínez, M. 2001. Quaternary intra-arc extension in the central Trans-Mexican volcanic belt. Boletín GSA. 113 (6): 693-703.

Szynkaruk, E., Garduño-Monroy, V.H., Bocco, G. 2004. Active fault systems and tectono-topographic configuration of the central Trans-Mexican Volcanic Belt. Geomorphology. 61. 111 – 126.

Wells, D., Coppersmith, K. 1994. New empirical relationships among magnitude, rupture length, rupture width, rupture area and surface displacement. Boletín de la Sociedad Sismológica de América. 84(4): 974-1002.

Cross-section features of columnar joints in basalt in the Huasca de Ocampo, Hidalgo of Mexico

Shunshan Xu, Angel F. Nieto-Samaniego, **Paola A. Botero-Santa**, Susana A. Alaniz-Álvarez

Centro de Geociencias, Universidad Nacional Autónoma de México (UNAM),
Blvd. Juriquilla No. 3001. Querétaro, 76230, México, sxu@geociencias.unam.mx

Key words: columnar joint, transverse fracture, basalt.

Columnar jointing is a geologic feature that occurs in cooling lava that forms parallel, prismatic columns. The columns are generally found in igneous rock bodies of basaltic sills and dikes. The cross-section of the columns is generally pentagonal or hexagonal but there are rare cases of formations with three to twelve sides. The horizontal parting surface of basaltic columnar joints in the Huasca de Ocampo shows polygonal pattern with an average number of side equal to 5. The hexagonality index (maturation parameter) changing from 0.94 to 1.42 increases with the increasing distance to the flow base in the low colonnade, which indicates a progressive maturation of columnar joints with time as described by Budkewitsch and Robin (1994). According to the first order morphologies on polygons, three types of transverse fracture are observed, namely plane polygon, upward convex polygon and upward concave polygon (Figure 1). They represent three different stress distributions within columns that are similar to the stress model proposed by Spry (1962).

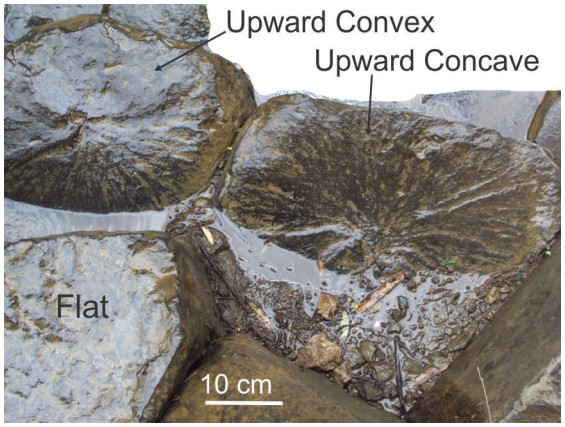

Fig. 1 – Three types of morphologies on polygons.

On some polygons, the concentric ring structures can be observed. In most cases, the form of rings alters depending on the distance between the ring and polygon edge. For small distance, the rings show polygonal shape and are nearly parallel to the column sides. For large distance, the rings demonstrate elliptical shape. For medium distance, the rings express rounded polygons (Fig. 2). The change of ring shape can be explained by crystallization-induced melt migration (Mattsson *et al.*, 2011; Bosshard *et al.*, 2012). In the three-dimension the ring structures is columnar form in the lower part, whereas in the upper part is cone shape (Fig. 2). The isotherms during cooling can be inferred as showing in the right lower part in Fig. 2 according to melt migration model.

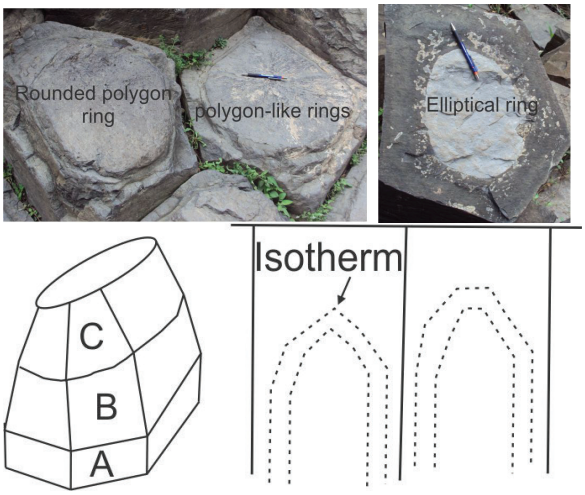

Fig. 2 – Upper: three types of ring structure. Lower: three-dimensional form of ring structures (left) and conjectured isotherms within columns during cooling.

On the other hand, the transverse fractures are perpendicular or somewhat oblique to the prism axis at angle 0°–25°. Most fractures are not beyond a column. However, some fractures cut across more than one column. On the transverse fractures, radiating striae and fine parallel laminations can be observed (Fig. 3). The mechanism of fine parallel laminations is not very clear. The radiating striae are the hackly fracture feature under tensional stress (*e.g.*, DeGraff and Aydin, 1987).

Figure 3. Radiating striae (left) and plume-like striae with a symmetric line (right). The arrow indicates propagation direction of the fracture.

The initial flaw points of radiating structures are usually encountered in the polygon centers, whereas a few of them are located on the edges of polygon (Fig. 3). The plume-like striae may express the typical tensional fractures (*e.g.*, DeGraff and Aydin, 1987). Therefore, the above features of transverse fractures are consistent with mechanism of tensional fracture. They formed after the columnar joints and were not resulted from the constitutional supercooling proposed by Gilman (2009), because the radiating striae exist not only within the ring structures but also in the rims on the polygons.

References

Bosshard, S.A., Mattsson, H.B., Hetényi, G., 2012. Origin of internal flow structures in columnar-jointed basalt from Hrepphólar, Iceland: I. Textural and geochemical characterization. Bull Volcanol 74, 1645-166.

Budkewitsch, P., Robin, P.Y., 1994. Modelling the evolution of columnar joints. J. Volcanol. Geotherm. Res. 59**,** 219–239.

DeGraff, J.M., Aydin, A., 1987. Surface morphology of columnar joints and its significance to mechanics and direction of joint growth. GSA Bulletin 99, 605-617.

Gilman, J., 2009. Basalt columns: Large scale constitutional supercooling? J. Volcanol. Geotherm. Res. 184**,** 347-350.

Mattsson, H.B. Caricchi, L., Almqvist, B.S.G., Caddick, M.J., Bosshard, S.A. Hetényi, G., Hirt, A.M., 2011. Melt migration in basalt columns driven by crystallization-induced pressure gradients. Nature Communications, DOI: 10.1038/ncomms.1298.

Spry, A., 1962. The origin of columnar jointing, particulary in basalt flows. Austral. J. Earth Sci. 8**,** 191–216.

Overview of Jagged Rock, a frozen plumbing system exposed in Hopi Buttes, Navajo Nation, USA

Giuseppe Re[1], James D.L. White[1] and Michael H. Ort[2]

[1] *Geology Department, University of Otago, Dunedin, New Zealand.* regi7084@student.otago.ac.nz
[2] *Geology Department, Northern Arizona University, Flagstaff, Arizona USA.*

Keywords: dike, intrusive complex, conduit initiation, stress regime.

The Hopi Buttes volcanic (HBVF) field consists of about 300 maar-diatreme and other monogenetic volcanic centers of Miocene age (~7 Ma), covering an area of around 2000 km^2. Intrusions and diatreme structures cross-cut flat-lying sedimentary rock of the nondeformed and tectonically stable Colorado Plateau. It is a superb site for studying maar-diatreme eruptive processes because a gradual increase in depth of erosion from NE to SW offers excellent exposure of different volcano structural levels, from tephra ring and thin distal eruptive proucts to root zones and feeder dikes.

Jagged Rock Complex (JRC) comprises mostly intrusive rocks extending over ~2 km^2 on the southern edge of HBVF. Current exposure is about 350 m below the pre-eruptive surface into the Petrified Forest Member of the Triassic Chinle Formation, made up of colourful fluvial deposits of mudstone interbedded with lenticular sandstone.

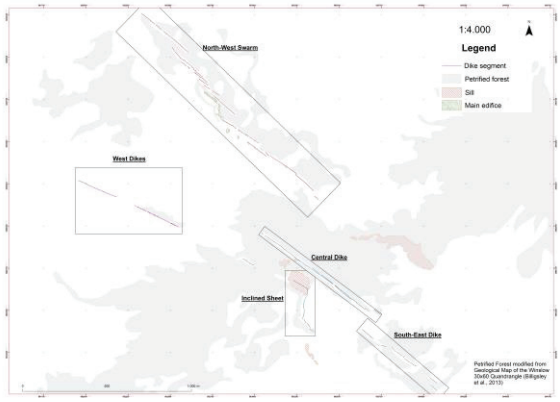

Fig. 1 – Map of the Jagged Rock Complex.

JRC reveals many volcanic features (Fig.1).

Two dike arrays are prominent in the western part of the complex, where the topography is about 10 to 30 meters lower than in the east. The north-west swarm consist of nine *en echelon* dike striking NW-SE for ~1.5 km, plus two larger massifs and three minor plugs near its midpoint. In the western zone, two collinear dikes, striking WNW-ESE for 700 m, are separated by a bridge 100 m long.

In the eastern part of the complex two dike arrays, the central and the south-eastern are surrounded by an inclined sheet. Both dikes strike NW-SE showing a weak *en echelon* arrangement. The former, 810 m long, is linked with a sill at one site, east of which it divides into two parallel dikes. The latter, 180 m long, consist of two collinear segment with a plug crops out between them. The inclined sheet is exposed near the central dike and the sheet's strike varies from N-S to WNW-ESE. Dip ranges between 40°-60° eastward. Its northern tip is linked with a sill that may link with the central dike, and its southern tip is very close to another sill segment. Lastly, a larger sill is located farther to the northeast. Both inclined sheets and sills are characterized by step-and-stair geometries.

Differences in geometry and texture across the complex allow us to assess geometrical relations among intrusive sheets, infer the stress regime at the time of emplacement, and investigate the transition between dikes and more- equant conduits.

Each dike has a slightly different texture, but all consist of coherent porphyritic igneous rock with phenocrysts of pyroxene+/-phlogopite (plentiful only in the NW swarm, 1-6 cm size) in a fine to medium grained groundmass (Fig. 2). Well-developed vesicles occur in dikes i) along external edges they are tiny and mostly round, ii) as symmetrical inner bands where they are dispersed commonly elongate with medium size (~1 cm), along with phenocryst concentrations, and iii) in a mid-dike zone of scattered fine to medium size, with no uniform shape.

Lithic fragments from 2-10 cm are present, and 20-30 cm cavities are common in the outer dike walls where lithic blocks have been eroded.

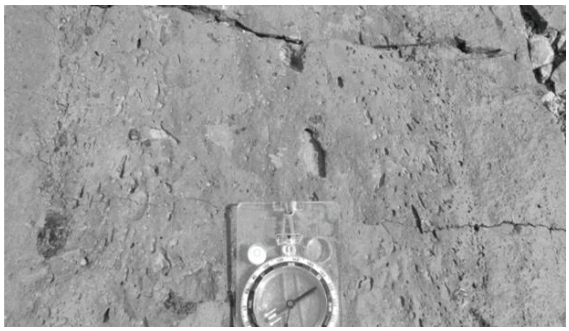

Fig. 2 – Texture of coherent rock in northern dike.

The contact with the country rock is commonly sharp, without evidence of deformed layers or baked margins in the host rock; chilled margins are common at dike margins. In places, evidence of explosive fragmentation take the form of medium-grained lapilli tuff composed of angular lithic and round-vesicled juvenile fragments. This fragmental rock is commonly associated with large amounts of country rock trapped as xenoliths within the dike.

Ingestion of sediments into coherent magma may have triggered explosive fragmentation. Evidence for this is visible in the western dike, where many 'buds' have domains of i) homogeneous coherent intensely welded juvenile rock, ii) scoriaceous lapilli tuff containing deformed sedimentary lithic blocks, and in places nondeformed lithic blocks (5-20 cm), and iii) lapilli tuff to tuff breccia with lithic and angular to rounded juvenile clasts (Fig.3). These textural features in buds may record the inception of fragmentation at the transition from dike to conduit.

Fig. 3 – Bud from eastern dike of western sector.

Each dike is segmented; segments most commonly overlap, have parallel segment tips, or bridge from one to another. The shapes of tips include both elongate horns and widened bulging.

The notable *en echelon* geometry of the NW swarm suggests emplacement into a shear stress regime. Delaney and Pollard (1981) and Pollard *et al.* (1982) showed that *en echelon* patterns can result from segmentation during propagation of a parent dike. This mechanism involves the rotation of the least stress axes (σ_3) in a tensile stress regime during dike propagation. The lateral growth, oblique to the propagation direction, of *en echelon* segments allows segment overlap until the mechanical interaction of adjacent segments limits this growth; the overlap of tips from neighboring segments works against further dilation.

JRC dike segments display diverse geometries. Along the lateral growth direction are many bends, often sharp and near segment terminations, giving chevron fold and zig-zag geometries. This folding in places also affects the vertical dike form as steps (bumps) and inflections (dimples) on exposed subvertical dike walls.

We infer that the stress field was highly variable, both in vertical and horizontal directions, during, and probably as a result of, dike propagation. Key roles may have been played by variations in the country rock's physical behaviour, which under certain stress conditions could have changed its rheology from ductile to brittle (Nygard *et al.*, 2006).

The eastern inclined sheet segments suggest a semi-circular saucer-shaped intrusion. Chevallier and Woodford (1999) claim that saucer-shaped intrusions are divided into: i) a sub-horizontal inner sill forming the base, ii) a steeply dipping inclined sheet cross-cutting the stratification, and iii) a sub-horizontal outer sill. At JRC parts of inclined sheet and outer sill are exposed, but no inner sill crops out, though it may be present below the current surface. In this interpretation, the central dike extends upward from the sill, and its emplacement could have been driven by deformation induced by sill growth. The step-and-stair surfaces may reflect the mud rock's response. During sill inflation sediments were compacted and strengthened. Once made resistant, they act as ramps, so they forced the sill to step upward during its lateral propagation.

Geometrical and textural features exposed at JRC offer excellent opportunities for analysis of dikes, inclined sheet propagation, and transitions from dikes to conduits with associated fragmentation. Such analysis is needed to better understand how magma is delivered to small volcanoes during and prior to eruption.

Acknowledgements

This work is supported by University of Otago Scholarship (GR) and MBIE through subcontract to GNS Science, NZ (JDLW).

References

Billingsley, G.H., Block, D., Redsteer, M.H., 2013. Geologic Map of the Winslow 30' × 60' Quadrangle, Coconino and Navajo Counties, Northern Arizona. USGS Scientific Investigations, Map 3247.

Chevallier, L.,Woodford, A., 1999. Morpho-tectonics and mechanism of emplacement of the dolerite rings and sills of the western Karoo, South Africa. South African Journal of Geology 102:43-54.

Delaney, P.T., Pollard, D.D., 1981. Deformation of host rocks and flow of magma during growth of minette dikes and breccia-bearing intrusions near Ship Rock, New Mexico. USGS Professional Paper 1202:1-61.

Nygård, R., Gutierrez, M, Bratli, R.K., Høeg, K., 2006. Brittle-ductile transition, shear failure and leakage in shales and mudrocks. Marine and Petroleum Geology 23:201-212.

Pollard, D. D., Segall, P., Delaney, P. T., 1982. Formation and interpretation of dilatant echelon cracks. Geological Society of America Bullettin 93:1291-1303.

Complex eruption of Late Pleistocene Las Cabras scoria cone (Michoacán, México): From magma mingling to cone breaching

Athziri Hernández Jiménez[1], Marie-Noëlle Guilbaud[1], Claus Siebe[1]

[1] *Departamento de Vulcanología, Instituto de Geofísica, Universidad Nacional Autónoma de México, Coyoacán, C.P. 04510, México D.F, México.* athzirih@ciencias.unam.mx

Keywords: Scoria cone, monogenetic volcanism, cone collapse, magma mingling.

The Las Cabras scoria cone is one of the ca. 1,100 monogenetic volcanoes existing in the Michoacán-Guanajuato volcanic field (MGVF) located in the central part of the subduction-related Trans-Mexican Volcanic Belt (Hasenaka and Carmichael, 1985). Although this volcano is morphologically similar to many other young scoria cones in this area, its products display peculiar sedimentary and textural features that motivated this study. Preliminary results of field work and bulk rock compositional analysis are presented here.

The eruption of the volcano included two main phases of activity: An explosive phase that built a ~300 m high scoria cone and deposited thick ash fallout exposed to the north of the cone, and an effusive phase that formed a >7 km long lava flow field that emerged from a mayor breach in the cone (Figs. 1 and 2). The area covered by the flows and their volume were estimated at 18.2 km^2 and 0.6 km^3 respectively, while the volume of the cone is only 0.06 km^3. Radiocarbon dating of paleosols (4 samples) directly below the fallout deposits yielded ages ranging between 27,400 and 21,800 y. B.P.

The lava surface displays peculiar elongated mounds or hummocks (Figs. 1 and 2) whose interior is exposed in quarries that reveal coarsely stratified, partly welded fallout products, rich in scoriaceous spatter-bombs (~1-2.5 m in size). These features are typical for proximal scoria cone deposits, hence the hummocks must have originally been part of the cone. The elongation of the two largest hummocks in the direction of the flow (Fig. 2) suggests that after detachment from the cone, these were carried on top of the lava flow. The hummocks probably formed as a result of the breaching of the cone at its eastern flank by the lava flow that then rafted the detached cone walls down-flow.

Extensive quarrying of the scoria-fallout deposits allowed to undertake a detailed analysis of the explosive phase(s) of the eruption. The exposed proximal fallout deposits of Las Cabras can be divided into three main units: A basal part dominated by thin fine-grained (ash and fine lapilli) layers and sporadic bombs, a middle part consisting of increasingly thicker (6-50 cm) and coarser grained (4-16 mm in size) layers, and an upper part characterized by thick (10-100 cm) layers, coarse clasts (16-64 mm), and large bombs (Fig. 3). Layers forming the basal part consist of a mixture of highly-vesicular and dense juvenile clasts, while accidental lithics first appear in the middle and get more abundant toward the upper part, where juveniles are mostly of the highly-vesicular type.

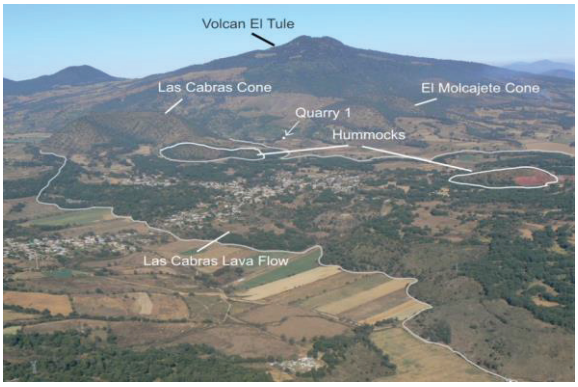

Fig. 1 – Aerial photograph of Las Cabras scoria cone and proximal deposits (hummocks, thick andesite lava flows). Note red color of scoria agglutinates exposed in quarry of hummock to the right. Photo taken by C.S. from the southeast.

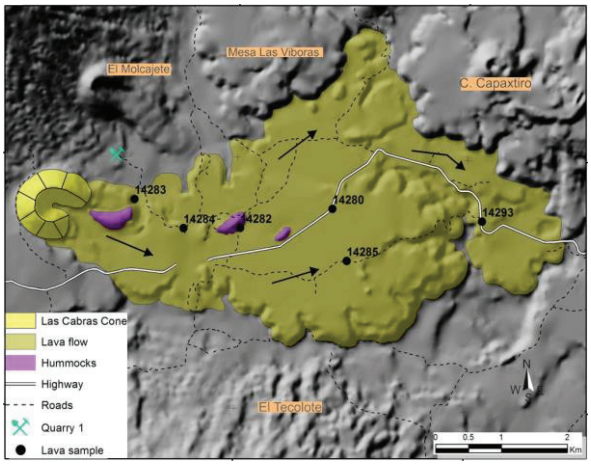

Fig. 2 – Map of Las Cabras breached scoria cone and associated lavas. Sampling locations and quarry displaying fallout sequence shown in Fig. 3 are also indicated.

Various sedimentary structures can be observed in the fine-grained basal part of the stratigraphic section. Among the most notorious is the presence of asymmetric erosion channels that are concentrated in

two stratigraphic levels of the section (Fig. 3). These are 10 to 18 cm deep, 30 to 40 cm wide, and display a near constant horizontal separation interval of 80 to 100 cm. Interestingly, the channels affect mostly the finest, most indurated layers of the sequence. These features differ from impact-sag structures that can be observed in the same part of the section and that were produced by large bombs that caused ductile and brittle deformation of the layers underneath.

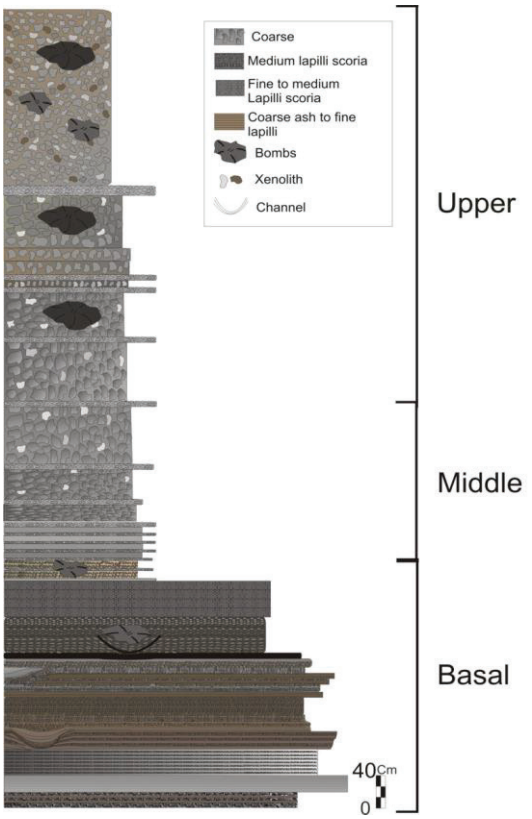

Fig. 3 – Stratigraphic section studied at quarry 1 (location on Fig. 1). Distinct parts described in the text are indicated.

Fresh lava samples collected at different distances from the vent, and scoria and bomb samples from different levels of the fallout sequence, were analyzed for bulk-rock chemical composition. The samples range from basaltic andesite to andesite, with scoria clasts spreading a slightly wider range towards more silicic compositions (56.4–63.0 SiO_2 wt.%) than lavas (56.9–60.4 SiO_2 wt.%). The mineralogy is similar for lava and scoria samples: Both contain Ol and Plag phenocrysts (<1-3 mm) in a matrix rich in plagioclase microlites. Ol is the dominant phenocryst phase (25 vol.% in lava, 30 vol.% in scoria) with Plag accounting for 15 vol.% in lava and 20 vol.% in scoria. Some bomb samples collected from the upper part of the section present marked flow banding (Fig. 4) indicating the mingling of two types of magma prior to explosive eruption. Interestingly, these peculiar bombs contain, in addition to Ol and Plag, phenocrysts of biotite (<4.1 mm).

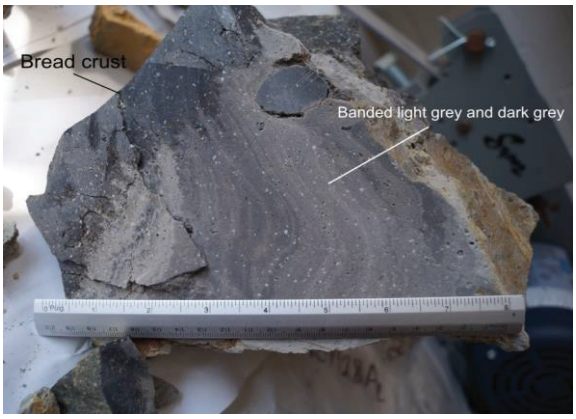

Fig. 4 – Fragment of bread-crust bomb with outer dark glassy rind and distinct interior displaying parallel flow-banding. Layers of micro-vesicular light-grey material alternate with denser dark-grey layers. Larger xenolithic enclaves (< 2 cm) surrounded by bands are common. All layers contain micro-phenocrysts of Plag (~2 mm), Ol (~1.5 mm), and biotite (~1 mm). The crust is richer in Plag than the core, but the core is richer in biotite.

These preliminary results show that the eruption of Las Cabras was unusual in many ways. The ductile deformation style (impact sags) and syn-depositional erosion channels preserved in the fallout deposits point toward torrential rain during the eruption, a fact that should be considered when reconstructing the paleo-climate of this region. On the other hand, the occurrence of bombs displaying flow-banding with layers of two different compositions within the deposits suggests that a complex magmatic system was feeding the eruption. All of the above indicate that monogenetic scoria cone eruptions in continental arc settings seem to be far more complex than usually assumed. This is important, when envisaging possible future eruptive scenarios and associated hazards.

Acknowledgements

Field and laboratory costs were defrayed from projects funded by the Consejo Nacional de Ciencia y Tecnología (167231 y 152294) granted to C.S. and M.N.G. respectively.

Reference

Hasenaka, T., Carmichael, I.S.E., 1985. The cinder cones of Michoacán-Guanajuato, central México: Their age, volume and distribution, and magma discharge rate. J. Volcanol. Geotherm. Res. 25, 105-124

Origin of the lava cone of Cerro Prieto, Baja California Norte

Laura García-Sánchez [1], José Luis Macías [1], José Luis Arece [2], Víctor Hugo Garduño-Monroy [3], Ricardo Saucedo [4], and Paul Layer [5]

[1] *Instituto de Geofísica, Universidad Nacional Autónoma de México (UNAM), Unidad Michoacán, Ex-Hacienda de San José de La Huerta C.P. 58190, Morelia, Michoacán, México.* monte_olimpo27@yahoo.com.mx
[2] *Instituto de Geología, UNAM, C.U., Mexico City, México.*
[3] *Instituto de Investigaciones en Ciencias de la Tierra, UMSNH, Morelia, México.*
[4] *Instituto de Geología, UASLP, San Luis Potosí, México.*
[5] *Geochronology Laboratory, U A F, Fairbanks, Alaska, USA.*

Key words: Phreatomagmatism, granulometry, lithic.

The Cerro Prieto Volcanic Complex (CPVC) is located ~ 30 km SE of Mexicali and west of the Cerro Prieto Geothermal Field (CPGF), Baja California Norte. It sits on a pull-apart basin that belongs to the transtensional tectonic system that includes the San Andres Fault System and the Salton Trough basin to the NW and the Eastern Pacific Dorsal to the SE (Fig. 1).

Locally, CPVC is situated on the NW-SE Cerro Prieto Fault, together with Imperial Fault form a pull-apart basin has been filled by Tertiary sediments from Colorado River and alluvial fan from Cucapá Range. These sediments overlaying granitic basement exposed in Cucapá Range.

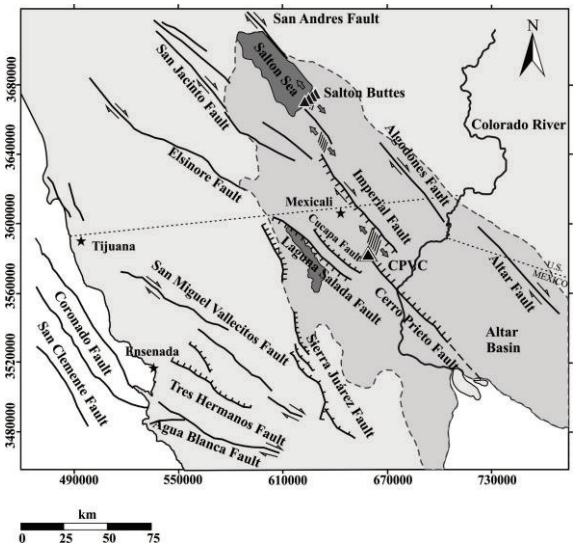

Fig. 1 – Regional tectonic map showing location of CPVC within Salton Trough basin, and main NW-SE faults belonging San Andres Fault System.

The volcanic complex consists of seven stratigraphic units. $^{40}Ar/^{39}Ar$ dating of two of these units suggested that volcanic activity of the complex occurred ~77,000 years ago with the extrusion of lava flows. The activity continued with the emission of domes and a dyke that were destroyed by an explosion. This explosion dispersed four beds and excavated a 300 m wide and 40 m deep crater forming a lava cone. Afterwards, the activity migrated ~650 m to the SW with the emission of three lava domes and a final fissure lava flow. Since then, reworking of volcanic material has produced debris and hyperconcentrated flows emplaced around the complex.

Petrography and geochemistry of rocks indicate that the CPVC erupted calc-alkaline magmas of dacitic composition (65.6-68.9 wt. % SiO_2), that in hand specimen have aphanitic texture with few phenocrysts of plg + opx + Ti-Fe ox + qtz.

Explosive activity

The explosion that formed the Cerro Prieto crater originated four fall deposits exposed around the cone flanks (Fig. 2). The deposits have unimodal distributions typical of fallout deposition. The components of these layers consists of abundant accidental lithics, broken isolated crystals of the lava cone and the dike, without juvenile components. Textural and morphological characteristics of particles observed under the SEM corroborated the absence of juvenile fragments (Fig. 3).

The geological environment in which CPVC is located, suggests that fall deposits may have originated for phreatic, phreatomagmatic or hydrothermal explosions, Sheridan and Wohletz, (1983); Barberi *et al.* (1992). According to the characteristic of the deposits described above we concluded that the Cerro Prieto crater was formed by a phreatic explosion due to the accumulation of vapor and water underneath the domes in association to the geothermal reservoir.

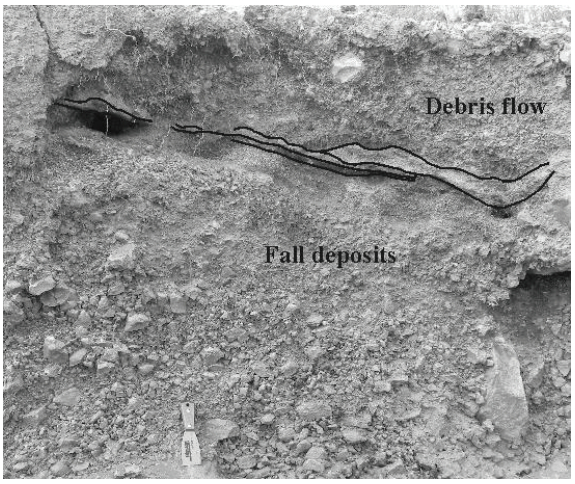

Fig. 2 – Picture showing the four fall deposits, consisting of lithic fragments from lava cone and dike. These deposits are partially remobilized and covered for a debris flow deposits.

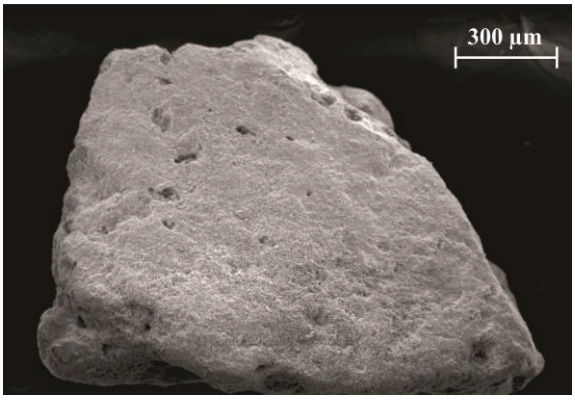

Fig. 3 – SEM picture showing the angular accidental lithic fragment belonging to one of the fall deposit.

References

Sheridan, M.F., Wohletz, K.H., 1983. Hydrovolcanism: Basic Considerations and review. Journal of Volcanology and Geothermal Research 17: 1-29.

Barberi, F., Bertagnini, A., Landi, P., Principe, C., 1992. A review on phreatic eruptions and their precursors. Journal of Volcanology 52: 231-246.

Maar fields along major rift fault escarpments: a genetic link?

Audray Delcamp[1], Hannes B. Mattsson[2], Matthieu Kervyn[1]

[1] *Department of Geography, DGGF-ESS, VUB, Brussels, Belgium.* delcampa@tcd.ie
[2] *Inst. f. Geochemie und Petrologie, ETH Zürich, Switzerland.*

Keywords: maar, carbonatite, East African Rift.

This abstract presents a starting project focused on East African maars. Several large maar fields are observed in Tanzania: south of Lake Natron (Natron rift), around the cities of Babati and Katesh (Manyara rift); in the Republic Democratic of Congo at the north of Lake Kivu and in Uganda, between Lake Edward, Lake George and Lake Albert. Those maars fields stand along major rift escarpments (*Fig. 1 and 2*). However neither description nor study on those large maars fields exist and their origin and formation mechanism are yet unknown. During preliminary field missions in Tanzania and in Uganda, we could observe that the landscape is covered by the volcanic products of the surrounding maars up to several kilometer distance, pointing to Late Pleistocene to Holocene age.

Local populations use the material for construction, and in Uganda several maars are source of drinking water. The maar fields are likely recent, on top of being a source of material and water reservoir, and their origin has thus to be unraveled since they present potential risk but also resources for population.

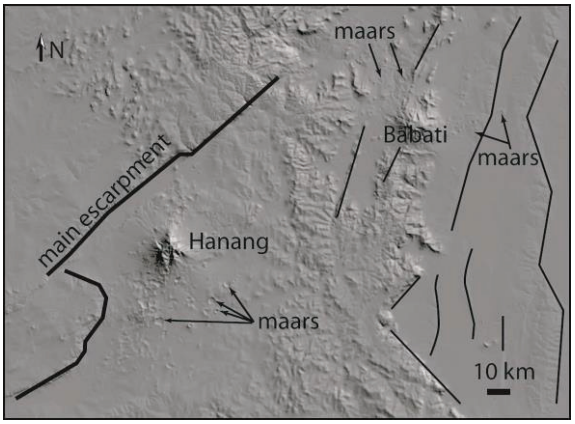

Fig. 1 – Maar field in Hanang and Babati area (Tanzania). Maar field is stretched along major rift escarpment (bold line) and faults (thin line).

Maars fields in Uganda and Tanzania are stretched along major fault escarpments and we could observe presence of carbonatite in several maars in Babati, Katesh. A recent publication (Berghuijs and Mattsson, 2013) notices similar juvenile magma composition at several maars in lake Natron area. In this study, the authors proposed that the fragmentation is likely due to the nature of the magma rather than triggered by magma-water interaction.

The objectives of the project are thus the following:

1/ to analyze the spatial distribution of maars within the field to highlight possible tectonic control on maar distribution

2/ to analyze the role of carbonatitic magma in fragmentation processes

3/ to define the recurrence timing of volcanic explosion in the scope of hazard assessment

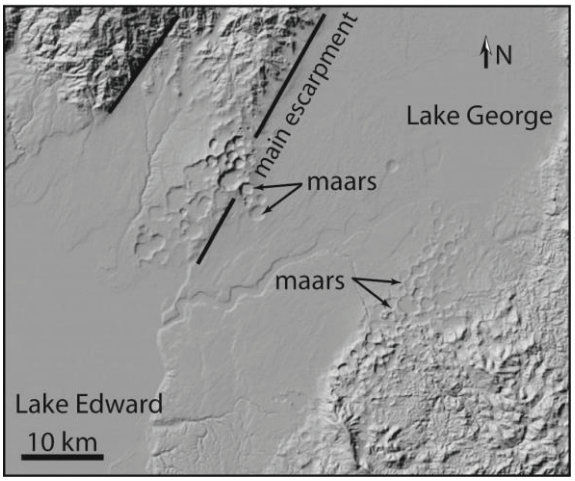

Fig. 2 – Maar field in the vicinity of Lake Edward and Lake George (Uganda). Note the amount and overlap of maar.

This project is thus reviving the controversial topic of explosion trigger for maar formation. Well admitted hypothesis is the magma-water contact as the cause of phreatomagmatism eruption (Morrissey *et al.* 2000). However, in some cases, it has been shown that high volatile content magma with low viscosity and rapid ascent could explain fragmentation mechanisms (Stoppa *et al.*, 2003; Berghuijs and Mattsson, 2013). If such mechanisms and volatile involvement happened to occur in Tanzania and in Uganda, one could propose of general maar formation for the East African Rift that needs to be taken into account for models and hazard

assessment. Such models could also be applied in other rift setting (*e.g.* western European Rift).

Fig. 3 – Detail of maar deposit at the base of Hanang volcano, Tanzania.

Acknowledgements

This project is funded by FWO post-doc program.

References

Berghuijs, J.F, Mattsson H.B., 2013. Magma ascent, fragmentation and depositional characteristics of "dry" maar volcanoes: Similarities with vent-facies kimberlite deposits. Journal of Volcanology and Geothermal Research, 252: 53-72.

Morrissey, M.M., Zimanowski, B., Wohletz, K., 2000. Phreatomagmatic Fragmentation, Encyclopedia of Volcanoes, Ed. H. Sigurdsson, Academic Press, San Diego, CA, 431-445.

Stoppa, F., Lloyd, F.E., Rosatelli, G, 2003. CO_2 as the propellant of carbonatite–kamafugite cognate pairs and the eruption of diatremic tuffisite. Periodico di Mineralogia, 72: 205–222.

Magma Emplacement Mechanism of the Puy de Dome Using Geophysical, Structural, Petrographic, and Geospatial Data

Daniel A. Garza[1], M.S. Petronis[1], Ben van Wyk de Vries[2]

[1] *Department of Environmental Sciences, New Mexico Highlands University, Las Vegas, New Mexico, United States.* dgarza3@live.nmhu.edu
[2] *Laboratoire des Magmas et Volcans, Blaise-Pascal Universitie, Clermont-Ferrand, Auvergne, France.*

Keywords: Geophysics, Magma emplacement, Lava dome.

The Puy de Dome is located in the south-central region of Auvergne, France. At 1,446 meters and ~10,000 years old, it is the largest volcanic structures in the Chaine des Puys (Boivin *et al.*, 2009). Despite being a local iconic landmark, and an internationally known volcano, the Puy de Dome has not been mapped in detail and the events relating to its emplacement mechanism remains unknown.

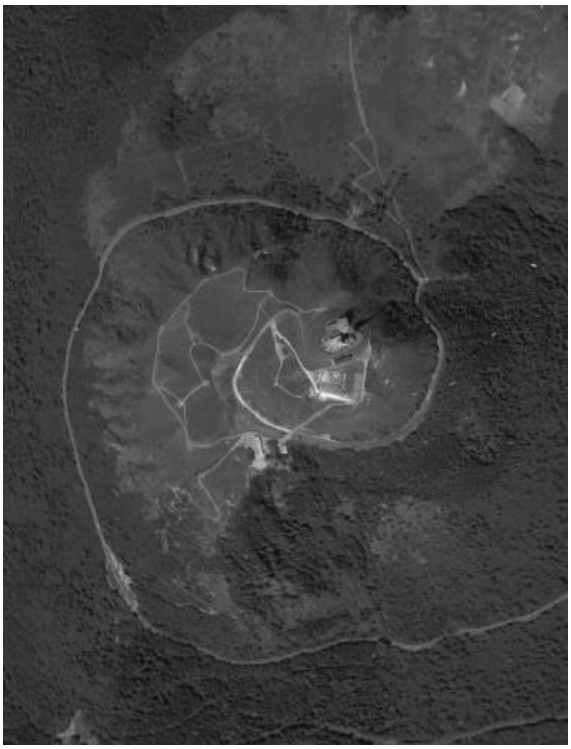

Fig 1- An aerial photo of the Puy de Dome volcano provided by Google Earth.

This study uses detailed geological mapping and various geophysical methods (anisotropy of magnetic susceptibility (AMS), rock magnetism, and paleomagnetism), petrographic observations, and geospatial data to unravel the history of the Puy de Dome.

Geologic mapping and imagery shows that the Puy de Dôme has a smooth NE-SSW facing side with the opposite side being a steeper ridged area.

The main fracture sets on the volcano are radial and slope parallel, but this simple arrangement is more complicated at a local scale.

A major ridge on the south side and a fault on the north side cut the volcano along the transition between the smooth and ridged sides. This is orientated NNE-SSW along the main lineament axis of this part of the Chaîne des Puys.

The western side is bounded by two ridges that are strongly foliated and have an approximate 270° bearing in the basal sections and rotate towards 290° towards the summit. The remainder of the ridges is massive and unfoliated, yet these ridges often have pinnacle blocks.

For the paleomagnetic work, 11 sites of 2x2.5cm drill core samples were collected via standard acquisition methods during the summer of 2013 and analyzed beginning February 2014. Preliminary AMS data shows strongly prolate fabrics for seven sites and impartial fabrics for the remaining four. Preliminary paleomagnetic data reveal two possible remanence directions, suggesting a hiatus in the eruption, highlighted by slight rotation. These data are currently interpreted as an original dome being deformed and pushed upwards and outwards by magma filling in the major faults. This deformation results in the two "hinges" on either side forming strong foliations and several minor faults, while the rest of the ridged area remains unfoliated. The ridge is aligned to the north with the Petit Puy de Dôme intrusions and to the south with the Grosmanaux Bulge (van Wyk de Vries *et al.*, 2012).The west side, bounded between the two shear zones, is the start of a westerly orientated lava flow, and the steep flank is the highly steep flow front. Over the flat summit is a small scarp, and a depressed area, that suggests a small graben formed at the summit in response to the developing lava flow. This morphology is similar to that of flank spreading. The main peak of the Puy de Dôme may be a spine erupted at the back of this graben through the eastern fault of the graben.

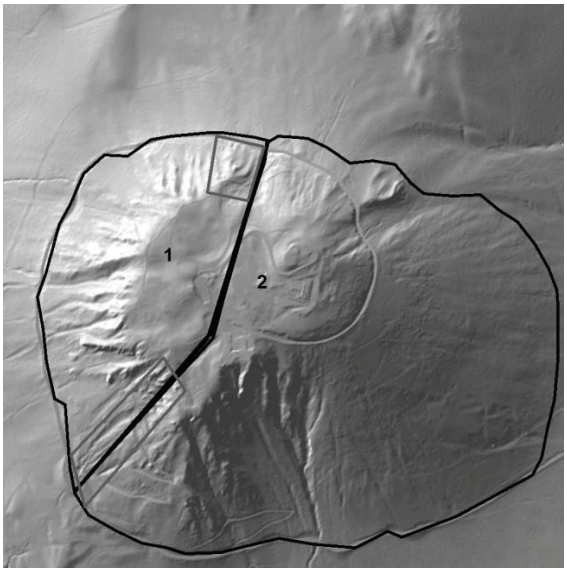

Fig 2- LiDAR map of the Puy de Dome showing the main fault that separates the sloping side (2) from the steep ridged side (1). Foliated "hinges" are boxed in near fault.

Thus, the Puy de Dôme was erupted from a NE-SW oriented fissure that pierced the surface after bulging and deforming nearby cones. The dome grew over this bulge and formed a slightly NE-SW elongated dome. This was buttressed on the NE and E side by the Peitit-Puy de Dôme Bulge, formed at the start of the eruption, but was free to extend SE to form the elongated ridge. The dome reached a height sufficient to flow laterally to the West and developed a bulge to this side as the flow initiated, but never managed to flow more than a few tens of meters before the eruption stopped.

As the dome grew, the outward dipping foliation favored shallow landslides one of which cut a significant scar in the southern flank. Another potential landslide is preserved on the west flank, and provides a fascinating example of impending dome collapse, stalled at the point of failure.

This study changes quite radically the model for the eruption of the Puy de Dôme and will provide the basic framework for interpreting ongoing geophysical work on the mountain, such as Muon tomogrpahy.

Acknowledgements

A special thank you to Gioachino Roberti and Tatum Herrero for their support and guidance in both the town of Clermont-Ferrand and in the field.

References

Boivin, P., Besson, J.C., Briot, D., Camus, G., De Goër de Hervé, A., Gourgaud, A., Labazuy, P., Langlois, E., de Larouzière, F.D., Livet, M., Mergoil, J., Miallier, D., Morel, J.M., Vernet, G., Vincent, P.M., (2009), Volcanologie de la Chaîne des Puys Massif Central Français, 5th Edition, scale 1 : 25 000, 1 sheet.

van Wyk de Vries, B, Grosse, P , Marquez, A , Petronis, M S, Kervyn, M , Delcamp, A , Mossoux, S, Troll, V R. (2012). The Chaîne des Puys: how complicated can monogentic get? (Invited) V44C-06 AGU FALL meeting December 2012

Contrasting style of tectonically-controlled monogenetic volcanism in Southern Andes: Cayutue cluster (41.5ºS)

Luis E. Lara[1, 2], Francisco Bucchi[1], and Rodrigo Mena[3]

[1] *Volcano Hazards Program, RNVV, SERNAGEOMIN, Santiago, Chile, luis.lara@sernageomin.cl*
[2] *CIGIDEN, National Research Center for Integrated Natural Disaster Management, Santiago, Chile*
[3] *Departamento de Geología, FCFM, Universidad de Chile, Santiago, Chile.*

Keywords: Monogenetic volcanism, maars, Southern Andes.

Arc-related monogenetic volcanism is present along the Southern Andean Volcanic Zone where minor eruptive centers are close to long-lived stratovolcanoes. Monogenetic volcanoes are especially common in the arc segment dominated by the Liquiñe-Ofqui Fault Zone (LOFZ), a *ca*. 1,200 km long active fault system and thus a tectonic control of this volcanic style has been proposed (Cembrano and Lara, 2009). In fact, some of the most remarkable clusters of monogenetic volcanoes are located on top of the LOFZ (Lara *et al.*, 2008). In addition, maars in Southern Andes occur close to the LOFZ, which suggests a hydraulic connection between the surface and the magma columns throughout the upper crust fault/fracture network.

Here we report on the contrasting eruptive style and morphology of monogenetic volcanoes forming the Cayutue cluster (41.5ºS) (Moreno *et al.* 1985; López-Escobar *et al.* 1995).

Cayutue cluster is located at the southern branch of the Todos Los Santos Lake (Fig. 1), east of the Osorno Volcano, and inside a graben formed by the master faults of the LOFZ (*e.g.*, Rosenau *et al.* 2006). It is formed by six subaerial pyroclastic cones (Cayutue-Cabeza de Vaca), the Pichilaguna maar and one recently discovered submerged pyroclastic cone. An unpublished AMS age of *ca*. 450 ky for the emerged centers prove they are some of the youngest clusters of the Southern Andes and thus eruptions sourced at monogenetic volcanoes should be considered in hazards assessment for this arc segment. Interestingly, a contrasting eruptive style can be observed in such small volcanic field, which calls attention to the interplay between magmatic processes (magma input in terms of volume and ascent rate) and tectonic processes related to the LOFZ. In addition, we expand on the morphological features of the subaqueous cone, surveyed by means of an echo sounder (Fig. 2) and a sidescan sonar. Preliminary results show it has the shape typical of subaerial scoria cones, possibly with trees in growing position on its surface, which is surprising taking into account the glacial origin of the lakes in this region, mostly formed after the Last Glacial Maximum. We thus infer a more complex landscape evolution of this region where magmatic, tectonic and climate-related processes play a role that could be revealed with a detailed study of volcanic successions in this outstanding monogenetic cluster.

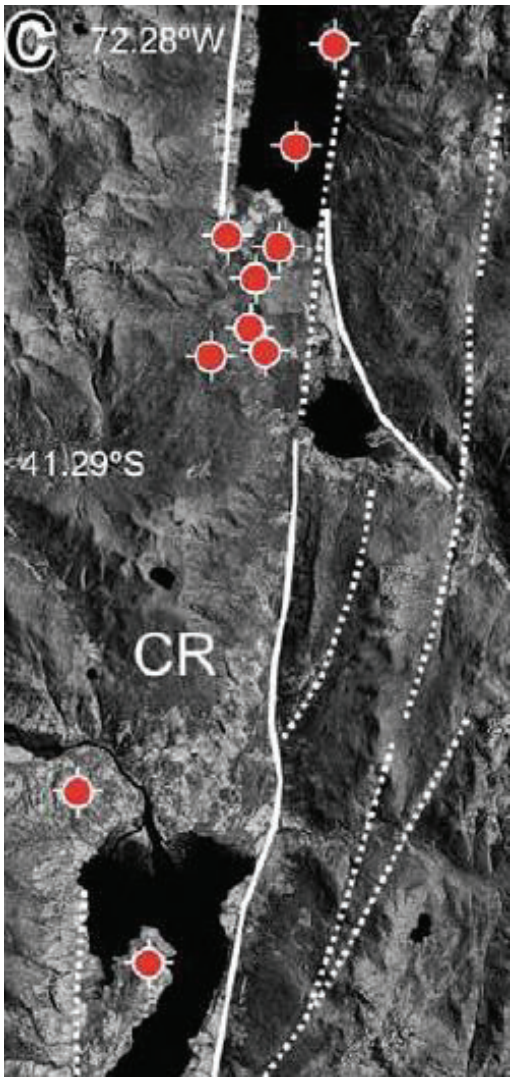

Fig. 1 – Cayutue cluster in Southern Andes with eruptive centers highlighted (after Cembrano and Lara, 2009). Note the location of a submerged volcano, whose presence extended consequences.

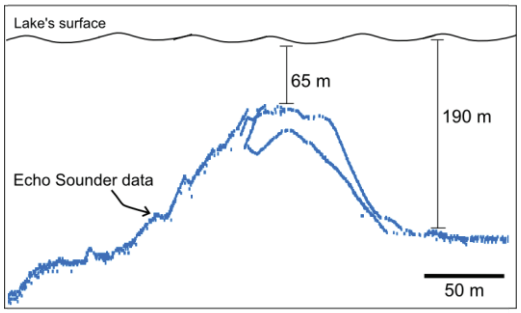

Fig. 2 – Echo sounder data showing the subaqueous cone.

Acknowledgements

We thank the FONDAP program of the Chilean National Science Foundation (CONICYT) for the financial support of our research through the grant FONDAP 15110017, and Volcano Hazards Program of SERNAGEOMIN.

References

Cembrano, J., Lara, L., 2009. The link between volcanism and tectonics in the southern volcanic zone of the Chilean Andes: A review. Tectonophysics. 471, 96 - 113.

Lara, L. E., Cembrano, J., & Lavenu, A. 2008. Quaternary Vertical Displacement along the Liquiñe-Ofqui Fault Zone: Differential Uplift and Coeval Volcanism in the Southern Andes?. International Geology Review, 50(11), 975-993.

López-Escobar, L., Parada, M. A., Hickey-Vargas, R., 1995. Calbuco Volcano and minor eruptive centers distributed along the Liquiñe-Ofqui Fault Zone, Chile (41°-42° S): contrasting origin of andesitic and basaltic magma in the Southern Volcanic Zone of the Andes.

Moreno, H., Varela, J., López, L., Munizaga, F., Lahsen, A. 1985. Geología y riesgo volcánico del volcán Osorno y centros eruptivos menores. Departamento de Geología y Geofísica, Universidad de Chile.

Rosenau, M., Melnick, D., Echtler, H., 2006. Kinematic constraints on intra-arc shear andstrain partitioning in the Southern Andes between 38°S and 42°S latitude. Tectonics 25, TC4013.

SESSION 3-2, 4, 5 and 6

ORAL PRESENTATIONS AND POSTERS
NOVEMBER 21, 2014

Ukinrek Maar Eruption, April 1977
Author: R. Russell, Alaska Department of Fish and Game
Source=http://www.avo.alaska.edu/image_full.php?id=13979 |Date=A

Inverse modeling aeromagnetic data from the El Pinacate Volcanic Field, Sonora, México: a 3D model of the crustal magnetization

Juan García Abdeslem[1]

[1] *CICESE, Departamento de Geofísica Aplicada, jgarcia@cicese.mx*

Keywords: El Pinacate, aeromagnetic data, 3D modeling.

The El Pinacate Volcanic Field (PVF) is located near the northern end of the Gulf of California, in the NW region of the State of Sonora, Mexico, and southern Arizona, in the USA (Figure 1). This volcanic field is within the El Pinacate and Gran Desierto de Altar, Biosphere Reserve, which is known for its unique physical and biological characteristics. The geological substratum that supports the rich biodiversity on this reserve is predominantly composed of volcanic rocks, sand and volcanic ashes that formed colors of special beauty, by the extensive areas of active dunes that surround the Santa Clara shield volcano, and Maar craters, such as the famous El Elegant Crater.

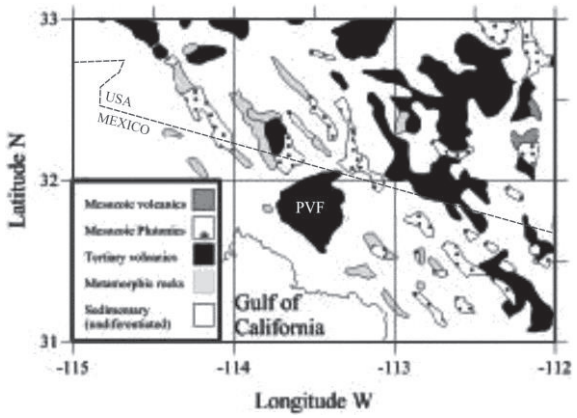

Fig. 1 – Location map of El Pinacate Volcanic Field and simplified geologic map.

The PVF (Gutman, 2011) contains remnants of two volcanic episodes that occurred in Early Miocene and Middle Miocene times (Vidal-Solano *et al.*, 2008). A volcanic episode in Pleistocene time a volcanic episode formed the Santa Clara shield volcano. This characteristic landform was constructed initially by basaltic volcanism that progressively changed to produce felsic lavas (trachyte) from the same parent magma (Lynch *et al.* 1993). Subsequently hundreds of basaltic cinder cones, spatter cones and maar craters have formed over the last million year.

One of the most impressive features in this volcanic field is the large amount of volcanic features: more than 400 cinder cones vents and 8 Maar craters (Figure 2). The spatial distribution cinder cones vents have been studied (Lutz and Gutman, 1995; Le Corvec *et al.*, 2013) with the aim of find statistically significant alignments of point like features, which may be related with the regional tectonic setting. Lutz and Gutman (1995) found that old vents exhibit structural control trending N10^{o}E, while vents younger than 0.4 Ma show control at N10^{o}E, N20^{o}W and N55^{o}W. These authors interpreted that the N10^{o}E alignments probably reflects the current Basin and Range stress regime, and that the N55^{o}W is possible related to extensional normal faulting associated with the opening of the Gulf of California. Le Corvec *et al.* (2013) found NS and NNW alignments that were interpreted as a result of the current strike slip tectonic setting

In this study I use aeromagnetic data from the Digital Magnetic Map of North America to infer, by linear inverse modeling, a 3D model of the crustal magnetization in the region of the PVF (Figure 3). These digital data provide residual total-field magnetic anomalies with respect of the International Reference Geomagnetic Field, have a spatial (grid cell size) resolution of 1 km, and were acquired at a nominal elevation of 300 m draped above the topography.

The linear inversion of aeromagnetic data from the PVF was carried using a cuboid model constituted by 14 layers of constant thickness, that extends from the topography down to 21 km BSL. At each layer is a regular array of rectangular prisms with horizontal dimensions of two by two km. The low magnetization intensity that resulted from the inversion suggests that the volcanic field is

constituted at depth by felsic rocks of low magnetic susceptibility, in agreement with inferences by Lynch *et al.* (1993), and suggesting a magma source partially depleted of magnetic minerals.

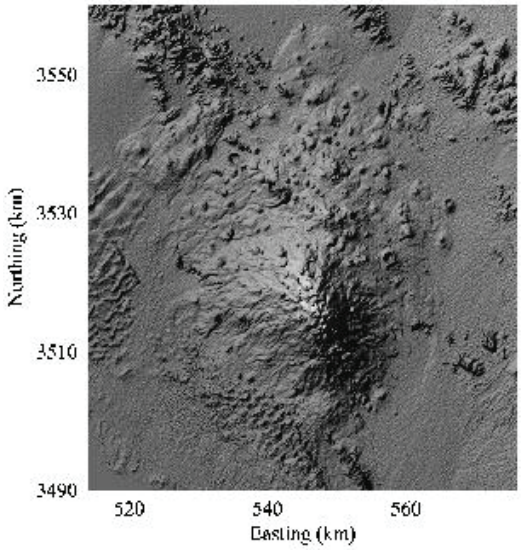

Fig. 2 – Topography at EPVF from SRTM data. TM projection with central meridian at -114°W.

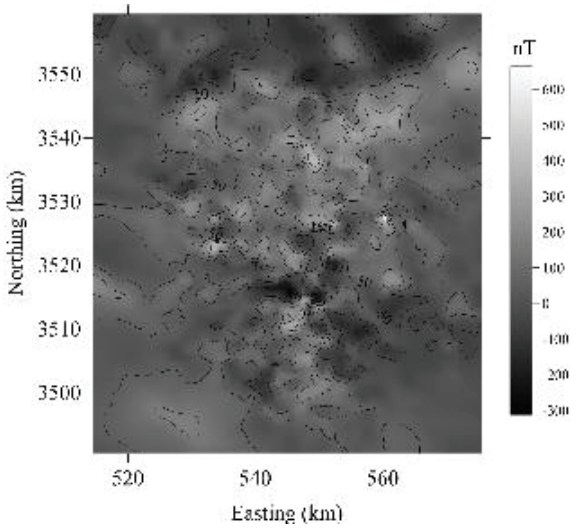

Fig. 3 – Magnetic anomaly at the PVF (nT).

The 3D representation of the magnetization intensity in the cuboid model, shown in Figure 4, suggests a zone of neutral buoyancy at about 12 km depth, and from this zone is detached the main body of the Santa Clara shield volcano.

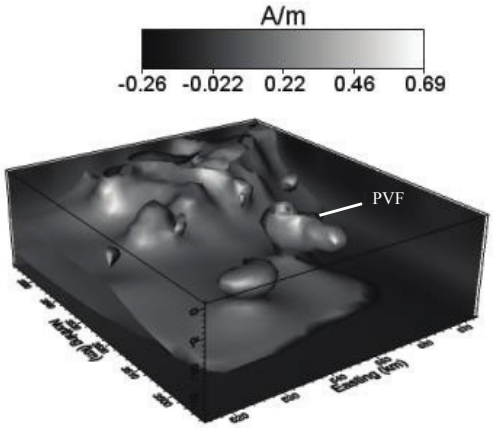

Fig. 4 – 3D model of magnetization. The gray isosurface represent a magnetization of 0.2 A/m, and it enclose regions of higher magnetization.

References

Gutman, J. T., 2011, Estudios geológicos en el Campo Volcánico de El Pinacate,: Publicaciones ocasionales No.5 UNAM, ERNO.

Lutz, T.M., Gutman, J. T. 1995, An improved method for determining and characterizing alignments of pointlike features and its implications for the Pinacate volcanid field, Sonora, México. Journal of Geophysical Research, 100, B9, 17659-17670.

Vidal-Solano J. R., Demant A., Paz Moreno F. A., Lapierre, H., Ortega-Rivera, M. A., Lee, J. K. W., 2008, Insights into the tectonomagmatic evolution of NW Mexico: Geochronology and geochemistry of the Miocene volcanic rocks from the Pinacate area, Sonora: GSA Bulletin, 120, 691-708.

Le Corvec, N., Sporli, K. B., Rowland, J., Lindsay, J., 2012, Spatial distribution and alignments of volcanic centers: Clues to the formation of monogenetic volcanic fields: Earth Science Reviews, http://dx.doi.org/10.1016/j.earscirev.2013.05.005.

Lynch, D. J., Musselman, T. E., Gutman, J. T., Patchett, P. J., 1993, Isotopic evidence for the origin of Cenozoic volcanic rocks in the Pinacate volcanic field, northwestern Mexico: Lithos, 29, 295-302.

Eruptive style and properties of magma feeding enigmatic medium-sized volcanoes in the Michoacán-Guanajuato Volcanic Field: Cerros El Metate and Paracho case studies

Magdalena Oryaëlle Chevrel, Claus Siebe, Marie-Noëlle Guilbaud, Juan Ramon de la Fuente, Sergio Salinas

Departamento de Vulcanología, Instituto de Geofísica, Universidad Nacional Autónoma de México, Coyoacán, C.P. 04510, México D.F., México. chevrel@geofisica.unam.mx

Keywords: shield volcano, dome, andesite, eruption style, monogenetic.

The Michoacán–Guanajuato volcanic field (MGVF) is situated in the west-central part of the Trans Mexican Volcanic Belt (TMVB). The MGVF covers 40,000 km^2 and is particularly interesting because the large active strato-volcanoes that are so typical for subduction-related volcanic arcs are almost absent. Instead, this area displays a high concentration of smaller volcanic vents. Over 1000 volcanic centers in the MGVF are small monogenetic scoria cones (few rare maars occur also) formed by Strombolian eruptions and associated lava flows. Another 400 are described as medium-sized volcanoes with a much larger volume (between 0.5 and 10 km^3, and up to 50 km^3) than scoria cones (average of 0.021 km^3; Hasaneka and Carmichael, 1985; Hasenaka 1994).

The nature of the medium-sized volcanoes is still under debate. Most of them were recognized as shields (shaped predominantly by effusive activity) crowned by a small lava dome or scoria cone, and others as composite (e.g. cones or domes built partly by lava flows and partly by pyroclastic deposits; Hasenaka, 1994). Their morphology is particularly interesting because their slopes are normally only between 5º and 10º, a figure that is similar or slightly steeper than that for Icelandic shields (Hasenaka 1994). However, unlike typical shields made of multiple thin basaltic flows, many shields in the MGVF are made of thick A'a to blocky andesite flows.

Eruption style and the resulting volcanic edifice morphology is largely controlled by the physical-chemical properties of the erupted magma (rheology, density, permeability, etc.) and its degree of interaction with water (e.g. phreato-magmatic eruptions). Rheology is the key parameter controlling magma dynamics. It depends on the chemical composition of the magma and its volatile content, temperature, amount of crystals, and the pressure gradient that is controlling bubble nucleation. Some differences must hence be expected between magmas giving rise to medium-sized volcanoes (e.g. effusive shields, domes, and composite edifices) and scoria cones in order to explain their specific eruption style.

In terms of composition and petrology, Hasenaka et al. (1994), pointed out that the products of scoria cones show a large diversity extending from calc-alkaline olivine basalts to andesites. In contrast, medium-sized volcanoes are restricted to a smaller compositional range in the calc-alkaline andesite domain and are characterized by containing Opx phenocrysts. Products from both types of volcanoes plot along the same compositional trend. Since lavas forming shields are frequently more differentiated, they suggested that these might have evolved by fractional crystallization of primitive calc-alkaline basalts of the type found in some of the scoria cones. Roggensack, (1992) argued that the correlation of Pb and Sr isotope ratios with high fractionation indices in rocks of the MGVF indicate that combined assimilation/fractional crystallization processes probably originated the shield lavas. The larger magma batches feeding the shields might rise more slowly, and hence have longer crustal residence times, allowing the magma to differentiate (and assimilate crust) and for bubbles to coalesce and gas to escape, reducing the explosivity of the eruptions. Furthermore, Hasenaka (1994) indicated that crystallization of Ol rather than Opx (in addition to Plag and Cpx) in the groundmass implies a higher H_2O-content for a given magma composition and cooling rate, suggesting that shields thus have relatively smaller H_2O-contents (reducing their explosivity) in comparison to scoria cones. However, this is in contradiction to Roggensack (1992) who concludes that magmas feeding both, scoria cones and shields, have similar volatile contents. The geochemical differences between both volcano types seem to be restricted to subtle variations and further investigations are needed to clear the question of their marked differences in eruption style.

The purpose of this study is to elucidate the eruption dynamics and physical properties of magmas feeding medium-sized volcanoes in the unique setting of the MGVF. With this in mind, two young and well-preserved typical medium-sized volcanoes, El Metate and Paracho, that in addition happen to be conveniently located in close proximity

to each other but display contrasting morphologies, were selected as case studies.

Cerro el Metate (N19°32'17", W101°59'33") is probably the youngest *"shield"* of the MGVF. Available ^{14}C-dates indicate that it is younger than 3700+/-50 yrs. B.P. The edifice consists of well-preserved lava flows (Fig. 1) of extraordinary thickness disposed radially around a summit dome (Hasenaka and Carmichael, 1986). Detailed mapping allowed us to reconstruct its eruptive activity and the sequence of emplacement of the different lava flows.

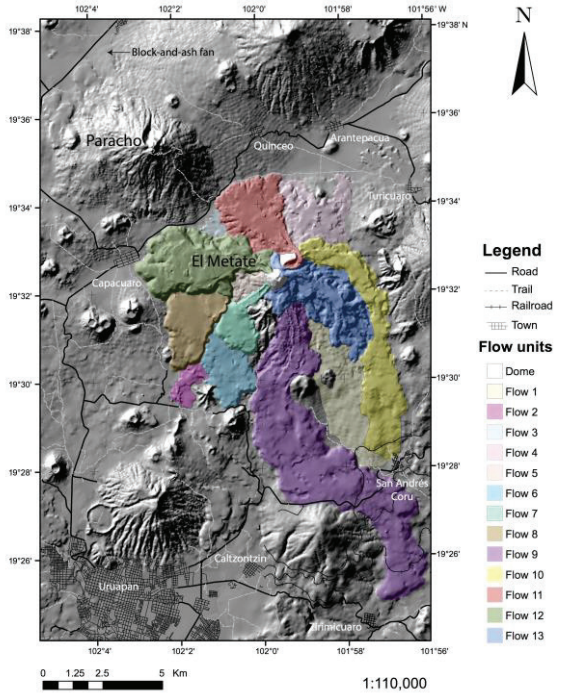

Fig. 1 – Hill-shade model of the study area showing the location of Cerro Paracho and Cerro El Metate (and the stratigraphic succession of its lava flows).

We have identified 13 individual lava flows that cover a total area of 103 km^2 with lengths ranging between 3 and 15 km and average thicknesses between 60 and 150 m. Individual volumes range between 0.5 and 3.5 km^3 for a total of 11 to 15 km^3. Effusion rates and emplacement durations of different flows were estimated using models proposed by Harris and Rowland (2009) and Kilburn and Lopes (1991). With maximum average effusion rates of 15 to 100 m^{3}s^{-1} the cumulative duration of each flow took at least 15 to 30 years. Such short emplacement times at El Metate are comparable to the nearby historical monogenetic Paricutin eruption (ca. 10 years) but its erupted lava volume is considerably larger (>11 km^3 for El Metate vs. ca. 0.8 km^3 for Paricutin). This has substantial implications, especially for evaluating future hazards.

To the NW and next to El Metate (Fig. 1), is Cerro Paracho (N19°35'23"; W 102° 2'27") dated at 0.06±0.01 Ma by the K-Ar method (Ban et al., 1992). It is much steeper and has a protruding summit dome. Lava flow surfaces are rarely preserved and a wide block-and-ash fan occurs at its lower slopes, where a deeply dissected valley originating near the summit reaches the surrounding plains. Its existence implies episodes of explosive activity. Although it has been catalogued as a monogenetic shield volcano, Paracho might be rather a composite dome as suggested by the extensive pyroclastic deposits occurring at its base. Chemical analyses revealed compositional similarity with its neighbor El Metate. This finding opens several questions, including: Why are the eruption styles so different? What are the rheological properties of the magmas that caused these differences? Do the magmas have the same source? And at a greater scale: Why do volcanoes of the MGVF display so many differences? Ultimately, are they all monogenetic and why are they so abundant in the MGVF?

Acknowledgements

Field and laboratory costs were defrayed by projects CONACyT-167231 and UNAM-DGAPA IN-109412-3 granted to C.S, as well as project CONACyT-152294 granted to M.N.G. The first author's stay in Mexico is funded by a UNAM-DGAPA postdoctoral fellowship.

References

Ban, M., Hasenaka, T., Delgado-Granados, H., 1992. K-Ar ages of lavas from shield volcanoes in Michoacán-Guanajuato, Mexico. Geof. Int. 31 (4): 467-473.

Harris, A. J. L., Rowland, S. K., 2009. Effusion rate controls on lava flow length and the role of heat loss: A review. Studies in Volcanology: The Legacy of George Walker. Special Publications of IAVCEI 2: 33–51.

Hasenaka, T., Carmichael, I.S.E., 1986. Metate and other shield volcanoes of the Michoacan-Guanajuato, Mexico. Trans. Am. Geophys. Union (EOS) 67: 44.

Hasenaka, T., Carmichael, I.S.E., 1985. The cinder cones of Michoacán-Guanajuato, central Mexico: Their age, volume and distribution, and magma discharge rate. J Volcanol. Geotherm. Res. 25: 105–124.

Hasenaka, T., 1994. Size, distribution and magma output rates for shield volcanoes of the Michoacán-Guanajuato volcanic field, Central Mexico. J. Volcanol. Geotherm. Res. 63: 13– 31.

Hasenaka, T., Ban M., Delgado-Granados, H., 1994. Contrasting volcanism in the Michoacán-Guanajuato volcanic field, Central Mexico: Shield volcanoes vs. cinder cones. Geof. Int. 33 (1): 125-138.

Kilburn C. R., Lopes R. M. C., 1991. General patterns of flow field growth: Aa and blocky Lavas. J. Geophys. Res. 96, No.B12: 19,721-19,732.

Basaltic ignimbrites in monogenetic volcanism

Gerardo J. Aguirre-Díaz[1], Joan Martí[2], Llorenç Planagomà[3], Adelina Geyer[2]

[1] *Centro de Geociencias, Universidad Nacional Autónoma de México, UNAM Campus Juriquilla, Querétaro, México.* ger@geociencias.unam.mx
[2] *Grupo de Volcanología, SIMGEO (UB-CSIC), Instituto de Ciencias de la Tierra Jaume Almera, Barcelona, Spain.*
[3] *Tosca S.L. Olot, Spain.*

Keywords: *Ignimbrites, monogenetic volcanism, La Garrotxa Volcanic Field.*

Ignimbrites are common products of explosive volcanism of intermediate and silicic magmas (Sparks et al., 1973). They also occur in eruptions of composite basaltic volcanoes (Freundt et al., 2000). However, they have not been yet described associated with monogentic volcanism. Commonly, monogenetic volcanism tends to generate lava flows, scoria and lapilli deposits, and different kinds of PDCs and explosion breccias when it has a phreatomagmatic character (Wohletz and Sheridan, 1983; Walker, 2000; Valentine and Gregg, 2008).

In the La Garrotxa volcanic field, the youngest area of the Catalan Volcanic Zone (Martí et al., 1992), a sector of the Neogene-Quaternary European rifts system located at the NE corner of Spain, we have indentified a particular group of pyroclastic density current deposits that show similar depositional and emplacement characteristics than silicic ignimbrites.

In this volcanic field, small-sized cinder cones were produced during monogenetic short-lived eruptions associated with widely dispersed fractures of short lateral extent (Martí et al., 2011). This volcanism is also characterised by important phreatomagmatic events that in many cases alternated with purely magmatic ones.

Among the wide variety of deposits generated by this volcanism, including scoria fallout, ballistic bombs and spatter, explosion breccias, ash fallout, and different types of pyroclastic density current deposits (PDC), it is characteristic the group of pyroclastic flows deposits which lithological and sedimentological characteristics resemble those from classical silicic ignimbrites.

Compared to the rest of PDC deposits present in the area, mostly emplaced from dilute pyroclastic surges generated during phreatomagmatic episodes (Martí et al., 2011), the ignimbritic deposits show very different lithological and sedimentological characteristics, indicating that they resulted from poorly expanded PDCs, probably also associated with phreatomagmatic phases. The deposits contain abundant vesiculated juvenile (scoria) fragments together with dense juvenile clasts and lithics, all them "floating" in an abundant matrix of ash and fine scoria lapilli (Fig. 1). There are several characteristics of these pyroclastic flow deposits that coincide with those described in typical silicic non-welded ignimbrites (Sparks et al., 1973; Wilson and Walker, 1982; Branney and Kokekaar, 1992) and than allow us to classify them as basaltic ignimbrites. These include: normal grading of lithic clasts, reverse grading of scoria fragments, presence of a ground surge (ground layer?), sharp erosional contact between the ground surge and the basal layer of the overlying scoriaceous part of the deposit, abundant ashy matrix, and presence of gas segregation structures. They are typically massive without a clear internal stratification, despite in some occasions the deposit is composed of several

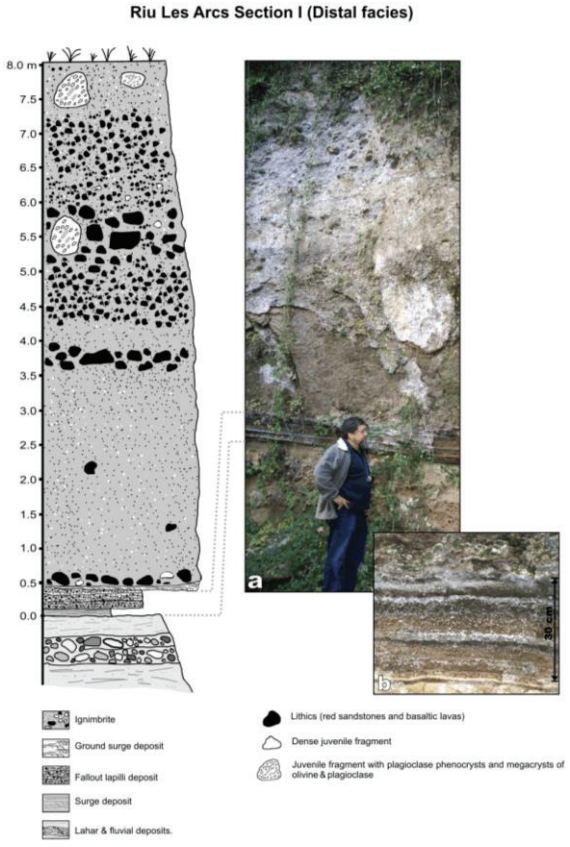

1Fig. 1 – Example of a basaltic ignimbrite sequence from La Garrotxa Volcanic Field.

flow units that give a stratified aspect to the whole sequence.

We propose that these pyroclastic flows or ignimbrites form during transient explosions when ground water comes into contact with magma during a steady phase of a magmatic eruption. The presence of well stratified lapilli deposits at the base of most of these ignimbrites indicates that their emplacement was preceded by a sustained high fire fountaining/short eruption column phase during a strombolian eruption. Massive disruption of subsurface water from a confined aquifer, probably due to decrease of pressure inside the conduit, caused a drastic change in the eruption dynamics suddenly increasing the explosivity of the magma, thus eroding the conduit and subsequently increasing the mass eruption rate, overloading the eruption column and making it to collapse over the crater and generating a dense PDC. The resulting flows were emplaced following topographic lows as highly concentrated pyroclastic flows that deposited several kilometres away as a plug flow when the initial momentum dissipated. The transient explosions may repeat several times during the eruption generating several flow units that formed composite sequences up to several tens of metres thick.

References

Branney, M.J. and Kokelaar, P., 1992. A re-appraisal of ignimbrite emplacement: progressive aggradation and changes from particulate to nonparticulate flow during emplacement of high-grade ignimbrite. Bulletin of Volcanology, 54: 504-520.

Freundt, A., Schmincke, H. U. 1995. Eruption and emplacement of a basaltic welded ignimbrite during caldera formation on Gran Canaria. Bulletin of Volcanology, 56, 640-659.

Freundt, A., Wilson, C.J.N., and Carey, S.N., 2000. Ignimbrites and block and ash flow deposits. In: Sigurdsson, H., ed., Encyclopedia of Volcanoes, p. 581-600.

Martí, J., Mitjavila, J., Roca, E. and Aparicio, A. 1992. Cenozoic magmatism of the Valencia trough (Western Mediterranean): relation between structural evolution and Volcanism". Tectonophysics, 203, 145-166.

Martí, J., Planagumà, Ll., Geyer, A., Canal, E., Pedrazzi, D., 2011. Complex interaction between Strombolian and phreatomagmatic eruptions in the Quaternary monogenetic volcanism of the Catalan Volcanic Zone (NE of Spain), Journal of Volcanology and Geothermal Research, 201, 178-193.

Sparks, R.S.J., et al., 1973. Products of ignimbrites eruptions. Geology, 1: 115-118.

Valentine, G. A. and Gregg, T. K. P., 2008. Continental basaltic volcanism - Processs and problems. Journal of Volcanology and Geothermal Research, 177, 857-873.

Walker, G. P. L., 2000. Basaltic volcanoes and volcanic systems. In: Sigurdsson, H (Ed), Encyclopedia of Volcanoes, Academic Press, San Francisco (CA), 283-289.

Wilson, C.J.N. and Walker, G.P.L., 1982. Ignimbrite depositional facies: the anatomy of a pyroclastic flow. Journal of the Geological Society of London, 139: 581-592.

Wohletz, K. M. and Sheridan, M. F. (1983): Hydrovolcanic explosions 2. Evolution of basaltic tuff rings and tuffs cones. American Journal of Science, 283: 385-413

.

Distribution of monogenetic phreato-magmatic volcanoes (maars, tuff cones, tuff rings) in the Mexican Volcanic Belt and their tectonic and hydrogeologic environment

Claus Siebe and Sergio Salinas

Departamento de Vulcanología, Instituto de Geofísica, Universidad Nacional Autónoma de México, C.U., México, D.F., Mexico.
csiebe@geofisica.unam.mx

Keywords: Monogenetic, phreato-magmatic, maars, Mexican Volcanic Belt.

The active Mexican Volcanic Belt (MVB) stretches across central Mexico for ca. 1200 km in an East-West direction from the coast at the Gulf of Mexico to the coast of the Pacific Ocean (Fig. 1). This volcanic arc is related to the subduction of the oceanic Cocos Plate underneath the continental North American Plate. It consists of a large number of Late Tertiary to Quaternary maars, scoria cones, domes, calderas, strato-volcanoes, the chemical and mineralogical composition of which is largely calc-alkaline. The belt traverses the southern part of the Mexican Altiplano, a highland characterized by normal faulting and horst-and graben structures. The resulting basins are/were often occupied by extensive (but shallow) lakes. Another particularity of the MVB is the abundance of scoria cones and other types of monogenetic volcanes, which outnumber by several orders of magnitude the much larger strato-volcanoes. Although the exact causes responsible for their great number (>3000) are still unknown, their high frequency of occurrence must be sought in the peculiar geometric configuration of the subduction zone (namely the obliqueness of the subduction vector, the flat subduction angle, the segmented nature of the subducting plate, and the resulting physical-chemical conditions prevailing in the mantle wedge).

We present an inventory of monogenetic phreato-magmatic volcanoes (maars, tuff-rings, tuff-cones) located within the MVB, that includes available data in regard to their main characteristics (morphological parameters, age, composition, type of substrate, etc.). This allows us to better address questions related to the tectonic and environmental causes that might explain their distribution in time and space.

Ordóñez (1905, 1906) was the first to study maars in central Mexico. In his pioneering work in the inter-montane basin of Serdán-Oriental, he was able to recognize the phreato-magmatic origin of maar tuff-deposits. This important breakthrough (Ordónez has been largely ignored by the volcanological community until today) did not become an established fact until much later (*e.g.* Lorenz, 1973; Sheridan and Wohletz, 1983). One of the reasons for this might be that in his writings, Ordónez did not use the term *maar*, known to geologists, but the local word *Axalapaxco* (=vessel of sand containing water, in *Náhuatl* language). Unfortunately, the number of detailed studies focusing on single maars in the MVB is still limited (*e.g.* Abrams and Siebe 1994, Carrasco-Núñez *et al.* 2006, Ort and Carrasco-Núñez 2009, Kshirsagar *et al.* 2014). Hence, several of their characteristics (*e.g.* chemical composition of juvenile components, radiometric age, etc.) are still largely unknown. Nonetheless, with the help of topographic maps and satellite images, we were able to identify a total of 88 monogenetic phreato-magmatic volcanoes in the entire MVB (including the Tuxtla Volcanic Field) for which we determined their spatial distribution, main morphological parameters, as well as tectonic and hydrogeologic environment (Tab. 1).

Our main finding is that maars are rare (ca. 3% of total monogenetic vents in the MVB). Almost one half (46.6%) is located in the Tuxtla Volcanic Field, in a littoral setting characterized by alluvial deposits near the Gulf of Mexico. Most of the other half are found clustered in only few (*e.g.* Serdán-Oriental, Valle de Santiago-Yuriria, Zacapu) of the many inter-montane lacustrine basins (tectonic grabens) that occur within the area of intersection between the Mexican Altiplano and the MVB (Fig. 1).

Apparently, optimal conditions for maar formation are frequently not met in these basins despite of the availability of sufficient ground/or surface water necessary to fuel such type of

Region	# of maars, etc	%	% of total monogenetic (*ca.* 3000)
Tepic Graben	3	3.4	0.11
Michoacán Guanajuato Volc. Field (Total=22)			
Zacapu basin	3	3.4	0.11
Scattered in MGVF	4	4.5	0.15
Valle de Santiago-Yuriria	15	17.0	0.57
Sierra Chichinautzin (Mexico Basin)	3	3.4	0.11
Puebla-Malinche	3	3.4	0.11
Serdán-Oriental Basin	16	18.2	0.61
Los Tuxtlas Volcanic Field	41	46.6	1.55
Total	**88**	**100.00**	**2.93**

Environment	# of maars, etc	%	% of total monogenetic (*ca.* 3000)
Fluvial	8	9.1	0.27
Intermontane Basin	39	44.3	1.30
Littoral	41	46.6	1.37
Total	**88**	**100**	**2.93**

Tab. 1 – Monogenetic phreato-magmatic volcanoes in the MVB according to region and environment. Note the low percentage of phreato-magmatic craters (ca. 3%) with respect to the total number of monogenetic constructs (ca. 3000, mostly scoria cones).

Fig. 1 – Distribution of phreato-magmatic volcanoes (maars, tuff rings, etc.) in the MVB (red hue). The largest concentration (41 craters) occurs in the Tuxtla Volcanic Field, followed by the inter-montane basin of Serdán-Oriental (16 craters).

eruptions. We hypothesize that monogenetic volcanoes (both scoria cones and phreato-magmatic vents) are absent in the interior of many of the basins (*e.g.* Chapala, Toluca, Cuitzeo) because the loose young sedimentary fill is less dense than the small batches of rising magma. If in addition, this non-compacted fill is thick, ascending magma will not reach the surface, because the fill will act as a density trap. Instead, a sill might form at the base of the sedimentary pile. This would explain, why in some cases (*e.g.* Zacapu, Yuriria, and Mexico basins) phreato-magmatic volcanoes occur only near the margins of the basin and also why warm springs are frequently found in the flat interior of a basin. In this context, the Serdán-Oriental basin is noteworthy, because both maars and scoria cones occur in close proximity to each other (in theory, they should be mutually exclusive). Although it is possible that groundwater availability might change strongly on a short lateral distance due to differences in hydraulic parameters of aquifers (*e.g.* permeability), it is also possible (as speculated before by Siebe 1986) that paleoclimate changes and their effect on groundwater conditions might be responsible for this apparent contradiction. Only systematic radiometric dating of the different types of monogenetic volcanoes in this area will solve this quest.

Acknowledgements

Field and laboratory costs were defrayed by projects CONACyT-167231 and UNAM-DGAPA IN-109412-3 granted to C.S. Data set for the Tuxtla Volcanic Field was kindly provided by K. Sieron.

References

Abrams, M., Siebe, C., 1994. Cerro Xalapaxco: an unusual tuff cone with multiple explosion craters, in central Mexico. J. Volcanol. Geoth. Res. 63: 183-199.

Carrasco-Nuñez, G., Ort, M.H., Romero, C., 2006. Evolution of hydrological conditions of a maar volcano (Atexcac crater, Eastern Mexico). J. Volcanol. Geoth. Res. 159: 179-197.

Kshirsagar, P., Siebe, C., Guilbaud, M.N., Salinas, S., 2014. Hydrogeological setting and stratigraphy of the Alberca de Guadalupe maar volcano at the SE margin of the Zacapu basin, Michoacán, México. 5IMC, Querétaro, México, Abstracts (this volume).

Lorenz, V., 1973. On the formation of maars. Bull. Volcanol. 37 (2): 183-204.

Ordóñez, E., 1905. Los Xalapazcos del estado de Puebla (1ª Parte). Imprenta y fototipia de la Secretaría de Fomento, México.

Ordóñez, E., 1906. Los Xalapazcos del Estado de Puebla: Segunda Parte. Imprenta y fototipia de la Secretaria de Fomento, México.

Ort, M.H., and Carrasco-Nuñez, G., 2009. Lateral vent migration during phreatomagmatic and magmatic eruptions at Tecuitlapa Maar, east-central Mexico. J. Volcanol. Geoth. Res. 181: 67-77.

Sheridan, M.F., Wohletz, K.H., 1983. Hydrovolcanism: Basic considerations and review. J. Volcanol. Geoth. Res. 17 (1): 1-29.

Siebe, C., 1986. On the posible use of maars and cinder cones as palaeoclimatic indicators in the closed basin of Serdán-Oriental, Puebla, México. J. Volcanol. Geoth. Res. 28: 397-400.

Hydrogeological setting and stratigraphy of the Alberca de Guadalupe maar volcano at the SE margin of the Zacapu basin, Michoacán, México

Pooja Kshirsagar, Claus Siebe, Marie-Noëlle Guilbaud and Sergio Salinas

[1] *Departamento de Vulcanología, Instituto de Geofísica, Universidad Nacional Autónoma de México, Coyoacán, C.P. 04510, México D.F.Mexico. pooja6vulcan@gmail.com*

Keywords: Maar, Zacapu, Hydrology.

Introduction

The Alberca de Guadalupe maar is one of the few phreato-magmatic volcanoes of the Plio-Quaternary Michoacán-Guanajuato Volcanic Field (MGVF). This large field (~40,000 Km^2) is located in the central part of the Trans-Mexican Volcanic Belt and includes >1000 monogenetic scoria cones and associated lava flows, ca. 300 shield volcanoes, and tens of lava domes (Hasenaka and Carmichael, 1985).

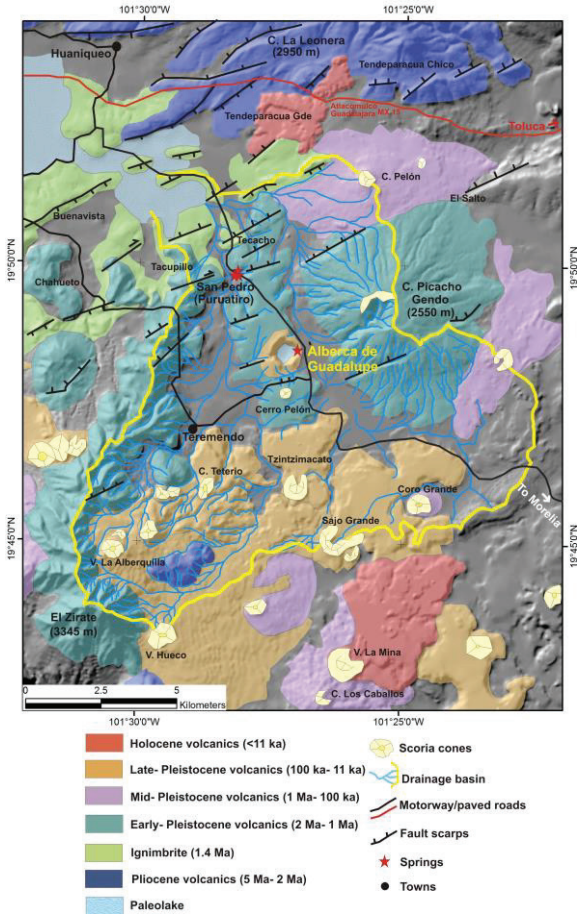

Fig. 1 – Geological Map of the Alberca de Guadalupe maar volcano.

Eruptive products in the MGVF are predominantly calc-alkaline andesites, but a wide range in compositions (ol-basalts to rhyolites, including exotic alkaline varieties) can be found. In contrast to the pervasively abundant scoria cones, so far only about 2 dozen phreato-magmatic monogenetic constructs (tuff rings, tuff cones, maars) have been identified in the MGVF. One half of these form a cluster near Valle de Santiago in the Lerma river valley at the northern margin of the MGVF (Aranda-Gómez *et al.*, 2013), while the others occur in a more scattered fashion. The scarcity of this type of volcano (only ca. 2% of all monogenetic volcanoes in the MGVF) is striking and implies that conditions favoring their formation are rarely met in this region. Here, we report on the Alberca de Guadalupe maar, a volcano that had never been studied in detail before, and provide data in regard to the peculiarities of its hydrogeological setting in order to better understand its origin.

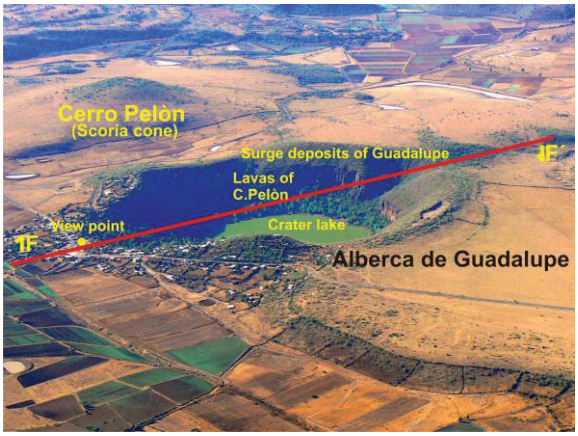

Fig. 2 – Aerial view of the Alberca de Guadalupe maar crater (view from the NE). The line indicates an E-W trending normal fault. Late Pleistocene surge deposits associated to crater formation are underlain by early Pleistocene lava flows from the Cerro Pelón scoria cone to the south of the crater.

Stratigraphy and geologic setting

Alberca de Guadalupe is one of three phreato-magmatic vents (the others are El Caracol and

Alberca de los Espinos) that occur within the catchment area of the lacustrine Zacapu basin, Michoacán. This large inter-montane basin (1980 m a. s. l.) owes its origin to a tectonic graben bound by ENE-WSW normal faults that are still active. It contained a wide, but shallow lake that was artificially drained in the late 19th century for the purpose of gaining agricultural land (Siebe *et al.*, 2012; Telford *et al.*, 2004).

Alberca de Guadalupe formed between 20,000 and 23,000 y BP (range indicated by 2 radiocarbon dates obtained on paleosols underlying surge deposits). It literally forms a hole in the general planar topography of the underlying early Pleistocene lava flows (Figs. 1, 2). The maar crater is ~1 km in diameter, ~140 m deep, and bears a ~9 m deep lake in its interior (Fig. 2). Outcrops near the rim display well-stratified sequences of alternating dry and wet surge deposits, as typically encountered at maar volcanoes. The deposits are rich in accidental lithics (angular andesite lava and ignimbrite clasts) constituting 51-88% of the deposit with few juveniles. The largest juvenile clasts are represented by decimeter-sized cauliflower-shaped bombs of basaltic-andesite composition (olivine, pyroxenes and plagioclase phenocrysts in a quenched glassy matrix; SiO_2 =54-58 wt.%). Dry surge deposits are friable, medium-to-coarse lapilli sized, mainly clast-supported and poorly sorted (Mdφ: -1.56 to -3.75, σφ: 1.43 to 3.23). In contrast, the wet surges are fairly indurated and consist of thin stratified layers of fine-ash with accretionary lapilli (~1 cm in diameter). The bedding of the deposits is frequently disrupted by ballistic impact-sag structures (Fig. 3).

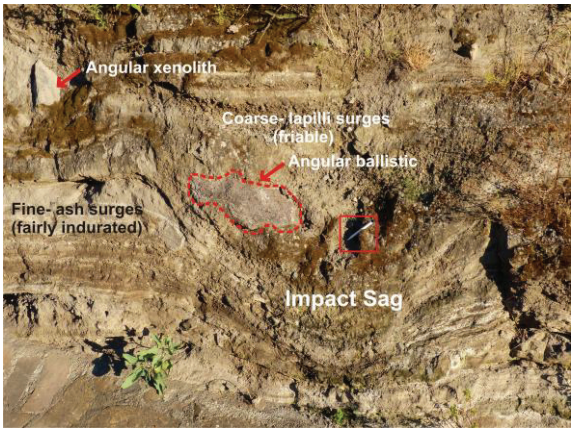

Fig. 3 – Typical surge deposits with ballistic impact sags, observable at outcrop on the road leading down to the crater-lake. Pen for scale (~18 cm) inside the square box.

An E-W trending regional fault that is parallel to a series of domino-style faults occurring throughout the graben system runs through the maar crater, down-throwing the northern part by ~30 m (Fig. 2). In addition to this main fault that probably served as a structural control to the conduit of the ascending magma feeding the eruption, several minor concentric listric faults can be observed cutting the deposits. These are related to inward slumping of the inner crater walls.

The unusual formation of this phreato-magmatic construct in the semi-arid highlands of Zacapu was favored by the local hydrological and topographical conditions, especially the shallow aquifer parameters (*e.g.* high permeability and flow direction) that allowed funneling enough ground-and-surface water along narrow valleys to the eruption site in order to fuel continuous phreato-magmatic explosions. Today, such groundwater conditions still prevail as attested by several high-discharge springs near Puruátiro, not far from the maar crater (Fig. 1), making it possible for such an event to occur again.

Thus, local hydrogeological and tectonic conditions explain the occurrence and evolution of this rare phreato-magmatic vent in the otherwise scoria cone dominated MGVF.

Acknowledgements

Field and laboratory costs were defrayed from projects funded by the Consejo Nacional de Ciencia y Tecnología (CONACyT-167231) and the Dirección General de Asuntos del Personal Académico UNAM-DGAPA IN-109412-3 granted to C.S. The first author's stay in Mexico was funded by a UNAM-DGAPA postdoctoral fellowship.

References

Aranda-Gómez, J.J., Levresse, G., Martínez, J.P., Ramos-Leal, J.A., Carrasco-Núñez, G., Chacón-Baca, E., González-Naranjo, G., Chávez-Cabello, G., Vega-González, M., Origel, G., Noyola-Medrano, C. 2013. Active sinking at the bottom of the Rincón de Parangueo Maar (Guanajuato, México) and its probable relation with subsidence faults at Salamanca and Celaya. Boletin de la Sociedad Geológica Mexicana 65(1): 169-188.

Hasenaka, T., Carmichael, I.S.E. 1985. The cinder cones of Michoacán-Guanajuato, Central Mexico: Their age, volume and distribution, and magma discharge rate. Journal of Volcanology and Geothermal Research 25: 105-124.

Siebe, C., Guilbaud, M.N., Salinas, S., Chedeville-Monzo, C. 2012. Eruption of Alberca de los Espinos tuff cone causes transgression of Zacapu lake ca. 25,000 yr BP in Michoacán, Mexico. 4IMC Conference, Auckland, NZ. Abstract volume. Geoscience Society of New Zealand Miscellaneous Publication 131A: 74-75.

Telford, R., Barker, P., Metcalfe, S., Newton, A. 2004. Lacustrine responses to tephra deposition: Examples from Mexico. Quaternary Science Reviews 23: 2337-2353.

Evolution of monogenetic volcanism around the Pátzcuaro Lake, Michoacán, México

Susana Osorio-Ocampo[1], José Luis Macías[1], Víctor Hugo Garduño-Monroy[2], Antonio Pola-Villaseñor[1], Silvestre Cardona[2] and Laura Garcia-Sanchez[1].

[1] *Instituto de Geofísica, Universidad Nacional Autónoma de México, Ex-Hacienda de San José de La Huerta C.P. 58190, Morelia, Michoacán, México.* susanaos2000@gmail.com
[2] *Instituto de Investigaciones en Ciencias de la Tierra, Universidad Michoacana de San Nicolás de Hidalgo, Morelia, Michoacán, México.*

Keywords: volcanism, monogenetic, spatio-temporal.

Mexico has one of the largest monogenetic volcanic fields on the world known as the Michoacán-Guanajuato Volcanic Field (MGVF) Hasenaka and Charmichael (1985). The MGVF holds more than 1,000 monogenetic cones distributed in 40,000 km^2. The activity of the MGVF began during late Pliocene and has continued to the present with the eruption of Paricutin Volcano occurred between 1943 and 1952.

This work presents the evolution of volcanism around the Pátzcuaro Lake located in the central part of the MGVF at 60 km west of Morelia, the capital city of the State of Michoacán (Fig. 1). The area covers a surface of 520 km^2 including the cities of Pátzcuaro and Tzintzuntzan and small villages as the Janitzio Island.

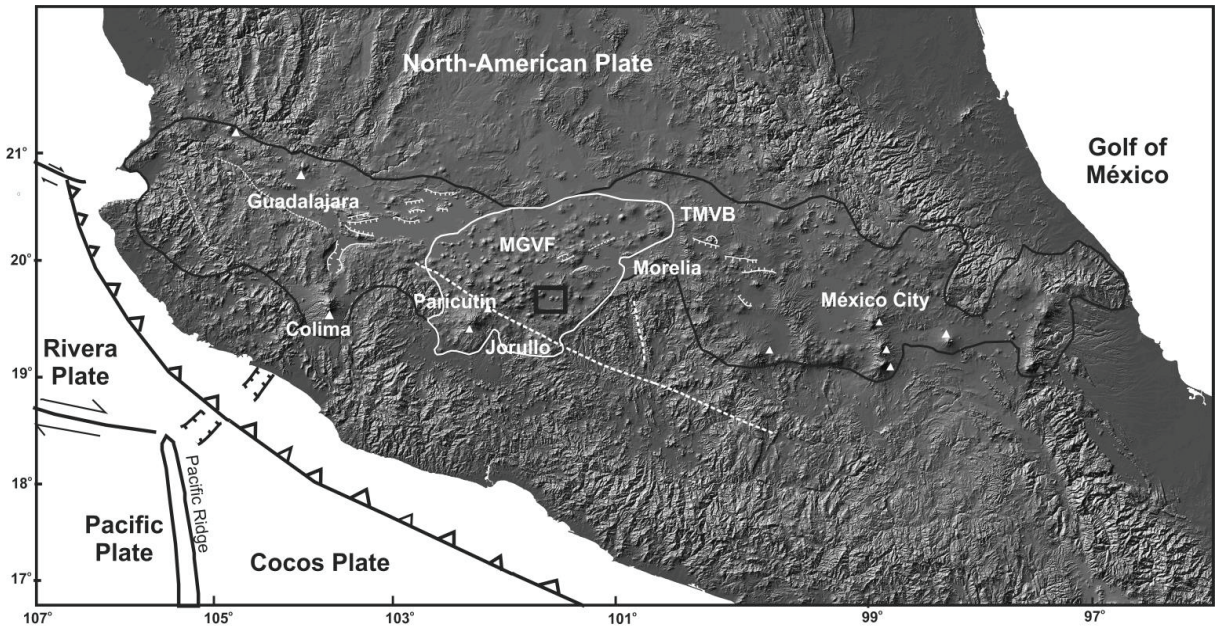

Fig 1. – General map of the central part of México showing the Transmexican Volcanic Belt (TMVB) and the Michoacan Guanajuato Volcanic Field MGVF. The black square inside MGVF represents de study area.

The area is transected by two faults systems: the oldest N-S faults belonging to the Basin and Range system while the younger NE-SW to E-W faults belong to the Morelia-Acambay Fault System (MAFS) Garduño *et al.* (2009). Several cones follow alignments parallel to these faults systems. The most recent faults are related to MAFS that respond to the regional stress σ^3, which determines the distribution of the current volcanism and is associated to two volcanic collapses of El Estribo and La Muela volcanoes (Fig. 2).

Detailed field mapping and stratigraphy aided by ^{14}C and $^{40}Ar/^{39}Ar$ dating allowed us to reconstruct the volcanic evolution of the area. There are 35 volcanic structures corresponding to 22 cinder cones, four small shield volcanoes, ten domes, two highly weathered landforms and several lava flows.

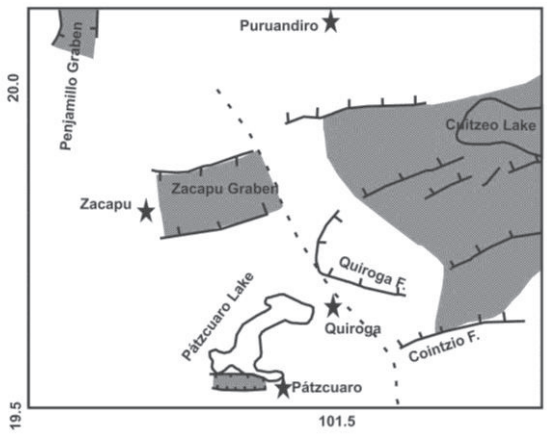

Fig 2. - Regional tectonic setting around Pátzcuaro, Garduño *et al.* (2009).

New dates allowed to determine that volcanic activity in the region started during the upper Pliocene and lower Pleistocene with the emplacement of lava domes ~2.5 Ma, followed by the construction of small shield volcanoes between ~1 and 0.4 Ma (Tariaqueri and Bosque volcanoes) during middle and upper Pleistocene. During late Pleistocene (~40 to 11 ka) were formed cinder cones due strombolian activity. Finally, during the Holocene four cinder cones were erupted (*e.g.* La Taza, 8 ka; Hasenaka and Carmichael (1985)) and the Chenadas cone (~7 ka).

The total volume produced by these volcanoes during the past 2.5 Ma was 35 km^3. We estimate effusion rates for 1 kyr of 0.003 km^3 during early Pleistocene, 0.04 km^3 for middle Pleistocene, 0.02 km^3 during late Pleistocene, and 0.14 km^3 during the Holocene.

The most abundant rocks of the volcanoes are andesitic in composition with silica contents varying from 57.12 to 62.54 wt % and a mineral association of plagioclase, olivine, clinopyroxene and orthopyroxene. In a smaller proportion occur dacites composed of plagioclase, hornblende and biotite with silica contents between 64.61 and 64.75 wt %. As a whole, silica ranges from 54.7 to 64.8 wt % with LILE (Large Ion Lithophile Elements) enrichments and depletions in Nb, Ta, and Ti typical patterns of calc-alkaline magmatic series of subduction environments.

Acknowledgements

All the Authors are kindly thanked for having submitted an abstract formatted according to this template. Many people had contributed to the development of this project. Particular thanks to the volcanology team of the Geophysical Institute Unidad Michoacán in Morelia, Michoacán lead by Dr. Macías for all the help, comments and useful discussions about this research. To the Instituto de Investigaciones en Ciencias de la Tierra from Universidad Michoacana de San Nicolás de Hidalgo in Morelia, Michoacán for the academic support.

References

Ego, F., Ansan, V., 2002. Why is the central Trans-Mexican volcanic belt (102–99 W) in transtensive deformation. Tectonophysics, 359: 189-208.

Ferrari, L., 2000. Avances en el conocimiento de la faja Volcánica Transmexicana durante la última década. Boletín de la Sociedad Geológica Mexicana, 53: 84-92.

Garduño-Monroy, V. H., Soria-Caballero, D. C., Israde-Alcántara, I., Hernández Madrigal, V. M., Rodríguez-Ramírez, A., Ostroumov, M., Mora-Chaparro, J. C., 2011. Evidence of tsunami events in the Paleolimnological record of Lake Pátzcuaro, Michoacán, México. Geofísica internacional, 50: 147-161.

Garduño-Monroy, V.H., Pérez-Lopez, R., Israde-Alcantara, I., Rodríguez-Pascua, M.A., Szynkaruk, E., Hernández-Madrigal V.M., García-Zepeda, M.L., Corona-Chávez P., Ostroumov, M., Medina-Vega, V.H., García-Estrada, G., Carranza, O., Lopez-Granados, E., Mora Chaparro, J.C., 2009. Paleoseismology of the southwestern Morelia-Acambay fault system, central México. Geofísica Internacional, 48: 319-335.

Gómez-Tuena, A., Orozco-Esquivel, M. T., Ferrari, L., 2005. Petrogénesis ígnea de la faja Volcánica Transmexicana. Boletín de la Sociedad Geológica Mexicana, 57:227-283.

Hasenaka, T., 1994. Size, distribution, and magma output rate for shield volcanoes of the Michoacán-Guanajuato volcanic field, Central Mexico. Journal of Volcanology and Geothermal Research, 63: 13-31.

Hasenaka, T., Carmichael, I., 1985a. The cinder cones of Michoacán Guanajuato central México.

Hasenaka, T., Carmichael, I., 1985b. A compilation of location, size, and geomorphological parameters of volcanoes of the Michoacan-Guanajuato volcanic field, central México. Geofísica Internacional, 24: 577-607.

Hasenaka, T., Carmichael, I., 1987. The Cinder Cones of Michoacán-Guanajuato, Central Mexico: Petrology and Chemistry. Journal of Petrology, 28: 241-269. Their age, volume, and distribution, and magma discharge rate. Journal of Volcanology and Geothermal Research, 25: 105-124.

Recent discovery of *Mammuthus columbi* embedded in volcanic ash in the Sierra Chichinautzin monogenetic field, Central México: Volcanological constraints for taphonomy

Marie-Noëlle Guilbaud[1], Lilia Arana-Salinas[1], Claus Siebe[1], Luis Alberto Barba-Pingarrón[2] and Agustín Ortiz[2]

[1] *Departamento de Vulcanología, Instituto de Geofísica, Universidad Nacional Autónoma de México, Ciudad Universitaria, Coyoacán, México DF, México.* m.guilbaud@geofisica.unam.mx
[2] *Instituto de Investigaciones Antropológicas, Universidad Nacional Autónoma de México, Ciudad Universitaria, Coyoacán, México, D.F., México.*

Keywords: Mammoth, scoria cone, geochronology.

Introduction

At the end of 2011, molars of a mammoth were found accidentally at a cornfield on the edge of a small ravine near the village of Santa Ana Tlacotenco, at the southeastern limit of Mexico City and on the northern slopes of the Sierra Chichinautzin volcanic field (Fig. 1). The systematic excavation at this location in March-May 2013 unearthed a near complete skeleton of *Mammuthus columbi* in an area of 40 m^2.

Although remains of this species of mammoth are frequently discovered in central Mexico, this new finding is at the southernmost and highest (ca. 2770 m asl) location yet found within the boundaries of the Mexico Basin (Fig. 1), sparking the interest of paleontologists.

In addition, the bones were found embedded in dark volcanic ash, raising the possibility of a relationship between the death of the animal and explosive activity at a neighboring scoria cone. The site is located at a short distance (<10 km) from several young volcanoes from which the ash embedding the bones could have originated (Fig. 1).

Stratigraphical, sedimentological, geochemical, and geochronological studies were conducted at the excavation pit and within a radius of 5 km around it in order to determine the tephra stratigraphy in the area and constrain the source of the "mammoth ash" and the age and taphonomy of the fossil remains.

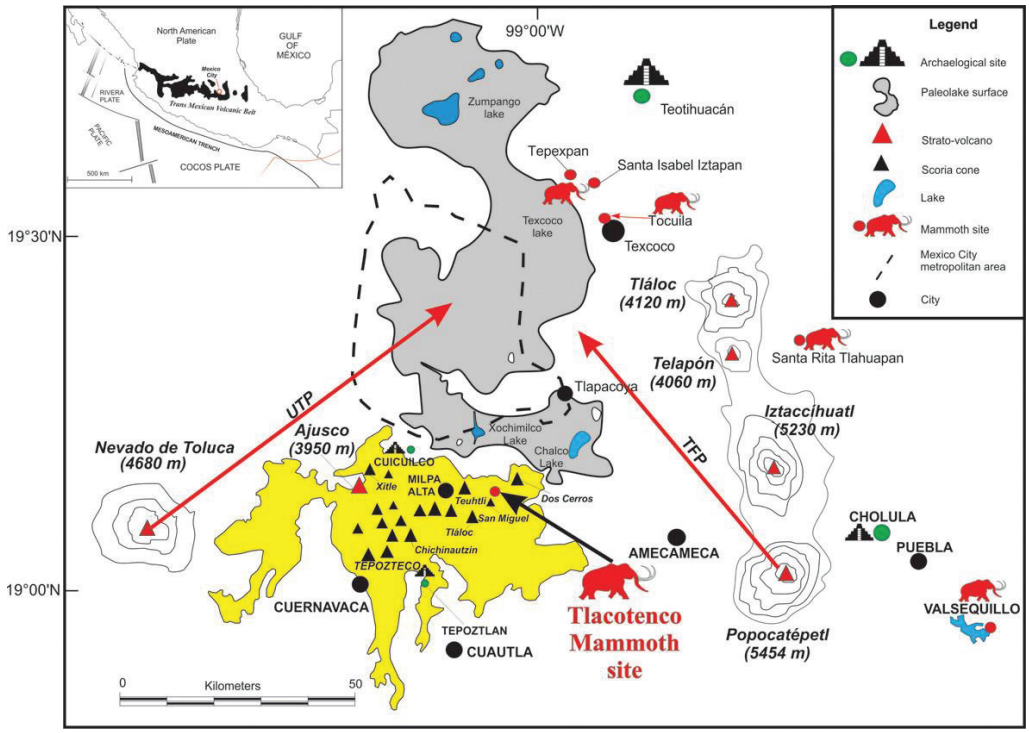

Fig. 1 – Location of the discovery site and other reported sites in the Mexico basin. In yellow is the Sierra Chichinautzin volcanic field, black triangles indicate the youngest scoria cones of this field.

A 4-Phase Model for Westeifel/Germany Alkaline Basalt Volcanoes with Initial Maar-Phase - Implications for Geoeducation

Peter Bitschene[1,2] and Bertram Schmidkonz[3]

[1] *Gerolstein Museum of Natural History, Hauptstraße 72, 54568 Gerolstein, Germany. info@naturkundemuseum-gerolstein.de*
[2] *TW Gerolsteiner Land GmbH, Gerolstein, Germany.*
[3] *Institute for Natural Sciences Education, InB, Chemistry, University of Koblenz-Landau, Germany.*

Keywords: *4-phase model, maar volcanism, geoeducation*

The Westeifel Volcanic Field (WEVOF) comprises roughly about 350 volcanic cones, lava flows, and maars, has an intraplate setting amidst the European plate, ranges in age from about 700.000 to 11.000 years BP, is nearly exclusively alkaline basaltic in composition, and is famous for being the region with the type location where the term "maar" has been coined (Steininger, 1820). Consequently, the First International Maar Conference was held there in 2000.

Looking closer at WEVOF's rocks and petrogenesis, there are interesting peculiarities such as small scale magma mixing (Woodland & Shaw, 2012), a complete suite of xenoliths from lithospheric upper mantle through all crustal levels (e. g. Haardt, 1914), and all kinds of carbonated mineral waters – the most famous one being "Gerolsteiner".

The scope of this presentation, however, is to show that the WEVOF not only is a prolific scientist's playground but also contributes its share to the region's economy and education through the valorization of its volcanic assets. Not at least in respect to a sustainable development of the region and to raise public awareness for its unique natural riches, it is necessary to deliver scientific findings with explicit volcanic content in an appealing way to the interested audience, but without loosing scientific correctness. The WEVOF also is an ideal alternative learning place for students of environmental and natural sciences, but its resources have to be put into value by appropriate information for teaching personnel (Bitschene & Schüller, 2011).

Here, a 4-phase model for the alkaline basaltic volcanism of the WEVOF is presented, which follows the need for a simple, comprehensive model, explaining the evolution of a monogenetic volcano or a small scale volcanic complex in the respective region. The model interprets landscapes, morphologies, outcrops, and deposits. It must be emphasized that the model is idealized, because not every volcano shows all four phases, and sometimes phases repeat several times in one volcano. Nevertheless, the model has been validated with pupils, students, scientists, and senior citizens.

The most prominent and representative WEVOF example is the "Rockeskyller Kopf volcanic complex", about three km NE of the town of Gerolstein. It is here, where a circular geo trail with well maintained outcrops and geo panels explains the morphologies, outcrops, and rocks using the 4-phase model (Bitschene *et al.*, 2012; Fig. 1). The close-by "Gees Drees", a carbonated mineral spring, shows the final phase with the gas emanations.

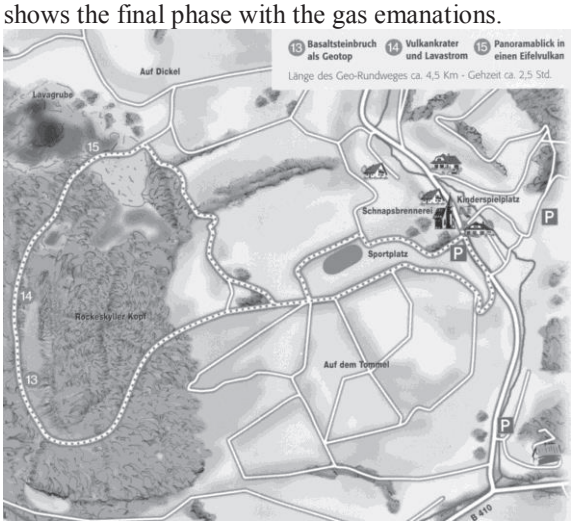

Fig. 1 – The circular geo-trail "Rockeskyller Kopf Volcanic Complex" with 3 geo sites, where phases I – III can be observed in the field and are explained with panels .

The 4-Phase-Model

Phase I: This initial volcanic activity in the lifetime of a WEVOF volcano in most cases is a hydro-volcanic eruption which opens the volcano's crater, and subsequently deepens it into the crust as long as ground water and magmatic heat and gas – and eventually magma – are available. The resulting morphology at the earth's surface is a funnel-shaped depression - a maar crater – which may be either dry or water-filled. The resulting tephra is composed of predominantly lithic clasts from the shattered wall rock, cognate basalt and upper mantle xenoliths may be present. The depositional processes are lateral mass flows, and surges. Phase I is the hydroclastic,

initial maar-building phase. Fig. 2 shows Phase I and II deposits, separated by an angular discordance.

Phase II: Ongoing explosive volcanic activity is then driven by fluid lava and volcanic gases leading to Strombolian-type eruptions. The resulting morphology is a cinder-and-ash-cone that is essentially composed of basaltic tephra. The maar crater is now filled by intra-crater basaltic tephra and covered with proximal basaltic tephra that eventually builds up a positive volcanic cone. The depositional process is mostly air-fall, with abundant spatter. Phase II is the pyroclastic, cone building Strombolian phase.

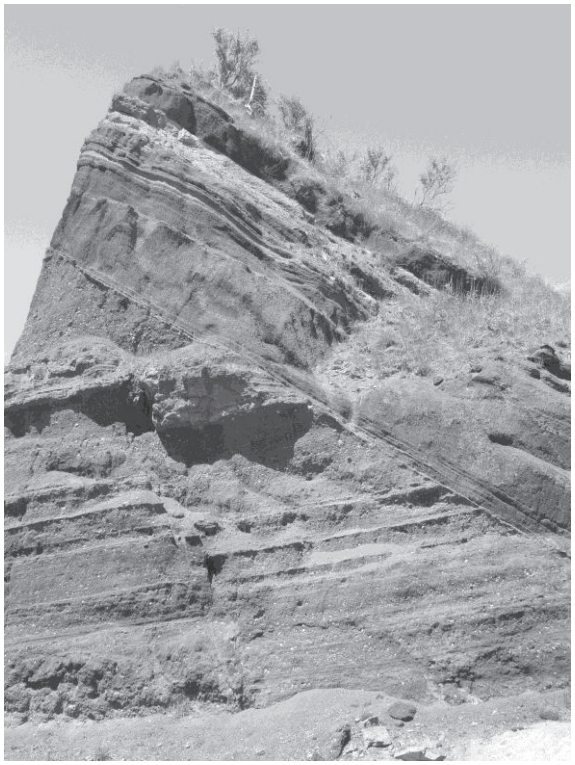

Fig. 2 - The "ship nose" outcrop at the Rockeskyller Kopf volcanic complex with Phase I (dip to the left) and phase II (dip to the right) deposits separated by a discordance which delineates the former maar crater wall.

Phase III: With rising lava output and diminishing input of water vapor and/or volcanic gases the explosive volcanic activity now turns into a quieter, effusive volcanic activity. The resulting landforms are basaltic lava plateaus and/or valley fillings. Phase III is the effusive, crater, pond and valley-filling phase.

Phase IV: Finally, the outpouring of lava stops, feeder dikes and lava lakes solidify or retreat, and the volcanic activity upon the Eifel's crust comes to an end. But within the crust, and especially within the upper mantle source region, activities continue, leading to the ongoing ubiquitous CO_2 outgassing. The volcanic outgassing can be seen as CO_2 bubbles in carbonated mineral water springs, and even cold water geysers. Phase IV is the final, CO_2-releasing Mofette phase, which is an indicator for the actually dormant but still breathing Eifel volcanism.

This 4-phase model for the WEVOF's volcanoes is simplified. Of course, some volcanoes have only seen phase I, leaving 75 maars behind, of which 10 are water-filled and thus prime geotouristic assets. Other volcanoes have seen repeated phase I through phase III volcanic activity, and in other cases phase I or phase III is missing. This model, however, can be applied for education and entertainment in the WEVOF, and maybe also in other monogenetic intraplate volcanic fields.

References

Bitschene, P. R., Schüller, A. 2011. Geo-Education and Geopark Implementation in the Vulkaneifel European Geopark. In Carena, S., Friedrich, A. M., Lammerer, B. (ed.): Geol. Field Trips in Central Western Europe. Geol. Soc. Amer., 22: 29-34.

Bitschene, P.R., Shaw, C.S.J.., Woodland, A.B. 2012. Der Vulkankomplex Rockeskyller Kopf im nationalen Geopark Vulkanland Eifel - Brennpunkt vulkanologischer Forschung und geotouristischer Inwertsetzung. In DVG (ed): Ein-Blicke – 25 Jahre Deutsche Vulkanologische Gesellschaft, 117-126.

Haardt, W.J. 1914. Die vulkanischen Auswürflinge und Basalte am Kyller Kopf bei Rockeskyll in der Eifel. Jb. Preuß. Geol. Landesanst., 35: 177-253.

Steininger, J. 1820. Die erloschenen Vulkane in der Eifel und am Niederrheine. 182 p., Mainz, Kupferberg

Shaw, C.S.J., Woodland, A.B. 2012. The role of magma mixing in the petrogenesis of mafic alkaline lavas, Rockeskyllerkopf Volcanic Complex, West Eifel, Germany. Bulletin of Volcanology 74: 359-376.

The Chaîne des Puys and Limagne Fault UNESCO World Heritage Project: a flagship project to raise awareness of monogenetic volcanism and tectonics

Cécile Olive[1], Benjamin van Wyk de Vries[2]

[1] *Conseil Générale du Puy de Dôme, Clermont-Ferrand, France. Cecile.OLIVE@cg63.fr*
[2] *Laboratoire Magmas et Volcans, Univierité Blaise Pascal, Clermont-Ferrand, France. b.vanwyk@opgc.fr*

Keywords: Chaîne des Puys, Limagne Fault, UNESCO World Heritage.

The Chaîne des Puys and Limagne fault UNESCO World Heritage project is a global partnership for raising the profile of monogenetic volcanism and rift tectonics.

Fig 1. - The central Chaîne des Puys seen from the Puy de Gouttes volcano.

The project was initiated in 2007, by the local Council of the Puy de Dôme Department in the Auvergne Region of France. Slowly the project developed from considering just the monogenetic volcanoes of the Chaîne des Puys, to encompass the Limagne Rift fault and numerous landforms that are related to the interaction of the volcanoes and the rifting. Thus, the project came to propose a tectono-volcanic ensemble, a mix of volcanism, tectonics and related surface process features.

This evolution was done to fit the project into the requirements of UNESCO, where important gaps in the World Heritage List had been identified. The project was thus conceived to fill these gaps, and to propose to the World Heritage list a novel nomination that fully illustrated major processes operating in the geological history of the Earth, backed with impressive educational facilities and a sound management plan.

The project was developed in close consultation with local stakeholders, to provide a sustainable structure, which could be used to assure the preservation, enhancement and development of the property.

The main international geological organizations, such as the IUGS, IAVECI, Smithsonian, AGU, were consulted, alongside many individual volcanologists and tectonicians. Thus, the project was developed with what UNESCO calls an 'upstream process' of constant assessment and adjustment.

The project, passed the French national selection process in 2012 and was submitted to UNESCO in 2013. The International Union for the Conservation of Nature (IUCN) was given the task of providing an expert review of the project and asked for 11 desktop reviews and a two-person field visit. The result of this was published in May 2014. At writing, the UNESCO committee will examine the projet in the light of this report in Qatar in June 2014.

Fig 2. - The Limagne Fault and the uplifted Chaîne des Puys seen from the Gravenoire volcano on the fault escapment.

Here we first provide an overview of the project and will then describe the IUCN review and the present reaction at UNESCO.

The Tectono-volcanic Ensemble of the Chaîne des Puys and the Limagne fault is made of a spectacular rift margin that uplifts an 80-strong chain of monogenetic volcanoes, with a superlative range of edifice types, a wide range of compositions and diverse eruptions types. The Interaction of the volcanism with the rift fault has produced distinctive landforms, such as relief inversion, that have sculpted the fault scarp. The whole ensemble can be

seen from a wide area in central France, with the iconic Puy de Dôme domination the chain.

From the 19th Century the Chaîne des Puys and Limagne Fault have been at the centre of discussion about the nature of volcanoes, and the origin of rifts. Part of this interest was due to the action of landowners and government agents such as Montlosier and Desmarest (who first realized that the chain were volcanoes), and national leaders such as Napoleon I, who was instrumental in the visit of Humphrey Davey and Michael Farady in 1805. The chain features largely in Scrope's 'Considerations on volcanoes' 1825, and of Bonney's 'Volcanoes their structure and significance' of 1899. The fault escarpment is discussed at length by Lyell in Principles of Geology (1830), although they did not recognize it yet as a rift.

The area has seen the development of a modern scientific – government - private partnership in research and education that has developed in parallel with the growth of an earth science centre of excellence, now the Laboratoire Magmas et Volcans.

In addition, local owners and users have taken an important part in the development of this partnership to help create a sustainable management of the area. Partnerships have been developed with other sites around the world to share best practice, especially in managing inhabited natural sites.

For over 30 years the area has been part of the evolving Auvergne Region Natural Volcano Park, for five years the central Puy de Dôme is a 'Grande site de France', equivalent to a national monument. Educational attractions grew up first as private - scientific partnerships (*e.g.* Lemptégy, Volvic, Maison de la Pierre) and then with greater public input like Vulcania and the Puy de Dome. The channeling of visitors has been accomplished by improved access by bus, and a new cog-railway up the Puy de Dôme.

The Project was submitted to UNESCO in April 2013, and was praised by World Heritage experts, the geological experts and the IUCN chosen field evaluators.

Surprisingly, the final IUCN report was totally negative. This report, however, shows a large number of gross errors and omissions:

-The monogenetic volcanoes of the Chaîne des Puys are described as only being scoria cones,
-No mention is made of the Limagne fault,
-No analysis of the erosional landforms is made,
-No mention of the domes, maars, tuff rings and intrusive topography is made,
-The volcanoes are compared with totally irrelevant landforms, such as the Grand Canyon,
-The Scientific Literature quoted is misinterpreted,

and many other errors.

The list of errors would infact take up much more than the 2 page abstract here.

The conclusion we and our Earth Science partners, like the IUGS, is that the IUCN panel do not understand geology. And this is clear from the makeup of the panel that contains no vulcanologist or tectonics expert.

In response,to the report all the major geoscience organizations, and many individual scientists have sent letters to UNESCO to point out the failings of the IUCN report and stating their continued support for the project. At present, the diplomatic and scientific discussion is going on at UNESCO.

We hope to bring you a positive outcome for this to the Maar Conference, and this presentation will examine the consequences to geoheritage of the present UNESCO reporting process, and the various discussions underway between the geoscience organizations and other conservation bodies.

This experience will serve as a model for any other geoheritage project developed around monogenetic volcanoes at UNESCO World Heritage and GEOPARK level.

Acknowledgements

All the geoscience Bodies that have supported the proejct: the ILP, IUGS, IAVCEI, the Monogenetic commission of IAVCEI, GEOPRISMS, Smithsonian, AGU, AIG, Also to some notable individuals, especially Karoly Nemeth, Joan Marti, Steve Sparks, Michael Ort, Mike Petronis, Tyrone Rooney, Claus Seibe, Servando de la Cruz Reyna, Hugo Delgado, Pablo Grosse, Matheiu Kervyn... and many more.

Geosites in a young lava flow field: the Reserva Ecológica del Pedregal de San Ángel and nearby areas, México City.

Marie-Noëlle Guilbaud[1], Jose Luis Palacio Prieto[2]

[1] *Departamento de Vulcanología, Instituto de Geofísica, Universidad Nacional Autónoma De México, Coyoacán, C.P. 04510, México D.F., m.guilbaud@geofisica.unam.mx*
[2] *Departamento de Geografía Física, Instituto de Geografía, Universidad Nacional Autónoma de México, Coyoacán, C.P. 04510, México D.F.*

Keywords: pahoehoe lavas, Sierra Chichinautzin, V. Xitle.

Introduction

The Pedregal de San Angel Ecological Reserve (REPSA) is a conservation area created in 1983 within the campus of the Universidad Nacional Autónoma de México (UNAM) located in the southern part of Mexico City. Initially encompassing an area of 1.245 km^2, the REPSA now covers a bit more than 2.37 km^2, a third part of the university campus.

The REPSA was created with the interest of maintaining an area of biological and cultural diversity containing the last remnants of natural ecosystems in southern Mexico Valley. Nevertheless, in addition to its biological interest, it is a site of geological and geomorphological significance to explain the evolution of the landscape of the southern portion of the Mexico Basin. The site also serves an important role for the recharge of shallow aquifers, and conserves evidence for early human settlements in the basin. The REPSA has thus many non-biological values that have not been adequately recognized and promoted until now.

The REPSA is located over the lava flows emitted ca. 1670 yrs ago by the Xitle scoria cone, the youngest volcano of the Sierra Chichinautzin monogenetic field that borders the south of the Mexico basin (Delgado et al. 1998, Siebe 2000). Considering that the urban area have expanded over most of the lavas, the REPSA represents one of the few remaining places where the original characteristics of the flows can be observed. In particular, the interior of the lavas is exceptionally well exposed at many cuts and quarries around the campus, making it one of the best areas in the world for the observation and study of basaltic lava flows (e.g., Walker 2009). While the surface morphology of Xitle lavas varies across the field, pahoehoe features dominate in the distal areas where the UNAM is constructed.

This study identified and characterized 9 geosites of significant value within and near the REPSA. The interests of the selected sites include volcano-stratigraphic features (sequences of lavas and pyroclastics), volcanological (lava flows, pyroclastic cones) and archaeological values. The sites also have educational value that can be incorporated into formal education schemes (as sites of interest in geology and geography courses) and informal (as information for non-specialized visitors) and contribute to the outreach of Earth Sciences, particularly Geology and Geomorphology.

Proposed geosites

The proposed geosites are located on Fig. 1 and are briefly described here. All sites are easily accessible, promoting their use for educational and touristic purposes.

1. Botanic Garden (*Jardín Botánico*).

Created in 1959, the UNAM Botanic Garden is considered the largest of Latin America. It is also a site where pahoehoe surface features are particularly well exposed, more specifically braided lava crust, tumuli, sheet lobes, inflation clefts and lava sutures. The construction of small paved paths within the garden facilitates the observation of the features.

2. Pumas quarry (*Cantera de los Pumas*).

Located near the university metro station, this site is the place of origin of the building blocks of the first UNAM buildings. Part of the site hosts the facilities of the university football team (Los Pumas). The main stratigraphic and volcanological values of the site is the exposure of a cut through 20 to 40 m of a pile of sheet to hummocky pahoehoe lava. Natural cold springs emerging from the base of the flows feed small lakes, making this site an enjoyable green area with significant esthetic as well as educational values.

3. Ecological path (*Senda Ecológica*)

Located next to UNAM scientific museum (Universum), this sites offers a “promenade” over the irregular surface of the Xitle lavas, allowing to observe the specific type of vegetation growing wildly on top of the lavas.

4. Sculptural site (*Espacio escultórico*)

This site consists of a circular structure with a diameter of 120 m that surrounds part of the lava field. Constructed for an esthetic purpose, this site also provides a view of the Xitle cone and Sierra Chichinautzin range in days with good visibility.

5. University entrance

This site presents a laterally extensive cut across a 5 m thick sheet lobe characterized by many suture zones and a variety of characteristic vesicular features. The paleosol with ceramic remains can be observed at some locations.

6. Baseball field

In this site a thick part of the paleosol underneath the lava can be observed, revealing pre-eruptive products.

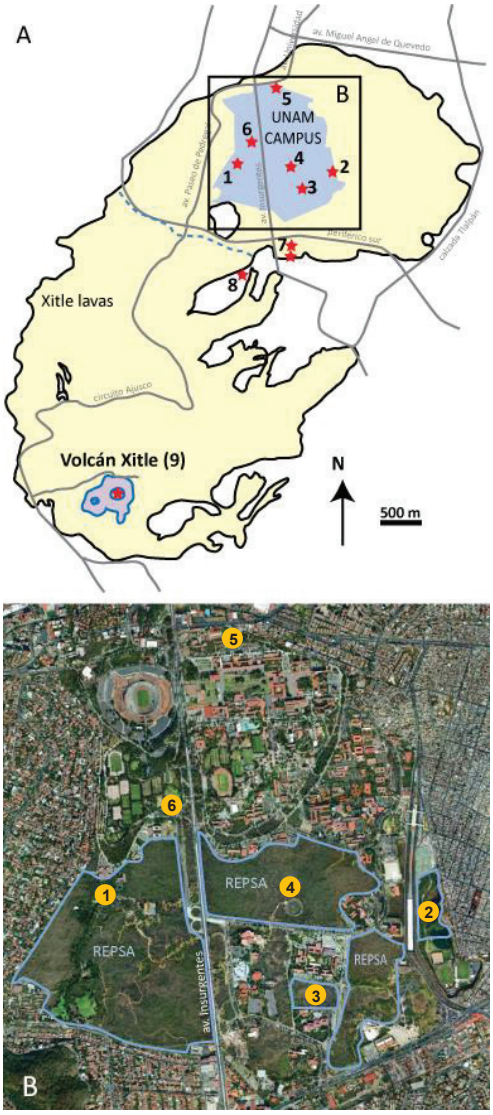

Fig. 1 – A. Location map of geosites (list in text). B. Geosites in UNAM campus and REPSA located on satellite image from Google Earth.

7. Cuicuilco: Pyramid and commercial center

This site of major archaeological interest was discovered in 1922. It represents some of the remains of an important population center that was partly buried by the Xitle lavas. Whether the site was abandoned much before or because of the Xitle eruption is still debated. Pillow lavas are exposed in a commercial center nearby.

8. Tlalpan parc

This public recreational area was established on the slopes of a small eroded scoria cone surrounded by the Xitle lavas. This pumice fallout deposits pre-dating the Xitle eruption can be observed. The lavas show there morphologies more similar to aa-type, for the greater slopes of the underlying terrain.

9. V. Xitle

V. Xitle is a well preserved 200 m high scoria cone established over a fissure. Small paths allow to climb the cone and observe proximal pyroclastic deposits and a deep crater. The distance reached by the flows, as well as their invasion by the city, can be appreciated in clear atmospheric conditions.

Conclusion

This study allowed to identify within and near the REPSA sites with important geological geomorphological values, along with archeological, historical and esthetic interests, that best characterize the landscape of the southern part of Mexico city. As in many other places, monogenetic volcanism has been frequent in this area in the past and will occur in the future, hence these geosites can serve to increase public consciousness.

Acknowledgements

Field costs were funded by UNAM-DGAPA (RR182312-2) granted to M.N.G.

References

Delgado H., Molinero R., Cervantes P., Nieto-Obregón J., Lozano-Santa Cruz R., Macías-González H.L., Mendoza-Rosales C., Silva-Romo G., 1998. Geology of Xitle volcano in southern Mexico-City, A 2000 year-old monogenetic volcano in an urban area: Revista Mexicana de Ciencias Geológicas, 15 (2), 115-131.

Siebe C., 2000. Age and archaeological implications of Xitle volcano, southwestern Basin of Mexico-City: Journal of Volcanology and Geothermal Research, 104 (1-4), 45-64.

Walker G.P.L., 2009. The endogenous growth of pahoehoe lava lobes and morphology of lava-rise edges: Studies in Volcanology: The Legacy of George Walker, edited by T. Thordarson et al., Spec. Publ. IAVCEI, 2, 17-32.

Kimberlite maar-diatreme volcanoes and diamonds, Fort à la Corne field, Canada: Process dependent tonnage, grade & value variation

Bruce Kjarsgaard

Geological Survey of Canada, Ottawa, Ontario, Canada. Bruce.Kjarsgaard@NRCan.gc.ca

Keywords: kimberlite, diatreme.

In the Fort à la Corne (FalC) kimberlite field, maar-diatreme volcanoes contain significant, high tonnage diamond deposits. There is inter- and intra-kimberlite variation with respect to deposit geometry, diamond grade (carats/100t), stone value ($US/carat) and stone size (stones/carat) that is volcanic process dependent.

The FalC kimberlite field, consisting of discrete volcanic events that span the age range 105 – 92 Ma, is hosted by a mid-Cretaceous sedimentary succession, in which the depositional environment (fluvial-deltaic, estuarine [Cantuar & Pense formations]; shallow-marine [Joli Fou & Viking formations]) is well understood (Harvey et al., 2009; Kjarsgaard et al., 2009). The kimberlite eruptive units at FalC are assigned to a specific stratigraphic formation, based on conformable depositional events. Due to the economic interest for kimberlite-hosted diamonds, there is a significant amount of information from drilling at FalC. Initially (1989 to 1998), information for an individual kimberlite body was based on single, or up to 3 or 4 widely spaced drill holes. Early volcanic models suggested the formation of large maar craters that were subsequently in-filled by pyroclastic rocks, up to 4 m.y. later. The magma for both postulated volcanic events (maar excavation and subsequent in-fill) was suggested to be fed via dykes, with no diatremes recognized. Subsequent exploration (post-1998) utilized a grid-drilling program (200 m), with additional 100 m or 50 m grid drilling on the thicker volcanic intersections, for selected kimberlites of economical interest. This resulted in the recognition that discrete 'feeder vent(s)' underlie the maar - volcanic edifice (Kjarsgaard et al., 2009). These 'feeder vents' should in fact be termed diatremes, using the nomenclature of White and Ross (2011).

A combination of drill-core logging, and 2-D and 3-D geophysics (magnetic, EM, seismic) is utilized to define the size, geometry and in-fill of three maar-diatreme complexes (Star, Orion South, Orion Central) in the FalC kimberlite field. Of importance is recognition that individual kimberlites are not simple monogenetic maar-diatremes; rather they should be considered polygenetic, or, stacked-monogenetic, with multiple volcanic episodes punctuated by sedimentation over a 4 – 10 m.y. time frame. Bulk sampling for diamonds by large diameter drilling (LDD: 24", 36", 48") and exploration shafts and drifts, within well defined volcanic units of the Star and Orion South kimberlites has enabled grade, tonnage, diamond value and average diamond size to be determined (Shore Gold, 2011).

At the Star kimberlite (surface expression ~2 x ~2.5 km), three diatremes are identified (late-Cantuar, early Joli Fou, mid/late Joli Fou). The late-Cantuar and early Joli Fou diatremes are funnel-shaped, with wall-rock contacts of ~50-60°, and similar diameters and depths of ~125, and ~200m, respectively. Diatreme in-fill is bedded (2 – 18 m) kimberlite, with minor slumps, grain flow deposits and large rotated wall rock blocks. In contrast, the mid Joli Fou diatreme is carrot-shaped, with ~80° wall rock contacts, and is ~100m x ~150m diameter and ~550 m deep. The upper ~100 m contains bedded (1 – 20 m) kimberlite, the lower ~450 m is massive, homogenous kimberlite. The diatremes for the early-Cantuar and Pense volcanic events at Star have not been located, but must be <100 m diameter, based on the grid drilling. Diamond grade and value varies significantly between volcanic units: early Cantuar ($355/c; 13.4 c/100t), early Joli Fou ($225/c; 8.6-16.1 c/100t), Pense ($175/c; 14.2 c/100t), mid/late Joli Fou ($200/c; 2.3 – 4.7c/100t). The early Joli Fou is subdivided into an inner area (diatreme and tuff ring, 16.1 c/100t) and an outer area (distal tuff ring deposits (8.6 c/100t). The diamond grade and average diamond size are related to the average olivine size in these proximal and distal kimberlite volcanic eruptive units.

At the Orion South kimberlite (surface expression ~1.5 x ~2.5 km) seven diatremes are identified along a 305° trend. A problem for defining diatreme geometry at Orion South is younger diatremes and volcanic events cut older diatremes, and some diatremes are very small and poorly defined based on drill data. The Pense diatreme, with massive in-fill, forms a flared funnel ~350 m diameter and at least 300 m deep, and underlies a tephra cone of ~900 m diameter and ~90 m (preserved) height. Two younger, steep walled

carrot-shaped early Joli Fou diatremes are separated by 1.3 km, and are ~100m diameter, in-filled with bedded kimberlite. The late Joli Fou diatreme is steep walled, filled with massive kimberlite, and of small size (<75 m dia.). Diamond grade and value varies significantly between volcanic units: Pense ($129/c; 5.8-9.3 c/100t), early Joli Fou ($192/c; 8.4-19.4 c/100t). The Pense is subdivided into an inner area (diatreme and tuff cone, 9.3 c/100t) and an outer area (distal tuff ring deposits (5.8 c/100t). The early Joli Fou is also subdivided into an inner area (diatreme and tuff ring, 19.4 c/100t) and an outer area (distal tuff ring deposits (8.4 c/100t). For both the Pense and early Joli Fou deposits, the diamond grade and average diamond size are related to the average olivine size in these proximal and distal kimberlite volcanic eruptive units.

Orion Central (#145 body; surface expression ~1 x ~.5 km) is just north of Orion South. Pittari et al. (2008) originally described two elongate crater structures (#145A, #145B). However, additional grid drilling reveals five diatremes, which are aligned along a ~325° azumith. In order of decreasing age, these are Cantuar, early Joli Fou-1, early Joli Fou-2 north, and eJF-2 south that is a twin diatreme, which is separated by in-situ sediments. Each of these diatremes is <100 m in diameter, based on the grid drilling. The location of a sixth diatreme that corresponds to another volcanic episode is unknown, but must also be of small (< 100 m) size. All of the Orion Central diatremes are interpreted as fairly steep walled (carrot-shaped rather than funnel-shaped). Diamond grade information is limited, mostly microdiamonds (from caustic fusion), and limited macrodiamonds (from LDD), but shows a strong relationship with volcanic eruptive unit.

In FalC, kimberlite diatremes are typically small, often less than 100 m diameter, and steep walled and carrot-shaped. Larger diatremes, up to ~350 m diameter are not as common and tend to be more funnel shaped. The diatremes underlie much larger volcanic edifices, which range in geometry from tuff cones to tuff rings. The size and geometry of the kimberlite edifice-maar-diatreme is process controlled (variably dry to phreatomagmatic eruptions) and there is also a strong relationship between process and diamond grade and average diamond size, the latter which heavily influences diamond value.

Acknowledgements

Shore Gold, De Beers Canada Exploration, Uranerz Exploration and Mining, and Kensington Resources are thanked for access and collaboration from 1991 to 2009.

References

Harvey, S., Kjarsgaard, B.A., McClintock, M., Shimell, M., Fourie, P.D., Du Plessis, P. and Read, G. (2009). Geology and evaluation of the Star and Orion South kimberlites, Fort à la Corne, Canada. Lithos, v. 112S, p. 47-60.

Kjarsgaard, B.A., Harvey, S., McClintock, M., Zonneveld, J.P., Du Plessis, P., D. McNeil, D. and Heaman, L.M. (2009). Geology of the Orion South kimberlite, Fort à la Corne, Canada. Lithos, v. 112S, p. 600-618.

Pittari, A., Cas, R.A.F., Lefebvre, N., Robey, J., Kurzlaukis, S., and Webb, K. (2008). Eruption processes and facies architecture of the Orion Central kimberlite complex, Fort a la corne fied, Saskatchewan: kimberlite mass flow deposits in a sedimentary basin. Journal of Volcanology and Geothermal Research, v. 174, p. 152-170.

Shore Gold (2011). Technical Report on the feasibility study and updated mineral reserve for the Star-Orion South Diamond Project, Fort à la Corne, Saskatchewan, Canada, 404 p.

White, J. and Ross, P-S. (2011). Maar-diatreme volcanoes: A review. Journal of Volcanology and Geothermal Research, v. 201, p. 1-29.

K E Y N O T E

Magma meets water: when does it explode - when not?

Bernd Zimanowski

Physikalisch Vulkanologisches Labor, Universität Würzburg, Pleicherwall 1, D-97070 Würzburg, Germany,
zimano@mail.uni-wuerzburg.de, www.vulkanologie.uni-wuerzburg.de

Keywords: experimental volcanology, magma-water interaction, thermal granulation, phreatomagmatic explosion.

Explosive magma-water interaction is generally accepted to be an important process of explosive phreatomagmatic volcanism and many colleagues believe that phreatomagmatic explosions are a key process in the formation of maar-diatreme volcanoes. Despite some work has been done in the past decades and the physics seem to be quite well understood (Büttner and Zimanowski, 1998, Büttner *et al.*, 2005, Wohletz *et al.*, 2013), some important open questions still need to be addressed, namely: what are the exact conditions for the transition from non-explosive to explosive magma-water contact and what role plays the water (or coolant) temperature? How big can single explosions get and from how deep (*e.g.* in a diatreme) can they therefore cause an eruption at the surface (Valentine *et al.*, 2014)?

Experiments on non-explosive magma-water interactions have demonstrated the importance of the water temperature (Figure 1). Water- (or in general watery coolant) temperatures control the stability of the insulating vapour films. The closer to the boiling point, the more stable is the film. This has a major influence on the time available for the formation of magma-water premixes. Thus, under otherwise identical conditions, larger premixes can form under hydrothermal conditions.

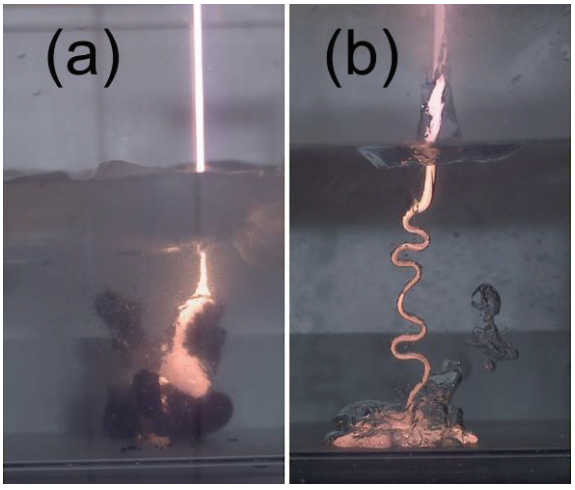

Fig. 1 – Jets of basaltic melt at 1200 °C poured into water: a) water temperature 3°C, b) water temperature at 90 °C. Frames taken from videos (300 Fps) at identical time after jet entry, size=15 x 26 cm.

The question if such premixes under increased coolant temperatures are more or less likely to explode still needs to be answered.

Phreatomagmatic explosion can generally described in 4 Phases: a) premix phase, where magma and water get in contact and form an explosive mix; b) trigger phase, where the onset of explosive heat transfer is initiated and "synchronized"; c) thermo-hydraulic explosion phase, where heat-transfer and magma fragmentation takes place in a positive feedback mechanism and where most of the explosion energy is released by shockwave-generation; d) expansion phase, where depressurization, steam generation and system expansion, initiate the following phreatomagmatic eruption (Figure 2).

Fig. 2 – Early part of post explosive expansion phase. High velocity cool particles separate from low velocity hot particles. Melt from basaltic eruption of Grimsvötn 2004 (Iceland) at 1200 °C. Frame from high-speed recording at 5000 fps, aperture time 100 µs, size=65 x 50 cm.

A modified setup featuring high speed high resolution data and video recording was developed at our laboratory to obtain more detailed information on trigger, heat transfer, and expansion times during explosive magma-water interactions. The setup also features direct observation of the onsets of the trigger, the explosion, and the system expansion. This way the time available for a coherent triggering can be measured, *i.e.* the time window between arrival of the trigger signal and system expansion. In

addition, the time available for the thermo-hydraulic fragmentation and heat transfer can now be measured in much higher precession, thus allowing to calculate the power generation and to test and improve thermodynamic models. The critical time between arrival of the trigger signal and system expansion measured ranged from 250 µs to 900 µs. This measurements so far are all done using water at room temperature. It is planned to retrofit the set-up with a device that allows coolant temperature control over a wide range (which is unexpectedly tasking). Nevertheless it is clear, that for a single phreatomagmatic pulse a premix volume is restricted to a specific size that can be synchronous triggered on a specific time scale. Thus, independent of the availability of magma and water, the intensity of a phreatomagmatic explosion is limited! If several premix volumes have formed apart from each other within an extended magmatic feeder-, it is very likely, that one explosion will trigger others. Unfortunately no experimental or observational data exist about whether such a scenario can lead to additional escalations. We hope that large scale experimentation, which will be undertaken by our friends and partners at the Natural Hazard Centre of SUNY at Buffalo, will cast more light into this problems in the near future.

References

Büttner, R., and Zimanowski, B., 1998, Physics of thermo-hydraulic explosions. Phys. Rev. E. 57, 5726-5729.

Büttner, R., Zimanowski, B., Mohrholz, C.O., and Kümmel, R., 2005, Analysis of thermohydraulic explosion energetics. J. Appl. Phys. 98, 043524.

Spitznagel, N., Dürig, T., and Zimanowski, B., 2013, Trigger- and heat-transfer times measured during experimental molten-fuel coolant interactions. AIP Advances 3, 102128, doi: 10.1063/1.4827023.

Valentine, G.A., Graettinger, A.H., and Sonder, I, 2014, Explosion depths for phreatomagmatic eruptions. Geophys. Res. Lett. Doi: 10.1002/2014GL0600096.

Wohletz, K., Zimanowski, B., and Büttner, R., 2013, Magma-water interactions, in Fagents, S.A., Gregg, T.K.P., and Lopes, R.M.C., eds., Modeling Volcanic Processes. Cambridge University Press (ISBN 978052 1895439), 230-257.

Tracing lithics in maar-diatreme deposits using experiments

Alison H. Graettinger[1], Greg Valentine[1], Ingo Sonder[1], Pierre-Simon Ross[2], James.D.L. White[3], J. Taddeucci[4]

[1] *University at Buffalo, Center for Geohazard Studies, Buffalo, NY, 14260, USA. ahgraett@buffalo.edu*
[2] *Institut National de la Recherche Scientifique, Centre Eau Terre Environnement, 490, Rue de la Couronne, Quebec, Quebec, Canada.*
[3] *Geology Department, University of Otago, Dunedin, New Zealand.*
[4] *Instituto Nazionale di Geofisica e Vulcanologia (INGV), Rome, Italy.*

Keywords: maar-diatreme, components, lithics.

Maar-diatreme volcanoes are characterized by a crater extending below the ground surface underlain by a downward tapering structure composed of mixtures of pyroclastic material and intrusions resulting from multiple subsurface explosions. The components within the diatreme include juvenile pyroclasts, country rock lithics and compound clasts. The distribution of country rock lithics within surficial deposits (i.e. tephra ring and distal ejecta) is dependent on their original configuration and the distribution of materials in the diatreme. Meter-scale blast experiments were used to investigate how materials from a layered substrate were distributed in subsurface and surface deposits as a result of individual and multiple subsurface explosions.

These experiments used chemical explosives at variable depths in constructed substrates of layered sands and gravels. Each experimental pad was used for between one and three blasts with measurements and sampling between each blast. The substrate layers were 15 cm thick and made of five distinct materials. Samples of ejecta were collected from two arrays of 0.25 m^2 boxes at 1 m intervals radiating from explosion epicenters. Additional samples were collected during excavation of the subcrater structure. These samples were used to determine the areal distribution of ejecta, the mass per unit area concentration of ejecta, the componentry of the ejecta and the componentry of diatreme deposits.

Ejecta deposits produced by these discrete blasts were divided up into three zones: proximal (constructional feature), medial (continuous blanket of ejecta) and distal (isolated clasts). The distribution of ejecta with distance from the crater is controlled by the scaled depth (the depth of charge placement divided by the cube root of the energy) and the presence or absence of a crater or retarc (inverted crater) (Ohba *et al.* 2002; Graettinger *et al.* 2014; Taddeucci *et al.* 2013). These topographic features exert a geometric effect on ejecta jets and represent conditions where the aggregate was already partially disrupted. The shape of the jet produced reflects the starting conditions (scaled depth, crater geometry) and the jet shape in turn influences the maximum extent of ejecta distribution. These trends showed some variation between the ejecta regions. The distance from the crater where medial ejecta was maximum with a scaled depth of 0.004 $m/J^{-1/3}$, corresponding to the optimal scaled depth for crater excavation (Fig. 1a; Bening and Kurtz 1967). Distal ejecta however showed a steady increase in distribution with decreasing scaled depth (Graettinger *et al.* 2014; Fig. 1b). The only explosions that produced extra-crater deposits were those with scaled depths of < 0.006 $m/J^{1/3}$. Medial ejecta dominates the volume of deposits from blasts through undisturbed experimental pads (Graettinger *et al.* 2014) and craters that had experienced at least three blasts. Other blast configurations produced predominantly proximal ejecta.

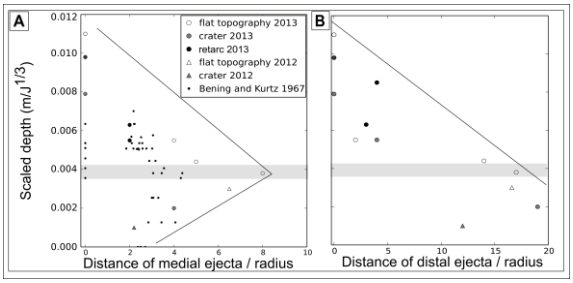

Fig. 1 – Distribution of ejecta with scaled depth (see text for definition). A) Medial ejecta distribution peaks with optimal scaled depth as crater size also peaks. Additional data from Bening and Kurtz (1967) blast experiments show similar trends. B) Distal ejecta distribution continues to increase as scaled depth decreases (adapted from Graettinger *et al.* 2014).

For blasts with large scaled depths subsidence pits were produced at the surface, and in the subsurface there was evidence of both upward and downward mixing. For deposits that produced extra-crater deposits there was an inverse stratigraphy of components in the proximal ejecta construction (tephra ring analog). Additionally, deeper materials were ejected close to and within the crater with progressively shallower material deposited further away (Fig. 2). The overwhelming bulk of proximal deposits were from layers above the blast, with

medial and distal ejecta typically containing material from only the top two layers. With one exception materials from the layer where the charge was located (and deeper) were absent in extra-crater deposits.

The componentry of the ejecta evolved with each progressive blast with progressively fewer clasts sourced from the top layer as it was removed from the crater area. This evolution also involved an increase in the abundance of deeper materials with subsequent blasts. Consequently, components that originated from the charge depth, or deeper, only made it out of the crater after repeated explosions in the same crater.

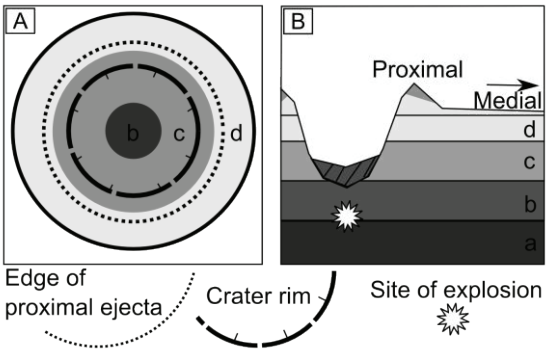

Fig. 2 – Idealized schematic of ejecta distribution resulting from blast experiments through layered stratigraphy where units are alphabetical from oldest to youngest. A) Map view of crater componentry and major constructional features. Deeper components occur within the crater and get shallower with distance from the crater. B) Cross-sectional view of crater with accentuated crater. Hatched material at bottom of crater is mixed shallow units (b,c,d) and proximal ring contains shallow material overlain by some deeper materials (c) .

The mixing of layered strata by subsurface explosions is a fitting analog for surface and subsurface structures of maar-diatreme volcanoes. These experiments indicate that extra-crater ejecta is sourced predominantly from layers above the explosion site. Deeper materials can be erupted from the crater after multiple explosions that have mixed the pyroclastic material within a diatreme. In the experiments, material was only ejected from the crater to form ejecta deposits when the scaled depth was fairly shallow supporting volume-based estimates of Valentine *et al.* (2014). Experiments such as these are important for integrating our understanding of physical processes and the deposits produced, particularly in systems where the bulk of processes occur in the subsurface. These experiments will also help with our interpretation of the geologic record, in particular how to interpret the presence of deep crustal lithics in tephra ring deposits. The presence of these clasts is indicative of the depth of diatreme activity, but do not indicate that they were emplaced directly by an explosion that occurred at the depth of origin. Additionally, the dataset collected from these experiments can be used to investigate the processes that occur at any discrete blast eruption where clast transport and deposition is dominated by ballistic processes.

Acknowledgements

This work was funded by the 3E Fund at the University at Buffalo.

References

Bening, R. G., and M. K. Kurtz (1967). The formation of a crater as observed in a series of laboratory-scale cratering experiments, report number PNE-5011, 63 pp., U.S. Army Eng. Nucl. Cratering Group, Livermore, Calif.

Graettinger, A.H.; Valentine, G.A.; Sonder, I.; Ross, P.-S.; White, J.D.L.; Taddeucci, J. (2014). Maar-diatreme geometry and deposits: Subsurface blast experiments with variable explosion depth, Geochemistry, Geophysics and Geosystems, 15, doi: 10.1002/2013GC005189.

Ohba, T., Taniguchi, H., Oshima, H., Yoshida, M., and Goto, A. (2002). Effect of explosion energy and depth on the nature of explosion cloud: A field experimental study, J. Volcanol. Geotherm. Res., 115, 33–42.

Taddeucci, J., Valentine, G.A., Sonder, I., White, J.D., Ross, P.-S., and Scarlato, P. (2013). The effect of pre-existing crater on the initial development of explosive volcanic eruptions: An experimental investigation, Geophys. Res. Lett., 40, 507–510, doi:10.1002/grl.50176.

Valentine, G.A., Graettinger, A.H., Sonder, I., (2014). Explosion depths for phreatomagmatic eruptions. Geophysical Research Letters, doi: 10.1002/2014GL060096.

Spatial distribution of ballistic clasts of the Atexcac Maar (central Mexico): implications for the morphology of the crater

Mario López and Gerardo Carrasco-Núñez

Centro de Geociencias, Universidad Nacional Autónoma de México, UNAM, Campus Juriquilla, Querétaro, México.
mario_lopr@geociencias.unam.mx

Keywords: maar volcanoes, ballistics, trajectories, facies.

Atexcac volcano is an explosion crater located in the central part of the Serdán-Oriental basin in the eastern Mexican Volcanic Belt. This basin is dotted with several volcanic structures such as basaltic cinder cones, rhyolitic domes and about a dozen of maar volcanoes of either basaltic or rhyolitic composition. The Atexcac crater has an elliptical shape with diameters between 1150 and 850 m, being the largest dimension in the ENE direction (Fig. 1). It was formed during phreatomagmatic explosions that reveals strong fluctuations in the availability of external water, temporal migration of the locus of explosions and periodic injection of magma (Carrasco-Núñez et al., 2007). The stratigraphy of Atexcac crater was described by Carrasco et al. (2007), who proposed 3 main sequences: pre-maar, integrated for a Mesozoic limestone basement, a lava flow, a cinder cone scoria, and a brown-tuff intercalated with silicic ash layers; the maar sequence, where we described the stratigraphic facies and measure ballistic blocks, and the post-maar sequence that contains a obsidian breccia and an uppermost soil.

Explosions forming the maar sequence in Atexcac crater were accompanied by ballistic blocks of different compositions. Velocities of those blocks were modeled, resulting at infrasonic speed (~ 0.3 Mach). The equations governing the travel of the ballistic blocks are based on the second law of Newton (Wilson, 1972):

$$\frac{\partial Vx}{\partial t} = -\frac{\rho_a . C_D . A . Vx^2}{2m} \qquad (1)$$

$$\frac{\partial Vy}{\partial t} = -\frac{\rho_a . C_D . A . Vy^2}{2m} - g \qquad (2)$$

Where ρ_a is air density, C_D is drag coefficient, A is cross section of fragment, Vx and Vy are components of the exit fragment´s velocity and m is the mass. This model assumes that the drag force due to resistance to atmospheric air is proportional to the square of the fragment´s velocity that is transported through this medium (Sherwood, 1967).

Maars are volcanic craters resulted from explosive interactions of an ascending magma body with external water contained in an aquifer that produce the successive deposition of fall and surges layers. The magma/ water interactions control the magma fragmentation in the phreatomagmatic explosions and, in some cases, these interactions are not efficient and may originate ballistics fragments of the country rock or fresh magma, which exit to the atmosphere with trajectories almost parabolic, rather hyperbolic, due to the resistance that offer the air when the fragments are transported through the atmosphere. Experimentally, ejection velocities in explosive molten-fuel-coolant interactions has been obtained by Büttner et al. (2002) and Zimanowski et al. (1997a) in 100 and 75 m/s, respectively. Self et al. (1980) estimated velocities of 100 m/s for large blocks at Ukinrek maars.

Fig. 1 – Panoramic view of Atexcac crater showing the elongation of the crater in the ENE direction. Photo was taken from northwest.

As the pyroclastic deposits (fall deposits and surge layers) forming the Atexac crater are mostly associated with dry conditions, no many bomb sags are formed and is not very easy to find conditions to infer ballistic trajectories. We only take into account ballistics with elongated shape because ballistic projectiles are ejected from the explosive locus following a parallel trajectory to its larger diameter, but they may turn around along this diameter during the travel. Thus, the projectile will remain with its major axis on direction of its trajectory. The resistance of air changes slightly the trajectory of ballistics when they are transported through the

atmosphere, varying from a parabolic to a hyperbolic trajectory.

Ballistics projectiles were emplaced on different facies of the stratigraphic sequence of Atexcac Maar. Six different volcanic facies were identified considering variations in grain size, structures and stratification. The facies dominated by the alternation of lapilli breccias and stratified ash are the most abundant. Ballistics were found in all types of facies. The larger ballistics (Fig. 2) are intrusive rocks (some with diameter larger than 2.3 m). The median diameter varies from 10 cm 1.4 m.

In order to reconstruct ballistic trajectories we used the so called Eject software, version 1.4 (Mastin, 2008) with the next considerations and assumptions: air drag coefficient for ellipsoidal shapes (Mironer, 1979); different densities of blocks (basalt, andesite, intrusive, juvenile and limestone); initial velocities of 100-120 m/s; ejection angle between 45 and 85 degrees and distance between of impact point and lake water level. We consider in the modeling, the most likely site of the ballistics exit, and for that we used angles of 45° and 85° and its midpoint. We defined two likely main zones of ballistic ejecta, one dominated by basalt and limestone blocks, and another one by andesite, intrusive and juvenile blocks.

Fig. 2 – One of the largest ballistic blocks (2.3 m in diameter for the longest dimension). It corresponds to an intrusive rock emplaced to the south wall of Atexcac crater. Source is to the right-hand side.

We present an inverse study inferring trajectories of ballistics blocks emplaced in different facies and try to explain the lateral migration of explosive locus during the evolution of this maar volcano. The inferences about alternation of different explosive locus try to explain the morphology of crater as it can be seen today.

Maar volcanoes are formed by fragmentation of the wall-rocks during explosive interactions and the ejection of large amounts of these wallrock clasts, together with juvenile casts, result in loss of mass at the level of explosions and the consequent wall rock instability. However, the generalized model where the collapse and downward displacement of the explosion foci is proposed (Lorenz, 1986) cannot be applied in the case of Atexcac crater. The variable vent sources proposed in this paper suggests an alternation of the explosive locus in different zones inside of crater. The explosions started in the southwest sector and migrated to the north and then a more chaotic trend occurred with sometimes simultaneous active vents. The study of ballistics may be a very good tool to analyze the evolution and morphology of a maar volcano like Atexcac and others in which there was a migration of the explosive locus.

Acknowledgements

This work was supported by CONACYT grant 15090 and PAPIIT IN-106314 and logistical support by Centro de Geociencias (UNAM). Reviews by Gerardo Aguirre were very useful for this work. We want to thank Lorena De León and Luis Rocha for helping us in the field.

References

Büttner, R., Dellino, P., La Volpe, L., Lorenz, V., Zimanowski, B., 2002. Thermohydraulic explosions in phreatomagmatic eruptions as evidenced by comparision between pyroclasts and products from Molten Fuel Interaction experiments. Journal of Geophysical Research 107: (B11).

Carrasco-Núñez, G., Ort, M., Romero, C., 2007. Evolution and hydorlogical conditions of a maar volcano (Atexcac crater, Eastern Mexico). Journal of Volcanology and Geothermal Research 159: 179-197.

Lorenz, V., 1986. On the growth of maars and diatremes and its relevance to the formation of tuff rings. Bulletin of Volcanology 48: 265-274.

Mastin, L., 2008. A simple calculator of ballistics trajectories for blocks ejected during volcanic eruptions, version 1.4, U.S. Geol. Sur. Open File Rep., 01-45.

Mironer, A., 1979. Engineering fluid mechanics: New York. McGraw-Hill, 592 p.

Self, S., Kienle, J., Huot, J.-P., 1980. Ukinrek maars, Alaska, II, deposits and formation of the 1977 craters. Journal of Volcanology and Geothermal Research 7: 39-65.

Sherwood, A., E., 1967. Effect of air drag on particles ejected during explosive cratering. Journal of Geophysical Research 72: 1783-1791.

Wilson, L., 1972. Explosive volcanic eruptions II, the atmospheric trajectories of pyroclasts. Geophysical Journal of the Royal Astronomical Society (London) 30: 381-392.

Zimanowski, B., Büttner, R., Lorenz, V., 1997a. Premixing of magma and water in MFCI experiments. Bulletin of Volcanology 68: 419-495.

Large-scale experients on overpressured jets justify the eruptive regime of superficial phreatomagmatic explosions

Pierfrancesco Dellino[1], Bernd Zimanowski[2]

[1] *Dipartimento di Scienze della Terra e Geoambientali, Università di Bari, Italy.* *pierfrancesco.dellino@uniba.it*
[2] *Physical Volcanology Laboratory, University of Wuerzburg, Germany.*

Keywords: overpressured jets, cocktail jets, pyroclastic density currents.

Large-scale experiments on overpressured jets, where the eruptive gas-particle mixture issues from the vent at a pressure much higher than atmospheric, are carried out and compared with experiments where the highly concentrated gas-particle mixture issues from the vent balanced in pressure with atmosphere (Dellino *et al.*, 2007). Ovepressured jets are strongly impulsive and upon issuing from the vent generate a radially expanding cloud that diffusely spreads on the ground resembling the cocktail jets structures (Fig. 1) of the eruptive clouds of recent phreatomagmatic eruptions. The cloud then propagates on the ground as a diluted pyroclastic density current. Most of the initial dilution in particle concentration is due to the in-air expansion of the cloud at the conduit exit. This is different from what happens with high-concentration eruptive columns that form by pressure balanced jets and evolve as collapsing fountains. At the collapse site, massive deposits are formed, whereas with increasing distance from the vent a turbulent current develops and lead to the formation of a fine laminated facies of deposits (Dellino *et al.*, 2010). Deposits formed by overpressured jets are always finely laminated with tractional structures, lacking in the massive layers. These difference in the eruptive regime and in the associated deposits can justify the difference from sustained pyroclastic flows formed by collapsinig fountains and impulsive diluted base surges associated with phreatomatmacig volcanism. The nature of overpressured jets is compatble with repeated superficial magma fragmentation events, which are typical of eruptions originating from magma interaction with a low-depth aquifer. The facies architecture of deposits can help intepreting ancient eruptions as due to pressure balanced collapsing columns or to impulsive overpressured jets, thus contributing to elucidate the regime and initial conditions of explosive volcanic events.

Fig. 1 – Formation of cocktail jets as a result of an ovepressured jets experiment.

References

Dellino, P., Buttner, R., Dioguardi, F., Doronzo, D.M., La Volpe, L., Mele, D., Sonder, I., Sulpizio, R., Zimanowski, B., 2010. Experimental evidence links volcanic particle characteristics to pyroclastic flow hazard. Earth and Planetary Science Letters 295: 314-320.

Dellino, P., Zimanowski, B., Buttner, R., La Volpe, L., Mele, D., Sulpizio, R., 2007. Large-scale experiments on the mechanics of pyroclastic flows: Design, engineering, and first results. Journal of Geophysical Research 112 DOI: 10.1029/2006JB004313

The formation of bomb-sags during phreatic eruptions: meso-scale experiments

Joshua Méndez[1], Andrew Gase[2], and Josef Dufek[1]

[1] *School of Earth and Atmospheric Sciences, Georgia Institute of Technology, Atlanta, Georgia, USA.* ub313@gatech.edu
[2] *Department of Geosciences, Boise State University, Boise, Idaho, USA.*

Keywords: maar, bomb-sag, keywords.

Bomb sags are impact features produced when volcanic bombs impact a water saturated substrate. These features are generally associated with phreatic eruptions. Because substantial amounts of water are involved in these eruptions, surge deposits often display signs of plastic deformation due to cohesion between grains. Consequently, when ejected bombs impact the syn-eruptive wet base surge deposits, they do not destroy the layering but merely deform it.

Previous work used experiments to relate impact energy to the depth of the bomb sag, both in wet and dry sediments (Manga et al., 2012). The experiments showed that the cohesive, deformed layers below bomb sags require water saturation of the volcanic deposit. They also demonstrated that over the energy range accessed in the lab experiments, the depth of the impact scales nearly linearly with the energy of the impactor. In their experiments, Manga et al., (2012) employed an empirical relationship between the substrate deformation and the impact velocity of a mock clast.

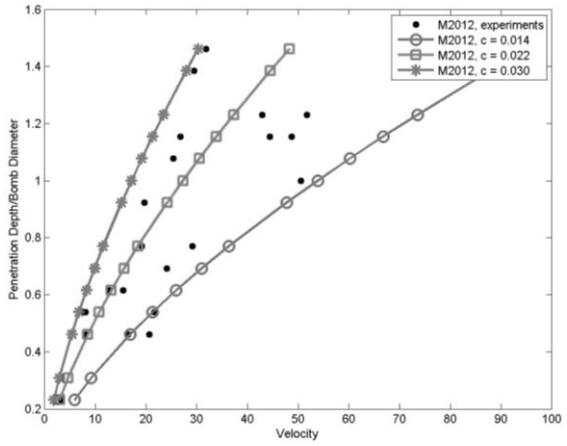

Fig. 1 – Relationship between the ratio of penetration depth to clast diameter and impactor velocity as presented in Manga et al., (2012).

Despite the crucial role of water in the development of impact sags, it is complicated to formulate energy dissipation relationships for wet granular media without any prior information of pore fluid distribution. As such, the empirical formulation for impacts into dry granular systems developed by Mitarai et al., (2006) was used by Manga et al., (2012) to relate the morphology of bomb sags and impactor velocity. In that work, they imposed all binder fluid influences into a proportionality constant, c. This treatment allowed Manga and others to relate the ratio of bed deformation to clast diameter, d/D, to the velocity of the clast at impact, V, in the following manner:

$$\frac{V^2}{gD} = \left(\frac{c}{dD}\right)^3 \left(\frac{\rho_b}{\rho_s}\right)^{-\frac{3}{2}} \left(\frac{1}{tan\,(\theta)}\right)^{-3} \qquad (1)$$

In Eq. (1) g is the acceleration due to gravity, ρ_s is the average substrate density, ρ_b is the density of the impactor, and θ is the angle of repose of the wet substrate particles. Experimentally, Manga et al., (2012) found c to be 0.022 +/- 0.008. Their results are shown in Fig. (1), which plots the dimensionless penetration depth (depth d divided by the bomb diameter D) as a function of the measured impact velocity.

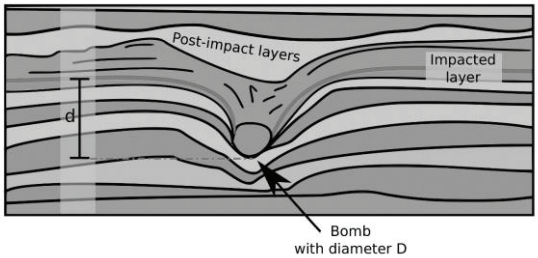

Fig. 2 – Schematic diagram of a typical bomb sag morphology, illustrating the measurements made in the field.

To explore the applicability of the model delineated above we composed a large bomb sag dataset (~200 bomb sags) from nine maars in Mexico and the United States. Seven of the nine maars are located in the Serdán-Oriental Volcanic Field (SOVF – Puebla-Veracruz, Mexico). Impacts in the deposits of Ubehebe Crater (UC - California, USA) and Large Soda Lake (LSO – Nevada) were also characterized. At each site, we measured the depth of penetration, d; the effective diameter of the

bomb, D; the composition of the bomb; the composition of the substrate; and, if possible, the angle of impact of the bomb. We take the penetration depth to be the vertical distance from the bottom of the bomb to the top of the impacted layer in the far-field (undeformed region approximately 10 bomb diameters away). The impacted layer is defined as the layer that is pinched immediately beneath the bomb. The effective bomb diameter is the average of the long and short axes. See Fig. (2).

Using the relationship in Eq. (1), impact velocities were calculated. Additionally, ejection velocities and ballistic trajectories were estimated using a numerical model similar to Eject!, which incorporates the effects of atmospheric drag. The main difference between Eject! and our model is how the drag coefficients are computed.

We calculate drag coefficients using the equations described in Parmar et al., (2010). This model makes use of the dimensionless Reynolds and Mach numbers.

While the range of values obtained previously for the substrate constant, c, provided reasonable impact velocities for the smallest of bombs in our dataset (D < 5 cm), they yielded extremely high velocities for larger bombs. Indeed, for some bomb sags, the velocities required to form the sags would have been in excess of terminal velocity. Given that the experiments used to ascertain the value of *c* (0.022 +/- 0.008) used impactors with diameters of 1-2 cm, we believe that Eq. (1) holds true for small impactors, but a different relationship must be used for bombs with a diameter larger than a few tens of millimeters.

In this work, we present our progress on developing an extended bomb-sag formation model applicable to larger clasts. To assess the interaction between larger bombs and a water-saturated substrate we constructed a pneumatic cannon capable of projecting clasts with diameters of up to 10 cm. Spherical clasts were machined from natural basalt. A 1 x 1 x 0.5 meter volume of wet sand was used as a substrate. The dimensions of the substrate bed were chosen to minimize edge effects. Experiments were conducted with different impact velocities (20 and 50 m/s) and a range of substrate granulometries.

Acknowledgements

The authors would like to acknowledge Julian McAdams for his help building the cannon and running experiments. We would also like to than Dr. Gerardo Carrasco Núñez for his information about accessing the SOVF maars and his time in the field.

References

Manga, M., Patel, A., Dufek, J., & Kite, E. S. (2012). Wet surface and dense atmosphere on early Mars suggested by the bomb sag at Home Plate, Mars. Geophysical Research Letters, 39(1).

Mitarai, N., & Nori, F. (2006). Wet granular materials. Advances in Physics, 55(1-2), 1-45.

Parmar, M., Haselbacher, A., & Balachandar, S. (2010). Improved drag correlation for spheres and application to shock-tube experiments. Aiaa Journal, 48(6), 1273-1276.

Geology and geochemistry of the Sierra de Santa Marta, Los Tuxtlas Volcanic Complex, Veracruz, Mexico

Sergio R. Rodríguez[1], Wendy V. Morales[1], and Claus Siebe[2]

[1] *Instituto de Geología, Universidad Nacional Autónoma de México, Ciudad Universitaria, Mexico City, Mexico.* srre@unam.mx
[2] *Instituto de Geofísica, Universidad Nacional Autónoma de México, Ciudad Universitaria., Mexico City, Mexico.*

Keywords: Los Tuxtlas, Geology, Geochemistry.

The Los Tuxtlas Volcanic Complex (LTVC) is located in the south of the Veracruz state, on the Gulf of Mexico coastal plain. It is a major topographic high composed by more than 500 scoria cones and several composite volcanoes. Most of the Los Tuxtlas volcanic products are alkaline basalts and their relation with the Trans Mexican Volcanic Belt has been under discussion (Fig. 1).

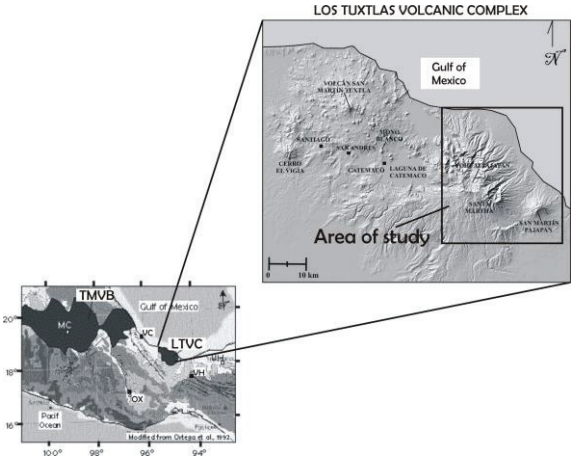

Fig. 1 – Spatial relation between the Trans-Mexican Volcanic Belt (TMVB) and the Los Tuxtlas Volcanic Complex.

The area of study is located to the east of the Catemaco lagoon and is known as Sierra de Santa Marta, which is composed of at least three NW-SE aligned composite volcanoes: San Martín Pajapan (1160 masl) to the south, Santa Marta (1460 masl), and Yohualtijapan (1460 masl) to the north.

Nelson and González-Caver (1992) separated the volcanic activity of Los Tuxtlas into two series: the younger volcanic series (< 0.8 Ma) and the older volcanic series. The K/Ar dates reported by these authors for the older series, which are the focus of this work, range between 7 and 2.6 Ma. Apparently there is no activity between 2.6 and 0.8 Ma. One of the purposes of this work is to compile a systematic rock sampling in order to fill this apparently lacking of data.

Using LIDAR images and field work we present a preliminary geological map of the San Martin Pajapan and Santa Marta Volcanoes. The geomorphological features of these volcanic edifices suggest strong erosional processes, and according to the debris flow deposits associated to the San Martín Pajapan volcano, a partial sector collapse (Fig. 2).

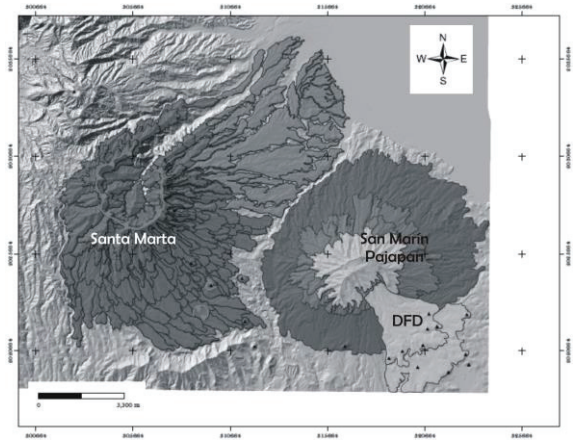

Fig. 2 – Preliminary geological map of the San Martín Pajan and Santa Marta volcanoes. The dark and light gray areas are mostly lavas. DFD: Debris flow deposits.

The geochemical composition of some of the lavas is presented in Table 1. The SiO_2 content of the lavas range between 46.14 % the lowest, and 56.35 % the highest.

Table 1- Major elements from Sierra de Santa Marta lavas.

Analyte Symbol	SiO2	Al2O3	Fe2O3(T)	MnO	MgO	CaO	Na2O	K2O	TiO2	P2O5	LOI	Total
SMTUX-6	51.57	16.5	10.04	0.141	6.06	10.13	3.33	0.85	0.916	0.2	0.52	100.3
SMTUX-17	52.18	14.74	8.5	0.155	8.5	11.26	1.88	0.82	0.523	0.11	0.11	98.79
SMTUX-18	46.14	12.76	11.64	0.175	12.67	10.13	2.69	1.11	1.763	0.44	-0.58	98.92
SMTUX-16	46.82	14.63	11.4	0.182	8.89	11.98	2.24	0.58	0.99	0.16	0.48	98.36
SMTUX-5	54.58	17.09	10.02	0.172	4.64	9.01	2.85	1.04	0.967	0.19	0.27	100.8
SMTUX-9	47.94	16.81	11.43	0.198	6.79	11.52	3.03	0.91	1.256	0.37	-0.15	100.1
SMTUX-4	56.35	16.65	8.19	0.153	3.85	7.94	3.05	1.3	0.922	0.24	1.21	99.85
SMTUX-2	49.12	16.69	10.58	0.167	6.77	11.83	3.19	0.88	1.275	0.27	-0.21	100.6
SMTUX-20	55.83	16.3	8.65	0.156	4.49	7.92	3.29	1.4	0.968	0.26	0.47	99.74
SMTUX-3	52.71	17.55	10.78	0.185	4.44	9.4	3.07	1	1.081	0.2	0.27	100.7
SMTUX-1	52.77	16.27	9.47	0.164	4.93	9.37	2.81	1.11	1.043	0.23	0.2	98.38
SMTUX-14	49.95	16.88	10.99	0.172	5.39	10.35	3.35	0.96	1.192	0.23	-0.01	99.45
SMTUX-11	48.16	16.1	12.31	0.202	6.94	12.47	2.68	0.87	1.113	0.25	-0.16	100.9
SMTUX-12	51.04	14.38	10.4	0.166	8.59	12.21	2.47	0.78	1.05	0.16	-0.27	101
SMTUX-8a	47.54	15.16	12.27	0.185	7.64	11.89	2.5	0.76	1.157	0.19	0.08	99.38
SMTUX-10	50.85	16.45	10.5	0.156	6.05	10.1	3.11	0.83	0.933	0.2	0.28	99.45
SMTUX-19	55.96	16.44	8.3	0.153	4.33	7.14	3.13	1.53	0.984	0.26	1.23	99.46

Most of the samples show a high alkaline content, which agrees with previous analyses of lavas from the LTVC.

Fig. 3 show the distribution of the samples that have been analyzed for major and trace elements and those which are being processing for $^{40}Ar/^{39}Ar$.

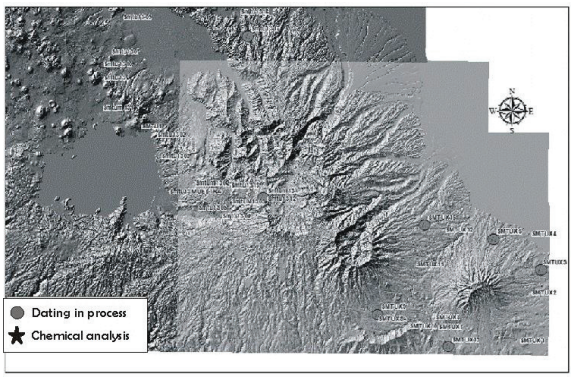

The main purpose of this work is to determine the possible geochemical and geochronological evolution of the volcanic edifices that constitute the Sierra de Santa Marta. As well, these data will be useful to understand the relation between the LTVC and the TMVB.

Acknowledgements

Project PAPIIT-UNAM IN109813.

References

Nelson, S.A. and González-Caver, E. (1992): Geology and K-Ar dating of the Tuxtla Volcanic Field, Veracruz, México. Bull. Volcanol., v.55, p.85-96.

Ortega-Gutiérrez, F., Mitre-Salazar, L.M., Roldán-Quintana, J., Aranda-Gómez, J.J., Morán-Zenteno, D., Alaniz-Alvarez, S.A., y Nieto-Samaniego, A.F., 1992. Texto explicativo de la quinta edición de la Carta Geológica de la República Mexicana escala 1:2,000,000: Universidad Nacional Autónoma de México, Instituto de Geología. Secretaría de Energía, Minas e Industria Paraestatal, Consejo de Recursos Minerales: 1-74.

Episodic volcanism in the West Eifel Volcanic Field: indicating an asthenospheric trigger

Michael W. Förster[1]

[1] *Johannes Gutenberg University, Institute for Geosciences, J.-J.-Becher-Weg 21, D-55099 Mainz, Germany.*
foermich@students.uni-mainz.de

Keywords: Tephrochronology, Thermobarometry, Eifel.

The West Eifel Volcanic Field, situated in southwest Germany was dominated by two phases of volcanism. The older phase formed the center of the volcanic field and occurred 750,000 to 400,000 BP. Following a hiatus of 300,000 years, a younger phase of volcanism started around 130,000 BP. This phase was dominated by two contrasting magma sources. The first was active during the older phase and is strongly foiditic, comprising magmas of melilitite, nephelinite and potassium-rich leucitite. The second source is less foiditic and comprises very mafic olivine nephelinites and sodic basanites. These two sources were described by Mertes and Schmincke (1985) as the F-suite and ONB-suite, respectively.

The last 130,000 years of the eruption history in the West Eifel Volcanic Field were determined from the positions of the ash-layers in the drill-cores of the **E**ifel **L**aminated **S**ediment **A**rchive (**ELSA**) project (Sirocko et al. 2013). The activity is concentrated in two brief periods of time. The positions of the ash-layers from the drill-cores show a characteristic pattern (see Fig. 2). Phreatomagmatic ashes from maar volcanoes were distinguished from strombolian scoria-cone ashes by their high abundance of accidentally introduced host-rock of up to 90 vol.-%. It is stated here, that each phase began with maar volcanoes and ended with the formation of scoria cones. Specifically, the first period began at 130,000 BP with a cluster of maar volcanoes forming until 100,000 BP and was followed by the eruptions of scoria-cones around 90,000 BP. After a lull in activity a second cluster of maar formation occurred from 60,000 BP to 40,000 BP followed by the formation of several large scoria-cones at 30,000 BP. Only one volcano erupted after the second period, the small Ulmener Maar at 11,000 BP.

The scoria cones belong to the younger ONB-suite, whereas the maar volcanoes with exception of Boos and Mosbruch belong to the F-suite. The thermobarometric equations of Lee et al. (2009) are used to calculate the depth of origin for both the F-suite and ONB-suite magmas. The calculated source region of the F-suite magma results in 2.0 to 2.5 GPa. This corresponds to 60 - 90 km depth for mean density of continental lithosphere. The calculated temperatures amount to 1250°C to 1320°C. The calculated depth of the ONB-suite magmas range from 3.2 to 3.8 GPa. That equals to 100 - 125 km depth with a temperature of 1430°C to 1480°C, grouping around the 1400°C adiabat (see Fig. 1). These two domains show clear differences in pressure and temperature: The ONB-suite magma comprises partial-melting at greater pressure and temperature than the F-suite. Both sources lie well below the solidus for dry melting (line starting at 1100°C), thus explaining the volumetric minor volcanism.

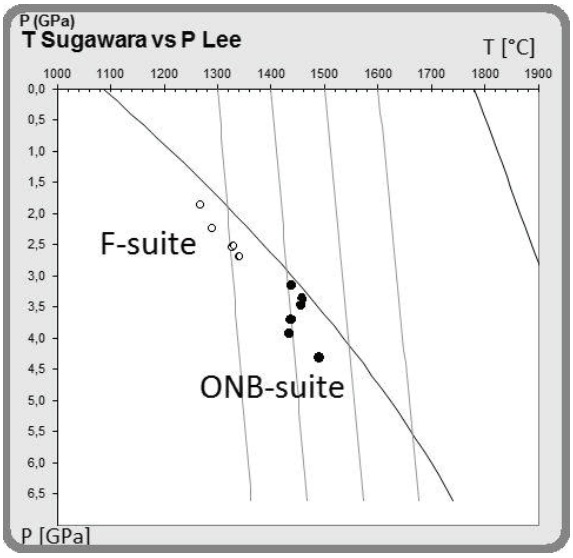

Fig. 1 – The thermobarometric calculations result in two pressure/temperature distributions for the magmas of the F-suite (open circles) and ONB-suite (filled circles) (modified after Lee et al. 2009, data from Mertes and Schmincke (1985)).

It is assumed here, that the formation of the F-suite magma ceased at the end of the older phase around 400,000 BP, in the West Eifel Volcanic Field. The sodium and magnesium-rich magma of the ONB-suite appeared here first about 80,000 BP. This very mafic melt rose from the asthenosphere and infiltrated the base of the lithosphere, generating high-Mg veins with type-I clinopyroxene megacrysts

as described by Shaw and Eyzaguirre (2000). The source of the F-suite is situated at the base of the lithosphere. ONB-suite magmas rose from the underlying asthenosphere and displaced the remaining batches of F-suite magma, triggering their eruption. Due to the high ascent rates of the volatile rich F-suite magmas, maar volcanoes were preferential formed by the rapid encounter of groundwater. The ONB-suite magmas are on the other hand characterized by less groundwater interaction- because their lower rising velocity caused evaporation prior to contact. As a result voluminous scoria cones are formed preferentially.

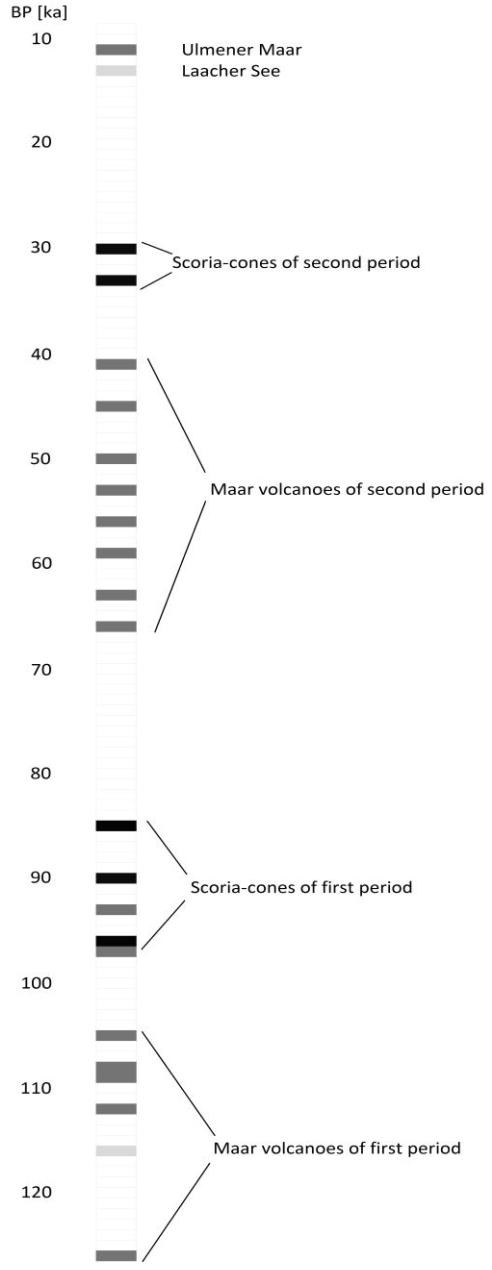

Fig. 2 – The activity pattern of the West Eifel Volcanic Field derived from the position of ash-layers in drill-cores: black - scoria-cone eruptions, grey - maar eruptions, light grey - plinian eruptions from the distant East Eifel Volcanic Field

References

Lee, C. T. A., Luffi, P., Plank, T., Dalton, H., & Leeman, W. P. (2009). Constraints on the depths and temperatures of basaltic magma generation on Earth and other terrestrial planets using new thermobarometers for mafic magmas. *Earth and Planetary Science Letters*, *279*(1), 20-33.

Mertes, H., & Schmincke, H. U. (1985). Mafic potassic lavas of the Quaternary West Eifel volcanic field. *Contributions to Mineralogy and Petrology*, *89*(4), 330-345.

Shaw, C. S., & Eyzaguirre, J. (2000). Origin of megacrysts in the mafic alkaline lavas of the West Eifel volcanic field, Germany. *Lithos*, *50*(1), 75-95.

Sirocko, F., Dietrich, S., Veres, D., Grootes, P. M., Schaber-Mohr, K., Seelos, K., ... & Grim, S. (2013). Multi-proxy dating of Holocene maar lakes and Pleistocene dry maar sediments in the Eifel, Germany. Quaternary Science Reviews, 62, 56-76.

Phreatomagmatic to magmatic activity in the 641 AD historical eruption in Al-Madinah City, Kingdom of Saudi Arabia

Hugo Murcia[1], Károly Németh[2], Nabil El-Masry[3], Peter Wameyo[4], Mohammed Rashad Moufti[3], Jan Lindsay[1], Shane Cronin[2], Ian Smith[1], Gabor Kereszturi[2]

[1] *School of Environment, The University of Auckland, New Zealand.* *hugofmurcia@gmail.com*
[2] *Volcanic Risk Solutions, Massey University, Palmerston North, New Zealand.*
[3] *Geohazards Research Center, King Abdulaziz University, Jeddah, Kingdom of Saudi Arabia.*
[4] *Institute of Earth Science and Engineering, The University of Auckland, New Zealand.*

Keywords: monogenetic volcanic field, Harrat Rahat, basalts.

Harrat Rahat is one of the largest intracontinental volcanic fields in Saudi Arabia. It is part of the Red Sea rift-related volcanism and lies inland and parallel to the western coast of the Arabian Peninsula. The field has evolved for 10 Ma with both monogenetic and polygenetic eruptions, producing a wide range of eruptive styles through both single and multiple aligned vents (Camp and Roobol, 1989; Moufti *et al.*, 2012). The field contains extensive lava flow fields and more than 960 recognizable pyroclastic cones (Runge *et al.*, 2014). Compositions range from basalt to trachyte, and eruption styles from effusive to explosive and from phreatomagmatic to purely magmatic.

One of the three known historical eruptions in the field occurred in 641 AD, and was located only 12 km away from the Holy Mosque of Al-Madinah (in the north of the Harrat), notably outside the area of lava coverage (Moufti *et al.*, 2013) (Fig. 1AB).

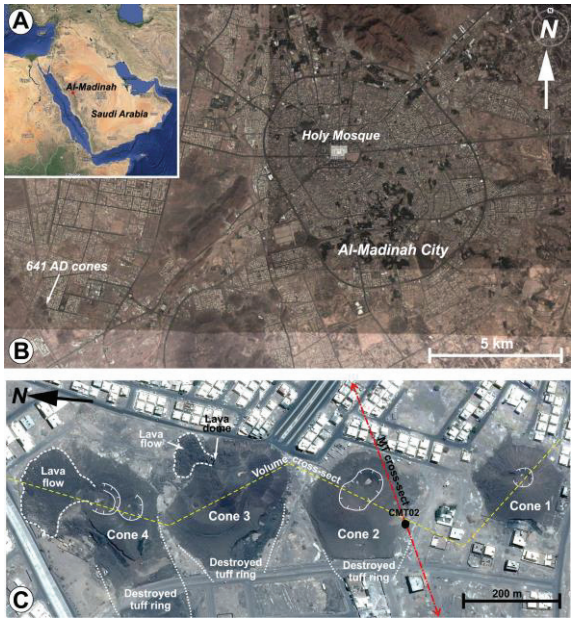

Fig. 1 – 641 AD eruption location. Note the location of Al-Madinah City in Saudi Arabia (**A**), the 641 AD pyroclastic cones within the urban area of the city (**B**), and a close-up of the cones (**C**). Images from Google Earth (08-12-2013)

This eruption emitted mafic products through a 0.8 km-long fissure and produced four small pyroclastic cones with deposits related to both phreatomagmatic and magmatic activity. Although the products are fresh and the cones well-preserved, anthropogenic activity has partially modified their morphology. This has masked the real extent of the base of some cones, whilst at the same time providing outcrops that allow sampling and description of the cones' internal structure. Whole-rock analyses reveal that the products of this eruption are alkali-basalts of intraplate affinity, displaying a narrow range in chemical composition (SiO_2 44.7- 45.9 wt.%; MgO 6.6-6.9 wt.%).

Satellite images combined with field observations, allowed us to define tuff rings at the base of cones 2, 3 and 4 (Fig. 1C). We infer that these resulted from phreatomagmatic explosive eruptions during the inception of the volcanism. Afterwards, predominately magmatic explosive eruptions dominated the activity. The tuff rings are characterized by base-surge deposits (Fig. 2) with a high content of accidental lithics derived from underlying alluvial sediments composed dominantly of gravels and pebbles from the Paleozoic crystalline basement. The upper magmatic parts of the cones are dominated by fall deposits with typical scoriaceous fragments and bombs. Cones 3 and 4 also display short lava flows (<160 m long; Fig. 1C) and a small single lava plug that shows that the final stage of activity was dominated by extrusion of degassed magma. The tuff ring deposits contain abundant cored (Fig. 2) and loaded bombs suggesting entrapment of cold wall-rocks by the rising low viscosity melt prior to fragmentation (c.f., Rosseel *et al.*, 2006). Overall, the eruption began in the north, progressing to the south, starting with phreatomagmatic activity and finishing with magmatic activity. This pattern reflects a rapid diminishing of available groundwater to sustain phreatomagmatism as the eruption progressed southwards.

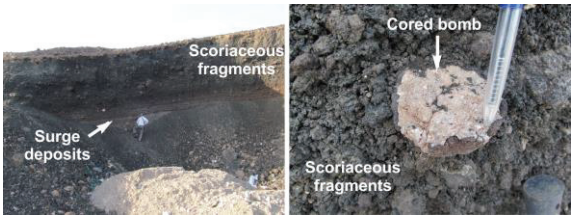

Fig. 2 – Typical deposits and fragments from the cones.

The interpretation described above is complemented by the results of a magnetotelluric survey semi-perpendicular to the eruption fissure (Fig. 1C) that shows evidence of a NE dipping fault plane, and also an alluvial channel located to the west of the cones (Fig. 3). We propose that in the case of cones 2, 3 and 4, magma interacted with the water of this channel and that the explosions deepened as the explosion locus migrated from west to east creating elongated volcanic centres, oriented perpendicular to the fissure. When the external water was exhausted, the eruption conduits became stable and built symmetric and magmatic-dominated edifices, and the new cone 1.

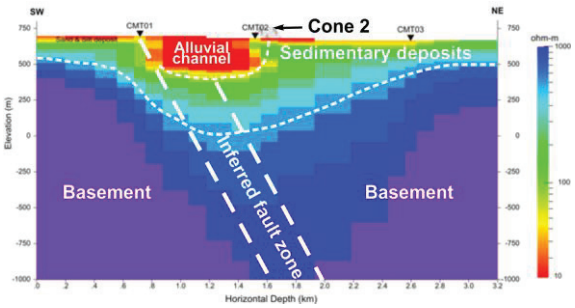

Fig. 3 – 2D inversion cross-section of magnetotelluric data obtained across the 641 AD four cones. Beneath the four cones a low resistivity zone is apparent down to about 500 m below the surface. Site CMT02 is located adjacent to cone 2. See Fig. 1C for cross-section location.

Analysis of the four cones and their eruptive products using a Light Detection and Ranging (LiDAR) Digital Elevation Model (DSM) was used to calculate a dense rock equivalent (DRE) volume of at least 0.0011 km^3, following the estimation method of Kereszturi *et al.* (2013) (Fig. 4). Individual cone volumes put these volcanoes among the smallest monogenetic volcanic cones on Earth (Kereszturi and Németh, 2012).

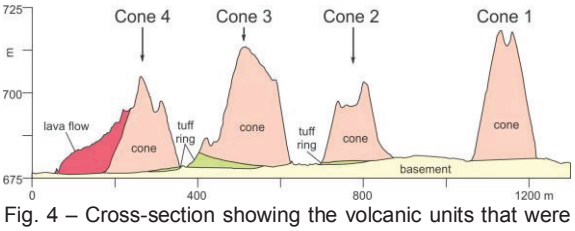

Fig. 4 – Cross-section showing the volcanic units that were used in the eruptive volume estimates. See Fig. 1C for cross-section location.

Overall, the erupted magma displays the same characteristics as the youngest basaltic eruptions in northern Harrat Rahat, which were affected mainly by fractional crystallization processes after partial melting in the garnet peridotite field at depths of around 100 km (Murcia *et al.*, in prep). These cones provide an analogy for possible future eruption scenarios and show that initial phreatomagmatic explosive eruptions are a realistic threat in the known, shallow aquifers and oasis areas surrounding the city of Al-Madinah.

Acknowledgements

This study is part of the Volcanic Risk in Saudi Arabia (VORiSA) project, which is a collaboration between King Abdulaziz University and The University of Auckland.

References

Camp V.E., Roobol M.J., 1989. The Arabian continental alkali basalt province: Part I: Evolution of Harrat Rahat, Kingdom of Saudi Arabia. The Geological Society of America Bulletin 101: 71-95.

Kereszturi, G., Németh, K., 2012. Monogenetic basaltic volcanoes: genetic classification, growth, geomorphology and degradation. In: K. Németh (Ed), Updates in Volcanology - New Advances in Understanding Volcanic Systems. In Tech Open, Rijeka, Croatia, pp. 3-88

Kereszturi, G., Németh, K., Cronin, S.J., Agustin-Flores, J., Smith, *I.E.*M., Lindsay, J., 2013. A model for calculating eruptive volumes for monogenetic volcanoes - Implication for the Quaternary Auckland Volcanic Field, New Zealand. Journal of Volcanology and Geothermal Research, 266: 16-33

Moufti M.R., Moghazi A.M., Ali K.A., 2012. Geochemistry and Sr–Nd–Pb isotopic composition of the Harrat Al-Madinah Volcanic Field, Saudi Arabia. Gondwana Research 21: 670-689.

Moufti M.R., Németh K., Murcia H., Al-Gorrry S.F., Shawali J., 2013. Scientific basis of the geoheritage and geotouristic values of the 641 AD Al Madinah eruption site in the Al Madinah volcanic field, Kingdom of Saudi Arabia. The Open Geology Journal 7: 31-44

Murcia, H., Lindsay, J.M., Smith, *I.E.*M., Moufti, M.R., Németh, K., Cronin, S.J., El-Masry, N.N, Niedermann, S., in prep. Melt source and magma ascent processes revealed by recent (<4500 yr) basaltic eruptions in northern Harrat Rahat, Kingdom of Saudi Arabia

Rosseel, J-B, White, J.D.L., Houghton, B.F., 2006. Conplex bombs of phreatomagmatic eruptions: Role of agglomeration and welding in vents of the 1886 Rotomahana eruption, Tarawera, New Zealand. Journal of Geophysical Research, 111: B12205

Runge M.G., Bebbington M.S., Cronin S.J., Lindsay J.M., Kenedi C.L., Moufti M.R.H., 2014. Vents to events: determining an eruption event record from volcanic vent structures for the Harrat Rahat, Saudi Arabia. Bulletin of Volcanology 76:1-16.

Geodynamic transection across northeast Asia: Focus on Changbai Volcanoes

Liu Jiaqi, Guo Zhengfu, Chu Guoqiang, Liu Qiang, Liu Jiali, Wu Jing, Guo Wenfeng, Sun Chunqing

Division of Cenozoic Geology and Environment, Institute of Geology and Geophysics Chinese Academy of Sciences, Beijing, China, liujq@mail.iggcas.ac.cn

Keywords: geodynamic transaction, Changbai Volcanoes.

It is very known that a geodynamic transection and integrated plate system from the Pacific Plate subduction zone via Japanese arc islands and back-arc basin to the east Eurasia continental margin with rifting system displays in Northeast Asia . Based on this geological background many huge earthquakes and volcanic eruptions often occurred in this area such as Fujiyama Volcano in Japan, Cheju Volcano in South Korea and Changbai Volcano .

The Changbai Volcano is huge volcanic group with some 12×103 km^2 area and hundreds volcanic cones crossed the boundary between China and Korea covered 41°-42.5° latitude north and 127°-129° longitude east. It is among largest active and dangerous volcanoes on the Globe and composed of three main volcanoes (eruptive centers): Tianchi (2755 m a.s.l.), Wangtian'e (2438m a.s.l.) and South Paotaishan (2434m a.s.l.), which distribution assumes as tripod. These three eruptive centers have similar magma system and different ages. They were built from the Early Miocene to the Recent by basaltic flow as lava plateau, trachyte composing of volcanic cones and pyroclastic deposits covering the tops of the mountains and other places. Tianchi volcano is younger than others. According to historic documents the largest eruption of Tianchi volcano occurred in 1014-1019 AD., after that there were still several eruptions until 1903 AD. The frequencies of Changbai volcanic eruptions corresponded to those of the Pacific, especially Japan. Now Changbai Volcano is locates in the nodes of thousand year eruption cycle and hundred year eruption cycle.

There is systematic magma evolution from basic basalt, intermediate trachyte to acid pantellerite with 87Sr/86Sr 0.704771-0.710096, 143Nd/144Nd 0.512487-0.512602, which indicated that the magma derived from rich mantle and finished a complete magmatic cycle. Geophysical data reveal a buried magmatic reservoir is lying below the volcanoes.

It is tectonic active phase in the Northeast Asia, even in the globe recently. The west Pacific fire ring is very active accompanied with frequent volcanic eruptions and earthquakes like M9 earthquake in Northeast Japan of March 11, 2011 and M 7.3 deep earthquake in Wangqing, Northeast China of June 28, 2002. Based on those geological surrounding the possibility of re-eruption of Changbai Volcano is going to strengthen. Therefore we must put attention to volcanic action.

.

San Diego maar, an isolated monogenetic volcano in the Central Cordillera of Colombia

Carlos Borrero[1], Hugo F. Murcia[2] and Javier Agustín-Flores[3]

[1] *Departamiento de Ciencias Geológicas Universidad de Caldas, Manizales, Colombia.* borrero_c@yahoo.com
[2] *School of Environment, The University of Auckland, Auckland, New Zealand.*
[3] *Volcanic Risk Solutions, Massey University, Palmerston North, New Zealand.*

Keywords: phreatic explosion, lava-dome, Colombia.

San Diego maar (Toro, 1988) is an isolated volcano located at 770 masl at the eastern flank of the Colombian Central Cordillera (5°38.586'N, 74°57.43'W), 89 km northeast from the current Cerro Machín- Cerro Bravo volcanic complex in the Caldas Department. The cordillera at this sector is composed of Paleozoic metamorphic basement and some Neogene volcanic intrusions. The present-day tuff ring is roughly semi-circular in shape with a maximum axis of 2,74 km and a minimum axis of 2,5 Km. The tephra rim reaches a maximum and minimum height of 1029 masl and 1011 masl respectively, and is characterized by steep inward-dipping walls. The maar has an inner lake partially filled with sediments, with an approximate depth of 48 m. On the northeastern sector of the maar, a dacitic dome was emplaced after the eruption of the maar. A collapse occurred in the northern sector of the dome edifice, which produced a small debris avalanche deposit in the northern part of the maar (Fig. 1).

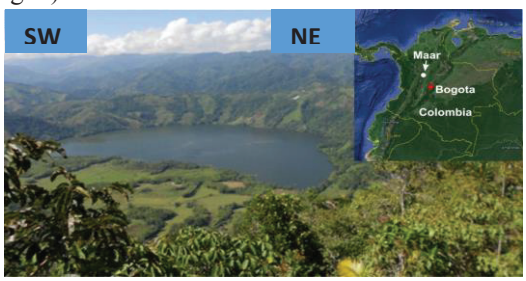

Fig. 1 – San Diego maar view. Photo taken from the dome top. Note the location of the maar (Fig. right side).

At the top of the eastern and northern sectors of the maar rim behind the dome, a deposition sequence is exposed along the roads to San Diego village. No time breaks are evident within the whole sequence suggesting a continuous volcanic activity. Based on sedimentary and stratigraphic characteristics, four lithofacies were identified. These lithofacies correspond to the outer-rim facies. Lithofacies I is characterized by a~ 1.5 m-thick, massive, poorly-sorted, unconsolidated bed composed by angular-to-subangular, lapilli-to-block-size fragments from the metamorphic and volcanic substrate. This lithofacies was observed only in the easternmost distal location with respect to the maar crater to a distance of 3,5 km. Lithofacies II (Fig. 2) is composed of a ~5 m-thick, stratified sequence of fine-to-coarse ash layers inter-bedded with very fine ash layers that display dune-bedding and slight cross-stratification. Lithofacies III are represented by a 2 m-thick succession of unconsolidated massive beds composed of coarse ash fragments with good sorting. Lithofacies IV, which is present in the eastern and northern tephra rim and by its continuity was recognized at eight outcrops, is characterized by a variable thickness (between 1,25 to 2,45 m) and composed of unconsolidated, poorly-sorted, massive beds that consist of lapilli to block-size fragments from the metamorphic and volcanic substrate. The unconsolidated deposits of the entire sequence are mildly-to-highly altered due to the prevalence of high humidity in the region.

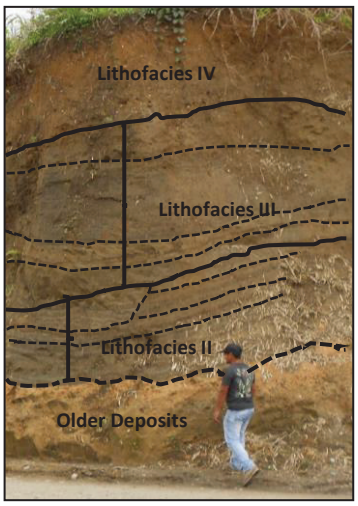

Fig. 2 – Sequence at San Diego village showing the main lithofacies of the deposits related to the San Diego maar. The outcrop is located at the top of the eastern sector of maar rim behind the dome (see Fig. 1).

Componentry analyses from the eastern maar´s rim sequence suggest that the dominant fragments of the whole deposit were sourced from the uppermost substrate lithologies in the area: Paleozoic metamorphic schists and the weathered Miocene-to-Pliocene andesitic volcanic rocks. Subordinated Late-Pliocene-ash flow particles are also present. Scanning electron microscope images also attest the

presence of the above fragments in the fine fraction that show blocky fragments with irregular shapes with conchoidal fractures and fragmented stepped surfaces probably as a consequence of their disruption and transport (cf. Wholetz, 1983).

The western and southern maar rim correspond exclusively to a unconsolidated and unsorted massive talus deposits composed by mega-blocks of metamorphic rocks; these deposits are related to crater wall collapse and slumping, common phenomenon in the steep inner crater walls of hard-substrate maars, and their lithofacial characteristics prevents the correlation with the eastern and northern outer rim sequence described above.

At the northeastern sector of the maar, an effusive eruption of a dome filled up to a third of the original crater. This dome displays a landslide crown in the northern face (Fig. 3), which is related to a gravitational collapse of part of the dome into the eastern sector of the maar crater; this collapse forms a small-volume debris avalanche deposit. The dome and the debris avalanche deposit are relatively fresh, and exhibit porphyritic rocks with quartz, plagioclase and amphibole crystal assemblage; whole-rock chemistry of this dome reveals dacitic composition (SiO_2 69.4 wt. %).

Fig. 3 – Northern side of the dome. This sector was affected by a gravitational collapse, which produced a small-volume debris avalanche deposit.

The morphological characteristics of the edifice appear to be comparable to those described for a maar (*e.g.* Fisher and Schmincke, 1984) of relatively large size. However, the deposits at San Diego maar are dominated by rather massive beds composed of brecciated material, which do not reflect the mode of transport of diluted pyroclastic density currents.

The lack of juvenile fragments and the nature of deposits may suggest that the formation of the maar may be related to a phreatic eruption. In this case, the water confined within an aquifer or a hydrothermal system was heated by the uprising dacitic magma causing its boiling with the subsequent violent expansion and disruption of the system. These explosions would have ejected jets of saturated steam with host rock fragments (Le Guern *et al*., 1980) depositing the phreatic breccias that apparently dominate the exposed outcrops. This type of explosions may produce limited base surges episodes (Barberi *et al*., 1992), obviously devoid of magmatic fragments. Lithofacies II may represent such a base surge-related episode. In addition, the deposition of four distinct lithofacies implies that there were at least four explosions with their own "blasts". Although the mechanisms of maar-forming phreatic eruptions are poorly understood, the phreatic steam-driven explosions are likely to be single episodes located at different sites within the area affected by magma heat. In this context, it cannot be envisage a downward penetration, and the formation of deep diatreme, as in the maar model by Lorenz (1986).

The silicic composition involved in the eruption and the location of the maar in a relatively high terrain are not typical of maars that are usually associated to basaltic compositions and located in low valleys related to good hydraulic conditions (Lorenz, 1986). These, together with the large size of San Diego maar, provide important information in the hazard assessment related to this type of eruptions.

Acknowledgements

The Vicerrectoría de Investigaciones, Caldas University supported this project. IIES, Caldas University provided the SEM images. Whole-rock chemistry was carried out at The Univ. of Auckland.

References

Barberi, F., Bertagnini, A., Landi, P., Principe, C. (1992). A review on phreatic eruptions and their precursors. J. Volcanol. Geothermal R., 52, 231-246.

Le Guern, F., Bernard, A., & Chevrier, R. M. (1980). Soufriere of Guadeloupe 1976–1977 eruption—Mass and energy transfer and volcanic health hazards. Bull. Volcanologique, 43, 577-593.

Fisher, R.V., Schmincke, H.U., 1984. Pyroclastic Rocks, Springer-Verlag, Berlin, 472 p.

Lorenz, V. 1986. On the growth of maars and diatremes and its relevance to the formation of tuff rings. Bull. Volcanology, 48: 265-274.

Toro, G. 1988. Etude du volcan San Diego (Caldas) et des dépots de Nariño (Antioquia), Colombie. Contributions a l'etude des tephras en climats tropicaux humides. Memoire de fin d'etudes, Université de Liége, Belgique, 91 p.

Wohletz, K.H., 1983. Mechanisms of hydrovolcanic pyroclasts formation: grain size, scanning electron microscopy, and experimental studies. J. Volcanol. Geothermal R., 17: 31-63.

Alternation between Strombolian activity and phreatomagmatism in Valle de Santiago, Mexico

Nick Varley[1] and Adrián García[1]

[1] *Facultad de Ciencias, Universidad de Colima, Colima, Mexico. nick@ucol.mx*

Keywords: maar, scoria cone, aquifer.

Valle de Santiago features a remarkable collection of maars which erupted between about 1.175 and 0.073 Ma (Murphy 1982), as well as a number of scoria cones and shield volcanoes. It is by far the largest concentration of maars in the huge Michoacán-Guanajuato Volcanic Field. They are orientated in two principles directions, roughly NW-SE and W-E. Current conditions do not reflect the previous hydrological situation, with dramatic reductions in the phreatic level having occurred, especially recently due regional overexploitation. The lakes which could be still observed recently in the maars have virtually disappeared.

This study concentrates on deposits surrounding the Cerro Bateo scoria cone to the south of the distributed volcanic field, which is 2.2 km from the southernmost well-formed maar Hoya Álvarez. The eruption of the scoria cone has been reported as pre-dating the maar eruptions, though no direct samples were dated. Observations have revealed a complex alternation between typical scoria and extensive pyroclastic surge deposits (fig. 1 and 2), some of which contain accretionary lapilli, whilst others are strongly welded. Two possibilities are being investigated: whether the deposit results from conditions fluctuating between dry conditions with typical Strombolian eruptions from the Cerro Bateo scoria cone and changes within the conduit system allowing the infiltration of an aquifer resulting in phreatomagmatic eruptions; or that there were contemporaneous eruptions from this vent and Hoya Álvarez, which produced the surge deposits. An eruption with two vents, the ejecta from each one reflecting whether there was a significant interaction with the local aquifer or not was observed in the Eifel district (Houghton and Schmincke, 1989).

The composition of both Cerro Bateo and Hoya Álvarez is alkali-basalt, meaning more detailed petrology needs to be considered to determine the source of different layers. Previous dating in the region by Murphy (1982) combined with assumptions, probably based upon stratigraphic position and erosional evidence, places the eruption of Cerro Bateo in the region of 6 Ma, whereby Hoya Álvarez was assumed to be around 0.4 – 1 Ma, which precludes the contemporaneous option if the dates have been correctly conceived. The physical properties of the different layers will help to decipher the puzzle.

Fig. 1 – Section of Cerro Bateo deposit, showing surge with scoria above and below.

Hoya Álvarez exhibits an interesting sequence of pyroclastic surges in the exposed tuff ring. Figure 3 shows some sedimentary structures reflected the high water-content at the time of deposition. Two older maars also can be observed to the east, which represent other candidates to be considered as sources for the surge layers.

It is more common that the magma-water interaction dominates early phases of activity of a monogenetic volcano; however, it depends on the local hydrology (*e.g.* Di Traglia *et al.* 2009). At Cerro Bateo there is an apparent alternation between the

deposits associated with wet and dry eruptions, with large surges emplaced in the middle of the stratigraphic column. Upcoming fieldwork will gather further evidence to establish the mechanism controlling these frequent variations.

Fig.2 – Scoria and surge deposits at Cerro Bateo

Fig.3 – Surge deposits in the tuff ring of Hoya Álvarez showing sedimentary structures.

References

Di Traglia, F., Cimarelli, C., de Rita, D. and Gimeno Torrente, D., 2009. Changing eruptive styles in basaltic explosive volcanism: Examples from Croscat complex scoria cone, Garrotxa Volcanic Field (NE Iberian Peninsula). Journal of Volcanology and Geothermal Research, 180(2-4): 89-109.

Murphy, G.P. 1982. The chronology, pyroclastic stratigraphy, and petrology of the Valle de Santiago maar field, central Mexico. M.Sc. Thesis, University of California, Berkeley, USA.

Houghton, B.F. and Schmincke, H.U., 1989. Rothenberg scoria cone, East Eifel: a complex Strombolian and phreatomagmatic volcano. Bulletin of Volcanology, 52(1): 28-48.

Hidromagmatic volcanism at Deception Island (Antarctica): implications for volcanic hazard

Dario Pedrazzi[1,2], Gerardo Aguirre Díaz[2], Stefania Bartolini[1], Joan Martí[1] and Adelina Geyer[1]

[1] *Centro de Geociencias, Universidad Nacional Autónoma de México , UNAM, Campus Juriquilla, Querétaro, México.* d_pedrazzi@yahoo.com
[2] *Institute of Earth Sciences Jaume Almera, ICTJA-CSIC, Group of Volcanology.SIMGEO (UB-CSIC), Lluís Solé i Sabarís s/n, 08028, Barcelona, Spain.*

Keywords: Hydromagmatism, Deception Island, Volcanic Hazard.

Deception Island, the southernmost island in the South Shetland Archipelago (Antarctica), is located at the southwestern end of the Bransfield Strait, a young (<1.4 Ma) back-arc basin (Fig. 1) (Barker 1982, Lawver *et al.* 1995).

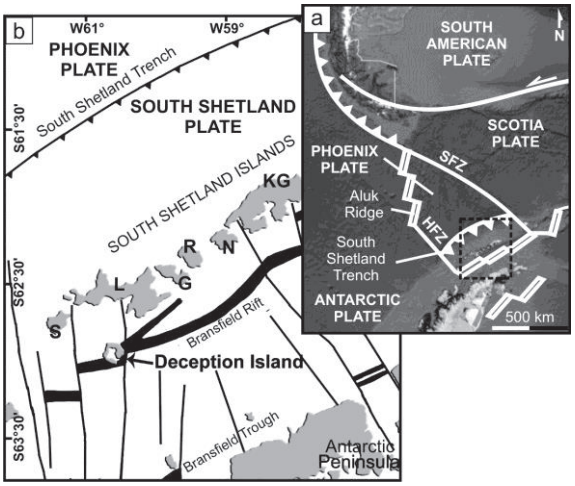

Fig. 1 – (a) Simplified regional tectonic map and location of the South Shetland Islands Archipelago (modified from Ibañez *et al.* 2003). HFZ-Hero Fracture Zone, SFZ-Shetland Fracture Zone; (b) geological Setting of the South Shetland Islands Archipelago and location of Deception Island (modified from Grad *et al.* 1992). KG-King George Island, N-Nelson Island, R-Robert Island, G-Greenwich Island, L-Livingstone Island, S-Snow Island.

The basin is volcanically active and the main volcanic Quaternary edifices of the archipelago are Deception, Bridgeman and Penguin Islands. Numerous small volcanic centers are recognized as well on Livingston, Greenwich and King George Islands (Weaver *et al.* 1979, Smellie *et al.* 1984, Fisk 1990, Keller and Fisk 1992, Smellie *et al.* 1995, Gràcia *et al.* 1996).

Deception Island is a <0.75-Ma (Valencio *et al.* 1979, Smellie 1988) horseshoe-shaped volcanic edifice, interpreted as a tectonic fault-controlled collapse caldera (Martí *et al.* 2013). Three volcanic phases are recognized: 1) pre-caldera that built a shield volcano, 2) syn-caldera characterized by pyroclastic density currents and 3) post-caldera, during which different vents were formed inside or around the caldera depression (Smellie 2001, Martí *et al.* 2013) (Fig. 2). This work focuses on this last phase. More than 20 eruptions have been identified over the past two centuries (Roobol 1980, Pallàs *et al.* 2001) with the most representative episodes related to Kroner Lake (1829-1912), 1967, 1969 and 1970 eruptions (Fig. 2).

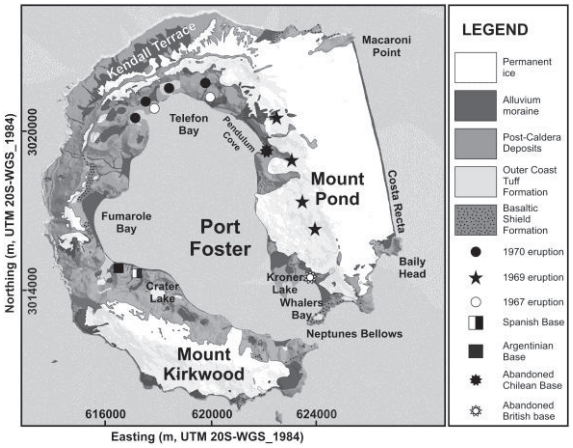

Fig. 2 – Simplified geological map of Deception Island. Location of the former and current scientific stations and the most recent volcanic episodes are also included.

On the one hand, the Kroner Laker eruption (1829-1912) (Roobol 1973), located in Whalers Bay, close to the Neptunes Bellows (Fig. 2) is characterized by a monotonous sequence of mainly juvenile fallout with subordinate PDCs deposits. The eruption probably took place at shallow sea-water with the formation of a crater open to the sea.

The 1967 episode lasted about two days and generated three overlapping pyroclastic cones with water-filled craters in the northwestern corner of Telefon Bay from initial submarine vents, while a further centre was located close to sea-level between Telefon Bay and Pendulum Cove (Fig. 2). Mainly fallout deposits characterize the eruption with bombs, blocks, lapilli and ash of magmatic/hydromagmatic origin (Baker *et al.* 1975).

The 1969 episode occurred at Mount Pond (Fig. 2) from a short-lived (<48 hours) explosive activity

from several small pyroclastic vents formed along a series of en echelon fissures, creating a large and sudden discharge of melted ice water that overflowed the glacier (Smellie 2002).

The 1970 eruption, located in the same general area as the one of 1967 (Fig. 2), led to the formation of conical shape craters at onshore locations and "maar-like" craters in shallow seawater (Baker *et al.* 1975). No direct observation of the duration of the eruption is reported, because it occurred when Deception Island was unoccupied. Similarly to the 1967 episode, a sequence of fallouts with subordinate PDCs deposits of phreatomagmatic origin characterizes the eruption (Pedrazzi *et al.* 2014).

These volcanic episodes demonstrate that similar explosive events lead to different eruptive phenomena and associated hazards. The British and Chilean scientific bases at Port Foster (Fig. 2) were destroyed by the 1967 and 1969 eruptions. The 1970 eruption occurred when the island was unoccupied but it was similar to the episode of 1967 (Pedrazzi *et al.* 2014). The Kroner Lake eruption shows the same characteristics as the shallow seawater eruptions of 1967 and 1970.

Similar eruptions may occur in the future on Deception Island, and may be a serious hazard to the increasing number of people that visit the island during certain periods of the year and to the scientific installations that operate there.

Acknowledgements

This research was supported by the MICINN grant CTM2011-13578-E. AG is grateful for her Juan de la Cierva Grant (JCI-2010-06092) and Ramón y Cajal contract (RYC-2012-11024).

References

Baker, P., McReath, I., Harvey, M., Roobol, M., Davies, T., 1975. The geology of the South Shetland Islands: volcanic evolution of Deception Island. BritishAntarctic Survey Scientific Reports 78: 81 pp.

Barker, P.F., 1982. The Cenozoic subduction history of the Pacific margin of the Antarctic Peninsula: ridge crest–trench interactions. Journal of the Geological Society 139(6): 787-801.

Fisk, M.R., 1990. Volcanism in the Bransfield Strait, Antarctica. Journal of South American Earth Sciences 3(2–3): 91-101.

Gràcia, E., Canals, M., Lí Farràn, M., José Prieto, M., Sorribas, J., Team, G., 1996. Morphostructure and evolution of the central and Eastern Bransfield Basins (NW Antarctic Peninsula). Marine Geophysical Researches 18(2-4): 429-448.

Grad, M., Guterch, A., Sroda, P., 1992. Upper crustal structure of Deception Island area, Bransfield Strait, West Antarctica. Antarctic Science 4(04): 469-476.

Ibáñez, J.M., Almendros, J., Carmona, E., Martınez-Arévalo, C. and Abril, M., 2003. The recent seismo-volcanic activity at Deception Island volcano. Deep Sea Research Part II: Topical Studies in Oceanography 50(10–11): 1611-1629.

Keller, R.A., Fisk, M.R., 1992. Quaternary marginal basin volcanism in the Bransfield Strait as a modern analogue of the southern Chilean ophiolites. Geological Society, London, Special Publications 60(1): 155-169.

Lawver, L., Keller, R., Fisk, M., Strelin, J., 1995. Bransfield Strait, Antarctic Peninsula Active Extension behind a Dead Arc. In: B. Taylor (Editor), Backarc Basins. Springer US: pp. 315-342.

Martí, J., Geyer, A., Aguirre-Diaz, G., 2013. Origin and evolution of the Deception Island caldera (South Shetland Islands, Antarctica). Bull Volcanol 75(6): 1-18.

Pallàs, R., Smellie, J.L., Casas, J.M., Calvet, J., 2001. Using tephrochronology to date temperate ice: correlation between ice tephras on Livingston Island and eruptive units on Deception Island volcano (South Shetland Islands, Antarctica). The Holocene 11(2): 149-160.

Pedrazzi, D., Aguirre, G., Bartolini, S., Martí, J., Geyer, A. 2014. The 1970 eruption on Deception Island (Antarctica): eruptive dynamics and implications for volcanic hazards. Journal of the Geological Society: in press.

Roobol, M.J., 1973. Historic volcanic activity at Deception Island. British Antarctic Survey Bulletin 32: 23-30.

Roobol, M.J., 1980. A model for the eruptive mechanism of Deception Island from 1820 to 1970. British Antarctic Survey Bulletin 49: 137-156.

Smellie, J.L., 1988 Recent observations on the volcanic history of Deception Island, South Shetland Islands. British Antarctic Survey Bulletin 81(83–85): pp. 83.

Smellie, J.L., 2001. Lithostratigraphy and volcanic evolution of Deception Island, South Shetland Islands. Antarctic Science 13(02): 188-209.

Smellie, J.L., 2002. The 1969 subglacial eruption on Deception Island (Antarctica): events and processes during an eruption beneath a thin glacier and implications for volcanic hazards. in: Smellie, J.L. and Chapman, M.G., eds. Volcano-ice interaction on Earth and Mars. GeologiaJ/ Society, London, Special Publication 202: 59- 79.

Smellie, J.L., Liesa, M., Muñoz, J.A., Sàbat, F., Pallàs, R., Willan, R.C.R., 1995. Lithostratigraphy of volcanic and sedimentary sequences in central Livingston Island, South Shetland Islands. Antarctic Science 7(01): 99-113.

Smellie, J.L., Pankhurst, R.J., Thomson, M.R.A., Davies, R.E.S., 1984. The geology of the South Shetland Islands. VI: Stratigraphy, geochemistry and evolution. British Antarctic Survey, London, ROYAUME-UNI: 85 pp.

Valencio, D.A., Mendía, J., Vilas, J.F., 1979. Palaeomagnetism and KAr age of Mesozoic and Cenozoic igneous rocks from Antarctica. Earth and Planetary Science Letters 45(1): 61-68.

Weaver, S., Saunders, A., Pankhurst, R., Tarney, J., 1979. A geochemical study of magmatism associated with the initial stages of back-arc spreading. Contr. Mineral.and Petrol. 68(2): 151-169.

The influence of monogenetic activity on prehispanic cultures, Los Tuxtlas Volcanic Field (Veracruz, Mexico).

Katrin Sieron[1], Franck Lavigne[2], Jairo Teinturier[2], Horacio Tapia McClung[3], Ignacio Mora González[1]

[1] *Centro de Ciencias de la Tierra, Universidad Veracruzana, Xalapa, México.* ksieron@uv.mx, ksieron@gmail.com,
[2] *Universidad de París I Panthéon-Sorbonne, France.*
[3] *LANIA, Xalapa, Mexico.*

Keywords: Los Tuxtlas, monogenetic volcanoes, prehispanic civilization.

Los Tuxtlas volcanic massif rises above the Veracruz basin up to 1700 m a.s.l. and includes the active San Martín Tuxtla volcano, 3 other larger but inactive volcanic centers, and at least 350 monogenetic volcanoes. The area has been occupied by prehispanic civilizations for more than 4850 years (*e.g.* Goman and Byrne, 1998; Stark and Arnold, 1997), although first settlements are only evidenced by agricultural traces in lake deposits.

The Los Tuxtlas region offered ground stone and fertile volcanic soils, but the prehispanic population also had to cope with the negative side effects of active volcanism.

Los Tuxtlas Volcanic Field (LTVF) shows a very high density of volcanic edifices (about 0.2 scoria cones/km^2 in an area of the currently active volcanic field) as evidenced by point- and kernel density analyses (*e.g.* Fig. 1).

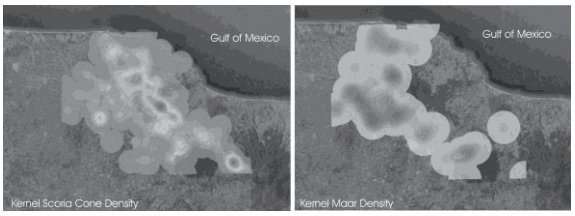

Fig. 1 – Kernel densities of scoria cones (left) and explosion craters (right) of Los Tuxtlas Volcanic field; search radius 3 and 4 km respectively. Greyscale color scheme indicates densities varying from 0.2-1.8 and 0.05 - 0.2, left and right image respectively.

The morphologically youngest monogenetic edifices are distributed apparently chaotically throughout the LTVF, but within the major NW-SE fault zone (see Fig. 2). Strombolian eruptions associated to scoria cone creation are the most common eruption type, although about ten per cent of recent volcanic eruptions have been phreatic and phreatomagmatic associated to explosion craters (mainly maars).

Early settlements in the Catemaco region. Eastern LTVF, (*e.g.* Bezuapan, Jaime-Riveron and Pool, 2009) have been affected by several monogenetic eruptions, including phreatomagmatic eruptions (Fig. 2), causing migration and abandonment of the affected area, and strongly diminished the population (Santley, 2007, Jaime-Riveron and Pool, 2009). This picture is supported by new radiocarbon dates (*e.g.* Las Animas scoria cone, see Fig. 2) After a few hundred years the affected area was repopulated and despite suffering other monogenetic eruptions, later civilizations stayed in the area, dealing with the effects of the eruption.

Prehispanic sites in the W LTVF have been affected in a similar way by several eruptions, which have been mentioned by several authors (*e.g.* Santley *et al.* , 2007; Jaime-Riveron and Pool, 2009), without indicating any specific source vents.

Further research, especially identifying stratigraphic relationships between the distinct monogenetic eruptions, complemented by radiocarbon dating is required to be able to obtain a complete picture of recent monogenetic volcanism in the LTVF. Dealing with volcanic hazards has been a topic for thousands of years in the Los Tuxtlas region and might explain migrations and abrupt cultural changes; interdisciplinary work offers a complete picture of cultural aspects.

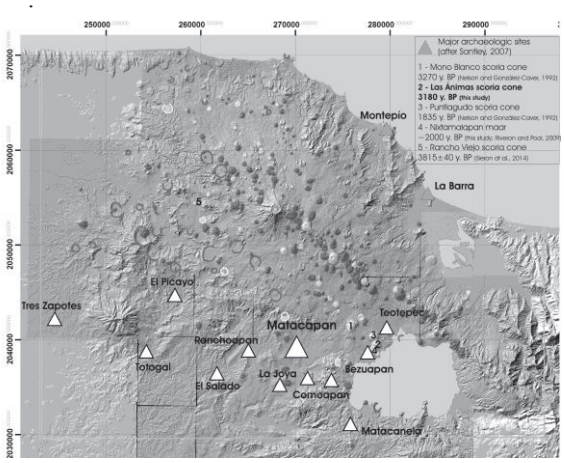

Fig. 2 – Active part of Los Tuxtlas Volcanic field. Scoria cones dark grey, explosion craters lines. Lighter grey colored monogenetic vents indicates very recent emplacement. Major archaeological sites are also indicated.

References

Goman, M. Byrne, R. 1998 A 5000-year record of agriculture and tropical forest clearance in the Tuxtlas, Veracruz, Mexico. The Holocene 8, 83-89.

Jaime-Riverón, O., Pool, C. 2009. The impact of volcanic hazards on the ancient Olmec and Epi-Olmec economies in the Los Tuxtlas region, Veracruz, Mexico. In: Jones, E.C., Murphy, A.D. (Eds.) In the Political Economy of Hazards and Disasters. Altamirano Press, Lanham, p. 133-154.

Nelson, S.A. y González-Caver, E. (1992): Geology and K-Ar dating of the Tuxtla Volcanic Field, Veracruz, Mexico. Bull. Volcanol., v.55, p.85-96.

Santley, R.S. 2007. The prehistory of the Tuxtlas. University of New Mexico Press. 261p.

Stark, B.L., Arnold III P.J. (eds.), Olmec to Atztec: Settlement patterns in the ancient Gulf lowlands. The University of Arizona Press.

The Bellecombe ash: Indications of explosive eruptions at Piton de La Fournaise, Reunion Island

Michael H. Ort[1], Andrea Di Muro[2], Laurent Michon[3], Patrick Bachelery[4],

[1] *SESES, Northern Arizona University, Flagstaff, Arizona, USA. michael.ort@nau.edu*
[2] *Observatoire Volcanologique du Piton de la Fournaise, IPGP, La Plaine des Cafres, La Réunion, France.*
[3] *Laboratoire Géosciences Réunion, Université de La Réunion, Saint-Denis, La Réunion, France.*
[3] *Laboratoire Magmas et Volcans, Université Blaise Pascal, Clermont-Ferrand, France.*

Keywords: Piton de la Fournaise, Bellecombe ash, explosive eruptions.

Piton de La Fournaise (PdF) is the currently active volcano of the Reunion hot spot about 800 km east of Madagascar. It is a dominantly effusive volcano today but evidence of past explosive phases is abundant. Historic explosive events occurred, most notably in 1791, 1860, 1961, 1986 and in 2007, with concomitant crater collapse in the summit area. Evidence of earlier explosive activity includes breccia deposits along the Enclos Fouqué caldera rim and the more widely dispersed Bellecombe ash (Bachelery, 1981). This abstract concentrates on this older activity because it may indicate what the volcano is capable of doing if the current effusive phase transitions back into a more explosive phase.

Modern (last 350 years) eruptive activity has typically involved magma ascending beneath the central cone and then either erupting there or along the northeast or southeast rift zones. This results in effusive eruptions of hours to half a year in length, with small volumes (0.1-240 Mm^3) and rare weak ash plumes (Michon et al. 2013). A variant on this style is when flank eruptions lead to summit collapse and the formation of pit craters or summit calderas, in some cases accompanied by explosive activity. A third style of eruption is decades-long effusive eruptions associated with summit lava lakes. These long-term events were associated with explosive phases in 1759, 1791, and 1860 CE. The deposits from modern explosive eruptions show evidence of the involvement of external fluids, such as dense and lithic-rich ashes and breccias draping underlying lavas and fountain deposits (scoria, Pele's hair, etc.). Notably, they contain only sparse clasts from the geothermal system possibly located ~500 m below the surface. Michon et al. (2013) interpret that the explosions emanate from shallower depths.

The older Bellecombe ashes are exposed over a larger area (out to 15 km downwind; Figure 1) than the modern ashes, whose deposits were emplaced during short-lived explosive events and are preserved only near the volcano summit caldera rim. The Bellecombe ashes were originally identified by Bachelery (1981) and described in more detail by Mohamed-Abchir (1996). Both interpreted the deposit as having been produced by a single large, dominantly phreatic eruption associated with a caldera collapse event. Recent dating shows that this type of ashfall was deposited over a time period from 4800 ka to 2800 ka (Morandi et al. 2014).

Inside the outer PdF caldera in the Plaine des Sables area west of PdF summit (Petit Carriere site), the Bellecombe ash consists of a 2.5-m-thick section of, from the base, ash pellet and lapilli fallout, massive and laminated fine ash beds with two one-clast-thick breccia layers, and bedded lapilli and ash, much of it reworked (Figure 2). Most beds show signs of water-magma interaction, including ash pellets and accretionary lapilli. The breccia layers are scoria from an immediately adjacent small scoria cone and, with undulatory contacts and, in some cases, incipient soil formation, are interpreted to represent significant hiatuses in the deposition. Vesicular ashes occur within the lower massive and laminated fine ash beds and are also interpreted to be the results of significant breaks in the eruption (years to decades), as their upper contacts are erosive and the lower contacts commonly gradational. Weak bedding and channels in the upper section reveal erosion and re-sedimentation off the adjacent scoria cone.

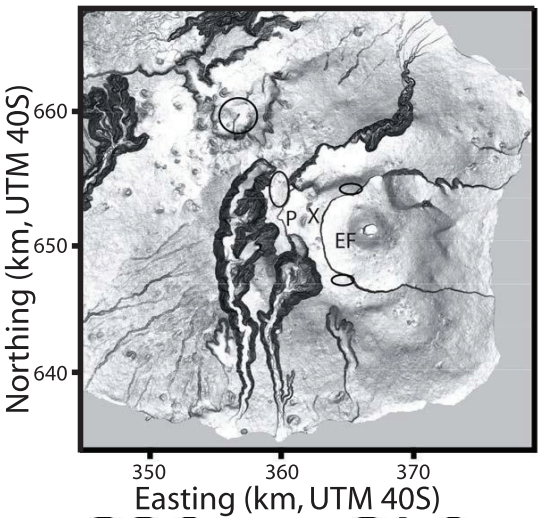

Fig. 1 – Map of Piton de La Fournaise, with circles showing distribution of Bellecombe deposits. EF: Enclos Fouqué (inner caldera), P: Plaine des Sables (outer caldera), X: Petit Carriere site.

Outside the caldera on the Plaine des Remparts, 2-4 km NW of Petit Carriere, a single bed, correlative with the upper ash pellet and laminated ash of Petit Carriere, dominates or is the only primary bed in the Bellecombe sequence in many locations. Massive or laminated fine-grained ash layers occur above and below this bed in many locations. These may correlate with the massive and laminated fine ash inside the caldera. In distal outcrops, 10-11 km downwind from Petit Carriere, >5 gray ashes interbedded with local scoria fallouts occur in sections along the main highway. Correlation of these beds to individual, more proximal beds of the Bellecombe ash has not been possible, but their presence and the occurrence within them of laminated fine ash and mud pellet layers suggests that Bellecombe-like eruptive behavior has been a recurring phenomenon at PdF.

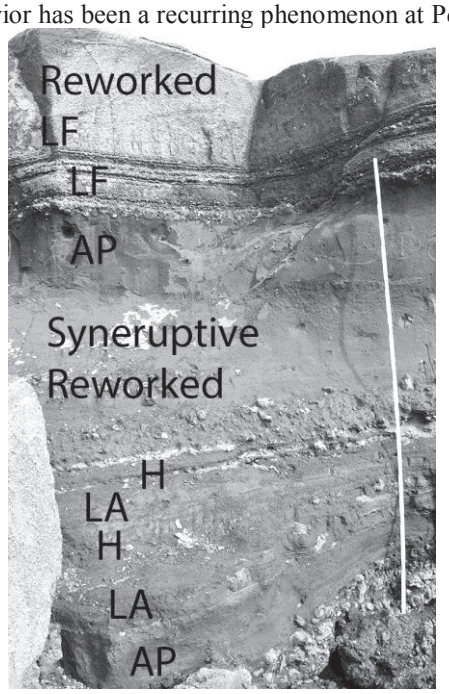

Fig. 2 – The lower Bellecombe ash section at Petit Carriere. AP: ash-pellet-rich bed, LA: laminated ash, H: eruptive hiatus (erosion, vesicular ash), LF: lapilli fallout.

A distinctive coarse breccia occurs along the inner caldera rim of PdF, with ash beds above and below it. The breccia is only found within a few hundred meters of the rim whereas the ash is 1-2 m thick in total and extends out farther, although it then is covered by or not preserved on top of lavas. The ash is massive, with many ash pellet beds, or laminated, and in near-caldera-rim sites, cross-bedded coarse-ash deposits are interpreted as deposits of dilute pyroclastic density currents (PDC). The ash beds may correlate with the lower part of the Petit Carriere sequence.

Abundant gray ash may represent a magmatic (hot rock) component, but the Bellecombe ash also has ash and lapilli of gabbro, thought to come from an intrusive body ≥2000 m below the surface (Upton et al. 2000), and hydrothermally altered grains that likely come from a geothermal system between the top of the gabbro body and the water table, about 500 m below the surface of the summit.

The Bellecombe ashes are the products of water:magma interaction. The abundant ash pellets, blocky juvenile fragments, and dilute PDC deposits are typical of such interaction. The deposit distribution downwind is consistent with a low wind-directed eruption column, with the planar laminated ash indicating moist deposition over an extended period (months). The distribution and the dilute-PDC flow direction indicators locate the lower eruption sequence vent in the inner caldera whereas the upper sequence was likely sourced in the outer caldera, just to the west of Petit Carriere.

We interpret the Bellecombe ash sequence to be indicative of multiple explosive eruptions from PdF. The breccia near the caldera rim and associated ash may be from a N-S fissure during lateral (seaward) flank sliding. A second eruption produced the upper part of the Petit Carriere sequence and much of the deposits exposed to the northwest. Based upon the many ash beds in the distal exposures, this style of explosive eruption has occurred repeatedly in the past at PdF. The current effusive eruptive style of PdF is not the only possibility for the future. Extended eruptions of wet ash could produce lingering hazards in the downwind direction and lahars can affect inhabited areas at lower elevations, while the associated explosions could make the caldera, a popular tourist destination, hazardous.

References

Bachèlery, P. 1981. Le Piton de la Fournaise (Ile de la Réunion). Etude volcanologique, structurale et pétrologique. University of Clermont-Ferrand, Clermont-Ferrand, Ph.D. thesis, 255 pp.

Michon, L., DiMuro, A., Villeneuve, N., Saint-Marc, C., Fadda, P., Manta, F. 2013. Explosive activity of the summit cone of Piton de la Fournaise volcano (La Réunion island): A historical and geological review. Journal of Volcanology and Geothermal Research 263:117–133.

Mohamed-Abchir, A. 1996. Les Cendres de Bellecombe: un évènement majeur dans le passé récent du Piton de la Fournaise, Ile de la Réunion. PhD thesis, Université de Paris VII, 248 pp.

Morandi, A., Principe, C., Di Muro, A., Leroi, G., Michon, L., Bachelery, P. In press. Pre-historic explosive activity at Piton de La Fournaise volcano. Bachelery, P., Lenat, J.F., Di Muro, A., Michon, L., Eds., "Active Volcanoes of the World" series, Springer.

Upton, B.G.J., Semetb, M.P., Joron, J.-L. 2000. Cumulate clasts in the Bellecombe Ash Member, Piton de la Fournaise, Réunion Island, and their bearing on cumulative processes in the petrogenesis of the Réunion lavas. Journal of Volcanology and Geothermal Research 104:297-318.

Eruption sequence forecasting and hazard mapping of volcanic fields

Gábor Kereszturi*, Károly Németh, Jonathan Procter, Shane J. Cronin and **Javier Agustín-Flores**

*Volcanic Risk Solutions, Institute of Agriculture and Environment, Massey University, Private Bag 11 222, Palmerston North, New Zealand. * g.kereszturi@yahoo.com*

Keywords: volcanic hazard, phreatomagmatism, tuff ring, scoria cone.

Monogenetic basaltic volcanism is characterised by a complex array of behaviours in the spatial distribution of magma output, temporal variability in magma flux and eruptive frequency. The most difficult aspect of planning for volcanic hazards in an urbanised monogenetic field is the unknown location of the next eruption. New eruption sites can only be broadly forecast based on vent spatial-density methods (Connor and Hill, 1995). Quantifying the spatial variability of hazard in volcanic fields could provide an advance toward more robust hazard preparedness. Aside from variations in eruption volume or composition, one of the key factors dictating hazard in a distributed field is the interaction of magma with the near surface geology, hydrology and landscape. Specifically, it is recognised that the most explosive eruptions in basaltic volcanic fields are normally related to phreatomagmatism, especially when magmas first break through to the surface in saturated country rock environments (Lorenz, 2007). Past emergency management planning approaches in the AVF, have used eruption scenarios developed by expert elicitation and incorporated within Bayesian Event Tree for Eruption Forecasting (BET_EF) (Lindsay *et al.* , 2010). Combining this with specific models for new eruption locations is precluded by the absence of any spatio-temporal relationship seen in the AVF. Since future vent-opening cannot be forecast based on past volcanism, an alternative approach is to develop a spatial-susceptibility map.

Combining near-surface multi-component geological and geographic data within a Geographical Information System (GIS) is common for a range of studies, such as flood and landslide susceptibility mapping. This approach has not yet been adapted for specifically determining eruption hazard types and likely eruption sequence. Here a spatial hazard model is developed for the AVF by combining; (1) a spatial model combining factors promoting phreatomagmatic explosive eruptions; and (2) a spatial distribution of past eruptive volumes for phreatomagmatic eruptions.

To create a spatial model for phreatomagmatic eruption susceptibility four main factors were combined: (a) thickness of water-saturated and porous sediments, specifically Pliocene-Recent alluvial and intertidal deposits, (b) elevation, (c) distance from present coastline, and (d) distance from known fault lines.

The correspondence of thick deposits (≥20 m) of Pliocene-Recent unconsolidated sediments (Fig. 1A) to dominantly phreatomagmatic volcanism was recognised in the southern part of the AVF (*e.g.* Agustín-Flores *et al.* , 2014). These sediments host the most productive aquifers in the area, with aquifers in the deeper Miocene sediments restricted to jointed/fractured areas and porous volcanic deposits being mostly thin, surficial units (Agustín-Flores *et al.* , 2014).

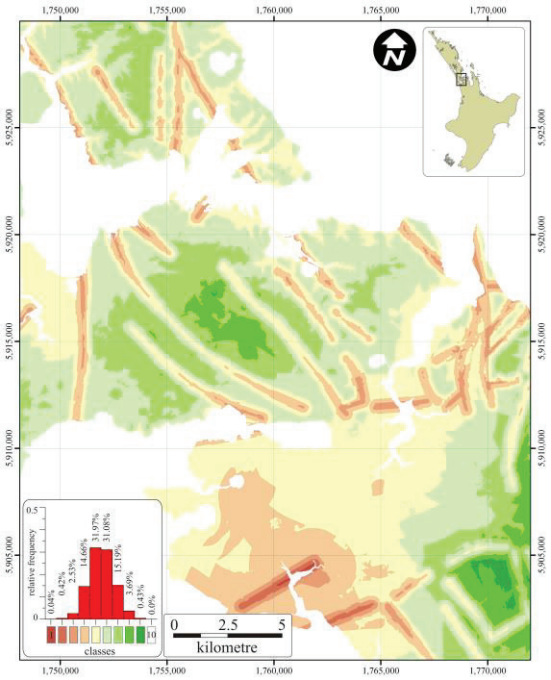

Fig. 1 – Classified susceptibility map for phreatomagmatic vent opening phase for the AVF.

The topography of the field was determined form a Light Detection and Ranging (LiDAR) derived Digital Surface Model (DSM), with the present day shoreline defined at 0 m a.s.l. Coastal margins in volcanic fields often show high concentrations of phreatomagmatic volcanoes, as well as depressions. Fault locations (Fig. 1D) were taken from Kenny *et al.* (2012), recognising

that these structural weak zones in country-rock, host aquifers and thus favour magma-water interactions. Based on these factors promoting phreatomagmatism, a susceptibility map was created by overlaying each information layer, provisionally weighted equally. The only areas not covered in this approach are submarine sites. The susceptibility for phreatomagmatic eruptions in the AVF was subdivided into ten classes (1 = high, 10 = low).

In order to develop a spatial model for eruption sequence forecasting for the AVF, the volumes of past phreatomagmatic eruptions from Kereszturi *et al.* (2013), were interpolated between vent locations to create a field estimate. This volume surface was overlain with the susceptibility map to extract median phreatomagmatic volumes for each susceptibility class. There is a strong correlation between eruptive volumes with the susceptibility class (Fig. 2). This correlation can thus be used to forecast potential phreatomagmatic eruption volumes based on location.

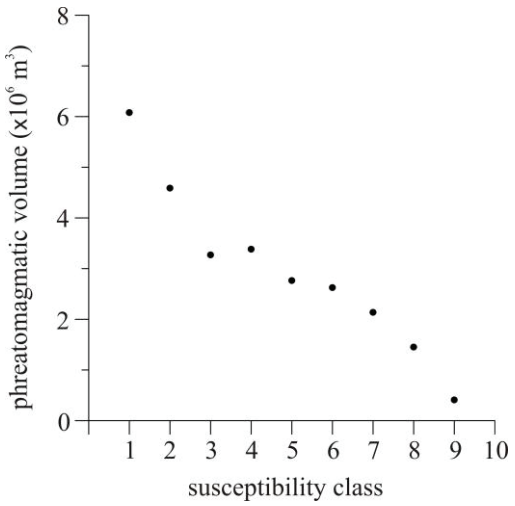

Fig. 2 – Scatter graph showing the relationship between susceptibility classes for phreatomagmatic eruptions and the median volume estimated from the interpolated raster of phreatomagmatic phases.

The susceptibility map for the AVF (Fig. 1) shows a low potential for phreatomagmatic eruptions in the North Shore, Central Auckland and the Hunua Ranges. Relatively higher local susceptibilities within these areas occur along fault lines and/or where the alluvium reaches ≥20 m thickness. The Manukau Lowlands shows the highest susceptibility for phreatomagmatic eruptions. Large potential eruption areas within the AVF are under the sea (~300 km^2), where initial Surtseyan style volcanism is also expected.

Volcanic hazard preparation in monogenetic fields can be improved by forecasting the likely volcanic phenomenon on a spatial basis, especially in a densely populated city. This eruption style susceptibility mapping technique can be directly integrated into the BET_EF approach, providing a more detailed picture of potential volcanic hazards, based on multiple influencing factors (*e.g.* lithology, topography, faults and sea proximity).

This approach must still be adapted for changing environmental features that may influence eruption susceptibility, for example, in the current AVF sea level is higher than throughout most of its eruptive history during the late Pleistocene glaciations. For forecasting phreatomagmatic eruptions, for instance active monitoring of groundwater levels and flows could be factored in. Hazard evaluation can also be improved by better understanding physical influences on magma-water interaction, for example identifying specific eruption magnitudes in relation to different country rock substrates (*e.g.* Agustín-Flores *et al.* , 2014). Extending this approach to volcanic fields with other climatic and geological settings would ensure a more complex understanding of volcanic hazard for monogenetic volcanic fields.

Acknowledgements

GK gratefully acknowledges the Institute of Agriculture and Environment, PhD Fellowship at Massey University.

References

Agustín-Flores, J., Németh, K., Cronin, S.J., Lindsay, J.M., Kereszturi, G., Brand, B.D., Smith, I.E.M., 2014. Phreatomagmatic eruptions through unconsolidated coastal plain sequences, Maungataketake, Auckland Volcanic Field (New Zealand). Journal of Volcanology and Geothermal Research 276, 46-63.

Connor, C.B., Hill, B.E., 1995. Three nonhomogeneous Poisson models for the probability of basaltic volcanism: Application to the Yucca Mountain region, Nevada, U.S.A. Journal of Geophysical Research: Solid Earth 100, 10107-10125.

Kereszturi, G., Németh, K., Cronin, J.S., Agustin-Flores, J., Smith, I.E.M., Lindsay, J., 2013. A model for calculating eruptive volumes for monogenetic volcanoes – Implication for the Quaternary Auckland Volcanic Field, New Zealand. Journal of Volcanology and Geothermal Research 266, 16-33.

Kenny, J.A., Lindsay, J.M., Howe, T.M., 2012. Post-Miocene faults in Auckland: insights from borehole and topographic analysis. New Zealand Journal of Geology and Geophysics 55, 323-343.

Lindsay, J., Marzocchi, W., Jolly, G., 2010. Towards real-time eruption forecasting in the Auckland Volcanic Field: application of BET_EF during the New Zealand National Disaster Exercise 'Ruaumoko'. Bulletin of Volcanology 72: 185-204.

Lorenz, V., 2007. Syn- and posteruptive hazards of maar–diatreme volcanoes. Journal of Volcanology and Geothermal Research 159, 285-312.

Eruptive volumes, lava flow morphology and numerical simulation of the 1256 AD Al-Madinah eruption, Kingdom of Saudi Arabia

Gábor Kereszturi[1], **Károly Németh[1]**, Mohammed Rashad H. Moufti[2], Annalisa Cappello[3], Gaetana Ganci[3], Ciro Del Negro[3], Jonathan Procter[1], Hani Mahmoud Ali Zahran[4]

[1] *Volcanic Risk Solutions, Institute of Agriculture and Environment, Massey University, Private Bag 11 222, Palmerston North, New Zealand.* g.kereszturi@yahoo.com
[2] *Geological Hazard Research Center, King Abdulaziz University, Jeddah, Kingdom of Saudi Arabia.*
[3] *Istituto Nazionale di Geofisica e Vulcanologia, Catania, Italy.*
[4] *National Center for Earthquakes and Volcanoes, Saudi Geological Survey, Kingdom of Saudi Arabia.*

Keywords: morphology, basalt, effusion.

Emplacement of lava flows is mainly influenced by their rheology, which is a function of parameters, such as extrusion temperature, composition, crystallinity, volatile content, effusion rate and topography (Griffiths and Fink 1993; Kerr *et al.* 2006; Harris and Rowland 2009). In many cases, emplacement processes are strongly influenced by topography, such as documented on the steep flanks of Mt. Etna (Favalli *et al.* 2005).

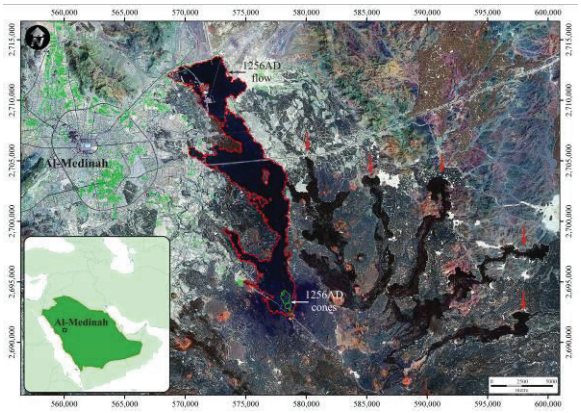

Fig. 1 – Overview pan-sharpened LANDSAT image of the 1256AD lava flow in the Harrat Rahat, Saudi Arabia. Other recent lava flows are indicated by red arrows.

The interplay between such parameters imprints signatures on the lava flows that may vary on multiple scales, and are defined by existent lava structures and lava textures. The lava structures includes lava rises, lava tubes, tumuli, breakout flows (*e.g.* Murcia *et al.* 2014), occurring at a km to m scale. Lava textures refer to smooth, spiny, blistered, clinker, agglutinated surfaces (*e.g.* Murcia *et al.* 2014), occurring at a much finer scale of m to mm. As a whole, these lava structure and texture define the surface morphology or morphotypes that are related to the classical definition of the lava flows, such as pahoehoe, a'a and blocky (*e.g.* Rossi 1997). These morphotypes may be used to reconstruct the thermodynamics and kinematics of the lava flows.

The emplacement of a lava flow can be modeled numerically using a variety of input data on rheology, viscosity, eruptive volumes and effusion curves. In terms of modeling, there are two types of codes available for simulations. Codes that use topography to predict lava flow emplacement processes (*e.g.* inundation at a specific location). These codes account only for the maximum elevation change of the topography as a first-order proxy of lava flow pathway detection (Favalli *et al.* 2005). The other type of codes, such as MAGFLOW (Del Negro *et al.* 2008), that can model rheological changes during the emplacement of a lava flow (*e.g.* solidification rates, spreading and channelizing of flow). Consequently, these codes can predict flow path for lava, occurring on low relief areas.

Volcanic hazard mapping of potentially active monogenetic volcanic fields requires a careful implementation of field-derived data of lava flows (*e.g.* mapping, flow morphometry, flow volume) into a numerical model. This aspect of constructing volcanic hazard maps is important in the Harrat Rahat, Saudi Arabia (Fig. 1). The youngest manifestation of volcanism formed an extensive lava flow associated with small to medium size scoria cones in the northern part of the Harrat Rahat (Camp *et al.* 1987; Murcia *et al.* 2014). Most of the Holocene eruptions in the Harrat Rahat produced very similar eruption styles (*e.g.* fire-fountaining to Strombolian and violent Strombolian eruptions), dominated by an emplacement of lava flows. Due to the abundance of effusive activity of the area, Harrat Rahat requires a volcanic hazard map for lava flows. As input data for lava flow simulations using MAGFLOW (Del Negro *et al.* 2008), an analysis of lava flow morphometry and eruptive volumes of the most recent lava flow field emplaced 1256 AD in the proximity to the City of Al-Madinah (Fig. 1) was carried out. This is to establish the emplacement conditions of the 1256 AD flow (*e.g.* volume- vs. cooling-limited regime, and influences on lava flow emplacement processes), and to provide supporting data for choosing an appropriate lava flow simulation code for future volcanic hazard mapping.

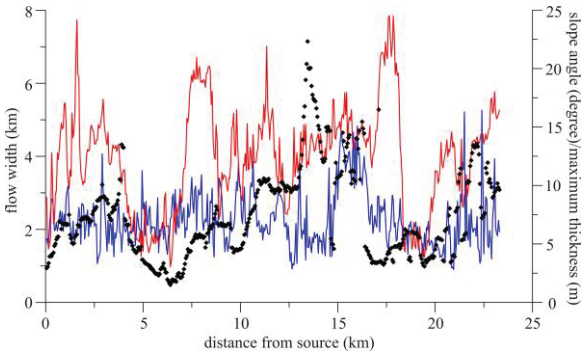

Fig. 2 – Down flow change of the flow width of the main along perpendicular transects (black diamond) as a function of slope angle of pre-eruptive surface (blue line) and maximum thickness (red line).

The outline of the scoria cones and lava flow was mapped out at the scale of 1:500, using high resolution orthophotos (0.6 m), Landsat TM satellite image, high resolution (0.5 m) Light Detection and Ranging (LiDAR) Digital Surface Model (DSM) and their derivatives, such as hillshade and slope angle maps, and previous mapping by Camp *et al.* (1987). The lava flow and scoria cone bulk volumes were extracted from the LiDAR DSM using two first order trend surface fitted to spot heights captured outside of the lava flow field. This pre-eruptive surface and the LiDAR DSM consequently defined a bulk eruptive volume of 0.018 km^3 and 0.4 km^3 for the scoria cone and lava flow, respectively. Based on the historical description, the lava flow emplacement took place in ca. 52 days, resulting in a ca. 89 m^3/s average effusion rates. A Geographical Information System-based (GIS) morphometric analysis of the main lava flow channel was carried out, determining the flow width, thickness and slope of the pre-eruptive terrain. The results show that there is no or limited correlation of the flow width with the pre-eruptive topography (Fig. 2). Slope angle values along transects are highly variable due to the fine-details of topography captured by the high-resolution LiDAR DSM. The overall inclination of the pre-eruptive terrain is, however, less than 1 degree. There is a mild correlation between lava flow width and the maximum flow thickness (Fig. 2). Lava flow maximum thickness tends to be thicker when the flow width increases. This potentially points out a limited dependence of flow emplacement processes on pre-eruptive topography. Comparing the maximum length of the main flow channel of 23 km with the empirical relationship of flow length with the average effusion rate, it can be concluded that the flow emplaced in the cooling-limited regime. Therefore, the flow attained its maximum length in accordance with the effusion rates before the magma supply dropped (Harris and Rowland 2009).

Based on the preliminary results on the lava flow morphometry and volumes, the most appropriate numerical code for lava flow simulation is a code, such as MAGFLOW (Del Negro *et al.* 2008), that is able to model rheological changes during lava flow emplacement. This code requires input parameters, such as solidification temperature, density, emissivity, specific heat, water content, total volume, effusive curve, source location, and pre-eruptive topography. In the future this code can be tested to simulate lava flows in the broader area of the Harrat Rahat.

Acknowledgements

GK is thankful for the logistic support from the Geohazards Research Center of the King Abdulaziz University, Jeddah.

References

Camp, V., Hooper, P., Roobol, M.J., White, D.L., 1987. The Madinah eruption, Saudi Arabia: Magma mixing and simultaneous extrusion of three basaltic chemical types. Bulletin of Volcanology 49, 489-508.

Del Negro, C., Fortuna, L., Herault, A., Vicari, A., 2008. Simulations of the 2004 lava flow at Etna volcano using the magflow cellular automata model. Bulletin of Volcanology 70, 805-812.

Favalli, M., Pareschi, M.T., Neri, A., Isola, I., 2005. Forecasting lava flow paths by a stochastic approach. Geophysical Research Letters 32, DOI: 10.1029/2004GL021718.

Griffiths, R.W., Fink, J.H., 1993. Effects of surface cooling on the spreading of lava flows and domes. Journal of Fluid Mechanics 252, 667-702.

Harris, A.J.L., Rowland, S.K., 2009. Effusion Rate Controls on Lava Flow Length and the Role of Heat Loss: A Review, in: Hoskuldsson, A., Thordarson, T., Larsen, G., Self, S., Rowland, S. (Eds.), The Legacy of George P.L. Walker, Special Publications of IAVCEI 2. Geological Society of London, London, United Kingdom, pp. 33-51.

Kerr, R.C., Griffiths, R.W., Cashman, K.V., 2006. Formation of channelized lava flows on an unconfined slope. Journal of Geophysical Research: Solid Earth 111, B10206.

Murcia, H., Németh, K., Moufti, M.R., Lindsay, J.M., El-Masry, N., Cronin, S.J., Qaddah, A., Smith, I.E.M., 2014. Late Holocene lava flow morphotypes of northern Harrat Rahat, Kingdom of Saudi Arabia: Implications for the description of continental lava fields. Journal of Asian Earth Sciences 84, 131-145.

Rossi, M.J., 1997, Morphology of the 1984 open-channel lava flow at Krafla volcano, northern Iceland: Geomorphology, v. 20, p. 95-112.

Maarmuseum Manderscheid - Not just a museum and maars, but also an important multiplier for geotourism!

Martin Koziol

Maarmuseum Manderscheid, Wittlicher Strasse 11, D-54531 Manderscheid. maarmuseum@t-online.de

Keywords: natural history museum, geotourist service, environmental education.

The quaternary volcanic field of the West Eifel includes about 270 volcanic sites (Meyer, 2013) of which more than 75 have already been identified as maar volcanoes / craters. They are the huge craters which are formed, scattered across the landscape, when rising magma makes explosive contact with surface and ground water. The West Eifel is one of the classic maar areas of the world, showing activity from 1 million years back in the past until 10,000 years ago. Apart from these recent maars, there are at least three older maars, among them the oldest maar of the Eifel, the Eckfeld-Maar that dates back 45 million years. They all belong to the tertiary High Eifel volcanic field that was active some 45-35 million years ago (Wagner *et al.*, 2012)

With the *exhibition* at the Maarmuseum Manderscheid – a natural history museum -opened in 1999 we would like to show visitors the enormous natural variety and international significance of these quaternary and tertiary maars of the Eifel for the region itself and science. The exhibition shows the genesis, history and development of the Eifel-maars in the past and present. At Maarmuseum Manderscheid, the maars - unique testimonies to ancient times - present themselves in a transparent manner. Spectacular simulation shows provide information about geological facts from new perspectives. One highlight of the exhibition is the large-scale model of a maar (Fig. 1) with audio-visual performances!

Fig. 1 – Interior view of the Museum / Manderscheid.

In addition, the museum presents the originals of fossils from the world-famous Eocene ”Eckfeld Maar”, such as the ”Eckfeld Horse”, a pre-horse skeleton bearing a fetus. With the help of the 30.000 fossils, the once tropical landscape of the Eifel has been reconstructed in a large diorama

The Museum is responsible for a hiking trail called the *GeoRoute Volcanic Eifel around Manderscheid*. (Fig. 3) The 140 km long GeoRoute is divided into three sections: the ”Volcanic route”, the ”Sandstone route” as well as the ”Devon route”, with information about the nature and geology of this famous region in the west of the Eifel displayed on special boards

We are not just a Museum, but also a geotourist service undertaking, however, without any intention of making a profit! We use this many-sided and world-famous volcanism in the Eifel purposefully for tourism in our region and its service providers – hotels, youth hostels, camp sites – so that its value will be experienced. School classes and hiking groups book trained *GeoRangers* through the Museum for a small fee who accompany them on their field trip and explain the geological outcrops in a clear and comprehensible manner. Special highlights are the abandoned lava pits of the Mosenberg volcanoes by “Bettenfeld” which were transformed into a *Volcano adventure park* conceived by the Museum in 2013 (Fig. 2)

Fig. 2 – Volcano adventure park Mosenberg / Bettenfeld.

There you see a cross section through a scoria cone with its colors and forms. This outcrop is supplemented by an educational trail with the different volcanic rocks of the Eifel and an outdoor classroom. From there the volcanic wall is to be seen in bad weather and explained with the help of the information boards installed. The *VulkaMaar- Trail* is a signposted quality hiking trail running directly through the adventure park. Hikers can thus be led to this highlight that is free of charge and open throughout the year. The experience on the spot can be repeated and deepened once again in the Museum on your own or with the help of a guided tour appropriate for one's age.

In addition, since 2001 the Museum has been active in *environmental education* and accepted by the state authorities as an extramural place of learning and environmental education institution. The environmental education topics are linked together and promoted by a study group active in several regions.

The *Museum's collection consists of regional fossils, minerals and rocks*. The fossils come from the devonian argillaceous slate or limestone of the Eifel, or from fossil-bearing lake sediments from maars all over the world. In the case of the minerals and rocks, the focus is entirely on the Eifel volcanoes. This collection is supplemented by a library with many scientific works, periodicals, maps and books about the Eifel and volcanism.

Maarmuseum Manderscheid has *co-operation agreements with the State Collection of Nature of Rhineland-Palatinate*, the German Helmholtz-GeoResearchCenter Potsdam and the *Huguangyan Maar Geopark* in South China. We are a member of geoscientific and museum associations. We support universities with their research, field trips and seminars in the Eifel directly on the spot. Small conferences and study group meetings can be held here.

All activities are strategically integrated into the *European Nature- and GeoPark Vulkaneifel* and the tourist agencies of the region. The geological museums in Strohn, Daun, Hillesheim, Jünkerath and Gerolstein also belong to the GeoPark. The marketing and product development of these institutions are concentrated, promoted and central marketed by this GeoPark.

"Collect, preserve, research and present" are the principles that (must) direct a structured museum! Nestling in a unique volcanic landscape, Maarmuseum Manderscheid is the only museum worldwide that deals with the thrilling origin and development of maars. And that not only for museum and scientific purposes, but for the geotourist benefit of the Eifel!!

Acknowledgements

Mayor Wolfgang Schmitz (District of Manderscheid), Mayor Günter Krämer (Town of Manderscheid), State Collection of Nature of Rhineland-Palatinate, German Helmholtz-GeoResearchCenter Potsdam and a lot of culture interested people have provided support for the last 15 years. We thank Andrea Brockes for helping by the English translation.

Internet: www.maarmuseum.de / www.geopark-vulkaneifel.de / www.vulkanerlebnis-mosenberg.de

References

Meyer, W. (2013). Geologie der Eifel. 4. Edition, XIV, 704 pp., 157 figures, 12 tables, 8 panels.

Wagner, W.H., Kremb-Wagner, F., Koziol, M. & Negendank, J.F.W. (2012). Trier und Umgebung. 3. Edition, X, 396 pp., 170 figures, 13 tables, Collection of Geol. Leaders, Vol. 60

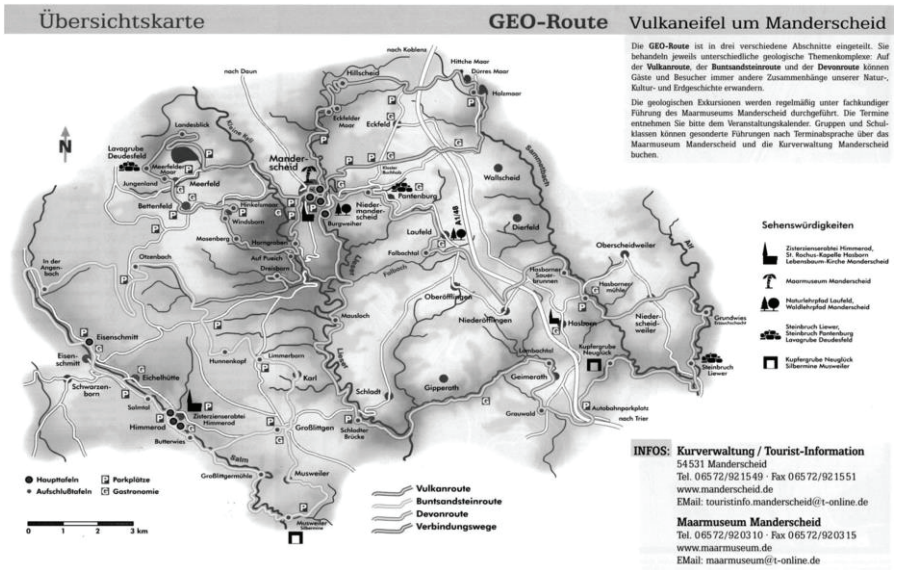

Fig. 3 – Overview map of the GeoRoute Manderscheid.

Lemptégy Volcano: How a hill top removal became a major geo-educational facility

Cécile Olive[1], Audray Delcamp[2], Benjamin van Wyk de Vries[3]

[1] *Conseil Générale du Puy de Dôme, Clermont-Ferrand, France.* Cecile.OLIVE@cg63.fr
[2] *Department of Geography, Vrije Univieristiteit Brussel, Belgium.* delcampa@tcd.ie
[3] *Laboratoire Magmas et Volcans, Univierité Blaise Pascal, Clermont-Ferrand, France.* b.vanwyk@opgc.fr

Keywords: Lemptégy, Chaîne des Puys, geoheritage.

Quarrying and mining can be be disastrous for local scenery and geological heritage, but if done with care and consideration, can enhance the value of a site.

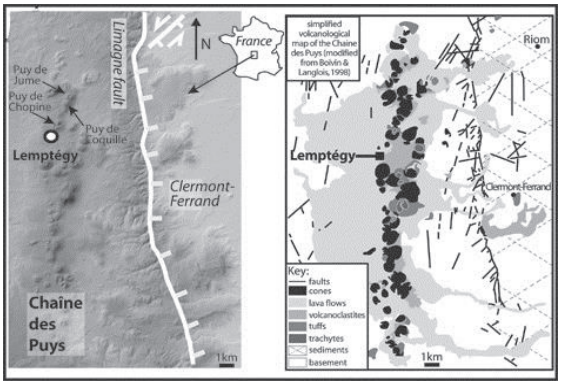

Fig. 1 – The Chaîne des Puys and Limagne fault topography, the monogenetic volcanoes and the structure, with the location of Lemptégy.

Here we show the history of the Lemptégy volcano, which has become a major geological treasure, for education, tourism and research (Delcamp *et al.* 2007, 2014; Mathieu et al 2008; Petronis et al 2013), through intelligent quarrying.

Fig. 2 – Lemptégy volcano seen from the air.

The first mention of Lemptégy volcano, a 32,000 year old (Boivin *et al.*, 2009) small scoria cone in the Chaîne des Puys (Auvergne, France), comes from an 1815 when de Ramond (de Ramond 1815) used a small roadside excavation to prove that it's trachyte breccia covering was just a layer above a scoria core.

Quarrying was a local affair until 1948, when a major extraction phase began to help in post war reconstruction. Local owners employed local labor, who had a close, traditional relationship with the land.

In the 1980's increased mechanization lead to greater extraction, and attracted the attention of local geologists, who found superb cross-sections of the tephra chronology of the Chaîne des Puys, and who began to realize that the geological details being uncovered were of exceptional value.

Fig. 3 – Lemptégy volcano. A school party in front of a horst and graben sequence with an unconformity. This site is part of the French national school curriculum.

Starting with university excursions, then school visits, the quarry began to accept the passage of the public, until in 1993 when it opened as a tourist and educational attraction with specialist guides and a dedicated exhibition. This has continually expanded, and has become the main activity at the volcano, since extraction ceased in 2007.

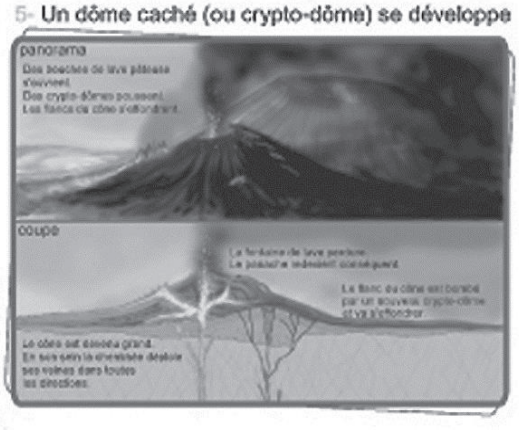

Fig. 4 – An example of a sketch of Lemptégy from the volcano exhibition, illustrating the development of intrusions, cryptodomes and flank eruptions.

Over the last 30 years the extraction has been done with the aim of enhancing the value of the site as a geological feature, so that features such as dykes, vents, conduits, lava flows, faults, alteration, bombs and stratigraphy were preserved, or preferentially excavated. This could only have been done by a close collaboration and understanding between the operators and scientists. Lemptégy is now a major educational and tourist attraction, with over 100,000 visitors a year. It forms part of the recommended national curriculum in France, still attracts cutting edge research.

Fig. 5 – A young visitor gets to grips with density and vesiculation in bombs!

All this would not have been possible without the sense of place, the pride and understanding of the local owners and their close relationship with the scientists.

The most recent development has been the production of a 20 minute 4-D documentary film that describes the evolution of the volcanoes around Lemptégy and the history of the quarry.

The symbiotic relationship between extractors and scientists at Lemptégy has served as an example for other local quarries, where similar relationships are developing, and is now providing an example worldwide of responsible intelligent mining, through the framework of the UNESCO World Heritage project 'The Tectono-volcanic Ensemble of the Chaîne des Puys and the Limagne Fault'.

Acknowledgements

The Lemptégy Volcano team and especially Philippe Montiel and Nathalie Villedieu, and Stéphanie, and Aurélie.

References

Boivin, P., Besson, J.C., Briot, D., Camus, G., De Goër de Hervé, A., Gourgaud, A., Labazuy, P., Langlois, E., de Larouzière, F.D., Livet, M., Mergoil, J., Miallier, D., Morel, J.M., Vernet, G., Vincent, P.M., (2009(, Volcanologie de la Chaîne des Puys Massif Central Français, 5th Edition, scale 1 : 25 000, 1 sheet.

de Ramond, P.,1815, Les Monts dômes, Memoirs Academy of Science Inst., France, p. 1-138.

Delcamp, A. van Wyk de Vries, B, Kervyn, M., (2014). The Endogenous and exogenous growth of the the monogenetic Lemptégy volcano, chaîne des Puys, France (in press. GEOSPHERE).

Matheiu L, van Wyk de Vries B, *Holohan E, Troll (2008) Dykes, cups, saucers and sills: analogue experiments on magma intrusion into brittle rocks 271, 1-4 (2008) 1-13.

Petronis MS, *Delcamp A, van Wyk de Vries B (2009) Magma Emplacement at Lemptegy Volcano, Chaine Des Puys, France based on Structures, Anisotropy of Magnetic Susceptibility and Paleomagnetic Data AGU Fall meeting San Fransisco V23E-2154

Petronis MS, Delcamp A, van Wyk de Vries B (2013) Magma emplacement Lemptégy scoria cone (Chaîne des Puys, France). Bul Volc. On line Sept 2013

Did a maar shelter the Antic port of Agde, France ? A volcanological perspective

Jean-Philippe Degeai[1], Benoît Devillers[2]

[1] *CNRS UMR5140 ASM, 390 route de Pérols, 34970 Lattes, France. jean-philippe.degeai@cnrs.fr*
[2] *Université Montpellier 3, Département de Géographie, route de Mende, 34199 Montpellier Cedex, France.*

Keywords: maar-diatreme structure, isopach maps, kriging models.

The Antic city of Agàthe (Agde, South of France), a major trading post in the Western Mediterranean during the Greek and Roman periods, was founded ca. 550 cal BC by the Phocaeans on a Lower Pleistocene basaltic plateau superimposed or surrounded by scoria cones and maars (fig. 1). These monogenetic volcanoes, that extend seaward from offshore magnetic prospection, erupted during a low sea-level along the Northwestern Mediterranean shelf, in the southern part of the Cenozoic French Massif Central Volcanic Field (Degeai, 2004).

Archaeological excavations between the scoria cone of the Mont Saint-Loup and the Cape of Agde unveiled ancient quarries where occurred an active basalt exploitation for an old millstone industry, while underwater archaeological surveys enabled the discovery of several Antic shipwrecks along the Cape of Agde and in the Luno pond, including one with its full cargo of basalt millstones (Lugand and Bermond, 2001). Questioning about favorable geological settings in coastal domain in order to find a natural harbor susceptible to shelter the unlocalized Antic port infrastructures of Agàthe led to a volcanological study of the multi-vent volcanic complex of Agde.

A geological database was established from the lithostratigraphic analysis of 131 drilling sites cross-cutting the volcanic products in the area of Agde. The raw data are available from the French Geological Survey (BRGM). A deep-drilling of 1,602 m-depth to the west of the Luno pond allows to describe the regional stratigraphy cut through by the internal structure of volcanoes, and notably the diatreme underlying a maar crater (White and Ross, 2011). In addition, field investigations were undertaken to recognize the petrography of deposits.

A series of seven geological cross-sections through the onshore volcanic area shows the stratigraphic relationships between the different volcanoes. A first phase of phreatomagmatic activity formed two ca. 1 km-diameter maars and several small vents filled with lava lake. The syn-eruptive maar crater of the Mont Saint-Loup was then buried under scoria cones, while a lava flow obstructed the palaeovalley of the Hérault River to the west.

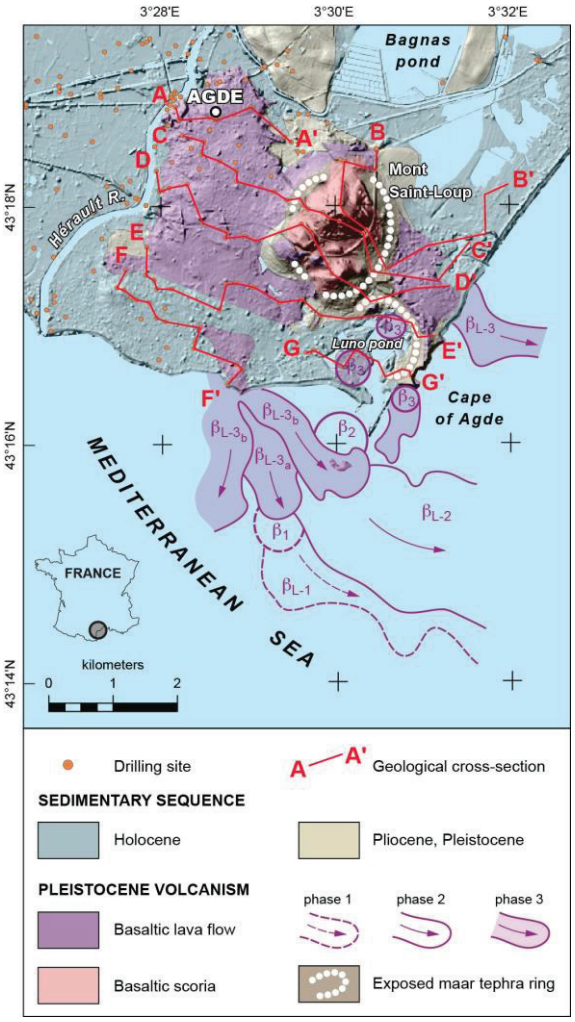

Fig. 1 – Geological setting and location of drilling sites.

A new maar-diatreme volcano was identified in the Luno pond to the west of the Cape of Agde. It is underlined by a ring-dyke along the border fault in the eastern part of the maar crater. This ring-dyke intruded the phreatomagmatic deposits composed of multiple unconsolidated to consolidated planar or cross-bedded horizons, with yellowish ashes partly palagonitized. Petrographic analysis of lithic clasts in the tephra ring of a maar can supply information

about the depth of the explosion locus at the root of the diatreme (Valentine, 2012).

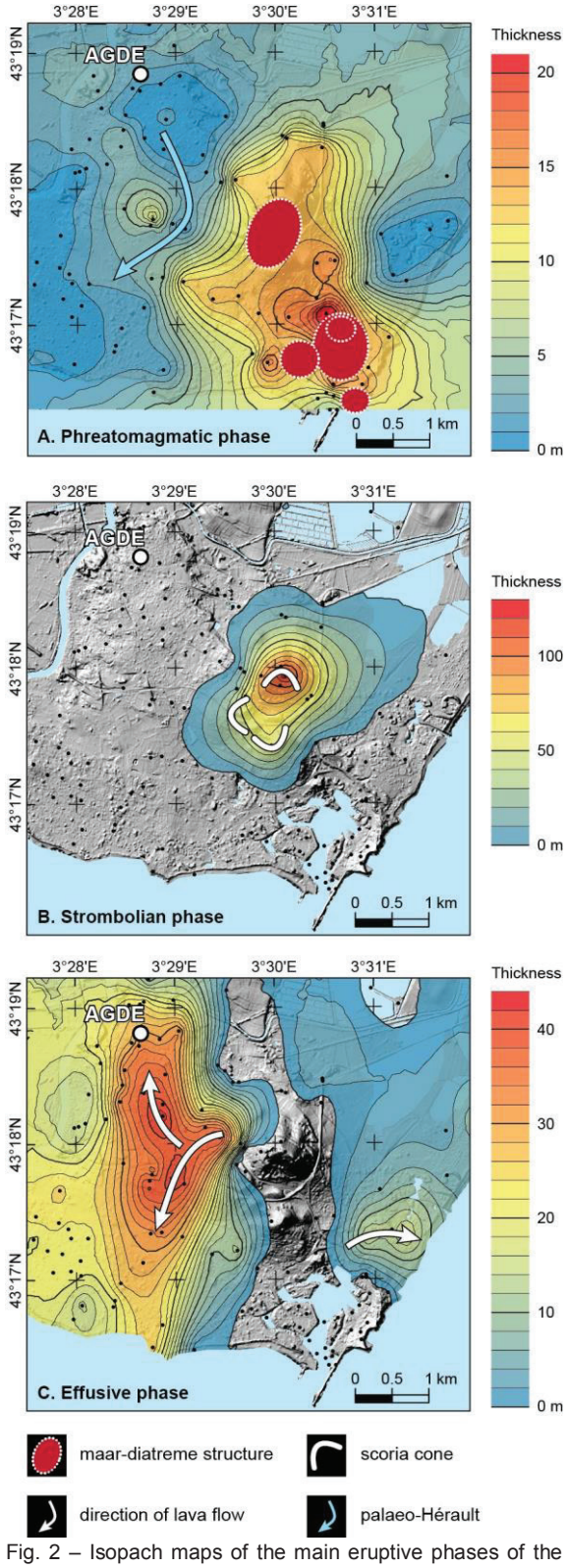

Fig. 2 – Isopach maps of the main eruptive phases of the Agde volcanic system.

Sedimentary lithics in the deposits of the tephra ring along the beach of "La Grande Conque" near the Cape of Agde suggest that the diatreme under the Luno maar crater is a deep-seated structure with a root-zone probably deeper than 1,000 m.

Geostatistical analyses from the stratigraphic database were furthermore performed in order to reconstruct the volume and shape of the main volcanic units. Kriging methods using isotropic and anisotropic exponential models were applied to three units: the phreatomagmatic deposits from the tephra rings, the scoria cones, and the basalt lava flow (fig. 2). The pre-eruptive topography of the palaeovalley of the Hérault River was reconstructed with the ANUDEM numerical model.

The bulk volume of tephra ejected from the maar craters was assessed using the isopach areas for the proximal deposits in the pyroclastic ring and an exponential decay law for the distal tephra-fall deposits (Pyle, 1989; Fierstein and Nathenson, 1992; Sulpizio, 2005). According to the calculation of one or two segments for the distal thinning, this yields a total volume of 0.67-0.86 km^3 ejected during the phreatomagmatic phase.

Acknowledgements

This work is a part of the research program DYLITAG (LabEx ARCHIMEDE) funded by a grant from the French program "Investissements d'Avenir" (ANR-11-LABX-0032-01).

References

Degeai, J.-P., 2004. Mesure de l'érosion post-éruptive autour des craters de maars en inversion de relief dans le Massif central français. Géomorphologie – Relief, Processus, Environment 10/4: 285-304.

Fierstein, J., Nathenson, M., 1992. Another look at the calculation of fallout tephra volumes. Bulletin of Volcanology 54: 156-167.

Lugand, M., Bermond, I., 2001. Carte Archéologique de la Gaule, Agde et le basin de Thau, 34/2. Académie des Inscriptions et Belles-Lettres, Paris, 448 p.

Pyle, D.M., 1989. The thickness, volume and grainsize of tephra fall deposits. Bulletin of Volcanology 51: 1-15.

Sulpizio, R., 2005. Three empirical methods for the calculation of distal volume of tephra-fall deposits. Journal of Volcanology and Geothermal Research 145: 315-336.

Valentine, G.A., 2012. Shallow plumbing systems for small-volume basaltic volcanoes, 2: Evidence from crustal xenoliths at scoria cones and maars. Journal of Volcanology and Geothermal Research 223-224: 47-63.

White, J.D.L., Ross, P.-S., 2011. Maar-diatreme volcanoes: a review. Journal of Volcanology and Geothermal Research 201: 1-29.

Maar volcanoes of the Cameroon Volcanic Line (Central Africa)

Robert Temdjim and Jean-Pierre Tchounkoue

Department of Earth Sciences, Faculty of Sciences, University of Yaounde I, P.O. Box 812 Yaoundé, Cameroon. rtemdjim@yahoo.fr

Keywords: Central Africa, Cameroon Volcanic Line, maar volcanoes.

The Cameroon Volcanic Line is a Y-shaped tectonomagmatic megastructure of Cenozoic-Quaternary age in Western Central Africa. Its continental segment consists of more than sixty Cenozoic anorogenic ring complexes (70-30 Ma; Ngako *et al.*, 2006) and twelve main volcanic centres from Tertiary (51.8 Ma) to Recent (Wandji *et al.*, 2009) set within a succession of horsts and grabens. Its oceanic sector is composed of four major volcanoes installed in the Atlantic Ocean (Bioko, Pagalu, Sao Tomé and Principe; Fig. 1). These result in a major active N30°E tectono-magmatic structure that stretches for more than 1600 km, achieving a width up to 100 km at some places. It extends from Pagalu Island in the gulf of Guinea to Lake Chad in the interior of Africa. Such an active alkaline intraplate structure in both oceanic and continental lithospheres is a unique feature in Africa and even over the World. Only the Mount Cameroon volcano located at the boundary of the continental and oceanic sectors of the Cameroon Volcanic Line is still magmatically active (Suh *et al.*, 2003). In the continental domain, a succession of volcanic horsts is interrupted by trenches and plains (Noun, Kumba, Tombel, Wum, etc.) where numerous, very recently active, monogenetic volcanoes occur.

In Cameroon (Fig. 1), the maar volcanoes are, after scoria cones, the second most common type of subaerial volcanoes. Within the past 30 years, the most disastrous natural hazards and risks were mainly linked to volcanic toxic gas emanations from maar lakes. During this period, more than 30 maar volcanoes were identified, but not studied in detail : four basaltic maar volcanoes (Tison, Ngaoundaba, Ngagouba and Youkou) in the northern part, notably around the Ngaoundere area in the Adamawa Volcanic Massif (Temdjim *et al.*, 2003) which constitutes the north-eastern continental end of the Y-shaped tectono-magmatic structure. The Mbalang-Djalingo maar is located at 18 km east of Ngaoundere; it is the unique trachytic volcano of phreatomagmatic origin reported in Cameroon (Temdjim *et al.*, 2000).

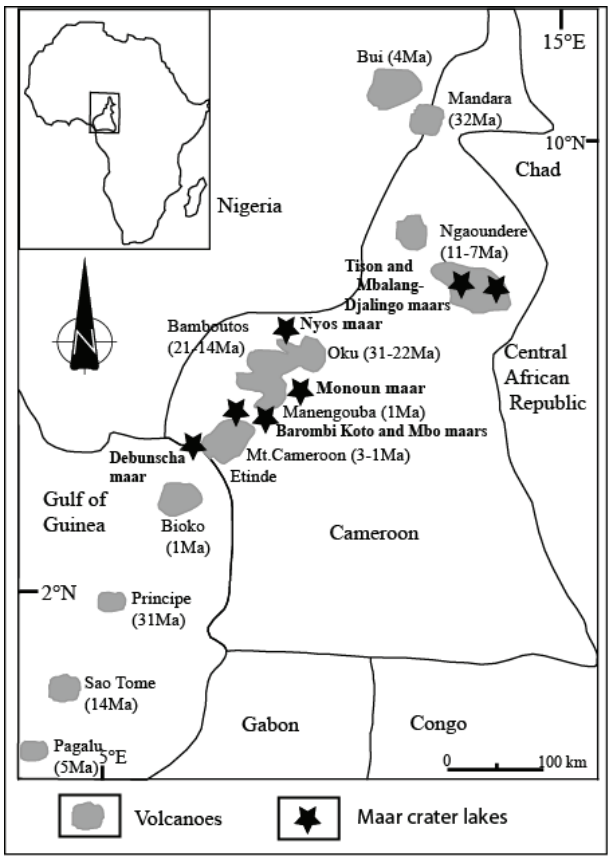

Fig. 1 – Location of the Barombi-Mbo, Barombi-Koto, Debunscha, Mbalang-Djalingo Monoun, Nyos and Tison maar volcanoes along the Cameroon volcanic line. My = million years.

The other maar volcanoes are located in different volcanic centres within the southern sector of the Cameroon volcanic line, and house deep lakes such as : lakes Baleng, Banefo, Barombi-Mbo, Barombi-Koto, Debunscha, Disoni, Edip, Elum, Kuk, Mbwandong, Ménené-East, Ménemé-West, Mfouet, Monoun, Wum, Nchout-Monoun, Négop-Ghang, Nfou, Ngouondam, Nji, Njimbouot, Njipipa-West, Njipipa-South, Nkoambeng-North, Oku, Tchoua and Yupé.

The Nyos (Kling *et al.*, 1987) and Monoun (Sigurdsson *et al.* 1987) are by far, the best known maar crater lakes in Cameroon Volcanic because of hazardous gas that killed at least 37 and 1746 persons respectively at Monoun (15th august 1984) and Nyos (21st august 1986) and a large number of domestic and wild animals. In spite of these catastrophes, maar volcanism in Cameroon is still poorly know. On the other hand, the Nyos maar is also one of the most important volcanoes due to the occurrence of various types of mantle xenoliths (spinel lherolites, spinel harzburgites olivine websterites, and spinel wehrlites) in its phreatomagmatic deposits (Temdjim, 2012).

References

Kling, G.W., Clark, M.A, Compton, H.R, Evans, W.C., Humphrey, A.M., Koenigsberg, E.J., Lockwood, J.P., Tuttle, M.L. and Wagner, G.N. (1987). The 1986 lake Nyos gas disaster in Cameroon, West Africa. *Science 236, 169-175.*

Ngako V., Njonfang E., Aka F.T., Affaton P., Nnange J.M., 2006. The north-south Paleozoic to Quaternary trend of alkaline magmatism from Niger-Nigeria to Cameroon: complex interaction between hotspots and Precambrian faults. J. Afri. Earth Sci., 45, 241-256.

Sigurdsson, H., Devine, F.M., Tchoua, T.S., Pringle, M.K.W., Evans, W.C., 1987. Origin of the Lethal gas bust from Lake Monoun, Cameroon. Journal of Geothermal Research 31, 1–16.

Suh, C.E., Sparks, R.S.J., Fitton, J.G., Ayonghe, S.N., Annen, C., Nana, R., Luckman, A., 2003. The 1999 and 2000 eruptions of Mount Cameroon: eruption behaviour and petrochemistry of lavas. Bulletin of Volcanology 65, 267-287.

Temdjim, R. 2012. Ultramafic xenoliths from Lake Nyos area, Cameroon volcanic line, West-central Africa. Petrography, mineral chemistry, equilibration conditions and metasomatic features. Chemie der Erde – Geochemistry, vol. 72, n°1, 39-60.

Temdjim Robert, Kengne Fodouop et Jean-Pierre Nguetkam (2003). Les risques volcaniques associés à l'activité magmatique récente sur le plateau de l'Adamaoua (Nord-Cameroun), Ligne du Cameroun. Revue de Géographie du Cameroun ; vol. XV, n° 1, 68 – 77.

Temdjim Robert, Tchouankoué Jean.Pierre et Tchoua Félix-M. (2000). Découverte d'un maar trachytique dans la ligne volcanique du Cameroun : Le maar Mbalang-Djalingo dans le district volcanique de Ngaoundéré (Adamaoua, Centre Cameroun). Bulletin de la Société Volcanologique Européenne, vol. 4, 9-14.

Wandji, P., Tsafack, J.P.F., Bardintzeff, J.M., Nkouathio, D.G., Kagou Dongmo, A., Bellon, H., Guillou, H.,2009. Xenoliths of dunites, wehrlites and clinopyroxenite in the basanites fron Batoke volcanic cone (Mount Cameroon, Central Africa): petrogenetic implications. Miner. Petrol. 96, 81-98.

Multiphase numerical modeling of debris jets: implications for diatreme evolution

Matthew R. Sweeney[1], Greg A. Valentine[1,2], Ingo Sonder[1,2], and Abani K. Patra[2,3]

[1] *Department of Geology, University at Buffalo, Buffalo, NY 14260 USA. ms428@buffalo.edu*
[2] *Center for Geohazards Studies, University at Buffalo, Buffalo, NY 14260 USA.*
[3] *Department of Mechanical and Aerospace Engineering, University at Buffalo, Buffalo, NY 14260 USA.*

Keywords: diatreme, debris jets, numerical modeling.

Maar-diatreme volcanoes are the result of explosive subsurface interactions between magma and water that cut deeply into country rock. Multiple explosions throughout the life of these volcanoes result in a crater whose floor is below the pre-eruptive surface (maar) and a subterranean vent structure that extends downward from the crater floor (diatreme). Diatremes constitute the host environment for explosive fragmentation and structures within them can provide important information regarding the eruptive history of a volcano. However, our understanding of the relationship between such structures and eruption dynamics remains limited, particularly in regards to transport length scales and mixing following subsurface explosions. Here, we present results from two-dimensional numerical modeling of phenomena known as "debris jets", which are mixtures of vent-filling debris, vapor, and liquid water that form above explosion sites, with the goals of 1) quantifying the length scales of debris jet activity in diatremes as a function of depth and source conditions and 2) determining how material is mobilized and redistributed in a diatreme.

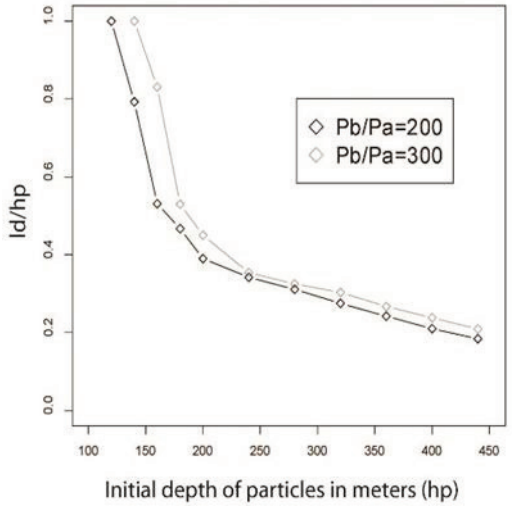

Fig- 1 – Vertical extent of debris jet deposits as a function of pressure and depth in two sets of simulations. Pb/Pa is the ratio of initial debris jet pressure to atmospheric pressure. ld/hp is the ratio of the deposit height to original depth of the particles, hence, ld/hp=1 implies the debris jet breached the surface.

A two-dimensional computational domain is discretized into an axisymmetric, uniform, structured mesh and a bed of close-packed particles is introduced into the lower portion of the domain, meant to represent the vent-filling debris in diatremes during an eruption. A volume of high-pressure gas, which is modeled as water vapor, is introduced into the particles as an initial condition and the particles that lie within the extent of the initial high-pressure area are tracked separate from the rest of the domain and taken as an analogue for the source, or juvenile material in a natural volcano (*e.g.* Andrews *et al.* 2014).

Simulations were done to investigate the vertical transport scales of debris jets as a function of both initial pressure and initial volume of the gas. The depth of the particle domain is incrementally increased from 100m by 20m until 200m, and then is incrementally increased from 200m to 440m by 40m. The vertical extent of the "juvenile" material relative to the initial depth of particles (ld/hp) was recorded (Figure 1). Two sets of simulations were done with different initial pressures to simultaneously investigate the effect of initial pressure on debris jet transport. In each case, ld/hp decreases as the initial depth of particles increases. The rate that ld/hp decreases changes as a function of of the initial depth as well. At initial depths of less than 200m the slope of the ratio becomes significantly steeper indicating that shallower explosions (<200m) form debris jets that travel farther than deep explosions. A 50% increase in initial pressure has a minimal effect on the results.

The volume of gas formed from an explosive interaction between magma and water significantly affects debris jet emplacement due to the strong coupling between volume and energy (see Valentine *et al.* 2014). Using a range of energy values, we arrive at a range of volumes of gas expected to be formed following an explosion in a diatreme. Using this range, we are then able to investigate the effect the initial volume of gas has on debris jet length scales. We find that for typical volumes, breached jets do not occur at depths greater than 300m.

However, for anomalously large volumes of gas, we find that jets that originated as deep as 400m can breach the surface. Recent work by Valentine *et al.* (2014) combining relationships between scaled depth of explosions and energy constraints of phreatomagmatic explosions has shown that most eruptions in maar-diatreme systems are likely sourced by explosions in the upper ~200m of the diatreme and shallower ones (<100m) are likely to dominate deposition onto tephra rings. Both of these results are consistent with the numerical modeling done in this work.

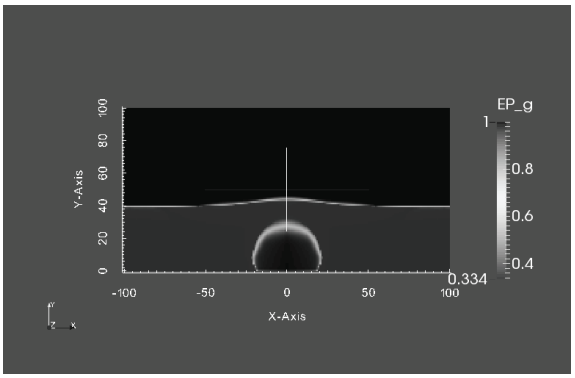

Fig. 2 – Gas volume fraction following release of high-pressure in the bottom of the domain in a shallow model run. Large cavity forms and surface deformation is observed. Scale bars are in meters.

In addition to the vertical transport scales of debris jets, we investigated the effects that the passage of a debris jet has on the distribution of material within a diatreme. We divide the computational domain into identical layers, but mark them such that we can follow them individually to observe meter scale mixing dynamics. We looked at how the width of the domain as well as the shape and location of the initial gas pressure affects the mixing and nature of the resulting deposit. We found that even within the vertically focused debris jet deposit, it was common for a solids species to be present well below its initial position in the initial layering configuration. This phenomenon was observed at Standing Rocks West diatreme by Lefebvre *et al.* (2013) where wall rock clasts in debris jet deposits were found up to 200m below their original stratigraphic unit. This was attributed to space generated at shallow depths encouraging wall-rock collapse as well as evidence for continual mixing of vent-filling debris during the eruption. However, we have shown that through major amounts of subsidence and lesser amounts of entrainment following the formation and passage of a jet, material from one particular layer (20m thick) can be redistributed vertically throughout the entire domain (>100m) in the debris jet deposit (defined as 10m from the central axis). Even so, the debris jet deposit is dominated by the material sourced at (i.e. juvenile), or directly adjacent to, the site of high pressure release. Specifically, the source material and the two nearest solids species never represent less than 33% of the deposit and they usually represent much more. This result is in agreement with both field work (*e.g.* Ross and White (2006)) and experimental work (*e.g.* Andrews *et al.* 2014) done studying debris jet composition and emplacement. Andrews *et al.* (2014) showed that following the release of a high-pressure volume of gas a two-stage process of cavitation and granular uprush occurs, which promotes segregation of the source material and host material. Here, we reproduce this phenomena in all our model runs (Figure 2 and 3), but also show that entrainment does play a noticeable, albeit small, role in transporting particles toward the surface.

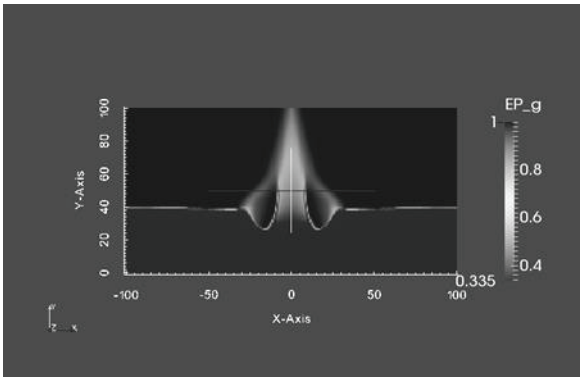

Fig. 3 – Gas volume fraction 3 seconds into the same model run as Figure 2. Following cavitation, a vertical granular uprush is observed, which breaches the surface. Compare to phenomena observed by Andrews *et al.* (2014).

References

Andrews, R.G., White, J.D.L., Dürig,T., Zimanowski, B., 2014. Discrete blasts in granular material yield two-stage process of cavitation and granular fountaining. *Geophysical Research Lett*ers *41*: 422-428, doi:10.1002/2013GL058526.

LeFebvre, N.S., White, J.D.L., Kjarsgaard, B.A., 2013. Unbedded diatreme deposits reveal maar-diatreme-forming eruptive processes: Standing Rocks West, Hopi Buttes, Navajo Nation, USA. Bulletin of Volcanology 75: 739, doi:10.1007/s00445-013-0739-9.

Ross, P.-S., White, J.D.L., 2006. Debris jets in continental phreatomagmatic volcanoes: A field study on their subterranean deposits in the Coombs Hill vent complex, Antarctica. Journal of Volcanology and Geothermal Research 149: 62-84, doi:10.1016/j.jvolgeores.2005.06.007.

Valentine, G.A., Graettinger, A.H., Sonder I., 2014. Explosion depths for phreatomagmatic eruptions. *Geophysical Research Letters*, doi: 10.1002/2014GL06009

The effects of the host-substrate on phreatomagmatic eruptions and the formation of maar-diatremes

Elodie Macorps[1], Greg A. Valentine[1], Alison H. Graettinger[1], Benjamin van Wyk de Vries[2]

[1] *Dept. of Geology and Center for Geohazards Studies, University at Buffalo, Buffalo, NY 14260 USA, elodiema@buffalo.edu*
[2] *Laboratoire Magma et Volcans, Université Blaise Pascal, Clermont-Ferrand, France*

Keywords: phreatomagmatic, maar-diatreme, host-substrate

Understanding maar-diatreme volcanoes that result from the explosive interaction between magma and groundwater, a type of phreatomagmatic activity, is crucial for volcanic hazard analysis. The type of substrate controls the type of aquifer in which external water is sitting before the interaction with magma. This notion is related to the degree of cohesion into particles that comprise the host-substrate. We therefore distinguish "hard" versus "soft" substrate as the two end-members for water availability where: (1) a joint aquifer refers to a hard rock environment in which the faults and structure weaknesses are hydraulically active, and (2) a soft-rock environment where unconsolidated sediments are water-saturated up to - or close to the surface (Lorenz, 2003). Because of the difference in the groundwater availability, the substrate in which the phreatomagmatic explosion occurs can significantly affect the surface morphology (Sohn and Park (2005). Auer *et al.* (2007) established a conceptual model of the two end-member maar-diatreme volcanoes based on the two opposite environments for water availability: hard rock versus wet, unconsolidated sediment maar-diatremes.

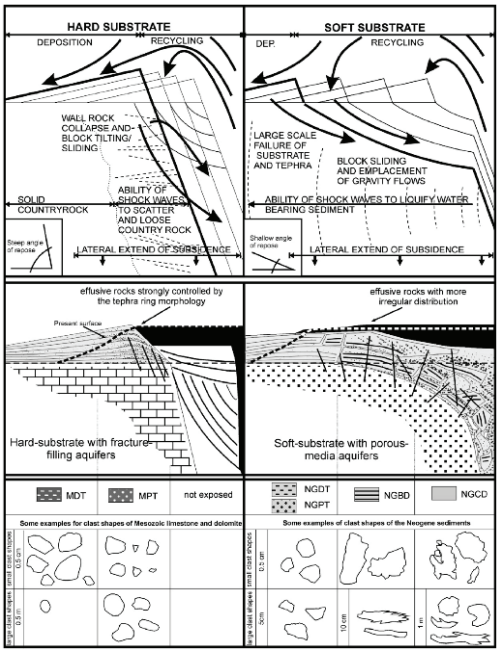

Figure 1 - General model for hard versus soft maar-diatreme volcano (Auer *et al.*, 2007)

However, other field-studies of maar-diatreme volcanoes suggest that the end-member model incompletely describes the products of these eruptions. (Delpit *et al.*, 2014; Ross *et al.*, 2013; Valentine and de Vries, 2014). The results of these studies present an inconsistency with the conceptual models. Because of the disagreement between the proposed model and field observations, it seems crucial to deepen the knowledge on the effects of the host substrate on maar-diatreme volcanoes and phreatomagmatic eruptions.

This study intends to analyze the effect of the host-substrate on the eruptive jet, the ejecta deposits, the crater, and the diatreme structures, focusing on differences between hard and soft substrates.

Valentine *et al.* (2012), Ross *et al.* (2013), and Graettinger *et al.* (2014) present results of meter-scale experimental studies modeling phreatomagmatic eruptions at different scaled depths. Scaled depth refers to a quantitative notion used to describe the location of a subsurface explosion at a specific energy.

$$D = d/E^{(1/3)}, \quad (1)$$

This is mathematically represented in equation (1) where d is the depth of charge burial, E = the energy of the explosion, and D expressed in $m/J^{1/3}$.

The experiments have been performed on two different dates; first in 2012 (Ross *et al.*, 2013; Valentine *et al.*, 2012) and then spring 2013 (Graettinger *et al.*, 2014). The different materials and weather conditions for the experiment settings in 2012 versus 2013 enable the comparison of the substrate influence on the maar-diatreme structure, the eruptive jet features, and ejecta deposits. In the experiments of spring 2012, Valentine *et al.* (2012) and Ross *et al.* (2013) used a top layer composed of crushed asphalt product that developed some strength because many asphalt particles stuck together in the daytime heat. The experimental pads in 2012 can therefore be associated to a "hard" substrate as opposed to the experiments in spring 2013 that are associated to a "soft" substrate. Despite the pad materials, the same experimental settings

(*i.e.* explosive charge and scaled-depth) have been used for pad 1 and pad 3, which enable the comparison of the results between these two experimental datasets focusing on the substrate influence.

Pad 1

The pad 1 – 2012 records large clasts in the ejecta (~50 cm); ten times larger than the biggest clasts in pad 1 – 2013 (~5 cm). The eruptive jet width is, on average, 3 times larger in pad 1 – 2012 than in pad 1 – 2013 (12 m and 4 m, respectively). It appears, therefore, that the eruptive jet width and the ejecta clast sizes tend to be higher when the explosions originate in a more cohesive substrate rather than in a soft substrate. However, there is no major difference in the eruptive jet height and the greatest distance of ejecta between the 2012 and 2013 dataset.

Looking at the crater and subsurface structures, the crater is larger and deeper for the 2012 explosion; however the subsurface structure is deeper in pad 1 – 2013 with a similar wall slope to pad 1 – 2012. A deeper diatreme in soft substrate contradicts the conceptual model of Auer *et al.* (2007) and concurs with prior field observations (Valentine and de Vries, 2014).

Pad 3

Pad 3 had three successive explosions referred to as blasts 1, 2, and 3 for both 2012 and 2013 experiments. The first major difference observed for P3B1 (pad 3 blast 1) between the two datasets is the presence of a retarc, which is a pile of material in a depression, that formed above the pad in 2013, but not in 2012. The 2013 retarc is also associated with a larger crater diameter than in 2012. For the second and third blasts, the crater results are wider in pad 3 from 2012 than from 2013. The eruptive jet maximum height is about 4 times higher for the three blasts in 2012. P3B1 – 2012 presents bigger clasts in the ejecta and a wider eruptive jet. In P3B2 and P3B3, the difference in clast sizes and jet width between the two dataset is less important. This can be interpreted as the hard substrate behaving as a soft substrate after a previous disruption of the host-substrate decreasing the overall particle cohesion.

An upcoming meter-scale experimental study of phreatomagmatic successive explosions in a hard substrate will yield additional results that will be used for a more specific comparison with pad 3 – 2013.

This preliminary study suggests that there are notable differences between the two end-member types of substrate for maar-diatreme formation such as the size of the largest clasts in the ejecta, the width of the eruptive jet, the crater diameter, and the subsurface maximum depth. The combinations of these differences from the resulting pads appear to be more complex than the previous conceptual model proposed.

Acknowledgments

This work is part of a master thesis supported by the University at Buffalo and the Center of Geohazard studies, Buffalo, NY.

References

Auer, A., Martin, U., and Nemeth, K., 2007, The Fekete-hegy (Balaton Highland Hungary)"soft-substrate" and "hard-substrate" maar volcanoes in an aligned volcanic complex–Implications for vent geometry, subsurface stratigraphy and the palaeoenvironmental setting: Journal of Volcanology and Geothermal Research, v. 159, no. 1, p. 225-245.

Delpit, S., Ross, P.-S., and Jr, B. C. H., 2014, Deep bedded ultramafic diatremes in Missouri River Breaks volcanic field, Montana, USA: more than 1 km of syn-eruptive subsidence.

Graettinger, A., Valentine, G., Sonder, I., Ross, P. S., White, J., and Taddeucci, J., 2014, Maar-diatreme geometry and deposits: Subsurface blast experiments with variable explosion depth: Geochemistry, Geophysics, Geosystems.

Ross, P.-S., White, J., Valentine, G., Taddeucci, J., Sonder, I., and Andrews, R., 2013, Experimental birth of a maar–diatreme volcano: Journal of Volcanology and Geothermal Research, v. 260, p. 1-12.

Sohn, Y. K., and Park, K. H., 2005, Composite tuff ring/cone complexes in Jeju Island, Korea: possible consequences of substrate collapse and vent migration: Journal of Volcanology and Geothermal Research, v. 141, no. 1, p. 157-175.

Valentine, G. A., and de Vries, B. v. W., 2014, Unconventional maar diatreme and associated intrusions in the soft sediment-hosted Mardoux structure (Gergovie, France): Bulletin of Volcanology, v. 76, no. 3, p. 1-16.

Valentine, G. A., White, J. D., Ross, P. S., Amin, J., Taddeucci, J., Sonder, I., and Johnson, P. J., 2012, Experimental craters formed by single and multiple buried explosions and implications for volcanic craters with emphasis on maars: Geophysical Research Letters, v. 39, no. 20.

Scaling methods for multi-blast craters in pre-existing morphology

Ingo Sonder, Alison Graettinger and Greg Valentine

Center for Geohazards Studies, University at Buffalo, Buffalo, New York, USA. ingomark@buffalo.edu

Keywords: *crater scaling*, blast experiments, maar-diatremes.

Maar-diatreme volcanoes are primarily formed by the interaction of magma and groundwater in multiple explosive events. In order to understand processes involved in the formation of such structures experiments detonating several discrete chemical explosive charges in one crater structure were conducted. The chemical explosive used, a PETN/TNT mix, has a higher specific energy, and a higher detonation speed compared to an MFCI explosion which is commonly associated with maar forming processes. Therefore the experiments represent an upper limit for the influence of the processes "explosivity" on the whole process. Experimental conditions consisted of test beds made from several stratified, compacted aggregates. In the, so far, 24 experiments the explosive charges were fired at same lateral locations with varying depth of burial. The time separating the blasts was large, so that the material came to rest between the blasts. Resulting crater morphologies and structures were documented by manual measurement and semi automatic photogrammetry for each blast. Experiments were recorded by a diverse set of sensors including high-speed/high-definition cameras, seismic and electric field sensors, normal- and infrasound microphones.

After all blasts were completed resulting structures were excavated and analyzed. The measured sensor signals were evaluated and related to blast energies, depths of burial and crater morphologies.

Former experiments in volcanology and military research (*e.g.* Goto *et al*., 2001, Holsapple & Schmmid, 1980, Bening & Kurtz, 1967) considered craters of single blasts at a given lateral position and found empirical relationships emphasizing the importance of length scaling with the cube root of the blasts energy E. For example the depth of burial producing the largest crater radius—the 'optimal' depth—is proportional to $E^{1/3}$, as is the corresponding radius. The dependencies on $E^{1/3}$ could be roughly confirmed (Valentine *et al*., 2012, Taddeucci *et al*., 2013, Graettinger *et al*., 2014). Also the scaled depth correlated with the sensor signals capturing the blasts dynamics. However, significant scatter was introduced by the pre-existing morphologies. Especially in the case of shallow blasts it is difficult to define the charges depth of burial.

A suitable re-definition for the charges depth of burial ('eruption depth'), accounting for a pre-existing (crater) morphology, the measured dependencies of morphology and blast dynamics on E can be improved significantly. Correlating the distribution of material confining the charge, and its distance to the latter, a confinement potential can be defined that helps to distinguish between inertial and frictional forces. Already the potential is useful as a method to reasonably define an effective depth of charge burial (eruption depth).

The presented multiblast experiments are one of few opportunities to observe the whole range of processes involved in the formation of craters, from subsurface processes to ejecta ballistics. They are expected to provide means to relate eruption dynamics and pre-eruptive settings to endmembers like subsurface structures or ejecta distributions.

Fig. 1 – Snapshot of a blast conducted at 'optimal' depth of burial.

Acknowledgements

This project was funded by the 3E fund of the University at Buffalo.

References

Bening, R. G., Kurtz, M. K., 1967. The Formation of a Crater as Oberved in a Series of Laboratory Sized Experiments U.S. Army Engineer Nuclear Cratering Group, Accession Number : ADA382385.

Büttner, R., Zimanowski, B., 1998 Physics of Thermo-hydraulic Explosions. Physcal Review E, 57: 5726-5729.

Goto, A., Taniguchi, H., Yoshida, M., Ohba, T., Oshima, H., 2001. Effects of explosion energy and depth to the formation of blast wave and crater: Field Explosion Experiment for the understanding of volcanic explosion Geophys. Res. Lett., 28: 4287-4290.

Graettinger, A. H., Valentine, G. A., Sonder, I., Ross, P.-S., White, J. D. L., Taddeucci, J., 2014. Maar-diatreme geometry and deposits: Subsurface blast experiments with variable explosion depth. Geochemistry, Geophysics, Geosystems, 15: 740-764.

Holsapple, K. A., Schmidt, R. M. 1980. On the scaling of crater dimensions: 1. Explosive processes Journal of Geophysical Research: Solid Earth, 85: 7247-7256.

Taddeucci, J., Valentine, G. A., Sonder, I., White, J. D. L., Ross, P.-S., Scarlato, P., 2013. The effect of pre-existing craters on the initial development of explosive volcanic eruptions: an experimental investigation Geophys. Res. Lett., 40, 507-510

Valentine, G. A., White, J. D. L., Ross, P.-S., Amin, J., Taddeucci, J., Sonder, I., Johnson, P. J., 2012. Experimental craters formed by single and multiple buried explosions and implications for maar-diatreme volcanoes Geophys. Res. Lett., 39: L20301.

Morphology and dynamics of explosive vents through cohesive rock formations

Olivier Galland[1], Galen R. Gisler[1], and Øystein T. Haug[2]

[1] *Physics of Geological Processes, Department of Geosciences, University of Oslo, Sem Selandsvei 24, Oslo, Norway, olivier.galland@fys.uio.no*
[2] *Now at GFZ German Research Centre for Geosciences, Helmholtz Centre Potsdam, Telegrafenberg, C 224, D-14473 Potsdam, Germany.*

Keywords: explosive vents, laboratory models, numerical models, dimensional analysis.

Shallow explosive volcanic processes, such as kimberlite volcanism, phreatomagmatic and phreatic activity, produce volcanic vents exhibiting a wide variety of morphologies, including vertical pipes and V-shaped vents. So far, most studies on explosive eruption dynamics have focused on the processes within existing magmatic conduits, *i.e.* magma degassing and fragmentation, assuming that the walls were infinitely rigid (Melnik et al., 2005, Starostin et al., 2005, Dellino et al., 2007). Other studies addressed the formation of maar-diatremes through loose (cohesionless) material, though natural rocks are cohesive (*e.g.* Woolsey et al., 1975; Ross et al., 2008; Gernon et al., 2009; Nermoen et al., 2010). Hence, these studies were not suitable for unraveling the formation of explosive vents through realistically cohesive rock formations.

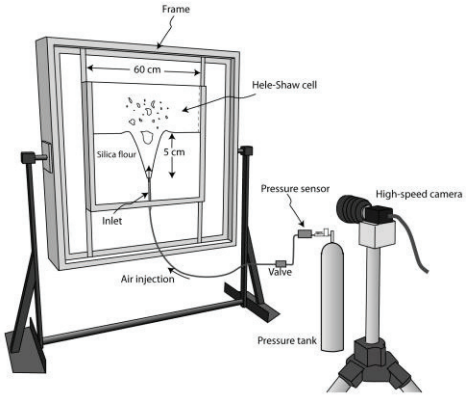

Fig. 1 – The caption(s) of the figure(s) should be typed in this format. The font to be used is Arial 8 pt.

In this study we report on experimental and numerical models designed to capture a range of morphologies in an eruptive system through cohesive material (Haug et al., 2013; Galland et al., in press). Using dimensional analysis, we identified key governing dimensionless parameters, in particular the gravitational stress-to-fluid pressure ratio (Π_2 = P/ρgh), and the fluid pressure-to-host rock strength ratio (Π_3 = P/C). We used combined experimental and numerical models together to test the effects of these parameters.

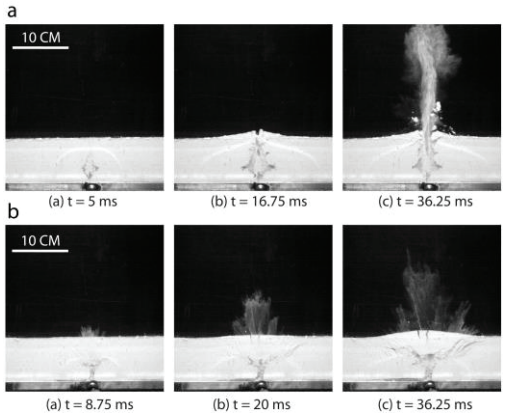

Fig. 2 – **a**. Snapshots of experiment with relatively high pressure compared to overburden thickness (high Π_2). The air carves straight through the layer. **b**. Snapshots of experiment with relatively low pressure compared to overburden thickness (low Π_2). Diagonal fractures propagate towards the surface.

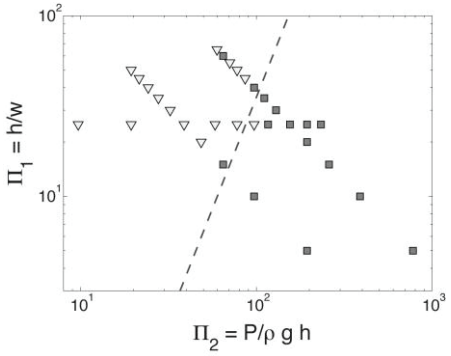

Fig. 3 – Phase diagram of vent morphology as a function of dimensionless parameters. Open triangles: V-shaped vents; Grey squares: vertical vents.

The experiments were used to test the effect of Π_2 on vent morphology and dynamics (Figure 1). Two distinct morphologies were observed in the experiments: vertical pipes (Figure 2a) and diagonal fractures (Figure 2b). A dimensionless phase diagram demonstrates a separation between morphologies, with vertical structures occurring at high values of Π_2, and diagonal ones at low values of Π_2 (Figure 3).

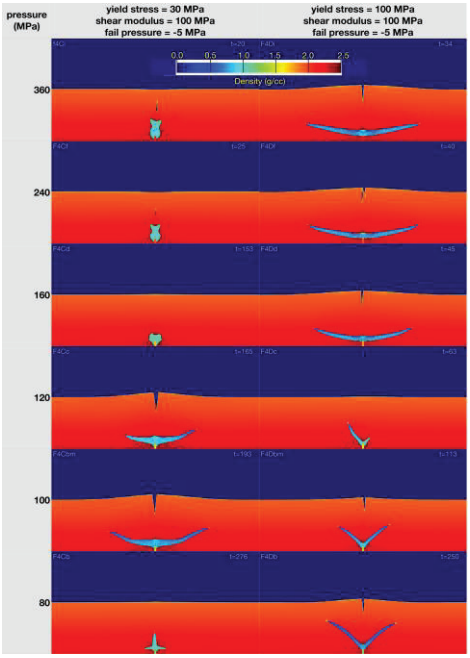

Fig. 4 – Phase diagram showing snapshots of numerical simulations. It is observed that for high values of Π_3 (upper left corner), vertical pipes are produced, whereas for low values of Π_3 (lower right corner) V-shaped vents are produced.

The numerical simulations were used to test the effect of Π_3 on vent morphology and dynamics. In the numerical models we see three distinct morphologies: vertical pipes are produced at high values of Π_3, diagonal pipes at low values of Π_3, while horizontal sills are produced for intermediate values of Π_3 (Figure 4).

The distribution of stress (Figure 5) reveal that vertical pipes form by plasticity-dominated yielding for high-energy systems (high Π_2 and Π_3), whereas diagonal and horizontal vents dominantly form by fracturing for lower-energy systems (low Π_2 and Π_3).

Although our models are 2-dimensional, they suggest that circular pipes result from plastic yielding of the host rock in a high-energy regime, whereas V-shaped volcanic vents result from fracturing of the host rock in lower energy systems.

Acknowledgements

This work was supported by Center of Excellence grant from the Norwegian Research Council to PGP. The authors gratefully acknowledge the technical support of Olav Gundersen. The staff of the workshop of the Physics Department at the University of Oslo built the experimental box. The authors gratefully thank Prof. Knut Jørgen Måløy for lending the high speed camera to Ø. Haug.

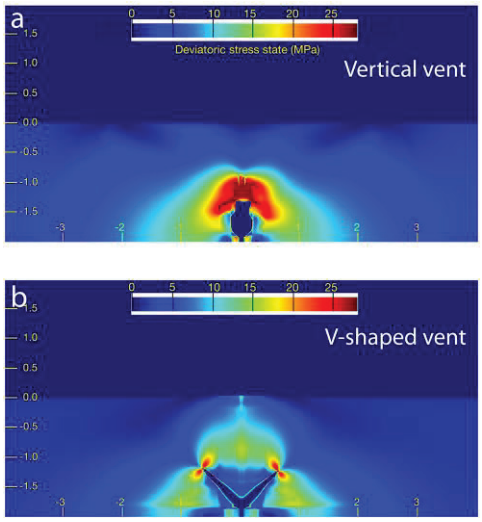

Fig. 5 – a. Map of deviatoric stress associated with vertical vent (high Π_3). The stresses are distributed over a broad zone, highlighting plasticity-dominated process. b. Map of deviatoric stress associated with V-shaped vent (low Π_3). The stresses are concentrated at the tips of fractures, highlighting elasticity-dominated process.

References

Dellino, P., B. Zimanowski, R. Büttner, L. La Volpe, D. Mele, and R. Sulpizio, 2007. Large-scale experiments on the mechanics of pyroclastic flows: Design, engineering, and first results, Journal of Geophysical Research, 112.

Galland, O., Gisler, G.R., and Haug, Ø.T., in press. Morphology and Dynamics of explosive vents through cohesive rock formations. Journal of Geophysical Research.

Gernon, T. M., M. A. Gilbertson, R. S. J. Sparks, and M. Field, 2009. The role of gas-fluidisation in the formation of massive volcaniclastic kimberlite. Lithos, 112 Supplement 1(0): 439-451.

Haug, Ø. T., O. Galland, and G. R. Gisler, 2013. Experimental modelling of fragmentation applied to volcanic explosions. Earth and Planetary Science Letters 384(0): 188-197.

Melnik, O., A. A. Barmin, and R. S. J. Sparks, 2005. Dynamics of magma flow inside volcanic conduits with bubble overpressure buildup and gas loss through permeable magma. Journal of Volcanology and Geothermal Research 143(1-3): 53-68.

Nermoen, A., O. Galland, E. Jettestuen, K. Fristad, Y. Y. Podladchikov, H. Svensen, and A. Malthe-Sørenssen, 2010. Experimental and analytic modeling of piercement structures. Journal of Geophysical Research 115(B10): B10202.

Ross, P. S., J. D. L. White, B. Zimanowski, and R. Büttner, 2008. Multiphase flow above explosion sites in debris-filled volcanic vents: Insights from analogue experiments. Journal of Volcanology and Geothermal Research 178(1): 104-112.

Starostin, A. B., A. A. Barmin, and O. E. Melnik, 2005. A transient model for explosive and phreatomagmatic eruptions. Journal of Volcanology and Geothermal Research 143(1-3): 133-151.

Woolsey, T. S., M. E. McCallum, and S. A. Schumm, 1975. Modeling of diatreme emplacement by fluidization. Physics and Chemistry of the Earth 9: 29-42.

X-Ray diffraction study of ash samples from the Popocatépetl volcano

José Luis González[1], Luis Manuel Arévalo[2], Alejandra Quintanilla[1], Karla E. Barquera[1], Yleana Claudia Martínez[1], Ricardo Agustín[3]

[1] *Colegio de Geofísica, FI-BUAP, Puebla, México.* jose.gogu@gmail.com
[2] *Facultad de Ciencias físico Matemáticas, BUAP, Puebla, México.*
[3] *Centro Universitario de Vinculación y Trasferencia de Tecnología OTC- BUAP, Puebla, México.*

Keywords: Popocatépetl, volcanic ash, x-ray difraction.

We present the results of the x-ray diffraction study of ashes from the Popocatépetl volcano, wich was very active on May 7th, 2013, and a large amount of ash fell down over the metropolitan area of the Puebla city. The ash samples were collected with the help of students from the Applied Geophysics laboratory from the the Benemérita Universidad Autónoma de Puebla (BUAP). Sampling was done one hour after the deposit of the ash.

The studied samples were collected from eight different points located in: 1) Puebla´s metropolitan area, 2) San Nicolás de los Ranchos (two samples), and 3) Atlixco (Puebla).

Studies performed in the ash samples are: measurement of electric and magnetic properties, Raman spectroscopy, and X-ray diffraction.

Preliminary results show consistencies in ten parameters, including presence of: albite, enstatite, forsterite, iron oxide and magnetite , as shown in the Figs. 1-4 .

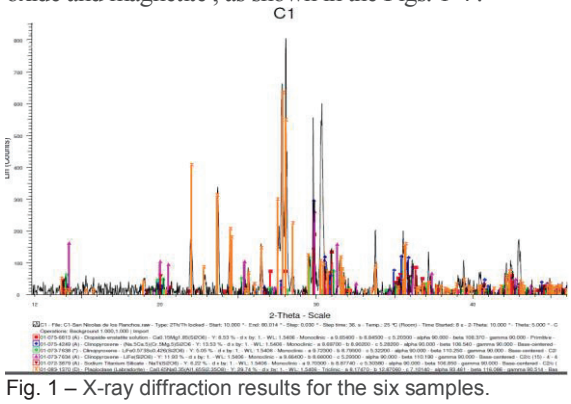

Fig. 1 – X-ray diffraction results for the six samples.

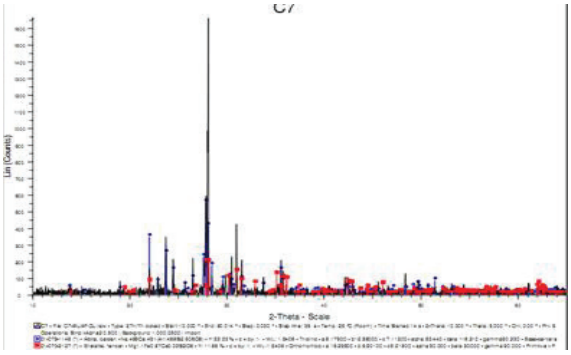

Fig. 2 – X-ray diffraction graph for the sample collected at the campus of the BUAP.

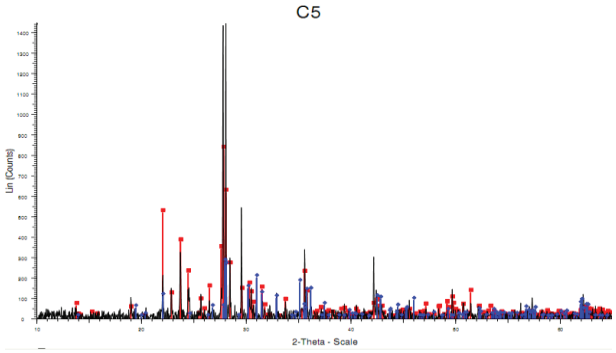

Fig. 3 – X-ray diffraction graph for the Loma Encantada sample.

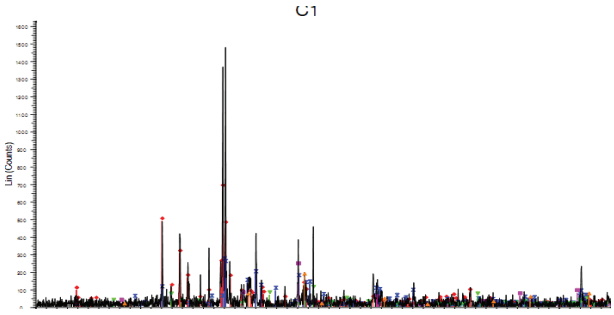

Fig. 4 – X-ray diffraction graph for the sample collected in San Nicolás de los Ranchos.

We are currently comparing the results obtained in the studies of 2012 and 2013 ash samples. Our data includes the results of X-ray and Raman spectroscopy.

References

Brindley, George W., Brown, George, eds. 1980, Crystal structures of clay minerals and their X-ray identification, Mineralogical Society. ISBN 0903056089.

Drenth, Jan, 1999, Principles of protein x-ray crystallography. Springer. ISBN 0387985875.

Helliwell, John R., 1992, Macromolecular crystallography with synchrotron radiation. Cambridge University Press. ISBN 0-521-33467-5.

Stout, George H.; Jensen, Lyle H. 1989, X-ray structure determination — A practical guide. John Wiley & sons. ISBN 0-471-60711-8.

AUTHORS INDEX

AUTHORS INDEX (CONT.)

This book was printed in Hidalgo Producciones Gráficas S.A. de C.V.,
Querétaro, México, with a print run of 300 copies.
October, 2014

We acknowledge our sponsors for their support to this meeting: